DEVELOPMENT OF A PREDICTIVE EQUATION OF STATE FOR EQUILIBRIUM AND VOLUMETRIC PROPERTIES OF DIVERSE MOLECULES AND THEIR MIXTURES

By

AGELIA M. ABUDOUR

Bachelor of Science in Chemical Engineering
Alzawia University
Subrata, Libya
2001

Master of Science in Chemical Engineering
Tripoli University
Tripoli, Libya
2007

Submitted to the Faculty of the
Graduate College of the
Oklahoma State University
in partial fulfillment of
the requirements for
the Degree of
DOCTOR OF PHILOSOPHY
December, 2014

DEVELOPMENT OF A PREDICTIVE EQUATION OF STATE FOR EQUILIBRIUM AND VOLUMETRIC PROPERTIES OF DIVERSE MOLECULES AND THEIR MIXTURES

Dissertation Approved:

Dr. Khaled A. M. Gasem

Dissertation Adviser

Dr. Robert L. Robinson, Jr.

Dr. Josh D. Ramsey

Dr. Martin Hagan

ACKNOWLEDGEMENTS

First of all, I would like to express my grateful appreciation to my advisor Dr. Khaled Gasem. His continuous support, constructive guidance, knowledge, and experience have greatly contributed to the success of this work. I am proud to be his student.

I would like to extend my thanks and appreciation to my co-advisor Dr. Robert Robinson, Jr. for his valuable suggestions and encouragement. Also, I extend my thanks to the committee members Dr. Josh Ramsey and Dr. Hagan for their time and efforts in reviewing this work.

I would like to thank Dr. Sayeed Mohammad for his valuable advice, support and significant contribution. I would also like to thank Dr. Brian Neely for his advice and helpful discussions. My special thanks go to my colleagues, Dr. Krishna Yerramsetty, Dr. Solomon Gebreyohannes, and Mr. Pongtorn Charoensuppanimit for their support and help. I also thank all many friends I made over the years, whose friendship I truly appreciate.

I also acknowledge the support of the U.S. Department of Energy and the Coal-Seq Consortium to our research group that made this project possible.

I like to express my greatest appreciation and love to my husband, Abdulwahab, for his patience and understanding, and to my daughters and son, Rahf, Rana, Rafa and Ahmed, who make it all an enjoyable experience.

Finally, I dedicate this research effort to all members of my family, especially my parents whose inspiration, encouragement, moral and financial support made my ambitions throughout the years a reality.

Name: AGELIA M. ABUDOUR

Date of Degree: DECEMBER, 2014

Title of Study: DEVELOPMENT OF A PREDICTIVE EQUATION OF STATE FOR EQUILIBRIUM AND VOLUMETRIC PROPERTIES OF DIVERSE MOLECULES AND THEIR MIXTURES

Major Field: CHEMICAL ENGINEERING

Abstract:

Accurate prediction of the phase equilibrium and volumetric properties of pure fluids and their mixtures is essential for chemical process design and related applications. Although experiments provide accurate data at specific phase conditions, such data are limited and do not meet the ever-expanding industrial needs for process design and development. Therefore, a need exists for models that can provide accurate predictions of a wide range of thermodynamic properties.

Cubic equations of state (CEOS) are widely used for calculations of thermodynamic properties; however, they often require experimental data for system-specific model tuning. An attractive alternative is to develop *predictive* equations of state that can estimate these properties based *solely* on the molecular structure - the most basic information that is generally available. In this work, the Peng-Robinson (PR) EOS is the focus of such development.

The two main objectives of this study are to (1) develop improved generalized models for critical properties, acentric factor and vapor-liquid equilibria (VLE) property predictions using a theory-framed quantitative structure-property relationship (QSPR) modeling approach and (2) develop a new volume-translation function with a scaling-law correction to predict liquid density for pure fluids and mixtures of diverse molecules.

To facilitate model development, a comprehensive databases of experimental measurements was assembled for pure-fluid critical properties, acentric factors, and liquid densities as well as VLE and liquid densities of binary mixtures. QSPR models were then developed to provide *a priori* predictions for the critical properties, acentric factor and VLE properties. The newly developed QSPR models for the critical properties provided predictions within twice the experimental errors. Similarly for VLE predictions, the QSPR models resulted in approximately twice the errors obtained through the data regression analyses of the VLE systems considered. Also, a new volume-translation method for the PR EOS was developed. The volume-translation function parameter was generalized in terms of molecular properties of each fluid. Then, the volume-translated PR EOS was extended to predict liquid densities of diverse mixtures employing EOS conventional mixing rules. The volume-translation approach developed in this work has been shown capable of providing accurate predictions of liquid densities in the saturated as well as single-phase regions for pure fluids and mixtures over large ranges of pressure and temperature. Specifically, the new volume-translated PR EOS yielded errors that are three to six times lower than the corresponding predictions from the untranslated model.

TABLE OF CONTENTS

CHAPTER PAGE

CHAPTER PAGE

LIST OF TABLES

TABLE PAGE

TABLE PAGE

TABLE PAGE

LIST OF FIGURES

FIGURE PAGE

FIGURE PAGE

FIGURE PAGE

CHAPTER I

INTRODUCTION

1.1 Rationale

Accurate vapor-liquid equilibrium (VLE) and volumetric property predictions are essential for designing and modeling chemical processes. Equilibrium systems involve different molecules, different types of interactions, and different phase conditions. Consequently, they produce different types of phase behavior. The complexity of the phase behavior encountered necessitates different computational frameworks, and different models to serve different applications. Herein, EOS modeling is considered for two targeted applications:

A. Energy sector: Thermophysical property predictions are routinely required and carried out in the refining and petrochemical processes. Further, the phase equilibrium models are an important part of reservoir simulation work and design of enhanced gas and oil recovery processes.
B. Computer-aided molecular design (CAMD): Thermodynamic and physical properties are essential inputs to all CAMD applications. CAMD is the general term used to describe the process of designing molecules that have specific desired properties. A successful CAMD process requires an accurate prediction platform to compute the relevant properties of the generated candidate molecules.

Experimental measurements are the most reliable method for determining these required properties of pure and mixed substances. However, experiments can be time consuming and expensive. As such, a need exists for reliable predictive models to determine accurately the vapor-liquid equilibrium and volumetric properties without the need for extensive experimentation. Cubic equations of state (CEOS) such as Soave-Redlich-Kwong (SRK) [1] and Peng-Robinson (PR) [2] are widely used in the chemical industry to perform reservoir simulations and process design calculations due to the inherent simplicity and efficiency of CEOS. To be sufficiently accurate, these models frequently require system-specific model tuning using available experimental data, thus limiting their predictive capabilities. A potentially attractive method is to predict *a priori* the input model parameters of CEOS from the molecular structure of the constituent molecules. If successful, this strategy will ensure that the CEOS model becomes *entirely predictive* in nature, thus providing a much needed capability for practical work. Developing a predictive CEOS entails an integrated effort to develop the various components of the computational algorithm. Specifically, the predictive CEOS will require structure-based predictive models for (a) model input variables such as pure-fluid critical properties (b) binary interaction parameters used in the mixing and combining rules and (c) volume-translation for liquid densities.

Accurate critical properties and acentric factor are required inputs in a CEOS. In fact, these pure-fluid properties have a significant influence on the phase behavior predictions from a CEOS [3]. Riazi et al [4] showed that large errors in the predicted thermophysical properties can result from small errors in the critical properties and acentric factors. Traditionally, critical properties have been determined experimentally by techniques of varying complexities. However, experimental determination of critical properties of the ever increasing number of chemicals requires significant time and cost investments. Therefore, several approaches, empirical as well as semi empirical, have been suggested in the literature to estimate these properties. These include group-

contribution methods and correlations using structural parameters [5-11]. However, such methods are limited by their range of applicability and/or by poor suitability for generalization. Recently, quantitative structure–property relationship (QSPR) modeling has shown the ability to predict thermophysical properties based solely on chemical structure information [12-16]. Although QSPR models are successful in predicting thermophysical properties, the majority of such existing models were developed based upon limited data and hence their general predictive capabilities are limited. Therefore, the proposed study aims to develop predictive QSPR models for pure-fluid critical properties based on a comprehensive database containing diverse molecular classes. Further, the proposed study will utilize improved algorithms developed recently [17] for enhancing their accuracy significantly when used for *a priori* predictions.

Predicting phase equilibrium properties using a CEOS often requires adjustable parameters in the mixing rules, and these adjustable parameters are referred to as the binary interaction parameters (BIPs). The BIPs account for the unlike molecular interactions in mixtures composed of diverse molecular species. In fact, an accurate description of phase equilibria of mixtures is generally sensitive to the mixing rules and the BIPs in the CEOS [18]. These BIPs, in general, cannot be predicted *a priori* from existing theory, but they are typically regressed from experimental measurements of the binary pairs which form the systems of interest. Thus, the need for developing reliable generalized models to estimate EOS BIPs exists. QSPR modeling has shown potential for providing accurate predictions of fluid properties based on the molecular structure. The proposed study aims to generalize the BIPs of the PR EOS using QSPR modeling; thereby, a predictive, structure-based model capable of describing the phase behavior of diverse systems at various conditions can be developed. In fact, this capability is essential in the overall development of a predictive CEOS.

Another aspect of CEOS model development is to provide the prediction of liquid densities, which are generally inaccurate due to the two-parameter nature of CEOS. To overcome this

deficiency, several volume-translation approaches have been proposed, and these range from a constant correction term to more complex forms that are both temperature and density dependent [10, 18-30]. Temperature-dependent volume-translation methods provide improved saturated liquid density predictions. However, these methods do not perform as well in the single-phase, compressed liquid region [28, 31]. Further, the use of a temperature-dependent volume-translation function with CEOS can lead to thermodynamic inconsistencies such as isotherm cross-overs [28, 31-33] and negative isochoric heat capacities, C_V, at high pressures [32-34] in the compressed liquid region. The proposed study will develop a volume-translation method based on a scaling law correction and will eliminate the inherent deficiencies in existing literature methods for volume translation.

Apart from the simple volume-translation method of Peneloux et al. [20], only a few volume-translation methods in the literature have been extended to mixtures. Tsai and Chen [23] and Lin and Duan [25] extended their volume-translation methods to mixtures, but only at atmospheric pressure conditions. Since most volume-translation methods available in the literature have been developed and tested only for pure fluids, a need exists for a reliable volume-translation method that can provide accurate predictions of saturated and single-phase liquid densities for mixtures. Thus, the proposed study will include an extension of the volume-translation method to diverse binary mixtures. The applicability of the developed model will be demonstrated using a comprehensive database for liquid densities of binary mixtures.

The aim of this research is thus to develop a QSPR-based, predictive CEOS with generalized models for the CEOS input variables, binary interaction parameters and volume translation. The developed model would, in principle, be applicable for vapor-liquid, liquid-liquid equilibria, volumetric properties and calorimetric properties. However, the scope of this work is limited to vapor-liquid equilibrium and volumetric property predictions with the newly developed predictive CEOS.

1.2 Goals and Objectives

The goal of this research is to develop and evaluate the efficacy of a structure-based predictive EOS based on the Peng-Robinson equation. This was accomplished by equipping the PR EOS with a new volume-translation function and generalizing the model input parameters using QSPR methodologies. To accomplish this goal, the following objectives and their associated tasks were undertaken:

A. Assembling experimental databases

Several databases were assembled for conducting this study, including

- Pure-fluid critical properties and acentric factor
- High- and low-pressure vapor-liquid equilibrium (VLE)
- Pure-fluid and mixture liquid densities

The databases were chosen such that there is a sufficient representation of all major classes of molecules of interest to chemical design and processes, with wide temperature and pressure ranges.

B. Applying QSPR methodology to develop predictive models for selected thermophysical properties

A new QSPR model was developed that is capable of *a priori* predictions of the pure-fluid thermophysical properties including the critical properties (critical temperature (T_c), critical pressure (P_c), and critical compressibility factor (V_c)) and acentric factor (ω). The model was applied for diverse molecules using large databases of the selected thermophysical properties.

C. Generalizing the binary interaction parameters in the PR EOS using the QSPR methodology

Structure-based generalized models were developed for *a priori* predictions of VLE for a diverse set of binary mixtures over wide conditions of pressure, temperature and composition. Specifically, the QSPR modeling was used to provide structure-based parameters for the PR EOS model.

D. Developing a new volume-translation function with scaling-law correction

A new volume-translation method for the PR EOS was developed that can be used to obtain reliable predictions of liquid densities in *both* saturated and single-phase regions of diverse chemical species over extended ranges of temperature and pressure. The volume-translation function parameter was generalized in terms of molecular properties of each fluid. Then, the volume-translated Peng-Robinson equation-of-state (VTPR EOS) was extended to predicting liquid densities of diverse mixtures over large ranges of pressure and temperature using conventional mixing rules.

This research work provided a modified PR EOS model capable of accurate *a priori* predictions of vapor-liquid equilibrium and volumetric properties of pure fluids and mixtures over a wide range of temperatures and pressures for use in numerous applications such as refining, reservoir simulation, and design of enhanced gas and oil recovery processes. Further application includes providing thermodynamic and physical properties of candidate molecules in computer-aided molecular design (CAMD) processes.

1.3 Thesis Organization

This dissertation is written in the "manuscript style," and it is divided into five stand-alone chapters. Chapter 1 provides the rationale and the objectives of this work. Chapter 2 presents the development of non-linear QSPR models for the prediction of critical temperature, critical pressure, critical volume and acentric factor. The results for the four properties are presented and discussed in this chapter. Chapter 3 deals with application of PR EOS modeling of high-pressure

phase equilibria of coalbed gas + water mixtures. In this chapter, generalized correlations for the BIPs in the PR EOS in terms of temperature were developed. Chapter 4 focuses on PR EOS binary parameter generalizations using the QSPR methodology for 916 VLE systems. Chapter 5 presents the development of a new volume-translation method for the PR EOS to predict the pure-fluid liquid densities in the saturated and the single-phase region. Chapter 6 describes the extension of the volume-translation method to mixture liquid density predictions using EOS conventional mixing rules. The final chapter contains conclusions and recommendations from this study.

REFERENCES

1. G. Soave, Equilibrium constants from a modified Redlich-Kwong equation of state, Chemical Engineering Science, 27 (1972) 1197-1203.
2. D.Y. Peng, D.B. Robinson, A new two-constant equation of state, Industrial & Engineering Chemistry Fundamentals, 15 (1976) 59-64.
3. A.S. Teja, R.J. Lee, D. Rosenthal, M. Anselme, Correlation of the critical properties of alkanes and alkanols, Fluid Phase Equilibria, 56 (1990) 153-169.
4. M.R. Riazi, T.A. Al-Sahhaf, M.A. Al-Shammari, A generalized method for estimation of critical constants, Fluid Phase Equilibria, 147 (1998) 1-6.
5. A.P. Kudchadker, B.J. Zwolinski, Vapor pressure and boiling points of normal alkanes, C21 to C100, Journal of Chemical & Engineering Data, 11 (1966) 253-255.
6. A.L. Lydersen, Estimation of critical properties of organic compounds, in: Eng. Exp. Stn. Rep. 3, WI, University of Wisconsin College Engineering: Madison, 1955.
7. K.G. Joback, R.C. Reid, Estimation of pure-component properties from group-gontributions, Chemical Engineering Communications, 57 (1987) 233-243.
8. K.A.M. Gasem, Binary vapor-liquid phase equilibrium for carbon dioxide + heavy normal paraffins (interaction parameters, density predictions, pure hydrocarbon properties), in, Oklahoma State University, United States -- Oklahoma, 1986.
9. C. Tsonopoulos, Z. Tan, The critical constants of normal alkanes from methane to polyethylene: II. application of the flory theory, Fluid Phase Equilibria, 83 (1993) 127-138.

10. K. Magoulas, D. Tassios, Thermophysical properties of normal-alkanes from C1 to C20 and their prediction for higher ones, Fluid Phase Equilibria, 56 (1990) 119-140.

11. J.J. Marano, G.D. Holder, General equation for correlating the thermophysical properties of n-paraffins, n-olefins, and other homologous series. 2. Asymptotic behavior correlations for PVT properties, Industrial & Engineering Chemistry Research, 36 (1997) 1895-1907.

12. C. Hansch, T. Fujita, p-σ-π Analysis. A method for the correlation of biological activity and chemical structure, Journal of the American Chemical Society, 86 (1964) 1616-1626.

13. A.R. Katritzky, V.S. Lobanov, M. Karelson, Normal boiling points for organic compounds: correlation and prediction by a quantitative structure−property relationship, Journal of Chemical Information and Computer Sciences, 38 (1998) 28-41.

14. A.R. Katritzky, L. Mu, M. Karelson, QSPR treatment of the unified nonspecific solvent polarity scale, Journal of Chemical Information and Computer Sciences, 37 (1997) 756-761.

15. D.T. Stanton, L.M. Egolf, P.C. Jurs, M.G. Hicks, Computer-assisted prediction of normal boiling points of pyrans and pyrroles, Journal of Chemical Information and Computer Sciences, 32 (1992) 306-316.

16. M.D. Wessel, P.C. Jurs, Prediction of normal boiling points for a diverse set of industrially important organic compounds from molecular structure, Journal of Chemical Information and Computer Sciences, 35 (1995) 841-850.

17. K.M. Yerramsetty, B.J. Neely, K.A.M. Gasem, A non-linear structure–property model for octanol–water partition coefficient, Fluid Phase Equilibria, 332 (2012) 85-93.

18. G.F. Chou, J.M. Prausnitz, A phenomenological correction to an equation of state for the critical region, AIchE Journal, 35 (1989) 1487-1496.

19. J.J. Martin, Cubic equations of state-which?, Industrial & Engineering Chemistry Fundamentals, 18 (1979) 81-97.

20. A. Peneloux, E. Rauzy, R. Freze, A consistent correction for Redlich-Kwong-Soave volumes, Fluid Phase Equilibria, 8 (1982) 7-23.

21. H.B. de Sant'Ana, P. Ungerer, J.C. de Hemptinne, Evaluation of an improved volume translation for the prediction of hydrocarbon volumetric properties, Fluid Phase Equilibria, 154 (1999) 193-204.

22. P. Watson, M. Cascella, D. May, S. Salerno, D. Tassios, Prediction of vapor-pressures and saturated molar volumes with a simple cubic equation of state .2. The VanderWaals-711 EOS, Fluid Phase Equilibria, 27 (1986) 35-52.

23. J.-C. Tsai, Y.-P. Chen, Application of a volume-translated Peng-Robinson equation of state on vapor-liquid equilibrium calculations, Fluid Phase Equilibria, 145 (1998) 193-215.

24. J. Ahlers, J. Gmehling, Development of an universal group contribution equation of state: I. Prediction of liquid densities for pure compounds with a volume translated Peng–Robinson equation of state, Fluid Phase Equilibria, 191 (2001) 177-188.

25. H. Lin, Y.-Y. Duan, Empirical correction to the Peng–Robinson equation of state for the saturated region, Fluid Phase Equilibria, 233 (2005) 194-203.

26. P. Ungerer, C. Batut, Prédiction des propriétés volumétriques des hydrocarbures par une translation de volume améliorée, Oil & Gas Science and Technology - Rev. IFP, 52 (1997) 609-623.

27. J.-C. de Hemptinne, P. Ungerer, Accuracy of the volumetric predictions of some important equations of state for hydrocarbons, including a modified version of the Lee-Kesler method, Fluid Phase Equilibria, 106 (1995) 81-109.

28. H. Baled, R.M. Enick, Y. Wu, M.A. McHugh, W. Burgess, D. Tapriyal, B.D. Morreale, Prediction of hydrocarbon densities at extreme conditions using volume-translated SRK and PR equations of state fit to high temperature, high pressure PVT data, Fluid Phase Equilibria, 317 (2012) 65-76.

29. P.M. Mathias, T. Naheiri, E.M. Oh, A density correction for the Peng—Robinson equation of state, Fluid Phase Equilibria, 47 (1989) 77-87.

30. K. Frey, M. Modell, J. Tester, Density-and-temperature-dependent volume translation for the SRK EOS: 1. Pure fluids, Fluid Phase Equilibria, 279 (2009) 56-63.

31. K. Liu, Y. Wu, M.A. McHugh, H. Baled, R.M. Enick, B.D. Morreale, Equation of state modeling of high-pressure, high-temperature hydrocarbon density data, The Journal of Supercritical Fluids, 55 (2010) 701-711.

32. M.A. Trebble, P.R. Bishnoi, Accuracy and consistency comparisons of ten cubic equations of state for polar and non-polar compounds, Fluid Phase Equilibria, 29 (1986) 465-474.

33. O. Pfohl, Evaluation of an improved volume translation for the prediction of hydrocarbon volumetric properties, Fluid Phase Equilibria, 163 (1999) 157-159.

34. W.R. Ji, D.A. Lempe, Density improvement of the SRK equation of state, Fluid Phase Equilibria, 130 (1997) 49-63.

CHAPTER II

QUANTITATIVE STRUCTURE-PROPERTY RELATIONSHIP (QSPR) MODELS FOR PREDICTION OF PURE-FLUID CRITICAL PROPERTIES AND ACENTRIC FACTOR

2.1 Introduction

Pure-fluid physical properties including critical properties and acentric factor are important for designing and modeling chemical processes. The critical properties and acentric factor are required to calculate reduced state variables in the corresponding states theory and to determine equation-of-state parameters for predicting properties such as vapor pressure, phase density, heat of vaporization, viscosity, interfacial tension and phase equilibrium [1]. In fact, pure-fluid critical properties and acentric factors have a significant influence on the accuracy of phase behavior predictions [2]. Riazi et al. [3] showed that large errors in the predicted thermophysical properties could result from small errors in the critical properties and acentric factors.

Traditionally, critical properties have been determined experimentally by techniques of varying complexity. However, experimental determination of critical properties can be time consuming and costly. Moreover, these properties are difficult to measure for complex and large molecules that chemically degrade before they reach critical conditions [1, 4]. Therefore, reliable models capable of providing a *priori* predictions for the critical properties and acentric factor are of significant value.

Several approaches, empirical as well as semi-empirical, have been suggested in the literature to estimate the critical properties and acentric factor. However, the models are restricted to a limited number of classes of molecules. Gasem [5] and Gasem et al. [6] developed empirical correlations (the asymptotic behavior correlation to predict the critical properties and acentric factor of *n*-paraffins. Tsonopolous and Tan [7] developed correlations for predicting the critical properties of *n*-alkanes. Teja et al. [2] utilized the limiting property value approach for correlating the critical temperature and the critical pressure. Marano and Holder [8] extended the ABC model developed by Gasem and co-workers [5, 6] to a number of homologous series beyond alkanes. Kontogeorgis and Tassios [9] correlated the critical temperature and the critical pressure with the molecular weight.

Although the methods mentioned above have been applied to estimate the critical properties and acentric factor, are empirical in nature and often require accurate experimental data as input. Thus, the usefulness of these correlations is affected adversely when the required thermophysical data are unavailable or must be estimated using other correlations. Further, these models are specific to particular subclasses of compounds and perform poorly when applied to a diverse set of compounds. Therefore, researchers have turned their attention to structure-property relationship models that can predict the property values based solely on the molecular structure of the compound of interest.

A review of the available literature indicated that most current calculation methods for critical properties and acentric factor are based on the group-contribution approach. These methods employ the concept that a molecule is composed of functional groups rather than individual atoms. In other words, the thermophysical behavior of a molecule is determined by interactions between the functional group fragments present in the molecule. However, one of the drawbacks of these methods is that they cannot distinguish between isomeric forms of similar compounds since the isomers are described by the same set of groups. Despite their limitations, significant

efforts have been made to apply these methods for the prediction of critical properties and acentric factor. Riedel [10] and Kudchadker et al. [11] developed models for the critical properties of paraffins. Joback [12] proposed a more general group-contribution method to correlate the critical properties. The group contribution method proposed by Joback has been modified by Ambrose and Ghiasse [13] and Lydersen and Tsochev [14] and their group-contribution models are the most widely used for the prediction of critical properties. Other group-contribution models by Somayajulu [15] and Poling et al. [1] have utilized the boiling point to estimate critical properties. Ourique and Telles [16] presented an acentric factor prediction method for organic molecules. Although group-contribution methods have been extensively applied to specific sets of molecules, they often lack the accuracy desirable for a diverse set of molecules.

Recently, the quantitative structure–property relationship (QSPR) models, where the entire molecule is parameterized using molecular descriptors calculated through molecular mechanics, have been used effectively to correlate varied and often complex thermophysical properties of molecules. QSPR models have been able to predict successfully thermophysical properties such as normal boiling point, melting point and vapor pressure. Although structure-property relationships do not eliminate completely the need for experimental validation, a dramatic reduction in the number of molecules requiring synthesis and validation is realized. Numerous QSPR models have been proposed in the literature to predict varied and often complex thermophysical properties of molecules [17-21].

Needham et al. [22] utilized connectivity indices in their model to correlate the critical properties of over 70 organic molecules. Turner et al. [23] developed non-linear QSPR model with eight descriptors to predict the critical pressures and temperatures of 165 diverse molecules. Espinosa et al. [24] developed non-linear QSPR models with eight descriptors for critical pressure and temperature predictions of 530 diverse compounds. Their developed model yielded predictions of

critical temperatures for 530 diverse compound. Ren [25] applied atom-type topological indices to a QSPR model for predicting acentric factor of 74 molecules. However, the model was limited to alkanes with up to nine carbon atoms. Boozarjomehry et al. [26] used specific gravity and normal boiling point to predict critical properties and acentric factor of 194 molecules. Recently, Godavarthy [27] developed a QSPR model for predicting the critical properties using a reasonably sized dataset. However, this model was not tested sufficiently using an external test set. Gharagheizi et al. [28] applied a group contribution method to estimate critical properties and acentric factor of diverse chemical compounds. However, they employed a large number of descriptors (about 150 descriptors) as model inputs, which can increase the probability for over fitting and chance correlation. Although QSPR models are successful in predicting critical properties and acentric factor, the majority of such models were developed using limited data, and therefore, their general predictive capabilities are limited.

In this work, new QSPR models were developed that are capable of *a priori* predictions of pure-fluid critical properties (critical temperature (T_c), critical pressure (P_c), and critical volume (V_c)) and acentric factor (ω). This work differs from other literature efforts in that (a) a comprehensive database containing diverse molecular classes is used for model development, (b) descriptor selection is performed using non-linear algorithms (c) the developed models are further validated by employing an external test set of compounds not used for developing the model.

The remaining sections are organized as follows: Section 2 presents the QSPR methodology used, Section 3 discusses the results obtained, Section 4 compares the results of the current model with other different models from the literature and Section 5 presents the conclusions from this study.

2.2 Quantitative Structure-property Relationship (QSPR) Methodology

The development of a QSPR model involves several interconnected strategies. A flowchart outlining the steps involved in QSPR model development is presented in Figure 2.1. The

following steps are part of any QSPR model development effort: (a) database development, (b) molecular structure generation and optimization, (c) descriptor generation, (d) descriptor reduction, (e) QSPR model development and (f) QSPR model validation. In a recent work, Yerramsetty [29] has provided details of each of these steps. However, for the sake of completeness, a summary of these steps is outlined below.

2.2.1 Database Development

A reliable database is the prime requirement for developing a robust model and evaluating its performance. The critical properties and acentric factor experimental data were compiled from the DIPPR [30] database. The assembled dataset is representative of all major classes of organic molecules of interest to chemical design applications.

The database contained critical properties of 2030 molecules including experimental, predicted and smoothed data. The focus of the study was to develop models for molecules commonly encountered in refining processes; therefore, inorganic compounds, salts and elements were excluded. Since the predictive capability of the QSPR model depends strongly on the accuracy of the experimental data used in the model development process, only *experimental* data with low uncertainty values (<5%) were included in the database used for model development. The experimental data with high uncertainty values (>5%) as well as predicted and smoothed data taken from the DIPPR [30] database were then used for secondary external validation purposes. Figures 2.2–2.5 illustrate the error distribution for the experimental, predicted and smoothed error values obtained from DIPPR database for each of the critical properties.

2.2.2 Structure Generation, Optimization, and Descriptor Calculation

After development of a suitable database, structures are generated for the molecules. ChemBioDraw Ultra 11.0 [31] software was used to generate two-dimensional (2-D) structures of the molecules. Each 2-D structure was then used to generate three-dimensional (3-D) structures.

The 2-D structure can lead to several conformations of 3-D structure; however, only the 3-D conformation with the lowest energy is the stable state of the molecule. Thus, the molecular energy of the 3-D conformations was minimized using the OpenBabel genetic algorithm-based (GA) conformal search [32, 33] that employs the MMFF94 force field method [34].

The optimized structures were provided as inputs to the DRAGON [35] software to generate up to 3000 molecular descriptors for each molecule. A variety of constitutional, topological, geometrical, electrostatic and other descriptors are generated. The number of descriptors calculated for each molecule depends on the structural complexity of the molecule. Typically, only a few of these descriptors are significant in describing a specific property under investigation. Thus, a descriptor reduction approach was used to find the most significant descriptors.

2.2.3 Descriptor Reduction and Model Development

The descriptor reduction approach involves a hybrid strategy, which results in a non-linear wrapper based model, where descriptor reduction and model development are performed simultaneously. Specifically, a hybrid algorithm that combines evolutionary programming (EP) and differential evolution (DE) was used as a wrapper around artificial neural networks (ANNs). To search for the best descriptor subsets from a large number of molecular descriptors, the method begins with an initial population of single hidden layer ANNs (individuals) that have been divided into four different niches. Niches are mutually exclusive sub-populations in the original population, which are not allowed to exchange genetic material. The ANNs in the initial population are assigned random descriptor subsets as inputs. These ANNs then undergo (a) single-point mutation on the descriptor subsets, (b) modified differential evolution (MDE) operations on the descriptor subsets, (c) retraining with different initial weights and (d) change in the number of hidden neurons, over successive generations. The ANNs that can accurately predict

the target property are favored over inaccurate ANNs to remain in the population. The details on the actual descriptor reduction algorithm employed in the current study are also available in a recent work [29].

In the model development process, the entire data set was divided into four sub-sets (training, validation, internal test, and external test sets). The proportion of data for the different data sets was: 50% for the training set, 15% for the internal validation set, 10% for the internal test set and the remaining 25% for the external test set. The data division was performed by ensuring adequate representation of all the functional group interactions in all the datasets.

All data, excluding external test, was used in the descriptor reduction and model development process. The validation data set is used to avoid over-fitting by applying an early-stopping method [36, 37]. In addition, the internal test data was used to select the best ANNs during the descriptor reduction algorithm. The external test set data was set aside in the model development process and used to assess the generalization (*a priori* prediction) capability of the developed model.

In the current work, the entire data set excluding the external test set data was split into training (T), internal validation (V) and internal test sets (IT). The root-mean-squared error (RMSE) values between the predicted and target values were calculated for each of these subsets. The following objective function (OF) was then computed based on these RMSE values:

$$OF = RMSE_T + RMSE_V + RMSE_{IT} \tag{2.1}$$

Where the RMSE is calculated by the following equation:

$$RMSE = \left(\frac{\sum_{i=1}^{NDP} \left(M_p - M_t \right)_i^2}{NDP} \right)^{1/2} \tag{2.2}$$

where, NDP is the number of data points, M_t and M_p are the target and predicted properties, respectively

2.2.4 Creating Ensembles

An artificial neural network (ANN) may exhibit instability and the predictive performance of ANN is dependent strongly on the training data and the training parameters. Therefore, a single outlier in the training data could have disproportional effect on the generalization ability of the final model. To prevent this, ensembling of ANNs was utilized, where the predictions of different ANNs are averaged to result in the final predictions [38-40]. In this work, the final ensemble models consisted of 20 different ANNs, each having the same descriptors as inputs but different network architectures and weights.

2.2.5 Model Validation

The developed QSPR models were validated by employing an external test set of compounds not used in the model development process as emphasized by Tropsha *et al.* [41]. In this study, two different external test sets were used to better test the generalization capability of our developed models. The primary external data set (external test set 1) represent 25% of the dataset used in the model development process. This dataset was compiled by including experimental data from DIPPR that contained estimated errors of less than 5%. The secondary external data set (external test set 2) contained experimental data with estimated errors higher than 5%, as well as predicted and smoothed data with estimated errors less than 25. The performance of the developed models on these data sets would indicate the generalization capability (*a priori* prediction) of the final models.

2.3 Results and Discussion

QSPR models were developed to predict critical temperature (T_c), critical pressure (P_c), critical volume (V_c), and acentric factor (ω) of a diverse organic dataset containing over 1500 molecules**.** The predictive capabilities of these models were evaluated by comparing the property prediction errors, as described by the root-mean-squared error (RMSE), absolute average deviation (AAD) and percentage absolute average deviation (%AAD).

$$\text{bias} = \frac{\sum_{i=1}^{NDP}\left(M_{cal} - M_{exp}\right)_i}{NDP} \tag{2.3}$$

$$\%\,AAD = \frac{100}{NDP}\sum_{i=1}^{NDP}\left|\frac{M_{exp} - M_{cal}}{M_{exp}}\right|_i \tag{2.4}$$

where, NDP is the number of data points, M_{exp} and M_{cal} are the experimental and calculated properties, respectively.

2.3.1 Critical Temperature

One of the key tasks in QSPR modeling is determining the number of descriptors that is needed to accurately predict target values. Therefore, different-descriptor models were developed for predicting the critical temperature. Specifically, 10-descriptor, 15-descriptor and 20-descriptor models were tested, but no significant difference was observed among these models. Therefore, for the sake of simplicity, 10-descriptor models were used in the current study. We observed that using fewer than 10 descriptors provides a model with a significant increase in the errors for the training set. Therefore, 10-descriptor-model was chosen as the number of input descriptors for the critical temperature.

Table 2.1 provides the list of molecular descriptors used as inputs in developing the QSPR model for predicting critical temperature. Four of the ten descriptors are 2-D matrix-based descriptor types. These descriptors are calculated by including the relationship of edge adjacency in

the molecular graph of a chemical compound [42]. The list also includes descriptor types such as atom-centered fragments, information indices and molecular properties. Additional information on these descriptors may be found in the documentation of DRAGON [35].

Figure 2.6 (a) shows a comparison between the experimental and predicted T_c values in the modeling set. The correlation coefficient (R^2) between the experimental and predicted values is 0.99, indicating that the predicted T_c values are in good agreement with the experimental values. Similarly, Figures 2.6 (b) and (c) compare the experimental T_c values with the predicted T_c values in the primary external test and the secondary external test sets, respectively. The R^2 values between the experimental and predicted values for the primary external and the secondary external data sets are 0.97 and 0.85, respectively. Since data with lower uncertainty levels were used for the primary external data set, the level of agreement for this dataset is better than that for the secondary external data set, which contained data with higher experimental uncertainties or errors.

Table 2.5 presents the summary results for the critical temperature predictions using QSPR model for the modeling and primary external test sets. As shown in Table 2.5, the errors for the critical temperature predictions in the external test set were within two times the errors in the training set. Table 2.6 presents the summary results for the critical temperature predictions using QSPR model for the secondary external test set. The results are presented based on the experimental errors reported in the DIPPR database. For data with errors of less than 1%, the generalized model provided predictions with 1.8% AAD. Overall, the QSPR model resulted in 4.1 %AAD for the secondary external test set, which is higher than the deviations in the primary external test set (2.4 %AAD).

Figure 2.7 shows the distribution of deviations in predicted T_c obtained for data used in model development, primary external data and secondary external data sets. The model predictions are

within 5% AAD for most molecules, indicating the high accuracy of the developed model. As expected, the secondary external data set has higher errors than the primary external data set.

2.3.2 Critical Pressure

Similar to the models for critical temperature, 10-descriptor, 15-descriptor, and 20 descriptor-models were tested, but no significant difference was observed among the models. Therefore, 10-descriptor models were used in the current study. Table 2.2 provides the list of molecular descriptors used as inputs in developing the QSPR model for predicting critical pressure. Two of the significant descriptors are 2-D matrix-based descriptor types. Further, walk and path counts is one of the significant descriptors, which is used as a criterion for molecular complexity [43]. Another significant descriptor, ZM1MulPer (first Zagreb index by multiplicative perturbation vertex degrees) [44], is a topological index that takes into account the valence electrons in the atoms and describes the branching and the size of the molecule. The list also includes other descriptors types such as GETAWAY descriptors, RDF descriptors, WHIM descriptors and atom-type E-state indices.

Figure 2.8 (a) shows a comparison between the experimental and predicted P_c values in the modeling set. The correlation coefficient (R^2) between the experimental and predicted values is 0.99. The figure indicates that the predicted P_c values are in good agreement with the experimental values. Figures 2.8 (b) and (c) compare the experimental and predicted P_c values in the primary and secondary external test sets, respectively. The R^2 values between the experimental and predicted values for the primary and secondary external datasets are 0.97 and 0.89, respectively. The higher errors for some molecules in the secondary external data set could be due to the larger experimental uncertainty in the data for those molecules. Although the level of agreement for the external set is lower than that for the modeling set, these results are still

indicative of the capability of the developed QSPR model for generalized predictions on new systems not used in the model development process.

Table 2.5 presents the summary results for the critical pressure predictions using QSPR model for the modeling data and primary external test sets. As shown in Table 2.5, the overall errors for the modeling set (2.1%AAD) and primary external test set (4.3%AAD) are within the uncertainty of 5% reported in the DIPPR database. This also indicates the capability of the model for generalized *a priori* predictions. Table 2.6 presents the summary results for the critical pressure predictions using QSPR model for the secondary external test set. Overall, the QSPR model predicted the critical pressure within 7.6 %AAD for the secondary external test sets, which is reasonable since the maximum uncertainty in the data is about 10%.

Figure 2.9 shows the distribution of errors in predicted P_c obtained for data used in model development, primary external data and secondary external data sets. The predictions are generally within 5% for the data used in model development and primary external test sets, which demonstrates the capability of the model for generalized *a priori* predictions.

2.3.3 Critical Volume

For predicting critical volume, 5-descriptor, 10-descriptor and 15-descriptor-models were tested and no significant differences were observed among these models. Therefore, 5-descriptor models were used in the current study. Table 2.3 provides the list of the molecular descriptors that were used as inputs in developing the QSPR model for predicting V_c. In particular, 3-D matrix-based descriptors and McGowan volume appear to be significant in predicting critical volume. The McGowan volume is calculated from the individual atomic sizes and number of bonds in each molecule [45]. The result also includes 2-D matrix based descriptors, atom-centered fragments and topological indices.

Figures 2.10 (a)-(c) present a comparison between the experimental and predicted V_c values in the modeling, the primary external test and the secondary external test sets, respectively. The R^2 values between the experimental and predicted values are 1, 0.99 and 0.99 for the data used in model development, the primary external test and the secondary external test sets, respectively.

Table 2.5 presents summary results for the critical volume predictions using QSPR model for the modeling and primary external test sets. As can be seen from Table 2.5, the %AAD value for the primary external test set (2.8%) is about twice the error for the modeling set (1.6%), which indicates that the developed QSPR model was capable of accurate predictions of critical volume. Table 2.6 presents the summary results for the critical volume predictions using QSPR model for the secondary external test set. As expected, the developed model provided worse predictions on this dataset than those on the primary external dataset, due to the larger error uncertainty in the secondary external test set. In particular, the QSPR model yielded 5.8 %AAD for the secondary external test sets, which is reasonable since the maximum uncertainty in the most of these data is 10%. Figure 2.11 shows the distribution of error in predicted V_c for data used in model development, primary external data and secondary external data sets. Similar to T_c and P_c predictions, most of the molecules have lower than 5% error in the predictions for data used in model development and primary external test set, which demonstrates the capability of the model for generalized *a priori* predictions.

2.3.4 Acentric Factor

As the previous models, 5-descriptor, 10-descriptor, 15-descriptor, and 20 descriptor-models were tested. No significant difference was observed when more than 10 descriptors were used. We also observed that using less than 10 descriptors provides a model with a significant increase in the errors for the training set. Therefore, 10-descriptor-model was chosen as the number of input descriptors for the acentric factor. Table 2.4 provides the list of molecular descriptors that were

used as inputs in developing the QSPR model for predicting acentric factor. Topological indices and constitutional indices are significant in predicting the acentric factor. Topological descriptors are derived from hydrogen-suppressed molecular graphs, in which the atoms are represented by vertices and the bonds by edges [44]. Constitutional descriptors are reflecting the chemical composition of a compound without any information about its molecular geometry or atom connectivity [44]. 3D-MoRSE descriptors, RDF descriptors and 2D Atom Pairs were also used as input in developing the QSPR model for predicting the acentric factor. Additional information on these descriptors may be found in the documentation of DRAGON [35].

Figures 2.12 (a)-(c) show a comparison between the experimental and predicted acentric factor values in the data used in model development, the primary external test and the secondary external test sets, respectively. The R^2 value between the experimental and predicted acentric factor was 0.95 for data used in model development, which indicates that the developed model was capable of representing the data well. The R^2 values for the primary and secondary external test sets were 0.79 and 0.80, respectively.

Table 2.5 provides the errors in acentric factor predictions for the data used in model development and primary external test sets. As shown in Table 2.5, the developed QSPR model was capable of predicting the acentric factor values within 12.3 %AAD, which is considerably higher than the corresponding value for the critical temperature, critical pressure and critical volume. The higher errors could be due to the larger experimental uncertainty in the acentric factor data. The acentric factor predictions using QSPR model for the secondary external test set are shown in Table 2.6. Similar predictions were obtained for both external test sets (16.3 %AAD). From the error distribution plot shown in Figure 2.13, it can be seen that the majority of the molecules have errors higher than 5%.

2.4 Comparison of Critical Properties and Acentric Factor Predictions from Different Methods

In this section, we present comparisons of the critical properties and acentric factor predictions from different methods. Specifically, we compared our models with nine other models for the critical properties and acentric factor predictions from the literature. In this comparison, the literature models were developed based on databases that differ from that used in the present study. Therefore, the predictions from the literature models expected to be different. The comparisons provided here are intended to serve only as a guide to the relative accuracies of these models.

Table 2.7 presents the summary results for the comparison of critical properties and acentric factor predictions from different models. In particular, the literature models of Gasem [5], Marano and Holder [8], Constantinou and Gani [46], Turner et al. [23], Espinosa et al. [24], Yuan et al. [47], Godavarthy [27], Sola et al. [4], and Gharagheizi et al. [28] were used for comparisons. Gasem and co-workers [5, 6] developed the Asymptotic Behavior Correlation (ABC) model framework to predict the physical properties of n-paraffins. Their model yielded of 0.08 %AAD for T_c, 0.38 %AAD for P_c, 0.59 %AAD for V_c, and 0.68 %AAD for ω regarding about 16 paraffins. Marano and Holder [8] extended the ABC model developed by Gasem and co-workers [5, 6] to n-Paraffins and n-Olefins. Their model developed based on a data set of about 16 paraffins and about 8 olefins. Constantinou and Gani (1994) developed an advanced group-contribution method based on the UNIFAC groups. They added second order group contributions to overcome the limitation of UNIFAC which cannot distinguish special configurations such as isomers, multiple groups located close together, and resonance structures at the first order. They applied their method for 251 to 285 molecules and they reported errors of 0.85, 2.89, and 1.79 %AAD for T_c, P_c, and V_c, respectively.

The estimation of critical pressures and temperatures on the basis of a back-propagation neural network model correlation (Non-linear QSPR model) was developed by Turner et al. [23] using a data set of 165 compounds (alcohols, ketones, esters, carboxylic acids, aldehydes, phenols, ethers, nitriles, and amines). For critical temperature, the authors developed an improved eight-descriptor non-linear QSPR model with an observed RMSE of 7.3 K for the 132 training, 7.7 K for 15 cross-validation, and 9.9 K for the 18 external set compounds, respectively. They also developed an eight-descriptor non-linear QSPR model for critical pressure which gave RMSE of 1.5, 1.4, and 2.4 bar for 132 training set, 15 cross-validation set, and 18 external set compounds, respectively. For both the critical temperature and pressure good results were obtained, even though the critical pressure, as stated by the authors, is much more difficult to model. On the other hand, the database considered by the authors includes a lot of hydrocarbons with little presence of other organic compounds.

Non-linear QSPR models with eight descriptors were developed by Espinosa et al. [24] for critical pressure and temperature predictions. Their developed model yielded predictions of critical temperatures for 530 diverse compounds with 5.6 %AAD while their model of critical pressures for 463 compounds gave predictions of 7.7 %AAD. A five-descriptor linear QSPR model was obtained by Yuan et al. [48] for the prediction of critical temperature of 139 hydrocarbon compounds with RMSE of 16.3 K. A four-descriptor linear model gave a correlation of critical pressure for 129 hydrocarbon compounds with RMSE of 1.9 bar.

Godavarthy [27] developed non-linear QSPR models for the critical properties predictions of diverse organic compounds. They obtained reliable results with an average absolute deviation of 1.2% (539 compounds) for T_c, 3.4% (539 compounds) for P_c, and 2.2% (273 compounds) for V_c. Their models show promising results in predicting the critical properties compared to previously published results. However, these models were not tested sufficiently using an external test set. Sola et al. obtained linear QSPR models with eight descriptors for the critical temperatures and

pressures of diverse compounds. They have reported RMSE of 12.6 and 9.7 K for the critical temperature training and validation sets, respectively, and 2.5 and 2.8 bar for critical pressure.

Recently, Gharagheizi et al. [28] developed a new model based on the artificial neural network group-contribution method (ANNGC) for predicting critical properties and acentric factors of around 1700 chemical compounds. As shown in Table 2.7, the resultant non-linear QSPR models are capable of giving excellent predictions of the critical properties and acentric factor of diverse compounds. Specifically, the average absolute deviations of their models are about 0.9% for T_c, 1.1% for P_c, 1.4% for V_c, and 3.7% for the acentric factor. However, they employed a large number of descriptors (about 150 descriptors) as model inputs, which can increase the probability for over fitting and chance correlation.

In this work, we present non-linear QSPR models for the prediction of critical properties and acentric factor for a diverse dataset. For model development, only *experimental* data with low uncertainty values (<5%) were included in the database. The resultant QSPR models are capable of predicting critical properties and acentric factor of the diverse set of molecules with average absolute percent deviations of 2, 3, 2 and 12 for critical temperature, critical pressure, critical volume and acentric factor, respectively. The developed models were validated by employing an external test set of compounds not used for developing the model. Comparable results were obtained with respect to other QSPR models despite the different composition of the database, confirming the versatility and robustness of the QSPR method.

2.5 Conclusion

Four non-linear models for the prediction of the critical temperature, critical pressure, critical volume and acentric factor were developed using QSPR methodology. Ten molecular structural descriptors were utilized as inputs in each of the QSPR models for T_c, P_c and ω. Five descriptors were used as inputs for the V_c model. The developed models were capable of predicting the

critical properties and acentric factor values with errors of 1.7%, 2.1%, 1.6% and 10.8% AAD for critical temperature, critical pressure, critical volume and acentric factor, respectively. Unlike models for predicting T_c, P_c and V_c, the developed model for predicting ω has higher prediction errors due to the larger experimental uncertainties of the data. The resulting models from this work can be used to predict *a priori* the critical temperature, critical pressure, critical volume of new molecules with reasonable accuracy.

To test the generalization capability of the developed QSPR models, two different external test sets were used. The primary external data set (external test set 1) was compiled by including experimental data from DIPPR that had estimated errors less than 5%, and the secondary external data set (external test set 2) contained experimental data with estimated errors higher than 5% as well as predicted and smoothed data with larger uncertainties. The predictions of the critical properties in the primary external test set were within two times the error in the model training set. As expected, due to the larger uncertainties in the secondary external data test set, the developed models exhibited larger differences with this dataset than those on the primary external dataset.

Table 2.1. Descriptors Used As Inputs for the ANNs in the Final Ensemble for Estimating Critical Temperature

No.	Descriptor Name	Descriptor	Type of Descriptor
1	SM2_B(p)	spectral moment of order 2 from Burden matrix weighted by polarizability	2D matrix-based descriptors
2	C-002	CH2R2	Atom-centred fragments
3	SIC0	Structural Information Content index (neighborhood symmetry of 0-order)	Information indices
4	Ho_D	Hosoya-like index (log function) from topological distance matrix	2D matrix-based descriptors
5	AMR	Ghose-Crippen molar refractivity	Molecular properties
6	B04[C-O]	Presence/absence of C - O at topological distance 4	2D Atom Pairs
7	nROH	number of hydroxyl groups	Functional group counts
8	SpMaxA_Dz(i)	normalized leading eigenvalue from Barysz matrix weighted by ionization potential	2D matrix-based descriptors
9	SpAD_B(e)	spectral absolute deviation from Burden matrix weighted by Sanderson electronegativity	2D matrix-based descriptors
10	ALOGP	Ghose-Crippen octanol-water partition coeff. (logP)	Molecular properties

Table 2.2. Descriptors Used As Inputs for the ANNs in the Final Ensemble for Estimating Critical Pressure

No	Descriptor Name	Descriptor	Type of Descriptor
1	MWC08	molecular walk count of order 8	Walk and path counts
2	SM3_Dz(Z)	spectral moment of order 3 from Barysz matrix weighted by atomic number	2D matrix-based descriptors
3	ZM1MulPer	ZM1MulPer	first Zagreb index by multiplicative perturbation vertex degrees
4	NsOH	number of sulfenic (thio-) acids	Functional group counts
5	VR2_B(m)	normalized Randic-like eigenvector-based index from Burden matrix weighted by mass	2D matrix-based descriptors
6	H3v	H autocorrelation of lag 3 / weighted by van der Waals volume	GETAWAY descriptors
7	RDF010m	Radial Distribution Function - 010 / weighted by mass	RDF descriptors
8	L2u	2nd component size directional WHIM index / unweighted	WHIM descriptors
9	SsF	Sum of sF E-states	Atom-type E-state indices
10	Hy	Hy	hydrophilic factor

Table 2.3. Descriptors Used As Inputs for the ANNs in the Final Ensemble for Estimating Critical Volume

No	Descriptor Name	Descriptor	Type of Descriptor
1	AVS_RG	average vertex sum from reciprocal squared geometrical matrix	3D matrix-based descriptors
2	Vx	Vx	McGowan volume
3	SpPosA_Dz(i)	normalized spectral positive sum from Barysz matrix weighted by ionization potential	2D matrix-based descriptors
4	O-057	phenol / enol / carboxyl OH	Atom-centred fragments
5	BAC	Balaban centric index	Topological indices

Table 2.4. Descriptors Used As Inputs for the ANNs in the Final Ensemble for Estimating Acentric Factor

No	Descriptor Name	Descriptor	Type of descriptor
1	ON1V	overall modified Zagreb index of order 1 by valence vertex degrees	Topological indices
2	ATS1s	ATS1s	Broto-Moreau autocorrelation of lag 1 (log function) weighted by I-state
3	nN	number of Nitrogen atoms	Constitutional indices
4	Mor02i	signal 02 / weighted by ionization potential	3D-MoRSE descriptors
5	nO	number of Oxygen atoms	Constitutional indices
6	RDF070v	Radial Distribution Function - 070 / weighted by van der Waals volume	RDF descriptors
7	Eig09_EA(bo)	eigenvalue n. 9 from edge adjacency mat. weighted by bond order	Edge adjacency indices
8	Hy	Hy	hydrophilic factor
9	F01[Cl-Si]	Frequency of Cl - Si at topological distance 1	2D Atom Pairs
10	F10[O-O]	Frequency of O - O at topological distance 10	2D Atom Pairs

Table 2.5. Summary Results Obtained for QSPR Modeling of Critical Properties and Acentric Factor Using an Ensemble Model

	N[a]	% Split	ND[b]	Ensemble Network		
				RMSE	%AAD	AAD
T_c (K)						
Modeling Data	337	73%	10	13	1.7	9
External Test Set	125	27%		22	2.4	14
Overall	**462**	**100%**		**16**	**1.9**	**10**
P_c (bar)						
Modeling Data	242	73%	10	1.4	2.1	2.7
External Test Set	90	27%		2.3	4.3	1.6
Overall	**332**	**100%**		**1.7**	**3.1**	**1.2**
V_c (m^3/kmol)						
Modeling Data	152	70%	5	0.007	1.6	0.005
External Test Set	64	30%		0.013	2.8	0.008
Overall	**216**	**100%**		**0.009**	**1.8**	**0.006**
ω						
Modeling Data	156	70%	10	0.1	10.8	0.1
External Test Set	66	30%		0.2	16.3	0.1
Overall	**222**	**100%**		**0.1**	**12.3**	**0.1**

([a]) N = Number of Molecules
([b]) ND = Number of Descriptors

Table 2.6. QSPR Model Predictions for the Critical Properties and Acentric Factor for the Secondary External Test Set Based on Experimental Errors Reported in DIPPR

DIPPER Error Range	T_c (K)		P_c (bar)		V_c (m^3/kmol)		ω	
	N[a]	%AAD (QSPR)	N	%AAD (QSPR)	N	%AAD (QSPR)	N	%AAD (QSPR)
< 0.2%	46	2.2	6	4.6	-	-	-	-
< 1%	57	1.8	38	2.6	-	-	-	-
< 3%	161	3.4	71	4.2	-	-	-	-
< 5%	737	3.7	162	6.6	-	-	-	-
< 10%	200	5.6	972	7.3	38	5.3	122	14.2
< 25%	112	7.2	199	12.0	10	7.4	53	21.1
Total	**1313**	**4.1**	**1448**	**7.6**	**48**	**5.8**	**175**	**16.3**

([a]) N = Number of Molecules

Table 2.7. Comparison of Critical Properties and Acentric Factor Predictions from Different Models

Researchers	Ref.	Model Type	Type of Compound	T_c (K)			P_c (bar)			V_c (m^3/kmol)			ω		
				N[a]	ND[b] (NP)[c]	%AAD (RMSE)	N	ND (NP)	%AAD (RMSE)	N	ND (NP)	%AAD (RMSE)	N	ND (NP)	%AAD (RMSE)
Gasem 1986	[8]	(ABC)[d]	n-paraffin	17	- (5)	0.08 (0.52)	16	- (5)	0.38 (0.13)	16	- (5)	0.59 (0.005)	15	- (5)	0.68 (0.004)
Marano and Holder 1997	[11]	(ABC)	n-paraffin	16	- (6)	0.05 (0.08)	16	- (6)	0.73 (0.046)	16	- (6)	0.64 (0.001)	16	- (6)	1.4 (0.002)
			n-olefin	9	- (6)	0.1 (0.24)	8	- (6)	1.03 (0.98)	8	- (6)	0.52 (0.001)	15	- (6)	1.8 (0.003)
Constantinou and Gani 1994	[71]	Group contribution	Organic	285	-	0.85 (6.98)	269	-	2.89 (2.02)	251	-	1.79 (0.01)	-	-	-
Turner et al. 1998	[47]	Non-linear QSPR	Organic	165	8 -	1.4 (7.6)	165	8 -	4.5 (5.0)	-	-	-	-	-	-
Espinosa et al. 2001	[48]	Non-linear QSPR	Organic	530	8 -	5.6 (29.2)	463	8 -	7.7 (3.9)	-	-	-	-	-	-
Yuan et al. 2003	[72]	Linear QSPR	Hydrocarbon	139	5 -	- (16.1)	129	5 -	- (1.9)	90	4	- (0.015)	-	-	-
Godavarthy 2004	[51]	Non-linear QSPR	Organic	539	10 -	1.2 9.3	539	10 -	3.4 1.7	273	5	2.2 0.009	-	-	-
Sola et al. 2008	[36]	Linear QSPR	Organic	153	8 -	1.5 (12)	139	8 -	4.9 (2.6)	-	-	-	-	-	-
Gharagheizi et al. 2011	[67]	ANN group contribution	Organic	1697	149 -	0.9 -	1696	149 -	1.1 -	1706	166	1.4 -	1691	166	3.7 -
This work		Non-linear QSPR	Organic	462	10 -	1.9 (16)	332	10 -	3.1 (1.7)	216	5	1.8 (0.009)	222	10	12.3 (0.1)

([a]) N = Number of Molecules
([b]) ND = Number of Descriptors
([c]) NP = Number of Parameters
([d]) (ABC) = Asymptotic Behavior Correlation

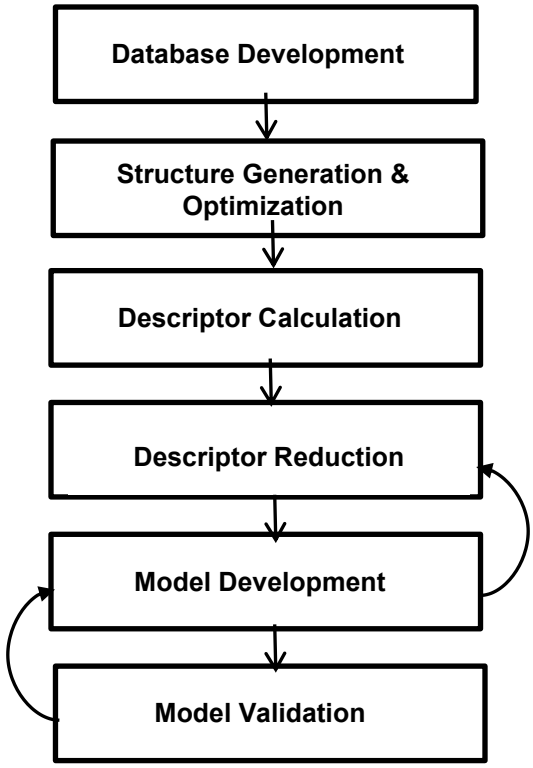

Figure 2.1. Steps Involved in Development of a QSPR Model

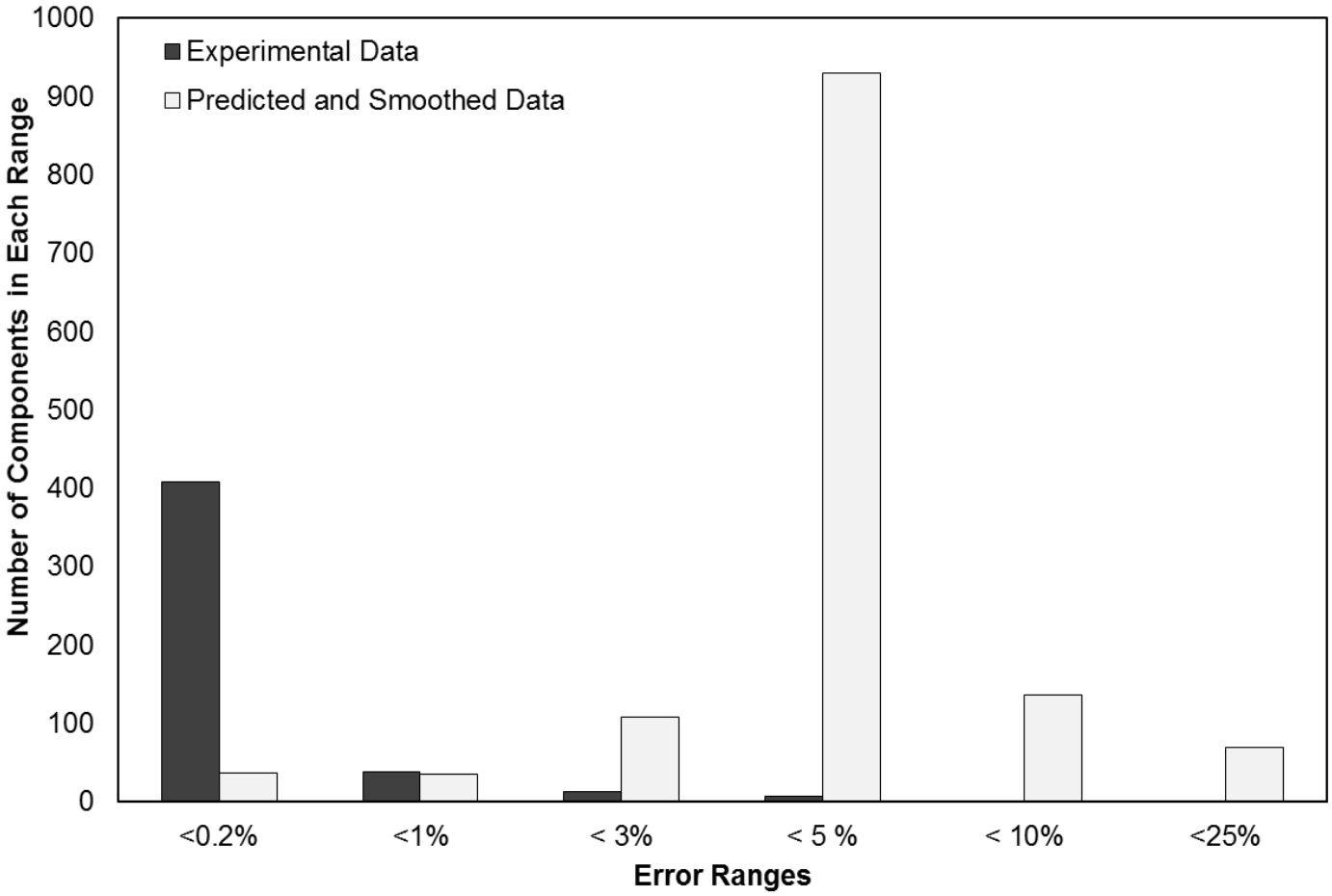

Figure 2.2. The Distribution of the Experimental Error Values Obtained from DIPPR Database for the Critical Temperature (T_c)

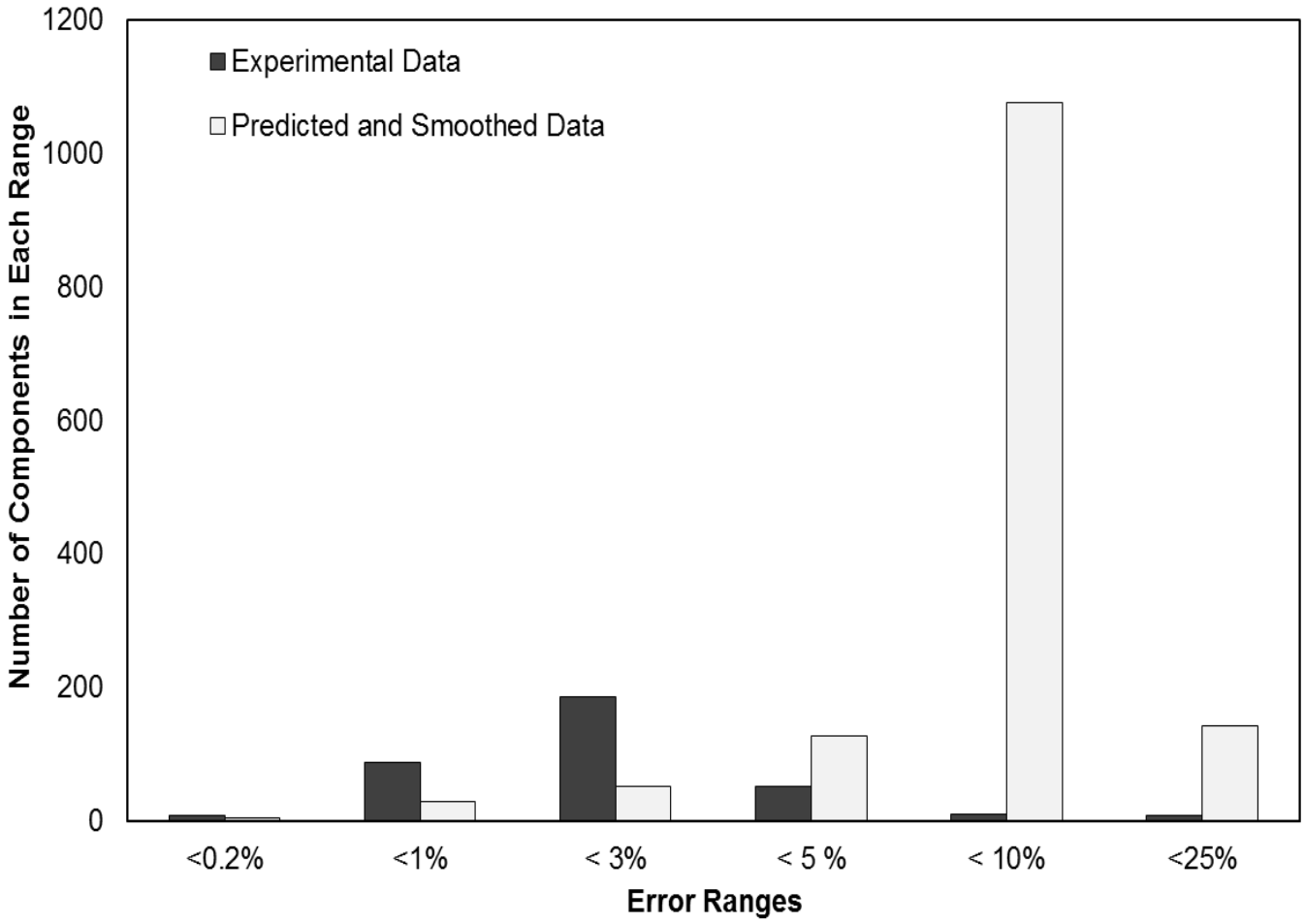

Figure 2.3. The Distribution of the Experimental Error Values Obtained from DIPPR Database for the Critical Pressure (P_c)

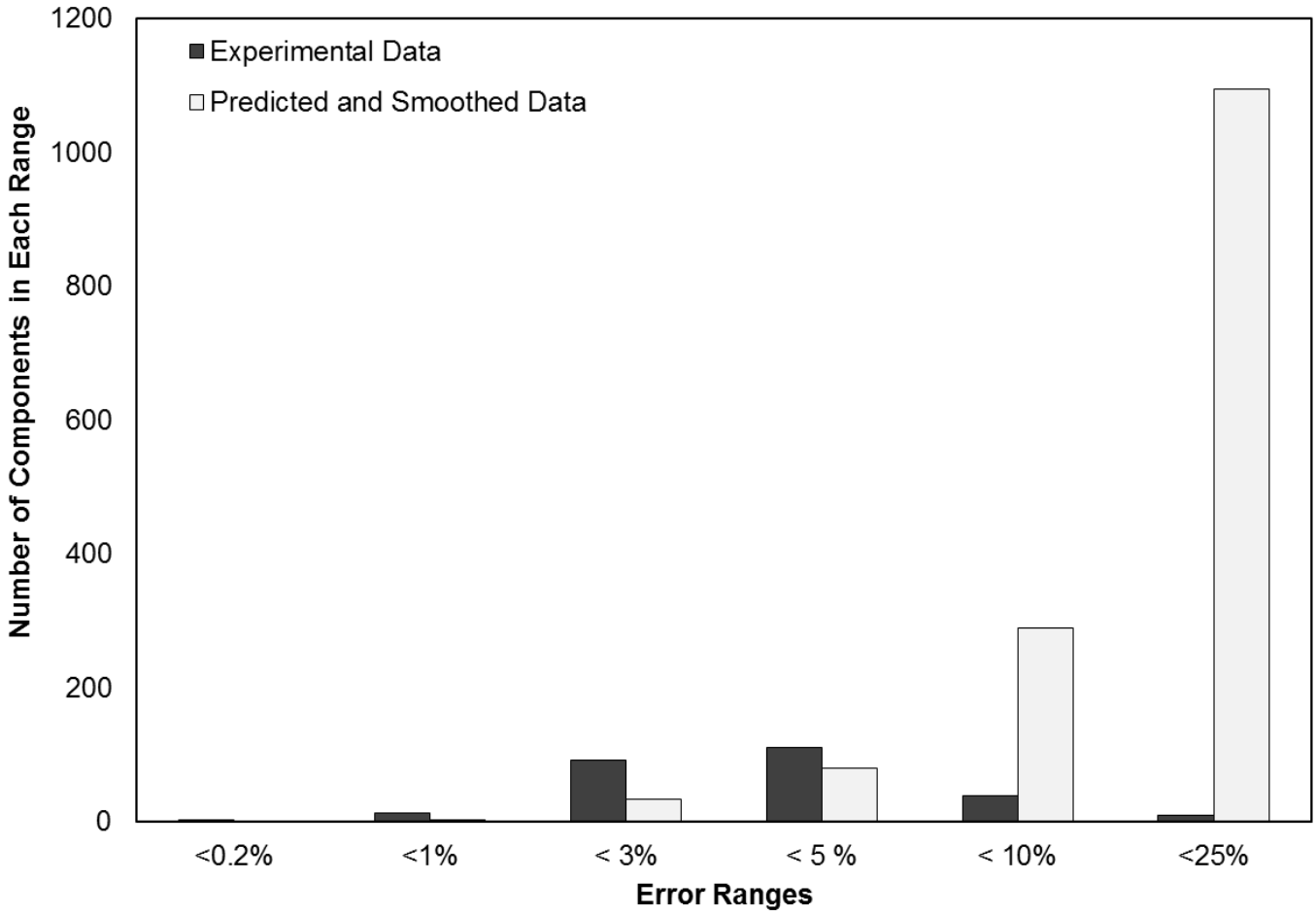

Figure 2.4. The Distribution of the Experimental Error Values Obtained from DIPPR Database for the Critical Volume (V_c)

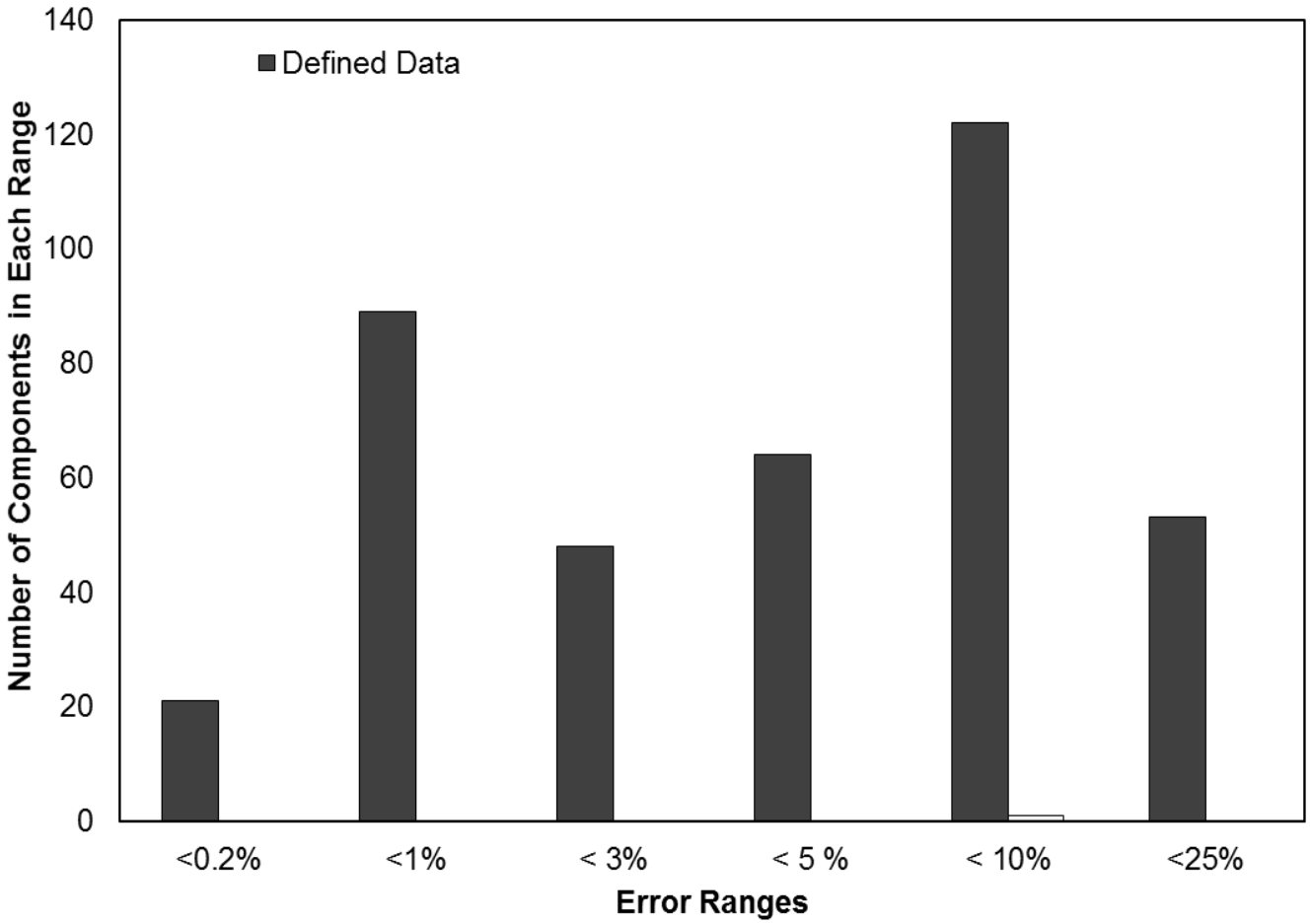

Figure 2.5. The Distribution of the Experimental Error Values Obtained from DIPPR Database for the Acentric Factor (ω)

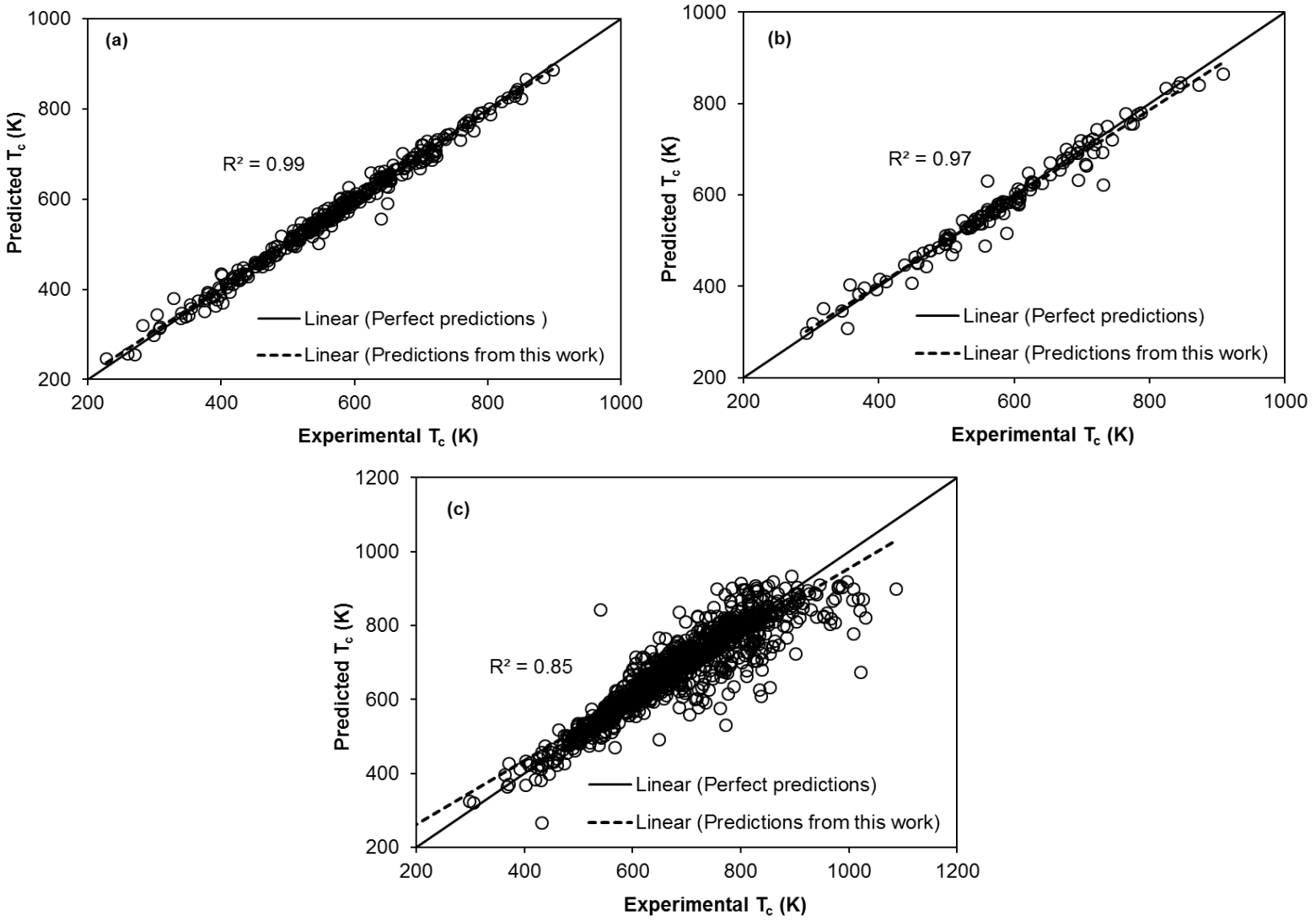

Figure 2.6. Comparison of the Experimental and Predicted T_c from QSPR Model for (a) Modeling Data (Training, Validation, and Internal Data Sets), (b) Primary External Test Set, (c) Secondary External Test Set

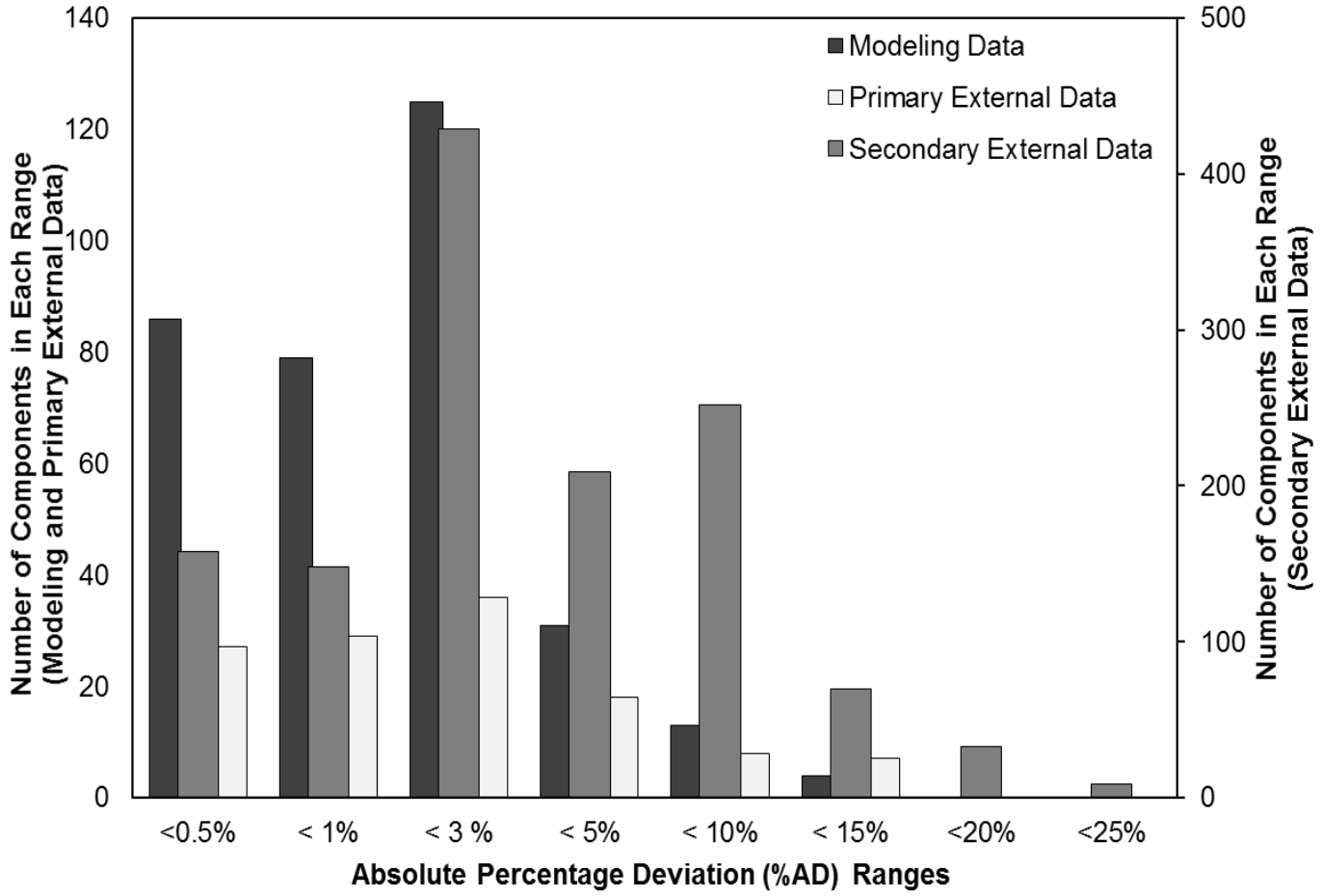

Figure 2.7. Distribution of Error in Predicted T_c (K) Obtained using the QSPR Model for Modeling Data, Primary External Data, and Secondary External Data Sets

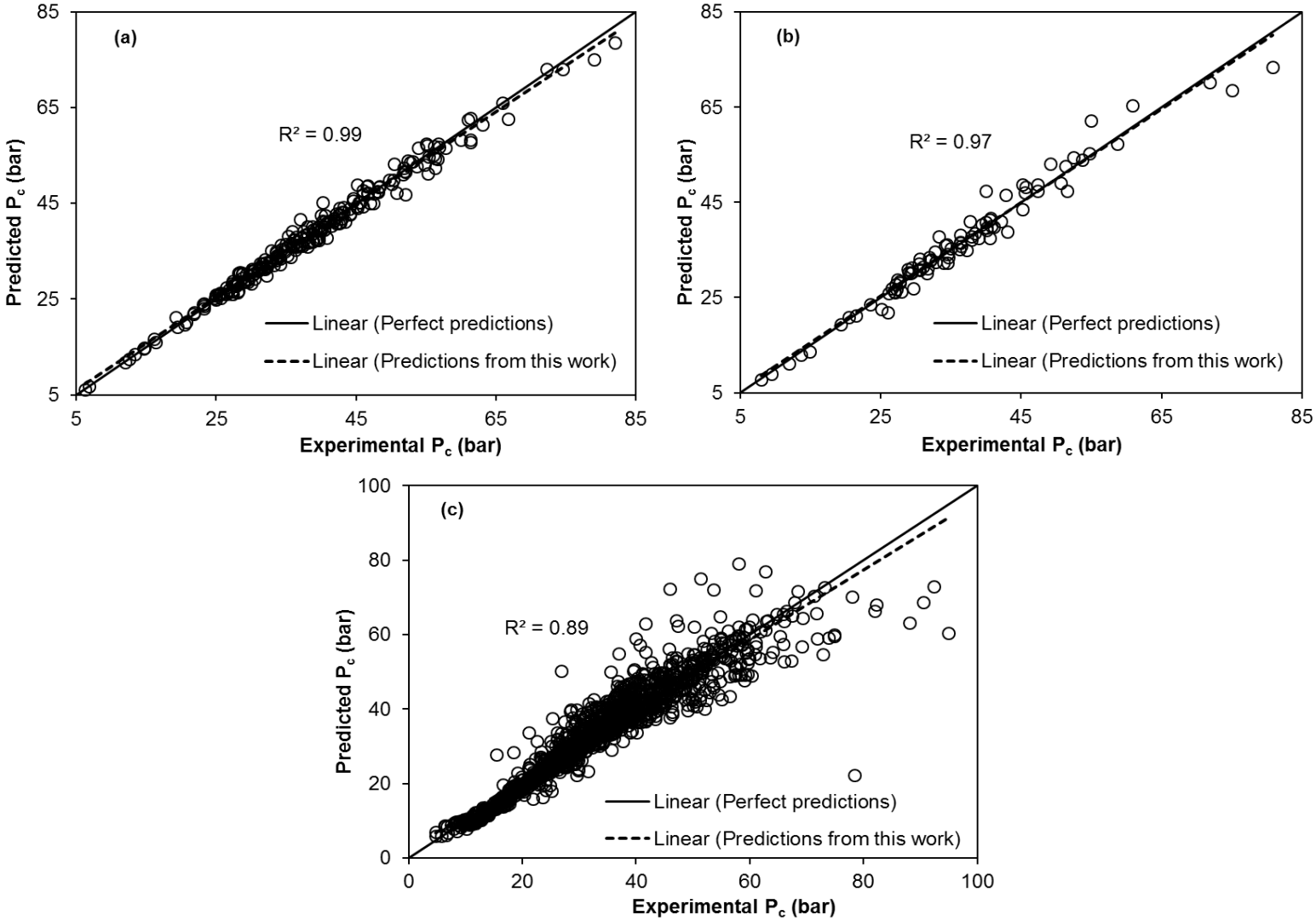

Figure 2.8. Comparison of the Experimental and Predicted P_c from QSPR Model for (a) Modeling Data (Training, Validation, and Internal Data Sets), (b) Primary External Test Set, (c) Secondary External Test Set

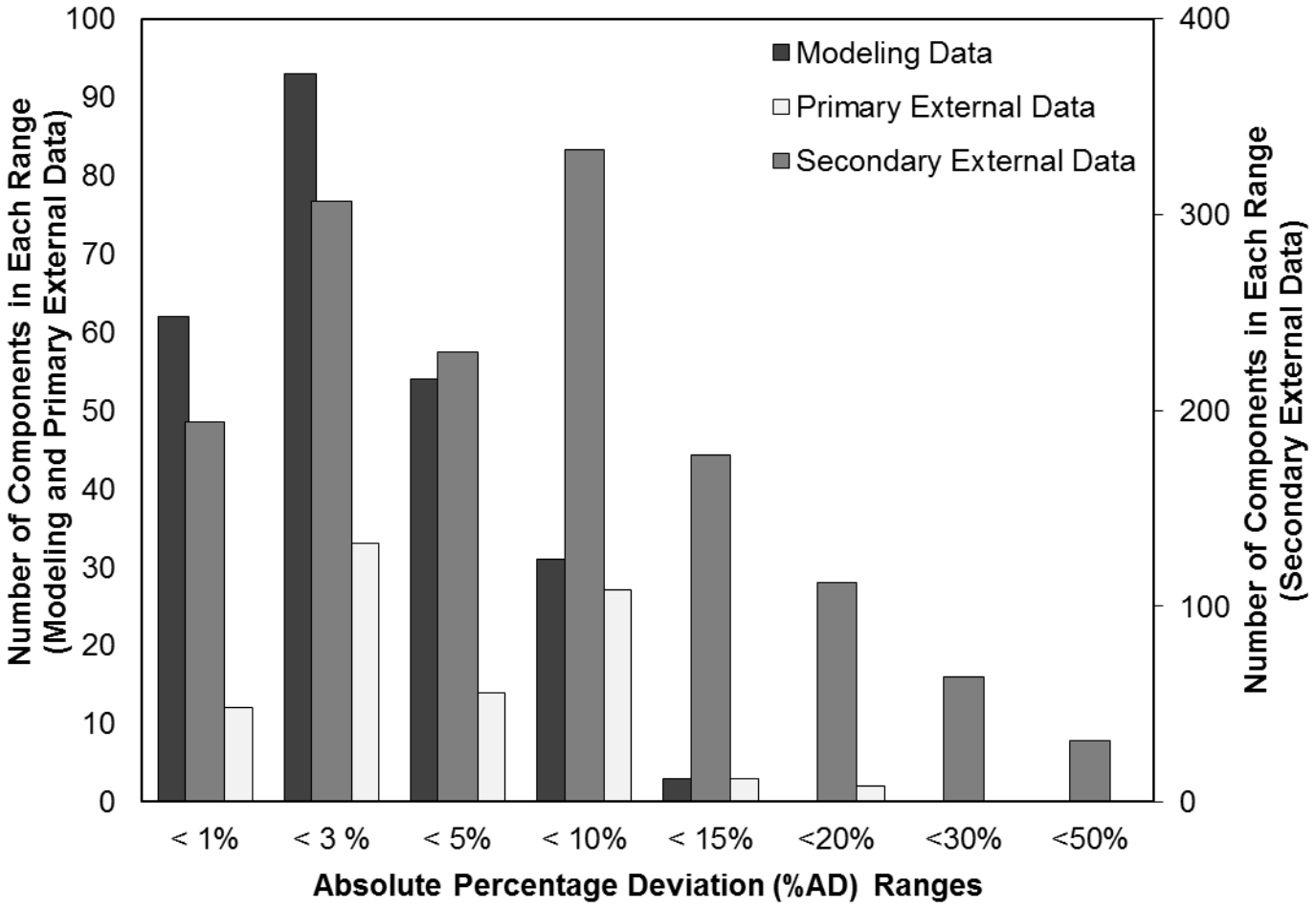

Figure 2.9. Distribution of Error in Predicted P_c (bar) Obtained using the QSPR Model for Modeling Data, Primary External Data, and Secondary External Data

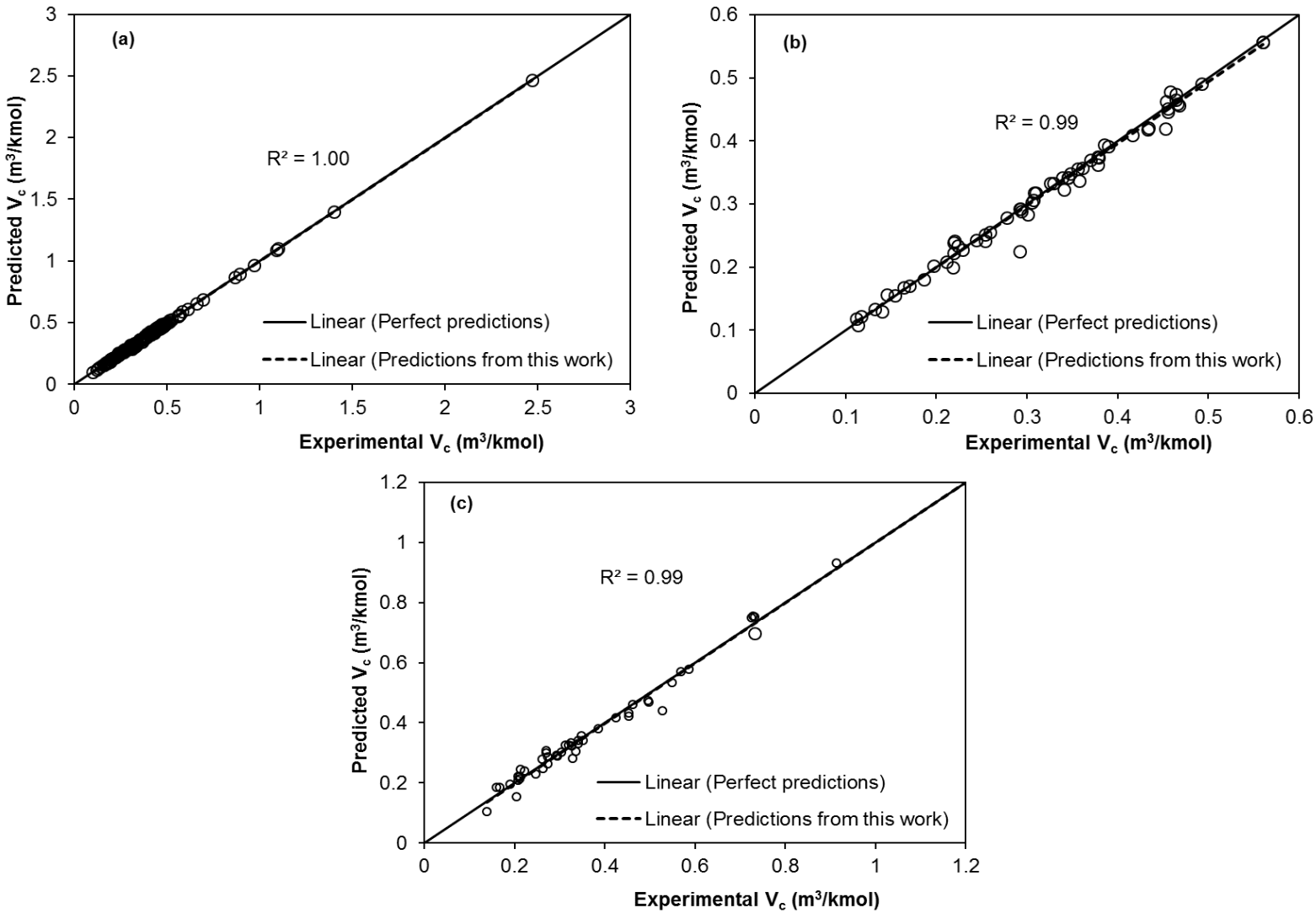

Figure 2.10. Comparison of the Experimental and Predicted V_c from QSPR Model for (a) Modeling Data (Training, Validation, and Internal Data Sets), (b) Primary External Test Set, (c) Secondary External Test Set

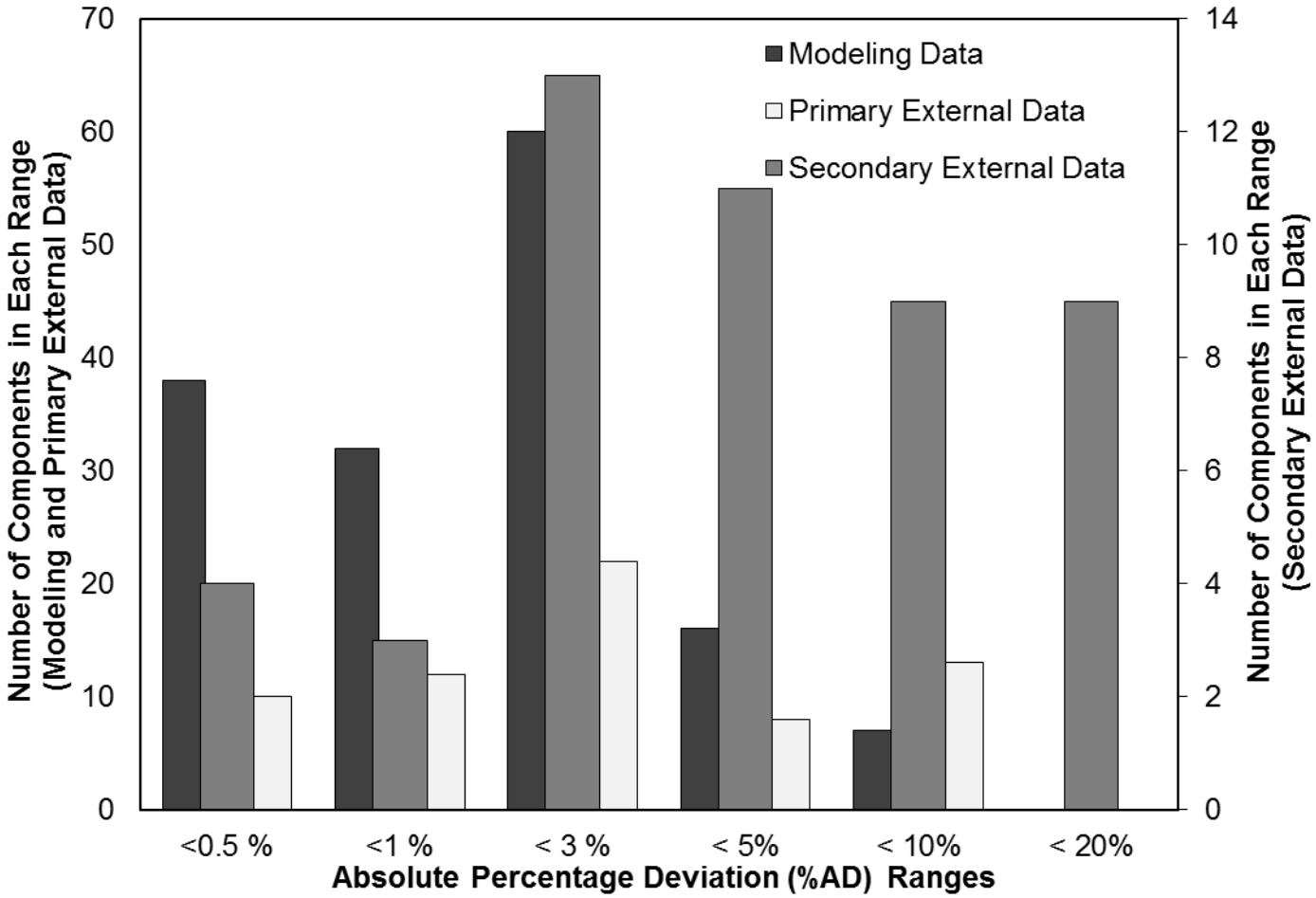

Figure 2.11. Distribution of Error in Predicted V_c (m^3/kmol) Obtained using the QSPR Model for Modeling Data, Primary External Data, and Secondary External Data Sets

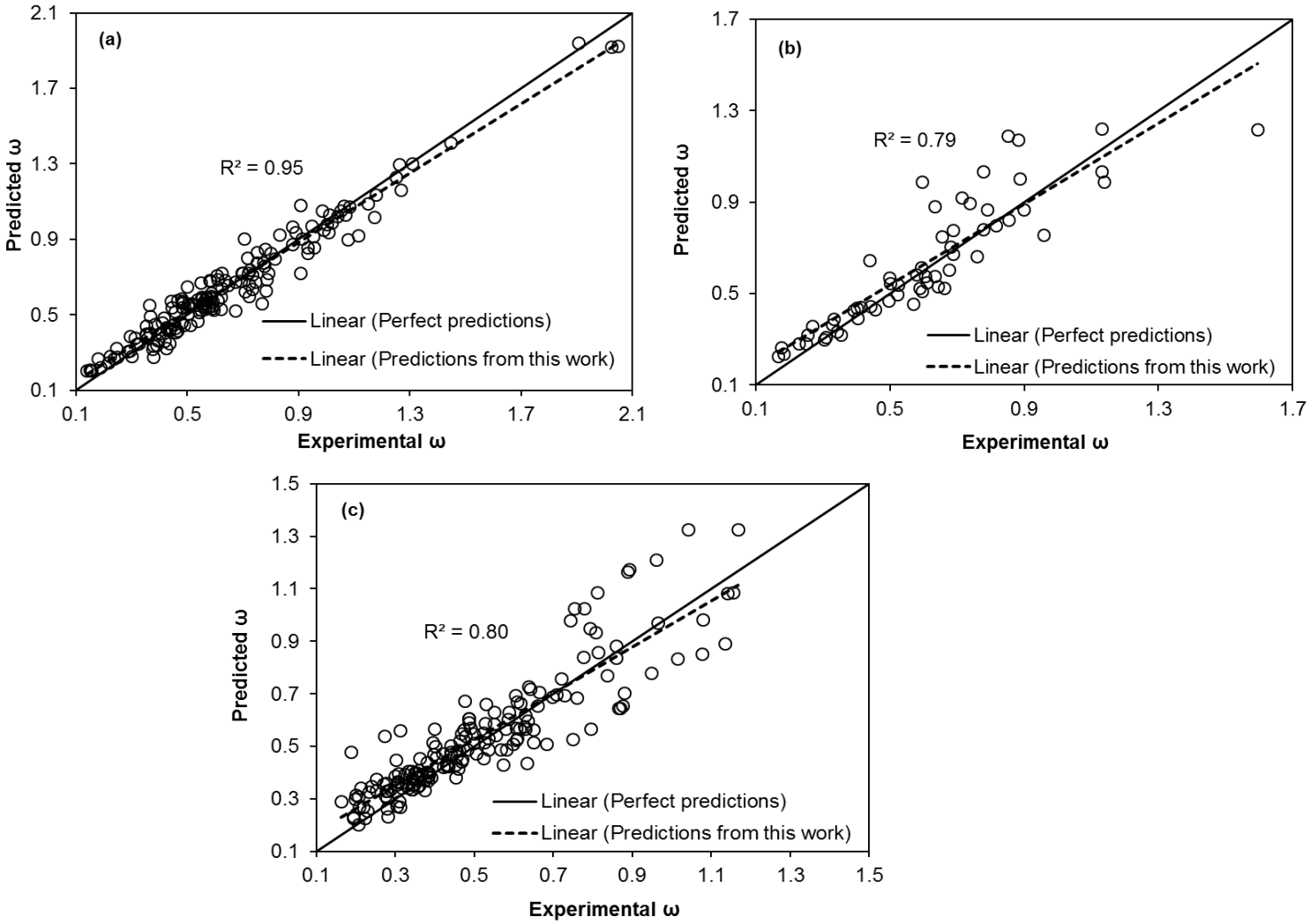

Figure 2.12. Comparison of the Experimental and Predicted ω from QSPR Model for (a) Modeling Data (Training, Validation, and Internal Data Sets), (b) Primary External Test Set, (c) Secondary External Test Set

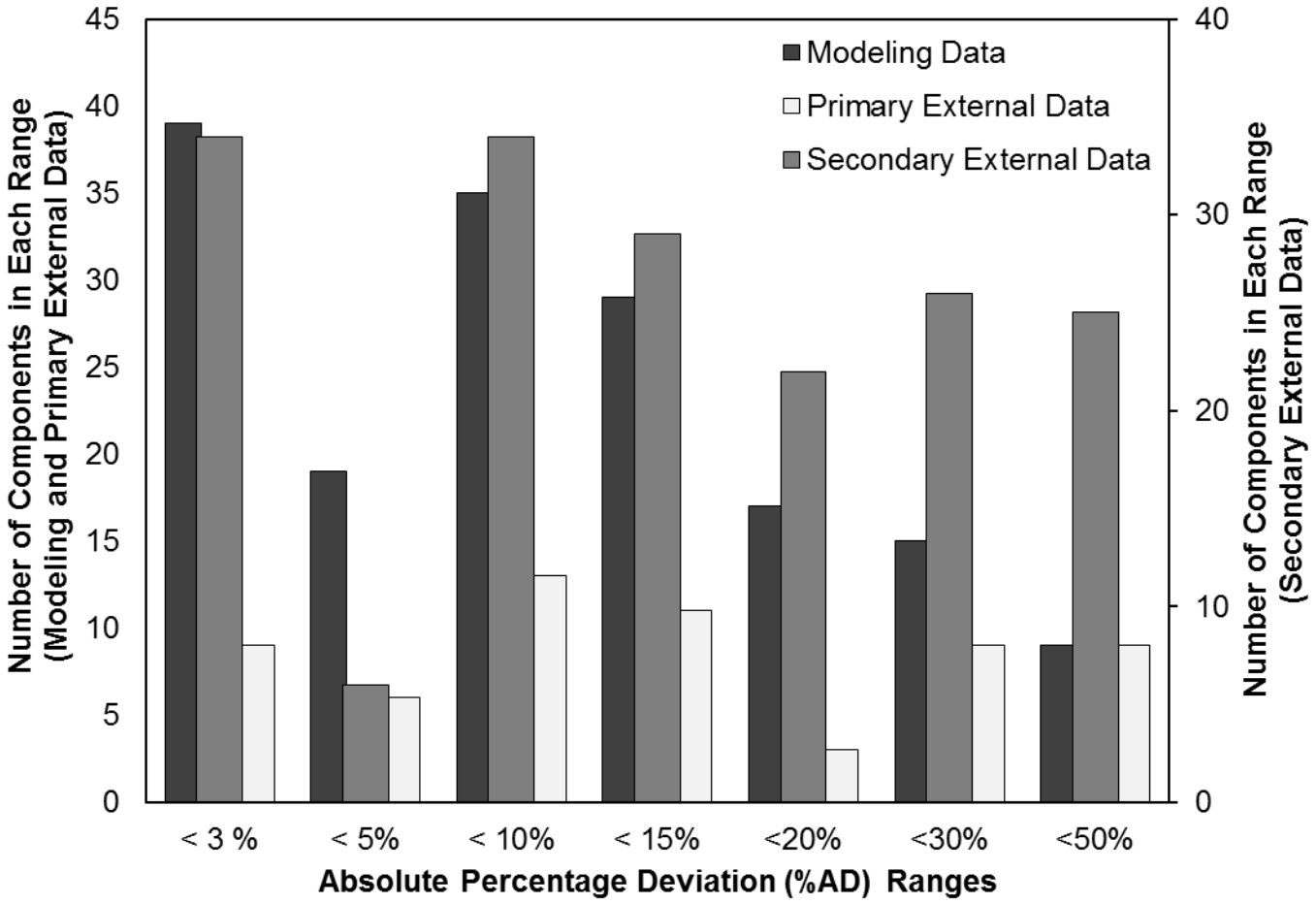

Figure 2.13. Distribution of Error in Predicted ω Obtained using the QSPR Model for Modeling Data, Primary External Data, and Secondary External Data

REFERENCES

1. B.E.P. Poling, J. M.; O'Connell, J. P., Properties of gases and liquids, 5th ed., McGraw-Hill, New York,, 2001.
2. A.S. Teja, R.J. Lee, D. Rosenthal, M. Anselme, Correlation of the critical properties of alkanes and alkanols, Fluid Phase Equilibria, 56 (1990) 153-169.
3. M.R. Riazi, T.A. Al-Sahhaf, M.A. Al-Shammari, A generalized method for estimation of critical constants, Fluid Phase Equilibria, 147 (1998) 1-6.
4. D. Sola, A. Ferri, M. Banchero, L. Manna, S. Sicardi, QSPR prediction of N-boiling point and critical properties of organic compounds and comparison with a group-contribution method, Fluid Phase Equilibria, 263 (2008) 33-42.
5. K.A.M. Gasem, Binary vapor-liquid phase equilibrium for carbon dioxide + heavy normal paraffins (interaction parameters, density predictions, pure hydrocarbon properties), in, Oklahoma State University, United States -- Oklahoma, 1986.
6. K.A.M. Gasem, C.H. Ross, R.L. Robinson, Prediction of ethane and CO_2 solubilities in heavy norma paraffins using generalized-parameter Soave and Peng-Robinson equations of state, The Canadian Journal of Chemical Engineering, 71 (1993) 805-816.
7. C. Tsonopoulos, Z. Tan, The critical constants of normal nlkanes from methane to polyethylene: II. Application of the flory theory, Fluid Phase Equilibria, 83 (1993) 127.
8. J.J. Marano, G.D. Holder, General equation for correlating the thermophysical properties of n-paraffins, n-olefins, and other homologous series. 2. Asymptotic behavior correlations for PVT properties, Industrial & Engineering Chemistry Research, 36 (1997) 1895-1907.

9. G.M. Kontogeorgis, D.P. Tassios, Critical constants and acentric factors for long-chain alkanes suitable for corresponding states applications. A critical review, Chemical Engineering Journal, 66 (1997) 35-49.

10. L. Riedel, Berechung der kritischen daten der verzweigten paraffin-kohlenwasserstoffe, Chemie Ingenieur Technik, 35 (1963) 433-439.

11. A.P. Kudchadker, W.D. Holcomb, B.J. Zwolinski, Correlation studies on vapor pressures and critical properties for isomeric alkanes, Journal of Chemical & Engineering Data, 13 (1968) 182-188.

12. K.G. Joback, R.C. Reid, Estimation of pure-component properties from group-gontributions, Chemical Engineering Communications, 57 (1987) 233-243.

13. D. Ambrose, N.B. Ghiassee, Vapour pressures and critical temperatures and critical pressures of some alkanoic acids: C1 to C10, The Journal of Chemical Thermodynamics, 19 (1987) 505-519.

14. A.L. Lydersen, V. Tsochev, Critical temperatures and pressures and high temperature vapour pressures of seven alcohols, Chemical Engineering & Technology, 13 (1990) 125-130.

15. G.R. Somayajulu, Estimation procedures for critical constants, Journal of Chemical & Engineering Data, 34 (1989) 106-120.

16. J.E.S. Ourique, A.S. Telles, Estimation of properties of pure organic substances with group and pair contributions, Brazilian Journal of Chemical Engineering, 14 (1997).

17. C. Hansch, T. Fujita, p-σ-π Analysis. A method for the correlation of biological activity and chemical structure, Journal of the American Chemical Society, 86 (1964) 1616-1626.

18. A.R. Katritzky, V.S. Lobanov, M. Karelson, Normal boiling points for organic compounds: correlation and prediction by a quantitative structure−property relationship, Journal of Chemical Information and Computer Sciences, 38 (1998) 28-41.

19. A.R. Katritzky, L. Mu, M. Karelson, QSPR treatment of the unified nonspecific solvent polarity scale, Journal of Chemical Information and Computer Sciences, 37 (1997) 756-761.

20. D.T. Stanton, L.M. Egolf, P.C. Jurs, M.G. Hicks, Computer-assisted prediction of normal boiling points of pyrans and pyrroles, Journal of Chemical Information and Computer Sciences, 32 (1992) 306-316.

21. M.D. Wessel, P.C. Jurs, Prediction of normal boiling points for a diverse set of industrially important organic compounds from molecular structure, Journal of Chemical Information and Computer Sciences, 35 (1995) 841-850.

22. D.E. Needham, I.C. Wei, P.G. Seybold, Molecular modeling of the physical properties of alkanes, Journal of the American Chemical Society, 110 (1988) 4186-4194.

23. B.E. Turner, C.L. Costello, P.C. Jurs, Prediction of critical temperatures and pressures of iIndustrially important organic compounds from molecular structure, Journal of Chemical Information and Computer Sciences, 38 (1998) 639-645.

24. G. Espinosa, D. Yaffe, A. Arenas, Y. Cohen, F. Giralt, A fuzzy ARTMAP-based quantitative structure−property relationship (QSPR) for predicting physical properties of organic compounds, Industrial & Engineering Chemistry Research, 40 (2001) 2757-2766.

25. B. Ren, Application of novel atom-type AI topological indices to QSPR studies of alkanes, Computers & Chemistry, 26 (2002) 357-369.

26. R.B. Boozarjomehry, F. Abdolahi, M.A. Moosavian, Characterization of basic properties for pure substances and petroleum fractions by neural network, Fluid Phase Equilibria, 231 (2005) 188-196.

27. S.S. Godavarthy, Design of improved solvents for extractive distillation, in: Chemical Engineering, Oklahoma State University, Stillwater, 2004.

28. F. Gharagheizi, A. Eslamimanesh, A.H. Mohammadi, D. Richon, Determination of critical properties and acentric factors of pure compounds using the artificial neural

network group contribution algorithm, Journal of Chemical & Engineering Data, 56 (2011) 2460-2476.

29. K.M. Yerramsetty, Quantitative structure-property relationship modeling & computer-aided molecular design: Improvements & applications, in, Oklahoma State University, United States -- Oklahoma, 2012, pp. 309.

30. DIPPR Project 801, Physical and thermodynamic properties of pure chemicals, in, 2005.

31. ChemBioOffice 11.0, in, CambridgeSoft, 2008.

32. R. Guha, M.T. Howard, G.R. Hutchison, P. Murray-Rust, H. Rzepa, C. Steinbeck, J. Wegner, E.L. Willighagen, The blue obeliskInteroperability in chemical informatics, Journal of Chemical Information and Modeling, 46 (2006) 991-998.

33. M. Stievano, N. Elvassore, High-pressure density and vapor–liquid equilibrium for the binary systems carbon dioxide–ethanol, carbon dioxide–acetone and carbon dioxide–dichloromethane, The Journal of Supercritical Fluids, 33 (2005) 7-14.

34. T.A. Halgren, Merck molecular force field. I. Basis, form, scope, parameterization, and performance of MMFF94, Journal of Computational Chemistry, 17 (1996) 490-519.

35. T. SRL, Dragon Professional 6.0.9, in, 2011.

36. L. Prechelt, Automatic early stopping using cross validation: quantifying the criteria, Neural Networks, 11 (1998) 761-767.

37. C. Rich, L. Steve, G. Lee, Overfitting in neural nets: backpropagation, conjugate gradient, and early stopping, in, 2000.

38. K.M. Yerramsetty, Quantitative structure-property relationship modeling & computer-aided molecular designimprovements & applications /by Krishna M. Yerramsetty, in: Chemical Engineering, Oklahoma State University, Stillwater, 2012, pp. 290.

39. D.K. Agrafiotis, W. Cedeño, V.S. Lobanov, On the use of neural network ensembles in QSAR and QSPR, Journal of Chemical Information and Computer Sciences, 42 (2002) 903-911.

40. C. Merkwirth, H. Mauser, T. Schulz-Gasch, O. Roche, M. Stahl, T. Lengauer, Ensemble methods for classification in cheminformatics, Journal of Chemical Information and Computer Sciences, 44 (2004) 1971-1978.

41. A. Tropsha, P. Gramatica, V.K. Gombar, The importance of being earnest: Validation is the absolute essential for successful application and interpretation of QSPR models, QSAR Comb. Sci., 22 (2003) 69-77.

42. E. Estrada, A. Ramírez, Edge adjacency relationships and molecular topographic descriptors. Definition and QSAR applications, Journal of Chemical Information and Computer Sciences, 36 (1996) 837-843.

43. G. Rücker, C. Rücker, Walk counts, labyrinthicity, and complexity of acyclic and cyclic graphs and molecules, Journal of Chemical Information and Computer Sciences, 40 (1999) 99-106.

44. R. Todeschini, V. Consonni, Handbook of molecular descriptors, Wiley-VCH, New York, 2000.

45. M.H. Abraham, J.C. McGowan, The use of characteristic volumes to measure cavity terms in reversed phase liquid chromatography, Chromatographia, 23 (1987) 243-246.

46. L. Constantinou, R. Gani, New group contribution method for estimating properties of pure compounds, AIChE Journal, 40 (1994) 1697-1710.

47. H. Yuan, C. Cao, Topological indices based on vertex, edge, ring, and distance: application to various physicochemical properties of diverse hydrocarbons, Journal of Chemical Information and Computer Sciences, 43 (2003) 501-512.

CHAPTER III

MODELING HIGH-PRESSURE PHASE EQUILIBRIA OF COALBED GASES / WATER MIXTURES WITH THE PENG-ROBINSON EQUATION OF STATE[1]

3.1 Introduction

Simulations of enhanced coalbed methane recovery and CO_2 sequestration in unmineable coalbeds require reliable phase equilibrium models that can predict accurately the phase behavior of mixtures of coalbed gases (methane, nitrogen and carbon dioxide) with water. The typical phase conditions in a coalbed reservoir are either near-critical or supercritical for the coalbed gases. Thus, an equation of state (EOS) model that is capable of describing the vapor-liquid equilibria (VLE) of these systems at high pressures is desirable.

Cubic equations of state such as Soave-Redlich-Kwong [1] and Peng-Robinson [2] are widely used in the natural gas and petroleum industries to perform reservoir simulations due to their computational efficiency and reliable predictive capability when appropriate model tuning is performed. Such model tuning typically involves the regression of binary interaction parameters that appear in the EOS mixing rules, since accurate description of phase equilibria of mixtures is sensitive to the mixing rules in the EOS [3]. Recently, efforts have been made to extend the use of cubic equations of state with the classical mixing rules with one or two parameters to model the complex phase equilibrium problems for polar and non-polar components [4].

[1] The material in this chapter has been reproduced with permission from A.M. Abudour, S.A. Mohammad, K.A.M. Gasem, Modeling high-pressure phase equilibria of coalbed gases/water mixtures with the Peng–Robinson equation of state, Fluid Phase Equilibria, 319 (2012) 77-89.

In this work, the Peng-Robinson equation of state (PR EOS) was applied to model the high-pressure phase equilibria of the three binary mixtures of interest in the present work. The PR EOS was selected because of its simplicity and widespread utilization in reservoir simulation-related work. Although the PR EOS has been used in the literature to describe phase equilibria for a variety of systems ranging from simple, non-polar mixtures to complex systems with varying degrees of success [5], there appear to be limited studies in the literature that include a detailed study of the three coalbed binary systems considered in this work. These binary systems have been studied by several authors using different thermodynamic approaches and models [6-19]. However, the studies that utilized cubic equations of state [6, 7, 10-13, 19] were conducted on a limited database and did not cover the entire P-T-x-y region of interest in coalbed reservoir studies. Therefore, this work presents a detailed investigation on the capabilities of a cubic equation of state (PR EOS) in predicting and correlating the high-pressure phase equilibria of these systems.

The current work involved (1) assembling an expanded database for the three binary systems mentioned above covering the phase conditions that are generally encountered in coalbed methane work (2) investigating both the ultimate correlative and the predictive capabilities of the PR EOS for these systems and (3) developing expressions to describe the temperature dependence of the binary interaction parameters in the PR EOS for each of the three systems. Since such a detailed study on these systems appears to be unavailable currently in the literature (to our knowledge), the current work aims to fill the gap in the existing literature when dealing with high-pressure phase equilibria of coalbed gas + water mixtures.

Coalbed gas + water mixtures represent polar + non-polar systems that may require two adjustable binary interaction parameters for model tuning. In general, the two interaction parameters cannot be predicted *a priori* from existing theory. Thus, they are typically regressed from available experimental data. Several empirical correlations have been developed for a

variety of mixtures. In particular, empirical correlations have been presented for carbon dioxide + hydrocarbon mixtures [20-22] and several gas + solvent mixtures [23-27]. Further, the interaction parameters in the EOS are generally found to be temperature-dependent; correlations have been presented for several systems [6, 21, 26-28]. The interaction parameters are almost universally assumed to be independent of pressure.

We performed several case studies to investigate the ultimate correlative as well as the predictive capabilities of the PR EOS. The case studies varied in the number of interaction parameters used and both temperature-dependent and -independent forms were included. These studies are described in the following order: Section 2 describes the PR EOS model, Section 3 discusses the VLE database assembled as part of this study, then presents the case studies undertaken and the expressions developed for the temperature dependence of the interaction parameters. Finally, Section 4 presents the conclusions from this study.

The phase equilibria of gas + water mixtures discussed in this study is applicable for the *free-gas* phase in a coalbed reservoir or the *bulk-gas* phase in an adsorption isotherm experiment. This is quite different from the *adsorbed-phase* equilibrium found in coalbeds. In several of our previous works, we have presented models for predicting adsorption equilibria of gases on coals [29-32]. Recently, a model for modeling competitive adsorption of gas + water adsorbed mixtures has also been presented [33]. The current study deals exclusively with the phase equilibria of free-gas phase found in coalbeds and thus, applies to the fluid phase behavior of those portions of the reservoir that are not under the influence of adsorptive forces.

3.2 Peng-Robinson Equation of State

The PR EOS [2] is given as

$$p = \frac{RT}{v-b} - \frac{a(T)}{v(v+b)+b(v-b)} \tag{3.1}$$

where

$$a(T) = \frac{0.457535\alpha(T)R^2T_c^2}{P_c^2} \tag{3.2}$$

$$b = \frac{0.077796RT_c}{P_c} \tag{3.3}$$

where p is the pressure, T is the temperature, v is the molar volume, a and b are EOS parameters, T_c is the critical temperature, P_c is the critical pressure and R is the universal gas constant.

In Equation (3.2), the term α(T) was calculated with the following expression developed in an earlier work at Oklahoma State University (OSU) [34]:

$$\alpha(T) = \exp\left((A + BT_r)\left(1 - T_r^{C+D\omega+E\omega^2}\right)\right) \tag{3.4}$$

where ω is the acentric factor, T_r is the reduced temperature and A through E are correlation parameters with values of 2.0, 0.836, 0.134, 0.508 and -0.0467, respectively. These values are based on accurate description of saturation pressures for several pure components including methane, nitrogen, carbon dioxide and water and conditions encountered in coalbed methane (CBM) operations.

3.2.1 Mixing Rules

Mixing rules are crucial for extending the PR EOS from pure-gas to mixtures. The familiar one-fluid mixing rules were used and are given as [35]

$$a = \sum_i \sum_j z_i z_j a_{ij} \tag{3.5}$$

$$b = \sum_i \sum_j z_i z_j b_{ij} \tag{3.6}$$

$$a_{ij} = \sqrt{a_i a_j}\left(1 - C_{ij}\right) \tag{3.7}$$

$$b_{ij} = \frac{\left(b_i + b_j\right)}{2}(1 + D_{ij}) \tag{3.8}$$

where z denotes the molar fraction in the liquid or the vapor phase. In the above equations, C_{ij} and D_{ij} are adjustable binary interaction parameters that are regressed from experimental data. The most widely-used method is to employ a single interaction parameter, C_{ij}; that is, C_{ij} is taken as constant and D_{ij} is set to zero. While the use of the second interaction parameter, D_{ij}, poses an additional complexity, it is necessary for precise representations of the phase behavior of these systems. Although more complex mixing rules have been proposed [36, 37], the classical mixing rules (with one or two parameters) are used more frequently in EOS applications in reservoir simulators due to their simplicity.

3.3 Results and Discussion

3.3.1 Pure-Fluid Equation-of-State Parameters

The values of critical temperature (T_c), critical pressure (P_c) and acentric factor (ω) for each fluid, along with binary interaction parameters (C_{ij} and D_{ij}), constitute the necessary model input variables for the PR EOS. The values of the input variables for the pure coalbed gases and water were taken from the National Institute of Standards and Technology [38]. Table 3.1 presents the pure-fluid physical properties used in this study.

3.3.2 VLE Literature Database Employed

A reliable database is a prime requirement for developing a robust model and evaluating its performance. Reviews of experimental data for high-pressure phase equilibria of mixtures

containing coalbed gases and water have been published by several authors [11-18, 39-42]. In a series of papers, Dohrn and co-workers [39-41] presented a comprehensive review of experimental data for several binary systems.

Herein, an expanded database was assembled that contains vapor-liquid equilibrium measurements for the three binary systems mentioned above. The database was compiled from published experimental data in the literature and is documented in Tables 3.2-3.4. These tables list the ranges of temperature, pressure and composition of the coexisting phases, together with the sources of data for carbon dioxide + water, methane + water and nitrogen + water, respectively. The temperature range for the data considered extends from 273.15 K to about 430 K and pressures up to 20.7 MPa were included. These ranges of pressure and temperature cover the phase conditions that are expected in coalbed reservoir systems.

Of the three binary systems considered, methane and nitrogen display very low solubility in water. Specifically, the molar fractions of methane and nitrogen in the water-rich phase were in the order of 10^{-5} to 10^{-3}. In comparison, carbon dioxide has higher solubility in water and the molar fractions of carbon dioxide in the water-rich phase were in the order of 10^{-3} to 10^{-1}.

The experimental uncertainties for the phase equilibrium data contained in the database appear to range from about 1-5% for liquid-phase compositions and 2-6% for the vapor-phase compositions for the three binary systems. Note that some authors did not report uncertainty in their data and/or have reported only reproducibility rather than the estimated accuracy of the measurements. Tables 3.2-3.4 list the experimental error levels for the data (in verbatim footnotes in the tables), where they were reported by the respective authors.

3.3.3 Data Reduction Method

Binary interaction parameters for the coalbed gases + water systems were regressed using a large database described above. Since most of the available data is in the form of solubilities (T-p-x)

with few vapor phase measurements, only the measured T-p-x data were used in the model evaluations for the methane + water and nitrogen + water systems. In contrast, both the T-p-x and T-p-x-y data were used for carbon dioxide + water systems based on more complete data for vapor phase compositions.

The objective functions given below by Equation (3.9) or (3.10) were used in the regressions. The form of objective function depended on the type of data employed in the regressions.

When only liquid-phase data were available, the objective function, OF, was

$$OF = \sum_{i=1}^{NDP} \left(\frac{x_{cal} - x_{exp}}{x_{exp}} \right)_i^2 \tag{3.9}$$

When both liquid and vapor phase data were available, the objective function was

$$OF = \sum_{i=1}^{NDP} \left[\left(\frac{x_{cal} - x_{exp}}{x_{exp}} \right)_i^2 + \left(\frac{y_{cal} - y_{exp}}{y_{exp}} \right)_i^2 \right] \tag{3.10}$$

where, NDP is the number of data points, x_{exp} and x_{cal} are the experimental and calculated liquid mole fractions, respectively, y_{exp} and y_{cal} are the experimental and calculated vapor mole fractions, respectively. A non-linear regression procedure based on the Marquardt [43, 44] method was utilized in this work. The results are presented and analyzed in terms of the average absolute percentage deviations (%AAD), the average absolute deviations (AAD) and percentage deviations (%DEV).

$$\%\,AAD = \frac{100}{NDP} \sum_{i=1}^{NDP} \left| \frac{x_{cal} - x_{exp}}{x_{exp}} \right|_i \tag{3.11}$$

$$AAD = \frac{1}{NDP} \sum_{i=1}^{NDP} \left| x_{cal} - x_{exp} \right|_i \tag{3.12}$$

$$\%\,\mathrm{DEV} = \frac{100}{\mathrm{NDP}} \sum_{i=1}^{\mathrm{NDP}} \left(\frac{x_{cal} - x_{exp}}{x_{exp}} \right)_i \tag{3.13}$$

3.3.4 Model Evaluation

An equilibrium algorithm, GEOS [45], was used to conduct flash calculations to determine the equilibrium liquid and vapor compositions of the gas + water mixtures. To evaluate the correlative and predictive capabilities of the PR EOS in modeling these mixtures at high-pressures, six distinct case studies were formulated. These case studies/scenarios are listed in Table 3.5. As shown in the table, the case studies progress systematically in the number of interaction parameters used in the model and both temperature-independent and temperature-dependent parameters were investigated. For the cases listed in Table 3.5, no generalization of the parameters is included; rather, specific parameter values were evaluated as required by the model for a given case. The generalization of the temperature dependence of the PR EOS parameters is discussed in a later section.

Case 1 represents an initial evaluation of the PR model in which its "raw" predictive capability (no interaction parameters) is assessed. In Case 2, the application of a single, constant interaction parameter, which is a common industrial practice, is considered for each binary mixture, independent of temperature. Case 3 addresses the improvements realized when a separate, constant pair of interaction parameters is considered for each binary mixture, independent of temperature. Case 4 is more complex than Case 2, since a separate, single interaction parameter is used for each isotherm of each binary mixture; this allows for variation of the parameter with temperature. Case 5 enhances Case 4 by including a single, constant value for the interaction parameter D_{ij} for each binary system. Case 6 represents the ultimate correlative capability of the equation of state; two interaction parameters are evaluated for each isotherm of each binary

mixture, thus allowing both parameters to vary with temperature. The interaction parameters for each case were obtained using the objective functions given by Equation (3.9) or (3.10).

In the following discussion, the results are presented in terms of the liquid-phase composition of the coalbed gas (denoted as "x_1") and the vapor-phase composition of water (denoted as "y_2"). Thus, the results are expressed in terms of errors in the *lower-concentration component* in each phase. Further, as mentioned earlier, the solubility of these gases in water is small. Therefore, the *percentage* deviations in the predictions would appear large compared to *absolute* deviations. In the results presented below, both percentage and absolute deviations are provided for a meaningful comparison of the magnitude of errors in the predictions.

3.4 Results and Discussion

For the carbon dioxide + water system, both T-p-x and T-p-x-y data were used in the model evaluations. For the methane + water and nitrogen + water systems, only the measured T-p-x data were used in the model evaluations. Tables 3.6-3.8 present summary results for the six cases described above for the three systems. As shown in these tables, the basic predictive capability of PR EOS (Case 1) is clearly inadequate for liquid-phase compositions for the three systems. The prediction errors for Case 1 ranged from about 65% AAD to 97% AAD in the liquid-phase compositions for the three binary systems. These correspond to an AAD in x_1 of 9.2×10^{-3} to 3.0×10^{-6} for the three binary systems. The predictions for vapor-phase compositions in Case 1 yielded %AADs ranging from 14 to 30 for the three binary systems.

When one or two constant interaction parameters, independent of temperature, were included in the PR EOS (Cases 2 and 3), moderate improvements in predictions were obtained. For Case 2, the %AADs in liquid-phase compositions ranged from about 41 to 73 for the three binary systems. The predicted vapor-phase compositions for Case 2 yielded %AADs that varied from about 19 to 46. The predictions from Case 3 were largely similar to Case 2. Overall, Cases 1 to 3

have highlighted that the PR EOS predictions have insufficient accuracy even with the inclusion of two temperature-independent interaction parameters. Thus, the inclusion of temperature-dependence for one or both the interaction parameters appears necessary. This aspect was investigated in Cases 4 to 6 below.

Case 4 includes the temperature-dependence of a single interaction parameter (i.e. a single C_{ij} was fitted to each isotherm). The temperature-dependence of C_{ij} has been recognized as a significant factor in improving the cubic EOS predictions [20, 21]. When the predictions from Case 4 are compared to those of Case 2 (constant value of C_{ij}), a large reduction in deviations was observed. Specifically, the %AAD in liquid-phase compositions was reduced from 47 to 2.2 for carbon dioxide + water, from 73 to 1.5 for methane + water and from 52 to 0.27 for nitrogen + water. The %AADs for Case 4 correspond to an AAD in x_1 of 2.4 x 10^{-4}, 1.4 x 10^{-5}, 0.95 x 10^{-6} for the carbon dioxide + water, methane + water and nitrogen + water systems, respectively. Figure 3.1 illustrates the temperature dependence of C_{ij} for the three systems, where C_{ij} increases with temperature. Similar observations were made earlier for PR EOS by Robinson et al. [46] for hydrocarbon + water mixtures. Further, the values of C_{ij} for the carbon dioxide + water system were negative up to a temperature of about 400 K and then became positive at higher temperatures.

A temperature-dependent C_{ij} with a constant-valued D_{ij}, was included as Case 5. In particular, constant values of D_{ij} = -0.21, -0.005, and 0.07 were determined for carbon dioxide + water, methane + water, and nitrogen + water systems, respectively. The inclusion of a constant D_{ij} did not yield significant improvement in the predicted phase compositions in the three binary systems. The only exception was the predictions for the vapor-phase compositions in the carbon dioxide + water system, where %AAD was reduced from about 30% (without D_{ij}) to about 8% (with D_{ij}). Further, the introduction of D_{ij} altered the values of C_{ij}, wherein the C_{ij} values

increased (from those of Case 4) and were positive over the entire range of temperatures considered in this work.

Two temperature-dependent parameters were included in Case 6. The representations for carbon dioxide + water and methane + water systems were of similar precision. In contrast, the regressions for the nitrogen + water system appear to be more precise. This could relate to the smaller range of concentrations of nitrogen in water. Overall, however, Case 6 did not provide any significant improvements over the predictions in Case 4 and 5. Thus, the inclusion of D_{ij} appears to be largely unnecessary for the three binary systems. As mentioned earlier, the only exception to this finding was the vapor-phase compositions in carbon dioxide + water system, where the inclusion of D_{ij} appeared to be useful.

The inclusion of one temperature-dependent parameter (C_{ij}) provides significant improvements to the predictions in the liquid-phase compositions for these systems. These results are in agreement with the conclusion reached by Søreide and Whitson [7]. Overall, Case 4 is adequate for methane + water and nitrogen + water systems, while Case 5 is recommended for carbon dioxide + water systems. The results of this work have shown that using one temperature–dependent interaction parameter is necessary and adequate for methane + water and nitrogen + water systems for the conditions considered here. In contrast, the carbon dioxide + water system benefits from using two interaction parameters, where one of them (D_{ij}) may be set to a constant value, as in Case 5.

The results also indicate that the effects of C_{ij} and D_{ij} on the predicted vapor-phase compositions for methane + water and nitrogen + water systems are insignificant when compared with the effects on the liquid-phase compositions. Further, some of the binary interaction parameter values were large (in magnitude). Since these interaction parameters were originally intended to be small corrections to the simple combining rules, their large magnitudes may point to the inadequacy of

the simple mixing/combining rules. Additional work would be necessary to fully explore the sensitivity of these results to the particular mixing rules in the PR EOS applied to these systems.

3.4.1 Generalization of Binary Interaction Parameters

Based on the results discussed above, expressions were developed to describe the temperature dependence of the two binary interaction parameters in the PR EOS. Specifically, we investigated both linear and quadratic forms of temperature dependence for the two interaction parameters. Further, both temperature and inverse of temperature forms were investigated for the temperature dependence. Our analysis indicated that a linear expression in temperature was reasonable and adequate to describe the temperature dependence of the two interaction parameters for the range of conditions considered in this work.

The results from Cases 4-6 were used to develop correlations for the two interaction parameters. The trends observed in the optimized PR EOS interaction parameters, as shown in Figures 3.1-3.4, suggest that some degree of generalization is possible. Table 3.9 presents the temperature-dependent correlations developed in this study. Figures 3.1-3.4 depict these correlations for the three systems. As evident from the figures, the expressions reproduced the regressed parameters reasonably well. Both T-p-x and T-p-y data were used in the generalization of interaction parameters for the three binary systems.

As shown in Table 3.6 for the carbon dioxide + water system, improved predictions were realized when temperature-dependence was used for C_{ij} along with a constant D_{ij} of -0.21 (Case 5). This is signified by a reduction in %AAD for liquid-phase compositions from 8.9 using one interaction parameter to 5.2 using two interaction parameters. Further, the predictions for vapor-phase compositions improved significantly when a constant D_{ij} was used. An inspection of the results reveals that Case 5 appears adequate for this binary system, since little improvement is realized by the additional complexity of Case 6.

The results for the methane + water and nitrogen + water systems also indicate that the inclusion of a single temperature-dependent interaction parameter is adequate for these binary systems. Tables 3.7 and 3.8 present the predictions for these systems obtained through the newly developed temperature-dependence correlations. Figures 3.1 and 3.4 present the temperature dependences for C_{ij} and D_{ij} for the three binary systems. As shown in Figure 3.4, the D_{ij} values are close to zero for methane + water and nitrogen + water systems, which indicates that the second parameter is not required for these systems. In contrast, carbon dioxide + water system shows a clear temperature dependence on the parameter $D_{ij,}$ where it ranges from -0.24 to -0.19.

As expected, the use of generalized expressions resulted in slight loss of accuracy in predictions. Overall, the generalized predictions yielded deviations that are two-three times larger than the deviations obtained from direct regressions of the liquid-phase compositions. For the nitrogen + water system, the %AAD for liquid-phase compositions was 3-4 as compared to about 0.3 in direct regressions; thus, the deviations were much larger for this binary system. Note that these %AADs correspond to an AAD in x_1 of about 1.4×10^{-5}.

Table 3.9 presents the coefficients for the linear correlations to describe the temperature dependence of interaction parameters. As mentioned earlier, quadratic forms for the temperature dependence were also investigated and the results are shown in Tables 3.6-3.8. Table 3.10 lists the coefficients for the quadratic correlations. Since the quadratic forms did not yield significant improvements to the predictions over those when the linear form was used, we elected to use the linear forms in the remainder of this work. The results discussed are all based on the linear temperature-dependence for the interaction parameters.

Figures 3.5 (a) and (b) present the deviations in the predicted liquid-phase compositions as a function of temperature and pressure, respectively, in the carbon dioxide + water system. Figure 3.5 is based on Case 5, where C_{ij} is temperature-dependent and a constant value of -0.21 was used

for D_{ij}. The corresponding plots for methane + water and nitrogen + water mixtures are presented in Figures 3.6 and 3.7, respectively. Figures 3.6 and 3.7 are both based on Case 4 for the respective binary system, where C_{ij} is temperature-dependent and D_{ij} was set to zero. Figure 3.5 shows that the generalized predictions for carbon dioxide + water system in Case 5 are quite comparable to direct parameter optimization/regressions, which is quite promising for the generalization. The linear correlation for temperature-dependence yielded a R^2 value of 0.98 and this enabled us to obtain generalized predictions of similar accuracy to the direct optimization of the interaction parameter C_{ij}. For the methane + water and nitrogen + water systems shown in Figures 3.6 and 3.7, respectively, the generalized predictions had slightly larger errors when compared to direct regressions. Nonetheless, the generalized predictions provided %AADs of about 4 to 7% for these systems.

In summary, the generalized parameters yielded slightly less accurate predictions than those from the regressed parameter cases. Nevertheless, the generalized expressions allow useful predictions throughout the range of pressures and temperatures considered in this work with reasonable accuracy, especially in the absence of experimental data for these systems.

3.4.2 Generalized Predictions and Experimental Uncertainties

It is also instructive to compare the accuracy of predictions to the reported experimental uncertainties of the data used in the generalization. The generalized predictions for the liquid-phase composition of carbon dioxide + water binary mixtures had a %AAD of 5.2 (Case 5), which is within three times the typical experimental uncertainties of about 2% for this system. Similarly, the generalized predictions for the liquid-phase composition of methane + water mixtures yielded a %AAD of 6.6 (Case 4), which is well within three times the typical experimental errors of about 2-5% for this binary mixture. For the nitrogen + water system, the generalized predictions for liquid-phase composition produced %AAD of about 3.8 or an AAD of

about 1.4 x 10^{-5} (Case 4). This compares with an experimental error for nitrogen solubility in the water-rich phase of about 1.5%. Thus, the generalized predictions for the liquid-phase compositions were, in general, within three times the errors in the measurements used in the analysis. However, for the vapor-phase compositions of water in these systems, the percentage errors in the predictions were large due to the small amounts of water present especially for the methane and nitrogen mixtures with water.

The present work focuses on the high-pressure phase equilibrium (T-p-x-y) of three binary mixtures encountered in enhanced coalbed methane recovery and carbon dioxide sequestration studies. Currently, we are also developing accurate prediction models for the PVT behavior of these mixtures as part of our overall goal of developing phase equilibrium models that would be useful in coalbed reservoir simulation studies. Such accurate phase equilibrium models are a prerequisite for conducting realistic simulation studies to predict gas production and CO_2 sequestration in coalbeds. Recently, we began efforts in this direction and expect to present our findings in a future study.

3.5 Conclusions

The PR EOS was employed to model the high-pressure phase equilibria of coalbed gas + water mixtures at conditions encountered in coalbed methane work. An expanded database of vapor-liquid equilibrium measurements was assembled for the binary mixtures methane + water, nitrogen + water and carbon dioxide + water. Six specific case studies were conducted to investigate the correlative and predictive capabilities of the PR EOS for these systems. New expressions were developed for the temperature dependence of interaction parameters in the PR EOS.

Results indicate that the PR EOS is capable of accurate description of phase equilibria of these systems; however, the level of precision depends on the degree of complexity used in

representing the interaction parameters in the mixing rules. Overall, the predictions provided average absolute percentage errors of about 0.3-1.7% for the liquid-phase compositions when two interaction parameters were used. Further, the predictions using the temperature-dependent expressions yielded average absolute percentage errors of about 3-6% for these systems. In general, the generalized predictions for the liquid-phase compositions were within three times the experimental uncertainties in the data employed in the analysis. Further, the predictions for the vapor-phase composition of water were noticeably less accurate due to the low concentrations of water in the gas-rich phase.

Table 3.1. Pure-Fluid Properties Used in Model Evaluations

Component	**T_c, K**	**P_c, MPa**	**ω**
Carbon Dioxide	304.12	7.374	0.225
Methane	190.56	4.599	0.011
Nitrogen	126.20	3.398	0.037
Water	647.15	22.064	0.344

Table 3.2. Binary VLE Database for the CO_2 (1) + H_2O (2) System Used in Model Evaluations

Temperature Range, K	Pressure Range, MPa	CO_2 Liquid Mole Fraction Range	CO_2 Vapor Mole Fraction Range	NDP	Footnotes	Source
278.15–351.15	0.19–9.3	0.0026-0.02488	-	27	-	[13]
278.15–318.15	0.465–8.0	0.00182-0.0279	-	47	-	[19]
278.15–318.15	0.465–8.0	-	0.975-0.9993	30	-	[19]
323.15–353.15	4–14.0	0.0080-0.0217	0.9857-0.9966	29	1	[47]
373.15-433.15	0.33-3.48	0.00047- 0.0093	0.2680-0.9550	28	-	[48]
288.71- 422.04	0.69–20.27	0.00049-0.0263	0.3260-0.9992	34	2	[49]
344.15	10-20	0.0166- 0.0213	-	4	3	[50]
323.15–348.15	10.13–15.2	0.0156-0.0210	0.9910-0.9945	4	-	[51]
332.15	33.4–198.9	0.00946-0.0249	-	6	-	[52]
278.15–293.15	6.44–19.68	0.025–0.0331	-	16	4	[53]
323.15	6.8–17.7	0.0165-0.02262	0.9936-0.9966	8	5	[54]
323.15-373.15	25.3–20.26	0.0043-0.0230	-	19	-	[55]
285.15–323.15	25.3–20.26	0.0093- 0.0311	-	38	-	[56]
323.15	10.1–20.1	0.02075-0.0235	0.9932-0.9945	2	-	[57]
288.15–298.15	6.08–20.27	0.0024–0.00301	-	25	6	[58]
288.15–313.15	5.17–20.27	-	0.9942-0.9978	41	6	[58]
273.35-313.15	0.1013	0.00136-0.00036	-	3	7	[59]
303.15-333.15	10-20	0.0185-0.0257	-	12	-	[60]
298.15-423	4.79	0.0062-0.021	-	9	8	[61]
298–348	4.79	0.0096-0.021	-	11	8	[62]
374–393	2.3–18.95	0.0038-0.020	-	9	-	[63]
323.15– 423.15	20	0.020-0.023	0.940-0.990	3	-	[64]
273–323	0.1-0.114	0.00035-0.00139	-	18	-	[65]
277–283	2.0–4.2	0.0181-0.23	-	9	-	[66]
298.15-348.15	0.1-20.27	-	0.7695-0.9987	26	-	[67]
298.15–373.15	1.733–5.15	-	0.9723-0.9985	22	-	[68]
298.2–323.2	0.059–0.53	0.00034-0.00332	-	54	-	[69]
352.85–393.45	2.11–10.18	0.0034–0.0166	-	18	-	[70]

Comments on experimental uncertainties from the above sources

1. The relative uncertainties are typically ≈1–2% for the solubility of carbon dioxide in the liquid phase and ≈2– 6% for the mole fraction of the water in the vapor phase.
2. It is estimated that all compositions of the binary system, carbon dioxide + water, have been determined with an accuracy of ±1%.
3. An overall experimental uncertainty for the solubility of liquid CO_2 in water is ±2%

4. The uncertainties of the measurements are 1.55% for the solubility of liquid CO_2 in water.
5. The CO_2-rich compositions of the minor component were reproducible to within ±1.5 % and the liquid phase compositions of the minor component were generally reproducible to within ±1.0%. The accuracy of the compositions is estimated to be within 2 times the reproducibility.
6. Consideration of the instrumental errors indicates that the solute ($CO_{2)}$ mole fractions in the water-rich and CO_2-rich phases are believed to be accurate to within about ± 0.3% and ±l% of the stated values, respectively.
7. It is estimated that the measured solubility of liquid CO_2 in water was determined with an accuracy of ±0.2%.
8. It is estimated that the measured solubility of liquid CO_2 in water was determined with an accuracy of ± 0.5%

Table 3.3. Binary VLE Database for the CH_4 (1) + H_2O (2) System Used in Model Evaluations

Temperature Range, K	Pressure Range, MPa	CH_4 Liquid Mole Fraction Range	CH_4 Vapor Mole Fraction Range	NDP	Footnotes	Source
275.11–313.11	0.97–18.0	0 .0002- 0.0025	-	16	-	[12]
324.65–398.15	10.13–20.7	0.00143- 0.0023	-	13	1	[71]
274.19–285.68	0.567–9.08	0.00056- 0.00188	-	18	2	[72]
285.1–348.4	0.1013	0.000015- 0.00003	-	11	-	[73]
324.15-375.15	5.6-20.6	0.000887- 0.00230	-	5	3	[74]
344.15	20	0.002183	-	1	-	[75]
313.35–373.29	0.34–9.3	0.00005- 0.00154	-	26	-	[76]
283.2–303.2	2.0–20.16	0.00056-0.00311	-	13	-	[77]
298.15–323.15	30-80	0.00051-0.00162	-	6	4	[78]
278.15–318.15	0.1013	0.000018-0.000039	-	9	-	[79]
278.15–308.15	0.1013	0.000021-0.000039	-	4	5	[80]
298.15–303.15	0.317–5.17	0.00006- 0.00113	-	17	-	[81]
298.2–410.93	2.23–17.75	0.00032- 0.0026	-	36	-	[82]
297.5–430.6	1.327–2.56	0.00021- 0.000308	0.7147-0.998	5	6	[83]
279.35–298.75	0.1013	0.000025-0.000038	-	5	-	[84]
278.2–318.2	0.1013	0.000019-0.000039	-	3	7	[85]
274.8–312.8	0.1013	0.000021-0.000044	-	6	-	[86]
291.15–310.15	0.1013	0.000021-0.000028	-	6	8	[87]
273.15–283.15	0.1013	0.000034-0.000044	-	2	-	[88]
278.15–298.15	0.1013	0.000025-0.000039	-	5	-	[89]
283.15–303.15	0.1013	0.000023-0.000035	-	5	-	[90]
298.15	0.1013	0.0000255	-	1	9	[91]
273.91–302.70	0.1013	0.000023-0.000045	-	35	-	[92]
278.15–298.15	0.1013	0.000025-0.00004	-	5	-	[93]
298.15	3.62–17.4	0.00077-0.00449	-	11	-	[94]
310.93–344.26	4.14–20.68	0.000759-0.0025	-	6	10	[95]
298.15	2.41–5.17	0.00057-0.0011	-	3	-	[96]
323.15-423.15	1.38-13.79	0.00017-0.0021	0.6454-0.9986	9	11	[49]
423.15	4.9–19.6	0.0008-0.003	-	4	-	[97]

Table 3.3. Binary VLE Database for the CH_4 (1) + H_2O (2) System Used in Model Evaluations *(Continued)*

Temperature Range, K	Pressure Range, MPa	CH_4 Liquid Mole Fraction Range	CH_4 Vapor Mole Fraction Range	NDP	Footnotes	Source
283.08-318.12	0.992-17.5	-	0.990-0.9997	29	-	[98]
282.98-313.12	0.51-2.846	-	0.993-0.999	17	-	[99]
298.15-338.15	2.5-12.5	0.000405- 0.0022	0.9902- 0.9994	15	-	[100]
310.93	8.29- 20.86	-	0.9985- 0.9994	6	-	[101]
298.15-373.15	2.35-9.34	-	0.98- 0.999	12	-	[102]

Comments on experimental uncertainties from the above sources

1. The average deviation of the solubility for CH_4 was about 0.4%.
2. Depending on the experimental conditions, the equilibrium endpoint value of dissolved methane in water is determined within 6% except for the measurements at pressures of 10.02 bar and 5.65 bar where the accuracy was 8% and 12% respectively.
3. The accuracy of the measured solubility data is estimated as 5% for CH_4
4. It is estimated that all compositions of the binary system, methane-water, were determined with an accuracy of 5 %.
5. The reproducibility for the solubility of CH_4 in this work is to within ± 0.3%.
6. The reproducibility for the solubility of CH_4 was found to be better than 0.5 %.
7. An over-all precision of ±2% is estimated for the methane solubility.
8. It is estimated that the measured solubility for CH_4 was determined with an accuracy of ±1.5%.
9. The maximum error in the measured solubility data for CH_4 is of the order of ±0.4%.
10. It is estimated that the measured solubility for CH_4 was determined with an accuracy of ±2%.
11. It is estimated that all compositions of the binary system, methane-water, have been determined with an accuracy of ±1%.

Table 3.4. Binary VLE Database for the N_2 (1) + H_2O (2) System Used in Model Evaluations

Temperature Range, K	Pressure Range, MPa	N_2 Liquid Mole Fraction Range	N_2 Vapor Mole Fraction Range	NDP	Footnotes	Source
298.15	4.517–11.74	0.00049- 0.00115	-	7	1	[103]
274.19–363.02	0.97–7.04	0.000074- 0.00107	-	52	-	[11]
303.15	1.103-5.89	0.00011- 0.00064	-	5	-	[104]
298.15	2.53–20.27	0.000279-0.00181	-	4	-	[105]
324.65	10.13-20.27	0.00081-0.00147	-	2	-	[106]
278.15–313.15	0.1013	0.0000099-0.000017	-	8	-	[79]
276.25–302.65	0.1013	0.0000109-0.000018	-	5	2	[107]
323.15-423.15	10.13-20.27	0.000784-0.00174	-	7	3	[108]
323.15-423.15	10.13-20.27	-	0.9659-0.999	7	-	[108]
276.25–310.2	0.1013	0.000009-0.000018	-	6	-	[109]
311.15	0.1013	0.00001028	-	1	-	[110]
273.73–303.86	0.1013	0.000011-0.0000187	-	10	-	[111]
298.15-311.15	0.1013	0.0000102-0.000012	-	9	-	[112]
338	7.088–20.32	0.00079-0.00143	-	6	-	[113]
324.65-398.15	10.13-20.67	0.000777-0.00149	-	6	4	[71]
298.15–373.15	2.53–20.27	0.000204-0.00181	-	16	5	[114]
293.33	0.1013	0.0000126	-	1	-	[115]
273.68–325.16	0.1013	0.000009-0.0000187	-	24	-	[116]
294.35	0.1013	0.00001256	-	1	6	[117]
289.35–290.35	0.1013	0.000013-0.0000134	-	2	-	[118]
298.15	0.1013	0.00001166	-	2	-	[119]
278.2-298.2	0.1013	0.000011-0.000017	-	5	-	[120]
285.65–345.65	0.1013	0.0000087-0.000015	-	12	7	[73]
275.01–300.16	0.1013	0.000011-0.000018	-	33	8	[121]
276.7–308.3	0.1013	0.0000099-0.000018	-	7	-	[122]
336.3–432.9	0.534–1.737	0.0000248-0.000277	-	13	-	[123]
310.9-422.04	0.345-13.79	0.000023-0.0012	0.9214-0.999	11	9	[124]
310.95-366.45	0.34-13.79	-	0.767-0.9993	10	-	[125]
298.15-373.15	2.109-10.15	-	0.98-0.999	13	-	[102]
282.86-363.08	0.499-4.96	-	0.874-0.999	35	-	[126]

Comments on experimental uncertainties from the above sources

1. The uncertainty in N_2 solubility is ≈ 1% -1.5%.
2. The solubility of nitrogen in distilled water has been determined with an estimated accuracy in α (Bunsen Coefficient) of 0.5%.
3. The average deviation of N_2 solubility in most of the results below 423.15 K was in the neighborhood of 0.75%. This increased slightly at the higher analysis temperatures to about 1 to 2.0%.
4. The average deviation of the solubility for N_2 was about 0.4%.
5. The solubility of nitrogen in distilled water has been determined with an estimated accuracy in (Absorption Coefficient (Cc of gas at S. T. P. per g. of water) of ±0.005.
6. The solubility of nitrogen in distilled water has been determined with an estimated accuracy in α (Bunsen Coefficient) of ±0.03.
7. The estimated reproducibility for the solubility of N_2 (cc of gas at S. T. P. per kg of water) is ± 0.005.
8. The solubility of nitrogen in distilled water has been determined with an estimated precision in α (Bunsen Coefficient) of ±0.002.
9. It is estimated that all compositions of the binary system, N_2-water, were determined with an accuracy of ±1%.

Table 3.5. Specific Cases Used in the Peng-Robinson Equation of State Model Evaluations

Case	Description
1. $C_{ij} = 0$, $D_{ij} = 0$	This provides the "raw predictive ability" of the model, using basic mixing rules with no interaction parameters.
2. C_{ij} = Constant, $D_{ij} = 0$	A single, constant value C_{ij} is determined for each binary mixture, independent of temperature.
3. C_{ij} = Constant, D_{ij} = Constant	A separate, constant pair of values, C_{ij} and D_{ij}, is determined for each binary mixture, independent of temperature.
4. C_{ij} (T), $D_{ij} = 0$	A separate value C_{ij} is determined for each binary system at each temperature.
5. C_{ij} (T), D_{ij} = Constant	A separate value C_{ij} is determined for each binary system at each temperature, along with a single, constant value of D_{ij}.
6. C_{ij} (T), D_{ij} (T)	A separate pair of values, C_{ij} and D_{ij}, is determined for each binary system at each temperature.

Table 3.6. Summary of Results for Peng-Robinson Equation of State for Carbon Dioxide (1) + Water (2) System (Liquid and Vapor Phase Compositions)

Case	Parameters	Liquid Composition of CO_2 (x_1)			Vapor Composition of Water (y_2)		
		NDP	%AAD	AAD × 10^3	NDP	%AAD	AAD × 10^3
Model Representations							
1	$C_{ij} = 0$, $D_{ij} = 0$	500	66	9.2	105	52	8.4
2	$C_{ij} = -0.08$, $D_{ij} = 0$	500	47	5.8	105	46	7.1
3	$C_{ij} = 0.27$, $D_{ij} = -0.21$	500	41	1.9	105	11	3.6
4	C_{ij} (T), $D_{ij} = 0$	500	2.2	0.24	105	30	6.1
5	C_{ij} (T), $D_{ij} = -0.21$	500	1.7	0.18	105	8.2	3.5
6	C_{ij} (T), D_{ij} (T)	500	1.6	0.14	105	7.7	3.4
Temperature Generalizations (Linear Equations from Table 3. 9)							
4	C_{ij} (T), $D_{ij} = 0$	500	8.9	1.16	224	71	12.9
5	C_{ij} (T), $D_{ij} = -0.21$	500	5.2	0.58	224	14	2.6
6	C_{ij} (T), D_{ij} (T)	500	5.0	0.57	224	13	2.5
Temperature Generalizations (Quadratic Equations from Table 3.10)							
4	C_{ij} (T), $D_{ij} = 0$	500	8.7	1.35	224	70	12.7
5	C_{ij} (T), $D_{ij} = -0.21$	500	3.7	0.42	224	13	2.5
6	C_{ij} (T), D_{ij} (T)	500	3.6	0.41	224	12	2.4

Table 3.7. Summary of Results for Peng-Robinson Equation of State for Methane (1) + Water (2) System (Liquid and Vapor Compositions)

Case	Parameters	Liquid Composition of CH_4 (x_1)			Vapor Composition of Water (y_2)		
		NDP	%AAD	AAD × 10^5	NDP	%AAD	AAD × 10^3
Model Representations							
1	$C_{ij} = 0$, $D_{ij} = 0$	281	87	59	29	30	4.6
2	$C_{ij} = -0.20$, $D_{ij} = 0$	281	73	56	29	24	3.9
3	$C_{ij} = -0.19$, $D_{ij} = 0.005$	281	71	54	29	22	3.8
4	C_{ij} (T), $D_{ij} = 0$	281	1.5	1.4	29	21	2.9
5	C_{ij} (T), $D_{ij} = -0.005$	281	1.5	1.3	29	20	2.8
6	C_{ij} (T), D_{ij} (T)	281	1.4	0.9	29	20	2.7
Temperature Generalizations (Linear Equations from Table 3.9)							
4	C_{ij} (T), $D_{ij} = 0$	281	6.6	5.7	93	41	2.5
5	C_{ij} (T), $D_{ij} = -0.005$	281	6.5	5.6	93	39	2.4
6	C_{ij} (T), D_{ij} (T)	281	6.2	5.5	93	38	2.2
Temperature Generalizations (Quadratic Equations from Table 3.10)							
4	C_{ij} (T), $D_{ij} = 0$	281	3.5	3.1	93	39	2.3
5	C_{ij} (T), $D_{ij} = -0.005$	281	3.5	3.0	93	38	2.2
6	C_{ij} (T), D_{ij} (T)	281	3.5	3.0	93	37	2.2

Table 3.8. Summary of Results for Peng-Robinson Equation of State for Nitrogen (1) + Water (2) System (Liquid and Vapor Compositions)

Case	Parameters	Liquid Composition of N_2 (x_1)			Vapor Composition of Water (y_2)		
		NDP	%AAD	AAD × 10^6	NDP	%AAD	AAD × 10^3
Model Representations							
1	$C_{ij} = 0$, $D_{ij} = 0$	256	97	29	11	23	2.7
2	$C_{ij} = -0.65$, $D_{ij} = 0$	256	52	27	11	19	1.8
3	$C_{ij} = -0.72$, $D_{ij} = 0.008$	256	50	22	11	19	1.7
4	C_{ij} (T), $D_{ij} = 0$	256	0.27	0.95	11	15	0.7
5	C_{ij} (T), $D_{ij} = 0.07$	256	0.26	0.91	11	14	0.6
6	C_{ij} (T), D_{ij} (T)	256	0.25	0.88	11	13	0.5
Temperature Generalizations (Linear Equations from Table 3.9)							
4	C_{ij} (T), $D_{ij} = 0$	256	3.8	14	76	29	2.60
5	C_{ij} (T), $D_{ij} = 0.07$	256	3.7	12	76	27	2.42
6	C_{ij} (T), D_{ij} (T)	256	3.6	12	76	25	2.36
Temperature Generalizations (Quadratic Equations from Table 3.10)							
4	C_{ij} (T), $D_{ij} = 0$	256	2.6	8.9	76	27	2.49
5	C_{ij} (T), $D_{ij} = 0.07$	256	2.5	8.7	76	25	2.32
6	C_{ij} (T), D_{ij} (T)	256	2.4	8.5	76	24	2.23

Table 3.9. Temperature Dependences of C_{ij} and D_{ij} (Linear Correlations)

System	Case 4			Case 5			Case 6			
	$C_{ij} = AT + B$		D_{ij}	$C_{ij} = AT + B$		D_{ij}	$C_{ij} = AT + B$		$D_{ij} = AT + B$	
	A	B		A	B		A	B	A	B
CO_2 + water	0.00112	-0.4616	0	0.00106	-0.08943	-0.21	0.00058	0.08149	0.00029	-0.31262
CH_4 + water	0.00268	-1.1212	0	0.00268	-1.10780	-0.005	0.00131	-0.70571	0.00057	-0.17253
N_2 + water	0.00328	-1.6798	0	0.00319	-1.90187	0.07	0.00174	-1.18560	0.00043	-0.13659

Table 3.10. Temperature Dependences of C_{ij} and D_{ij} (Quadratic Correlations)

System	Case 4				Case 5			
	$C_{ij} = AT^2 + BT + C$			D_{ij}	$C_{ij} = AT^2 + BT + C$			D_{ij}
	$A \times 10^6$	$B \times 10^3$	C		$A \times 10^6$	$B \times 10^3$	C	
CO_2 + water	-2.0625	2.53834	-0.7028	0	-2.6597	2.8931	-0.3999	-0.21
CH_4 + water	-4.2482	5.53403	-1.5906	0	-4.2522	5.5331	-1.5777	-0.005
N_2 + water	3.7711	5.82466	-2.1008	0	-3.7773	5.7387	-2.3236	0.07

Table 3.10. Temperature Dependences of C_{ij} and D_{ij}

(Quadratic Correlations) *(Continued)*

System	Case 6					
	$C_{ij} = AT^2 + BT + C$			$D_{ij} = AT^2 + BT + C$		
	$A \times 10^7$	$B \times 10^3$	C	$A \times 10^6$	$B \times 10^3$	C
CO_2 + water	-7.8864	1.12241	-0.0102	-1.1703	1.09373	-0.4486
CH_4 + water	-3.9129	1.57171	-0.7489	-1.4201	1.52416	-0.3295
N_2 + water	-7.1626	2.22225	-1.2656	-0.9966	1.09759	-0.2479

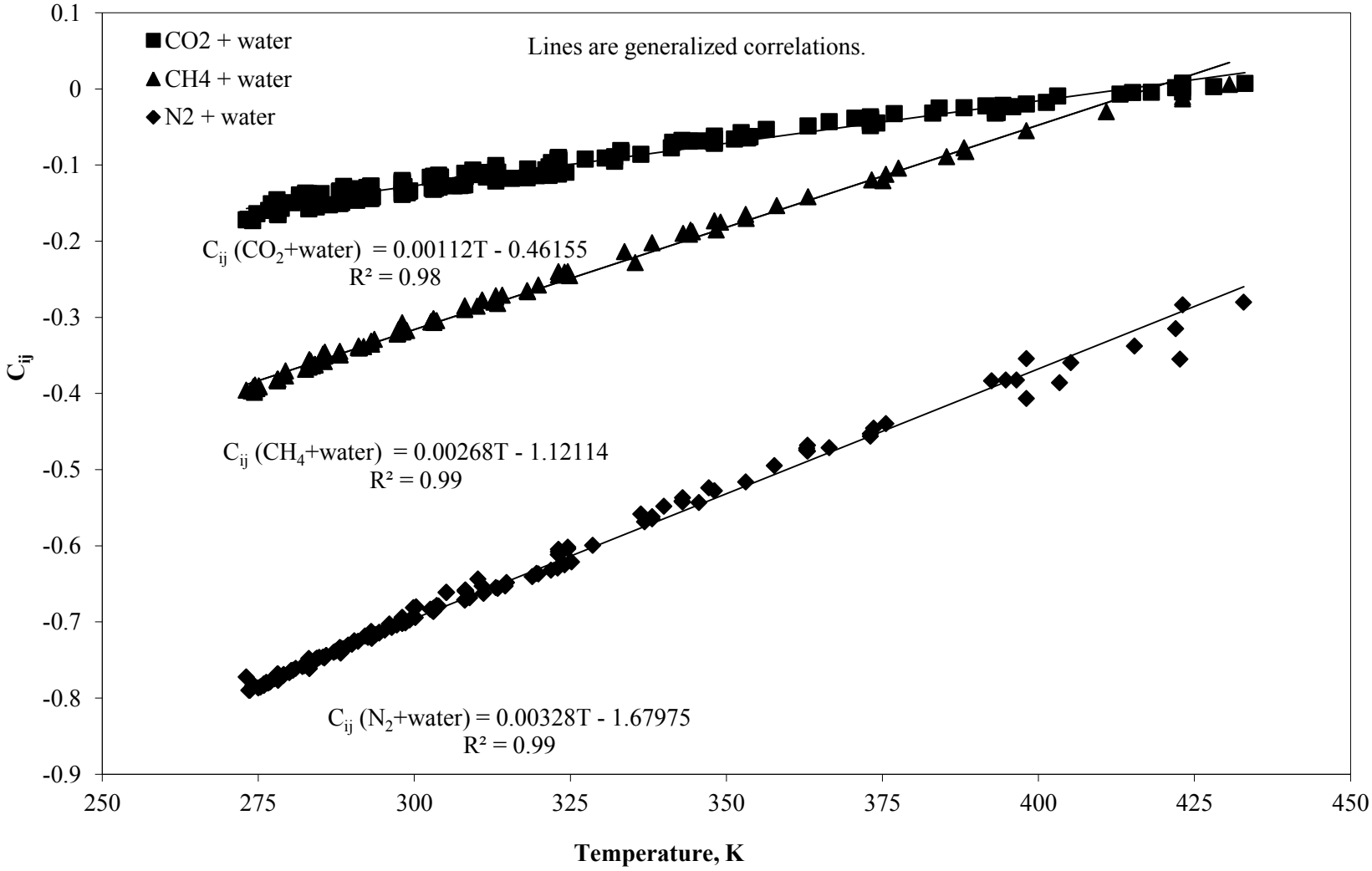

Figure 3.1. Generalized Parameter C_{ij} for the Three Binary Systems
Case 4: C_{ij} (T), D_{ij} = 0

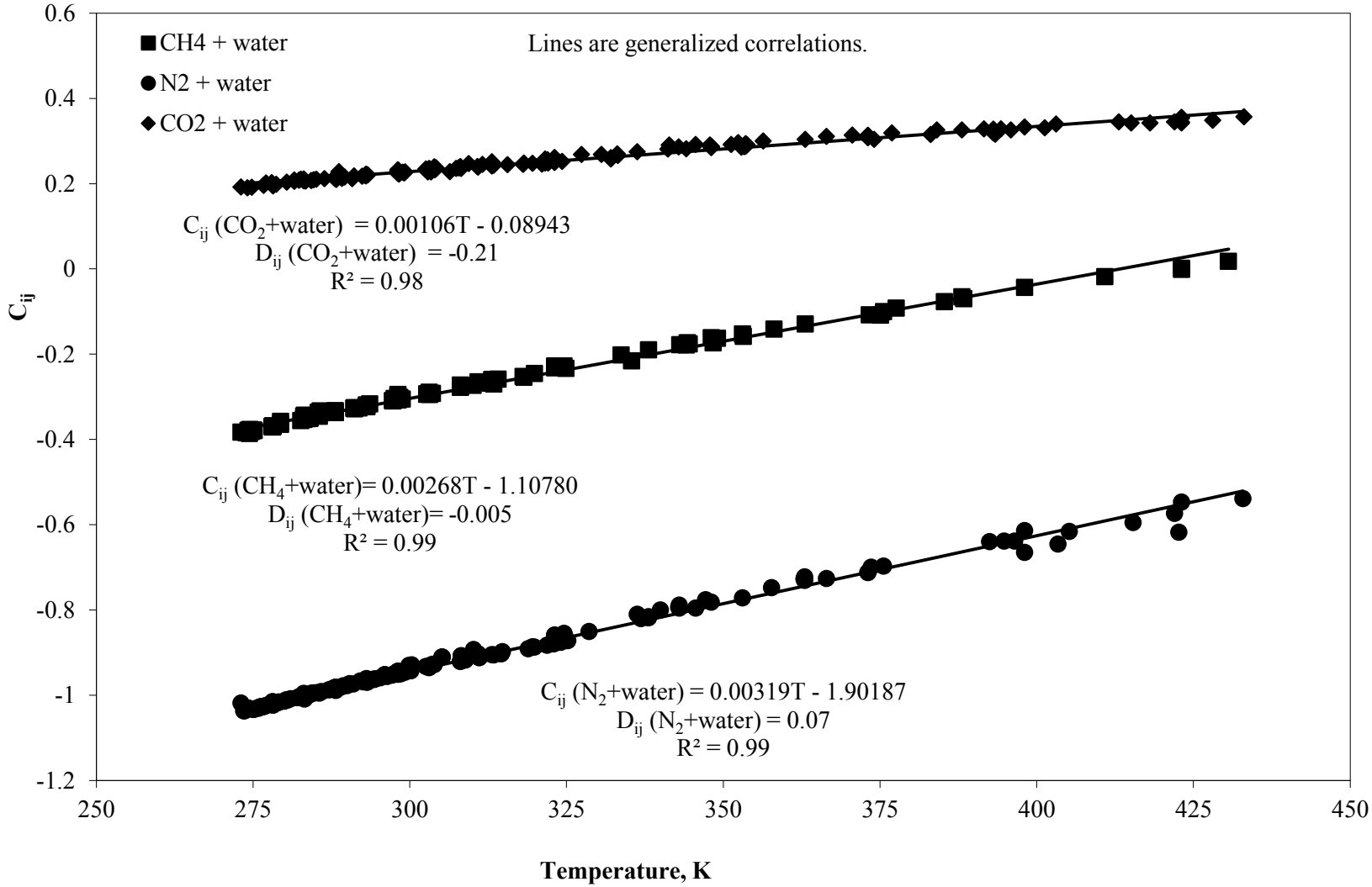

Figure 3.2. Generalized Parameter C_{ij} for the Three Binary Systems
Case 5: C_{ij} (T), D_{ij} = Constant

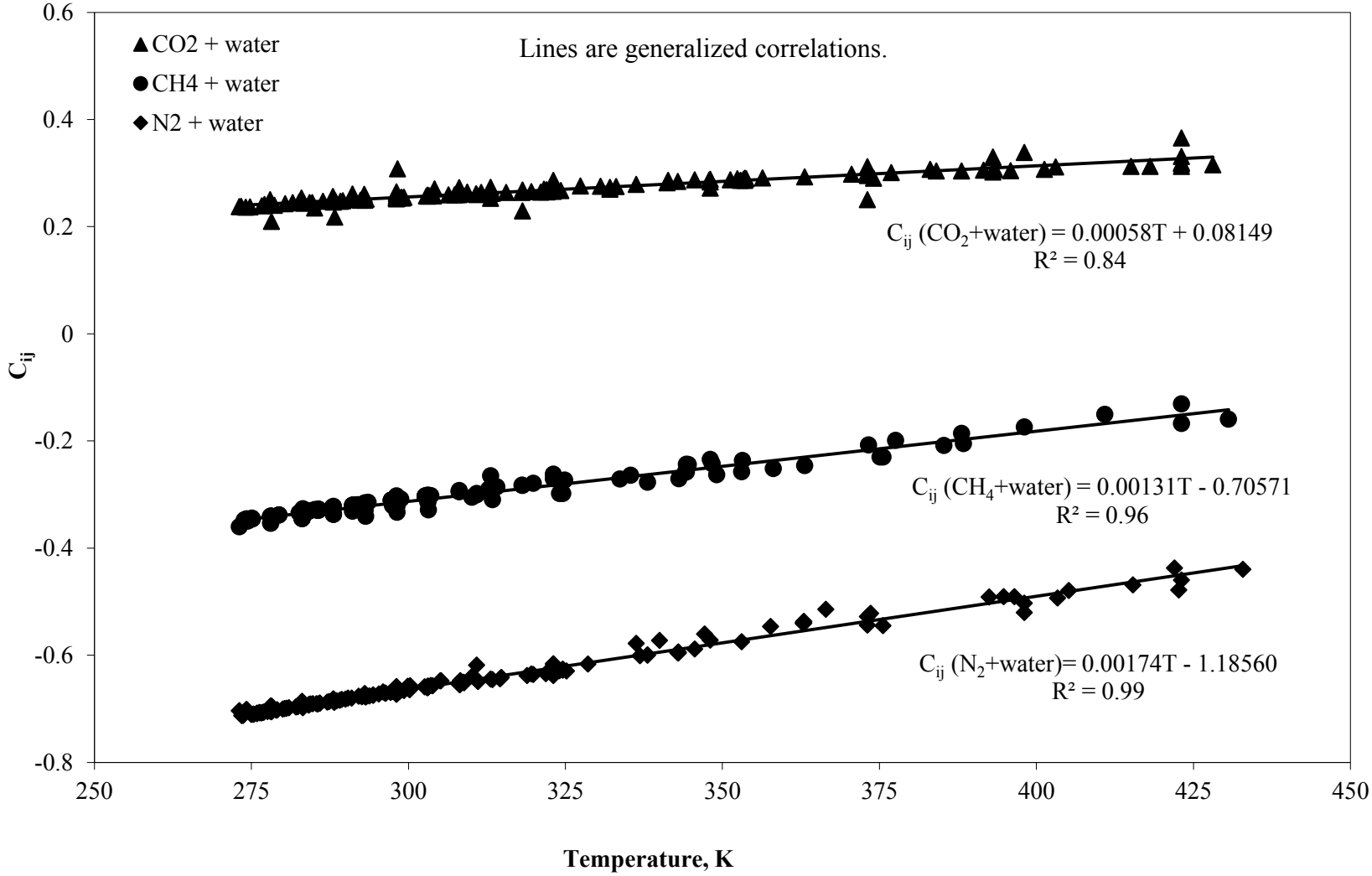

Figure 3.3. Generalized Parameter C_{ij} for the Three Binary Systems
Case 6: C_{ij} (T), D_{ij} (T)

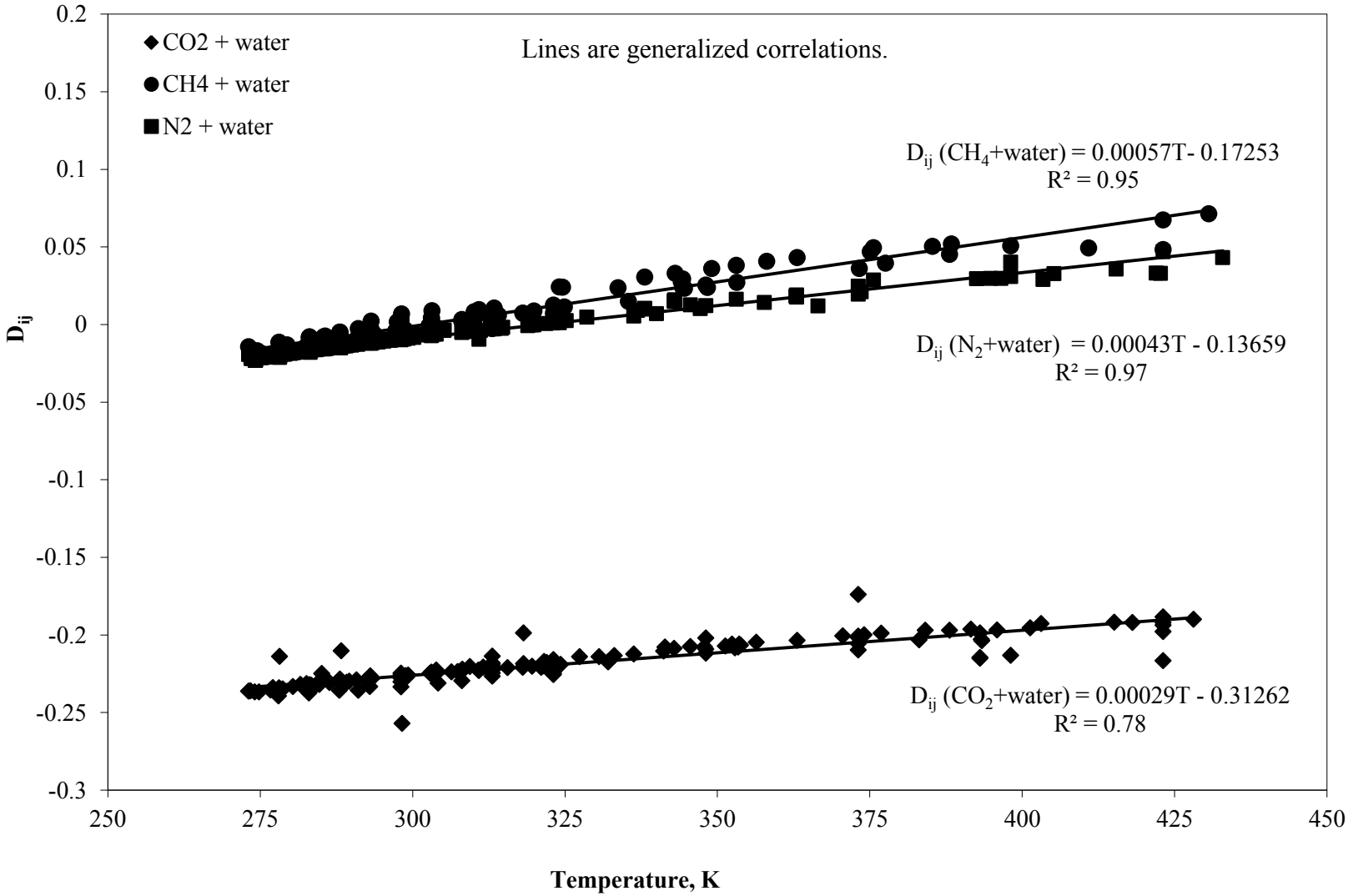

Figure 3.4. Generalized Parameter D_{ij} for the Three Binary Systems
Case 6: C_{ij} (T), D_{ij} (T)

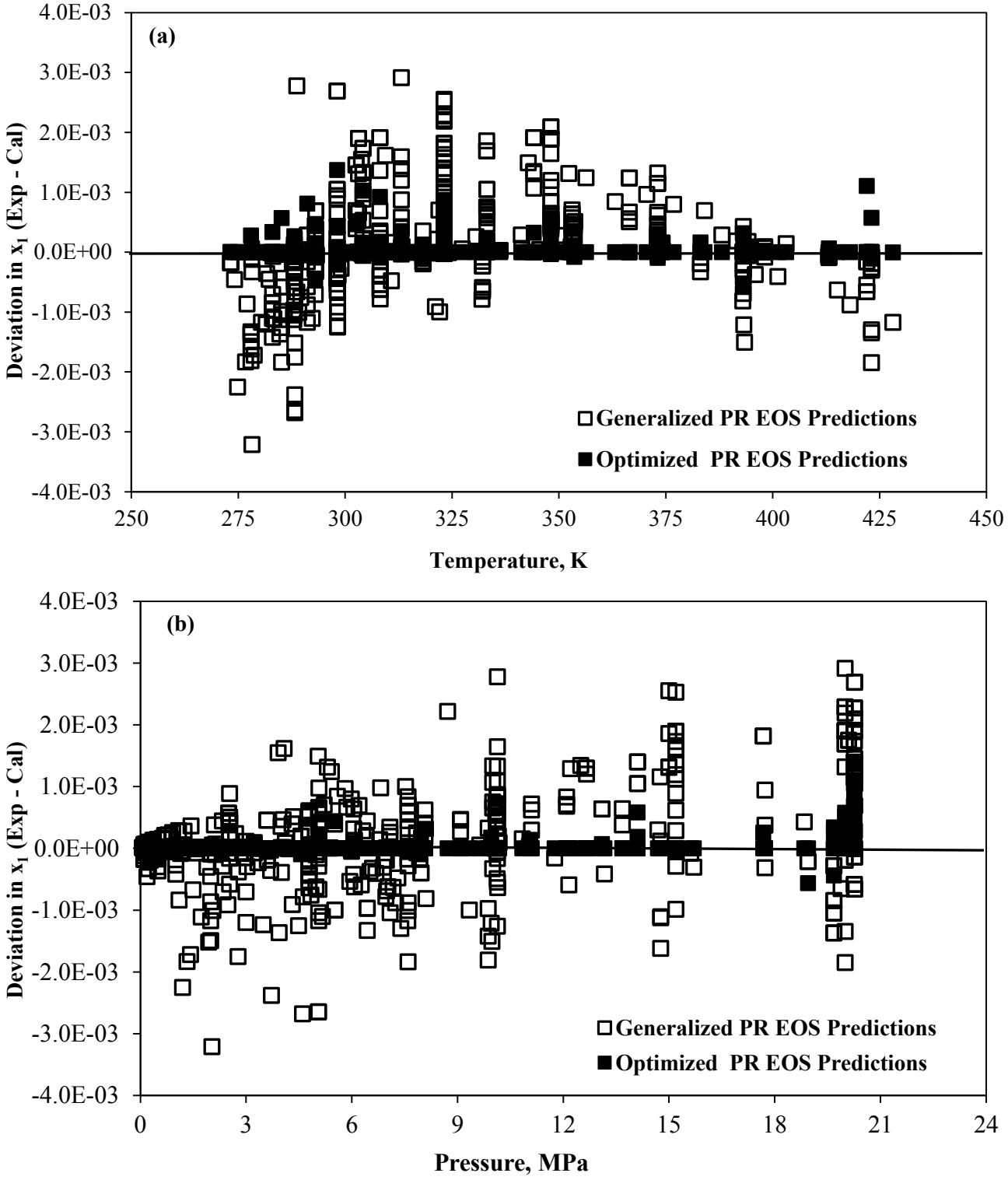

Figure 3.5. Deviations in x_1 for the Carbon Dioxide + Water System Using the Peng-Robinson Equation of State, Case 5: C_{ij} (T), D_{ij} = -0.21
(a) Deviations as a Function of Temperature
(b) Deviations as a Function of Pressure

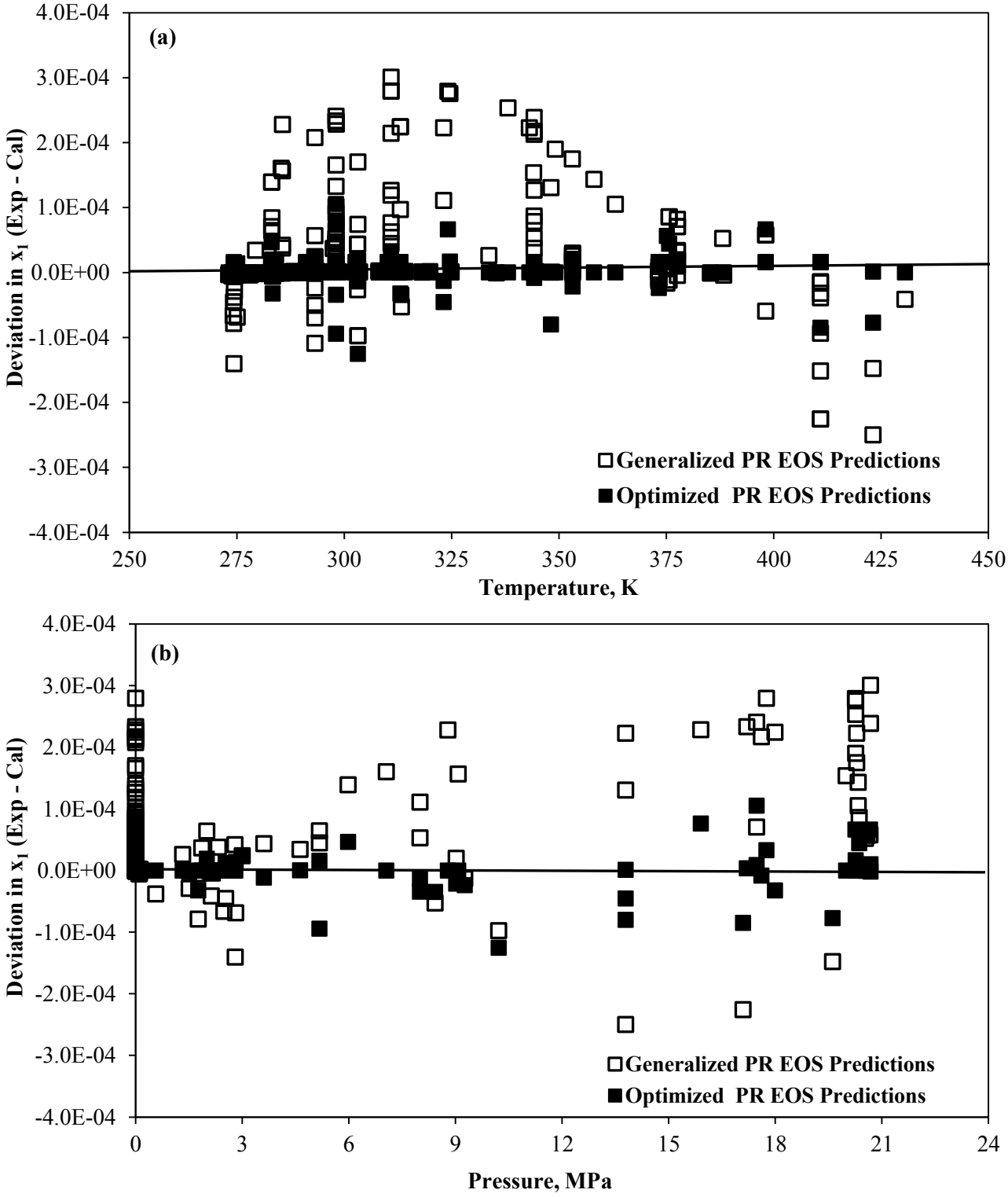

Figure 3.6. Deviations in x_1 for the Methane + Water System Using the Peng-Robinson Equation of State, Case 4: C_{ij} (T), $D_{ij} = 0$
(a) Deviations as a Function of Temperature
(b) Deviations as a Function of Pressure

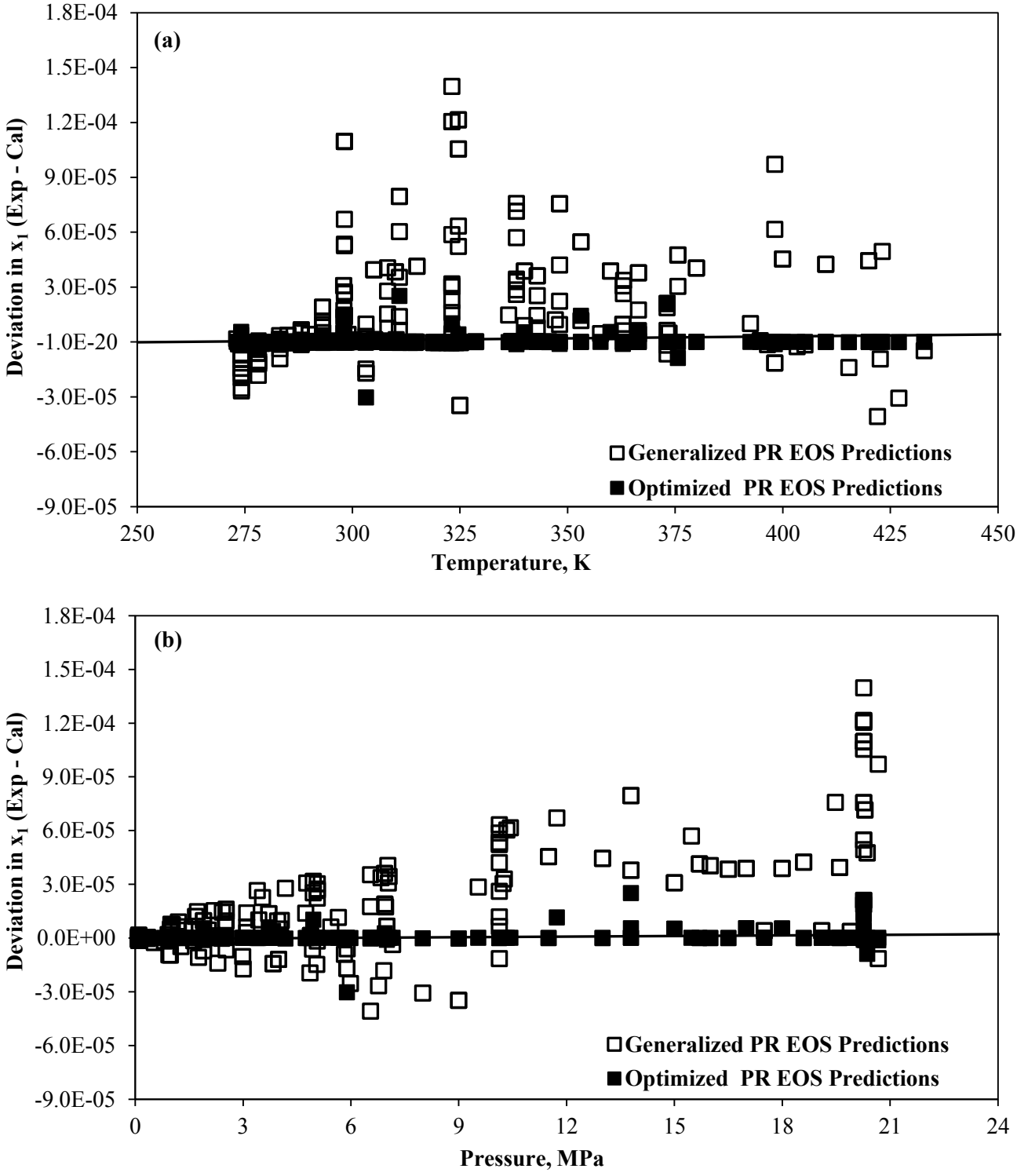

Figure 3.7. Deviations in x_1 for the Nitrogen+ Water System Using the Peng-Robinson Equation of State, Case 4: C_{ij} (T), D_{ij} = 0
(a) Deviations as a Function of Temperature
(b) Deviations as a Function of Pressure

REFERENCES

1. G. Soave, Equilibrium constants from a modified Redlich-Kwong equation of state, Chemical Engineering Science, 27 (1972) 1197-1203.
2. D.Y. Peng, D.B. Robinson, A new two-constant equation of state, Industrial & Engineering Chemistry Fundamentals, 15 (1976) 59-64.
3. G.F. Chou, J.M. Prausnitz, A phenomenological correction to an equation of state for the critical region, AIchE Journal, 35 (1989) 1487-1496.
4. J.O. Valderrama, The state of the cubic equations of state, Industrial & Engineering Chemistry Research, 42 (2003) 1603-1618.
5. P. Ghosh, Prediction of vapor-liquid equilibria using Peng-Robinson and Soave-Redlich-Kwong equations of state, Chemical Engineering & Technology, 22 (1999) 379-399.
6. G.D. Pappa, C. Perakis, I.N. Tsimpanogiannis, E.C. Voutsas, Thermodynamic modeling of the vapor-liquid equilibrium of the CO2/H2O mixture, Fluid Phase Equilibria, 284 (2009) 56-63.
7. I. Søreide, C.H. Whitson, Peng-Robinson predictions for hydrocarbons, CO_2, N_2, and H_2S with pure water and NaCI brine, Fluid Phase Equilibria, 77 (1992) 217-240.
8. C. Perakis, E. Voutsas, K. Magoulas, D. Tassios, Thermodynamic modeling of the vapor-liquid equilibrium of the water/ethanol/CO_2 system, Fluid Phase Equilibria, 243 (2006) 142-150.
9. J.J. Carroll, A.E. Mather, The system carbon dioxide-water and the Krichevsky-Kasarnovsky equation, Journal of Solution Chemistry, 21 (1992) 607-621.

10. K.A. Evelein, R.G. Moore, R.A. Heidemann, Correlation of the phase behavior in the systems hydrogen sulfide-water and carbon dioxide-water, Industrial & Engineering Chemistry Process Design and Development, 15 (1976) 423-428.

11. A. Chapoy, A.H. Mohammadi, B. Tohidi, D. Richon, Gas solubility measurement and modeling for the nitrogen + water system from 274.18 K to 363.02 K, Journal of Chemical & Engineering Data, 49 (2004) 1110-1115.

12. A. Chapoy, A.H. Mohammadi, D. Richon, B. Tohidi, Gas solubility measurement and modeling for methane-water and methane-ethane-n-butane-water systems at low temperature conditions, Fluid Phase Equilibria, 220 (2004) 113-121.

13. A. Chapoy, A.H. Mohammadi, A. Chareton, B. Tohidi, D. Richon, Measurement and modeling of gas solubility and literature review of the properties for the carbon dioxide-water system, Industrial & Engineering Chemistry Research, 43 (2004) 1794-1802.

14. Z.H. Duan, R. Sun, An improved model calculating CO_2 solubility in pure water and aqueous NaCl solutions from 273 to 533 K and from 0 to 2000 bar, Chemical Geology, 193 (2003) 257-271.

15. L.W. Diamond, N.N. Akinfiev, Solubility of CO_2 in water from -1.5 to 100 degrees C and from 0.1 to 100 MPa: evaluation of literature data and thermodynamic modelling, Fluid Phase Equilibria, 208 (2003) 265-290.

16. Z.H. Duan, Z.G. Zhang, Equation of state of the H_2O, CO_2, and H_2O-CO_2 systems up to 10 GPa and 2573.15 K: Molecular dynamics simulations with ab initio potential surface, Geochimica Et Cosmochimica Acta, 70 (2006) 2311-2324.

17. Z. Duan, S. Mao, A thermodynamic model for calculating methane solubility, density and gas phase composition of methane-bearing aqueous fluids from 273 to 523 K and from 1 to 2000 bar, Geochimica Et Cosmochimica Acta, 70 (2006) 3369-3386.

18. S. Mao, Z. Duan, A thermodynamic model for calculating nitrogen solubility, gas phase composition and density of the N_2-H_2O-NaCl system, Fluid Phase Equilibria, 248 (2006) 103-114.

19. A. Valtz, A. Chapoy, C. Coquelet, P. Paricaud, D. Richon, Vapour-liquid equilibria in the carbon dioxide-water system, measurement and modelling from 278.2 to 318.2 K, Fluid Phase Equilibria, 226 (2004) 333-344.

20. K. Kato, K. Nagahama, M. Hirata, Generalized interaction parameters for the Peng-Robinson equation of state: Carbon dioxide--n-paraffin binary systems, Fluid Phase Equilibria, 7 (1981) 219-231.

21. K.A.M. Gasem, R.L. Robinson Jr., Prediction of phase behavior for CO_2 plus heavy normal paraffins using generalized-parameter Soave and Peng-Robinson equations of state, in: Proceedings of the 1985 AICHE Spring National Meeting and Petro Expo '85, Houston, TX, 1985.

22. K.A.M. Gasem, C.H. Ross, R.L. Robinson, Prediction of ethane and CO_2 solubilities in heavy norma paraffins using generalized-parameter Soave and Peng-Robinson equations of state, The Canadian Journal of Chemical Engineering, 71 (1993) 805-816.

23. J.O. Valderrama, E.A. Molina, Interaction parameter for hydrogen-containing mixtures in the Peng--Robinson equation of state, Fluid Phase Equilibria, 31 (1986) 209-219.

24. J.O. Valderrama, S. Obaid-Ur-Rehman, L.A. Cisternas, Application of a new cubic equation of state to hydrogen sulfide mixtures, Chemical Engineering Science, 42 (1987) 2935-2940.

25. J.O. Valderrama, S. Obaid-ur-Rehman, L.A. Cisternas, Generalized interaction parameters in cubic equations of state for CO_2-n-alkane mixtures, Fluid Phase Equilibria, 40 (1988) 217-233.

26. J.O. Valderrama, L.A. Cisternas, V. Milena E, B. María A, Binary interaction parameters in cubic equations of state for hydrogen-hydrocarbon mixtures, Chemical Engineering Science, 45 (1990) 49-54.

27. W. Schulze, A simple generalization of the binary temperature-dependent interaction parameters in the Soave-Redlich-Kwong and Peng-Robinson equations of state for helium-mixtures, Fluid Phase Equilibria, 87 (1993) 199-211.

28. J.A.P. Coutinho, G.M. Kontogeorgis, E.H. Stenby, Binary interaction parameters for nonpolar systems with cubic equations of state: a theoretical approach 1. CO_2/hydrocarbons using SRK equation of state, Fluid Phase Equilibria, 102 (1994) 31-60.

29. F. Hall, C. Zhou, K.A.M. Gasem, R.L. Robinson, Jr. , Adsorption of pure methane, nitrogen, and carbon dioxide and their binary mixtures on wet fruitland coal, in: SPE Eastern Regional Conference & Exhibition, SPE Paper 29194, Charleston, S.C., 1994.

30. J.E. Fitzgerald, Z. Pan, M. Sudibandriyo, R.L. Robinson, Jr., K.A.M. Gasem, S. Reeves, Adsorption of methane, nitrogen, carbon dioxide and their mixtures on wet Tiffany coal, Fuel, 84 (2005) 2351-2363.

31. S.A. Mohammad, J.S. Chen, R.L. Robinson, K.A.M. Gasem, Generalized simplified local-density/Peng-Robinson model for adsorption of pure and mixed gases on coals, Energy & Fuels, 23 (2009) 6259-6271.

32. M. Sudibandriyo, S.A. Mohammad, R.L. Robinson Jr., K.A.M. Gasem, Ono–Kondo lattice model for high-pressure adsorption: Pure gases, Fluid Phase Equilibria, 299 (2010) 238-251.

33. S.A. Mohammad, K.A.M. Gasem, Modeling the competitive adsorption of CO_2 and water at high pressures on wet coals, Energy & Fuels, 26 (2012) 557-568.

34. K.A.M. Gasem, W. Gao, Z. Pan, R.L. Robinson, Jr., A Modified temperature dependence for the Peng-Robinson equation of state, Fluid Phase Equilibria, 181 (2001) 113-125.

35. J.M. Prausnitz, R.N. Lichtenthaler, E.G. Azevedo, Molecular thermodynamics of fluid-phase equilibria, 3rd ed., Prentice-Hall, New Jersey, 1999.

36. P.M. Mathias, H.C. Klotz, J.M. Prausnitz, Equation-of-state mixing rules for multicomponent mixtures: the problem of invariance, Fluid Phase Equilibria, 67 (1991) 31-44.

37. J. Schwartzentruber, H. Renon, Equations of state: how to reconcile flexible mixing rules, the virial coefficient constraint and the "Michelsen-Kistenmacher syndrome" for multicomponent systems, Fluid Phase Equilibria, 67 (1991) 99-110.

38. E.W. Lemmon, M.O. McLinden, D.G. Friend, Thermophysical properties of fluid systems in: P.J. Linstrom, W.G. Mallard (Eds.) NIST Chemistry WebBook, NIST Standard Reference Database Number 69, National Institute of Standards and Technology,Gaithersburg MD, 20899, http://webbook.nist.gov (retrieved October 5, 2011).

39. R. Dohrn, G. Brunner, High-pressure fluid-phase equilibria - experimental methods and systems investigated (1988-1993), Fluid Phase Equilibria, 106 (1995) 213-282.

40. M. Christov, R. Dohrn, High-pressure fluid phase equilibria - Experimental methods and systems investigated (1994-1999), Fluid Phase Equilibria, 202 (2002) 153-218.

41. R. Dohrn, S. Peper, J.M.S. Fonseca, High-pressure fluid-phase equilibria: Experimental methods and systems investigated (2000-2004), Fluid Phase Equilibria, 288 (2010) 1-54.

42. N. Spycher, K. Pruess, J. Ennis-King, CO_2-H_2O mixtures in the geological sequestration of CO_2. I. Assessment and calculation of mutual solubilities from 12 to 100 degrees C and up to 600 bar, Geochimica Et Cosmochimica Acta, 67 (2003) 3015-3031.

43. D.W. Marquardt, An algorithm for least-squares estimation of nonlinear parameters, Journal of the Society for Industrial and Applied Mathematics, 11 (1963) 431-441.

44. L.W. Jackson, A comparison of selected gradient methods for solving the nonlinear least squares problem, in: Computing and Information Sciences, Oklahoma State University, Stillwater, OK, 1978.

45. K.A.M. Gasem, GEOS, in, Oklahoma State university, Stillwater, OK, 1988-1999.

46. D.B. Robinson, D.Y. Peng, S.Y.K. Chung, The development of the Peng - Robinson equation and its application to phase equilibrium in a system containing methanol, Fluid Phase Equilibria, 24 (1985) 25-41.

47. A. Bamberger, G. Sieder, G. Maurer, High-pressure (vapor plus liquid) equilibrium in binary mixtures of (carbon dioxide plus water or acetic acid) at temperatures from 313 to 353 K, Journal of Supercritical Fluids, 17 (2000) 97-110.

48. G. Muller, E. Bender, G. Maurer, Vapor-liquid- equilibrium in the ternary-system ammonia-carbon dioxide-water at high water contents in the range 373 K to 473 K, Berichte Der Bunsen-Gesellschaft-Physical Chemistry Chemical Physics, 92 (1988) 148-160.

49. P.C. Gillespie, G.M. Wilson, Vapor-liquid and liquid-liquid equilibria : water-methane, water-carbon dioxide, water-hydrogen sulfide, water-npentane, water-methane-npentane, in: Research report RR-48, Gas Processors Association, Tulsa, 1982.

50. A. Dhima, J.C. de Hemptinne, J. Jose, Solubility of hydrocarbons and CO_2 mixtures in water under high pressure, Industrial & Engineering Chemistry Research, 38 (1999) 3144.

51. R. Dsouza, J.R. Patrick, A.S. Teja, High-pressure phase-equilibria in the carbon-dioxide normal-hexadecane and carbon-dioxide water-systems, Canadian Journal of Chemical Engineering, 66 (1988) 319-323.

52. Z.W. Li, M.Z. Dong, S.L. Li, L.M. Dai, Densities and solubilities for binary systems of carbon dioxide plus water and carbon dioxide plus brine at 59 degrees C and pressures to 29 MPa, Journal of Chemical and Engineering Data, 49 (2004) 1026-1031.

53. H. Teng, A. Yamasaki, M.K. Chun, H. Lee, Solubility of liquid CO_2 in water at temperatures from 278 K to 293 K and pressures from 6.44 MPa to 29.49 MPa and densities of the corresponding aqueous solutions, Journal of Chemical Thermodynamics, 29 (1997) 1301-1310.

54. J.A. Briones, J.C. Mullins, M.C. Thies, B.U. Kim, Ternary phase-equilibria for acetic acid-water mixtures with supercritical carbon-dioxide, Fluid Phase Equilibria, 36 (1987) 235-246.

55. R. Wiebe, V.L. Gaddy, The solubility in water of carbon dioxide at 50, 75 and 100 degrees, at pressures to 700 atmospheres, Journal of the American Chemical Society, 61 (1939) 315-318.

56. R. Wiebe, V.L. Gaddy, The solubility of carbon dioxide in water at various temperatures from 12 to 40 degrees and at pressures to 500 atmospheres - Critical phenomena, Journal of the American Chemical Society, 62 (1940) 815-817.

57. R. Dohrn, A.P. Bunz, F. Devlieghere, D. Thelen, Experimental measurements of phase-equilibria for ternary and quaternary systems of glucose, water, CO_2 and ethanol with a novel apparatus, Fluid Phase Equilibria, 83 (1993) 149-158.

58. M.B. King, A. Mubarak, J.D. Kim, T.R. Bott, The mutual solubilities of water with supercritical and liquid carbon-dioxide, Journal of Supercritical Fluids, 5 (1992) 296-302.

59. A.E. Markham, K.A. Kobe, The solubility of carbon dioxide and nitrous oxide in aqueous salt solutions, J. Am. Chem. Soc., 63 (1941) 449–454.

60. S. Bando, F. Takemura, M. Nishio, E. Hihara, M. Akai, Solubility of CO_2 in aqueous solutions of NaCl at (30 to 60) degrees C and (10 to 20) MPa, Journal of Chemical and Engineering Data, 48 (2003) 576-579.

61. S.D. Malinin, N.A. Kurovskaya, Investigation of CO_2 solubility in solutions of chlorides at elevated-temperatures and pressures of CO_2, Geokhimiya, (1975) 547-550.

62. S.D. Malinin, N.I. Savelyeya, The solubility of CO_2 in NaCl and $CaCl_2$ solutions at 25, 50, and 75 8C under elevated CO_2 pressures, Geokhimiya 6(1972) 643– 653.

63. C.F. Prutton, R.L. Savage, The solubility of carbon dioxide in calcium chloride water solutions at 75-degrees, 100-degrees, 100-degrees, 120-degrees and high pressures, Journal of the American Chemical Society, 67 (1945) 1550-1554.

64. K. Todheide, E.U. Franck, Das Zweiphasengebiet und die kritische Kurve im System Kohlendioxid-Wasser bis zu Drucken von 3500 bar, Z. Phys. Chem., 37 (1963) 387– 401.

65. H.S. Harned, R. Davis, The ionization constant of carbonic acid in water and the solubility of carbon dioxide in water and aqueous salt solutions from 0 to 50 degrees, Journal of the American Chemical Society, 65 (1943) 2030-2037.

66. P. Servio, P. Englezos, Effect of temperature and pressure on the solubility of carbon dioxide in water in the presence of gas hydrate, Fluid Phase Equilibria, 190 (2001) 127-134.

67. R. Wiebe, V.L. Gaddy, Vapor phase composition of carbon dioxide-water mixtures at various temperatures and at pressures to 700 atmospheres, J. Am. Chem. Soc., 63 (1941) 475–477.

68. C.R. Coan, A.D. King, Solubility of water in compressed carbon dioxide, nitrous oxide, and ethane-evidence for hydration of carbon dioxide and nitrous oxide in gas phase, Journal of the American Chemical Society, 93 (1971) 1857-1862.

69. C. Campos, H.G.D. Villardi, F.L.P. Pessoa, A.M.C. Uller, Solubility of carbon dioxide in water and hexadecane: experimental measurement and thermodynamic modeling, Journal of Chemical and Engineering Data, 54 (2009) 2881-2886.

70. J.A. Nighswander, N. Kalogerakis, A.K. Mehrotra, Solubilities of carbon-dioxide in water and 1 wt-percent NaCl solution at pressures up to 10-MPa and temperatures from 80 ^{o}C to 200 ^{o}C, Journal of Chemical and Engineering Data, 34 (1989) 355-360.

71. T.D. O'Sullivan, N.O. Smith, Solubility and partial molar volume of nitrogen and methane in water and in aqueous sodium chloride from 50 to 125 deg. and 100 to 600 atm, The Journal of Physical Chemistry, 74 (1970) 1460-1466.

72. K. Lekvam, P.R. Bishnoi, Dissolution of methane in water at low temperatures and intermediate pressures, Fluid Phase Equilibria, 131 (1997) 297-309.

73. T.J. Morrison, F. Billett, The salting-out of non-electrolytes .2. the effect of variation in non-electrolyte, Journal of the Chemical Society, (1952) 3819-3822.

74. J. Gao, D.Q. Zheng, T.M. Guo, Solubilities of methane, nitrogen, carbon dioxide, and a natural gas mixture in aqueous sodium bicarbonate solutions under high pressure and elevated temperature, Journal of Chemical and Engineering Data, 42 (1997) 69-73.

75. A. Dhima, J.C. de Hemptinne, G. Moracchini, Solubility of light hydrocarbons and their mixtures in pure water under high pressure, Fluid Phase Equilibria, 145 (1998) 129-150.

76. J. Kiepe, S. Horstmann, K. Fischer, J. Gmehling, Experimental determination and prediction of gas solubility data for methane plus water solutions containing different monovalent electrolytes, Industrial & Engineering Chemistry Research, 42 (2003) 5398.

77. L.K. Wang, G.J. Chen, G.H. Han, X.Q. Guo, T.M. Guo, Experimental study on the solubility of natural gas components in water with or without hydrate inhibitor, Fluid Phase Equilibria, 207 (2003) 143-154.

78. C. Yokoyama, S. Wakana, G. Kaminishi, S. Takahashi, Vapor liquid equilibria in the methane diethylene glycol water-system at 298.15 and 323.15-K, Journal of Chemical and Engineering Data, 33 (1988) 274-276.

79. B.A. Cosgrove, J. Walkley, Solubilities of gases in H_2O and $2H_2O$, Journal of Chromatography, 216 (1981) 161-167.

80. W.Y. Wen, J.H. Hung, Thermodynamics of hydrocarbon gases in aqueous tetraalkylammonium salt solutions, Journal of Physical Chemistry, 74 (1970) 170-180.

81. J.R. Duffy, N.O. Smith, B. Nagy, Solubility of natural gases in aqueous salt solutions.1. Liquidus surfaces in the system CH_4-H_2O-$NaCl_2$-$CaCl_2$ at room temperatures and at pressures below 1000 psia, Geochimica Et Cosmochimica Acta, 24 (1961) 23-31.

82. O.L. Culberson, J.J. McKetta, Phase equilibria in hydrocarbon-water systems. 3 - the solubility of metane in water at pressures to 1000 psia, Transactions of the American Institute of Mining and Metallurgical Engineers, 192 (1951) 223–226.

83. R. Crovetto, R. Fernández-Prini, M.L. Japas, Solubilities of inert gases and methane in H_2O and in D_2O in the temperature range of 300 to 600 K, J. Chem. Phys., 76 (1982) 1077-1086.

84. R.W. Bunsen, in: H.L. Clever, C.L. Young (Eds.) Solubility Data Series, Pergamon Press, Oxford, 1855, pp. 7.

85. D.B. Wetlaufer, R.L. Coffin, S.K. Malik, L. Stoller, Nonpolar group participation in denaturation of proteins by urea + guanidinium salts. Model compound studies, Journal of the American Chemical Society, 86 (1964) 508.

86. W.F. Claussen, M.F. Polglase, Solubilities and structures in aqueous aliphatic hydrocarbon solutions, Journal of the American Chemical Society, 74 (1952) 4817-4819.

87. A. Lannung, J.C. Gjaldbaek, The solubility of methane in hydrocarbons, alcohols, water and other solvents, Acta Chemica Scandinavica, 14 (1960) 1124-1128.

88. A.Y. Namiot, in: H.L. Clever, C.L. Young (Eds.) Solubility Data Series, Pergamon Press, Oxford, 1961, pp. 14.

89. A. Bennaim, J. Wilf, M. Yaacobi, Hydrophobic interaction in light and heavy-water, Journal of Physical Chemistry, 77 (1973) 95-102.

90. A. Bennaim, M. Yaacobi, Effects of solutes on strength of hydrophobic interaction and its temperature-dependence, Journal of Physical Chemistry, 78 (1974) 170-175.

91. B.M. Moudgil, Somasund.P, I.J. Lin, Automated constant pressure reactor for measuring solubilities of gases in aqueous-solutions, Review of Scientific Instruments, 45 (1974) 406-409.

92. S. Yamamoto, J.B. Alcauskas, T.E. Crozier, Solubility of methane in distilled water and seawater, Journal of Chemical and Engineering Data, 21 (1976) 78-80.

93. J.A. Muccitelli, W.Y. Wen, Solubility of methane in aqueous-solutions of triethylenediamine, Journal of Solution Chemistry, 9 (1980) 141-161.

94. O.L. Culberson, A.B. Horn, J.J. McKetta, Phase equilibria in hydrocarbon-water systems - the solubility of ethane in water at pressures to 1200 pounds per square inch, Transactions of the American Institute of Mining and Metallurgical Engineers, 189 (1950) 1-6.

95. B. Amirijafari, J.M. Campbell, Solubility of gaseous hydrocarbon mixtures in water, Soc. Petrol. Eng. J. , 1 (1972) 21–27.

96. R.K. Stoessell, P.A. Byrne, Salting-out of methane in single-salt solutions at 25-degrees-c and below 800 psia, Geochimica Et Cosmochimica Acta, 46 (1982) 1327-1332.

97. R.G. Sultanov, V.G. Skripka, A.Y. Namiot, Phase equilibrium and critical effect of water-methane system under increased temperature and pressure, Zhurnal Fizicheskoi Khimii, 46 (1972) 2160.

98. A. Chapoy, C. Coquelet, D. Richon, Corrigendum to “Revised solubility data and modeling of water in the gas phase of the methane/water binary system at temperatures from 283.08 to 318.12 K and pressures up to 34.5 MPa”: [Fluid Phase Equilibria 214 (2003) 101–117], Fluid Phase Equilibria, 230 (2005) 210-214.

99. A.H. Mohammadi, A. Chapoy, D. Richon, B. Tohidi, Experimental measurement and thermodynamic modeling of water content in methane and ethane systems, Industrial & Engineering Chemistry Research, 43 (2004) 7148-7162.

100. N.L. Yarym-Agaev, R.P. Sinyavskaya, I.I. Koliushko, L.Y. Levinton, Phase-equilibria in the water methane and methanol methane binary-systems under high-pressures, Zh. Prikladnoi Khim., 58 (1985) 165-168.

101. R.H. Olds, B.H. Sage, W.N. Lacey, Phase equilibria in hydrocarbon systems - Composition of the dew-point gas of the methane-water system, Industrial and Engineering Chemistry, 34 (1942) 1223-1227.

102. M. Rigby, J.M. Prausnitz, Solubility of water in compressed nitrogen argon and methane, Journal of Physical Chemistry, 72 (1968) 330.

103. R.P. Kennan, G.L. Pollack, Pressure-dependence of the solubility of nitrogen, argon, krypton, and xenon in water, Journal of Chemical Physics, 93 (1990) 2724-2735.

104. N.O. Smith, S. Kelemen, B. Nagy, Solubility of natural gases in aqueous salt solutions. 2. Nitrogen in aqueous NaCl, $CaCl_2$, Na_2SO_4 and $MgSO_4$ at room temperatures and at pressures below 1000 psia, Geochimica Et Cosmochimica Acta, 26 (1962) 921-926.

105. R. Wiebe, V.L. Gaddy, C. Heins, Solubility of nitrogen in water at 25 degrees C. from 25 to 1000 atmospheres, Industrial and Engineering Chemistry, 24 (1932) 927-927.

106. Osulliva.Td, N.O. Smith, B. Nagy, Solubility of natural gases in aqueous salt solutions-3 N_2 in aqueous NaCl at high pressures, Geochimica Et Cosmochimica Acta, 30 (1966) 619.

107. E. Douglas, Solubilities of oxygen argon + nitrogen in distilled water, Journal of Physical Chemistry, 68 (1964) 169-174.

108. A.W. Saddington, A.W. Krase, Vapor-liquid equilibria in the system nitrogen-water, Journal of the American Chemical Society, 56 (1934) 353-361.

109. L.E. Farhi, T. Homma, A.W.T. Edwards, Determination of dissolved N_2 in blood by gas chromatography and (a-a)N_2 difference, Journal of Applied Physiology, 18 (1963) 97-106.

110. J.A. Hawkins, C.W. Shilling, Nitrogen solubility in blood at increased air pressures, Journal of Biological Chemistry, 113 (1936) 273-278.

111. C.N. Murray, J.P. Riley, T.R.S. Wilson, Solubility of gases in distilled water and sea water. I. Nitrogen, Deep-Sea Research, 16 (1969) 297-310.

112. D.D. Van Slyke, R.T. Dillon, R. Margara, Studies of gas and electrolyte equilibria in blood - XVIII. Solurility and physical state of atmospheric nitrogen in blood cells and plasma, Journal of Biological Chemistry, 105 (1934) 571-596.

113. W.C. Eichelberger, Solubility of air in brine at high pressures - at 1000 to 3500 pounds per square inch gage and at 25-degrees-c to 65-degrees-c, Industrial and Engineering Chemistry, 47 (1955) 2223-2228.

114. R. Wiebe, V.L. Gaddy, C. Heins, The solubility of nitrogen in water at 50, 75 and 100 degrees from 25 to 1000 atmospheres, Journal of the American Chemical Society, 55 (1933) 947-953.

115. G. Hufner, Investigations on the absorption of nitrogen-gas and hydrogen through watery solutions, Zeitschrift Fur Physikalische Chemie--Stochiometrie Und Verwandtschaftslehre, 57 (1907) 611-625.

116. C.J.J. Fox, On the coefficients of absorption of nitrogen and oxygen in distilled water and seawater, and of atmospheric carbonic acid in sea-water, Transactions of the Faraday Society, 5 (1909) 68-86.

117. C. Bohr, The solubility of gas in concentrated sulfuric acid and in mixtures of sulfuric acid and water, Zeitschrift Fur Physikalische Chemie--Stochiometrie Und Verwandtschaftslehre, 71 (1910) 47-50.

118. C. Muller, The absorption of oxygen, nitrogen and hydrogen in watery solutions of non-electrolytes, Zeitschrift Fur Physikalische Chemie--Stochiometrie Und Verwandtschaftslehre, 81 (1912) 483-503.

119. R.J. Wilcock, R. Battino, Solubility of oxygen-nitrogen mixture in water, Nature, 252 (1974) 614-615.

120. L. Braun, The absorption of nitrogen and hydrogen in acqueous solutions of various dissociated materials, Zeitschrift Fur Physikalische Chemie--Stochiometrie Und Verwandtschaftslehre, 33 (1900) 721-739.

121. C.E. Klots, B.B. Benson, Solubilities of nitrogen, oxygen, and argon in distilled water, Journal of Marine Research, 21 (1963) 48-57.

122. W.E. Adeney, H.G. Becker, The determination of the rate of solution of atmospheric nitrogen and oxygen by water. Part I, Philosophical Magazine, 38 (1919) 317-337.

123. J. Alvarez, R. Crovetto, R. Fernandezprini, The dissolution of N_2 and of H_2 in water from room temperature to 640 K, Berichte der Bunsengesellschaft/Physical Chemistry Chemical Physics, 92 (1988) 935-940.

124. P.C. Gillespie, G.M. Wilson, Vapor-liquid equilibrium data on water-substitute gas components: N_2-H_2O, H_2-H_2O, CO-H_2O, H_2-CO-H_2O, and H_2S-H_2O, in, Research report RR-48, Tulsa, 1980.

125. A.Y. Namiot, M.M. Bondareva, Solubility of Gases in Water, Gostekhizdat, (1959).

126. A.H. Mohammadi, A. Chapoy, B. Tohidi, D. Richon, Water content measurement and modeling in the nitrogen plus water system, Journal of Chemical and Engineering Data, 50 (2005) 541-545.

CHAPTER IV

GENERALIZED BINARY INTERACTION PARAMETERS FOR THE PENG-ROBINSON EQUATION OF STATE[2]

4.1 Introduction

Accurate vapor-liquid equilibrium (VLE) predictions are essential for designing and modeling chemical processes. Such equilibrium systems can involve a variety of different molecules, types of interactions and phase conditions. Consequently, they produce different types of phase behavior. The complexity of the phase behavior encountered necessitates different computational frameworks. Although experiments provide accurate data at specific phase conditions, such data are limited and cannot be expected to meet the ever-expanding industrial needs for process design and development [1]. Therefore, a need exists for models that can provide accurate predictions of vapor-liquid equilibrium for a wide variety of systems exhibiting varied phase behaviors.

Two approaches are commonly used in describing VLE behavior of systems. The first approach utilizes an equation of state (EOS) to describe the phase behavior for both the liquid and vapor phases. The second approach utilizes an activity coefficient model to describe the liquid phase while a different model, usually an equation of state, is used to describe the vapor phase. The EOS model has been successful in describing systems containing nonpolar and slightly polar components over broad ranges of temperature and pressure. In contrast, activity coefficient models have been preferred to describe highly non-ideal systems.

[2] The material in this chapter has been reproduced with permission from A.M. Abudour, S.A. Mohammad, K.A.M. Gasem, Generalized binary interaction parameters for the Peng–Robinson equation of state, Fluid Phase Equilibria, 383 (2014) 156-173.

The activity coefficient model approach has been applied successfully at low temperatures where the liquid phase is relatively incompressible and up to moderate pressures [2]. However, this model is deficient in describing phase behavior at higher pressures. Further, an activity coefficient model is incapable of describing the phase behavior in the near-critical region of a mixture. An equation of state model is capable of reasonable predictions of phase behavior in near-critical region [3]. Additional problems result when the activity coefficient model is used for supercritical components [4]. Therefore, an EOS model applicable to both liquid and vapor phases over a wide range of temperatures and pressures provides several advantages relative to the activity coefficient approach. For the above reasons, an EOS model was used in this work to investigate the model's capability to predict phase behavior of highly non-ideal systems.

Cubic equations of state (CEOS) such as Soave-Redlich-Kwong (SRK) [5] and Peng-Robinson (PR) [6] are widely used in the chemical industry to perform reservoir simulations and process design calculations due to their inherent simplicity and efficiency. The accurate description of phase equilibrium from a CEOS often requires adjustable parameters in the mixing rules, which are referred to as the binary interaction parameters (BIPs). The BIPs account for the unlike molecular interactions in mixtures composed of widely differing molecular species. In fact, an accurate description of phase equilibria of mixtures is generally sensitive to the mixing rules and these parameters in the CEOS [7].

Several mixing rules for EOS parameters have been proposed [8-14]. Nevertheless, the one-fluid mixing rules are simple and relatively accurate for many systems. The CEOS with these mixing rules can be utilized to represent several systems within the experimental precision in many applications [10]. While the use of one interaction parameter is sufficient for some binary systems, other systems, especially those exhibiting polarity and dissimilarity in molecular sizes, require two binary parameters. Although these simple mixing rules are not as accurate as theoretically-based mixing rules such as Wong-Sandler mixing rules[14] in representing

asymmetric mixtures [15], their simplicity continues to make them attractive, especially when binary interaction parameters (BIPs) are utilized. Therefore, we elected to use the classical one-fluid mixing rules in this study for describing the vapor-liquid equilibria of binary systems.

The classical one-fluid mixing rules require binary interaction parameters (C_{ij}, D_{ij}) that account for deviations from simple mixing rules. These parameters, in general, cannot be predicted *a priori* from existing theory, but they can be regressed from experimental measurements on the binary pairs that form the systems of interest. These parameters can have a dramatic effect on the predicted properties of systems and are often required for accurate predictions. Therefore, the need exists for developing reliable generalized models to estimate EOS BIPs.

Several attempts have been made to generalize the binary parameters for a variety of systems. In our previous work [16], we developed generalized correlations for predicting the high-pressure phase equilibria of systems of coalbed gases (methane, nitrogen and carbon dioxide) with water. Several parameter generalizations of varying complexity have been presented for asymmetric mixtures [17-19]. In particular, Gao et al [19] developed generalized-parameter correlations for the conformal combining parameters (N_{ij}) of the PR EOS for asymmetric binary mixtures involving methane, ethane, nitrogen, hydrogen, carbon monoxide and carbon dioxide in the *n*-paraffins (C_4–C_{44}). A group contribution method has been developed for estimating the temperature dependent binary interaction parameters for mixtures containing alkanes, aromatics and naphthenes [20-22]. This model is limited by the relatively small number of group interaction parameters that are available. Lashkarbolooki et al. [23] developed an artificial neural network model for prediction of phase equilibria of binary systems containing carbon dioxide and hydrocarbon systems.

Although several models for generalizing the binary parameters have been proposed in the literature, the existing models suffer from a limited range of applicability and poor generalization

when applied to systems for which no data exist. Thus, a generalized model to estimate the interaction parameters of binary systems *a priori* is required. An accurate generalized model can be obtained when the property models account for molecular structural variations observed in fluid mixtures. One approach that has gained importance is the use of quantitative structure-property relationship (QSPR) and artificial neural networks (ANNs) models to correlate the desired property in terms of molecular structure. Several QSPR models have been proposed in the literature to predict varied and often complex pure-fluid physical properties of molecules [24-28]. However, little work has been done to date on QSPR models for mixtures. To our knowledge, generalized models to estimate the BIPs of PR EOS for diverse and a large number of binary systems over wide ranges of pressure and temperature have not been presented previously. In this work, the BIPs of the PR EOS were generalized using QSPR methodology as outlined in a later section. Thus, a structure-based model capable of *a priori* prediction of phase behavior for about 1000 binary systems was developed.

This work aims to (a) assess the correlative capabilities of the PR EOS model of describing the phase equilibria of the systems studied using regressed BIPs (C_{ij} and D_{ij}) in the one-fluid mixing rules (b) develop a QSPR model that can estimate *a priori* the binary interaction parameters of the PR EOS for a wide variety of systems and (c) evaluate the model predictions using an external test set that was not used in the model development.

The remaining sections are organized as follows: Section 2 presents the PR EOS model and the mixing rules used in this study, Section 3 presents details of the QSPR methodology used to generalize the model parameters, Section 4 discusses the results obtained for correlating and predicting vapor-liquid equilibria for low and high-pressure systems and Section 5 presents the conclusions from this study.

4.2 Peng-Robinson Equation of State

The PR EOS [6] is given as

$$p = \frac{RT}{v-b} - \frac{a(T)}{v(v+b)+b(v-b)}$$

(4.1)

where

$$a(T) = \frac{0.457535\alpha(T)R^2T_c^2}{p_c^2} \tag{4.2}$$

$$b = \frac{0.077796\,RT_c}{p_c} \tag{4.3}$$

where p is the pressure, T is the temperature, v is the molar volume, a and b are EOS parameters, T_c is the critical temperature, P_c is the critical pressure and R is the universal gas constant.

The α(T) term in Equation (4.2) was calculated with the following expression developed in an earlier work [29]:

$$\alpha(T) = \exp\left(\left(A + BT_r\right)\left(1 - T_r^{C+D\omega+E\omega^2}\right)\right) \tag{4.4}$$

where ω is the acentric factor, T_r is the reduced temperature and A through E are correlation parameters with values of 2.0, 0.836, 0.134, 0.508 and -0.0467, respectively.

4.2.1 Mixing Rules

To apply the PR EOS to mixtures, mixing rules are used to calculate the values of *a* and b *parameters*. The classical one-fluid mixing rules were used and are given as [30]

$$a = \sum_i \sum_j z_i z_j a_{ij} \tag{4.5}$$

$$b = \sum_i \sum_j z_i z_j b_{ij} \tag{4.6}$$

$$a_{ij} = \sqrt{a_i a_j}\left(1 - C_{ij}\right) \tag{4.7}$$

$$b_{ij} = \frac{\left(b_i + b_j\right)}{2}(1 + D_{ij}) \tag{4.8}$$

where z denotes the molar fraction in the liquid or the vapor phase. In Equations (4.7) and (4.8), C_{ij} and D_{ij} are adjustable binary interaction parameters (BIPs) that are regressed from experimental vapor-liquid equilibria data. When *i* equals *j*, C_{ij} and D_{ij} values are zero. The most widely-used method is to use a single interaction parameter, C_{ij}, and frequently it is sufficient for the purpose. The BIPs, C_{ij} and D_{ij}, have values typically near zero for systems of non-polar compounds of similar molecular size. However, non-zero values of C_{ij} and D_{ij} are generally required in the phase-equilibrium calculations for systems consisting of compounds with large differences in molecular size and shape and for systems containing polar compounds such as water [31]. Although several other mixing rules have been proposed [8-14], the classical one-fluid mixing rules are used more frequently in EOS applications due to their simplicity and efficiency.

4.3 QSPR Methodology

The development of a QSPR model for BIPs of the PR EOS involves several distinct steps which include: (a) database development, (b) PR EOS binary interaction parameter regression, (c) molecular structure generation and optimization, (d) descriptor generation, (e) descriptor reduction, (f) QSPR model development and (g) QSPR model validation. The details of each of these steps have been provided in our previous works [32]. However, for the sake of completeness, a summary of each of each step is outlined below.

Figure 4.1 presents a flowchart outlining the steps involved in QSPR model development. The modeling process begins by compiling a representative binary VLE database. The binary interaction parameters of the PR EOS are then regressed for each binary system. Then, two-dimensional (2-D) molecular structures of components in each binary system are generated and optimized to find the three-dimensional (3-D) conformation with the least energy. These optimized molecular structures are used to calculate molecular descriptors for each component by using DRAGON [33] and CODESSA [34]. In particular, the current DRAGON [33] software is capable of generating about 4,800 descriptors for each component. This large number of generated molecular descriptors is reduced to find the most significant descriptors for predicting the BIPs. These descriptors are then used to develop an artificial neural network (ANN) model. A detail description for each of these different steps follows.

4.3.1 Database Development

Experimental data are essential for developing a reliable phase behavior model. Further, the predictive capability of a QSPR model depends strongly on the accuracy of the experimental data used in the model development process. An experimental VLE database was compiled from available sources covering a sufficient various functional groups and, thus, the compiled database is well suited to test the efficacy of our approach. An earlier study [35] provides additional details of the VLE database used in this study.

Our VLE database consists of a total of 916 binary systems formed from various combinations of 140 different compounds totaling over 33,000 data points (Oklahoma State University, OSU-VLE Database-III) [35]. The experimental VLE data were taken from DECHEMA [36] and NIST-TDE [37]. A majority of the assembled data were low-pressure binary VLE systems. Out of a total of 916 systems, the data for 856 systems were low-pressure binary VLE data (about 0.0005-6 bar) and the remaining 60 systems contained high-pressure binary VLE data (about 1-58 bar) where

the highest pressure is near the critical pressure of the system studied. The range of temperatures for the database used was about 182-554 K. Details of this binary VLE experimental database, along with the temperature, pressure and composition ranges for each binary system, can be found in Table S1 of the Supplementary Material available with the web edition of this work.

The values of the pure-fluid physical properties, including the critical properties (critical temperature (T_c), critical pressure (P_c)) and acentric factor (ω) for each component, constitute the necessary model input variables for the PR EOS. The values of the input variables for the pure components were taken from DIPPR [38].

Figure 4.2 illustrates the VLE data distribution of the binary systems in the OSU database-III based on chemical classes. The compounds were classified in a similar manner as the UNIFAC functional group classification approach [39]. The database is composed of compounds belonging to 31 chemical classes. Figure 4.2 shows the number of available binary systems for each type of functional-group interaction. As shown in the figure, systems containing alcohol or alkane components are highly represented in the database due to the relatively large amounts of data for these systems.

4.3.2 Binary Interaction Parameter Regression

The PR EOS binary interaction parameters for the 916 binary systems were obtained by regressing the data for each system in our database. To determine the optimum values of the BIPs in the PR EOS model, regression analyses using an equal-fugacity equilibrium framework were conducted subject to mass balance constraints:

$$p^V = p^L$$

$$T^V = T^L \tag{4.9}$$

$$\hat{f}_i^V = \hat{f}_i^L$$

where $\hat{f}_i$ is the fugacity of component i in the mixture, T is the temperature, p is the pressure, and the superscripts, and V and L indicate vapor and liquid phases, respectively. In the regression analyses, the EOS approach was employed for VLE systems.

$$\hat{\phi}_i^V p y_i = \hat{\phi}_i^L p x_i \tag{4.10}$$

Where x_i and y_i are the liquid and vapor mole fractions of any component i, $\hat{\phi}_i^V$ and $\hat{\phi}_i^L$ are the component fugacity coefficients in the vapor and liquid phase, respectively.

An equilibrium algorithm, GEOS [40], was used to conduct bubble-point calculations to determine the bubble-point pressures of the systems studied. A non-linear regression procedure based on the Marquardt method [41, 42] was utilized in this work. Since much of the available data is in the T-p-x form (no vapor phase measurements), only the measured T-p-x data were used in the data reductions. The following objective function, OF, given below by Equation (4.11) was used in the regressions.

$$OF = \sum_{i=1}^{NDP} \left(\frac{p_{cal} - p_{exp}}{p_{exp}} \right)_i^2 \tag{4.11}$$

where NDP is the number of data points, p_{exp} and p_{cal} are the experimental and calculated bubble-point pressures, respectively.

4.3.3 Descriptor Calculation

Two-dimensional (2-D) molecular structures were generated for each component in the database using ChemDraw Ultra 11.0 [43]. Each 2-D structure was then used to generate a three-dimensional (3-D) structure. The 2-D structure can lead to several conformations of 3-D

structures; however, only the 3-D conformation with the lowest energy is the stable state of the molecule. Thus, the molecular energy of the 3-D conformations was minimized by using the OpenBabel genetic algorithm-based (GA) conformal search [44, 45] that employs the MMFF94 force field method [46]. Details on the GA-based conformal search are summarized in the OpenBabel documentation [47]. The optimized molecular structures were then used to generate molecular descriptors for each component. For each component, up to 2344 molecular descriptors were generated using DRAGON [33] and 598 descriptors were generated using CODESSA [34]. Details on the descriptors calculated by DRAGON can be found elsewhere [33]. Numerous successful QSPR models based on DRAGON and CODESSA descriptors have been proposed in the literature [24-28].

4.3.4 Descriptor Input Set up

The structural descriptors generated from DRAGON [33] and CODESSA [34] were used as input values in the development of the QSPR model. For each binary system, the input descriptor set was prepared by calculating the absolute *differences* in the individual descriptors for the compounds in the binary pair of molecules [35]. The absolute differences were used to ensure that the QSPR model remains internally consistent; that is, if an imagined binary system consists of identical compounds, the QSPR model will correctly predict zero values for the BIPs (if i=j, C_{ij} = D_{ij} =0).

4.3.5 Descriptor Reduction and Model Development

As mentioned earlier, DRAGON and CODESSA are capable of calculating a large number of molecular descriptors for each component. However, most of these descriptors have negligible influence in describing a specific property of a component. Therefore, descriptor reduction methodologies are used to reduce the number of descriptors by finding those that are most significant for describing a given property of interest.

In the current work, a sequential regression analysis [32] was used to identify the most significant descriptors for describing the BIPs, C_{ij} and D_{ij}. The sequential regression analysis identified thirty descriptors as significant in describing these parameters. The descriptors identified in this step were then used to construct an artificial neural network (ANN) model. A detailed discussion on our descriptor reduction methodology can be found in a previous work [32].

In the ANN model development process, the input dataset was divided into training, validation, internal test and external test sets that contained 50%, 15%, 10%, 25% of the data, respectively. The data was divided based on the functional-group interactions to ensure that all four data sets had sufficient representation of each of the functional-group interactions present in the database. The current work uses the back-propagation algorithm for training the multi-layer perceptron network [48]. An early-stopping method [49, 50] was used to avoid over-fitting by the application of training and internal validation sets. During initial phases of the ANN training, the errors in both the training and validation sets decrease; however, when the ANNs begins to over-fit the data, the error for the validation set begins to increase. The ANN training was stopped after a fixed number of iterations in which the error on the cross-validation set increased continuously, and the ANN parameters at the minimum of the cross-validation error were retained. Further, to ensure optimal ANN training and avoid local minima, multiple randomizations of the data and initializations of the initial ANN parameters (weights and biases) were used [51]. The Nguyen-Widrow algorithm [52] was used to initialize weights and biases and these were updated using a Levenberg-Marquardt optimization technique [48]. A detailed description of the ANN algorithm is available in a previous work [32].

4.3.6 Creating Ensembles

An Artificial Neural Network (ANN) can sometimes be unstable and its predictive performance is dependent strongly on the training data and the training parameters. Therefore, a single outlier in

the training data could have disproportional effect on the generalization ability of the final model. To prevent this, ensembling of ANNs was utilized, where the predictions of different ANNs are averaged to result in the final predictions [53-55]. In this work, the final ensemble model consisted of 20 different ANNs, each having the same descriptors as inputs but with different network architecture and weights.

4.3.7 Model Validation

The developed QSPR model was validated by employing an external test set of compounds not used in the model development process, as emphasized by Tropsha *et al.*[56]. The performance of the developed model on this external dataset indicates the generalization capability (*a priori* predictions) of the final model.

4.3.8 Model Evaluation

To evaluate the correlative and predictive capabilities of the PR EOS in modeling the systems studied, three distinct case studies were formulated. These case studies are listed in Table 4.1. As shown in the table, the case studies progress systematically in the number of interaction parameters used in the model. Case 1 represents an initial evaluation of the PR model in which its "raw" predictive capability (no interaction parameters) is assessed. In Case 2, the application of a single, constant interaction parameter independent of temperature, which is a common industrial practice, is considered for each binary system. Case 3 employs a separate, constant pair of interaction parameters independent of temperature for each binary system. The interaction parameters for each case were obtained using the objective function given by Equation (4.11).

As mentioned above, our VLE database consisted of 916 binary systems with a wide range of functional-group interactions, including aliphatic and aromatic hydrocarbons, water, alcohols, ethers, sulphides and nitrile compounds. Therefore, three models were studied to test the capabilities of the PR EOS and the generalized PR-QSPR model in modeling binary systems,

including separately: all systems, highly non-ideal non-aqueous systems, and aqueous systems. The three models are presented in Table 4.2. Model 1 represents the PR EOS and PR-QSPR model evaluation for all the systems studied (916 systems). In Model 2, the aqueous systems are excluded (861 systems). Model 3 addresses the ability of the PR EOS and PR-QSPR model for the aqueous systems (55 systems).

Parameters in our models were determined based on the objective function, OF, of Equation (4.11) the root-mean-square of the fractional deviations in pressures. In the following discussion, the results are also expressed and analyzed in terms of the root-mean-squared error (RMSE), bias and average absolute percentage deviations (%AAD).

$$\mathrm{RMSE} = \left(\frac{\sum_{i=1}^{\mathrm{NDP}} \left(p_{\mathrm{cal}} - p_{\mathrm{exp}} \right)^2}{\mathrm{NDP}} \right)^{1/2} \tag{4.12}$$

$$\mathrm{bias} = \frac{\sum_{i=1}^{\mathrm{NDP}} \left(p_{\mathrm{cal}} - p_{\mathrm{exp}} \right)}{\mathrm{NDP}} \tag{4.13}$$

$$\%\,\mathrm{AAD} = \frac{100}{\mathrm{NDP}} \sum_{i=1}^{\mathrm{NDP}} \left| \frac{p_{\mathrm{cal}} - p_{\mathrm{exp}}}{p_{\mathrm{exp}}} \right|_i \tag{4.14}$$

where, NDP is the number of data points, p_{exp} and p_{cal} are the experimental and calculated bubble-point pressures, respectively.

4.4 Results and Discussion

Table 4.3 presents a summary of results for the cases listed in Table 4.1, where overall model statistics are given for the bubble-point pressures for the three cases. The results are classified

into system-based (overall average predictions calculated based on the number of binary systems) and point-based (overall average predictions calculated based on number of data points) average.

As shown in Table 4.2, the prediction capability of PR EOS in the absence of interaction parameters, $C_{ij} = D_{ij} = 0$ (Case 1) resulted in large deviations for the predicted bubble-point pressures, especially for highly non-ideal and aqueous systems. This illustrates that interaction parameters are necessary for modeling of systems composed of dissimilar molecular species.

4.4.1 Single Parameter, C_{ij}, Representations

The use of a single interaction parameter, C_{ij}, specific to each binary system (Case 2) provides improved results for the 916 binary systems (Model 1). As indicated in Table 4.3, the results show a marked improvement compared to Case 1 with a reduction in overall errors from 18% to 5%AAD. Further, the errors decreased from 28% to 7% for highly non-ideal systems, and from 87% to 14% for aqueous systems. This demonstrates the value of interaction parameters, especially for asymmetric mixtures or mixtures containing polar components [17].

4.4.2 Two Parameter (C_{ij} and D_{ij}) Representations

To account for molecular size effects and polarity, a second interaction parameter, D_{ij}, was introduced into the co-volume mixing rules [57, 58]. Case 3 involves use of a separate, constant pair of values, C_{ij} and D_{ij}, which are determined for each binary system, independent of temperature.

Table 4.3 presents the results obtained for PR EOS using C_{ij} and D_{ij} binary parameters (Case 3). While a significant improvement is observed in in comparison with Case 1, the results indicate only a minor improvement over the use of single parameter C_{ij} (Case 2). Although the overall %AADs for Case 3 (4%) are comparable to Case 2 (5%), a closer inspection of the results reveals

that Case 3 provides some improvement in the representations for aqueous systems. Specifically, the errors for aqueous systems were about 11% for Case 3, compared to 14% for Case 2.

Figure 4.3 presents the %AAD distribution of bubble-point pressure representations for Cases 2 and 3 classified by functional-group interactions. Results for each case of each functional-group interaction are shown in variations of grey based on the error ranges given in the figure key. As shown in the figure, both cases provided comparable results when the components of a system are composed of the same functional group (diagonal elements of the triangular matrix). However, Case 2 results in higher errors for highly non-ideal systems when compared to Case 3. This is due to the fact that the use of a single interaction parameter (C_{ij}) is insufficient for systems exhibiting higher polarity or dissimilarity in the molecular species [59, 60]. The introduction of D_{ij} (Case 3) to account for the dissimilarity in molecular size improves the results for some highly non-ideal systems. However, both Case 2 and Case 3 yielded high errors for systems containing water. Although the PR EOS sufficiently models the phase behavior of the pure components of these systems, the phase behavior of a mixture of these components is poorly modeled. The poor predictions for these systems may be attributed to inherent deficiencies in the applied mixing rules and, thus, mixing rules other than the classical one-fluid mixing rules may be required for such systems.

Detailed information on bubble-point pressure representations as well as values of the optimized BIPs (C_{ij} and D_{ij}) for Cases 2 and 3 for the entire database used in this study is provided in Table S1 of the Supplementary Material available with the web edition of this paper.

4.4.3 PR-QSPR Generalized Predictions

The regressed BIPs obtained from PR EOS for both Cases 2 and 3 were used as targets in the development of QSPR models. This goal was to produce model generalizations capable of predicting bubble-point pressure within two times the error from direct data regressions. As

mentioned above, three models were developed and no significant difference was observed in the errors among the three models. Therefore, model 1, in which all the systems (916 systems) were included, was chosen in the current study.

In the QSPR model development process for Case 3, where both BIPs (C_{ij} and D_{ij}) have constant values, a sequential regression process was performed in order to improve the predictive capability of the generalized model. In this work, the QSPR model development started by using the initial regressed BIPs as targets (1^{st} iteration). Then, the regression process was repeated by regressing only one of the BIPs (C_{ij} or D_{ij}) while fixing the other at the generalized value from the QSPR model. The BIPs found in this step were then used as targets to develop a new QSPR model (2^{nd} Iteration). These alternating regression and QSPR modeling steps are repeated multiple times until no significant improvement in predictive capability is observed. The final model for this case (Case 3) was chosen after ten iterations of the regression process.

A set of 30 molecular descriptors obtained from the sequential regression model [32] was used as inputs for the ANNs in the final ensemble model. Tables 4.4-4.6 list the molecular descriptors found significant in estimating the parameters C_{ij} (Case 2), C_{ij} and D_{ij} (Case 3), respectively. The molecular descriptors were calculated using DRAGON [33] and CODESSA [34]. The descriptors listed constitute the descriptors for both the components of the system. The most significant descriptors found in predicting the BIPs were geometric, topological indices, 2D autocorrelations, quantum chemical and GETAWAY descriptors. Additional information on these descriptors may be found in the documentation of DRAGON [33].

Figures 4.4(a)-(b) compare the regressed C_{ij} values from PR EOS with the predicted C_{ij} values from QSPR model for Case 2 in the training and validation sets. The correlation coefficients (R^2) between the regressed and predicted values for the training and the validation sets are 0.97 and 0.90, respectively. The figures indicate that the predicted PR-QSPR model parameters are in good

agreement with the regressed PR EOS parameters. Figure 4.4(d) compares the regressed C_{ij} values from PR EOS with the predicted C_{ij} values from QSPR model for Case 2 in the external test set. The R^2 value between the regressed and predicted values for the external test set is 0.81. Although the level of agreement for the external set is lower than that for the training and validation sets, these results are still indicative of the capability of the developed QSPR model for generalized predictions on new systems not used in the model development process.

Similarly, Figures 4.5(a)-(c) and 4.6(a)-(c) compare the regressed C_{ij} and D_{ij} values from PR EOS with the predicted C_{ij} and D_{ij} values from QSPR model (10^{th} iteration model) for Case 3 in the training, validation and external test sets.

Table 4.7 presents the summary results for the bubble-point pressure predictions using PR-QSPR model (Case 2) for the training, validation, internal test and external test sets. The table provides the results for all systems in the database, and also for subsets composed of highly non-ideal non-aqueous systems and for aqueous systems. As expected, the generalized model predictions contain slightly higher errors than the regressed model. Nevertheless, the generalized models provide reasonable results and permit predictions for systems for which no experimental data exist. As shown in Table 4.7, the errors for the bubble-point pressure predictions in all data sets were less than two times those calculated in the PR EOS regressions (Case 2). The PR-QSPR model resulted in 6.7, 9.4, 10.7 and 10.5 %AADs for the training, validation, internal test and external test sets, respectively.

Figures 4.8(a)-(c) illustrate the generalized model predictions for equilibrium phase compositions of n-heptane + ethylbenzene, 1,3-butadiene + butane, chloroform + methyl acetate and isopentane + N,N-dimethylformide systems, respectively. Figure 4.8 is based on Case 2, where C_{ij} is a constant value and D_{ij} equal to zero. The figures also show a comparison between the PR-QSPR generalized model and PR EOS representations with one interaction parameter. As evident from

the figures, the PR-QSPR generalized model developed in this work provides predictions comparable to direct regressions for the equilibrium phase compositions. Further, the predictions from the PR-QSPR model are in good agreement with the experimental composition values for each system. This illustrates the capability of the PR-QSPR model for predicting various types of phase behavior including highly-non ideal systems.

Table 4.8 shows the summary results for the bubble-point pressure predictions using PR-QSPR model (Case 3) for the training, validation, internal test and external test sets. The errors for the bubble-point pressure predictions were within about two times the errors obtained in the PR EOS regressions (Case 3), indicating that a QSPR modeling approach is effective in generalizing PR EOS binary parameters for *a priori* property predictions. Table 4.8 indicates that the bubble-point pressure predictions from Case 3 were generally similar to Case 2. The only exception was a minor improvement in the predictions for aqueous systems, where the errors were reduced from about 22% (Case 2) to about 19%AAD (Case 3).

Figure 4.7 shows the %AAD distribution of bubble-point pressure predictions obtained from PR-QSPR model for Cases 2 and 3 classified by functional-group interaction. The matrix indicates that the PR-QSPR model resulted in prediction of bubble-point pressure between 5-10%AAD for most of the functional-group interactions present in the database.

Figures 4.9(a)-(d) illustrate the model predictions from Cases 2 and 3 for chloroform + diisopropyl ether, N,N-dimethylformide + 1-propanol , 2-methyl 1-propanol + bromobenzene, and hexane + n-decane systems, respectively. As shown in the figure, the PR-QSPR model for Cases 2 and 3 provide comparable predictions.

4.4.4 PR-QSPR Model Predictions for High-pressure Data

The PR-QSPR model was developed based on 916 systems as mentioned earlier. An additional higher-pressure VLE database was assembled for 22 systems including nearly ideal, highly non-

ideal and aqueous systems. These data were not used in the generalized model development and, thus, they provide a test of the generalization performed in this work. The generalized BIPs obtained from QSPR model were used to predict the bubble-point pressures for these systems.

Table 4.9 presents the high-pressure and low-pressure VLE databases for the 22 systems. The table lists the ranges of temperature and pressure for both databases. The table also presents comparison of PR-QSPR model predictions for high-pressure data and low-pressure data of these 22 systems. The results are shown for Cases 2 and 3 (Model 1). As indicated by the %AADs in Table 4.9, the bubble-point pressures are reasonably accurate for high-pressure data, considering that the model development was based on predominantly low-pressure data. Overall, the PR-QSPR model provided predictions with a %AAD of 8 and 7 for Cases 2 and 3, respectively, for high-pressure data. In comparison, the PR-QSPR model yielded predictions with a %AAD of about 10 for low- pressure data, as shown in Table 4.9.

Figures 4.10(a)-(d) illustrate the prediction of vapor-liquid equilibrium for hydrogen sulfide + methanol, benzene + toluene, pentane + acetone, 1-propanol + p-xylene systems, respectively at high pressures. The figure shows comparison between the PR-QSPR model predictions from Cases 2 and 3. As shown in Figure 4.10(a) for benzene + toluene system, the PR-QSPR models for both Cases 2 and 3 provide comparable predictions since the components of the system have same functional groups and the system is nearly-ideal. However, when the components of a system belong to different functional groups, Case 3, which accounts for the dissimilarity in molecular sizes, provides better predictions than Case 2 as shown in Figure 4.10(b) for hydrogen sulfide + methanol system. For 1-propanol + p-xylene system shown in Figure 4.10(d), both cases provide good predictions at 334 K compared to the experimental data. However, the generalized predictions for both cases show larger errors at 494 K, especially when the mole fraction of 1-propanol is more than 80 %; however, this high temperature is near the critical temperature of the system.

In summary, the generalized PR-QSPR model presented in this study has been shown to provide predictions for the bubble-point pressures within twice the errors calculated in the PR EOS regression analysis for both cases 2 and 3. This was demonstrated by testing the generalized PR-QSPR model for a variety of binary systems composed of diverse molecular species over range of temperatures and pressures. As evident from the above results, cases 2 and 3 provide comparable predictions. However, Case 3 was generally superior to Case 2 for systems exhibiting higher polarity or dissimilarity in the molecular species.

4.5 Conclusions

The PR EOS with the classical one-fluid mixing rules was employed to model the vapor-liquid equilibria of 916 binary systems composed of diverse molecular species. QSPR modeling approach was applied to generalize the binary interaction parameter of PR EOS model. A total of 30 molecular structural descriptors were utilized as inputs in the QSPR model.

Results indicate that the PR-QSPR model is capable of providing useful predictions of bubble-point pressures of binary systems. In particular, the results reveal that the predicted bubble-point pressures from the PR-QSPR model were within twice the errors calculated in the PR EOS regression analysis. The generalized model was further validated by predicting bubble-point pressures for high-pressure VLE data of 22 systems. The model provided predictions for these data comparable to predictions obtained for the low-pressure data used in model development. Thus, the PR-QSPR model developed in this work has been shown capable for *a priori* predictions of VLE for a diverse set of binary systems over wide conditions of pressure, temperature and composition.

Table 4.1. Specific Cases Used in the Peng-Robinson Equation of State Evaluations

Case	Description
1. $C_{ij} = 0$, $D_{ij} = 0$	This provides the "raw" predictive capability of the model, using the mixing rules with no interaction parameters.
2. C_{ij} = Constant, $D_{ij} = 0$	A single, constant value C_{ij} is determined for each binary system, independent of temperature.
3. C_{ij} = Constant, D_{ij} = Constant	A separate, constant pair of values, C_{ij} and D_{ij}, is determined for each binary system, independent of temperature.

Table 4.2. Models Used in the Peng-Robinson Equation of State and PR-QSPR Model Evaluations

Model	No. of systems	Description
1.	916	*All* 916 binary systems were included in the modeling process
2.	861	Aqueous systems *were excluded* in the modeling process
3.	55	*Only aqueous systems* were included in the modeling process

Table 4.3. Summary of Results for PR EOS Predictions (Case 1) and Representations (Case 2 and Case 3) of Bubble-point Pressure

Bubble-point Pressure, bar									
	System Based					Point Based			
Model	**Data set**	**No. sys**	**RMSE**	**Bias**	**%AAD**	**NDP**	**RMSE**	**Bias**	**%AAD**
Case 1 (C_{ij} = 0, D_{ij} = 0)									
1 (all data)	Highly non-ideal	348	26	5.3	28	14536	41	15	39
	Water systems	55	76	46	87	4310	76	57	94
	All data	916	19	2.7	18	33290	29	7	23
Case 2 (C_{ij} = Constant, D_{ij} = 0)									
1 (all data)	Highly non-ideal	348	3	0.22	7	14536	12	0.2	9
	Water systems	55	8	1.38	14	4310	8	0.7	19
	All data	916	2	0.08	5	33290	8	0.1	6
2 (non-aqueous systems)	Highly non-ideal	311	0.3	-0.03	6	11219	0.3	-0.04	6
	All data	861	0.2	-0.01	4	29488	0.2	-0.02	4
3 (aqueous systems)	Water systems	55	8	1.38	14	4310	8	0.7	19
Case 3 (C_{ij} = Constant, D_{ij} = Constant)									
1 (all data)	Highly non-ideal	348	0.1	-0.03	5	14536	0.14	0.14	7
	Water systems	55	0.2	0.01	11	4310	0.21	0.58	12
	All data	916	0.1	-0.01	4	33290	0.10	0.06	5
2 (non-aqueous systems)	Highly non-ideal	311	0.2	-0.02	5	11219	0.21	-0.03	5
	All data	861	0.1	-0.01	4	29488	0.14	-0.01	4
3 (aqueous systems)	Water systems	55	0.2	0.01	11	4310	0.21	0.58	12

Table 4.4. The Descriptors Used As Inputs for the ANNs in the Final Ensemble for Estimating the PR EOS Model Parameter (C_{ij}) for Case 2 (Model 1)

Descriptor Name	Descriptor	Source	Type of Descriptor
Moment of inertia C	Moment of inertia C	CODESSA	Geometric
ALOGP	Ghose-Crippen octanol-water partition coeff. (logP)	DRAGON	Molecular properties
ON0V	overall modified Zagreb index of order 0 by valence vertex degrees	DRAGON	Topological indices
HOMO - LUMO energy gap	HOMO - LUMO energy gap	CODESSA	Quantum Chemical
Min (>0.1) bond order of a N atom	Min (>0.1) bond order of a N atom	CODESSA	Quantum Chemical
HACA-1 [Zefirov's PC]	HACA-1 [Zefirov's PC]	CODESSA	Electrostatic
ATSC4p	Centred Broto-Moreau autocorrelation of lag 4 weighted by polarizability	DRAGON	2D autocorrelations
GATS1e	Geary autocorrelation of lag 1 weighted by Sanderson electronegativity	DRAGON	2D autocorrelations
X0Av	average valence connectivity index of order 0	DRAGON	Connectivity indices
P_VSA_i_2	P_VSA-like on ionization potential, bin 2	DRAGON	P_VSA-like descriptors
R3m	R autocorrelation of lag 3 / weighted by mass	DRAGON	GETAWAY descriptors
X4A	average connectivity index of order 4	DRAGON	Connectivity indices
Min electroph. react. index for O atom	Min electroph. react. index for a O atom	CODESSA	Quantum Chemical
FHDSA Fractional HDSA (HDSA/TMSA)[Quantum-Chemical P_C]	FHDSA Fractional HDSA (HDSA/TMSA) [Quantum-Chemical PC]	CODESSA	Quantum Chemical
PDI	packing density index	DRAGON	Molecular properties
Mor13i	signal 13 / weighted by ionization potential	DRAGON	3D-MoRSE descriptors
RTu+	R maximal index / unweighted	DRAGON	GETAWAY descriptors
Mor11m	signal 11 / weighted by mass	DRAGON	3D-MoRSE descriptors
WiA_B(p)	average Wiener-like index from Burden matrix weighted by polarizability	DRAGON	2D matrix-based descriptors
SpMax3_Bh(m)	largest eigenvalue n. 3 of Burden matrix weighted by mass	DRAGON	Burden eigenvalues
TPSA(NO)	topological polar surface area using N,O polar contributions	DRAGON	Molecular properties
GATS4e	Geary autocorrelation of lag 4 weighted by Sanderson electronegativity	DRAGON	2D autocorrelations
LUMO energy	LUMO energy	CODESSA	Quantum Chemical
Min atomic state energy for a O atom	Min atomic state energy for a O atom	CODESSA	Quantum Chemical
Max resonance energy for a H-N bond	Max resonance energy for a H-N bond	CODESSA	Quantum Chemical
E2p	2nd component accessibility directional WHIM index/weighted by polarizability	DRAGON	WHIM descriptors
Eta_sh_p	eta p shape index	DRAGON	ETA indices
C-028	R--CR--X	DRAGON	Atom-centred fragments
MATS2p	Moran autocorrelation of lag 2 weighted by polarizability	DRAGON	2D autocorrelations
Mor04p	signal 04 / weighted by polarizability	DRAGON	3D-MoRSE descriptors

Table 4.5. The Descriptors Used As Inputs for the ANNs in the Final Ensemble for Estimating the PR EOS Model Parameter (C_{ij}) for Case 3 (Model 1)

Descriptor Name	Descriptor Description	Source	Type of Descriptor
VE2_G/D	average coefficient of the last eigenvector from distance/distance matrix	DRAGON	3D matrix-based descriptors
GATS1e	Geary autocorrelation of lag 1 weighted by Sanderson electronegativity	DRAGON	2D autocorrelations
nROH	number of hydroxyl groups	DRAGON	Functional-group counts
SpAbs_B(m)	graph energy from Burden matrix weighted by mass	DRAGON	2D matrix-based descriptors
Psi_i_A	intrinsic state pseudoconnectivity index - type S average	DRAGON	Topological indices
C-007	CH2X2	DRAGON	Atom-centred fragments
GGI5	topological charge index of order 5	DRAGON	2D autocorrelations
PNSA-1 Partial negative surface area [Zefirov's PC]	PNSA-1 Partial negative surface area [Zefirov's PC]	CODESSA	Electrostatic
Max nucleoph. react. index for O atom	Max nucleoph. react. index for a O atom	CODESSA	Quantum Chemical
G3p	3rd component symmetry directional WHIM index / weighted by polarizability	DRAGON	WHIM descriptors
Eta_L	eta local composite index	DRAGON	ETA indices
MAXDP	maximal electrotopological positive variation	DRAGON	Topological indices
SpMax7_Bh(m)	largest eigenvalue n. 7 of Burden matrix weighted by mass	DRAGON	Burden eigenvalues
nHBonds	number of intramolecular H-bonds (with N,O,F)	DRAGON	Functional-group counts
Min e-n attraction for a H atom	Min e-n attraction for a H atom	CODESSA	Quantum Chemical
Max nucleoph. react. index for N atom	Max nucleoph. react. index for a N atom	CODESSA	Quantum Chemical
HACA-2 [Quantum-Chemical PC]	HACA-2 [Quantum-Chemical PC]	CODESSA	Quantum Chemical
Min electroph. react. index for O atom	Min electroph. react. index for a O atom	CODESSA	Quantum Chemical
Min resonance energy for a C-H bond	Min resonance energy for a C-H bond	CODESSA	Quantum Chemical
P_VSA_LogP_3	P_VSA-like on LogP, bin 3	DRAGON	P_VSA-like descriptors
C-024	R--CH--R	DRAGON	Atom-centred fragments
Cl-087	Cl attached to C2(sp3)	DRAGON	Atom-centred fragments
ALOGP	Ghose-Crippen octanol-water partition coeff. (logP)	DRAGON	Molecular properties
PCD	difference between multiple path count and path count	DRAGON	Walk and path counts
O-056	alcohol	DRAGON	Atom-centred fragments
nHDon	number of donor atoms for H-bonds (N and O)	DRAGON	Functional-group counts
ZM2Mad	second Zagreb index by Madan vertex degrees	DRAGON	Topological indices
Min total interaction for a H-O bond	Min total interaction for a H-O bond	CODESSA	Quantum Chemical
Eta_betaS	eta sigma VEM count	DRAGON	ETA indices
Mor30p	signal 30 / weighted by polarizability	DRAGON	3D-MoRSE descriptors

Table 4.6. The Descriptors Used As Inputs for the ANNs in the Final Ensemble for Estimating the PR EOS Model Parameter (D_{ij}) for Case 3 (Model 1)

Descriptor Name	Descriptor Description	Source	Type of Descriptor
FHDSA Fractional HDSA (HDSA/TMSA)[Quantum-Chemical PC]	FHDSA Fractional HDSA (HDSA/TMSA) [Quantum-Chemical PC]	CODESSA	Quantum Chemical
SpAbs_B(m)	graph energy from Burden matrix weighted by mass	DRAGON	2D matrix-based descriptors
REIG	first eigenvalue of the R matrix	DRAGON	GETAWAY descriptors
GGI1	topological charge index of order 1	DRAGON	2D autocorrelations
Mor19m	signal 19 / weighted by mass	DRAGON	3D-MoRSE descriptors
E2v	2nd component accessibility directional WHIM index / weighted by van der Waals volume	DRAGON	WHIM descriptors
G3p	3rd component symmetry directional WHIM index / weighted by polarizability	DRAGON	WHIM descriptors
FHDCA Fractional HDCA (HDCA/TMSA)[Quantum-Chemical PC]	FHDCA Fractional HDCA (HDCA/TMSA) [Quantum-Chemical PC]	CODESSA	Quantum Chemical
nHDon	number of donor atoms for H-bonds (N and O)	DRAGON	Functional-group counts
P_VSA_LogP_7	P_VSA-like on LogP, bin 7	DRAGON	P_VSA-like descriptors
SpMax7_Bh(m)	largest eigenvalue n. 7 of Burden matrix weighted by mass	DRAGON	Burden eigenvalues
SM1_B(m)	spectral moment of order 1 from Burden matrix weighted by mass	DRAGON	2D matrix-based descriptors
RDF010e	Radial Distribution Function - 010 / weighted by Sanderson electronegativity	DRAGON	RDF descriptors
RDF010u	Radial Distribution Function - 010 / unweighted	DRAGON	RDF descriptors
H_Dz(p)	Harary-like index from Barysz matrix weighted by polarizability	DRAGON	2D matrix-based descriptors
P_VSA_LogP_3	P_VSA-like on LogP, bin 3	DRAGON	P_VSA-like descriptors
C-007	CH2X2	DRAGON	Atom-centred fragments
Wi_B(i)	Wiener-like index from Burden matrix weighted by ionization potential	DRAGON	2D matrix-based descriptors
Balaban index	Balaban index	CODESSA	Topological
Wi_B(m)	Wiener-like index from Burden matrix weighted by mass	DRAGON	2D matrix-based descriptors
Avg valency of a C atom	Avg valency of a C atom	CODESSA	Quantum Chemical
nCbH	number of unsubstituted benzene C(sp2)	DRAGON	Functional-group counts
MAXDP	maximal electrotopological positive variation	DRAGON	Topological indices
SM1_Dz(p)	spectral moment of order 1 from Barysz matrix weighted by polarizability	DRAGON	2D matrix-based descriptors
Mor03p	signal 03 / weighted by polarizability	DRAGON	3D-MoRSE descriptors
Avg 1-electron react. index for Br atom	Avg 1-electron react. index for a Br atom	CODESSA	Quantum Chemical
ATSC2m	Centred Broto-Moreau autocorrelation of lag 2 weighted by mass	DRAGON	2D autocorrelations
ZM1Per	first Zagreb index by perturbation vertex degrees	DRAGON	Topological indices
Relative number of O atoms	Relative number of O atoms	CODESSA	Constitutional
Chi_Dt	Randic-like index from detour matrix	DRAGON	2D matrix-based descriptors

Table 4.7. Summary of Results for Bubble-point Pressure Predictions Using PR-QSPR Model for Case 2 (C_{ij} = Constant, D_{ij} = 0)

Bubble-point Pressure, bar								
Data set	System Based				Point Based			
	No. sys	RMSE	Bias	%AAD	NDP	RMSE	Bias	%AAD
Model 1 (all data)								
Training Set	460	0.2	-0.02	6.7	20043	0.3	-0.04	8
Validation Set	167	0.2	-0.02	9.4	4982	0.1	-0.01	9
Internal Test Set	101	0.2	-0.02	10.7	2631	0.1	-0.02	10
External Test Set	188	2.7	-0.02	10.5	5634	11	0.19	14
Without Test Set	728	0.2	-0.02	7.9	27656	0.3	-0.03	8
Highly Non-ideal	348	2.1	-0.05	10.4	14536	7	0.01	12
Water Systems	55	5.1	-0.03	21.6	4310	5	0.16	26
All data	916	1.2	-0.02	8.4	33290	5	0.01	9
Model 2 (non-aqueous systems)								
Training Set	431	0.2	-0.02	5.9	17173	0.2	-0.02	6
Validation Set	156	0.1	-0.01	8	4682	0.1	-0.01	7
Internal Test Set	98	0.1	-0.01	8.9	2622	0.1	-0.01	9
External Test Set	176	0.2	-0.02	9.2	5011	0.2	-0.02	8
Without Test Set	685	0.18	-0.01	6.8	24477	0.2	-0.02	6
Highly Non-ideal	311	0.3	-0.04	8.6	11219	0.3	-0.05	8
All data	861	0.2	-0.01	7.3	29488	0.2	-0.02	7
Model 3 (aqueous systems)								
All data	55	6	-0.05	21	4310	6	0.3	27

Table 4.8. Summary of Results for Bubble-point Pressure Predictions Using PR-QSPR Model for Case 3 (C_{ij} = Constant, D_{ij} = Constant)

Bubble-point Pressure, bar								
Data set	System Based				Point Based			
	No. sys	RMSE	Bias	%AAD	NDP	RMSE	Bias	%AAD
Model 1 (all data)								
Training Set	460	0.2	-0.01	6.6	20043	0.2	-0.03	7
Validation Set	167	0.2	-0.01	10.8	4982	0.1	0.00	11
Internal Test Set	101	0.1	-0.01	11.3	2631	0.1	0.00	11
External Test Set	188	7.3	0.36	10.6	5634	0.4	-0.05	10
Without Test Set	728	0.2	-0.01	8.2	27656	0.2	-0.02	8
Highly Non-ideal	348	5.4	0.18	10.3	14536	0.4	-0.05	10
Water Systems	55	13.6	1.20	19.4	4310	14	-0.12	16
All data	916	3.3	0.07	8.7	33290	0.3	-0.02	8
Model 2 (non-aqueous systems)								
Training Set	431	0.2	-0.009	5.9	17173	0.2	-0.01	6
Validation Set	156	0.1	-0.003	9.5	4682	0.1	0.00	9
Internal Test Set	98	0.1	-0.003	10.3	2622	0.1	-0.01	10
External Test Set	176	0.3	0.001	10.4	5011	0.2	-0.01	9
Without Test Set	685	0.2	-0.007	7.4	24477	0.2	-0.01	7
Highly Non-ideal	311	0.3	-0.016	9.1	11219	0.2	-0.03	8
All data	861	0.2	-0.005	8.0	29488	0.2	-0.01	7
Model 3 (aqueous systems)								
All data	55	16	2	26	4310	15	0.31	30

Table 4.9. Summary of Results for Bubble-point Pressure Predictions Using PR-QSPR Model for Cases 2 and 3 (Model 1) for High-Pressure Data of 22 Systems in Comparison with the Results of Low-Pressure Data for the Same Systems

System	Low-pressure Data (Used in QSPR Model Development(Training & External))					High-pressure Data (External Data)					Ref.
	Temperature Range (K)	Pressure Range (bar)	NDP	% AAD, Bubble-point Pressure (bar)		Temperature Range (K)	Pressure Range (bar)	NDP	% AAD, Bubble-point Pressure (bar)		
				Case 2	Case 3				Case 2	Case 3	
Butane(1)+Ethanol(2)	298.45-345.65	0.08-8.81	72	16	11	353.26-423.2	1.1-29.71	44	17	8	[61]
Methanol(1)+Isobutene(2)	323.15-323.15	0.55-6.31	11	21	13	364.49-364.5	10.56-16.3	22	22	16	[62]
Butane(1)+Pentane(2)	298.15-298.15	0.73-1.08	12	2	6	358.4-463.9	10.3-31.03	82	3	2	[63]
Pentane(1)+Ethanol(2)	293.15-293.15	0.06-0.63	7	22	32	372.7-422.6	2.24-19.63	34	13	7	[64]
Hydrogen Sulfide(1)+Methanol(2)	298.15-348.15	0.17-58	26	9	5	298-448.1	0.17-112.0	55	6	4	[65]
Benzene(1)+Toluene(2)	353.25-383.76	1.01-1.01	13	2	1	393-553	1.51-38.61	26	4	4	[66]
Pentane(1)+1-Butanol(2)	303.15-303.15	0.01-0.82	15	14	10	468.2-513.2	8.33-29.39	19	10	3	[67]
Water(1)+Methanol(2)	337.65-373.15	1.01-1.01	21	2	4	423.2-523.2	10.52-86.1	18	3	4	[68,69]
Water(1)+2-Propanol(2)	308.93-323.86	0.13-0.13	24	18	8	423-523	5.17-61.36	45	17	9	[70]
Water(1)+Ethanol(2)	351.55-369.25	1.01-1.01	12	7	7	409.8-573.2	6.89-127.5	60	5	12	[71]
Pentane(1)+Acetone(2)	238.15-322.3	0.01-1.01	49	5	4	372.7-422.6	3.66-17.98	33	2	1	[72]
Pentane(1)+Benzene(2)	323.15-323.15	0.36-1.59	15	1	4	420.9-537.7	13.79-44.1	22	1	2	[73]
Hexane(1)+Benzene(2)	298.15-403.15	0.13-5.02	109	1	2	393.1-463.2	4.05-15.11	69	3	4	[74,75]
Benzene(1)+Heptane(2)	298.15-428.15	0.06-6.28	96	2	1	458-488	7.76-17.73	29	2	2	[76]
Butane (1)+1-Propanol(2)	330.18-330.19	3.87-5.54	12	18	9	343.2-433.3	3.6-31.61	19	18	4	[77]
1-Propanol (1)+Heptane(2)	357.35-371.55	1.01-1.01	21	10	6	423.2-498.2	3.73-29.2	45	9	6	[78,79]
1-Propanol(1)+p-xylene(2)	313.15-313.15	0.03-0.07	10	12	20	433.2-494.2	1.0-26.16	15	6	5	[80]
Methanol(1)+Benzene(2)	308.2-353.4	0.2-1.01	162	10	12	393-473	4.87-40.82	50	11	13	[81]
Dichloromethane(1)+Methanol(2)	310.95-331.75	1.01-1.01	11	8	15	398.2-398.2	7.37-12.23	15	10	14	[82]
1,3-butadien(1)+Cyclohexane(2)	303.15-413.15	0.16-9.49	62	3	7	383.2-413.2	10.1-35.4	15	2	4	[83]
Butane(1)+Hydrogen Sulfide(2)	182.33-182.33	0-0.15	7	17	16	366.5-418.2	13.5-80.7	38	3	29	[84]
1-Propanol(1)+Water(2)	333.15-368.15	0.23-1.01	28	23	12	373.2-523.2	1.1-54.31	20	17	10	[68]
Overall			**795**	**10**	**9**			**775**	**8**	**7**	

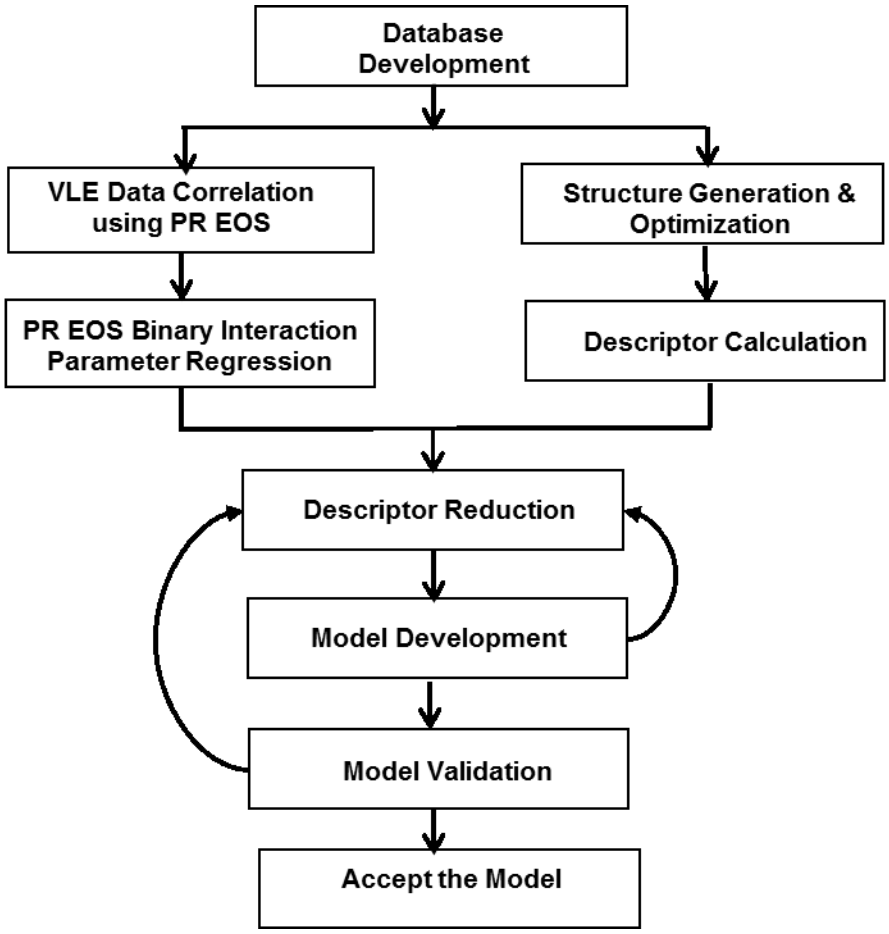

Figure 4.1. Steps Involved in Development of a QSPR Model

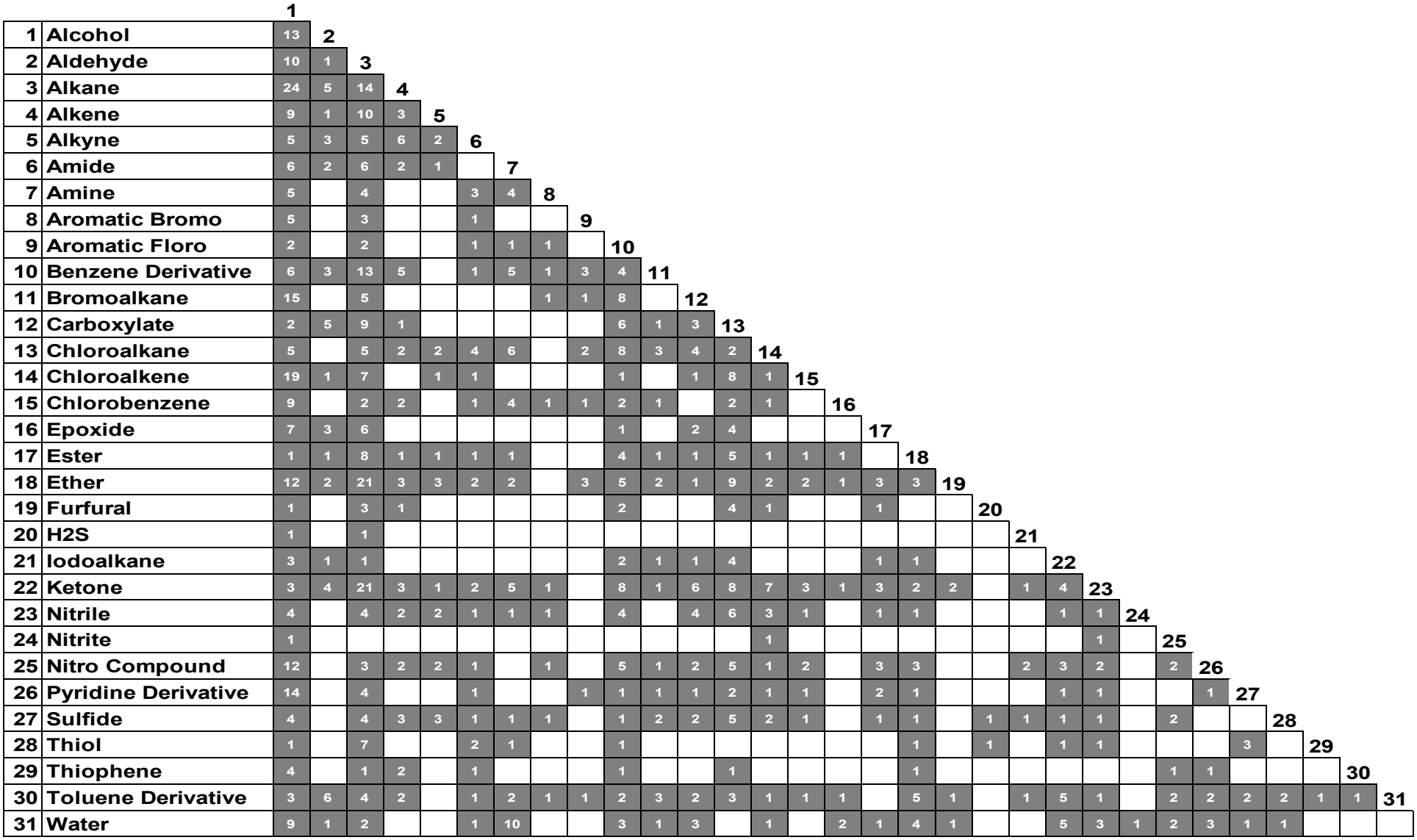

		1	2	3	4	5	6	7	8	9	10	11	12	13	14	15	16	17	18	19	20	21	22	23	24	25	26	27	28	29	30	31
1	Alcohol	13																														
2	Aldehyde	10	1																													
3	Alkane	24	5	14																												
4	Alkene	9	1	10	3																											
5	Alkyne	5	3	5	6	2																										
6	Amide	6	2	6	2	1																										
7	Amine	5		4			3	4																								
8	Aromatic Bromo	5		3			1																									
9	Aromatic Floro	2		2			1	1	1																							
10	Benzene Derivative	6	3	13	5		1	5	1	3	4																					
11	Bromoalkane	15		5					1	1	8																					
12	Carboxylate	2	5	9	1						6	1	3																			
13	Chloroalkane	5		5	2	2	4	6		2	8	3	4	2																		
14	Chloroalkene	19	1	7		1	1				1		1	8	1																	
15	Chlorobenzene	9		2	2		1	4	1	1	2	1		2	1																	
16	Epoxide	7	3	6							1		2	4																		
17	Ester	1	1	8	1	1	1	1			4	1	1	5	1	1	1															
18	Ether	12	2	21	3	3	2	2		3	5	2	1	9	2	2	1	3	3													
19	Furfural	1		3	1						2			4	1			1													
20	H2S	1		1																												
21	Iodoalkane	3	1	1							2	1	1	4				1	1													
22	Ketone	3	4	21	3	1	2	5	1		8	1	6	8	7	3	1	3	2	2		1	4									
23	Nitrile	4		4	2	2	1	1	1		4		4	6	3	1		1	1				1	1								
24	Nitrite	1													1									1								
25	Nitro Compound	12		3	2	2	1		1		5	1	2	5	1	2		3	3			2	3	2		2						
26	Pyridine Derivative	14		4			1			1	1	1	1	2	1	1		2	1				1	1			1					
27	Sulfide	4		4	3	3	1	1	1		1	2	2	5	2	1		1	1		1	1	1	1		2						
28	Thiol	1		7			2	1			1								1		1		1	1				3				
29	Thiophene	4		1	2		1				1			1					1							1	1					
30	Toluene Derivative	3	6	4	2		1	2	1	1	2	3	2	3	1	1	1		5	1		1	5	1		2	2	2	2	1	1	
31	Water	9	1	2			1	10			3	1	3		1		2	1	4	1			5	3	1	2	3	1	1			

Figure 4.2. Database Matrix of the Compounds in the OSU-VLE Database III

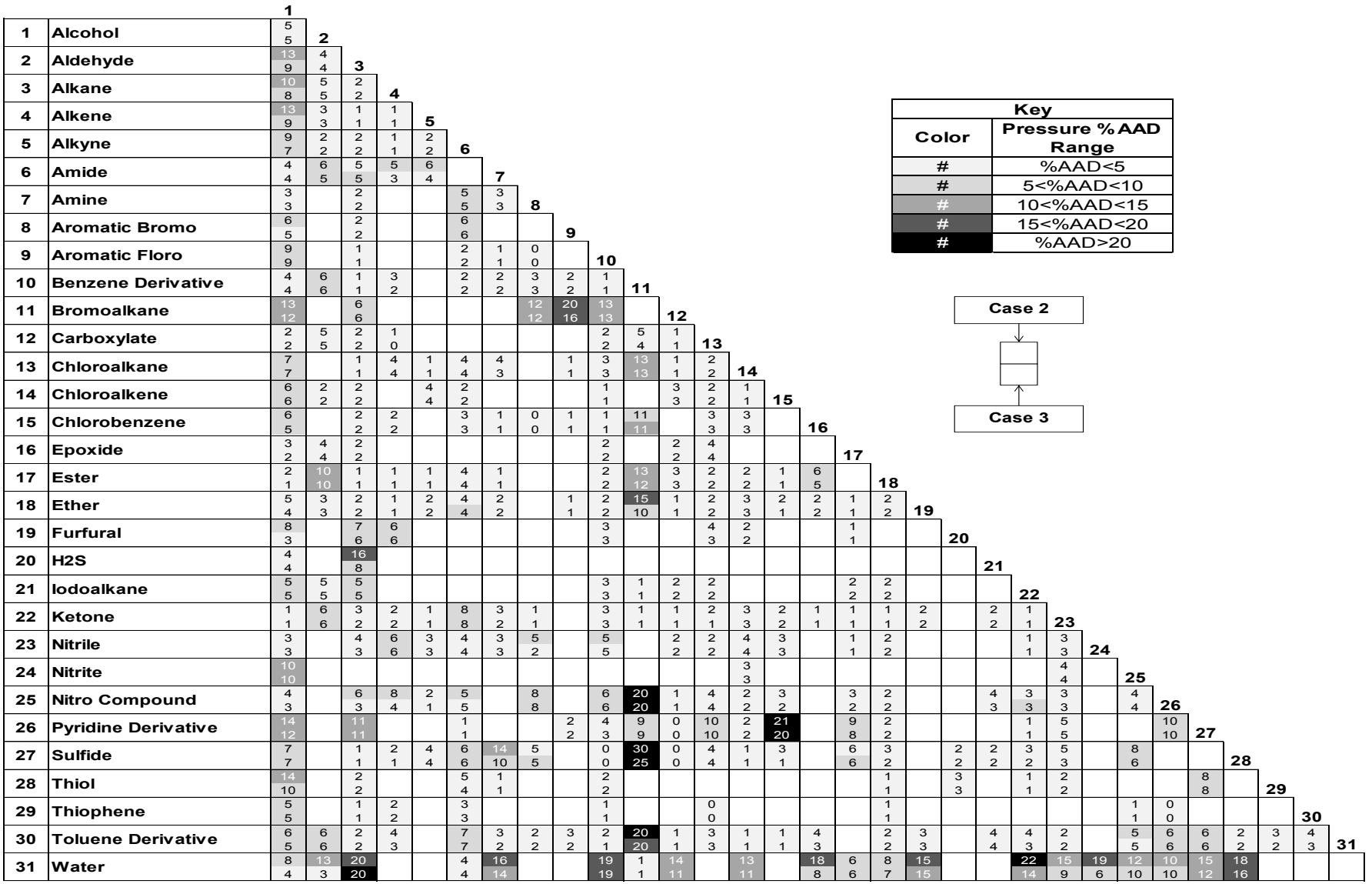

Figure 4.3. PR EOS Representations (Cases 2 and 3) of Bubble-point Pressure by Type of Interactions

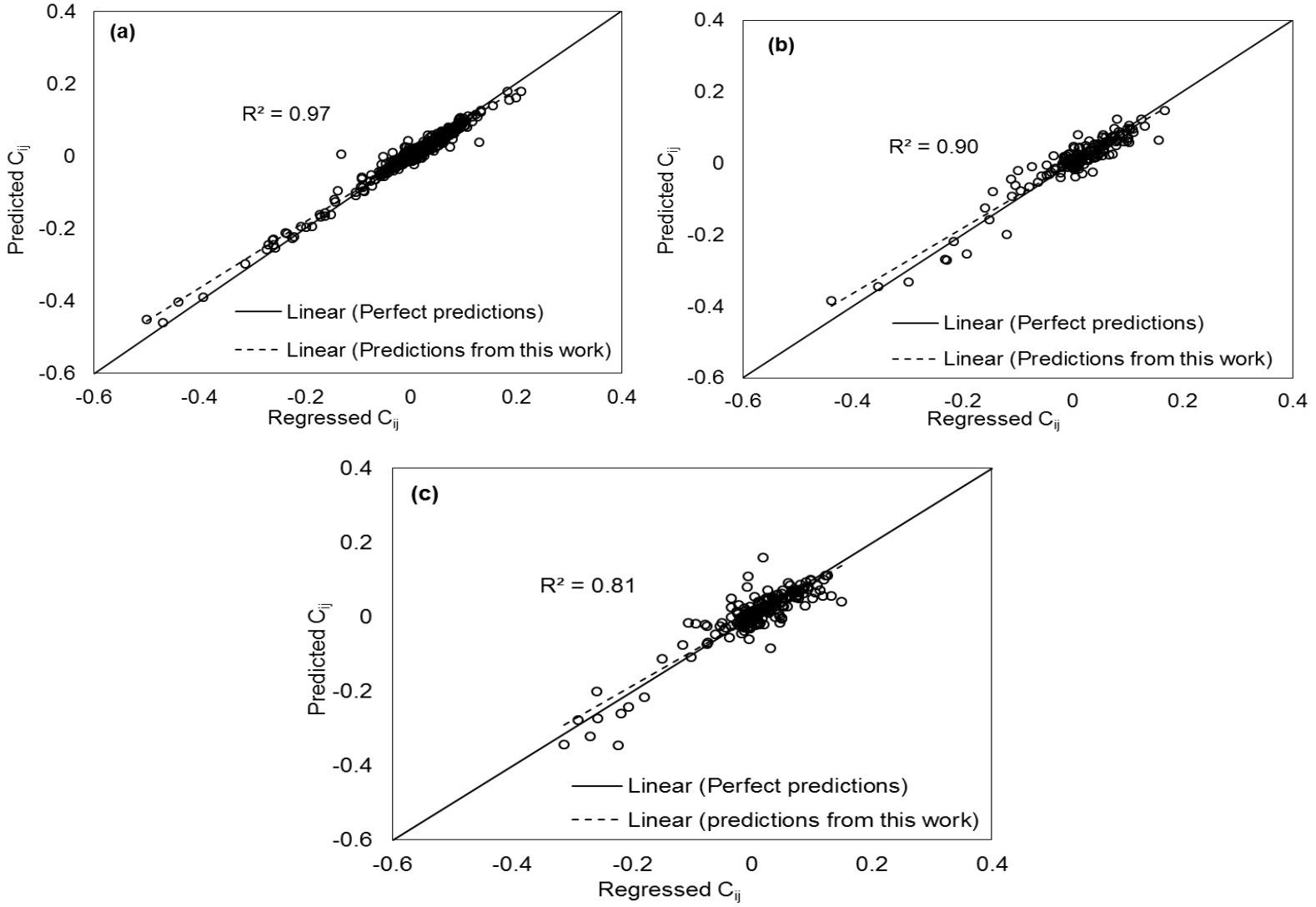

Figure 4.4. Comparison of the Regressed C_{ij} from PR EOS and the Predicted C_{ij} from QSPR Model for Case 2 in (a) Training Set (b) Validation Set (c) External Test Set

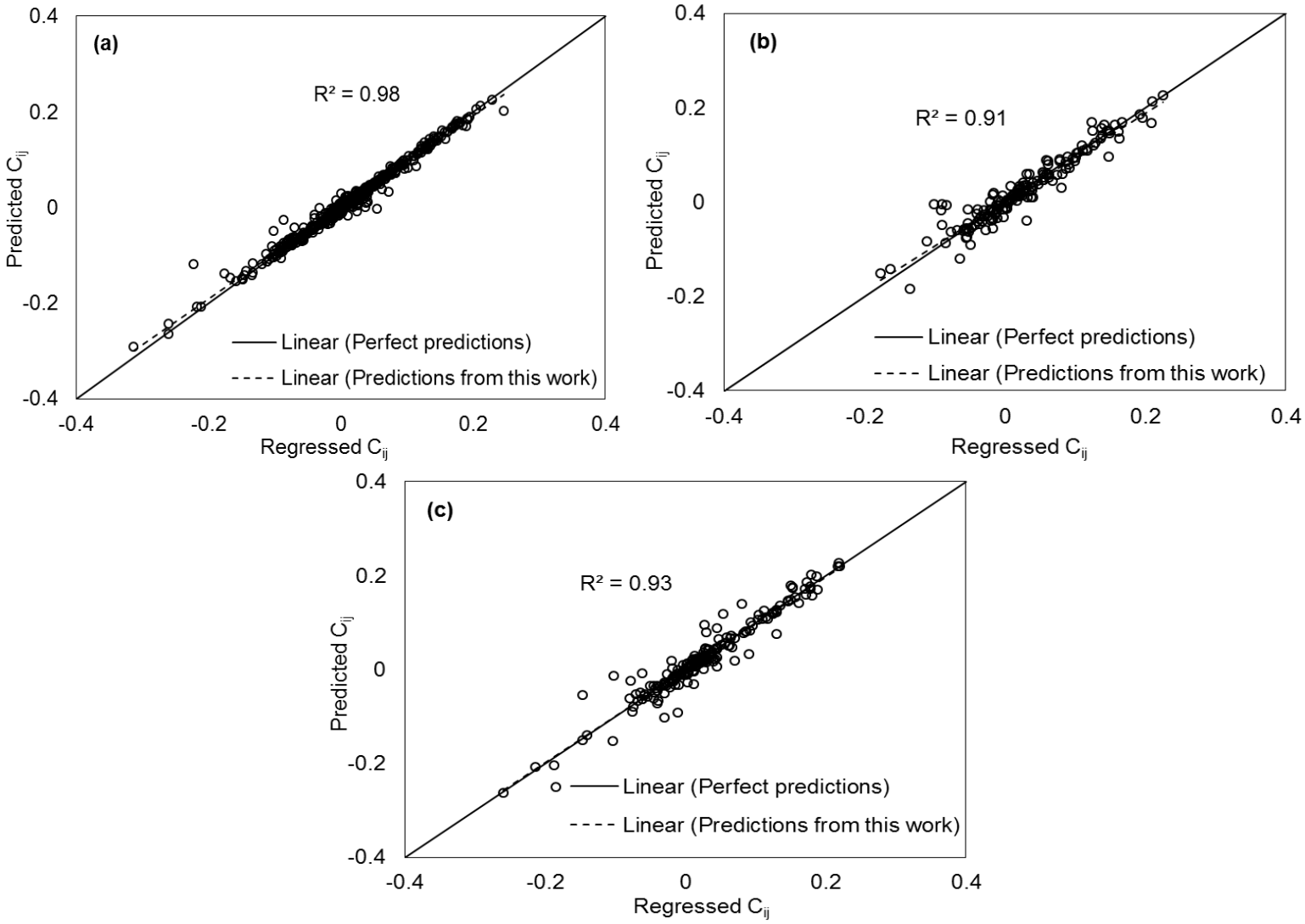

Figure 4.5. Comparison of the Regressed C_{ij} from PR EOS and the Predicted C_{ij} from QSPR Model for Case 3 in (a) Training Set (b) Validation Set (c) External Test Set

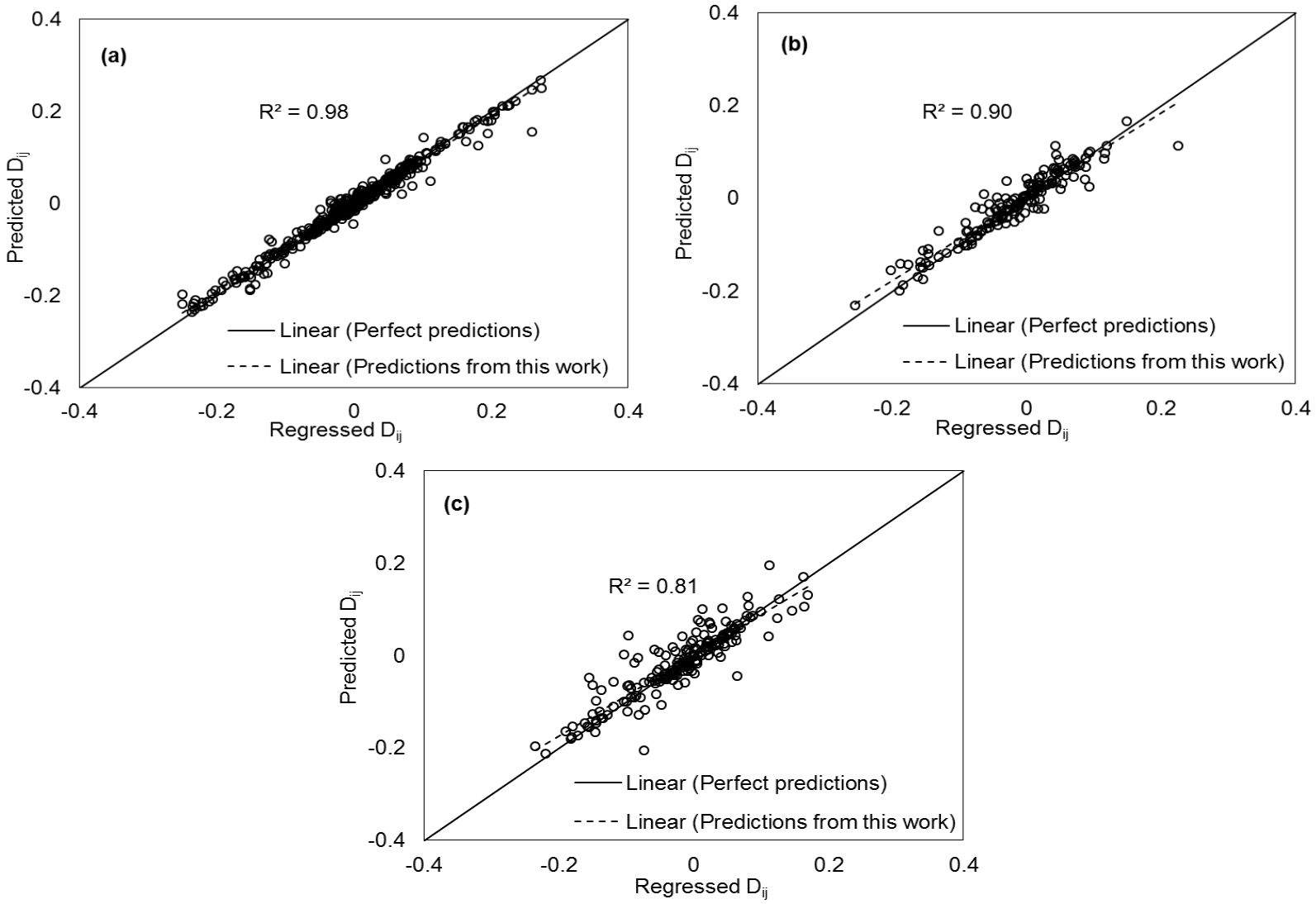

Figure 4.6. Comparison of the Regressed D_{ij} from PR EOS and the Predicted D_{ij} from QSPR Model for Case 3 in (a) Training Set, (b) Validation Set, (c) External Test Set

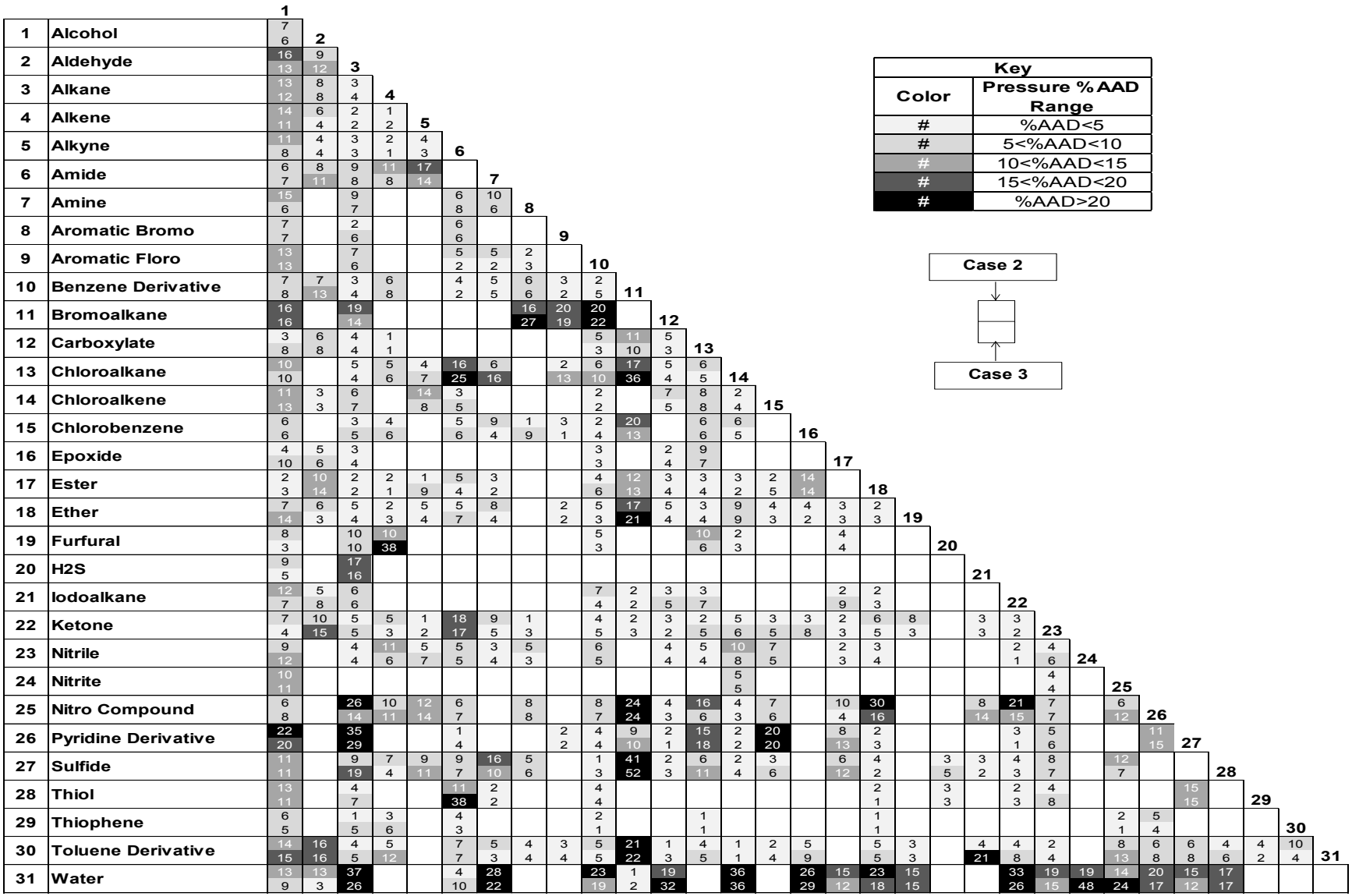

Figure 4.7. PR-QSPR Model Predictions (Cases 2 and 3) of Bubble-point Pressures by Type of Interaction

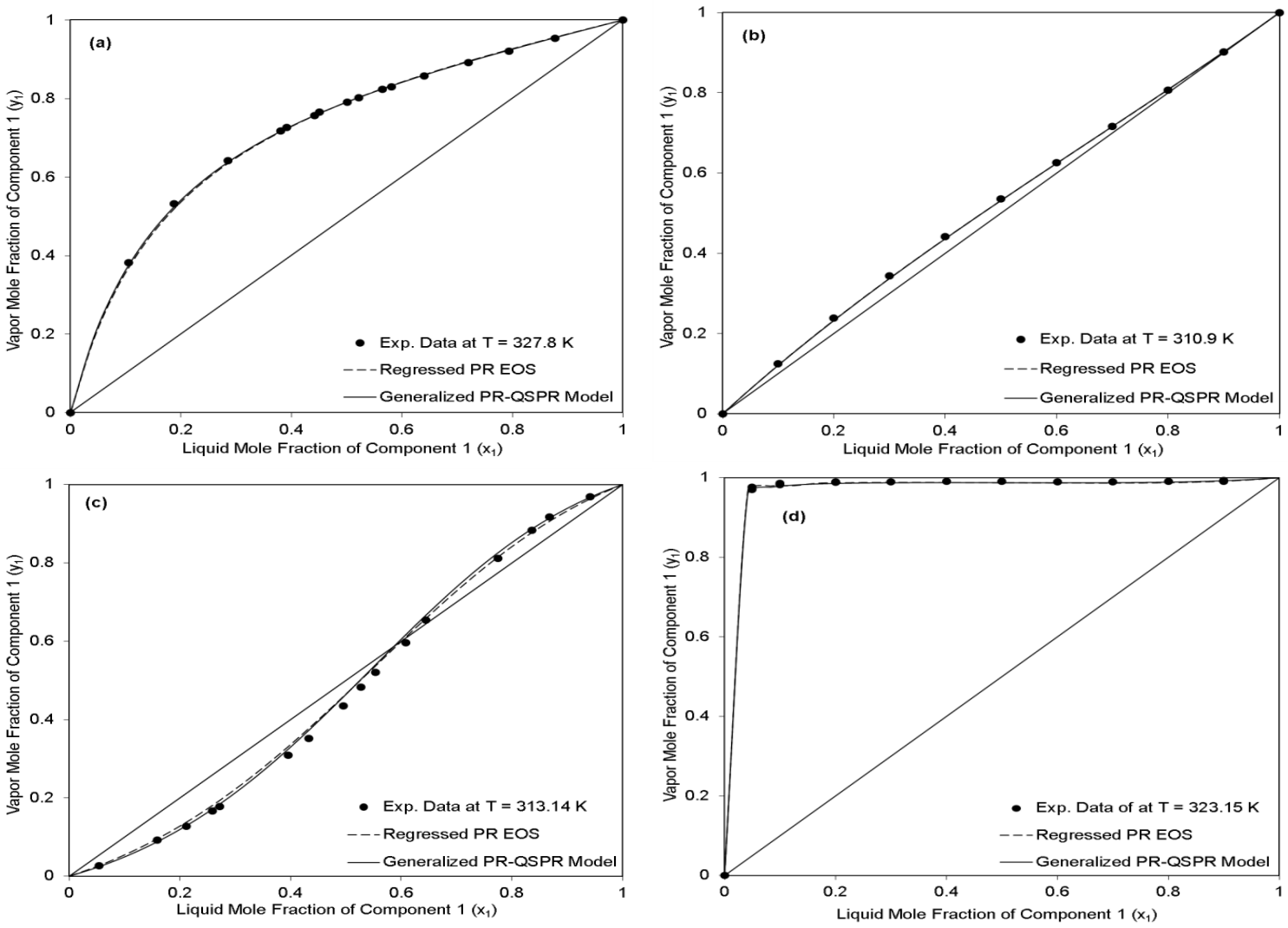

Figure 4.8. PR EOS Representations and PR-QSPR Model Predictions for Case 2 of Equilibrium Phase Compositions for (a) N-Heptane (1) + Ethylbenzene (2), (b) 1,3-Butadiene (1) + Butane (2), (c) Chloroform (1) + Methyl Acetate (2), (d) Isopentane (1) + N,N-Dimethylformide (2) Systems

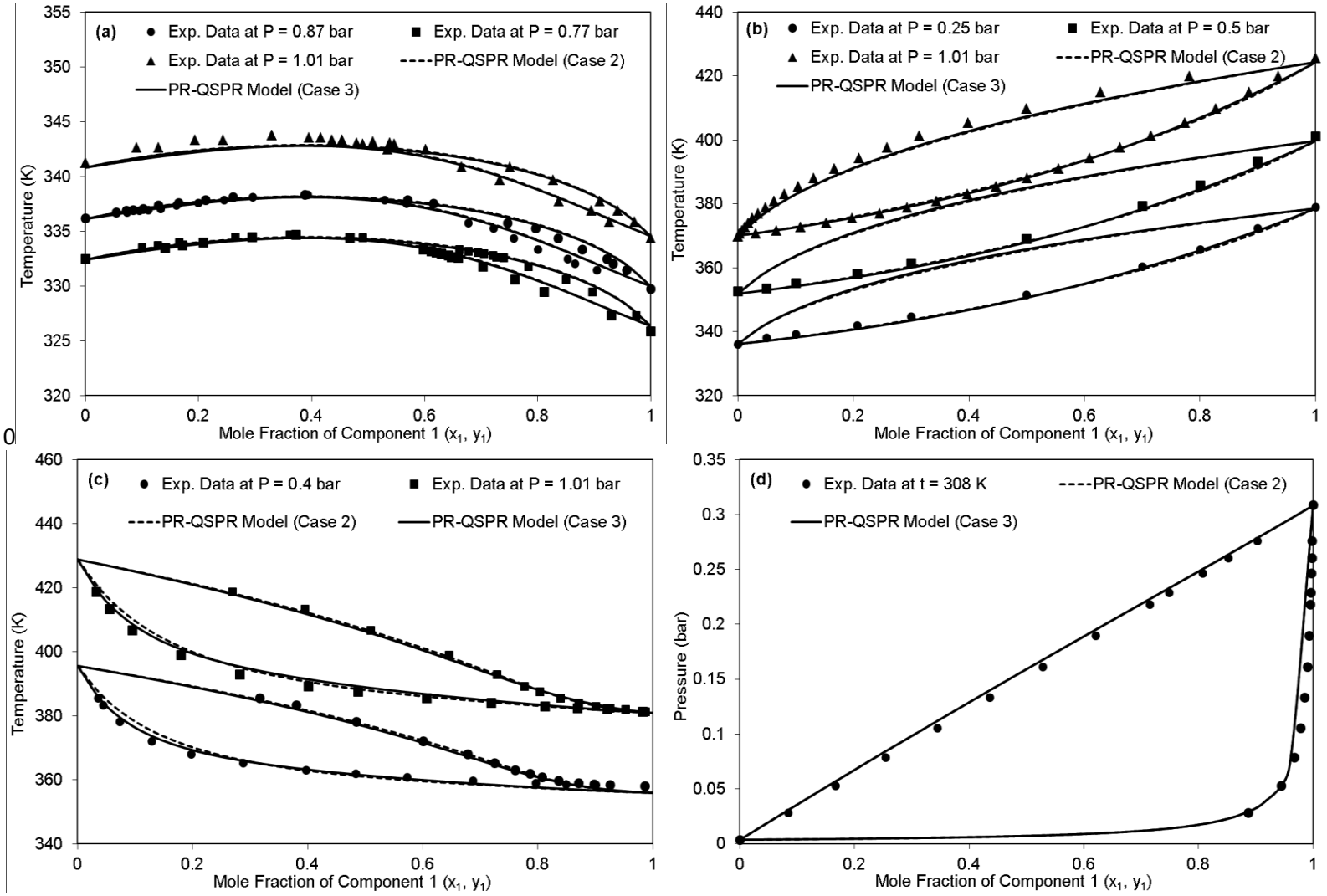

Figure 4.9. Predictions of Vapor-Liquid Equilibrium at Low Pressure Using the PR- QSPR Model for Cases 2 and 3 for (a) Chloroform (1) + Diisopropyl Ether (2), (b) N,N-Dimethylformide (1) + 1-Propanol (2), (c) 2-Methyl 1-Propanol (1) + Bromobenzene (2), (d) Hexane (1) + N-Decane (2) Systems

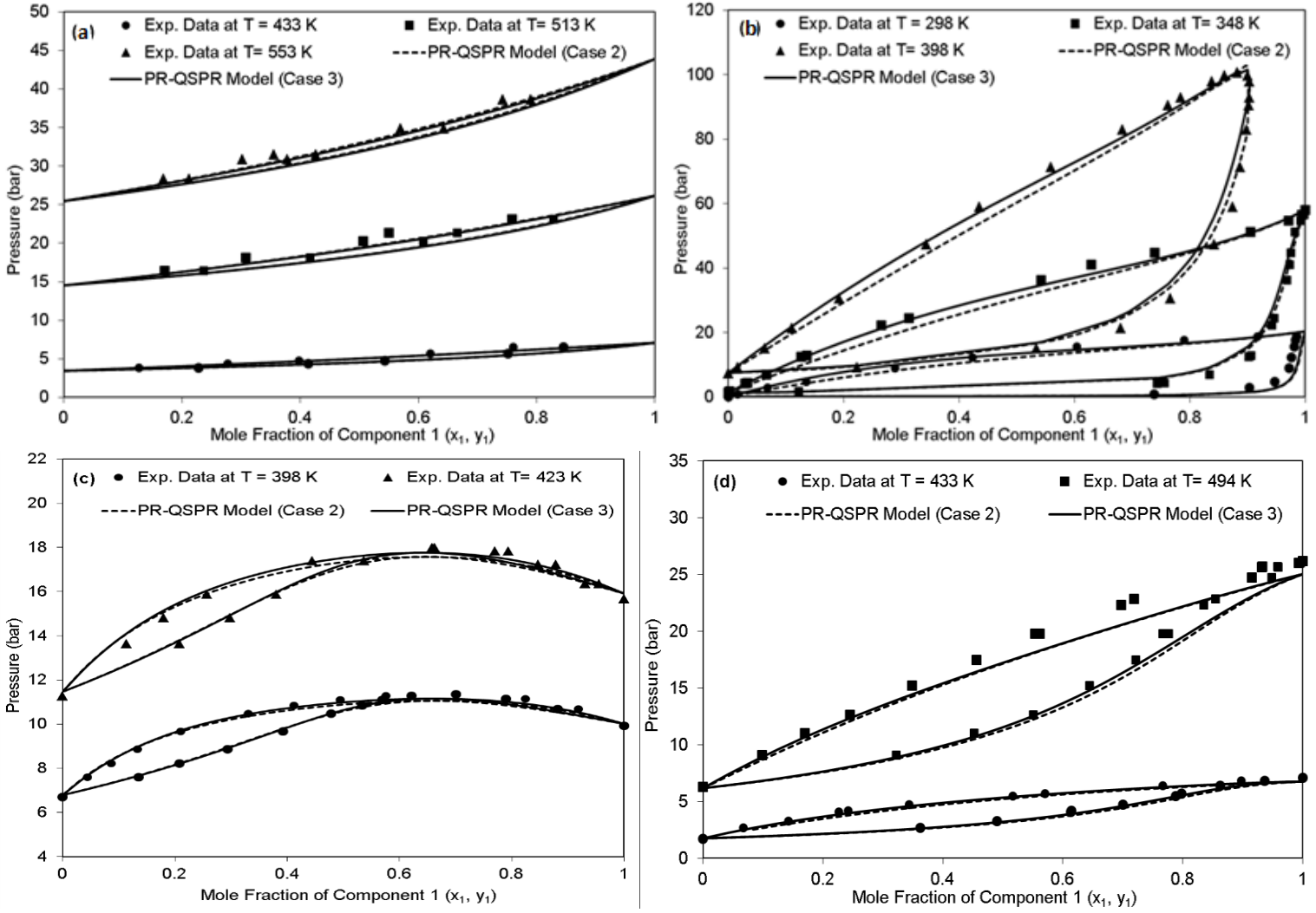

Figure 4.10. Predictions of Vapor-Liquid Equilibrium at High Pressure Using the PR- QSPR Model for Cases 2 and 3 for (a) Benzene (1) + Toluene (2), (b) Hydrogen Sulfide (1) + Methanol (2), (c) Pentane (1) + Acetone (2),(d) 1-Propanol (1) + P-Xylene Systems

REFERENCES

1. S. Zeck, D. Wolf, Requirements of thermodynamic data in the chemical industry, Fluid Phase Equilibria, 82 (1993) 27-38.
2. P.M. Mathias, T.W. Copeman, Extension of the Peng-Robinson equation of state to complex mixtures: Evaluation of the various forms of the local composition concept, Fluid Phase Equilibria, 13 (1983) 91-108.
3. R.A. Heidemann, A.M. Khalil, The calculation of critical points, AIChE Journal, 26 (1980) 769-779.
4. D. Abrams, F. Seneci, P. Chueh, J. Prausnitz, Thermodynamics of multicomponent liquid mixtures containing subcritical and supercritical components, Industrial & Engineering Chemistry Fundamentals, 14 (1975) 52-54.
5. G. Soave, Equilibrium constants from a modified Redlich-Kwong equation of state, Chemical Engineering Science, 27 (1972) 1197-1203.
6. D.Y. Peng, D.B. Robinson, A new two-constant equation of state, Industrial & Engineering Chemistry Fundamentals, 15 (1976) 59-64.
7. G.F. Chou, J.M. Prausnitz, A phenomenological correction to an equation of state for the critical region, AIChE Journal, 35 (1989) 1487-1496.
8. P.M. Mathias, H.C. Klotz, J.M. Prausnitz, Equation-of-state mixing rules for multicomponent mixtures: the problem of invariance, Fluid Phase Equilibria, 67 (1991) 31-44.
9. J. Schwartzentruber, H. Renon, Equations of state: how to reconcile flexible mixing rules, the virial coefficient constraint and the "Michelsen-Kistenmacher syndrome" for multicomponent systems, Fluid Phase Equilibria, 67 (1991) 99-110.

10. S.K. Shibata, S.I. Sandler, Critical evaluation of equation of state mixing rules for the prediction of high-pressure phase equilibria, Industrial and Engineering Chemistry Research, 28 (1989) 1893-1898.

11. P.T. Eubank, G.-S. Shyu, N.S.M. Hanif, New procedures for application of the Wong-Sandler mixing rules to the prediction of vapor-liquid equilibria, Industrial and Engineering Chemistry Research, 34 (1995) 314–323.

12. H. Orbey, S.I. Sandler, Reformulation of Wong-Sandler mixing rule for cubic equations of state, AIChE Journal, 41 (1995) 683-690.

13. C.H. Twu, J.E. Coon, J.R. Cunningham, A new generalized alpha function for a cubic equation of state Part 1. Peng-Robinson equation, Fluid Phase Equilibria, 105 (1995) 49–59.

14. D.S.H. Wong, S.I. Sandler, A theoretically correct mixing rule for cubic equations of state, AIChE Journal, 38 (1992) 671-680.

15. N. Trivedi, M. S. Thesis, in, Oklahoma State University, Stillwater, OK, 1996.

16. A.M. Abudour, S.A. Mohammad, K.A.M. Gasem, Modeling high-pressure phase equilibria of coalbed gases/water mixtures with the Peng–Robinson equation of state, Fluid Phase Equilibria, 319 (2012) 77-89.

17. K.A.M. Gasem, Binary vapor-liquid phase equilibrium for carbon dioxide + heavy normal paraffins (interaction parameters, density predictions, pure hydrocarbon properties), in, Oklahoma State University, United States -- Oklahoma, 1986.

18. K.A.M. Gasem, C.H. Ross, R.L. Robinson, Prediction of ethane and CO_2 solubilities in heavy norma paraffins using generalized-parameter Soave and Peng-Robinson equations of state, The Canadian Journal of Chemical Engineering, 71 (1993) 805-816.

19. W. Gao, R.L. Robinson Jr, K.A.M. Gasem, Alternate equation of state combining rules and interaction parameter generalizations for asymmetric mixtures, Fluid Phase Equilibria, 213 (2003) 19-37.

20. J.-N. Jaubert, F. Mutelet, VLE predictions with the Peng–Robinson equation of state and temperature dependent kij calculated through a group contribution method, Fluid Phase Equilibria, 224 (2004) 285-304.

21. J.-N. Jaubert, S. Vitu, F. Mutelet, J.-P. Corriou, Extension of the PPR78 model (predictive 1978, Peng–Robinson EOS with temperature dependent kij calculated through a group contribution method) to systems containing aromatic compounds, Fluid Phase Equilibria, 237 (2005) 193-211.

22. S. Vitu, J.-N. Jaubert, F. Mutelet, Extension of the PPR78 model (Predictive 1978, Peng–Robinson EOS with temperature dependent kij calculated through a group contribution method) to systems containing naphtenic compounds, Fluid Phase Equilibria, 243 (2006) 9-28.

23. M. Lashkarbolooki, Z.S. Shafipour, A.Z. Hezave, H. Farmani, Use of artificial neural networks for prediction of phase equilibria in the binary system containing carbon dioxide, The Journal of Supercritical Fluids, 75 (2013) 144-151.

24. A.R. Katritzky, L. Mu, M. Karelson, QSPR treatment of the unified nonspecific solvent polarity scale, Journal of Chemical Information and Computer Sciences, 37 (1997) 756-761.

25. A.R. Katritzky, V.S. Lobanov, M. Karelson, Normal boiling points for organic compounds: correlation and prediction by a quantitative structure−property relationship, Journal of Chemical Information and Computer Sciences, 38 (1998) 28-41.

26. M. Goodarzi, T. Chen, M.P. Freitas, QSPR predictions of heat of fusion of organic compounds using Bayesian regularized artificial neural networks, Chemometrics and Intelligent Laboratory Systems, 104 (2010) 260-264.

27. M. Bagheri, K. Yerramsetty, K.A.M. Gasem, B.J. Neely, Molecular modeling of the standard state heat of formation, Energy Conversion and Management, 65 (2013) 587-596.

28. F. Gharagheizi, QSPR studies for solubility parameter by means of genetic algorithm-based multivariate linear regression and generalized regression neural network, QSAR & Combinatorial Science, 27 (2008) 165-170.

29. K.A.M. Gasem, W. Gao, Z. Pan, R.L. Robinson, Jr., A modified temperature dependence for the Peng-Robinson equation of state, Fluid Phase Equilibria, 181 (2001) 113-125.

30. J.M. Prausnitz, R.N. Lichtenthaler, E.G. Azevedo, Molecular thermodynamics of fluid-phase equilibria, 3rd ed., Prentice-Hall, New Jersey, 1999.

31. C. Tsonopoulos, J.L. Heidman, High-pressure vapor-liquid equilibria with cubic equations of state, Fluid Phase Equilibria, 29 (1986) 391–414.

32. S. Golla, S. Madihally, R.L. Robinson Jr, K.A.M. Gasem, Quantitative structure–property relationship modeling of skin sensitization: A quantitative prediction, Toxicology in Vitro, 23 (2009) 454-465.

33. T. SRL, Dragon Professional 6.0.9, in, 2011.

34. A.R. Katritzky, V.L. Lobanov, M. Karelson, Codessa 2.7.8, in, 2007.

35. S. Gebreyohannes, Y. Dadmohammadi, B.J. Neely, K.A.M. Gasem, A comparative study of QSPR generalized activity coefficient model parameters for VLE mixtures, Under review (2014).

36. U.O. J. Gmehling, W. Arlt,, Vapor-liquid equilibrium data collection, chemistry data series, in: DECHEMA (Ed.), Frankfurt, Germany, 1977 - 2001.

37. NIST standard reference database 103b thermodata engine, in: NIST-TDE (Ed.), 2012.

38. Physical and thermodynamic properties of pure chemicals, in: DIPPR Project 801, 2011.

39. J. Gmehling, J. Li, M. Schiller, A modified UNIFAC model. 2. Present parameter matrix and results for different thermodynamic properties, Industrial & Engineering Chemistry Research, 32 (1993) 178-193.

40. K.A.M. Gasem, GEOS, in, Oklahoma State university, Stillwater, OK, 1988-1999.

41. D.W. Marquardt, An algorithm for least-squares estimation of nonlinear parameters, Journal of the Society for Industrial and Applied Mathematics, 11 (1963) 431-441.

42. L.W. Jackson, A comparison of selected gradient methods for solving the nonlinear least squares problem, in: Computing and Information Sciences, Oklahoma State University, Stillwater, OK, 1978.

43. CambridgeSoft, ChemBiooffice 11.0, in, 2008.

44. R. Guha, M.T. Howard, G.R. Hutchison, P. Murray-Rust, H. Rzepa, C. Steinbeck, J. Wegner, E.L. Willighagen, The blue obeliskInteroperability in chemical informatics, Journal of Chemical Information and Modeling, 46 (2006) 991-998.

45. Open Babel Package, in, http://openbabel.sourceforge.net/. 2011.

46. T.A. Halgren, Merck molecular force field. I. Basis, form, scope, parameterization, and performance of MMFF94, Journal of Computational Chemistry, 17 (1996) 490-519.

47. The Open Babel Developers, in: OBConformerSearch Class Reference, http://openbabel.org/dev-api/classOpenBabel11OBConformerSearch.shtml, 2007 (cited 26.07.11).

48. H. Demuth, M. Beale, M. Hagan, Neural Network Toolbox, in, MathWorks, Inc., 2010.

49. L. Prechelt, Automatic early stopping using cross validation: quantifying the criteria, Neural Networks, 11 (1998) 761-767.

50. C. Rich, L. Steve, G. Lee, Overfitting in neural nets: backpropagation, conjugate gradient, and early stopping, in, 2000.

51. M.S. Iyer, R.R. Rhinehart, A method to determine the required number of neural-network training repetitions, Neural Networks, IEEE Transactions on, 10 (1999) 427-432.

52. D. Nguyen, B. Widrow, Improving the learning speed of 2-layer neural networks by choosing initial values of the adaptive weights, in: Proceedings of the International Joint Conference on Neural Networks, 1990, pp. 21–26.

53. K.M. Yerramsetty, Quantitative structure-property relationship modeling & computer-aided molecular designimprovements & applications /by Krishna M. Yerramsetty, in: Chemical Engineering, Oklahoma State University, Stillwater, 2012, pp. 290.

54. D.K. Agrafiotis, W. Cedeño, V.S. Lobanov, On the use of neural network ensembles in QSAR and QSPR, Journal of Chemical Information and Computer Sciences, 42 (2002) 903-911.

55. C. Merkwirth, H. Mauser, T. Schulz-Gasch, O. Roche, M. Stahl, T. Lengauer, Ensemble methods for classification in cheminformatics, Journal of Chemical Information and Computer Sciences, 44 (2004) 1971-1978.

56. A. Tropsha, P. Gramatica, V.K. Gombar, The importance of being earnest: Validation is the absolute essential for successful application and interpretation of QSPR models, QSAR Comb. Sci., 22 (2003) 69-77.

57. E.A. Turek, R. S. Metcalfe, L. Yarborough and R. L. Robinson, Phase equilibria in CO2-multicomponent hydrocarbon systems: experimental data and an improved prediction technique, Society of Petroleum Engineers journal, 24 (1984) 308-324.

58. K.A.M. Gasem, R.L. Robinson Jr., Prediction of phase behavior for CO_2 plus heavy normal paraffins using generalized-parameter Soave and Peng-Robinson equations of state, in: Proceedings of the 1985 AIChE Spring National Meeting and Petro Expo '85, Houston, TX, 1985.

59. P.M. Mathias, A versatile phase equilibrium equation of state, Industrial & Engineering Chemistry Process Design and Development, 22 (1983) 385-391.

60. J.M. Prausnitz, Phase equilibria and fluid properties in the chemical industry, AIChE Proceedings 2nd International Cong, Part 2, (1980) 231.

61. C.-B. Soo, E.E. Ahmar, C. Coquelet, D. Ramjugernath, D. Richon, Vapor–liquid equilibrium measurements and modeling of the n-butane + ethanol system from 323 to 423 K, Fluid Phase Equilibria, 286 (2009) 79-87.

62. K. Hynynen, P. Uusi-Kyyny, J.-P. Pokki, M. Pakkanen, J. Aittamaa, Isothermal vapor liquid equilibrium for 2-methylpropene + methanol, + 1-propanol, + 2-propanol, + 2-butanol, and + 2-methyl-2-propanol binary systems at 364.5 K, Journal of Chemical & Engineering Data, 51 (2006) 562-568.

63. W.B. Kay, R.L. Hoffman, O. Davies, Vapor-liquid equilibrium relations of binary systems n-butane-n-pentane and n-butane-n-hexane, Journal of Chemical & Engineering Data, 20 (1975) 333-338.

64. S.W. Campbell, R.A. Wilsak, G. Thodos, (Vapor + liquid) equilibrium behavior of (n-pentane + ethanol) at 372.7, 397.7, and 422.6 K, The Journal of Chemical Thermodynamics, 19 (1987) 449-460.

65. A.-D. Leu, J.J. Carroll, D.B. Robinson, The equilibrium phase properties of the methanol-hydrogen sulfide binary system, Fluid Phase Equilibria, 72 (1992) 163-172.

66. J. Griswold, D. Andres, V. Klein, Determination of high-pressure vapor-liquid equilibria. The vapor-liquid equilibrium of benzene-toluene, Trans. Am. Inst. Chem. Eng, 39 (1943) 223.

67. Y. Kim, W. Bae, H. Kim, Isothermal vapor−liquid equilibria for the n-pentane + 1-butanol and n-pentane + 2-butanol systems near the critical region of the mixtures, Journal of Chemical & Engineering Data, 50 (2005) 1520-1524.

68. A.N. Shahverdiyev, J.T. Safarov, P-ρ-T and Ps-ρs-Ts properties of methanol + water and n-propanol + water solutions in wide range of state parameters, Physical Chemistry Chemical Physics, 4 (2002) 979-986.

69. P. Sentenac, Y. Bur, E. Rauzy, C. Berro, Density of methanol + water between 250 K and 440 K and up to 40 MPa and vapor−liquid equilibria from 363 K to 440 K, Journal of Chemical & Engineering Data, 43 (1998) 592-600.

70. F. Barr-David, B.F. Dodge, Vapor-liquid equilibrium at high pressures. The systems ethanol-water and 2-propanol-water, Journal of Chemical & Engineering Data, 4 (1959) 107-121.

71. D.S.K. Tsiklis, A. I.; Shenderei, L. I. , Phase equilibria in the system ethanol + ethylene + water at high pressures and temperatures, Khim. Prom-st. (Moscow), No. 5 (1960) 401-406.

72. S.W. Campbell, R.A. Wilsak, G. Thodos, Isothermal vapor-liquid equilibrium measurements for the n-pentane-acetone system at 372.7, 397.7, and 422.6 K, Journal of Chemical & Engineering Data, 31 (1986) 424-430.

73. J.M. Lenoir, H.G. Hipkin, Measured enthalpies for mixtures of benzene with n-pentane, Journal of Chemical & Engineering Data, 17 (1972) 319-323.

74. V.N.K. Rao, D.R. Swami, M.N. Rao, Vapor-liquid equilibria of benzene–n-hexane and benzene-cyclohexane systems, AIChE Journal, 3 (1957) 191-197.

75. M.S. Medani, M.A. Hasan, Thermodynamic properties of the n-hexane and benzene system at elevated temperatures, Journal of Applied Chemistry and Biotechnology, 27 (1977) 80-92.

76. K.L. Butcher, K.R. Ramasubramanian, M.S. Medani, Thermodynamic properties of the benzene and n-heptane system at elevated temperatures, Journal of Applied Chemistry and Biotechnology, 22 (1972) 1139-1155.

77. A. Deák, A.I. Victorov, T.W. de Loos, High pressure VLE in alkanol + alkane mixtures. Experimental results for n-butane + ethanol, +1-propanol, +1-butanol systems and calculations with three EOS methods, Fluid Phase Equilibria, 107 (1995) 277-301.

78. A. Zawisza, J. Vejrosta, High-pressure liquid-vapour equilibria, critical state, and p(V, T, x) up to 573.15 K and 5.066 MPa for (heptane+propan-1-ol), The Journal of Chemical Thermodynamics, 14 (1982) 239-249.

79. J. Oison, Thermodynamics of hydrogen-bonding mixtures 2. G E, H E, andS E of 1-propanol+ n-heptane, International journal of thermophysics, 16 (1995) 215-226.

80. A.-Q. Chen, G.J. Urbanus, K.-C. Chao, A new vapor-liquid equilibrium cell and VLE data for mixtures of 1-propanol+p-xylene, Fluid Phase Equilibria, 94 (1994) 281-288.

81. K.L. Butcher, M.S. Medani, Thermodynamic properties of methanol–benzene mixtures at elevated temperatures, Journal of Applied Chemistry, 18 (1968) 100-107.

82. J.R. Khurma, O. Muthu, S. Munjal, B.D. Smith, Total-pressure vapor-liquid equilibrium data for binary systems of dichloromethane with pentane, acetone, ethyl acetate, methanol, and acetonitrile, Journal of Chemical & Engineering Data, 28 (1983) 412-419.

83. M.S.K. Rozhnov, Phase and volume relationships in the butadiene plus hydrocarbon systems Prom-st. (Moscow), 43 (1967) 48.

84. A.D. Leu, D.B. Robinson, Equilibrium phase properties of the n-butane-hydrogen sulfide and isobutane-hydrogen sulfide binary systems, Journal of Chemical & Engineering Data, 34 (1989) 315-319.

CHAPTER V

VOLUME-TRANSLATED PENG–ROBINSON EQUATION OF STATE FOR SATURATED AND SINGLE-PHASE LIQUID DENSITIES[3]

5.1 Introduction

Cubic equations of state (CEOS) such as Soave-Redlich-Kwong (SRK) [1] and Peng-Robinson (PR) [2] are widely used in the natural gas industry to perform reservoir simulations due to their inherent simplicity and ease of use. However, the predictions for liquid densities from the CEOS are generally inaccurate due to their two-parameter nature. In particular, a two-parameter equation of state yields a constant critical compressibility factor, z_c, for all fluids, and this typically results in significant errors in liquid-phase densities. In fact, actual z_c values for most fluids are smaller than those predicted by most two-parameter CEOS. As a result, the predicted liquid densities from the cubic equations of state differ considerably from their true values, especially in the vicinity of the critical point. To overcome these deficiencies, several three-parameter CEOS have been proposed [3-7]. However, even with the inclusion of a third parameter in the CEOS, the predicted critical compressibility factor is larger than the actual value for several fluids [4, 7-9].

[3] The material in this chapter has been reproduced with permission from A.M. Abudour, S.A. Mohammad, R.L. Robinson Jr., K.A.M. Gasem, Volume-translated Peng–Robinson equation of state for saturated and single-phase liquid densities, Fluid Phase Equilibria, 335 (2012) 74-87.

An alternative approach is to introduce a "volume translation," as first suggested by Martin [10]. The method involves the application of a translation along the volume axis to improve the liquid density predictions without causing any changes in the vapor-liquid equilibrium predictions. Several volume-translation approaches have been proposed, and these range from a constant correction term to more complex forms that are both temperature and density dependent. Peneloux et al. [11] proposed a constant volume correction term for the SRK equation of state that improved liquid density predictions significantly at low reduced temperatures. However, the densities were over-predicted beyond a reduced temperature of about 0.7. Although the temperature-independent methods [10, 11] are the simplest form of volume translation, such constant-value volume corrections are generally insufficient at higher reduced temperatures and as the critical point is approached [12, 13].

Temperature-dependent volume-translation methods have been proposed by several authors [12, 14-19]. Watson et al. [14] used a volume-translation method for the van der Waals (vdW) EOS. Chou and Prausnitz [15] introduced a phenomenological correction to the SRK EOS for volumetric predictions by using a "distance function", d, to account for the differences between the predicted and actual values of densities. To ensure that the phase equilibrium calculations with the SRK EOS remain unaltered, the authors constrained their method to be a function of only temperature. Magoulas and Tassios [16] developed a temperature-dependent volume correction to the vdW and PR EOS for n-alkanes ranging from C_1 to C_{20}. Ungerer et al. [12, 20, 21] developed a volume-translation correction for the PR EOS and correlated the volume-translation parameter as a function of molecular weight. Tsai and Chen [17] used the PR EOS to calculate pure-fluid vapor pressures and saturated densities by introducing two additional parameters. Ahlers and Gmehling [18] and Lin and Duan [19] also presented temperature-dependent volume translations to the PR EOS and obtained improved liquid density predictions for non-polar and slightly polar fluids.

Although temperature-dependent volume-translation methods provide improved saturated liquid density predictions, these methods do not perform as well in the single-phase, compressed liquid region [22, 23]. Further, the use of a temperature-dependent volume-translation function with a cubic EOS can lead to thermodynamic inconsistencies such as isotherm cross-overs [22-25] and negative isochoric heat capacities, C_V, at high pressures [24-26] in the compressed liquid region.

Recently, Baled et al. [22] proposed a temperature-dependent volume correction to the SRK and PR EOS for predicting densities at very high temperatures and pressures. In a departure from other studies, the authors developed their volume-translation term based on single-phase densities alone at high pressures rather than the saturated liquid densities. The method provided improved density predictions in the single-phase region; however, the model showed relatively larger errors in the saturation region.

Volume-translation methods that are both temperature and density dependent have also been investigated by some authors. Mathias et al. [27] proposed a density-dependent volume correction term to the PR EOS, which was formally similar to that of Chou and Prausnitz [15]. The model developed by Mathias et al. [27] contains one adjustable parameter, which is unique to each compound. Kutney et al. [28] applied the volume-translation method to the hard-sphere van der Waals EOS for supercritical process modeling. Laugier et al. [29] applied volume correction to cubic equations of state and correlated liquid densities directly through the use of neural networks. Recently, Frey et al. [30] developed a density- and temperature-dependent volume translation for the SRK EOS. In their method, all derived properties such as the fugacity and enthalpy are calculated using a translated SRK EOS. However, even with the increased complexity, the method has been shown to provide only modest improvement of the SRK EOS at high temperatures and pressures [23].

The discussion above indicates that most volume-translation methods available in the literature have been developed either for the saturated or the single-phase region. Thus, there is a need for a volume-translation method that can provide accurate and reliable predictions for *both* saturated and single-phase liquid densities under high temperatures and pressures. Therefore, in this work, a volume-translation method is presented that can be used to obtain reliable predictions of liquid densities in both saturated and single-phase regions. As will be shown later, the method is capable of accurate predictions of liquid densities of a diverse class of molecules based solely on readily-available molecular properties (e.g., critical compressibility factor, acentric factor, dipole moment). The proposed method contains only one fluid-specific parameter that has been generalized in terms of the three molecular properties mentioned above.

The present work was motivated initially by our desire to provide accurate liquid densities for major coalbed gases (methane, nitrogen and carbon dioxide) and water. The encouraging results observed for these fluids led us to expand the scope of this work and *generalize* the method so that it would be applicable to a wider variety of compounds, including non-polar, strongly polar and asymmetric molecules. The remainder of this paper is organized as follows: Section 5.2 presents the volume-translation method developed in this work, Section 5.3 presents details of the database employed and the methods used to generalize the model and Section 5.4 discusses the results obtained for saturated and single-phase densities and includes validation results of the generalized model.

5.2 Volume-Translated Peng-Robinson Equation-of-State (VTPR EOS)

The original Peng-Robinson equation-of-state PR EOS [2] is given as

$$p = \frac{RT}{v-b} - \frac{a(T)}{v(v+b)+b(v-b)} \tag{5.1}$$

where

$$a(T) = \frac{0.457535\alpha(T)R^2T_c^2}{p_c^2} \tag{5.2}$$

$$b = \frac{0.077796RT_c}{p_c} \tag{5.3}$$

where p is the pressure, T is the temperature, v is the molar volume, a and b are EOS parameters, T_c is the critical temperature, P_c is the critical pressure and R is the universal gas constant. The term α(T) in Equation (5.2) was calculated with the following expression developed in an earlier work [31]:

$$\alpha(T) = \exp\left(\left(A + BT_r\right)\left(1 - T_r^{C+D\omega+E\omega^2}\right)\right) \tag{5.4}$$

where ω is the acentric factor, T_r is the reduced temperature and A through E are correlation parameters with values of 2.0, 0.836, 0.134, 0.508 and -0.0467, respectively.

A general volume-translation term for the equation of state can be represented as

$$v_{VTPR} = v_{PR} + c \tag{5.5}$$

where v_{VTPR} and v_{PR} are the translated and untranslated molar volumes and c is the volume-translation term.

Since the difference between the untranslated and the true volume increases as the critical point is approached, a "distance" function approach as suggested by Chou and Prausnitz [15] and Mathias et al. [27] was adopted in this work. Thus, the volume translation is dependent on the distance (or difference) between the critical point and a point on the pressure-density isotherm [15]. The dimensionless distance function, d, is given as [15]

$$d = \frac{1}{RT_c}\left(\frac{\partial p^{PR}}{\partial \rho}\right)_T \tag{5.6}$$

where T_c is the experimental critical temperature and ρ is the molar density. The distance function, d, is calculated from the untranslated PR EOS to avoid iterative solutions.

The distance function given by Equation (5.6) is constrained to be only temperature-dependent in the saturated region, i.e. the function is evaluated at the liquid phase conditions for translating both saturated liquid and vapor densities. As discussed elsewhere [11, 15], this ensures that the vapor pressures predicted by the original equation of state are preserved.

In this work, the partial derivative appearing in Equation (5.6) was always evaluated using the original (untranslated) PR EOS at the appropriate phase conditions. In the saturated (two-phase) region, the partial derivative was evaluated by using the untranslated saturated liquid density at the appropriate saturation temperature. In the single-phase regions of the phase diagram, the partial derivative was evaluated by using the untranslated density at the appropriate temperature and pressure for each point. Thus, in all cases, the distance function given by Equation (5.6) was evaluated in a consistent manner by conforming to the thermodynamic degrees of freedom given by the Gibb's phase rule. As will be shown in Section 5.3.4, this also ensures that the method presented here does not lead to inconsistencies that were observed previously for some of the volume-translation methods in the literature [22-25].

The volume-translation function is defined as [15]

$$v_{VTPR} = v_{PR} + c - \delta_c\left(\frac{0.35}{0.35 + d}\right) \tag{5.7}$$

In Equation (5.7), 0.35 is a universal constant for all fluids and δ_c is the volume correction at the critical temperature and is given as

$$\delta_c = \left(\frac{RT_c}{p_c}\right)\left(z_c^{EOS} - z_c^{exp}\right) \tag{5.8}$$

where T_c, P_c and z_c^{exp} are the experimental critical temperature, pressure and compressibility factor, respectively. Further, z_c^{EOS} has a universal value of 0.3074 for PR EOS.

A new expression was developed in this work for the volume-translation term, c, appearing in Equation (5.7). The expression is given as

$$c = \left(\frac{RT_c}{p_c}\right)\left(c_1 - (0.004 + c_1)\exp(-2d)\right) \tag{5.9}$$

where c_1 a constant, fluid-dependent parameter and d is the distance function given by Equation (5.6). As such, the volume translation developed in this work contains only one fluid-specific parameter, c_1, which was obtained by regressing data for saturated liquid densities of pure fluids.

5.2.1 Pure-Fluid Equation-of-State Parameters and Database Employed

The values of critical temperature, critical pressure, acentric factor, critical compressibility factor for each fluid constitute the necessary model input variables for the VTPR EOS. Further, the dipole moment of each fluid is an additional input variable for the generalized model. Table 5.1 presents the values of these properties, along with data sources for saturated liquid densities of the 65 fluids utilized in this work. Of these fluids, the data for 56 were taken from the National Institute of Standards and Technology [32] and the remaining nine were from the DIPPR database [33] and Frenkel et al. [34].

As shown in Table 5.1, the database includes several classes of chemical compounds. These include n-alkanes (e.g., propane and n-hexane), alkenes (e.g., ethylene), alcohols (e.g., methanol and propanol), ketones (e.g., acetone), aromatic (e.g., benzene and toluene), cyclic compounds (e.g. cyclohexane), long-chain hydrocarbons (e.g., eicosane), refrigerants (e.g., difluoromethane and chlorodifluoromethane), inorganic gases (e.g., N_2, O_2 and Ar), strongly polar molecules (e.g., ammonia, water) and several other classes. Overall, the compounds in the database cover a wide

range in terms of their structure, size, chain length, asymmetry and polarity and thus, are well suited to test the efficacy of our approach.

5.2.2 Data Reduction

The volume-translation parameter, c_1, was regressed for each fluid using the database discussed above. The regressions were performed using an objective function, OF, which minimizes the average absolute percentage deviation (%AAD) in saturated liquid densities, as given below:

$$OF = \%\,AAD = \frac{100}{NDP}\sum_{i=1}^{N}\left|\frac{\rho_L^{cal} - \rho_L^{exp}}{\rho_L^{exp}}\right|_i \tag{5.10}$$

where NDP is the number of data points and ρ_L^{cal} and ρ_L^{exp} are the calculated and the experimental saturated liquid densities, respectively. The resultant optimum c_1 parameters appear in Table 5.1.

5.2.3 Case Studies and Generalization Methodology

Our GEOS program [35] was used to calculate the saturated liquid densities of pure fluids. As indicated by Equation (5.9), the volume-translation term contains only one fluid-dependent parameter, c_1. The c_1 parameters were generalized in terms of molecular properties of each fluid. Typical examples for molecular properties that could be useful for this purpose include the acentric factor [36] and a polarity factor [37]. Ideally, the molecular properties used for generalization should account for the size, shape and polarity.

In this work, three specific cases were investigated to develop generalized models for the fluid-dependent parameter, c_1, as listed in Table 5.2. In Case 1, c_1 was generalized as a linear function of the critical compressibility factor, z_c. In Cases 2 and 3, neural network (NN) models were developed to predict c_1 from molecular descriptors or properties found to be significant for this purpose. In case 2, three molecular descriptors, including z_c, were used, In Case 3, c_1 was

generalized using six molecular descriptors, with z_c excluded from the pool of descriptors. The rationale behind these cases was to investigate systematically the effect of size, shape and polarity on parameter c_1. Since z_c for some fluids may not be available experimentally, the generalization in Case 3 was performed by excluding z_c as one of the molecular descriptors. In this manner, one linear and two non-linear generalized models were developed for additional analysis.

As mentioned above, neural network models were developed in Cases 2 and 3, which use molecular descriptors as input. In previous works, we have performed several studies for molecular modeling of thermophysical properties using a combination of molecular descriptors, genetic algorithms and neural networks [38-40]. These studies used the quantitative-structure-property-relationship (QSPR) modeling methodology to investigate the relation between molecular structure and thermophysical properties. The method involves generating (a) two- and three-dimensional molecular structures, (b) minimizing the energy of the three-dimensional structures, (c) calculating descriptors for each molecule using the optimized geometry/structure of each molecule, (d) searching for the most significant set of descriptors and (e) developing predictive models based on the set of descriptors that were found to be significant for the property being modeled. Our earlier studies [39, 41] provide details of each of these steps and, therefore, these aspects are not repeated here. In the following paragraphs, a brief overview is provided for each of the steps involved in molecular modeling.

For each molecule used in this study, two-dimensional (2-D) molecular structures were generated using ChemDraw Ultra 11.0 [42]. Each 2-D structure was then used to generate three-dimensional (3-D) structures. The 2-D structure can lead to several conformations of 3-D structure; however, only the 3-D conformation with the lowest energy is the stable state of the molecule. Thus, the molecular energy of the 3-D conformations was minimized by using the OpenBabel genetic algorithm-based (GA) conformal search [43, 44] that employs the MMFF94 force field method [45]. Details on the GA-based conformal search are summarized in the

OpenBabel documentation [46]. The optimized molecular structures were then used to calculate molecular descriptors for each molecule by using DRAGON software [47]. In particular, DRAGON 5.5 version was used that is capable of calculating up to 3000 descriptors for each molecule. In this manner, a large pool of descriptors is generated for each molecule. Typically, however, only a few of these descriptors are significant in describing a specific property under investigation. Therefore, descriptor reduction methodologies are used to find the most significant descriptors.

In the current work, a sequential regression analysis [41] was used to identify the most significant descriptors for describing the volume-translation parameter, c_1. The sequential regression analysis identified three to six descriptors as significant in describing the parameter c_1. The descriptors identified in this step were then used to construct the neural network models. The details of the neural network algorithm are also available in a previous work [41]. Briefly, multilayer neural networks were developed that utilized the back-propagation algorithm for training the network [48]. The feed-forward neural network model searches for the optimal network performance by varying the number of hidden neurons in the network. Further, the number of neurons was constrained such that the degrees of freedom (ratio of the number of network parameters to the number of data points) ratio remains greater than 2.0. The input dataset was randomly divided into training and cross-validation sets that contained 70% and 30% of the data, respectively. The model was trained on the training set alone and the error for the cross-validation set was monitored during the training process. During initial phases of the network training, the error on both the training and cross-validation sets decrease; however, when the network begins to over-fit the data, the error for the cross-validation set begins to increase. The network training was stopped after a fixed number of iterations in which the error on the cross-validation set increased continuously, and the network parameters at the minimum of the cross-validation error were retained. Further, to ensure optimal network training and avoid local minima, multiple

randomizations of the data and initializations of the initial network parameters (weights and biases) were used [49]. The Nguyen-Widrow algorithm [50] was used to initialize weights and biases, which were updated using a Levenberg-Marquardt optimization technique [48].

5.2.4 Volume-translation Methods from the Literature Used for Comparison

Predictions from our VTPR EOS are compared with three different temperature-dependent volume-translation methods for the PR EOS from the recent literature, as well as with the original PR and SRK EOS. The volume-translation methods from the literature used for comparison include those by Tsai and Chen [17], Ahlers and Gmehling [18] and Lin and Duan [19]. The volume translation proposed by Tsai and Chen [17] contains three parameters. One of these parameters is unique for each compound and the other two parameters are functions of acentric factor. The volume-translation function developed by Ahlers and Gmehling [18] includes three parameters that are functions of critical compressibility factor. The method of Lin and Duan [19] includes two parameters that are functions of critical compressibility factor. The method proposed in this work includes only one parameter that is dependent on the fluid, and the parameter was generalized in terms of critical compressibility factor, acentric factor and dipole moment.

Since the volume-translation methods from the literature were optimized on different databases, a comparison of their respective optimized models may not be very meaningful. Therefore, only the generalized models from different investigators will be compared with the generalized model developed in this work.

5.3 Results and Discussion

5.3.1 VTPR EOS Predictions for Saturated Liquid Densities

Table 5.1 lists the values of the fluid-dependent volume-translation parameter, c_1, for 65 fluids. Each parameter was obtained by regression of saturated liquid density data for the fluid with

which it is associated in the table. Table 5.2 presents the results obtained for the predictions of saturated liquid densities of the 65 fluids. The table lists each fluid, the range of reduced temperatures for each fluid used in the study, the number of data points (NDP) and the average percentage absolute deviation for the different methods. Overall, the VTPR EOS developed in this work is capable of representing saturated liquid densities of diverse classes of molecules with an overall %AAD of 0.6.

The largest %AAD of 1.49 was obtained for acetone and the smallest %AAD of 0.22 was obtained for carbon dioxide. As shown in Table 5.2, most refrigerants and alcohols have %AADs of less than 1.0. Further, the VTPR EOS provided %AADs of 1.16 and 0.91, respectively, for water and ammonia, which are highly polar. The cyclic compounds such as cyclopropane and cyclohexane had %AADs of 0.23 and 0.44, respectively. The predictions for aromatic compounds such as benzene and toluene showed %AADs of 0.68 and 0.53. The VTPR EOS provided %AADs of 0.87 and 1.17 for large chain compounds such as dodecane and eicosane, respectively.

Along with the results obtained in this work, Table 5.2 lists the %AADs obtained for the original PR and SRK EOS. The original PR and SRK EOS provided about 7 and 12% AADs, respectively, for these fluids, as shown in Table 5.2. The PR EOS is known to provide slightly better liquid density predictions for most fluids since the z_c for the PR EOS (0.3074) is closer to many fluids than the z_c for SRK EOS (0.3333).

5.3.2 Generalization of the VTPR EOS

The regressed values for c_1 parameter were then generalized in terms of molecular properties. Three different case studies were constructed for the generalization. In Case 1, the c_1 parameter was generalized in terms of the critical compressibility factor of each fluid, z_c. The generalized relation developed in Case 1 is given as:

$$c_1 = 0.4266\ z_c - 0.1101 \tag{5.11}$$

Table 5.2 presents the generalization results obtained in Case 1. The generalized model from Case 1 yielded predictions with an overall %AAD of 1.0 for 65 fluids. Figure 5.1 presents the generalized (linear) relation between z_c and c_1. The range of z_c values for the fluids was about 0.22 to 0.29, as evident from Figure 5.1. Tsai and Chen [17], Ahlers and Gmehling [18] and Lin and Duan [19] also generalized their volume-translation functions. Their generalized methods provided %AADs ranging from 1.6 to 3% for the database of this study, as shown in Table 5.2.

Case 1 of the VTPR EOS and the methods of Ahlers and Gmehling [18] and Lin and Duan [19] utilized the critical compressibility factor, z_c, for parameter generalization. The insufficiency of this parameter to fully characterize variations in molecular structure of polar fluids has been documented in the past by several investigators [36, 51-53], and attempts have been made to overcome such shortcomings. For more complex fluids, such as molecules with strong dipole moments and/or non-spherical force fields, at least one additional molecular parameter is necessary to account accurately for polar forces and asymmetry [54]. The traditional approach has been to utilize the acentric factor, ω, to account for the asymmetry due to its availability and the fact that it can be easily calculated from experimental data [36]. Other molecular characteristics, such as the dipole moment, can also be added to help in delineating the polarity effects of molecules.

In Cases 2 and 3, neural-network models were developed for generalizing c_1. Cases 2 and 3 provide a test of the value of including additional molecular properties to account for varied molecular structure, size and polarity. Several descriptors delineating the effects of molecular asymmetry, size, shape, charge, polarity and association were considered. Table 5.3 lists the case studies and the molecular properties or descriptors used in Cases 2 and 3. The descriptors found to be significant in Case 2 relate to either the asymmetry or the polarity of the molecule. Table 5.4

lists the structural descriptors for the molecules that were observed to be significant in Case 3. These descriptors relate to either the geometrical or topological characteristics of the molecule; additional information on these descriptors may be found in the documentation of DRAGON [55]. Figures 5.2 and 5.3 present the comparison of regressed and generalized values of c_1 parameter obtained in Cases 2 and 3, respectively. The figures depict the predictions for c_1 parameter for the fluids belonging to the training and cross-validation sets during the neural network training. Further, the legend entry "external set" refers to the set of 20 fluids used for external validation of the generalized model, as described in Section 5.3.3.

Although the overall %AADs for Cases 2 and 3 (0.8%) are comparable to Case 1 (1.1%), a closer inspection of the results reveals that Cases 2 and 3 provides improvement in the predictions for several polar and asymmetric compounds. For example, the %AAD for water (which is strongly polar) was about 1.2% for Cases 2 and 3, whereas Case 1 yielded a %AAD of 2% and the three literature methods listed in Table 5.2 produced %AADs ranging from 4 to 7 for water.

In summary, the generalized models presented in this work provide predictions comparable to direct optimizations for the saturated liquid densities. Specifically, the overall %AADs were 1.0, 0.8 and 0.8 for Cases 1, 2 and 3, respectively, which was lower than the deviations obtained from other literature methods listed in Table 5.2. Note that one of the parameters in the volume translation presented by Tsai and Chen [17] has a unique value for each fluid. Since this parameter was not generalized, some fluids listed in Table 5.2 could not be calculated using their method. Since the database contained much more data for non-polar compounds than polar compounds, the overall results of Ahlers and Gmehling [18] and Lin and Duan [19] methods were reasonable with overall %AADs of less than 2. However, closer inspection of Table 5.4 reveals that polar fluids such as water and alcohols showed significant deviations in these methods. Nonetheless, we note here that the literature methods used for comparison to this work were optimized and then subsequently generalized by the respective authors [17-19] using slightly

different databases than that used in the current work. As such, the predictions from their generalized methods used for comparison can be expected to be less optimal for the database used in this work. These comparisons are provided here only as a guide to the accuracy of the methods when applied to the fluids in our database.

5.3.3 Validation of the VTPR EOS

To validate the VTPR EOS model developed in this work, predictions were obtained for an additional data set of 20 fluids that included both polar and non-polar compounds. These compounds were not used in the generalized model development and thus, they provide a valuable test of the generalization performed in this work.

Table 5.5 lists these 20 fluids, their physical properties and the sources of the data. Table 5.6 presents the predictions obtained for these fluids for Cases 1-3. As shown in the table, the overall %AADs for these compounds range from 1-1.2 for Cases 1-3, which is only slightly larger than the deviations obtained for the fluids that were used in model development (Table 5.2). Further, the errors obtained were lower than other volume-translation methods listed in Table 5.6. As expected, the original PR and SRK EOS predictions produce large deviations for these fluids and the results are listed in Table 5.6 for comparison.

For polar fluids, considerable improvement over other methods was observed. For example, the saturated liquid densities of deuterium oxide (a polar compound) were predicted with %AAD of 0.82 (Case 2), whereas the deviations for this compound were much larger from other methods. In particular, the predictions had errors of 3.2% for the method presented in [18] and 7.8% for the method presented in [19]. The generalized VTPR model provided accurate predictions for several heavy hydrocarbons. The %AAD for octadecane was 1.2 for Case 2 and the corresponding statistics for the methods proposed in [18] and [19] were 3.98% and 4.26%, respectively. The improved results obtained in Case 2 for several polar and asymmetric molecules can be related to

the inclusion of acentric factor and dipole moment in describing the volume-translation parameter, c_1.

Figures 5.4-5.8 illustrate the distribution of errors in the predicted saturated liquid densities as a function of reduced temperature, based on Case 2. Figures 5.4 and 5.5 present the deviations for carbon dioxide and methane, respectively. Figures 5.6-5.8 present the error distributions for water, difluoromethane and octadecane, respectively. The predictions were comparable among different volume translation methods for methane (non-polar) and carbon dioxide (slightly polar). However, the predictions from VTPR EOS were considerably better for water and difluoromethane (polar fluids), as shown in Figures 5.7 and 5.8.

As evident from the discussion above, all three cases provided comparable predictions. However, Cases 2 and 3 were generally superior to Case 1 for polar and asymmetric fluids. When a combination of accuracy, simplicity and ease of use is considered, however, Case 2 appears to be the best choice since it provides accurate predictions based *solely* on readily-available molecular descriptors or properties; namely, critical compressibility factor, acentric factor and dipole moment. Apart from providing the least overall errors, the predictions from Case 2 also yielded a better distribution of errors among non-polar, polar and asymmetric compounds.

5.3.4 VTPR EOS Predictions for Single-Phase Liquid Densities

Most volume-translation methods are developed for the prediction of saturated liquid densities and they can provide reasonable liquid densities in the saturation region. When the same methods are used to predict liquid densities in the single-phase region, however, larger errors are observed. Further, most of the existing temperature-dependent volume-translation methods exhibit thermodynamic inconsistencies in the single-phase, compressed liquid region [24, 56]. In

particular, the methods lead to physically unrealistic isotherm cross-overs [22-25] and negative isochoric heat capacities in the compressed-liquid region at higher pressures [24-26]. Figures 5.9(a)-(c) illustrate the problem of isotherm cross-overs when different temperature-dependent volume-translation methods are used to predict densities in the compressed liquid region. As shown in these figures, the method developed by Tsai and Chen [17] predicts a cross-over of isotherms (273 K and 298 K) for carbon dioxide at about 500 bar, whereas the methods presented by Ahlers and Gmehling [18] and Lin and Duan [19] both predicted a cross-over at about 150 bar for the same set of isotherms. The original PR and SRK EOS do not predict isotherm cross-overs; however, the predictions contain large errors, as shown in Figures 5.10(a) and (b). In particular, the predicted densities show increasing deviation from the experimental data with an increase in pressure for both EOS.

The volume-translation method presented in this work does not lead to thermodynamic inconsistencies discussed above. To demonstrate this, Figure 5.11 presents the single-phase liquid density predictions obtained for carbon dioxide with the VTPR EOS developed in this work. As evident from the figure, the predictions do not lead to isotherm cross-overs or other inconsistencies. Further, the density predictions were reasonably accurate up to high pressures (2000 bar). The VTPR EOS predictions in the single-phase, compressed liquid region were tested at different temperatures for several of the fluids listed in Table 5.7 and no isotherm cross-overs were observed in any of the predictions up to pressures of 2000 bar. For brevity, these predictions are not reproduced here graphically.

Table 5.7 presents the predictions for compressed liquid densities for ten representative fluids. As shown in the table, the overall %AAD for these predictions was about 1.8 using Case 2 of the VTPR EOS. In comparison, the predictions with other volume-translation methods had deviations ranging between 6 to 7% for the same data set. Note

that these literature volume translation methods were developed for the saturated liquid densities and, as such, may not perform optimally for the single-phase liquid densities. For the same data set, the original PR and SRK EOS predictions for single-phase liquid densities contained errors of 11 to 14%.

Figures 5.12 to 5.15 present the distribution of errors in the compressed liquid density predictions as a function of reduced pressures for carbon dioxide, methane, pentane and water, respectively. The figures compare the results obtained with the VTPR EOS with several other volume-translation functions for the PR EOS as well as the original PR and SRK EOS. The three temperature-dependent volume-translation methods from the literature used for comparison showed large deviations from the experimental data at pressures higher than 100 bar for carbon dioxide, methane and pentane. Interestingly, the predictions obtained from the methods proposed by Tsai and Chen [17] and Ahlers and Gmehling [18] were closer to those from the VTPR EOS for water in the single-phase region, albeit with slightly larger errors, as shown in Table 5.7. Further, the saturated liquid density predictions for water from these two literature methods yielded higher errors especially in the critical region, as evident from Figure 5.6.

5.3.5 Phase Equilibrium Calculations for Pure Fluids with the VTPR EOS

As described above, the VTPR EOS was used to perform phase equilibrium calculations of pure fluids, including liquid and vapor phase densities in the saturation region. Further, the liquid and vapor densities in the single-phase region were also predicted for a representative set of fluids. Figures 5.16(a)-(c) present the results of these calculations for carbon dioxide, methane and water, respectively. As evident from these figures, the volume-translation method provides reasonably accurate predictions for the phase densities for these fluids. As mentioned earlier, the volume translation

presented in this work predicts vapor pressures that are unaltered from the original PR EOS. As such, the VTPR EOS may be used for both volumetric and phase equilibrium predictions of pure fluids.

The continuity and transition of the isotherm through the spinodal and unstable regions given by the VTPR EOS was also investigated. Figure 5.17 presents a representative isotherm for carbon dioxide at 5°C in the saturated region. The figure was generated by calculating the spinodal limits of the isotherm, the stable volume roots on the binodal or coexistence curve and several intermediate points along the isotherm. The figure shows both the stable volume roots on the coexistence curve and the spinodal limits for this isotherm. As shown in the figure, the VTPR EOS predictions did not exhibit any inconsistencies, unlike those that have been highlighted elsewhere [30]. For comparison, Figure 5.17 also illustrates the same isotherm for the original PR EOS.

Finally, we note that the method presented in this work may be extended to predict densities of liquid *mixtures* by using appropriate mixing rules. Preliminary results on a select group of mixtures appear to be promising. Additional development and refinement of the method when applied to mixtures is underway currently and would be part of a future publication.

In summary, the aim of this work was to develop a new volume translation method for the Peng-Robinson cubic equation and state (PR EOS). This work has addressed two major shortcomings of most existing volume translation methods for the PR EOS. The existing methods (a) were accurate either in the saturated region or in the single-phase region but not both and (b) most temperature-dependent methods produced isotherm-cross overs and other thermodynamic inconsistencies in the single-phase region at high

pressures. The method presented in this work has resolved both these inconsistencies and/or drawbacks of existing methods.

The scope of this work was to develop a robust volume translation method for the PR EOS. The method was intended for use in petroleum reservoir simulations, wherein the cubic equations of state are virtually indispensable due to their computational efficiency and speed. Other approaches such as the molecular-based equations of state may be used for general thermodynamic property predictions. Specific examples include the Statistical Associated Fluid Theory (SAFT) EOS [57, 58] and its extensions [59, 60]. However, these approaches have not been widely used in reservoir simulations due to their computational requirements, which can be prohibitive for such work. As such, the work presented here is specifically designed to be both accurate and computationally-efficient for practical applications in reservoir simulations.

5.4 Conclusions

A volume-translation method was presented for predicting pure-fluid liquid densities in the saturated and the single-phase region. The method consisted of only one fluid-specific parameter, which was generalized in terms of molecular properties such as critical compressibility factor, acentric factor and dipole moment. Three distinct cases were considered for generalization. They ranged from using linear correlations in terms of critical compressibility factor to the use of non-linear neural network models. The neural network models utilize three to six additional molecular properties of the selected fluid apart from the usual critical properties of each fluid.

The method was capable of precise representations of saturated liquid densities and yielded an overall %AAD of 0.6 for 65 fluids. The generalized model predicted the densities of the same data set with an overall %AAD of 0.8. The generalized model was

further validated by predicting densities of 20 fluids that formed an external data set. The model predicted the densities of these fluids with an overall %AAD of 1.0, which is quite comparable to predictions obtained for the fluids used in model development. The volume-translation method was also used to predict compressed liquid densities of a representative set of fluids. The method provided predictions with an overall %AAD of 1.8. Thus, the volume-translation approach developed in this work has been shown capable of providing reasonably accurate predictions of liquid densities in the saturated as well as single-phase regions. Further, the volume-translation approach presented in this work does not lead to thermodynamic inconsistencies such as isotherm cross-overs in the compressed liquid region at higher pressures unlike other temperature-dependent volume-translation methods.

Table 5.1. Physical Properties Data for Pure Fluids and Optimized Parameter c_1 (Equation 9) of the VTPR EOS

Compound	T_c (K)	P_c (bar)	ω	z_c	Dipole Moment	c_1	Physical Properties Data Ref.	Liquid Density Data Ref.
Carbon dioxide	304.13	73.773	0.22394	0.2746	0.000	0.00652	[32]	[32]
Nitrogen	126.19	33.958	0.037	0.2894	0.000	0.01386	[32]	[32]
Water	647.14	220.640	0.3443	0.2294	1.855	-0.01416	[32]	[32]
Methane	190.56	45.992	0.011	0.2863	0.000	0.01313	[32]	[32]
Ethane	305.33	48.718	0.0993	0.2776	0.000	0.00993	[32]	[32]
Propane	369.83	42.477	0.1524	0.2769	0.084	0.00778	[32]	[32]
Butane	425.13	37.960	0.201	0.2738	0.050	0.00642	[32]	[32]
Pentane	469.70	33.700	0.251	0.2684	0.370	0.00434	[32]	[32]
Hexane	507.82	30.340	0.299	0.2656	0.050	0.00306	[32]	[32]
Heptane	540.13	27.360	0.349	0.2632	0.000	0.00095	[32]	[32]
Octane	569.32	24.970	0.393	0.2565	0.070	0.00020	[32]	[32]
Nonane	594.55	22.810	0.443	0.2550	0.070	-0.00196	[32]	[32]
Decane	617.70	21.030	0.488	0.2501	0.070	-0.00230	[32]	[32]
Dodecane	658.10	18.170	0.574	0.2492	0.000	-0.00428	[32]	[32]
Ethylene	282.35	50.418	0.0866	0.2813	0.000	0.00995	[32]	[32]
Propylene	364.90	46.000	0.142	0.2800	0.366	0.00834	[32]	[32]
Propyne	402.38	56.260	0.204	0.2751	0.781	0.00426	[32]	[32]
Isobutane	407.81	36.290	0.184	0.2759	0.132	0.00706	[32]	[32]
2-Methylbutane	460.35	33.957	0.2296	0.2712	0.100	0.00689	[32]	[32]
2-Methylpentane	497.70	30.400	0.28	0.2706	-1.000	0.00414	[32]	[32]
Cyclohexane	553.64	40.750	0.20926	0.2729	0.300	0.00711	[32]	[32]
Cyclopropane	398.30	55.797	0.1305	0.2743	0.000	0.00631	[32]	[32]
Oxygen	154.58	50.430	0.0222	0.2879	0.000	0.01314	[32]	[32]
Argon	150.69	48.63	-0.00219	0.2895	0.000	0.01433	[32]	[32]
Xenon	289.73	58.420	0.00363	0.2895	0.000	0.01208	[32]	[32]
Fluorine	144.41	51.724	0.0449	0.2880	0.000	0.01215	[32]	[32]
Carbon monoxide	132.86	34.935	0.05	0.2915	0.100	0.01330	[32]	[32]
Sulfur dioxide	430.64	78.840	0.2557	0.2687	1.600	0.00333	[32]	[32]
Hydrogen sulfide	373.10	90.000	0.1	0.2847	0.970	0.01091	[32]	[32]
Sulfur hexafluoride	318.73	37.546	0.21	0.2782	0.000	0.00989	[32]	[32]
Methanol	512.64	80.970	0.5625	0.2240	1.700	-0.01264	[32]	[32]
Ammonia	405.40	113.330	0.25601	0.2440	1.470	-0.00777	[32]	[32]
Benzene	562.05	48.940	0.20921	0.2686	0.000	0.00526	[32]	[32]

Table 5.1. Physical Properties Data for Pure fluids and Optimized Parameter c_1 (Equation 5.9) of the VTPR EOS *(Continued)*

Compound	T_c (K)	P_c (bar)	ω	z_c	Dipole Moment	c_1	Physical Properties Data Ref.	Liquid Density Data Ref.
Toluene	591.75	41.263	0.266	0.2647	0.360	0.00288	[32]	[32]
Trichlorofluoromethane	471.11	44.076	0.18875	0.2790	0.450	0.00820	[32]	[32]
Dichlorodifluoromethane	385.12	41.361	0.17948	0.2764	0.510	0.00830	[32]	[32]
Chlorotrifluoromethane	302.00	38.790	0.1723	0.2768	0.510	0.00914	[32]	[32]
Tetrafluoromethane	227.51	37.750	0.1785	0.2807	0.000	0.01152	[32]	[32]
Dichlorofluoromethane	451.48	51.812	0.2061	0.2701	1.370	0.00571	[32]	[32]
Chlorodifluoromethane	369.30	49.900	0.22082	0.2683	1.458	0.00425	[32]	[32]
Difluoromethane	351.26	57.820	0.2769	0.2429	1.978	-0.00930	[32]	[32]
Fluoromethane	317.28	58.970	0.2012	0.2400	1.851	-0.00708	[32]	[32]
1,1,2-Trichloro-1,2,2-trifluoroethane	487.21	33.922	0.25253	0.2740	0.803	0.00614	[32]	[32]
1,2-Dichloro-1,1,2,2-tetrafluoroethane	418.83	32.570	0.2523	0.2757	0.658	0.00752	[32]	[32]
Chloropentafluoroethane	353.10	31.200	0.252	0.2730	0.520	0.00797	[32]	[32]
Hexafluoroethane	293.03	30.480	0.257	0.2815	0.000	0.00911	[32]	[32]
2,2-dichloro-1,1,1-trifluoroethane	456.83	36.618	0.28192	0.2681	1.356	0.00405	[32]	[32]
1-chloro-1,2,2,2-tetrafluoroethane	395.43	36.243	0.2881	0.2687	1.469	0.00507	[32]	[32]
Pentafluoroethane	339.17	36.177	0.3052	0.2684	1.563	0.00470	[32]	[32]
1,1,1,2-tetrafluoroethane	374.21	40.593	0.32684	0.2601	2.058	0.00075	[32]	[32]
1,1-Dichloro-1-fluoroethane	477.50	42.120	0.22	0.2706	2.014	0.00508	[32]	[32]
1-Chloro-1,1-difluoroethane	410.26	40.550	0.232	0.2679	2.140	0.00347	[32]	[32]
1,1,1-trifluoroethane	345.86	37.610	0.2615	0.2550	2.340	-0.00221	[32]	[32]
1,1-difluoroethane	386.41	45.168	0.27521	0.2520	2.262	-0.00360	[32]	[32]
Octafluoropropane	345.02	26.400	0.317	0.2755	0.140	0.00825	[32]	[32]
1,1,1,2,3,3-Hexafluoropropane	412.44	33.564	0.3794	0.2641	1.129	0.00257	[32]	[32]
Acetone	508.20	47.010	0.3065	0.2330	2.900	-0.00880	[33]	[33]
Eicosane	768.00	11.600	0.9069	0.2430	0.000	-0.00913	[33]	[33]
Ethanol	513.92	61.480	0.649	0.2430	1.700	-0.00424	[61]	[34]
Propanol 1	536.78	51.750	0.629	0.2540	1.700	-0.00049	[61]	[34]

Table 5.1. Physical Properties Data of Pure Fluids and Optimized Parameter c_1 (Equation 5.9) of VTPR EOS *(Continued)*

Compound	T_c (K)	P_c (bar)	ω	z_c	Dipole Moment	c_1	Physical Properties Data Ref.	Liquid Density Data Ref.
Propanol 2	508.30	47.620	0.665	0.2480	1.700	-0.00220	[61]	[34]
Butanol	563.05	44.230	0.59	0.2600	1.800	0.00073	[61]	[34]
Isobutanol	547.78	43.000	0.59	0.2580	1.700	0.00067	[61]	[34]
Pentanol	588.15	39.090	0.579	0.2620	1.700	0.00224	[61]	[34]
Carbonyl sulfide	378.77	63.700	0.0978	0.2731	0.715	0.00876	[32]	[32]

Table 5.2. VTPR EOS Predictions for Saturated Liquid Densities: Comparison with Other Methods

Compound	T_r range	NDP	%AAD in Saturated Liquid Density								
			PR	SRK	Generalized Method from			This Work			
					Ref.[17]	Ref.[18]	Ref.[19]	VTPR[a]	VTPR[b]	VTPR[c]	VTPR[d]
Carbon dioxide	0.712-0.999	357	4.4	12.6	1.9	0.78	0.84	0.22	0.47	0.58	0.39
Nitrogen	0.500-0.999	238	9.6	4.7	1.4	2.30	0.90	0.42	0.52	0.61	0.69
Water	0.423-1.000	243	19.7	28.9	7.2	3.59	6.95	1.16	2.00	1.16	1.17
Methane	0.477-0.999	250	9.1	4.5	1.2	2.20	0.75	0.33	0.80	0.34	0.35
Ethane	0.451-1.000	200	6.9	7.3	1.5	1.92	0.94	0.55	1.15	0.87	0.60
Propane	0.450-0.996	200	5.7	8.7	1.5	1.45	0.93	0.59	0.60	0.65	0.65
Butane	0.479-1.000	200	4.9	10.1	1.5	1.10	0.96	0.58	0.61	0.65	0.62
Pentane	0.450-0.997	200	3.7	11.7	1.6	1.50	0.96	0.66	0.66	0.69	0.67
Hexane	0.551-0.998	200	3.6	13.5	2.5	1.60	0.99	0.51	0.52	0.52	0.57
Heptane	0.555-0.998	200	4.0	15.2	1.5	2.10	1.10	0.43	1.15	0.68	0.62
Octane	0.562-0.998	200	5.2	16.1	1.6	1.40	1.35	0.66	0.96	0.97	0.85
Nonane	0.538-0.998	200	7.0	17.7	-	1.30	1.21	0.58	0.77	0.71	0.65
Decane	0.550-0.998	200	7.8	18.4	4.6	1.60	1.12	0.89	1.20	0.98	0.93
Dodecane	0.583-0.991	200	9.3	19.7	8.9	3.20	1.76	0.87	0.94	0.88	0.89
Ethylene	0.500-0.997	200	6.8	7.4	1.4	1.42	0.98	0.40	0.40	0.48	0.40
Propylene	0.500-0.998	200	5.8	8.6	1.9	0.99	1.34	0.51	1.01	0.95	0.70
Propyne	0.678-0.998	200	3.8	13.5	2.1	2.20	2.78	0.41	2.22	2.14	0.52
Isobutane	0.490-1.00	200	5.2	9.5	1.5	1.10	1.86	0.52	0.63	0.73	0.60
2-Methylbutane	0.434-0.991	200	4.9	9.5	1.8	1.65	1.12	0.71	1.06	1.01	1.08
2-Methylpentane	0.402-0.997	200	3.6	11.3	2.4	1.56	0.99	0.87	1.25	0.89	0.89
Cyclohexane	0.552-1.000	200	4.8	10.2	1.4	1.45	0.95	0.44	0.70	0.60	0.75
Cyclopropane	0.685-0.995	200	4.3	12.6	2.7	1.30	1.40	0.23	0.55	0.75	0.99

Table 5.2. VTPR EOS Predictions for Saturated Liquid Densities: Comparison with Other Methods *(Continued)*

Compound	T_r range	NDP	%AAD in Saturated Liquid Density								
			PR	SRK	Generalized Method from			This Work			
					Ref.[17]	Ref.[18]	Ref.[19]	VTPR[a]	VTPR[b]	VTPR[c]	VTPR[d]
Oxygen	0.400-0.999	200	9.7	4.0	1.9	1.85	0.97	0.54	0.61	0.54	0.58
Argon	0.556-1.000	200	9.1	4.9	1.5	2.10	1.32	0.31	0.67	0.34	0.49
Xenon	0.557-0.998	200	7.7	6.3	-	1.55	1.40	0.63	1.36	1.70	1.17
Fluorine	0.452-0.998	200	8.7	4.6	-	1.30	1.20	0.41	0.69	0.69	0.61
Carbon monoxide	0.513-0.998	200	9.2	4.4	-	1.10	0.99	0.40	0.86	0.42	0.59
Sulfur dioxide	0.551-0.995	200	3.0	13.2	1.8	1.40	1.46	0.47	1.29	0.99	0.46
Hydrogen sulfide	0.503-0.998	200	7.1	6.3	-	1.30	1.21	0.64	0.79	0.65	0.68
Sulfur hexafluoride	0.698-1.000	200	5.7	10.1	-	1.85	1.10	0.40	0.86	0.68	0.56
Methanol	0.546-0.998	200	17.9	27.3	6.1	3.50	4.30	0.87	2.87	0.87	1.00
Ammonia	0.482-0.997	200	12.9	22.9	12.4	2.40	4.20	0.91	1.82	0.91	0.91
Benzene	0.496-0.997	200	3.8	11.7	1.5	0.99	0.75	0.68	0.79	0.80	0.74
Toluene	0.500-1.000	200	3.2	13.5	2.8	1.20	0.89	0.53	0.54	0.54	0.53
Trichlorofluoromethane	0.480-1.000	200	5.6	8.7	1.4	0.92	1.23	0.54	1.10	1.00	1.59
Dichlorodifluoromethane	0.498-1.000	200	5.7	8.8	1.4	1.38	0.95	0.52	0.65	0.65	1.07
Chlorotrifluoromethane	0.500-1.000	200	6.2	8.2	-	1.95	0.92	0.53	0.87	0.88	0.81
Tetrafluoromethane	0.500-0.997	200	8.4	5.5	1.8	2.90	1.82	0.72	1.84	1.62	1.68
Dichlorofluoromethane	0.500-0.997	200	4.2	11.2	1.5	1.67	0.93	0.52	0.65	0.63	0.89
Chlorodifluoromethane	0.450-1.000	200	3.4	12.1	-	1.30	0.84	0.81	0.81	0.81	0.81
Difluoromethane	0.455-1.000	200	14.3	24.1	-	3.40	5.15	0.88	2.90	0.90	0.88
Fluoromethane	0.550-1.000	200	13.3	23.4	4.9	1.20	3.50	0.89	1.02	0.89	0.92
1,1,2-Trichloro-1,2,2-trifluoroethane	0.500-0.997	200	4.6	10.2	1.4	1.30	0.77	0.61	0.73	0.71	0.61
1,2-Dichloro-1,1,2,2-tetrafluoroethane	0.500-0.996	200	5.3	11.1	2.0	1.35	0.95	0.40	0.64	0.64	0.70
Chloropentafluoroethane	0.500-1.000	200	5.0	8.9	-	1.88	1.80	1.01	1.48	1.38	1.09

Table 5.2. VTPR EOS Predictions for Saturated Liquid Densities: Comparison with Other Methods *(Continued)*

Compound	T_r range	NDP	%AAD in Saturated Liquid Density								
			PR	SRK	Generalized Method from			This Work			
					Ref.[17]	Ref.[18]	Ref.[19]	VTPR[a]	VTPR[b]	VTPR[c]	VTPR[d]
Hexafluoroethane	0.597-1.000	200	6.3	8.4	-	0.98	0.92	0.55	0.93	0.95	0.72
2,2-dichloro-1,1,1-trifluoroethane	0.471-0.997	200	3.4	12.1	-	0.99	0.83	0.73	0.90	0.90	0.90
1-chloro-1,2,2,2-tetrafluoroethane	0.468-0.997	200	3.8	11.4	-	1.10	0.88	0.76	0.86	0.90	0.83
pentafluoroethane	0.510-0.997	200	3.8	11.8	-	1.20	0.82	0.59	0.64	0.70	0.60
1,1,1,2-tetrafluoroethane	0.502-1.000	200	4.6	15.5	-	1.20	0.92	0.71	0.71	0.72	0.72
1,1-Dichloro-1-fluoroethane	0.500-1.000	200	4.2	11.5	-	1.10	0.89	0.61	0.64	0.66	0.67
1-Chloro-1,1-difluoroethane	0.500-1.000	200	3.6	12.9	-	0.95	0.93	0.66	0.89	0.67	0.68
1,1,1-trifluoroethane	0.535-0.998	200	7.5	18.2	2.8	1.40	1.68	0.53	0.76	0.48	1.44
1,1-difluoroethane	0.450-1.000	200	8.7	19.1	2.7	1.45	2.06	0.87	1.33	0.87	0.87
Octafluoropropane	0.500-0.997	200	5.9	8.4	-	1.65	1.60	0.64	0.85	0.81	0.66
1,1,1,2,3,3-Hexafluoropropane	0.587-0.990	200	4.4	13.8	-	3.10	2.55	0.89	1.10	0.89	0.87
Acetone	0.541-0.997	140	14.0	23.9	3.6	2.60	2.44	1.49	2.86	1.56	1.46
Eicosane	0.600-0.993	120	14.1	23.7	7.1	3.85	4.50	1.17	2.82	1.16	1.17
Ethanol	0.500-0.995	93	9.5	19.7	5.3	2.80	2.80	0.43	1.82	0.69	0.54
1-Propanol	0.477-0.997	110	4.6	15.4	3.6	3.30	2.40	0.50	1.37	0.55	0.58
2-Propanol	0.503-0.997	90	6.5	17.1	3.1	2.50	2.60	0.51	2.43	0.71	2.04
Butanol	0.500-0.994	120	3.4	14.4	6.3	1.10	1.20	0.72	0.72	0.82	0.73
Isobutanol	0.511-0.996	110	3.4	14.4	6.1	1.45	1.98	0.86	1.12	0.86	0.89
Pentanol	0.476-0.990	85	2.0	12.7	1.6	1.45	1.80	1.13	1.20	1.16	1.22
Carbonyl sulfide	0.500-0.997	200	5.7	8.8	4.6	2.90	1.85	0.69	2.05	0.81	0.76
Overall		**12556**	**6.7**	**12.0**	**2.9**	**1.7**	**1.6**	**0.6**	**1.0**	**0.8**	**0.8**

(a) Based on optimized values from Table 5.1 (b) Based on generalized model using linear correlation (Case 1)
(c) Based on generalized model using neural network (Case 2) (d) Based on generalized model using neural network (Case 3)

Table 5.3. Case Studies for Model Generalization of VTPR EOS

Case No.	Description	Molecular Properties
1.	Linear model using one descriptor	critical compressibility factor
2.	Neural network model using 3 descriptors, including z_c	critical compressibility factor, acentric factor and dipole moment
3.	Neural network model using 6 descriptors without z_c	acentric factor, SM2_B(p), R2u+, dipole moment, Mor03m and HATS1p

Table 5.4. Description of the Molecular Properties Used in Case 3 of the Model Generalization of the VTPR EOS

Molecular Properties	Description	Type of Descriptor
SM2_B(p)	Spectral moment of order 2 from Burden matrix weighted by polarizability	2-D Topological Index
R2u+	R maximal autocorrelation of lag 2 / unweighted	Geometrical and Topological Index
Mor03m	Signal 03 / weighted by mass	3-D Geometrical Index
HATS1p	Leverage-weighted autocorrelation of lag 1 / weighted by polarizability	Geometrical and Topological Index

Table 5.5. Physical Properties Data and Generalized Parameter c_1 for Pure Fluids Used for Validation of the VTPR EOS

Compound	T_c (K)	P_c (bar)	ω	z_c	Dipole Moment	c_1 [a]	Physical Properties Data Ref.	Liquid Density Data Ref.
1,3-Butadiene	425	43.2	0.195	0.27	0	0.00512	[33]	[33]
Octene	566.9	26.63	0.3921	0.262	0.3	0.00122	[33]	[33]
1-Octyne	574	28.8	0.4233	0.267	0	0.00262	[33]	[33]
Cyclohexene	553.8	40.8	0.2081	0.273	0.6	0.00650	[33]	[33]
1,2-Dimethylbenzene	630.3	37.32	0.312	0.263	0.5	0.00242	[33]	[33]
Ethylcyclopentane	569.5	34	0.2701	0.269	0	0.00450	[33]	[33]
Methylcyclohexane	572.1	34.8	0.2361	0.27	0	0.00506	[33]	[33]
Deuterium oxide	643.89	216.71	0.364	0.2265	1.9	-0.01461	[33]	[32]
Dinitrogen monoxide	309.52	72.45	0.162	0.2743	0.1608	0.00713	[32]	[32]
Bromobenzene	670.15	45.19	0.2506	0.263	1.5	0.00231	[33]	[33]
Octafluorocyclobutane	388.38	27.775	0.3553	0.2775	0	0.00793	[32]	[32]
1,1,2,2,3-Pentafluoropropane	447.57	39.25	0.3536	0.2700	1.79	0.00464	[32]	[32]
1,1,1,3,3-Pentafluoropropane	427.2	36.4	0.3724	0.2657	1.549	0.00361	[32]	[32]
Trifluoromethane	299.29	48.32	0.263	0.2580	1.649	0.00009	[32]	[32]
1,1,1,3,3,3-Hexafluoropropane	398.07	32	0.3772	0.2667	1.982	0.00346	[32]	[32]
1,1,1,2,3,3,3-Heptafluoropropane	375.95	29.99	0.354	0.2813	1.456	0.00863	[32]	[32]
Tridecane	675	16.8	0.6174	0.247	0	-0.00527	[33]	[33]
Tetradecane	693	15.7	0.643	0.244	0	-0.00642	[33]	[33]
Pentadecane	708	14.8	0.6863	0.244	0	-0.00692	[33]	[33]
Octadecane	747	12.7	0.8114	0.243	0	-0.00846	[33]	[33]

([a]) c_1 values are from generalized Case 2

Table 5.6. Validation Results for VTPR EOS: Comparison with Other Methods

Compound	T_r range	NDP	%AAD in Saturated Liquid Density						
			PR	SRK	Generalized Method from		This Work		
					Ref.[18]	Ref.[19]	VTPR[b]	VTPR[c]	VTPR[d]
1,3-Butadiene	0.500-0.994	130	4.0	11.6	0.88	0.61	0.60	0.60	0.57
Octene	0.500-0.922	112	7.2	11.5	1.20	1.04	1.36	1.12	1.50
1-Octyne	0.600-1.000	120	3.8	12.4	1.30	1.24	0.94	1.74	1.80
Cyclohexene	0.500-0.996	124	4.4	11.0	0.90	0.45	0.69	0.65	1.22
1,2-Dimethylbenzene	0.500-1.000	150	3.2	14.3	0.89	0.82	0.74	0.92	1.12
Ethylcyclopentane	0.500-0.998	130	3.9	12.2	0.99	0.90	0.71	0.67	0.67
Methylcyclohexane	0.500-0.993	90	4.2	9.4	0.83	0.78	0.65	0.65	0.64
Deuterium oxide	0.500-0.997	200	20.6	29.8	3.20	7.80	1.43	0.82	0.95
Dinitrogen monoxide	0.589-1.000	200	4.8	10.8	0.85	0.62	0.53	0.44	1.10
Bromobenzene	0.500-0.997	120	3.5	14.8	1.20	0.95	0.73	0.89	1.75
Octafluorocyclobutane	0.600-0.998	200	5.5	9.4	1.30	0.78	0.56	0.48	1.10
1,1,2,2,3-Pentafluoropropane	0.500-0.990	200	3.5	10.4	1.41	1.07	1.20	1.31	1.35
1,1,1,3,3-Pentafluoropropane	0.500-0.995	200	3.2	12.8	1.50	0.88	0.66	0.71	0.83
Trifluoromethane	0.500-1.000	200	4.7	15.6	1.60	0.90	1.00	0.98	1.80
1,1,1,3,3,3-Hexafluoropropane	0.500-1.000	200	3.2	12.1	1.70	0.81	1.00	1.06	1.27
1,1,1,2,3,3,3-Heptafluoropropane	0.460-0.997	200	5.2	8.8	2.13	2.61	3.01	2.01	1.81
Tridecane	0.598-0.996	80	11.0	21.2	1.80	2.12	1.10	0.98	0.97
Tetradecane	0.602-0.995	76	12.3	22.4	2.20	2.95	1.36	1.13	1.29
Pentadecane	0.600-0.995	65	13.1	23.0	2.91	3.55	1.98	1.18	1.21
Octadecane	0.600-0.994	60	14.1	23.9	3.98	4.26	2.79	1.16	1.38
Overall		**2857**	**6.2**	**14.1**	**1.6**	**1.7**	**1.1**	**1.0**	**1.2**

([b]) Based on generalized model using linear correlation (Case 1) ([c]) Based on generalized model using neural network (Case 2)
([d]) Based on generalized model using neural network (Case 3)

Table 5.7. VTPR EOS Predictions for Single-Phase (Compressed) Liquid Densities: Comparison with Other Methods

Compound	Temperature Range, K	Pressure Range, bar	NDP	%AAD in Compressed Liquid Density						
				PR	SRK	Generalized Method from			This Work	
						Ref.[17]	Ref.[18]	Ref.[19]	Case 1	Case 2
Carbon dioxide	273-298	64.49-2000	118	5.1	7.4	10.3	15.2	15.6	0.6	0.7
Nitrogen	80-120	1.369-2000	80	11.7	2.0	4.2	5.2	5.6	1.9	2.0
Methane	100-180	1-2000	90	10.9	1.1	4.7	8.0	7.7	1.5	1.8
Pentane	320-420	2-2000	82	4.9	6.3	5.6	5.8	5.5	1.4	1.3
Decane	320-520	1-2000	80	4.5	14.3	5.3	5.8	4.1	2.2	2.1
Water	300-600	50-2000	170	19.0	27.8	4.3	3.1	6.1	3.2	2.3
Methanol	250-450	25-2000	123	18.5	27.2	18.4	2.8	4.2	2.0	3.0
Fluoromethane	200-300	1.325-600	104	10.9	20.5	2.4	9.2	5.7	0.5	0.8
Benzene	300-530	1-775	76	4.5	7.1	5.3	8.2	7.6	1.8	1.8
1-chloro-1,2,2,2-tetrafluoroethane	250-350	0.619-400	80	4.2	7.2	-	4.1	4.0	1.2	1.4
Overall			**1003**	**11.0**	**14.1**	**6.6**	**6.8**	**7.0**	**1.8**	**1.8**

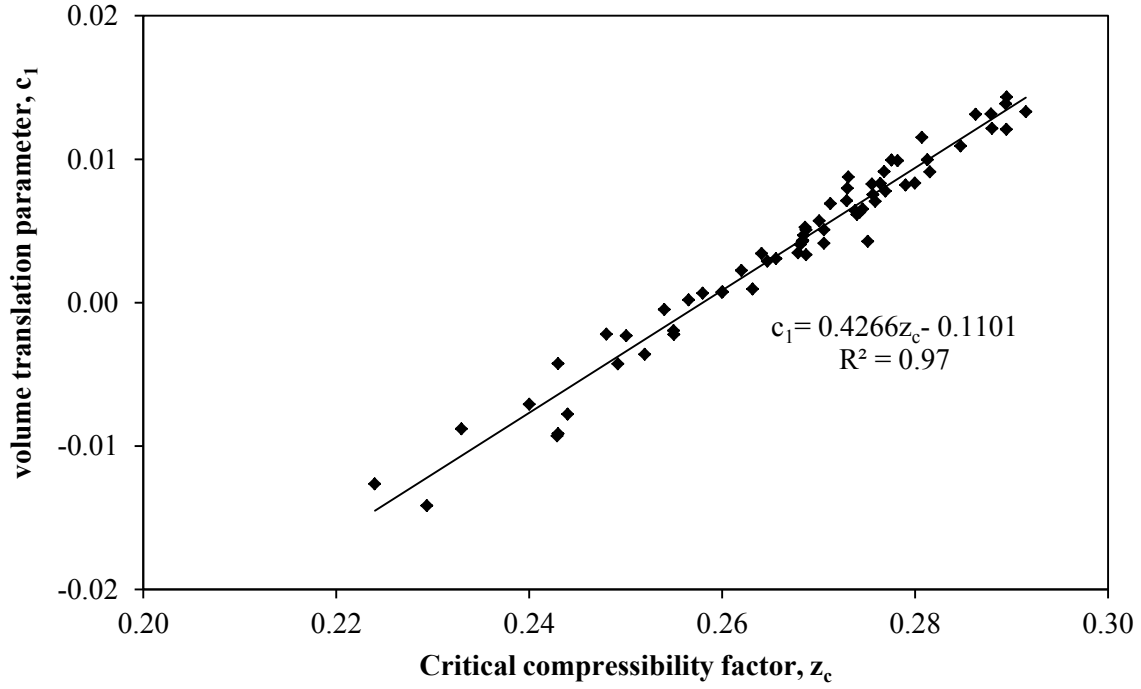

Figure 5.1. Correlation of the Volume Translation Parameter c_1 as a Function of the Critical Compressibility Factor z_c (Case 1)

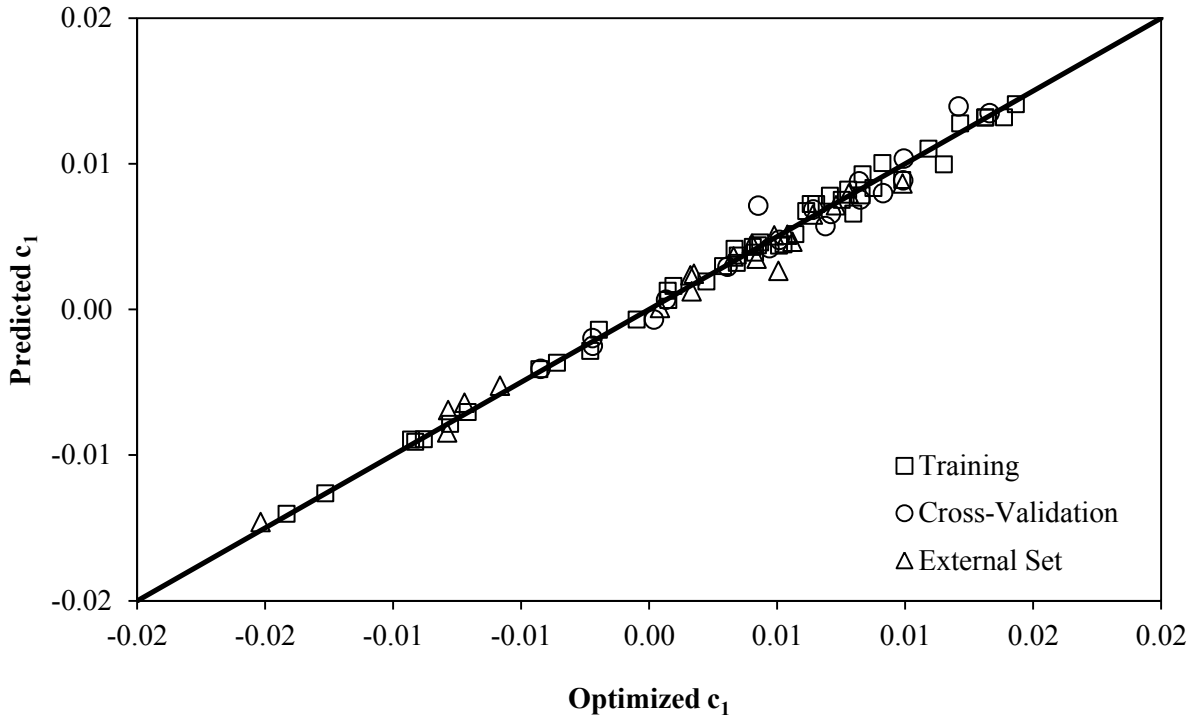

Figure 5.2. Comparison between the Optimized and Predicted Volume Translation Parameter, c_1 (Case 2)

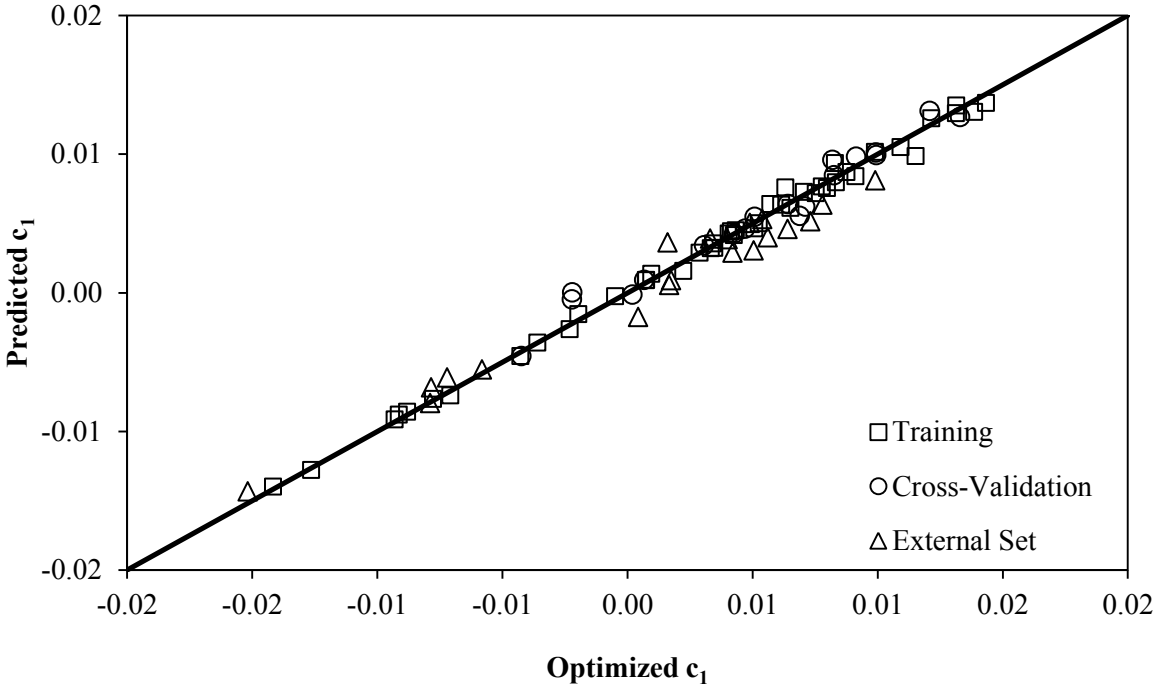

Figure 5.3. Comparison between the Optimized and Predicted Volume Translation Parameter, c_1 (Case 3)

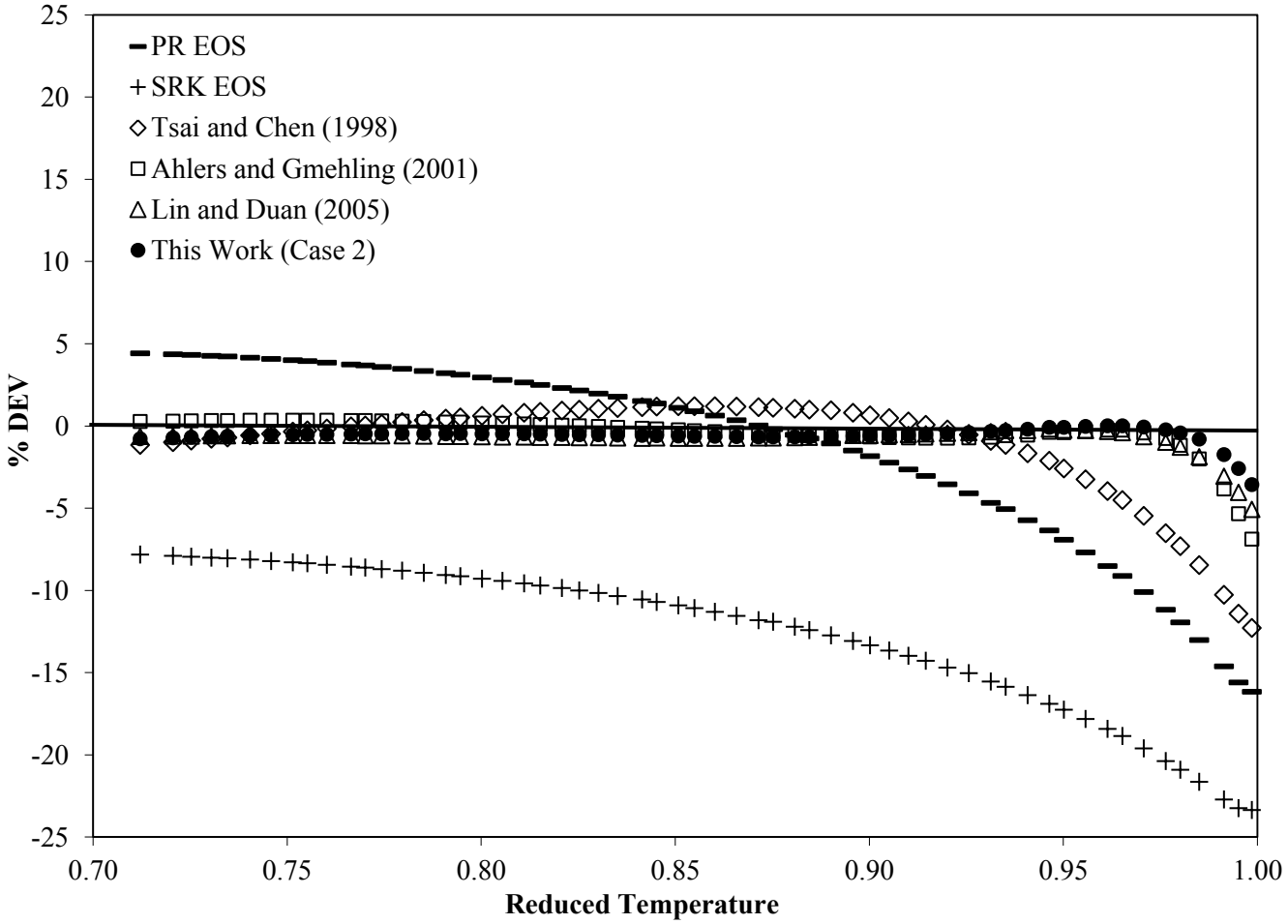

Figure 5.4. VTPR EOS Predictions for Saturated Liquid Densities of CO_2: Comparison with Different Methods

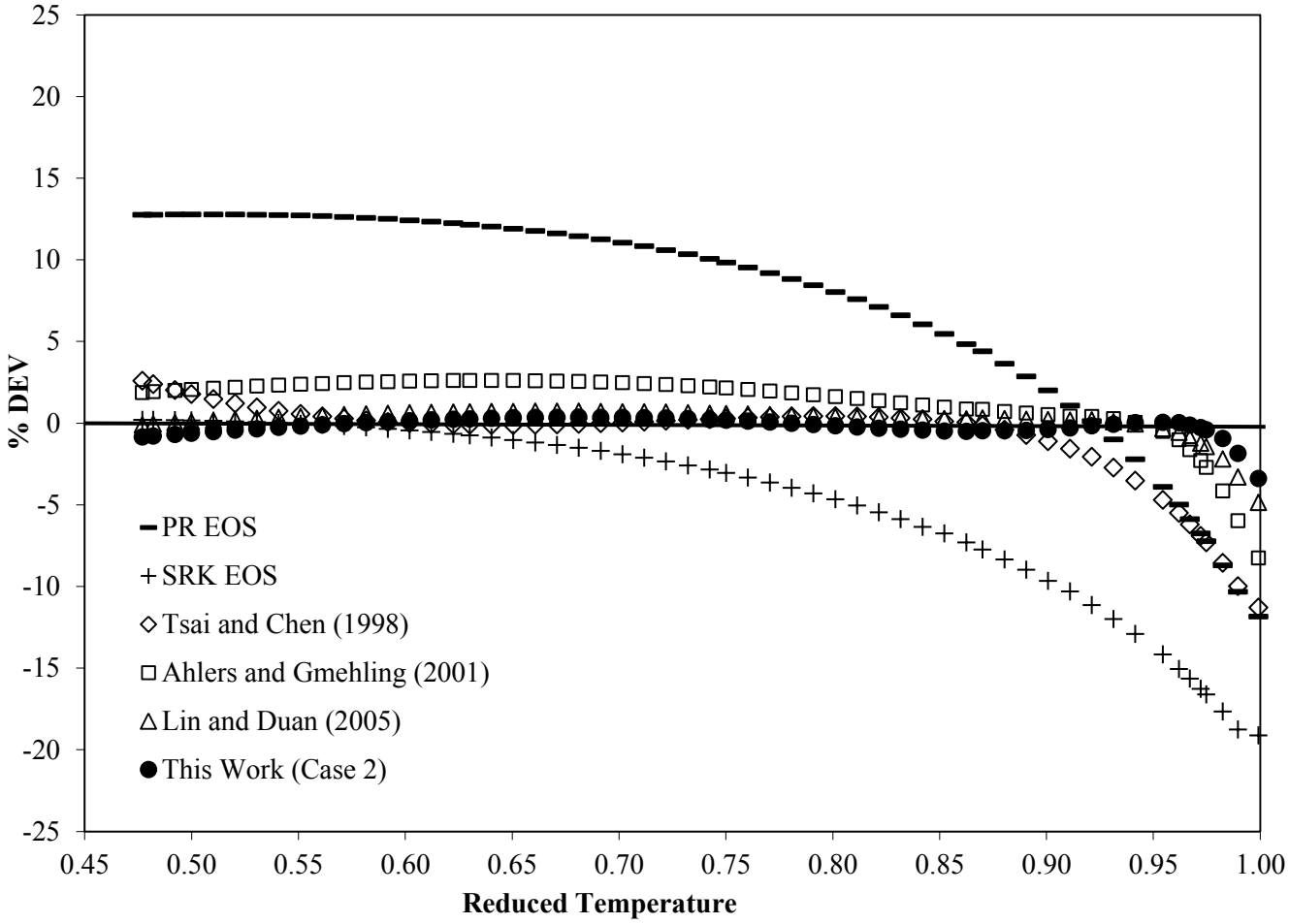

Figure 5.5. VTPR EOS Predictions for Saturated Liquid Densities of Methane: Comparison with Different Methods

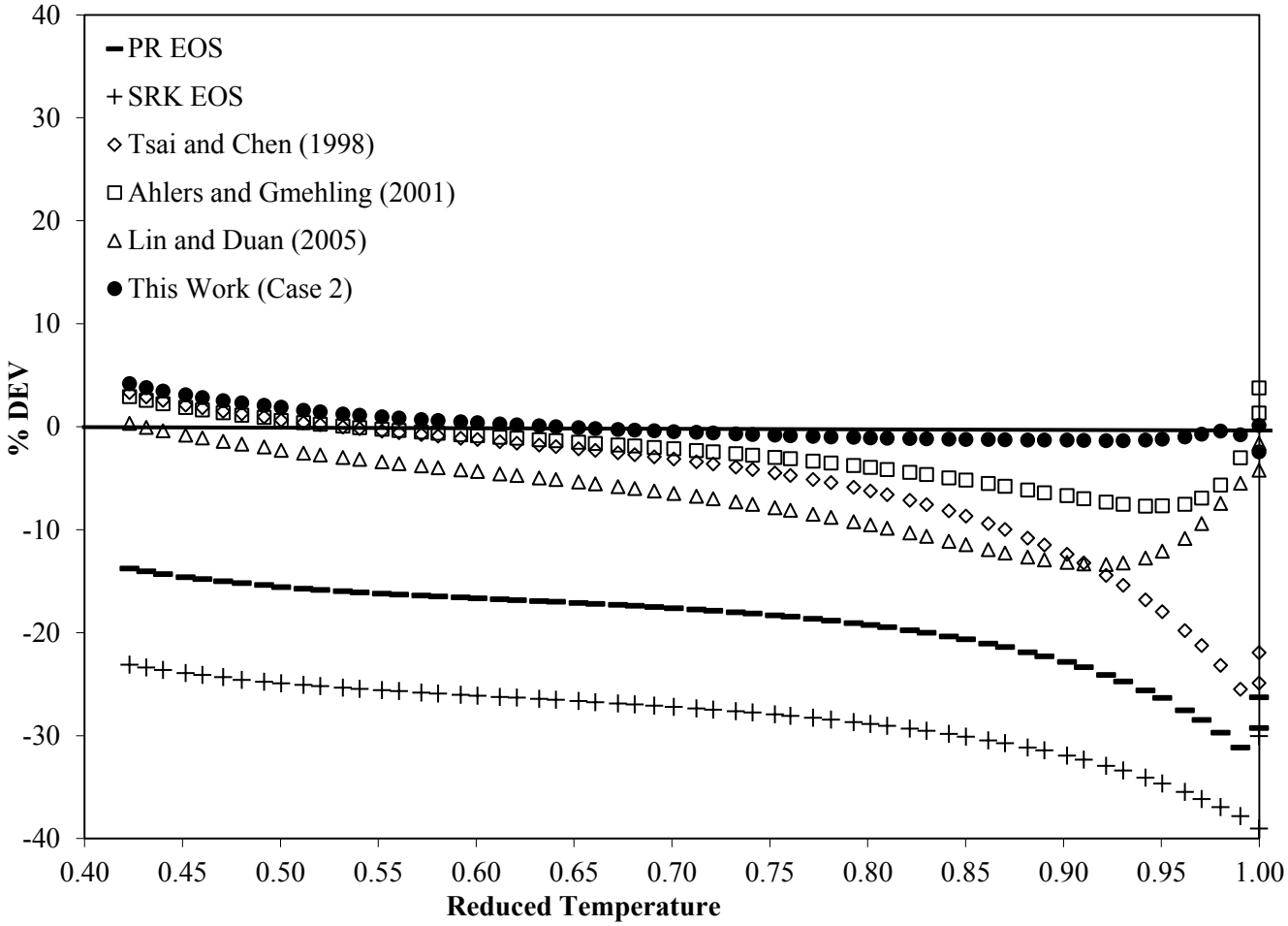

Figure 5.6. VTPR EOS Predictions for Saturated Liquid Densities of Water: Comparison with Different Methods

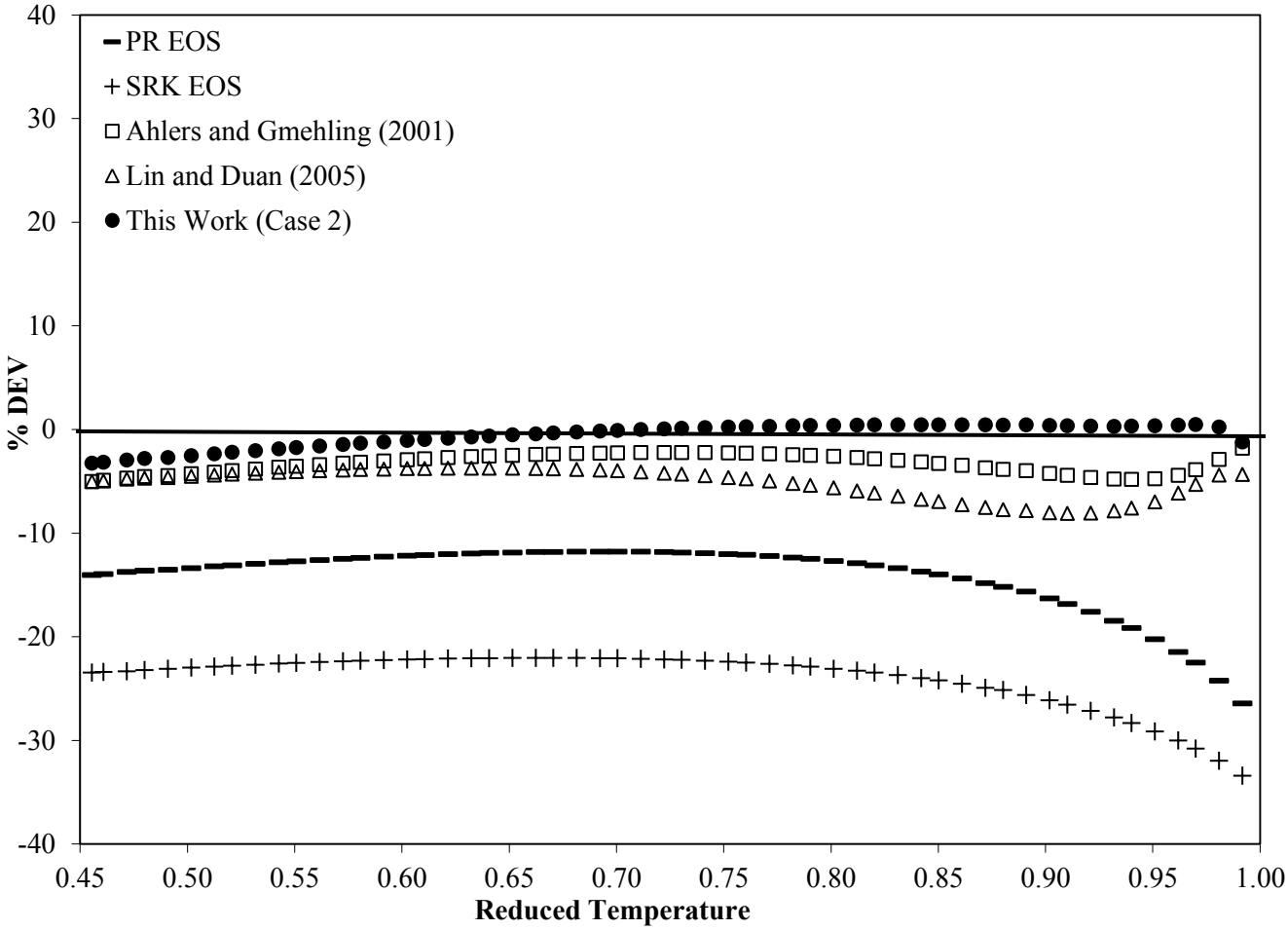

Figure 5.7. VTPR EOS Predictions for Saturated Liquid Densities of Difluoromethane: Comparison with Different Methods

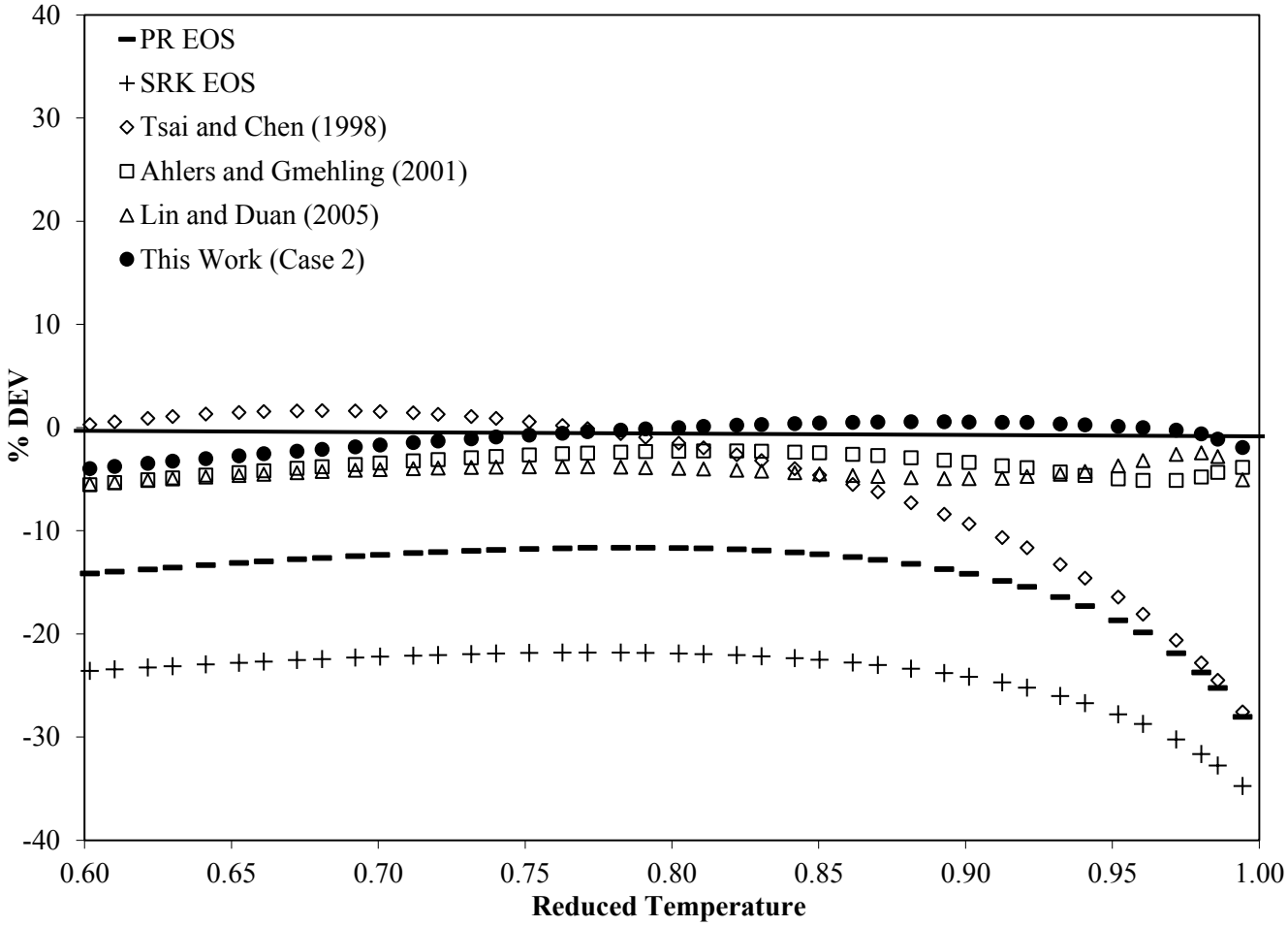

Figure 5.8. VTPR EOS Predictions for Saturated Liquid Densities of Octadecane: Comparison with Different Methods

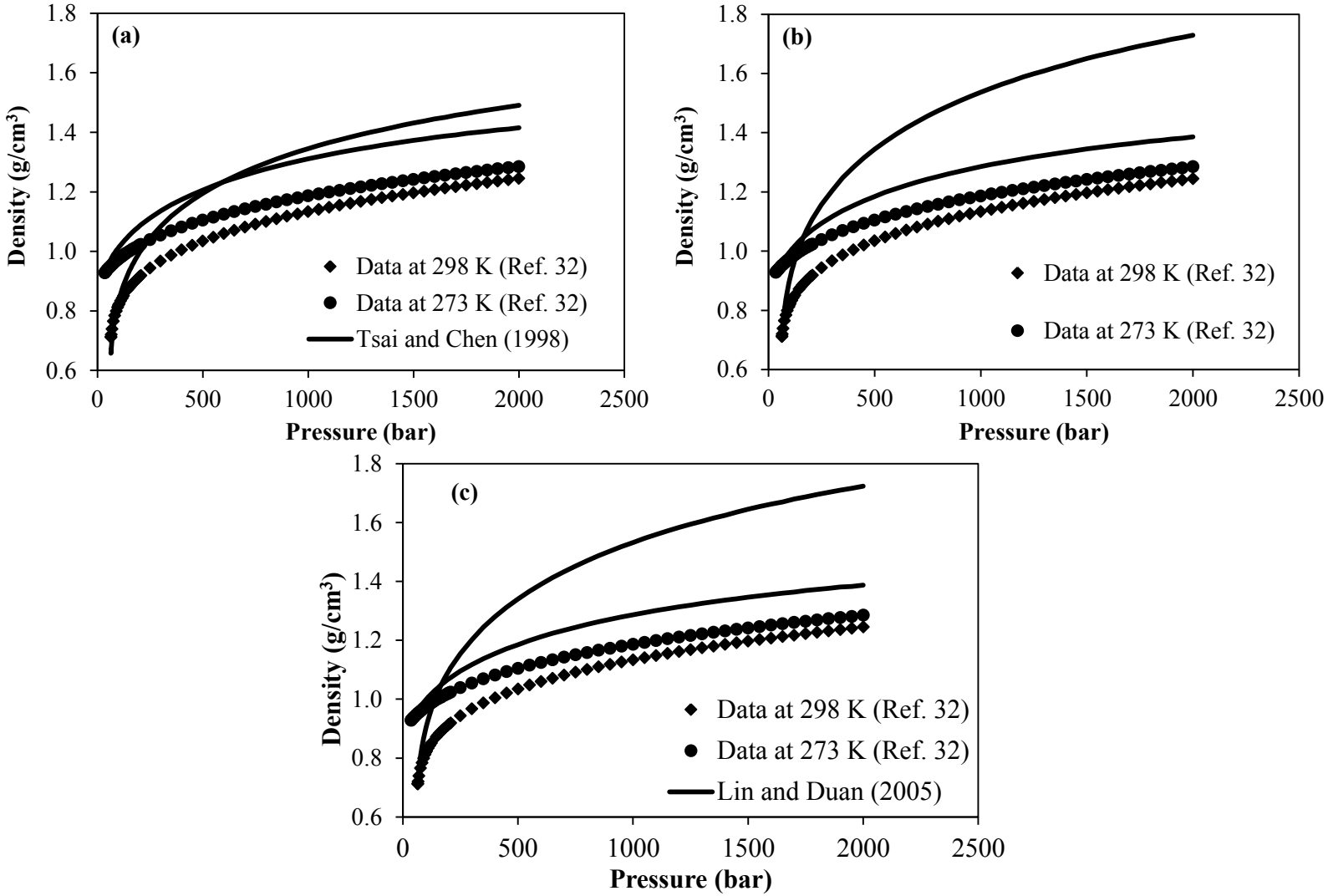

Figure 5.9. Single-Phase Liquid Densities of Carbon Dioxide Predicted by Temperature-Dependent Volume-Translation Methods (a) Tsai and Chen [17] (b) Ahlers and Gmehling [18] (c) Lin and Duan [19]

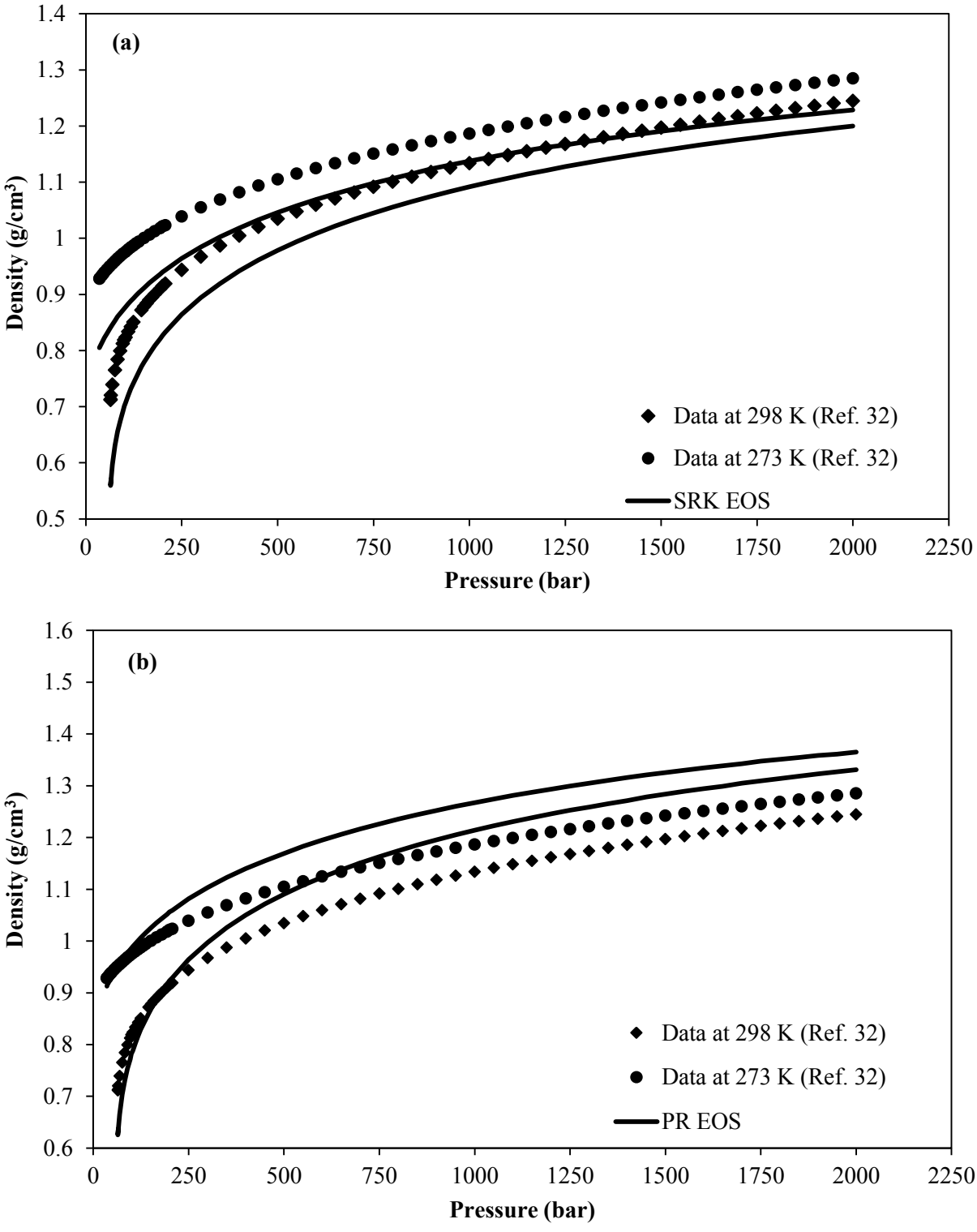

Figure 5.10. Single-Phase Liquid Densities of Carbon Dioxide Using (a) SRK EOS (b) PR EOS

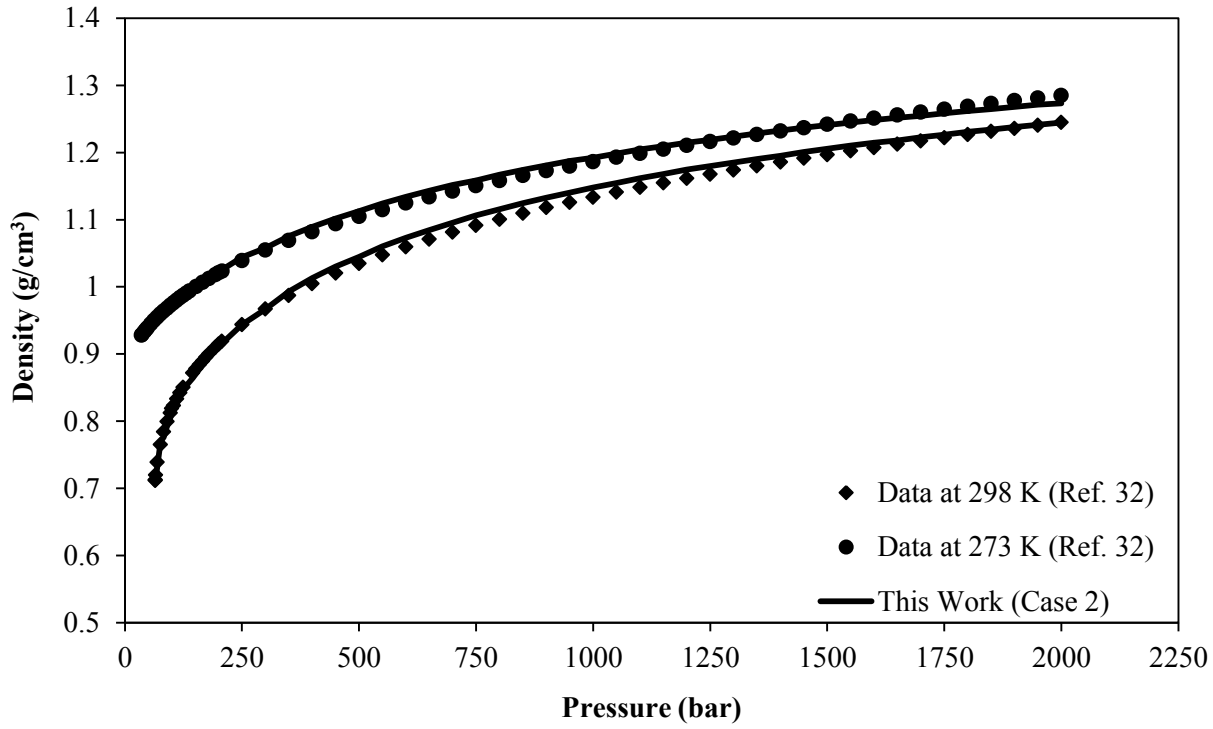

Figure 5.11. VTPR EOS Predictions for Single-Phase Liquid Densities of Carbon Dioxide

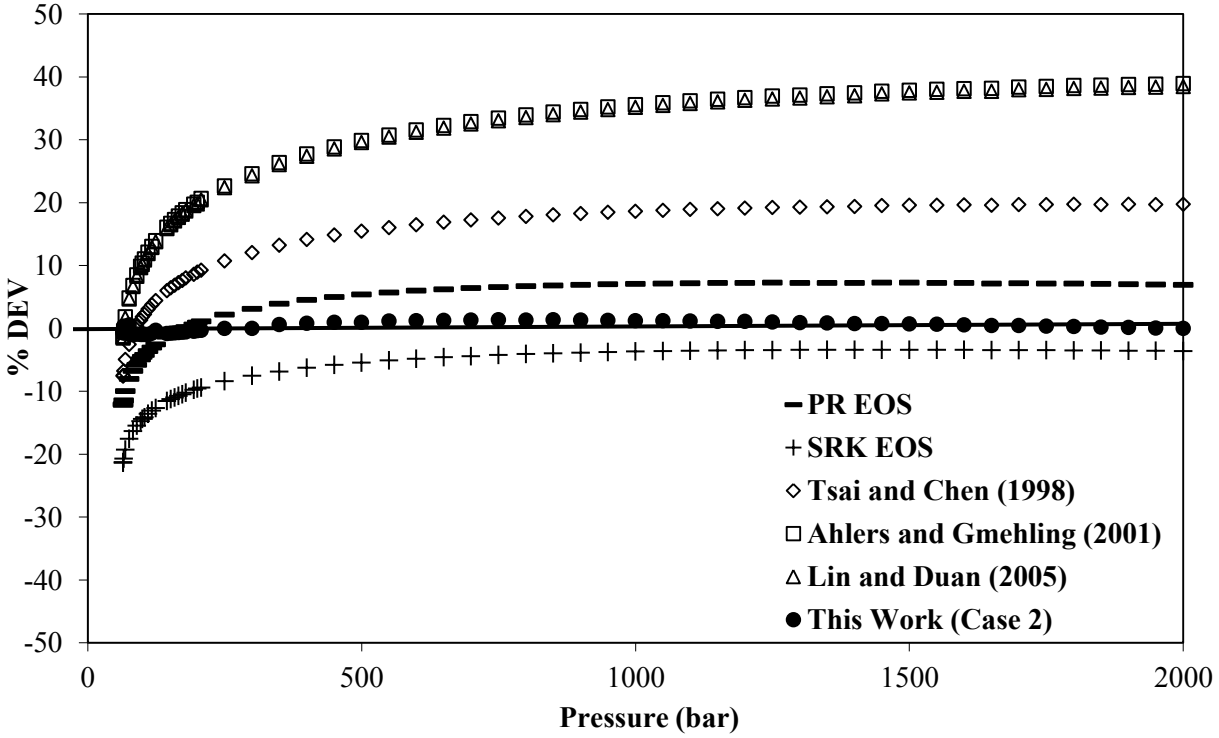

Figure 5.12. VTPR EOS Predictions for Single-Phase Liquid Densities of Carbon Dioxide at 298 K: Comparison with Different methods

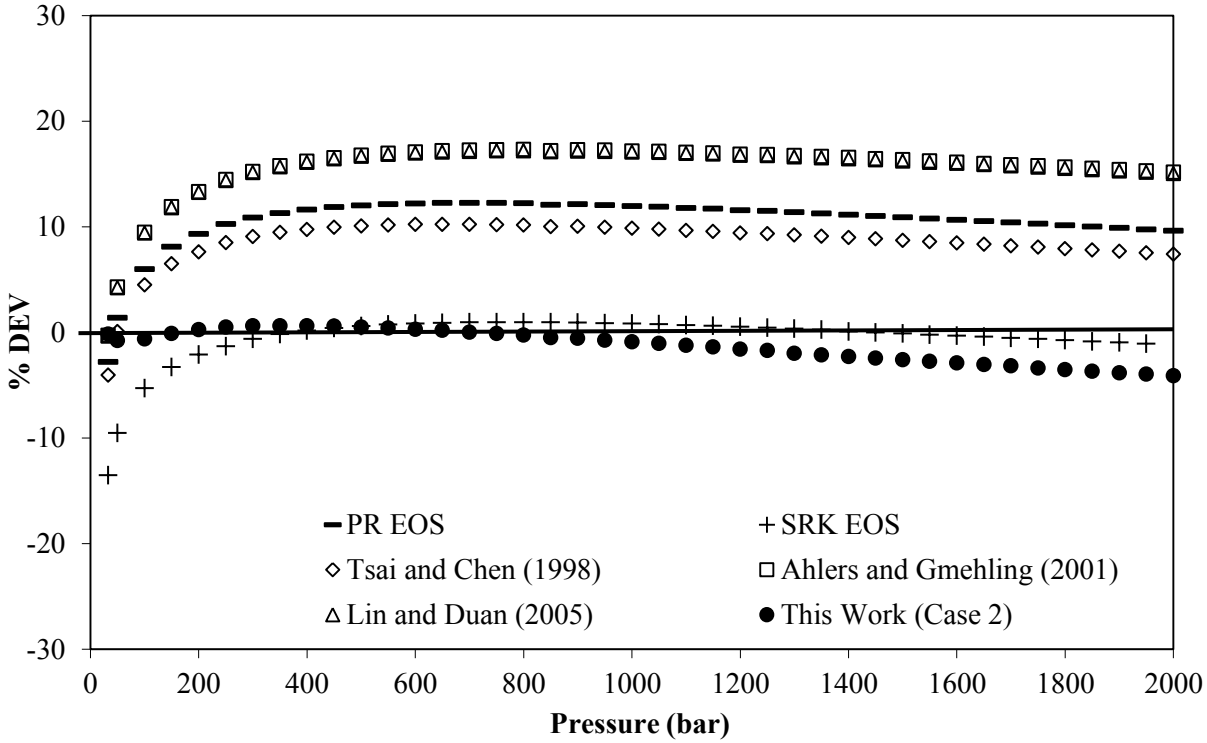

Figure 5.13. VTPR EOS Predictions for Single-Phase Liquid Densities of Methane at 180 K: Comparison with Different methods

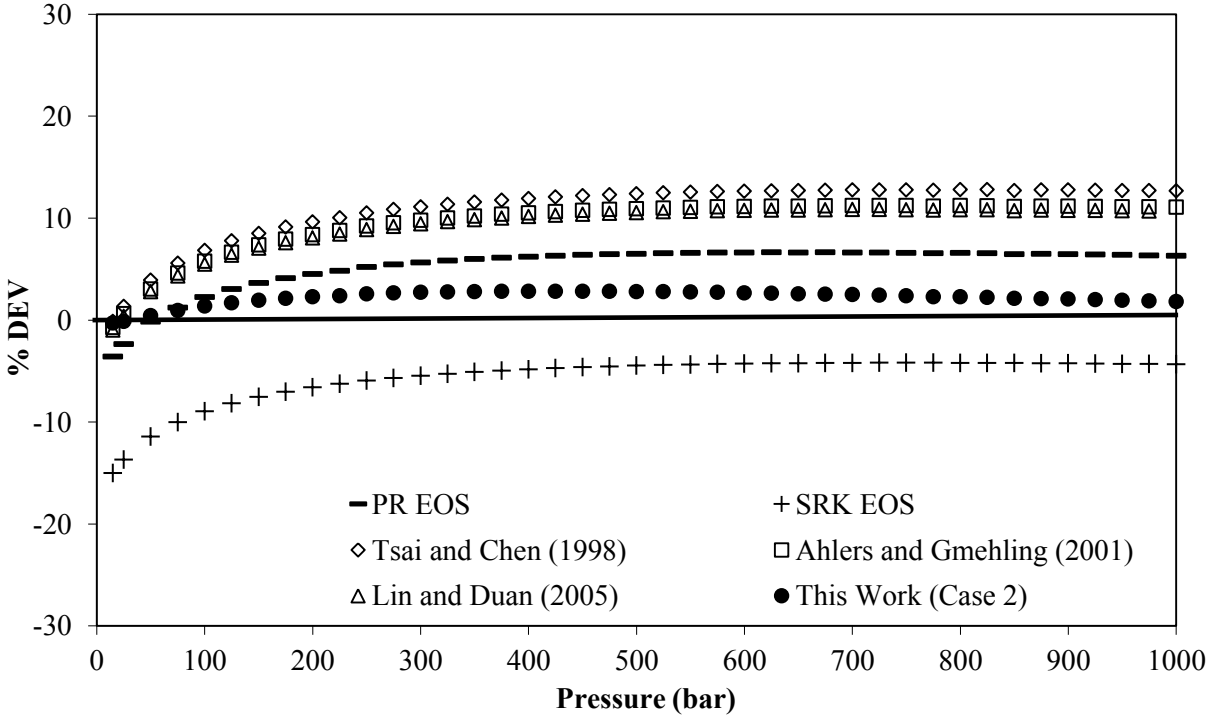

Figure 5.14. VTPR EOS Predictions for Single-Phase Liquid Densities of Pentane at 420 K: Comparison with Different methods

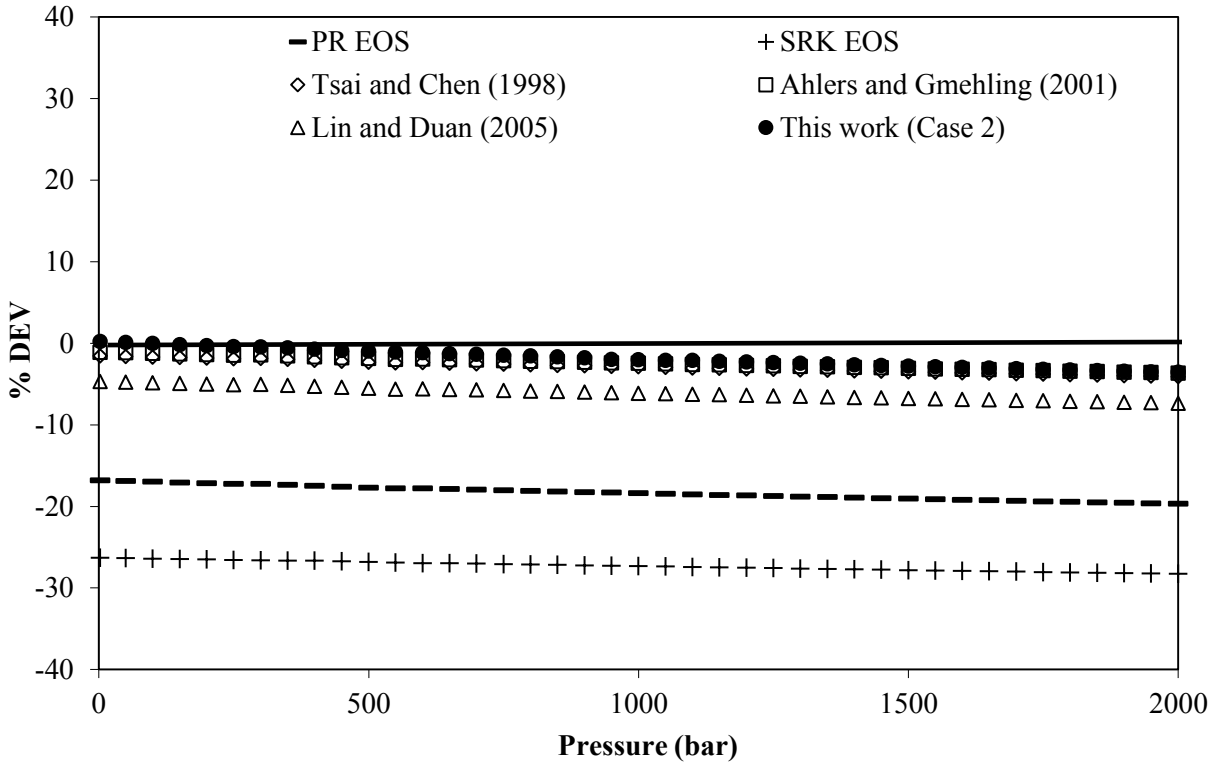

Figure 5.15. VTPR EOS Predictions for Single-Phase Liquid Densities of Water at 400 K: Comparison with Different methods

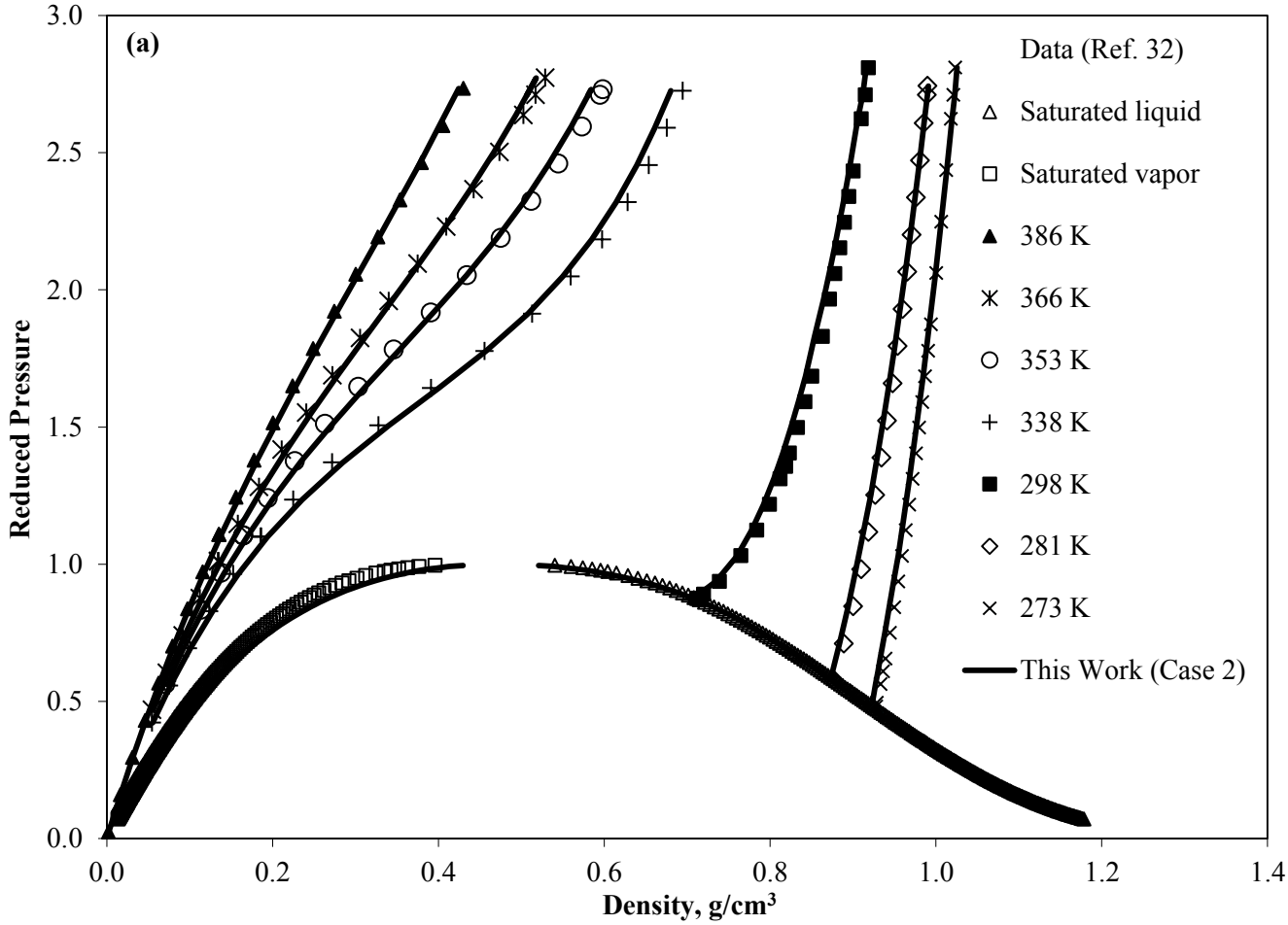

Figure 5.16(a). VTPR EOS Predictions for Carbon Dioxide: Phase Equilibrium Calculations and Volumetric Properties

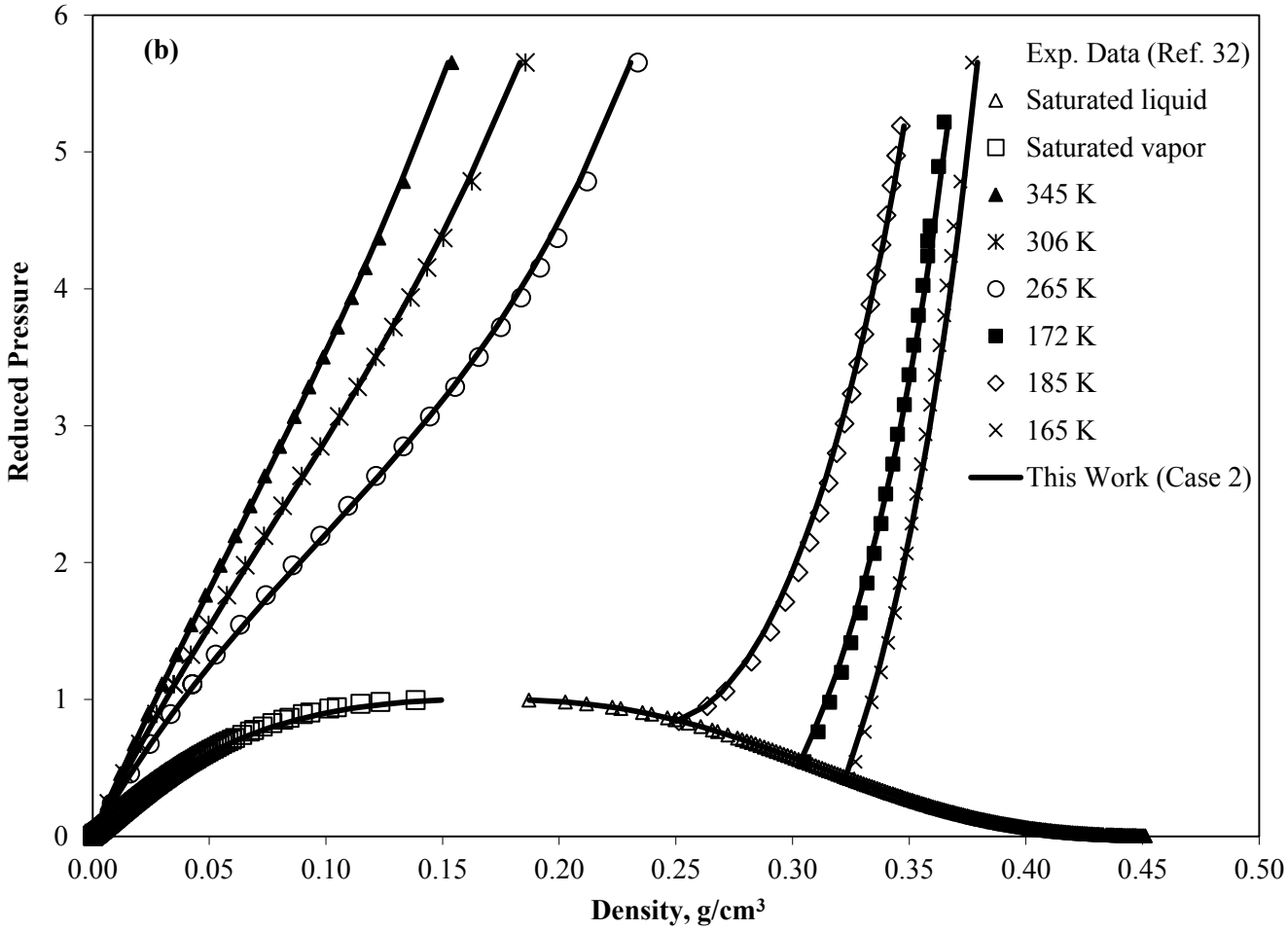

Figure 5.16(b). VTPR EOS Predictions for Methane: Phase Equilibrium Calculations and Volumetric Properties

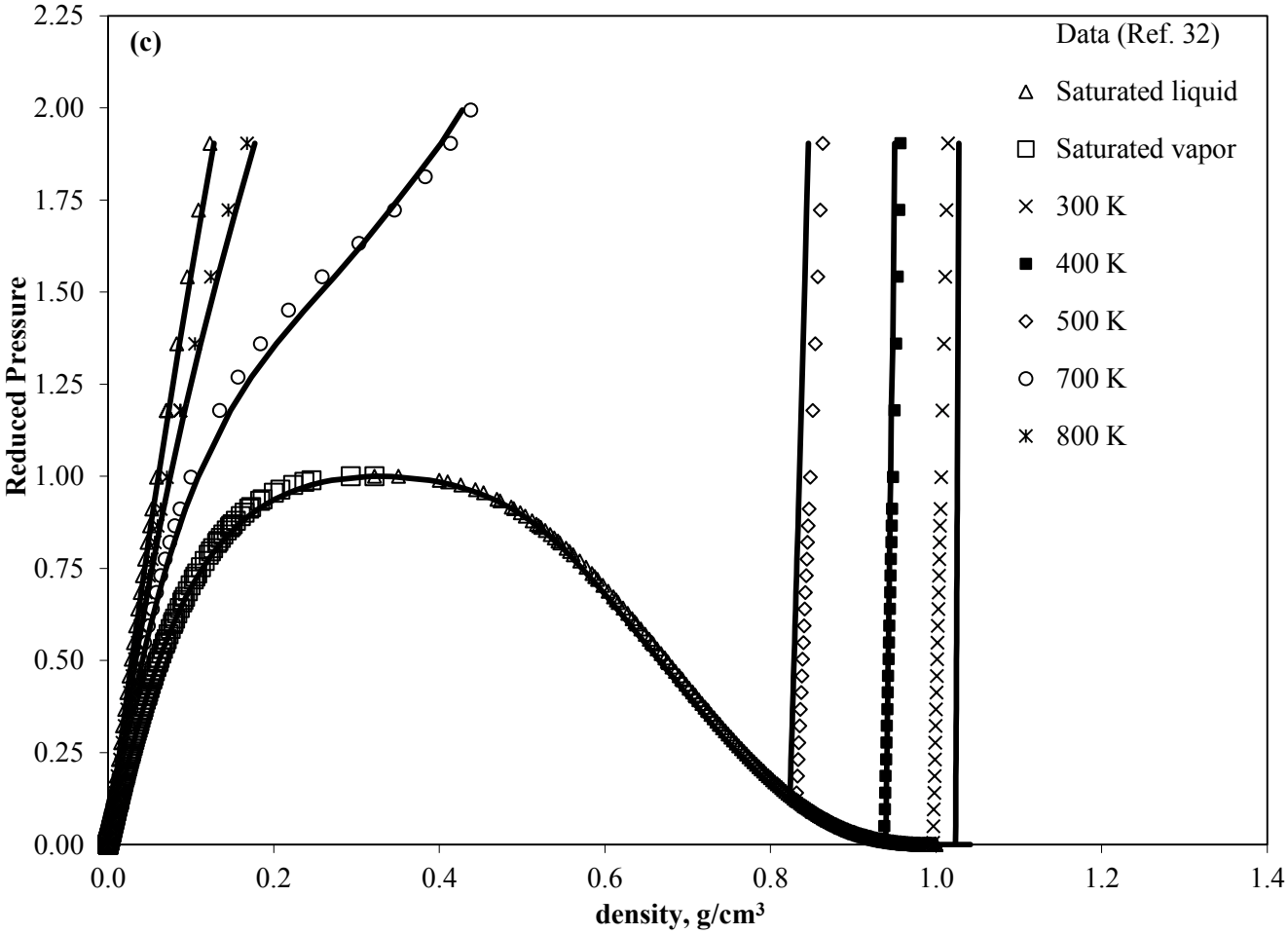

Figure 5.16(c). VTPR EOS Predictions for Water: Phase Equilibrium Calculations and Volumetric Properties

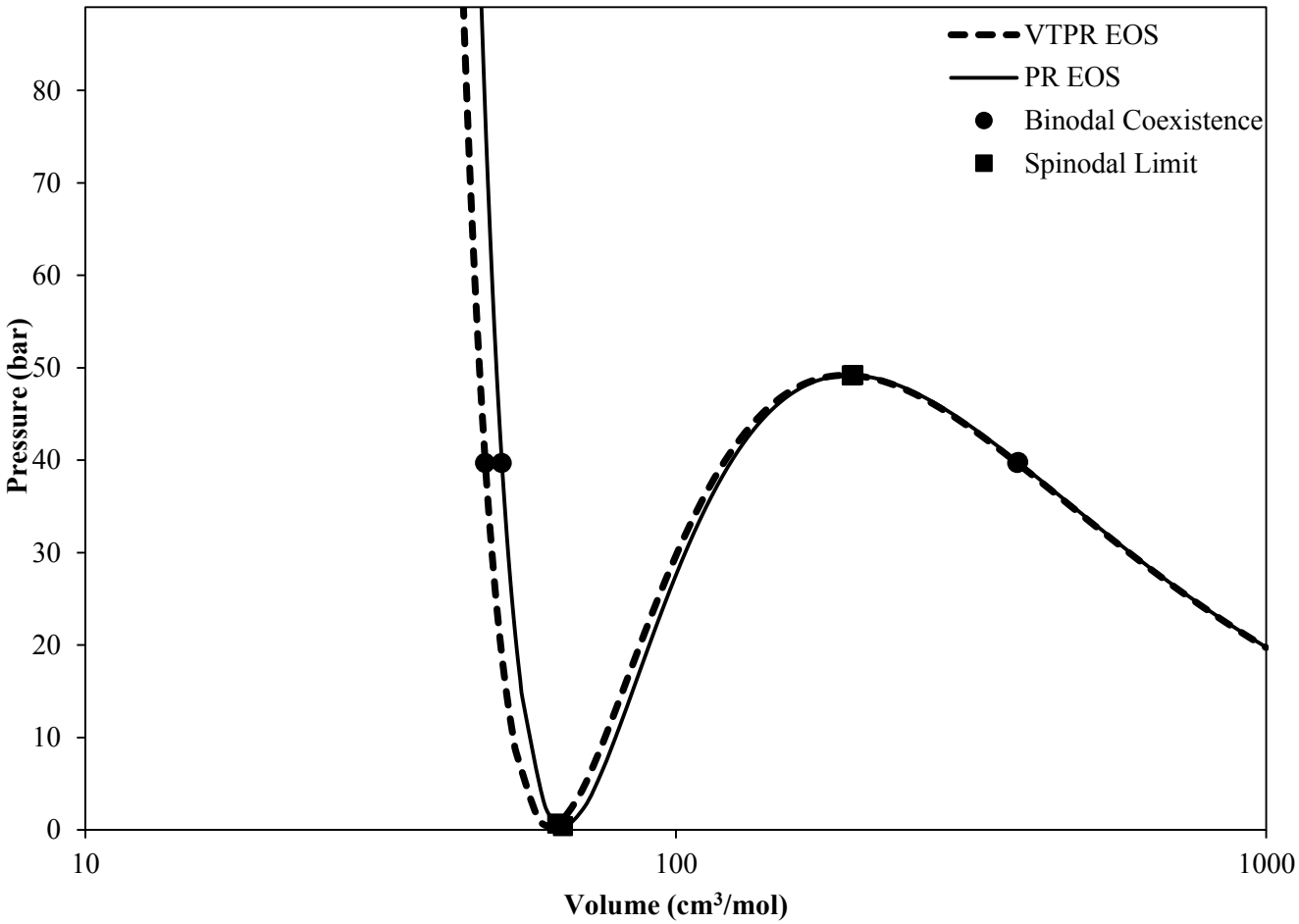

Figure 5.17. VTPR EOS Predictions for the Binodal and Spinodal Points for Carbon Dioxide at 5°C: Comparison with Original PR EOS

REFERENCES

1. G. Soave, Equilibrium constants from a modified Redlich-Kwong equation of state, Chemical Engineering Science, 27 (1972) 1197-1203.
2. D.Y. Peng, D.B. Robinson, A new two-constant equation of state, Industrial & Engineering Chemistry Fundamentals, 15 (1976) 59-64.
3. G.G. Fuller, A modified Redlich-Kwong-Soave equation of state capable of representing the liquid state, Industrial & Engineering Chemistry Fundamentals, 15 (1976) 254-257.
4. N.C. Patel, A.S. Teja, A new cubic equation of state for fluids and fluid mixtures, Chemical Engineering Science, 37 (1982) 463-473.
5. A. Harmens, H. Knapp, 3-parameter cubic equation of state for normal substances, Industrial & Engineering Chemistry Fundamentals, 19 (1980) 291-294.
6. J.O. Valderrama, L.A. Cisternas, A cubic equation of state for polar and other complex-mixtures, Fluid Phase Equilibria, 29 (1986) 431-438.
7. C.H. Twu, J.E. Coon, J.R. Cunningham, A new cubic equation of state, Fluid Phase Equilibria, 75 (1992) 65-79.
8. M.M. Abbott, Cubic equations of state, AIchE Journal, 19 (1973) 596-601.
9. R. Schmidt, W. Wagner, A new form of the equation of state for pure substances and its application to oxygen, Fluid Phase Equilibria, 19 (1985) 175-200.
10. J.J. Martin, Cubic equations of state-which?, Industrial & Engineering Chemistry Fundamentals, 18 (1979) 81-97.

11. A. Peneloux, E. Rauzy, R. Freze, A consistent correction for Redlich-Kwong-Soave volumes, Fluid Phase Equilibria, 8 (1982) 7-23.

12. H.B. de Sant'Ana, P. Ungerer, J.C. de Hemptinne, Evaluation of an improved volume translation for the prediction of hydrocarbon volumetric properties, Fluid Phase Equilibria, 154 (1999) 193-204.

13. P. Proust, E. Meyer, J.H. Vera, Calculation of pure compound saturated enthalpies and saturated volumes with the prsv equation of state - revised kappa-1 parameters for alkanes, Canadian Journal of Chemical Engineering, 71 (1993) 292-298.

14. P. Watson, M. Cascella, D. May, S. Salerno, D. Tassios, Prediction of vapor-pressures and saturated molar volumes with a simple cubic equation of state .2. The VanderWaals-711 EOS, Fluid Phase Equilibria, 27 (1986) 35-52.

15. G.F. Chou, J.M. Prausnitz, A phenomenological correction to an equation of state for the critical region, AIchE Journal, 35 (1989) 1487-1496.

16. K. Magoulas, D. Tassios, Thermophysical properties of normal-alkanes from C1 to C20 and their prediction for higher ones, Fluid Phase Equilibria, 56 (1990) 119-140.

17. J.-C. Tsai, Y.-P. Chen, Application of a volume-translated Peng-Robinson equation of state on vapor-liquid equilibrium calculations, Fluid Phase Equilibria, 145 (1998) 193-215.

18. J. Ahlers, J. Gmehling, Development of an universal group contribution equation of state: I. Prediction of liquid densities for pure compounds with a volume translated Peng–Robinson equation of state, Fluid Phase Equilibria, 191 (2001) 177-188.

19. H. Lin, Y.-Y. Duan, Empirical correction to the Peng–Robinson equation of state for the saturated region, Fluid Phase Equilibria, 233 (2005) 194-203.

20. P. Ungerer, C. Batut, Prédiction des propriétés volumétriques des hydrocarbures par une translation de volume améliorée, Oil & Gas Science and Technology - Rev. IFP, 52 (1997) 609-623.

21. J.-C. de Hemptinne, P. Ungerer, Accuracy of the volumetric predictions of some important equations of state for hydrocarbons, including a modified version of the Lee-Kesler method, Fluid Phase Equilibria, 106 (1995) 81-109.

22. H. Baled, R.M. Enick, Y. Wu, M.A. McHugh, W. Burgess, D. Tapriyal, B.D. Morreale, Prediction of hydrocarbon densities at extreme conditions using volume-translated SRK and PR equations of state fit to high temperature, high pressure PVT data, Fluid Phase Equilibria, 317 (2012) 65-76.

23. K. Liu, Y. Wu, M.A. McHugh, H. Baled, R.M. Enick, B.D. Morreale, Equation of state modeling of high-pressure, high-temperature hydrocarbon density data, The Journal of Supercritical Fluids, 55 (2010) 701-711.

24. M.A. Trebble, P.R. Bishnoi, Accuracy and consistency comparisons of ten cubic equations of state for polar and non-polar compounds, Fluid Phase Equilibria, 29 (1986) 465-474.

25. O. Pfohl, Evaluation of an improved volume translation for the prediction of hydrocarbon volumetric properties, Fluid Phase Equilibria, 163 (1999) 157-159.

26. W.R. Ji, D.A. Lempe, Density improvement of the SRK equation of state, Fluid Phase Equilibria, 130 (1997) 49-63.

27. P.M. Mathias, T. Naheiri, E.M. Oh, A density correction for the Peng—Robinson equation of state, Fluid Phase Equilibria, 47 (1989) 77-87.

28. M.C. Kutney, V.S. Dodd, K.A. Smith, H.J. Herzog, J.W. Tester, A hard-sphere volume-translated van der Waals equation of state for supercritical process modeling 1. Pure components, Fluid Phase Equilibria, 128 (1997) 149-171.

29. S. Laugier, F. Rivollet, D. Richon, New volume translation for cubic equations of state, Fluid Phase Equilibria, 259 (2007) 99-104.

30. K. Frey, M. Modell, J. Tester, Density-and-temperature-dependent volume translation for the SRK EOS: 1. Pure fluids, Fluid Phase Equilibria, 279 (2009) 56.

31. K.A.M. Gasem, W. Gao, Z. Pan, R.L. Robinson Jr, A modified temperature dependence for the Peng–Robinson equation of state, Fluid Phase Equilibria, 181 (2001) 113-125.

32. E.W. Lemmon, M.O. McLinden, D.G. Friend, Thermophysical properties of fluid systems in: P.J. Linstrom, W.G. Mallard (Eds.) NIST Chemistry WebBook, NIST Standard Reference Database Number 69, National Institute of Standards and Technology,Gaithersburg MD, 20899, http://webbook.nist.gov (retrieved October 5, 2011).

33. DIPPR, Physical and thermodynamic properties of pure chemicals, in: Project 801, 2005.

34. X.H. M. Frenkel, Q. Dong, X. Yan, R.D. Chirico, Physical Chemistry, Springer, NY, USA 2003.

35. K.A.M. Gasem, GEOS, in, Oklahoma State University, Stillwater, OK, 1988-1999.

36. B. Platzer, G. Maurer, A generalized equation of state for pure polar and nonpolar fluids, Fluid Phase Equilibria, 51 (1989) 223-236.

37. R.L. Halm, L.I. Stiel, A fourth parameter for the vapor pressure and entropy of vaporization of polar fluids, AIchE Journal, 13 (1967) 351-355.

38. S.S. Godavarthy, R.L. Robinson Jr, K.A.M. Gasem, SVRC–QSPR model for predicting saturated vapor pressures of pure fluids, Fluid Phase Equilibria, 246 (2006) 39-51.

39. S.S. Godavarthy, R.L. Robinson Jr, K.A.M. Gasem, Improved structure–property relationship models for prediction of critical properties, Fluid Phase Equilibria, 264 (2008) 122-136.

40. D. Ravindranath, B.J. Neely, R.L. Robinson Jr, K.A.M. Gasem, QSPR generalization of activity coefficient models for predicting vapor–liquid equilibrium behavior, Fluid Phase Equilibria, 257 (2007) 53-62.

41. S. Golla, S. Madihally, R.L. Robinson Jr, K.A.M. Gasem, Quantitative structure–property relationship modeling of skin sensitization: A quantitative prediction, Toxicology in Vitro, 23 (2009) 454-465.

42. CambridgeSoft, ChemBiooffice 11.0, in, 2008.

43. R. Guha, M.T. Howard, G.R. Hutchison, P. Murray-Rust, H. Rzepa, C. Steinbeck, J. Wegner, E.L. Willighagen, The blue obeliskInteroperability in chemical informatics, Journal of Chemical Information and Modeling, 46 (2006) 991-998.

44. M. Stievano, N. Elvassore, High-pressure density and vapor–liquid equilibrium for the binary systems carbon dioxide–ethanol, carbon dioxide–acetone and carbon dioxide–dichloromethane, The Journal of Supercritical Fluids, 33 (2005) 7-14.

45. T.A. Halgren, Merck molecular force field. I. Basis, form, scope, parameterization, and performance of MMFF94, Journal of Computational Chemistry, 17 (1996) 490-519.

46. P. Stringari, G. Scalabrin, D. Richon, Compressed and saturated liquid densities for the 2-propanol + water system, Journal of Chemical & Engineering Data, 53 (2008) 1789-1795.

47. DRAGON Professional 5.5, Talete SRL, in, 2010.

48. H. Demuth, M. Beale, M. Hagan, Neural Network Toolbox, MathWorks, Inc., 2010.

49. M.S. Iyer, R.R. Rhinehart, A method to determine the required number of neural-network training repetitions, Neural Networks, IEEE Transactions on, 10 (1999) 427-432.

50. D. Nguyen, B. Widrow, Improving the learning speed of 2-layer neural networks by choosing initial values of the adaptive weights, in: Proceedings of the International Joint Conference on Neural Networks, 1990, pp. 21–26.

51. V.L. Bhirud, A four-parameter corresponding states theory: Saturated liquid densities of anormal fluids, AIchE Journal, 24 (1978) 880-885.

52. G.Z.A. Wu, L.I. Stiel, A generalized equation of state for the thermodynamic properties of polar fluids, AIchE Journal, 31 (1985) 1632-1644.

53. H. Toghiani, D.S. Viswanath, A cubic equation of state for polar and apolar fluids, Industrial & Engineering Chemistry Process Design and Development, 25 (1986) 531-536.

54. J.M. Prausnitz, R.N. Lichtenthaler, E.G. Azevedo, Molecular thermodynamics of fluid-phase equilibria, 3rd ed., Prentice-Hall, New Jersey, 1999.

55. DRAGON Professional 6, Talete SRL., in, 2010.

56. L. Hnědkovský, I. Cibulka, On a temperature dependence of the van der Waals volume parameter in cubic equations of state, Fluid Phase Equilibria, 60 (1990) 327-332.

57. W.G. Chapman, K.E. Gubbins, G. Jackson, M. Radosz, New reference equation of state for associating liquids, Industrial & Engineering Chemistry Research, 29 (1990) 1709-1721.

58. W.G. Chapman, G. Jackson, K.E. Gubbins, Phase equilibria of associating fluids: chain molecules with multiple bonding sites, Molecular Physics, 65 (1988) 1057-1079.

59. S.H. Huang, M. Radosz, Equation of state for small, large, polydisperse, and associating molecules, Industrial & Engineering Chemistry Research, 29 (1990) 2284-2294.

60. J. Gross, G. Sadowski, Perturbed-Chain SAFT: An equation of state based on a perturbation theory for chain molecules, Industrial & Engineering Chemistry Research, 40 (2001) 1244-1260.

61. R.C. Reid, J.M. Prausnitz, B.E. Poling, The properties of gases and liquids, fourth ed., McGraw-Hill, 1987.

CHAPTER VI

VOLUME-TRANSLATED PENG-ROBINSON EQUATION OF STATE FOR LIQUID DENSITIES OF DIVERSE BINARY MIXTURES[4]

6.1 Introduction

Reliable, accurate thermodynamic models are necessary for design of chemical processes and for reservoir simulations in the petroleum and natural gas industry. Due to their inherent simplicity and computational efficiency, cubic equations of state (CEOS) such as the Soave-Redlich-Kwong (SRK) [1] and Peng-Robinson (PR) equations of state [2] are widely used in process design and reservoir simulations. However, a well-known deficiency in the two-parameter cubic equations of state is their inaccurate liquid density predictions. To address this problem, a translation in the calculated volume is frequently employed. Beginning with the works of Martin [3] and Peneloux et al. [4], several volume-translation approaches have been proposed in the literature. These range from a constant correction term to more complex forms that are both temperature and density-dependent [3-16]. In a recent work [17], we presented a new volume-translation function based on the dimensionless-distance approach of Mathias et al. [13] and Chou and Prausnitz [7]. The new volume-translation function contains only one fluid-specific parameter, and we have generalized this parameter in terms of molecular properties such as critical compressibility factor, acentric factor and dipole moment [17].

[4] The material in this chapter has been reproduced with permission from A.M. Abudour, S.A. Mohammad, R.L. Robinson Jr., K.A.M. Gasem, Volume-translated Peng-Robinson equation of state for liquid densities of diverse binary mixtures, Fluid Phase Equilibria, 349 (2013) 37-55.

The new volume-translated Peng-Robinson equation of state (VTPR EOS) provides accurate predictions of liquid densities in *both* the saturated- and single-phase regions for pure fluids of diverse classes of molecules. In addition, the VTPR EOS does not lead to thermodynamic inconsistencies, such as isotherm cross-overs in the compressed liquid region at high pressures, which were observed in some of the temperature-dependent methods in the literature [18].

An important aspect of volume-translation methods is their extension to mixtures. Apart from Peneloux's work [4], only a few volume-translation methods in the literature have been extended to mixtures. Tsai and Chen [14] and Lin and Duan [11] extended their volume-translation methods to mixtures, but only for atmospheric pressure conditions. Since most volume-translation methods available in the literature have been developed and tested only for pure fluids, a need exists for a reliable volume-translation method that can provide accurate predictions of saturated- and single-phase liquid densities for mixtures. Therefore, in this work, we extend the VTPR EOS from our previous work [17] to predict densities of diverse mixtures over large ranges of pressure and temperature. As is shown herein, the VTPR EOS appears capable of providing accurate predictions of liquid densities for binary mixtures comprised of diverse molecular species.

As discussed elsewhere [7], a successful application of volume translation to mixtures requires a satisfactory description of phase equilibria of the mixtures. Thus, in this work, we assembled both binary vapor-liquid equilibrium and mixture density data for the systems studied. One-fluid mixing rules fitted with regressed binary interaction parameters were used to obtain satisfactory description of vapor-liquid equilibria. Aside from these binary interaction parameters, the volume-translation method was extended

to mixtures to predict liquid densities without any further parameter fitting and/or regressions.

Numerous mixing rules for EOS parameters have been proposed [19-24]. However, the one-fluid mixing rules are simple and relatively accurate for many systems. The CEOS with these mixing rules can be utilized to represent several systems within the experimental precision in many applications [21]. Although these simple mixing rules are not as robust as theoretically-based mixing rules, such as Wong-Sandler mixing rules [23], in representing asymmetric mixtures [25], their simplicity continues to make them attractive, especially when binary interaction parameters (BIPs) are utilized. Therefore, we elected to use the classical one-fluid mixing rules in this study for describing the vapor-liquid equilibria of binary mixtures.

Although the VTPR EOS in this work is based on the dimensionless distance function approach of Chou and Prausnitz [7], this work differs from that of Chou and Prausnitz in several aspects. In particular, the method presented here

1. Does not require the additional complexity of a non-classical contribution to the Helmholtz energy.
2. Does not require mixture critical point calculations with the Heidmann and Khalil method [26] as part of the volume translation for mixtures.
3. Does not lead to isotherm cross-overs in the single-phase region at high pressures, as were observed in the original method.
4. Includes evaluations over comprehensive databases of vapor-liquid equilibrium and volumetric properties of diverse binary mixtures.
5. Includes evaluations in both the single-phase and saturated regions of the phase diagram.

Our analysis had shown that most temperature-dependent volume translation methods produce thermodynamic inconsistencies such as isotherm cross-overs in the single-phase region at higher pressures. In our earlier study on volume translation for pure fluids [17], an approach was presented that eliminates these inconsistencies. The current study includes that approach as part of the volume translation for mixtures. Further, Chou and Prausnitz applied a non-classical contribution to the Helmholtz energy in their study to improve the volume translation function in the vicinity of the critical point. However, as they noted [7], the non-classical contribution plays only a marginal role in volume translation for *mixtures*. Thus, we did not include the non-classical contribution in our study. In addition, the original method from Chou and Prausnitz involved mixture critical point calculations with the Heidmann and Khalil algorithm [26] at each composition as part of the volume translation for mixtures. Since numerous calculations of mixture critical points were required in the original method, we elected to apply the correlations presented by Chueh and Prausnitz [27] in an earlier study for estimating critical properties of mixtures. These correlations provide reasonably accurate estimates of mixture critical points for the purposes of volume translation. Thus, these modifications were introduced in the method presented in this study.

As mentioned previously, only few volume translation methods in the literature have been extended to mixtures. To our knowledge, a comprehensive analysis of volume translation for diverse binary mixtures over wide ranges of pressure and temperature has not been presented in the literature. In this study, the volume translation has been

1. Applied to predict mixture densities in *both* saturated- and single-phase regions over large ranges of pressure and temperature.

2. Applied to binary mixtures of diverse molecules ranging from simple, non-polar mixtures to mixtures containing highly-polar, asymmetric, aromatic and/or hydrogen-bonded fluids.
3. Employed to develop a unified framework for describing both vapor-liquid equilibria and phase densities of liquid mixtures.

The following sections are organized as follows. Section 6.2 presents the PR EOS model, the mixing rules, extension of the VTPR EOS to mixtures and details of the database employed. Section 6.3 discusses the results obtained for describing vapor-liquid equilibria and predicting liquid densities of the systems studied, Section 6.4 compares the performance of the current method with two other volume translation methods from the recent literature and Section 6.5 addresses phase equilibrium (P-T-ρ) calculations from our method.

6.2 Peng-Robinson Equation of State (PR EOS)

The Peng-Robinson equation of state (PR EOS) [2] is given as

$$p = \frac{RT}{v-b} - \frac{a(T)}{v(v+b)+b(v-b)} \tag{6.1}$$

where

$$a(T) = \frac{0.457535\alpha(T)R^2T_c^2}{p_c^2} \tag{6.2}$$

$$b = \frac{0.077796\,RT_c}{p_c} \tag{6.3}$$

where p is the pressure, T is the temperature, v is the molar volume, a and b are EOS parameters, T_c is the critical temperature, p_c is the critical pressure and R is the universal

gas constant. The term α(T) in Equation (6.2) was calculated with the following expression developed in our earlier work [28]

$$\alpha(T) = \exp\left(\left(A + BT_r\right)\left(1 - T_r^{C+D\omega+E\omega^2}\right)\right) \tag{6.4}$$

where ω is the acentric factor, T_r is the reduced temperature and A through E are correlation parameters with values of 2.0, 0.836, 0.134, 0.508 and -0.0467, respectively.

6.2.1 Mixing Rules

To apply the PR EOS to mixtures, classical one-fluid mixing rules were employed to calculate the values of a and b of the mixtures, as given by [29]

$$a = \sum_i \sum_j z_i z_j a_{ij} \tag{6.5}$$

$$b = \sum_i \sum_j z_i z_j b_{ij} \tag{6.6}$$

with the following combining rules

$$a_{ij} = \sqrt{a_i a_j}\left(1 - C_{ij}\right) \tag{6.7}$$

$$b_{ij} = \frac{\left(b_i + b_j\right)}{2}(1 + D_{ij}) \tag{6.8}$$

where z is the mole fraction of compound i in the phase of interest. The C_{ij} and D_{ij} in equations (6.7) and (6.8) are empirical "binary interaction parameters (BIPs)" that are determined from experimental vapor-liquid equilibrium data. These parameters account for deviations from simple combination rules for the EOS parameters. The simplest and most direct procedure is to use a single interaction parameter, C_{ij}, and frequently it is sufficient for the purpose. The binary interaction parameters, C_{ij} and D_{ij}, have values typically near zero for mixtures of non-polar

compounds of similar molecular size. However, non-zero values of C_{ij} and D_{ij} are generally required in the phase-equilibrium calculations for mixtures consisting of compounds with large differences in molecular size and shape and for mixtures containing polar compounds such as water [30]. Although several other mixing rules have been advanced [19-24], the classical mixing rules are used more frequently in EOS applications due to their simplicity.

6.2.2 Volume-Translated Peng-Robinson Equation of State (VTPR EOS)

The volume translation method for pure fluids developed in our previous work [17] was extended to mixtures in this study. For completeness, we briefly describe the volume translation function for pure fluids and then present its extension to mixtures.

6.2.2.1 Volume-Translation Function for Pure Fluids

A general volume-translation term for the equation of state can be represented as

$$v_{VTPR} = v_{PR} + c \tag{6.9}$$

where v_{VTPR} and v_{PR} are the translated and untranslated molar volumes and c is the volume-translation term.

To estimate the correction term for the volume, a dimensionless distance approach was suggested independently by Chou and Prausnitz [7] and Mathias et al. [13]. The dimensionless distance function, d, is given as [7]

$$d = \frac{1}{RT_c}\left(\frac{\partial p^{PR}}{\partial \rho}\right)_T \tag{6.10}$$

where T_c is the experimental critical temperature and ρ is the molar density. Further, the distance function, d, is calculated from the untranslated PR EOS to avoid iterative solutions. The

introduction of this parameter was designed primarily to improve results in the near-critical region, where cubic equations are known to have inherent inadequacies.

The distance function given by Equation (6.10) is constrained to be only temperature-dependent in the saturated region. In other words, the distance function is evaluated at saturated-liquid phase condition and is then used for translating *both* saturated liquid and vapor densities. Importantly, this ensures that the pure-fluid vapor pressures predicted by the original PR EOS are preserved [4, 7].

The volume-translation function is defined as [7]

$$v_{VTPR} = v_{PR} + c - \delta_c\left(\frac{0.35}{0.35 + d}\right) \tag{6.11}$$

In Equation (6.11), 0.35 is a universal constant for all fluids and δ_c is the volume correction at the critical temperature and is given as

$$\delta_c = \left(\frac{RT_c}{p_c}\right)\left(z_c^{EOS} - z_c^{exp}\right) \tag{6.12}$$

where T_c, p_c and z_c^{exp} are the experimental critical temperature, pressure and compressibility factor, respectively. Further, z_c^{EOS} has a universal value of 0.3074 for the PR EOS.

A new expression was developed in our earlier work [17] for the volume-translation term, c, appearing in Equation (6.11). The expression is given as

$$c = \left(\frac{RT_c}{p_c}\right)\left(c_1 - (0.004 + c_1)\exp(-2d)\right) \tag{6.13}$$

where c_1 is a *constant, specie-dependent* parameter and d is the distance function given by Equation (6.10). Thus, the volume-translation method presented above contains only one specie-specific parameter, c_1.

The parameter c_1 was generalized in terms of molecular properties such as critical compressibility factor (z_c), acentric factor and dipole moment. As described in our previous work on pure fluids, three different case studies were constructed for the generalization of pure-component c_1 [17]. In Case 1, the c_1 parameter was generalized in terms of the critical compressibility factor of each fluid, z_c. The generalized relation developed in Case 1 is given as

$$c_1 = 0.4266 z_c - 0.1101 \tag{6.14}$$

In Cases 2 and 3, neural network models were developed for generalizing c_1. Additional details on this development can be found in our previous work [17]. In this study, we have utilized the generalized values of the pure-component parameter, c_1.

6.2.2.2 Extension of Volume-Translation Function to Mixtures

The volume-translation method described above was extended to mixtures by adopting the same dimensionless distance function approach presented by Chou and Prausnitz [7]. Thus, the volume translation for mixtures is given as

$$v_{VTPR} = v_{PR} + c_m - \delta_{c_m}\left(\frac{0.35}{0.35 + d_m}\right) \tag{6.15}$$

where v_{VTPR} and v_{PR} are the translated and untranslated molar volumes and c_m is volume-translation term for mixtures and is given as

$$c_m = \left(\frac{RT_{cm}}{p_{cm}}\right)\left(c_{1m} - \left(0.004 + c_{1_m}\right)\exp\left(-2d_m\right)\right) \tag{6.16}$$

A linear mixing rule was used for c_{1_m} as proposed by Peneloux et al. [4]

$$c_{1_m} = \sum x_i c_{1_i} \tag{6.17}$$

where c_{1_i} is a specie-dependent parameter.

The dimensionless distance function for a binary mixture, d_m, is defined based the stability criterion and is given as [7]

$$d_m = \frac{1}{RT_{cM}}\left(\frac{\partial p^{PR}}{\partial \rho}\right)_T - \left(\frac{1}{RT_{cm}\rho^2}\right)\frac{a_{v1}^2}{a_{11}} \tag{6.18}$$

where T_{cm} is the critical temperature of the mixture, ρ is the molar density of the mixture, a is molar Helmholtz energy and the subscripts denote differentiation variables. In particular, the subscript v indicates differentiation with molar volume and subscript 1 indicates differentiation with the mole fraction of component 1. Similar to the case for pure fluids, the distance function, d_m, for mixtures is also calculated from the untranslated PR EOS to avoid iterative solutions. Note that in the limit of either pure 1 or pure 2, a_{11} becomes infinite and d_m reduces to distance, d, for a pure fluid [7]. The expressions for a_{v1} and a_{11} were derived based on the equations for Helmholtz energy derivatives found elsewhere [31].

In Equation (6.15), δ_{c_m} is the volume correction for a mixture at the critical point and is a function only of composition, x

$$\delta_{c_m} = v_{c_m}^{PR}(x) - v_{c_m}(x) \tag{6.19}$$

where $v_{c_m}^{PR}(x)$ is the mixture critical volume predicted from the PR EOS and $V_{c_m}(x)$ is the true critical volume.

The mixture critical volume, $v_{c_m}^{PR}(x)$ was calculated as

$$v_{c_m}^{PR}(x)=\left(\frac{RT_{c_m}}{p_{c_m}}\right)\left(z_c^{EOS}\right) \tag{6.20}$$

where T_{c_M} and p_{c_M} are the mixture critical temperature and pressure. For simplicity, z_c^{EOS} in Equation (6.20) was fixed at 0.3074 for the PR EOS.

The mixture true (experimental) critical volume was estimated by the following equation [27]

$$v_{c_m}(x)=\sum_i \theta_i v_{c_i} \tag{6.21}$$

where v_{c_i} is the critical volume of pure compound i and θ_i is the surface fraction of compound i defined as

$$\theta_i = \frac{x_i v_{ci}^{2/3}}{\sum_i x_i v_{ci}^{2/3}} \tag{6.22}$$

where x_i is mole fraction of compound i.

The critical temperature of the mixture, $T_{cm,}$ is calculated as proposed by Chueh and Prausnitz [27]:

$$T_{cm}=\sum_i \theta_i T_{ci} \tag{6.23}$$

where T_{ci} is the critical temperature of pure compound i.

The critical pressure of the mixture, $p_{cm,}$ is calculated using the correlation by Aalto et al. [32]:

$$p_{cm} = \frac{(0.2905\text{-}0.085\omega_m)RT_{cm}}{v_{cm}} \tag{6.24}$$

where ω_m is the acentric factor of the mixture and is calculated by the following equation

$$\omega_m = \sum_i x_i \omega_i \tag{6.25}$$

where ω_i is the acentric factor of compound i.

Similar to the case for pure fluids, the distance function given by Equation (6.18) and δ_{cm} given by Equation (6.19) are evaluated at saturated liquid phase conditions for translating both liquid and vapor densities in the saturated region. Further, the distance function and δ_{cm} in the single-phase region are calculated at the pressure and temperature of interest.

6.2.3 Databases Employed

Two databases were assembled for conducting this study. The first database contains vapor-liquid equilibrium data for binary mixtures that were included in this study. The second database is comprised of saturated- and single-phase liquid densities of binary mixtures. Details of the sources of binary vapor-liquid experimental data, along with the temperature, pressure and composition range for each binary system can be found in Table B.1 of the Appendix B. (Note that all tables with a B prefix appear in the Appendix B.) Overall, the database for vapor-liquid equilibrium measurements contains more than 5,000 data points. The database of liquid density measurements for

73 binary systems was compiled from experimental data in the literature and is documented in Table 6.1. The table lists the ranges of temperature, pressure, liquid phase composition and densities, together with the sources of data for liquid densities. Both saturated- and single-phase liquid densities for mixtures are included, depending on their availability from the original authors. Overall, this database for densities of liquid mixtures contains more than 13,000 data points.

As evident from Table 6.1, the database used in this study includes binary systems composed of diverse molecular species. Specifically, the database includes systems containing CO_2 (e.g., CO_2 + water), systems containing alcohols and ammonia with water (e.g., methanol + water and ammonia + water), systems containing acetone (e.g., acetone + alkane), systems containing refrigerant mixtures (e.g., R32 + R125), systems containing alkanes and/or cycloalkanes (e.g., propane + butane and cyclohexane + octane), systems containing benzene (e.g., benzene + methanol) and systems containing methane and nitrogen (e.g., methane + nitrogen). Overall, these binary systems cover a wide range in terms of molecular size, asymmetry and polarity and, thus, are well suited to test the efficacy of our approach.

6.2.4 Data Reduction

Binary interaction parameters for the binary systems were regressed using the large database documented in the Supplementary Material. Since the focus of this study is on liquid densities, only measured pressures, temperatures and liquid compositions (p-T-x) were used in the data reduction to determine the BIPs. The regressions were performed using an objective function, OF, which minimizes the sum of squared relative deviations in the predicted bubble-point pressures, as given below

$$OF=\sum_{i=1}^{NDP}\left(\frac{p_{cal}-p_{exp}}{p_{exp}}\right)_i^2 \tag{6.26}$$

where NDP is the number of data points, p_{exp} and p_{cal} are the experimental and calculated bubble-point pressures, respectively. A non-linear regression procedure based on the Marquardt [33, 34] method was utilized in this work. The results are presented and analyzed in terms of the average absolute percentage deviations (%AAD) and percentage deviations (%DEV) given as

$$\% \text{ AAD} = \frac{100}{\text{NDP}} \sum_{i=1}^{\text{NDP}} \left| \frac{M_{cal} - M_{exp}}{M_{exp}} \right|_i \tag{6.27}$$

$$\% \text{ DEV} = \frac{100}{\text{NDP}} \sum_{i=1}^{\text{NDP}} \left(\frac{M_{cal} - M_{exp}}{M_{exp}} \right)_i \tag{6.28}$$

where M_{cal} and M_{exp} are the calculated and experimental properties, respectively.

6.3 Results and Discussion

In this section, the capabilities of (a) the PR EOS to represent the vapor-liquid equilibrium of binary mixtures, and (b) the VTPR EOS to predict the liquid densities of binary mixtures are discussed. The PR and VTPR EOS were applied to 73 binary systems that include near-ideal through highly non-ideal systems. An equilibrium algorithm, GEOS [35], was utilized to conduct bubble-point pressure calculations for these systems. Further, the same algorithm was utilized to evaluate the liquid densities of the binary systems with the use of the VTPR EOS.

Several cases were investigated to test the capability of the PR EOS to represent the phase equilibria of binary mixtures. The case studies varied in terms of the number and types of BIPs used. Specifically, the cases involved the inclusion of a single, temperature-independent parameter C_{ij}, the addition of a second temperature-independent parameter, D_{ij}, and finally, a temperature-dependent C_{ij} was also considered. Our analysis showed that the use of a single temperature-independent

parameter C_{ij} provides reasonable predictions for bubble-point pressures of the systems studied. First, using a temperature-independent C_{ij} reduces the complexity with only a minor loss of accuracy in predictions. Second, using a single interaction parameter eliminates parameter inter-correlation that invariably exists when using multiple interaction parameters in the equation of state. The single exception is the CO_2 + water system, where a temperature-dependent C_{ij} and a constant D_{ij} (see Table B.2) produced significantly better representations.

Table 6.2 presents the summary results for the bubble-point pressure predictions. The table lists the binary systems, the number of data points (NDP) and the percentage absolute average deviation (%AAD) for the bubble-point pressures obtained, with and without using the BIPs. As evident from Table 6.2, the predictions improve for most binary systems when BIPs are used (as expected). Overall, the BIPs provided predictions with 2.3 %AAD compared to about 19% AAD when no BIPs are used. The largest improvement was obtained for systems containing CO_2, systems containing mixtures of alcohol or ammonia with water and systems containing acetone. In contrast, binary mixtures containing similar class of molecules such as alkanes or cycloalkanes or refrigerants produced reasonable results without the use of BIPs. Detailed information on bubble-point pressure predictions as well as values of BIPs for the entire database is provided in the Supplementary Material. Further, a brief discussion of these results is also provided for specific binary systems in the next section.

Our previous work on liquid density predictions for pure fluids had shown that all three generalized cases developed in that work provided comparable predictions for liquid densities of pure fluids [17]. However, when a combination of accuracy, simplicity and ease of use is considered, Cases 1 and 2 of that work appeared to be appropriate choices. Thus, both Case 1 (c_1 linear in z_c) and Case 2 (c_1 from neural network model

using molecular descriptors z_c, ω, and dipole moment) from our earlier work have been applied for the extension of density predictions to mixtures reported in this work.

The following sections contain results obtained through the use of PR EOS for vapor-liquid equilibrium calculations and VTPR EOS for mixture liquid density calculations. The discussion is organized to highlight examples of specific binary systems selected based on either their industrial importance or their unique characteristics such as asymmetry, polarity and hydrogen-bonded/association.

6.3.1 Systems Containing CO_2

Table B.2 lists the bubble-pressure predictions for systems containing CO_2. For CO_2 + water system, the inclusion of BIPs improved the results significantly (about 6 %AAD) relative to the case when no BIPs were used (about 48 %AAD). For this system, a detailed study was made in a recent work [36] to ascertain the capability of the PR EOS to represent the vapor-liquid equilibrium of this system. Our analysis [36] showed that the inclusion of a temperature-dependent C_{ij} along with a constant D_{ij} of -0.21 was needed for this binary system.

Table 6.3 presents the VTPR EOS predictions for saturated and single-phase liquid densities for the systems containing CO_2. Overall, the VTPR EOS provided predictions with 1.6 and 2 %AAD for Cases 1 and 2, respectively. In comparison, the original, untranslated PR EOS yielded predictions with about 12 %AAD.

Figure 6.1 illustrates the distribution of errors in the predicted single-phase liquid density for CO_2 + water binary system at two temperatures. The VTPR EOS predictions (shown only for Case 1 for all systems presented graphically) indicate a marked improvement over PR EOS with a reduction in deviations from about 13 to 2% for both isotherms over the range of pressures in Figure 6.1.

6.3.2 Mixtures of Alcohols or Ammonia with Water

Highly polar and hydrogen-bonding mixtures are known to pose a serious challenge to cubic equations of state. In this work, good predictions are shown for bubble-point pressures of complex systems (alcohol + water and ammonia + water) for the PR EOS with one-fluid mixing rules. Table B.3 shows the predictions of bubble-point pressures of binary systems containing mixtures of alcohol or ammonia with water. Figure 6.2 presents the results for the methanol + water binary system and provides an example of the influence of the BIP on vapor-liquid equilibrium calculations for a highly polar, hydrogen-bonded system. Figures 6.2(a) to (d) present the distribution of errors in the bubble-point pressure predictions. When no BIP is used, deviations of up to 60% were observed.

Table 6.4 presents the corresponding VTPR EOS predictions for single-phase liquid densities. Both Cases 1 and 2 of the VTPR EOS provided an overall error of about 2.5 and 3.3 %AAD with and without BIPs, respectively. The inclusion of BIPs provided an improvement to the density predictions for ammonia + water systems. In contrast, the alcohols + water systems showed minimal effect for the use of a BIP. Figure 6.3 presents the distribution of errors in the single-phase liquid density predictions for methanol + water and ammonia + water systems.

6.3.3 Systems Containing Acetone

Table B.4 shows the predictions of bubble-point pressures of these systems. Similar to most systems discussed above, the use of a single, temperature-independent BIP provided improved predictions of bubble pressures. Table 6.5 presents the VTPR EOS predictions for single-phase liquid densities for these binary systems. Errors of 8 and 1.3 %AAD were obtained for the PR and VTPR EOS, respectively. Figures 6.4(a)-(d)

illustrate the distribution of errors in the single-phase liquid density predictions for acetone(1) + heptane(2), acetone(1) + decane(2), acetone(1) + benzene(2), acetone(1) + toluene(2), respectively. Overall, the errors in density predictions from the VTPR EOS were as much as six times lower than the errors from the original, untranslated PR EOS.

6.3.4 Systems Containing Refrigerants

The binary systems composed of refrigerant mixtures are of interest in applications dealing with refrigerants as heat transfer fluids. Table B.5 presents the predictions of bubble-point pressures of the binary refrigerant mixtures. Since these binary systems contain relatively similar molecules, only marginal improvement is obtained, in general, in the bubble-point pressure predictions with the use of a BIP. However, a closer inspection of the results showed that the use of a BIP provided large improvement in the predictions for two binary systems. Specifically, the binary mixtures formed by R11 + R22 and R12 + R32 showed large reduction in errors when a single BIP was used. As shown in Table B.5, the inclusion of a BIP reduced the errors in bubble-point pressure predictions from 9 to 1.4 %AAD for R11 + R22 and from 15 to 2 %AAD for R12 + R32 systems. This could be attributed to the difference in polarity of the two molecules forming these mixtures. The dipole moments of all binary systems in Table B.5 were analyzed, revealing that when the *difference* in dipole moments of the two molecules was greater than about 0.5 debye, a single BIP provided a significant reduction in errors for these systems. All other binary systems in Table B.5 were composed of molecules with similar dipole moments.

Table 6.6 presents VTPR EOS predictions for saturated- and single-phase liquid densities for systems containing refrigerants. For the purposes of illustration, Figures 6.5(a) to (d) present the distribution of errors in liquid density predictions for R32(1) + R125(2) and R11(1) + R22(2) systems. Overall, the liquid density predictions for these

systems contained errors of about 1.8 %AAD for the VTPR EOS which is about four times lower than the errors from the PR EOS.

6.3.5 Systems Containing Alkanes and/or Cycloalkanes

Simple binary systems such as those containing mixtures of homologous alkanes or cycloalkanes were also analyzed for comparative purposes. Table B.6 shows the bubble-point pressure predictions for these systems. As expected, the PR EOS provides reasonable predictions in representing binary mixtures of alkanes and/or cycloalkanes without the use of a BIP. Nevertheless, the inclusion of a small BIP (in magnitude) provides predictions with roughly one-half the error than those without a BIP.

Table 6.7 presents the liquid density predictions from the VTPR EOS. The inclusion of a BIP has no effect on liquid density predictions for these systems. The VTPR EOS predicted the liquid densities of these binary systems with three times less error than the untranslated PR EOS. Figures 6.6(a) to (d) illustrate the error distribution of saturated liquid densities for binary systems composed of ethane, propane, butane and isobutane. Although the PR EOS provided reasonable predictions for the bubble-point pressures of these non-polar systems, the deviations for saturated liquid densities of these hydrocarbon systems were about 5%. In comparison, the VTPR EOS yielded predictions that were within about 1% AAD.

6.3.6 Systems Containing Benzene

Table B.7 contains the results of bubble-point pressure predictions for systems containing benzene. The binary mixtures of benzene with alcohols showed a marked improvement in bubble-point pressure predictions when a single BIP was included. For example, the benzene + butanol system yielded 1.3 and 18 %AAD with and without a BIP; other benzene + alcohol mixtures in Table B.7 also showed large reduction in

errors with the inclusion of a single BIP. In contrast, mixtures of benzene with alkanes that contained six to eight carbon atoms showed only marginal improvement in predictions when a single BIP was used.

Table 6.8 presents the corresponding VTPR EOS predictions obtained for liquid densities for these binary systems. The predictions for these systems appear insensitive to the inclusion of a BIP. Overall, the VTPR EOS predictions showed a slight improvement over the PR EOS with a reduction from 2.2 to 1.1 %AAD.

6.3.7 Systems Containing Mixtures of Methane or Nitrogen

Table B.8 presents the summary results for bubble pressure predictions for these systems. Interestingly, the inclusion of a small BIP provides improved predictions even for these relatively non-polar systems. For example, predictions for the methane + butane system have 1.3 and 3.4 %AAD with and without the use of a BIP. Further, binary mixtures of nitrogen with ethane, butane and cyclohexane contained much larger errors (with no BIPs) compared with the corresponding mixtures of these compounds with methane.

Table 6.9 presents the VTPR EOS predictions for saturated and single-phase liquid densities for these binary systems. The liquid density predictions are insensitive to BIPs, unlike the case for bubble pressure predictions for some of these systems. Overall errors of 1.4 and 7.6 %AAD were observed for the VTPR and PR EOS, respectively. For illustration purposes, Figures 6.7(a) and (b) present the distribution of errors in the predicted bubble-point pressures as a function of temperature and pressure, respectively, for methane(1) + nitrogen(2). Further, the errors in liquid densities for this binary system are illustrated in Figures 6.7(c) and (d).

6.4 Comparison of Liquid Mixture Density Predictions from Different Methods

In this section, we present comparisons of the liquid mixture density predictions from different methods. Specifically, we compared our generalized method with two other volume translation methods for the PR EOS from the recent literature. For this comparison, a total of 29 binary systems were selected for comparison over wide pressure and temperature ranges. These binary systems were selected from the different categories of binary mixtures (discussed in the previous section) and at least two binary systems were included from each category of mixtures. Thus, the binary systems ranged from simple, non-polar mixtures to highly-polar and hydrogen-bonded mixtures. Table 6.10 documents the binary systems used for comparison and also lists the pressure and temperature ranges for each binary system. Using these systems, predictions were obtained using the PR EOS for each volume translation method using the mixing rules employed by the original authors of the two literature methods. Further, predictions for both cases (with and without BIPs) were obtained for all the methods.

Table 6.11 presents the summary results for the comparison of liquid mixture density predictions from different methods. In particular, the literature methods of Lin and Duan [11] and Tsai and Chen [14] were used for comparisons. Predictions with the untranslated PR EOS are also listed in Table 6.11. As evident from the table, the volume translation method reported in this work is capable of providing about three to four times improved generalized predictions for the systems in Table 6.11, on average. We note, however, that the literature methods were optimized and then generalized based on databases that differ from that used in the present study. Therefore, the predictions from the literature methods can be expected to be less than optimal for the database used in this study. The comparisons provided here are intended to serve only as a guide to the relative accuracies of these methods when applied to the binary

mixtures in our database. Further, detailed comparisons with these methods for pure components were reported in our earlier work on pure-fluid volume translation [17] .

One of the parameters in the volume translation method of Tsai and Chen [14] has a unique value for each fluid. Since this parameter was not generalized by the original authors, predictions for five of the 29 mixtures in Table 6.11 could not be obtained with their method. Overall, the literature methods provided predictions with an overall error of 4.7 to 6.1 %AAD. In contrast, the method presented in this work provided predictions with an overall error of 1.7 %AAD. Further, the method presented in this study does not lead to any isotherm cross-overs in the single-phase region unlike the methods from Lin and Duan [11] and Tsai and Chen [14]. The isotherm cross-overs observed in both these methods were highlighted in an earlier study [17].

6.5 Phase Equilibrium Calculations and Volumetric Properties

For illustration purposes, we present example pressure-temperature-density (P-T-ρ) diagrams using the VTPR EOS. The P-T-ρ diagrams for CO_2 + water, methanol + water, ammonia + water and acetone + water binary systems are shown in Figures 6.8(a) to (d). The available experimental data for the respective systems are also plotted in these figures. The P-T-ρ diagrams at constant composition for a polar mixture (methanol + water) and a non-polar mixture (methane + nitrogen) are shown in Figures 6.9(a) and (b), respectively. As evident from these figures, the VTPR EOS provides reasonably accurate predictions for the liquid densities for these systems. In contrast, the PR EOS yielded predictions that contained larger errors.

Overall, the VTPR EOS presented in this study has been shown to provide three- to five-fold reduction in errors for liquid density predictions over those obtained with the original, untranslated PR EOS. This was demonstrated by testing the VTPR EOS for a

variety of binary mixtures composed of diverse molecular species. The BIP regressions for describing vapor-liquid equilibrium (VLE) showed that a single, temperature-independent BIP can have a significant effect on VLE predictions. However, the effect of BIPs on liquid density predictions is mixed and is dependent on the type of binary mixture studied. Nonetheless, the companion BIP regressions reported for these systems provide a unified framework wherein the same volume-translated EOS can be used for conducting *both* phase equilibrium and volumetric behavior calculations for a wide range of binary mixtures.

6.6 Conclusions

A volume-translation function was extended from pure fluids to predict liquid densities of mixtures and tested on 73 binary systems composed of diverse molecular species. Databases were compiled for both vapor-liquid equilibrium and liquid-phase density measurements for these systems. Results indicate that the volume-translation function for mixtures is capable of providing useful predictions of liquid densities of binary mixtures over large ranges of pressure. In particular, the results reveal that the predicted mixture densities from the volume-translated equation of state contain about three- to five-fold reductions in errors relative to the original, untranslated equation of state. The corresponding model results reported for bubble-point pressures ensure that the same model can be used successfully for conducting both phase equilibrium and volumetric property predictions for a wide variety of binary systems.

Table 6.1. Database of Binary Mixture Liquid Densities

System	Temperature Range (K)	Pressure Range (bar)	Compound (1) Liquid Mole Fraction Range	Liquid Density Range (g/cm^3)	NDP	Ref.
CO_2(1)+Water(2)	304.1	10-73.37	-	0.58 - 1.01	8	[37]
CO_2(1)+Water(2)	278.15–293.15	64.4–294.9	0.025-0.0331	1.01 - 1.03	24	[38]
CO_2(1)+Water(2)	288.15–298.15	6.08–20.27	0.0244-0.0301	1.02 - 1.03	25	[39]
CO_2(1)+Water(2)	352.85–471.2	21.1–102.1	0.0022-0.0166	0.84 - 0.96	33	[40]
CO_2(1)+Water(2)	332.15	33.4-198.9	0.00946-0.0249	0.99 - 1.01	6	[41]
CO_2(1)+Water(2)	332.15	33.4-285.9	0.00946-0.0249	0.99 - 1.01	29	[41]
CO_2(1)+Water(2)	283.8-333.19	10.8-306.6	0.02864	0.98 - 1.03	200	[42]
CO_2(1)+Butane(2)	283.1	3.578-41.334	0.0296-0.9254	0.31 - 0.6	10	[43]
CO_2(1)+Isobutane(2)	310.9-394.3	5.03-48.33	0.0251-0.8845	0.58 - 0.72	32	[44]
CO_2(1)+Decane(2)	344.3-377.6	63.85-164.65	0.457-0.925	0.59 - 0.72	45	[45]
CO_2(1)+Decane(2)	344.3	13.8-127.1	0.108-0.935	0.58 - 1.01	28	[46]
Methanol(1)+Water(2)	323.1-473.4	1-135.3	0.09879-0.8935	0.59 - 0.98	67	[47]
Methanol(1)+Water(2)	283-348.0	1-2215.4	0.25-0.75	0.74 - 1.08	295	[48]
Methanol(1)+Water(2)	320-400.0	1-2 000	0.2034-0.8005	0.72 - 1.01	326	[49]
Methanol(1)+Water(2)	283.1-348.1	1-2 215	0.15-0.75	0.79 - 1.04	229	[50]
Methanol(1)+Water(2)	256.9-443.5	10.61-405.23	0.1061-0.9061	0.69 - 1.02	934	[51]
Methanol(1)+Water(2)	282.5-393.2	16.66-213.86	0.1462-0.5739	0.80 - 0.92	134	[52]
Methanol(1)+Water(2)	287.1-417.1	37.21-299.27	0.059-0.708	0.76 - 0.97	401	[53]
Methanol(1)+Water(2)	320-420.0	1-2000	0.4993	0.76 - 0.95	150	[54]
1-Propanol(1)+Water(2)	283.1-308.1	0.9893	0.002-0.20	0.91 – 1.0	96	[55]
1-Propanol(1)+Water(2)	274-323	1.0132	0.00184-0.0061	0.78 - 1.0	24	[56]
1-Propanol(1)+Water(2)	298.1	1.0132	0.00079-0.02089	0.99 - 1.0	8	[57]
1-Propanol(1)+Water(2)	293.1-313.1	1.01	0.0018-0.00893	0.99 - 1.0	30	[58]

Table 6.1. Database of Binary Mixture Liquid Densities *(Continued)*

System	Temperature Range (K)	Pressure Range (bar)	Compound (1) Liquid Mole Fraction Range	Liquid Density Range (g/cm^3)	NDP	Ref.
1-Propanol(1)+Water(2)	298.1	1.01	0.0111-0.9042	0.8 - 1.0	25	[59]
1-Propanol(1)+Water(2)	283.1-348.15	1-2087	0.07-0.75	0.78 - 1.04	208	[50]
2-Propanol(1)+Water(2)	298.1	1.013	0.001072-0.016651	0.99 - 1.0	8	[57]
2-Propanol(1)+Water(2)	274-323.0	1.01	0.001636-0.005898	0.76 - 1.0	24	[56]
2-Propanol(1)+Water(2)	273-313	1.013	0.000056-0.003294	0.99 - 1.0	90	[60]
2-Propanol(1)+Water(2)	293.1-313.1	1.01	0.001798-0.008927	0.99 - 1.0	30	[58]
2-Propanol(1)+Water(2)	283.1-348.1	1-1906	0.06-0.75	0.76 - 1.04	187	[50]
Butanol(1)+Water(2)	273-313.0	1.013	0.000056-0.003294	0.99 - 1.0	89	[60]
Butanol(1)+Water(2)	293	1.0132	0.003113-0.70049	0.81 - 1.0	19	[61]
Butanol(1)+Water(2)	288.1-308.15	1.01	0.01-0.95	0.8 - 1.0	70	[62]
Butanol(1)+Water(2)	274-323.0	1.0132	0.001319-0.004798	0.79 – 1.0	24	[56]
Butanol(1)+Water(2)	278.1-323.15	1.01	0.005-0.015	0.98 - 1.0	30	[55]
Isobutanol(1)+Water(2)	298.1	1.013	0.001575-0.016465	0.99 - 1.0	7	[57]
Isobutanol(1)+Water(2)	298	1.0132	0.000877-0.020257	0.80 - 1.0	12	[63]
Isobutanol(1)+Water(2)	293	1.0132	0.003202-0.83417	0.80 - 1.0	23	[61]
Isobutanol(1)+Water(2)	273-313.0	1.013	0.000051-0.001852	0.99 - 1.0	79	[60]
Isobutanol(1)+Water(2)	274-323.0	1.01	0.001472-0.004782	0.78 - 1.0	24	[56]
Pentanol(1)+Water(2)	274-323	1.0132	0.001025-0.002905	0.79 - 1.0	24	[56]
Pentanol(1)+Water(2)	288-308	1.01	0.00045-0.00448	0.99 - 1.0	24	[64]
Pentanol(1)+Water(2)	298.1	1.013	0.001069-0.003529	0.99 - 1.0	9	[57]
Ammonia(1)+Water(2)	450-500.0	100-2000	0.1048-0.9102	0.35 - 0.93	218	[65]
Ammonia(1)+Water(2)	310-400.0	1-170	0.1016-0.8952	0.56 - 0.96	582	[66]

Table 6.1. Database of Binary Mixture Liquid Densities *(Continued)*

System	Temperature Range (K)	Pressure Range (bar)	Compound (1) Liquid Mole Fraction Range	Liquid Density Range (g/cm^3)	NDP	Ref.
Ammonia(1)+Water(2)	310-400.0	2-170	0.2973-0.8374	0.35 - 0.88	470	[67]
Acetone(1)+Hexane(2)	293.1	1.01	0.14153-0.93033	0.71 - 0.9	10	[68]
Acetone(1)+Hexane(2)	298.1	1.01	0.0504-0.9507	0.75 - 0.87	19	[69]
Acetone(1)+Hexane(2)	278.1-298.1	1.0132	0.0381-0.9413	0.77 - 0.86	38	[70]
Acetone(1)+Pentane(2)	303	3.45-96.5	0.25-0.75	0.74 - 0.89	24	[71]
Acetone(1)+Pentane(2)	298.1	1-100	0.49707	0.75 - 0.89	6	[72]
Acetone(1)+Heptane(2)	278.1-298.1	1.0132	0.053-0.978	0.72 - 0.79	48	[70]
Acetone(1)+Heptane(2)	298.1	1-100	0.49996	0.74 - 0.75	6	[72]
Acetone(1)+Heptane(2)	296	1.013	0.0903-0.9625	0.71 - 0.98	20	[73]
Acetone(1)+Octane(2)	278.1-298.1	1.0132	0.058-0.987	0.70 - 0.81	45	[70]
Acetone(1)+Octane(2)	293	1.013	0.201-0.955	0.70 - 0.79	11	[74]
Acetone(1)+Nonane(2)	288.1-308.1	1.0132	0.0421-0.9505	0.68 - 0.81	39	[75]
Acetone(1)+Decane(2)	288.1-308.1	1.0132	0.046-0.9507	0.71 - 0.72	36	[75]
Acetone(1)+Decane(2)	298.1	1-100	0.50373	0.68 - 0.79	6	[72]
Acetone(1)+Benzene(2)	273.0-363	27.58-220.6	0.2872-0.7838	0.66 - 0.77	72	[76]
Acetone(1)+Benzene(2)	293.1-343.3	1.013	0.0442-0.8332	0.66 - 0.77	43	[77]
Acetone(1)+Toluene(2)	273.0-363	27.58-220.6	0.325-0.8126	0.66 - 0.81	120	[78]
Acetone(1)+Toluene(2)	288.1-328.1	1.01	0.1-0.9	0.64 - 0.73	99	[79]
Acetone(1)+Toluene(2)	298.1-308.1	1.01	0.1371-0.9298	0.68 - 0.69	33	[80]
Acetone(1)+Sulfur dioxide(2)	298.1	1.01	0.09457-0.95135	0.79 - 1.30	17	[81]
Acetone(1)+Water(2)	288.1-318.1	1.01	0.9286-0.9994	0.76 - 0.80	62	[82]
Acetone(1)+Water(2)	283-433.0	1-1500	0.11734-0.41987	0.74 - 1.02	227	[83]
Acetone(1)+Water(2)	293-313	1.01	0.0134-0.9997	0.77 – 1.0	112	[84]

Table 6.1. Database of Binary Mixture Liquid Densities *(Continued)*

System	Temperature Range (K)	Pressure Range (bar)	Compound (1) Liquid Mole Fraction Range	Liquid Density Range (g/cm^3)	NDP	Ref.
R11(1)+R12(2)	288-333	5.75-15.75	0.1424-0.7794	1.21 - 1.48	66	[85]
R11(1)+R12(2)	230.0-425	6.86-698.07	0.4998	0.87 - 1.68	127	[86]
R11(1)+R13(2)	230.0-425	18.160 -695.19	0.4998	0.30 - 1.65	110	[86]
R11(1)+R22(2)	230.0-425	3.78-682.31	0.8336	1.11 - 1.59	140	[87]
R11(1)+R22(2)	232.0-422	3.45-89.16	0.8336	1.01 - 1.69	41	[87]
R12(1)+R114(2)	264.1-322.9	10.5-15.3	0.4874-0.8949	1.24 - 1.52	33	[85]
R12(1)+R32(2)	202.2-285.9	1.0113	0.12984	1.06 - 1.33	8	[88]
R32(1)+R125(2)	283.1-333.1	17.99-205.20	0.434-0.8814	0.80 - 1.3	240	[89]
R32(1)+R125(2)	277.1-397.1	59.04-297.28	0.69601	0.77 - 1.21	381	[90]
R32(1)+R125(2)	268.1-328.1	34.23-300.03	0.7069	1.09 - 1.19	194	[91]
R32(1)+R125(2)	294.7-333.8	14.529-39.782	0.60054-0.82895	0.79 - 1.14	44	[92]
R32(1)+R134a(2)	250-350	5.02-30.05	0.3953	0.99 - 1.30	36	[93]
R32(1)+R134a(2)	280-330	10-30.06	0.39531	0.99 - 1.21	22	[94]
R32(1)+R143a(2)	250-330	2.81-29.18	0.2483-0.7497	0.75 - 1.1	38	[95]
R32(1)+R143a(2)	250-330	5.04-30.13	0.2483-0.7497	0.76 - 1.11	93	[95]
R125(1)+R134a(2)	280.0-350	4.25-29.73	0.0866-0.9231	0.90 - 1.29	36	[93]
R125(1)+R143a(2)	279.99-329.99	7.74-28.29	0.0726-0.8631	0.84 - 1.25	35	[96]
Ethane(1)+Propane(2)	288.8	14.22-29.2	0.3094-0.8635	0.39 - 0.50	8	[97]
Ethane(1)+Propane(2)	268.4-343.9	15-82.78	0.65025	0.33 - 0.48	65	[98]
Ethane(1)+Propane(2)	283.1-322	27.6-96.5	0.2978-0.9498	0.27 - 0.51	315	[99]
Propane(1)+Butane(2)	288.8-327.6	6.44-11.24	0.311-0.844	0.46 - 0.57	8	[97]
Propane(1)+Butane(2)	343.1-418.1	17.237-42.747	0.1468-0.9258	0.25 - 0.46	65	[100]

Table 6.1. Database of Binary Mixture Liquid Densities *(Continued)*

System	Temperature Range (K)	Pressure Range (bar)	Compound (1) Liquid Mole Fraction Range	Liquid Density Range (g/cm^3)	NDP	Ref.
Propane(1)+Butane(2)	288.8-327.6	10-2000	0.2729-0.7308	0.37 - 0.70	321	[101]
Propane(1)+Isobutane(2)	288.75-327.55	3.27-16.69	0.1415-0.8464	0.46 - 0.56	10	[97]
Propane(1)+Isobutane(2)	280-440	10-2 000	0.2765-0.7468	0.35 - 0.70	318	[102]
Propane(1)+Isobutane(2)	240-380	4.751-70.811	70.811-0.75	0.36 - 0.62	271	[103]
Propane(1)+Pentane(2)	321.4-457.4	10.342-44.816	0.1470-0.8778	0.29 - 0.54	51	[100]
Propane(1)+Hexane(2)	348.1-495.4	4.497-49.802	0.144-0.922	0.23 - 0.61	74	[104]
Propane(1)+Propylene(2)	244-233	20.68-110.31	0.25-0.75	0.43 - 0.60	89	[105]
Butane(1)+Decane(2)	310.9-510.9	0.0050-49.229	0.0324-0.9751	0.25 - 0.72	72	[106]
Isobutane(1)+Butane(2)	288.8-327.6	1.966-7.103	0.2058-0.7979	0.52 - 0.58	8	[97]
Isobutane(1)+Butane(2)	240-380	3.12-70.032	0.25-0.75	0.43 - 0.64	313	[103]
Isobutane(1)+Butane(2)	280-440	10-2000	0.3761-0.7094	0.38 - 0.71	262	[107]
Pentane(1)+Cyclohexane(2)	293.1	1-100	0.50397	0.70 - 0.71	6	[108]
Pentane(1)+Cyclohexane(2)	298.1	1.013	0.06721-0.93387	0.62 - 0.77	16	[109]
Hexane(1)+Heptane(2)	333.1-343.1	0.275-1.054	0.102-0.905	0.61 - 0.65	20	[110]
Hexane(1)+Heptane(2)	298.1-348.1	1.0-400	0.124-0.874	0.61 - 0.71	208	[111]
Hexane(1)+Octane(2)	298.15	1.01	0.1-0.8954	0.66 - 0.70	9	[112]
Hexane(1)+Octane(2)	283.1-313.1	1.013	0.0835-0.9287	0.64 - 0.71	40	[113]
Hexane(1)+Decane(2)	283.1-313.1	1.013	0.1099-0.9207	0.65 - 0.73	33	[113]
Hexane(1)+Cyclohexane(2)	298.1-473.1	1.013	0.1962-0.7961	0.46 - 0.75	77	[114]
Hexane(1)+Cyclohexane(2)	293.2-573.2	0.98-490	0.19624-0.79619	0.38 - 0.79	86	[115]
Heptane(1)+Octane(2)	333.1-353.2	0.124-0.569	0.116-0.897	0.63 - 0.67	22	[110]
Heptane(1)+Octane(2)	283.1-313.1	1.0132	0.06956-0.92575	0.67 - 0.71	59	[116]
Cyclohexane(1)+Octane(2)	333.1-353.1	0.103-0.996	0.108-0.896	0.65 - 0.74	22	[110]
Cyclohexane(1)+Octane(2)	298.1-308.1	1.0132	0.0972-0.8971	0.69 - 0.77	33	[117]
Cyclohexane(1)+Octane(2)	308.1-313.1	1.01	0.1008-0.9153	0.69 - 0.76	22	[118]
Cyclohexane(1)+Nonane(2)	333.1-353.2	0.118-0.922	0.103-0.901	0.68 - 0.74	14	[110]

Table 6.1. Database of Binary Mixture Liquid Densities *(Continued)*

System	Temperature Range (K)	Pressure Range (bar)	Compound (1) Liquid Mole Fraction Range	Liquid Density Range (g/cm^3)	NDP	Ref.
Cyclohexane(1)+Heptane(2)	298.1-313.1	1.01	0.07702-0.97275	0.67 - 0.77	76	[119]
Cyclohexane(1)+Heptane(2)	298.1-353.1	1-1000.0	0.501	0.67 - 0.78	79	[120]
Benzene(1)+Methanol(2)	303-323	1.01	0.1723-0.8402	0.77 - 0.86	21	[121]
Benzene(1)+Methanol(2)	303-323	1.0132	0.1723-0.9428	0.77 - 0.86	27	[122]
Benzene(1)+Butanol(2)	298.1	1.01	0.05255-0.80826	0.81 - 0.87	10	[123]
Benzene(1)+Butanol(2)	288.1-313.1	1.01	0.0193-0.951	0.79 - 0.88	138	[124]
Benzene(1)+Isobutanol(2)	303	1.013	0.1012-0.8987	0.80 - 0.86	9	[125]
Benzene(1)+Pentanol(2)	283.1-328.1	1.013	0.0527-0.9494	0.79 - 0.88	72	[126]
Benzene(1)+Pentane(2)	298.1	1.0-100	0.48268	0.73 - 0.74	6	[72]
Benzene(1)+Pentane(2)	297	1.01	0.199-0.814	0.66 - 0.87	5	[127]
Benzene(1)+Hexane(2)	298.1-473.1	1.0132	0.216-0.815	0.47 - 0.82	77	[128]
Benzene(1)+Hexane(2)	298.1	1.0-100	0.53985	0.75 - 0.76	6	[72]
Benzene(1)+Heptane(2)	298-328	1.01	0.1-0.9	0.65 - 0.87	33	[129]
Benzene(1)+Octane(2)	298.1-328.1	1.01	0.04854-0.93266	0.67 - 0.87	64	[130]
Benzene(1)+Methylcyclohexane(2)	298.1-308.1	1.01	0.1018-0.896	0.76 - 0.87	33	[131]
Benzene(1)+Toluene(2)	298.1	1.01	0.12719-0.9275	0.86 - 0.87	9	[132]
Benzene(1)+Toluene(2)	273-343	1.01	0.54119	0.82 - 0.89	5	[133]
Benzene(1)+Toluene(2)	298.0-723	11.30-503.04	0.5	0.29 - 0.90	121	[134]
Methane(1)+Ethane(2)	140-270.1	4.908-66.263	0.0504-0.9408	0.22 - 0.53	15	[135]
Methane(1)+Ethane(2)	105-140	0.256-3.55	0.35457-0.68006	0.48 - 0.58	20	[136]
Methane(1)+Propane(2)	279-322	19.75-137.35	0.0242	0.46 - 0.52	21	[137]
Methane(1)+Propane(2)	105-130	0.27-3.3	0.29538-0.85796	0.47 - 0.66	20	[136]
Methane(1)+Butane(2)	316.1-479.3	91.44-481.39	0.3458-0.50340	0.29 - 0.41	66	[138]
Methane(1)+Butane(2)	115-140	1.27-6.023	0.77762-0.92788	0.43 - 0.55	19	[139]

Table 6.1. Database of Binary Mixture Liquid Densities *(Continued)*

System	Temperature Range (K)	Pressure Range (bar)	Compound (1) Liquid Mole Fraction Range	Liquid Density Range (g/cm^3)	NDP	Ref.
Methane(1)+Isobutane(2)	110-140	0.782-5.95	0.78329-0.92044	0.44 - 0.55	13	[139]
Methane(1)+Pentane(2)	310-440	27.57-344.73	0.1263-0.94	0.12 - 0.63	260	[140]
Methane(1)+Hexane(2)	348.1	22.7-115.6	0.0901-0.3996	0.52 - 0.59	10	[141]
Methane(1)+Cyclohexane(2)	294.3-444.3	41.36-689.47	0.1-0.9	0.14 - 0.80	644	[142]
Methane(1)+Carbon monoxide(2)	116.3-125	17-1600	0.203-0.707	0.4 - 0.79	140	[143]
Methane(1)+Nitrogen(2)	110.1-120	10-1379	0.294-0.68	0.41 - 0.91	369	[144]
Nitrogen(1)+Ethane(2)	150-271	10.12-101.04	0.0305-0.3581	0.30 - 0.6	14	[145]
Nitrogen(1)+Butane(2)	311.1-344.4	7.77-130.6	0.004-0.2678	0.49 - 0.56	28	[146]
Nitrogen(1)+Cyclohexane(2)	366.3-410.9	17.99-275.93	0.0169-0.2906	0.65 - 0.70	18	[147]
Nitrogen(1)+Methanol(2)	298	99.09-785.27	0.0105-0.122	0.79 - 0.84	27	[148]
Nitrogen(1)+Ammonia(2)	298-323	99.09-800	0.00138-0.0662	0.57 - 0.66	52	[149]
Nitrogen(1)+CO_2(2)	224.9-400.2	67.16-484.31	0.553	0.11 - 0.63	88	[150]
Overall Statistics					**13,679**	

Table 6.2. Summary Results Bubble-point Representations for Diverse Mixtures Using the PR EOS

System	NDP	% AAD in Bubble Pressure	
		No BIPs*	With BIPs**
Systems Containing CO_2	340	22	3.5
Systems Containing Mixtures of Alcohols or Ammonia with Water	927	71	5
Systems Containing Acetone	666	22	3
Systems Containing Refrigerants	843	1.8	1.0
Systems Containing Alkanes and/or Cycloalkanes	1073	3.0	1.2
Systems Containing Benzene	701	9	1.7
Systems Containing Mixtures of Methane or Nitrogen	745	5.6	1.6
Overall Statistics	**5295**	**19.5**	**2.3**

* No BIPs: $C_{ij} = D_{ij} = 0$

** With BIPs: C_{ij} = Constant or $C_{ij}(T)$, $D_{ij} = 0$ or Constant

Note: BIPs and detailed results for each system are provided in the Appendix B.

Table 6.3. VTPR EOS Predictions of Saturated- and Single-phase Liquid Densities: Systems Containing CO_2

System	NDP	%AAD in Liquid Density					
		PR EOS		VTPR EOS (Case 1)*		VTPR EOS (Case 2)**	
		No BIPs	With BIPs	No BIPs	With BIPs	No BIPs	With BIPs
CO_2(1)+Water(2)	8	14.7	14.0	1.1	0.5	1.0	1.8
CO_2(1)+Water(2)	24	13.6	12.2	0.3	2.0	2.4	4.3
CO_2(1)+Water(2)	25	14.2	13.0	0.5	1.1	1.6	3.2
CO_2(1)+Water(2)	33	14.9	14.5	2.1	1.8	1.2	1.3
CO_2(1)+Water(2)	6	15.4	14.7	2.1	1.2	0.1	0.9
CO_2(1)+Water(2)	29	15.7	14.9	2.5	1.5	0.4	0.7
CO_2(1)+Water(2)	200	14.1	12.9	0.8	1.3	1.7	3.4
CO_2(1)+Water(2)	8	14.7	14.0	1.1	0.5	1.0	1.8
CO_2(1)+Butane(2)	10	5.3	3.7	3.4	0.8	3.3	0.7
CO_2(1)+Isobutane(2)	32	4.9	7.4	4.8	1.4	4.8	1.4
CO_2(1)+Decane(2)	45	3.2	7.4	2.9	4.2	3.0	4.5
CO_2(1)+Decane(2)	28	3.4	7.1	2.5	3.2	3.7	3.6
Overall Statistics	**440**	**12**	**11**	**1.6**	**1.6**	**2.0**	**2.7**

* Case 1: Linear model for c_1 using one descriptor (z_c)

** Case 2: Neural network model for c_1 using 3 descriptors (z_c , ω, and dipole moment)

Table 6.4. VTPR EOS Predictions for Single-phase Liquid Densities: Systems Containing Mixtures of Alcohols or Ammonia with Water

System	NDP	%AAD in Liquid Density					
		PR EOS		VTPR EOS (Case 1)		VTPR EOS (Case 2)	
		No BIPs	With BIP	No BIPs	With BIP	No BIPs	With BIP
Methanol(1)+Water(2)	67	18	18	1.9	1.4	1.5	1.0
Methanol(1)+Water(2)	295	19	19	3.2	3.1	3.2	3.1
Methanol(1)+Water(2)	326	18	18	2.4	2.1	1.9	1.6
Methanol(1)+Water(2)	229	19	19	2.9	2.7	2.4	2.3
Methanol(1)+Water(2)	934	18	17	2.9	3.0	3.8	3.9
Methanol(1)+Water(2)	134	17	17	0.4	0.5	0.8	0.9
Methanol(1)+Water(2)	401	18	18	2.2	1.9	1.8	1.4
Methanol(1)+Water(2)	150	19	18	1.9	1.5	2.0	1.5
1-Propanol(1)+Water(2)	96	14	13	3.8	3.8	5.8	5.8
1-Propanol(1)+Water(2)	24	13	13	1.1	1.1	1.3	1.3
1-Propanol(1)+Water(2)	8	15	15	0.8	0.8	2.1	2.0
1-Propanol(1)+Water(2)	30	15	15	0.8	0.8	1.5	1.4
1-Propanol(1)+Water(2)	25	11	11	5.0	5.2	6.6	6.6
1-Propanol(1)+Water(2)	208	11	11	3.9	3.8	5.1	4.9
2-Propanol(1)+Water(2)	8	15	15	0.7	0.8	1.9	1.8
2-Propanol(1)+Water(2)	24	13	13	1.4	1.4	1.4	1.4
2-Propanol(1)+Water(2)	90	14	14	1.1	1.1	1.3	1.3
2-Propanol(1)+Water(2)	30	15	15	0.7	0.8	1.5	1.4
2-Propanol(1)+Water(2)	187	12	12	4.3	4.2	4.9	4.8
Butanol(1)+Water(2)	89	14	14	1.0	1.0	1.4	1.4
Butanol(1)+Water(2)	19	13	13	2.1	2.1	4.2	4.2
Butanol(1)+Water(2)	70	7	7	2.8	2.9	3.4	3.6
Butanol(1)+Water(2)	24	12	12	1.0	1.0	1.7	1.7
Butanol(1)+Water(2)	30	15	15	0.9	0.9	3.0	3.0
Isobutanol(1)+Water(2)	7	15	15	0.8	0.8	2.5	2.4
Isobutanol(1)+Water(2)	12	13	13	1.0	1.1	2.4	2.4
Isobutanol(1)+Water(2)	23	11	11	2.6	2.6	4.3	4.2
Isobutanol(1)+Water(2)	79	14	14	1.1	1.1	1.2	1.2
Isobutanol(1)+Water(2)	24	12	12	0.8	0.9	1.5	1.5

Table 6.4. VTPR EOS Predictions of Single-phase Liquid Densities: Systems Containing Mixtures of Alcohols or Ammonia with Water *(Continued)*

System	NDP	% AAD in Liquid Density					
		PR EOS		VTPR EOS (Case 1)		VTPR EOS (Case 2)	
		No BIPs	With BIP	No BIPs	With BIP	No BIPs	With BIP
Pentanol(1)+Water(2)	24	12	12	1.0	1.1	1.6	1.5
Pentanol(1)+Water(2)	24	15	15	1.0	1.0	1.3	1.2
Pentanol(1)+Water(2)	9	15	15	0.5	0.6	1.7	1.7
Ammonia(1)+Water(2	218	17	14	7.8	4.3	6.3	2.8
Ammonia(1)+Water(2	582	16	13	5.3	2.1	3.5	0.9
Ammonia(1)+Water(2	470	15	13	4.9	2.6	3.3	2.0
Overall Statistics	**4970**	**16**	**15**	**3.3**	**2.5**	**3.2**	**2.5**

Table 6.5. VTPR EOS Predictions for Single-phase Liquid Densities: Systems Containing Acetone

System	NDP	%AAD in Liquid Density					
		PR EOS		VTPR EOS (Case 1)		VTPR EOS (Case 2)	
		No BIPs	With BIP	No BIPs	With BIP	No BIPs	With BIP
Acetone(1)+Pentane(2)	24	3	4	3.5	2.2	2.2	1.2
Acetone(1)+Pentane(2)	6	3	4	2.9	1.8	1.9	0.7
Acetone(1)+Hexane(2)	10	4	5	2.6	1.5	1.6	1.0
Acetone(1)+Hexane(2)	19	4	5	2.6	1.5	1.8	1.1
Acetone(1)+Hexane(2)	38	4	5	2.0	1.5	1.5	1.1
Acetone(1)+Heptane(2)	48	6	6	2.4	1.5	1.5	1.0
Acetone(1)+Heptane(2)	6	5	6	2.2	1.4	1.5	0.7
Acetone(1)+Heptane(2)	20	6	7	2.5	1.5	1.4	0.9
Acetone(1)+Octane(2)	45	7	7	2.4	1.7	1.5	1.1
Acetone(1)+Octane(2)	11	8	8	2.5	2.1	1.6	1.2
Acetone(1)+Nonane(2)	39	8	8	2.3	1.7	1.4	1.2
Acetone(1)+Decane(2)	36	9	9	2.4	1.9	1.3	1.1
Acetone(1)+Decane(2)	6	9	10	2.2	1.8	0.5	0.1
Acetone(1)+Benzene(2)	72	5	5	2.3	2.0	1.8	1.7
Acetone(1)+Benzene(2)	43	5	5	0.9	0.8	0.7	0.7
Acetone(1)+Toluene(2)	120	6	6	1.5	1.1	1.5	1.2
Acetone(1)+Toluene(2)	99	5	6	1.1	0.7	0.7	0.6
Acetone(1)+Toluene(2)	33	6	6	0.9	0.7	0.7	1.0
Acetone(1)+Sulfur dioxide(2)	17	9	8	2.4	1.2	3.3	2.1
Acetone(1)+Water(2)	62	12	11	0.6	0.8	1.4	1.3
Acetone(1)+Water(2)	227	18	16	0.8	1.9	1.7	3.2
Acetone(1)+Water(2)	112	15	14	1.4	2.3	2.3	3.1
Overall Statistics	**1093**	**8.0**	**7.9**	**1.4**	**1.3**	**1.3**	**1.4**

Table 6.6. VTPR EOS Predictions for Single-Phase Liquid Densities: Systems Containing Refrigerants

System	NDP	%AAD in Liquid Density					
		PR EOS		VTPR EOS (Case 1)		VTPR EOS (Case 2)	
		No BIPs	With BIP	No BIPs	With BIP	No BIPs	With BIP
R11(1)+R12(2)	66	7	7	1.3	1.2	1.3	1.3
R11(1)+R12(2)	127	7	7	2.0	1.8	2.0	1.9
R11(1)+R13(2)	110	8	7	3.6	2.0	3.7	2.0
R11(1)+R22(2)	140	7	6	1.9	1.6	2.0	1.6
R11(1)+R22(2)	41	6	6	1.4	1.1	1.4	1.1
R12(1)+R114(2)	33	5	5	1.2	1.1	1.2	1.1
R12(1)+R32(2)	8	8	10	0.9	2.2	1.3	0.5
R32(1)+R125(2)	240	8	8	1.5	1.5	1.7	1.7
R32(1)+R125(2)	381	9	9	2.0	2.1	1.6	1.7
R32(1)+R125(2)	194	6	6	0.9	0.9	2.5	2.6
R32(1)+R125(2)	44	13	13	2.7	2.7	2.2	2.4
R32(1)+R134a(2)	36	6	6	0.5	0.5	1.3	1.4
R32(1)+R134a(2)	22	7	7	0.6	0.6	1.2	1.2
R32(1)+R143a(2)	38	11	11	3.1	3.2	2.1	2.2
R32(1)+R143a(2)	93	9	9	2.3	2.5	1.3	1.5
R125(1)+R134a(2)	36	4	4	1.7	1.7	1.8	1.9
R125(1)+R143a(2)	35	6	6	0.9	1.0	1.0	1.1
Overall Statistics	**1644**	**7.7**	**7.6**	**1.8**	**1.7**	**1.9**	**1.8**

Table 6.7. VTPR EOS Predictions for Saturated- and Single-phase Liquid Densities: Systems Containing Alkanes and/or Cycloalkanes

System	NDP	% AAD in Liquid Density					
		PR EOS		VTPR EOS (Case 1)		VTPR EOS (Case 2)	
		No BIPs	With BIP	No BIPs	With BIP	No BIPs	With BIP
Ethane(1)+Propane(2)	8	2.3	2.1	0.7	0.4	0.4	0.3
Ethane(1)+Propane(2)	65	4.0	4.2	1.0	1.0	0.8	0.8
Ethane(1)+Propane(2)	315	3.1	3.0	0.8	0.7	0.7	0.6
Propane(1)+Butane(2)	8	3.7	3.7	0.9	0.9	0.8	0.9
Propane(1)+Butane(2)	65	7.8	7.9	2.2	2.1	2.1	2.1
Propane(1)+Butane(2)	321	7.0	6.9	1.8	1.8	1.8	1.8
Propane(1)+Isobutane(2)	10	3.4	3.6	0.7	0.9	0.5	0.7
Propane(1)+Isobutane(2)	318	7.5	7.5	1.9	1.9	1.8	1.8
Propane(1)+Isobutane(2)	271	4.7	4.8	0.8	0.9	0.7	0.8
Propane(1)+Pentane(2)	51	6.1	7.6	1.3	2.1	1.3	2.1
Propane(1)+Hexane(2)	74	5.3	5.6	3.8	3.4	3.8	3.5
Propane(1)+Propylene(2)	89	6.5	6.4	1.0	0.9	1.0	0.9
Butane(1)+Decane(2)	72	5.7	5.8	2.3	2.1	2.4	2.2
Isobutane(1)+Butane(2)	8	4.5	4.6	1.2	1.3	1.1	1.1
Isobutane(1)+Butane(2)	313	4.7	4.7	1.1	1.1	1.0	1.0
Isobutane(1)+Butane(2)	262	6.8	6.9	1.9	2.0	1.9	1.9
Pentane(1)+Cyclohexane(2)	6	4.3	4.4	0.7	0.7	0.5	0.5
Pentane(1)+Cyclohexane(2)	16	4.2	4.2	0.7	0.7	0.6	0.6
Hexane(1)+Heptane(2)	20	1.3	1.4	1.3	1.4	1.7	1.8
Hexane(1)+Heptane(2)	208	0.9	1.0	0.7	0.7	0.9	0.9
Hexane(1)+Octane(2)	9	1.4	1.3	0.3	0.1	0.2	0.2
Hexane(1)+Octane(2)	40	1.5	1.4	0.5	0.5	0.5	0.5
Hexane(1)+Decane(2)	33	4.0	4.0	1.6	1.6	1.8	1.8
Hexane(1)+Cyclohexane(2)	77	3.4	3.4	1.0	1.1	1.1	1.1
Hexane(1)+Cyclohexane(2)	86	3.7	3.7	1.8	1.8	1.8	1.8
Heptane(1)+Octane(2)	22	1.3	1.3	0.9	0.9	1.1	1.1
Heptane(1)+Octane(2)	59	2.3	2.3	1.6	1.6	1.4	1.4
Cyclohexane(1)+Octane(2)	22	1.9	1.9	0.3	0.3	0.4	0.4
Cyclohexane(1)+Octane(2)	33	2.2	2.2	1.0	0.9	1.1	1.0

Table 6.7. VTPR EOS Predictions for Saturated and Single-Phase Liquid Densities: Systems Containing Alkanes and/or Cycloalkanes *(Continued)*

System	NDP	%AAD in Liquid Density					
		PR EOS		VTPR EOS (Case 1)		VTPR EOS (Case 2)	
		No BIPs	With BIP	No BIPs	With BIP	No BIPs	With BIP
Cyclohexane(1)+Octane(2)	22	2.2	2.2	0.7	0.7	0.8	0.8
Cyclohexane(1)+Nonane(2)	14	2.9	2.9	1.5	1.7	1.6	1.7
Cyclohexane(1)+Heptane(2)	76	1.9	2.0	0.9	0.8	0.7	0.6
Cyclohexane(1)+Heptane(2)	79	1.8	1.9	1.2	1.2	1.0	1.0
Overall Statistics	**3072**	**4.6**	**4.6**	**1.3**	**1.3**	**1.3**	**1.3**

Table 6.8. VTPR EOS Predictions for Saturated- and Single-phase Liquid Densities: Systems Containing Benzene

System	NDP	% AAD in Liquid Density					
		PR EOS		VTPR EOS (Case 1)		VTPR EOS (Case 2)	
		No BIPs	With BIP	No BIPs	With BIP	No BIPs	With BIP
Benzene(1)+Methanol(2)	21	6.0	6.5	3.2	2.7	2.5	2.0
Benzene(1)+Methanol(2)	27	7.2	7.6	3.7	3.2	2.6	2.1
Benzene(1)+Butanol(2)	10	1.6	1.3	0.9	0.7	0.6	0.5
Benzene(1)+Butanol(2)	138	1.3	1.0	0.7	0.5	0.5	0.4
Benzene(1)+Isobutanol(2)	9	1.3	0.8	1.2	0.8	0.8	0.5
Benzene(1)+Pentanol(2)	72	1.5	1.2	0.7	0.5	0.6	0.5
Benzene(1)+Pentane(2)	6	2.4	2.3	0.2	0.3	0.3	0.4
Benzene(1)+Pentane(2)	5	3.1	3.0	0.8	0.7	0.7	0.7
Benzene(1)+Hexane(2)	77	2.8	2.8	0.9	0.9	1.0	1.0
Benzene(1)+Hexane(2)	6	2.5	2.6	0.3	0.3	0.4	0.5
Benzene(1)+Heptane(2)	33	1.1	1.1	0.9	0.9	0.6	0.6
Benzene(1)+Octane(2)	64	1.6	1.6	0.9	0.8	0.8	0.8
Benzene(1)+ Methylcyclohexane(2)	33	3.5	3.4	0.4	0.4	0.4	0.4
Benzene(1)+Toluene(2)	9	1.4	1.4	1.0	1.0	1.1	1.0
Benzene(1)+Toluene(2)	5	1.7	1.7	0.6	0.6	0.6	0.6
Benzene(1)+Toluene(2)	121	3.2	3.1	2.0	2.1	2.0	2.1
Overall Statistics	**636**	**2.3**	**2.2**	**1.2**	**1.1**	**1.0**	**1.0**

Table 6.9. VTPR EOS Predictions for Saturated- and Single-phase Liquid Densities: Systems Containing Methane or Nitrogen

System	NDP	%AAD in Liquid Density					
		PR EOS		VTPR EOS (Case 1)		VTPR EOS (Case 2)	
		No BIPs	With BIP	No BIPs	With BIP	No BIPs	With BIP
Methane(1)+Ethane(2)	15	5.5	5.2	2.3	1.9	1.8	1.5
Methane(1)+Ethane(2)	20	9.8	9.7	0.5	0.5	1.0	1.1
Methane(1)+Propane(2)	21	5.2	5.1	1.2	1.2	1.0	1.0
Methane(1)+Propane(2)	20	8.7	8.5	2.4	2.5	3.1	3.2
Methane(1)+Butane(2)	66	1.9	1.6	0.7	0.9	0.9	1.1
Methane(1)+Butane(2)	19	9.5	9.2	2.0	2.2	3.0	3.2
Methane(1)+Isobutane(2)	13	9.6	9.5	2.0	2.1	3.0	3.1
Methane(1)+Pentane(2)	260	3.7	3.5	0.9	0.9	0.9	1.0
Methane(1)+Hexane(2)	10	1.0	1.1	0.8	0.7	0.8	0.7
Methane(1)+Cyclohexane(2)	644	6.6	6.5	1.3	1.5	1.5	1.5
Methane(1)+Carbon monoxide(2)	140	12.3	12.1	1.5	1.4	1.5	1.4
Methane(1)+Nitrogen(2)	369	12.1	11.9	1.4	1.3	1.5	1.3
Nitrogen(1)+Ethane(2)	14	5.4	5.7	2.4	2.6	2.2	2.4
Nitrogen(1)+Butane(2)	28	3.9	4.5	1.0	1.4	0.9	1.3
Nitrogen(1)+Cyclohexane(2)	18	4.6	5.3	0.7	0.8	0.6	0.7
Nitrogen(1)+Methanol(2)	27	15.1	15.1	1.0	1.0	1.5	1.5
Nitrogen(1)+Ammonia(2)	52	10.3	10.1	3.3	3.2	1.6	1.5
Nitrogen(1)+CO_2(2)	88	2.6	3.3	1.9	2.3	1.9	2.3
Overall Statistics	**1824**	**7.6**	**7.5**	**1.4**	**1.4**	**1.4**	**1.4**

Table 6.10. Binary Systems Used for Comparison of Liquid Mixture Density Prediction from Different Volume Translation Methods

System	Temperature Range (K)	Pressure Range (bar)	Compound (1) Liquid Mole Fraction Range	NDP	Ref.
CO_2(1)+Water(2)	352.85–471.2	21.1–102.1	0.0022-0.0166	33	[40]
Methanol(1)+Water(2)	320-420.0	1-2000	0.4993	150	[54]
1-Propanol(1)+Water(2)	293.1-313.1	1.01	0.0018-0.00893	30	[58]
2-Propanol(1)+Water(2)	293.1-313.1	1.01	0.001798-0.00893	30	[58]
Butanol(1)+Water(2)	278.1-323.15	1.01	0.005-0.015	30	[55]
Isobutanol(1)+Water(2)	274-323.0	1.01	0.00147-0.00478	24	[56]
Pentanol(1)+Water(2)	274-323	1.0132	0.00103-0.00291	24	[56]
Ammonia(1)+Water(2)	450-500.0	100-2000	0.1048-0.9102	218	[65]
Acetone(1)+Water(2)	283-433.0	1-1500	0.11734-0.41987	227	[83]
R11(1)+R12(2)	230.0-425	6.86-698.07	0.4998	127	[86]
R11(1)+R13(2)	230.0-425	18.160 -695.19	0.4998	110	[89]
R11(1)+R22(2)	230.0-425	3.78-682.31	0.8336	140	[90]
R32(1)+R125(2)	277.1-397.1	59.04-297.28	0.69601	381	[87]
R32(1)+R134a(2)	250-350	5.02-30.05	0.3953	36	[93]
Ethane(1)+Propane(2)	268.4-343.9	15-82.78	0.65025	65	[98]
Ethane(1)+Propane(2)	283.1-322	27.6-96.5	0.2978-0.9498	315	[99]
Propane(1)+Butane(2)	288.8-327.6	10-2000	0.2729-0.7308	321	[101]
Propane(1)+Isobutane(2)	280-440	10-2 000	0.2765-0.7468	318	[102]
Propane(1)+Pentane(2)	321.4-457.4	10.342-44.816	0.1470-0.8778	51	[100]
Isobutane(1)+Butane(2)	280-440	10-2000	0.3761-0.7094	262	[107]
Heptane(1)+Octane(2)	283.1-313.1	1.0132	0.06956-0.9258	59	[116]
Benzene(1)+Butanol(2)	288.1-313.1	1.01	0.0193-0.951	138	[124]
Benzene(1)+Hexane(2)	298.1-473.1	1.0132	0.216-0.815	77	[128]
Benzene(1)+Toluene(2)	298.0-723	11.30-503.04	0.5	121	[134]
Methane(1)+Ethane(2)	105-140	0.256-3.55	0.3546-0.6801	20	[136]
Methane(1)+Butane(2)	316.1-479.3	91.44-481.39	0.3458-0.5034	66	[138]
Methane(1)+Carbon monoxide(2)	116.3-125	17-1600	0.203-0.707	140	[143]
Methane(1)+Nitrogen(2)	110.1-120	10-1379	0.294-0.68	369	[144]
Nitrogen(1)+Methanol(2)	298	99.09-785.27	0.0105-0.122	27	[148]
Overall Statistics				**3909**	

Table 6.11. VTPR EOS Predictions for Liquid Mixture Densities: Comparison of Different Volume Translation Methods

System	NDP	%AAD in Liquid Density									
		PR EOS		VTPR EOS (Case 1)		VTPR EOS (Case 2)		Lin and Duan [11]		Tsai and Chen [14]	
		No BIPs	With BIPs	No BIPs	With BIPs	No BIPs	With BIPs	No BIPs	With BIPs	No BIPs	With BIPs
CO_2(1)+Water(2)	33	14.9	14.5	2.1	1.8	1.2	1.3	3.0	2.5	1.6	2.1
Methanol(1)+Water(2)	150	19.0	18.0	1.9	1.5	2.0	1.5	5.9	5.1	3.6	3.6
1-Propanol(1)+Water(2)	30	15.0	15.0	0.8	0.8	1.5	1.4	1.4	1.4	1.6	1.5
2-Propanol(1)+Water(2)	30	15.0	15.0	0.7	0.8	1.5	1.4	1.4	1.4	1.6	1.6
Butanol(1)+Water(2)	30	15.0	15.0	0.9	0.9	3.0	3.0	1.6	1.6	1.4	1.4
Isobutanol(1)+Water(2)	24	12.0	12.0	0.8	0.9	1.5	1.5	1.5	1.5	1.7	1.7
Pentanol(1)+Water(2)	24	15.0	15.0	1.0	1.0	1.3	1.2	1.2	1.2	1.9	1.9
Ammonia(1)+Water(2)	218	17.0	14.0	7.8	4.3	6.3	2.8	8.7	4.8	5.0	4.9
Acetone(1)+Water(2)	227	18.0	16.0	0.8	1.9	1.7	3.2	5.7	3.9	4.0	3.9
R11(1)+R12(2)	127	7.0	7.0	2.0	1.8	2.0	1.9	4.4	4.3	6.0	5.8
R11(1)+R13(2)	110	8.0	7.0	3.6	2.0	3.7	2.0	6.2	6.0	-	-
R11(1)+R22(2)	140	7.0	6.0	1.9	1.6	2.0	1.6	2.6	2.5	-	-
R32(1)+R125(2)	381	9.0	9.0	2.0	2.1	1.6	1.7	7.3	7.3	-	-
R32(1)+R134a(2)	36	6.0	6.0	0.5	0.5	1.3	1.4	1.9	1.9	-	-
Ethane(1)+Propane(2)	65	4.0	4.2	1.0	1.0	0.8	0.8	4.0	3.9	2.2	2.1
Ethane(1)+Propane(2)	315	3.1	3.0	0.8	0.7	0.7	0.6	5.9	5.8	2.6	2.6
Propane(1)+Butane(2)	321	7.0	6.9	1.8	1.8	1.8	1.8	9.4	9.1	11.5	11.2
Propane(1)+Isobutane(2)	318	7.5	7.5	1.9	1.9	1.8	1.8	10.0	9.9	12.8	12.7
Propane(1)+Pentane(2)	51	6.1	7.6	1.3	2.1	1.3	2.1	3.5	3.2	2.3	2.1

Table 6.11. VTPR EOS Predictions for Liquid Mixture Densities: Comparison of Different Volume Translation Methods (*Continued*)

System	NDP	%AAD in Liquid Density									
		PR EOS		VTPR EOS (Case 1)		VTPR EOS (Case 2)		Lin and Duan [11]		Tsai and Chen [14]	
		No BIPs	With BIPs	No BIPs	With BIPs	No BIPs	With BIPs	No BIPs	With BIPs	No BIPs	With BIPs
Isobutane(1)+Butane(2)	262	6.8	6.9	1.9	2.0	1.9	1.9	9.7	9.6	9.6	9.3
Heptane(1)+Octane(2)	59	2.3	2.3	1.6	1.6	1.4	1.4	1.6	1.6	1.5	1.5
Benzene(1)+Butanol(2)	138	1.3	1.0	0.7	0.5	0.5	0.4	0.7	0.5	0.4	0.4
Benzene(1)+Hexane(2)	77	2.8	2.8	0.9	0.9	1.0	1.0	1.3	1.3	1.0	1.0
Benzene(1)+Toluene(2)	121	3.2	3.1	2.0	2.1	2.0	2.1	5.9	5.9	9.9	9.8
Methane(1)+Ethane(2)	20	9.8	9.7	0.5	0.5	1.0	1.1	0.5	0.5	3.8	3.7
Methane(1)+Butane(2)	66	1.9	1.6	0.7	0.9	0.9	1.1	4.3	4.2	6.1	5.9
Methane(1)+Carbon Monoxide(2)	140	12.3	12.1	1.5	1.4	1.5	1.4	3.7	3.6	-	-
Methane(1)+Nitrogen(2)	369	12.1	11.9	1.4	1.3	1.5	1.3	5.6	5.4	4.2	4.1
Nitrogen(1)+Methanol(2)	27	15.1	15.1	1.0	1.0	1.5	1.5	1.2	1.2	11.0	11.0
Overall	**3909**	**9.0**	**8.6**	**1.9**	**1.7**	**1.9**	**1.7**	**6.1**	**5.6**	**4.8**	**4.7**

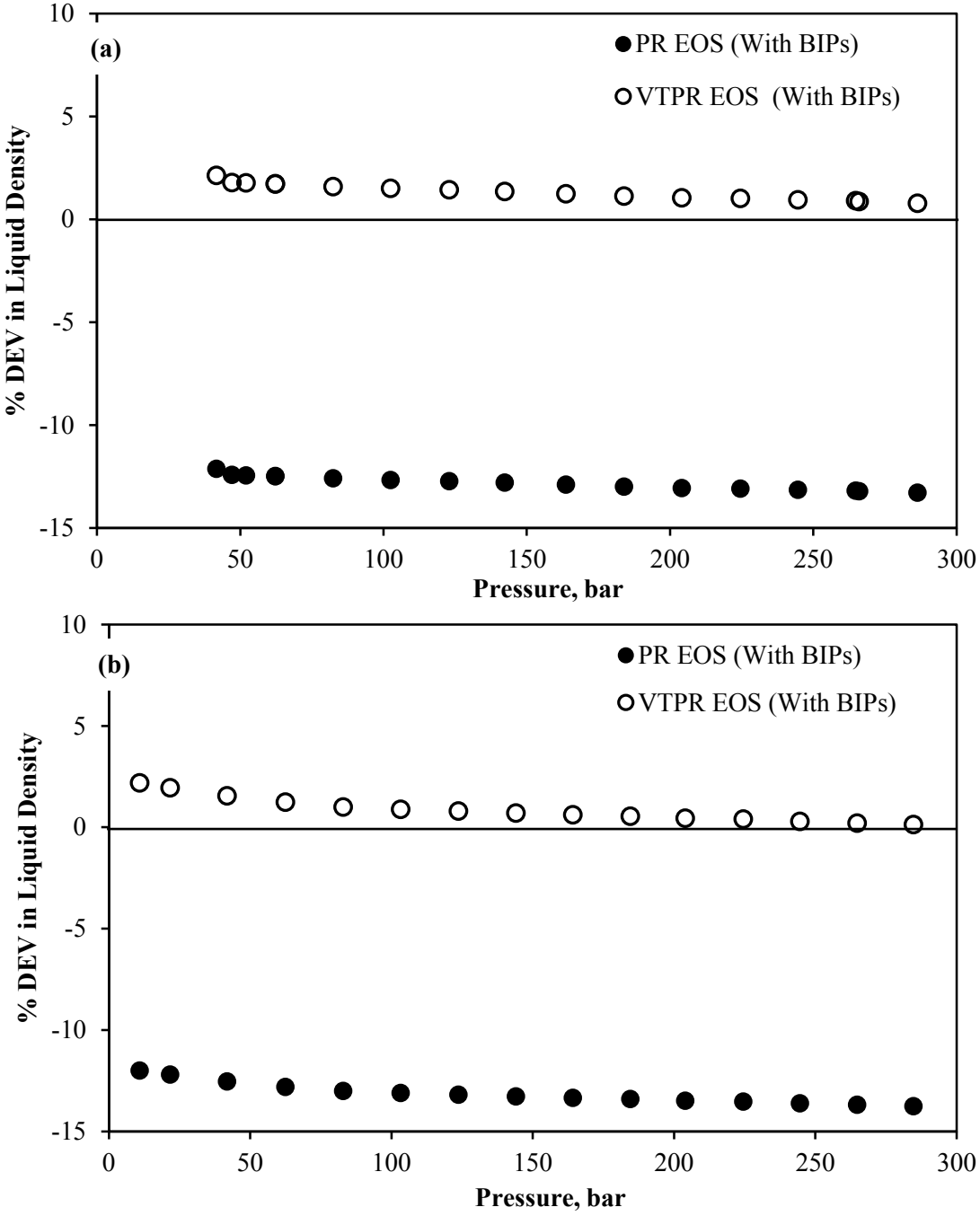

Figure 6.1. VTPR EOS Predictions* for Single-Phase Liquid Densities of CO_2 + Water System at x(1)=0.02864
(Experimental data from Hebach et al. [42])
(a) Deviations as a Function of Pressure at 284 K
(b) Deviations as a Function of Pressure at 313 K

***In all the figures, results are shown only for Case 1.**

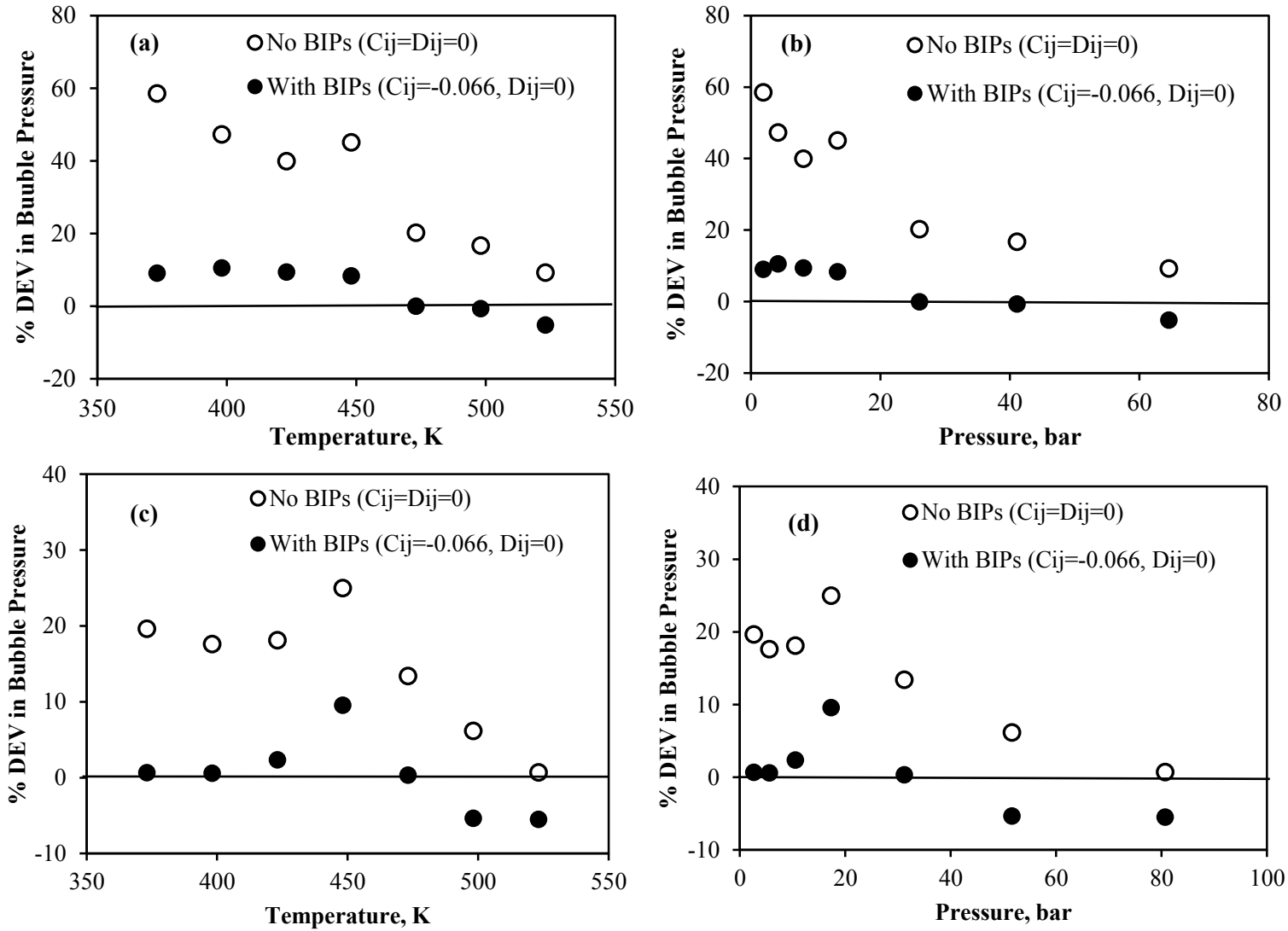

Figure 6.2. PR EOS Predictions for Bubble Pressure of Methanol (1) + Water (2) System (Experimental data from Shahverdiyev and Safarov [151])

a) Deviations as a Function of Temperature at x(1)=0.25 (b) Deviations as a Function of Pressure at x(1)=0.25

c) Deviations as a Function of Temperature at x(1)=0.5 (d) Deviations as a Function of Pressure at x(1)=0.5

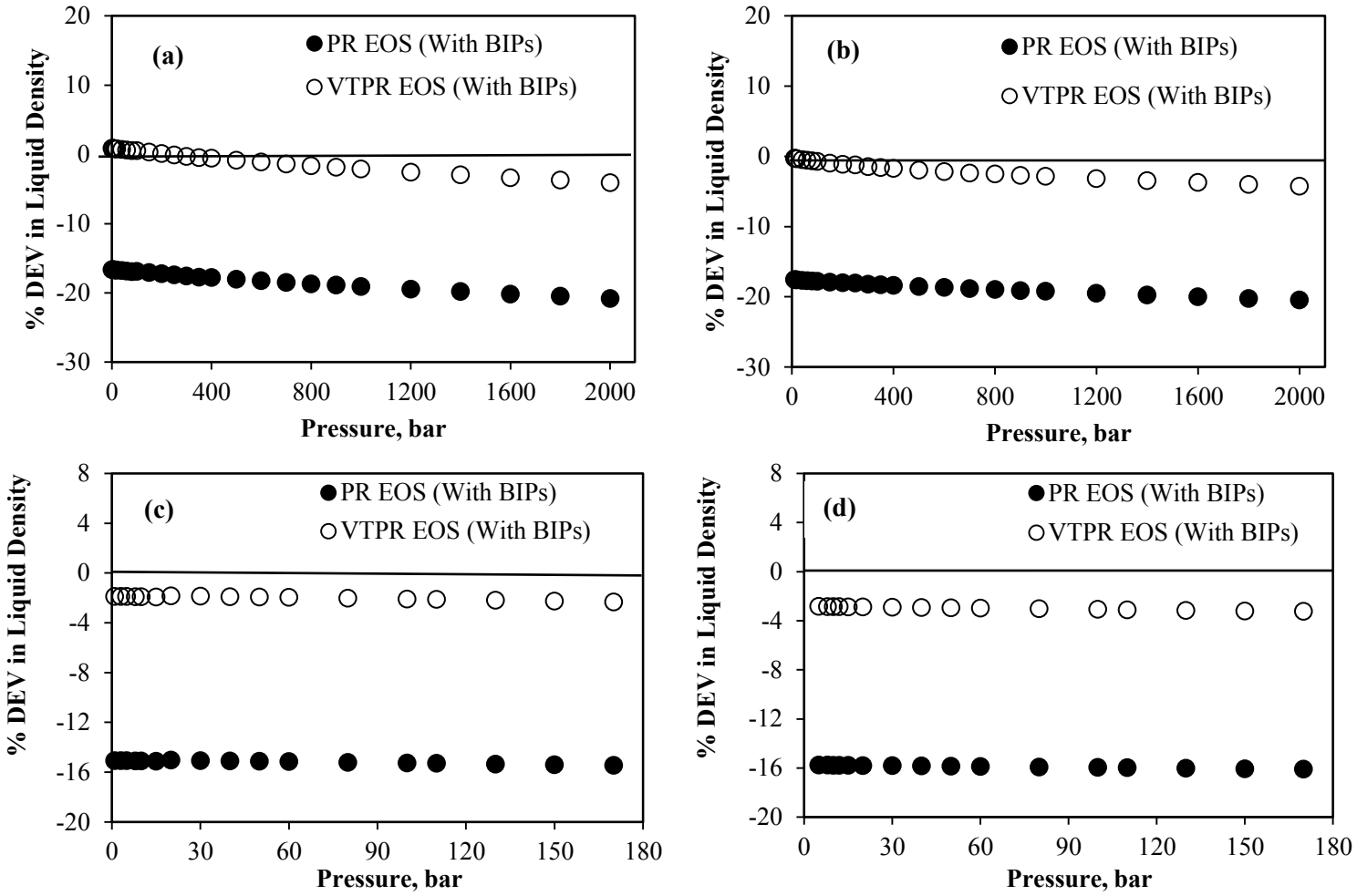

Figure 6.3. VTPR EOS Predictions for Single-phase Liquid Densities of Methanol + Water and Ammonia + Water Systems (Experimental Data from Osada et al.[54] and Munakata et al.[66])
(a) Methanol(1)+Water(2) System at 320 K and x(1)= 0.4993 (b) Methanol(1)+Water(2) System at 420 K and x(1)= 0.499
(c) Ammonia(1)+Water(2) System at 320 K and x(1)= 0.1016 (d) Ammonia(1)+Water(2) System at 380 K and x(1)= 0.1016

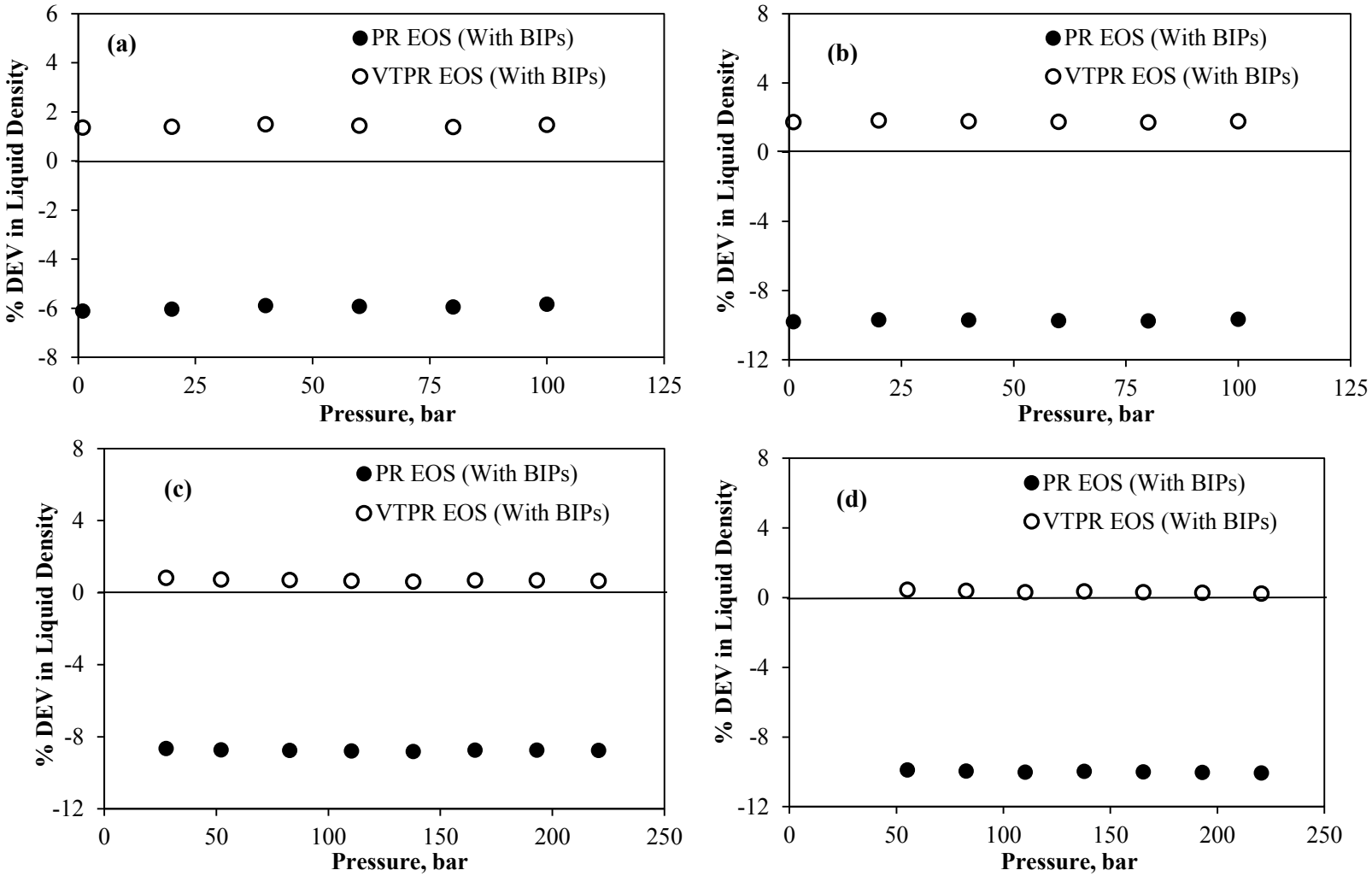

Figure 6.4. VTPR EOS Predictions for Single-Phase Liquid Densities: Systems Containing Acetone
(a) Acetone(1)+Heptane(2) System at 298 K and x(1)=0.5 (Experimental Data from Holzapfel et al.[72])
(b) Acetone(1)+Decane(2) System at 298 K and x(1)=0.5 (Experimental Data from Holzapfel et al.[72])
(c) Acetone(1)+Benzene(2) System at 273K and x(1)=0.78 (Experimental Data from Hanks et al.[76])
(d) Acetone(1)+Toluene(2) System at 273 K and x(1)=0.81 (Experimental Data from Gupta and Hanks [78])

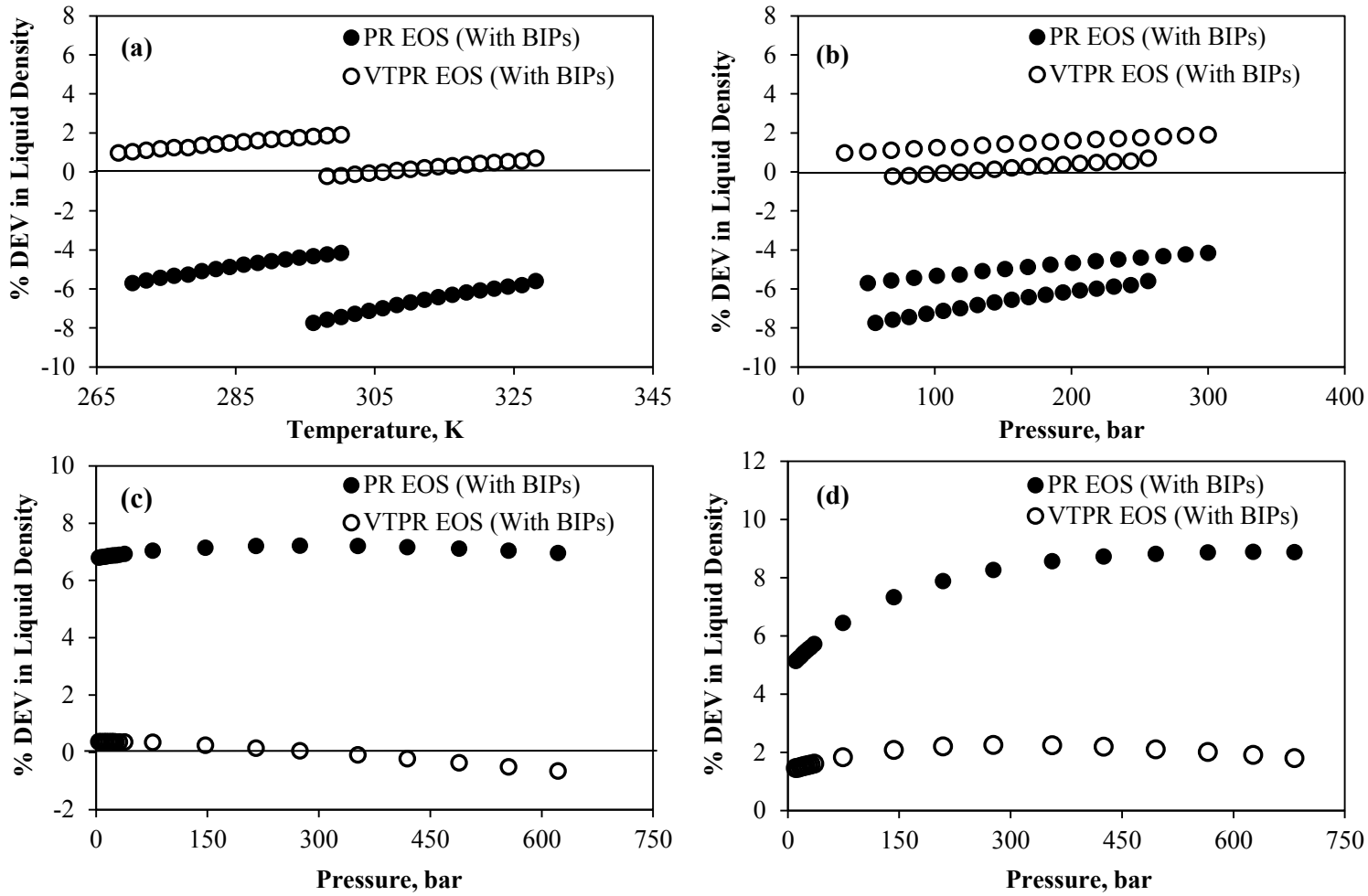

Figure 6.5. VTPR EOS Predictions for Single-Phase Liquid Densities of R32 + R125 and R11 + R22 Systems (Experimental Data from Matsuguchi et al. [91] and Yurttas et al. [87])
(a) Deviations as a Function of Temperature for R32(1)+R125(2) System at x(1)= 0.7069
(b) Deviations as a Function of Pressure for R32(1)+R125(2) System at x(1)= 0.7069
(c) Deviations as a Function of Pressure for R11(1)+R22(2) System at 270 K and x(1)= 0.83
(d) Deviations as a Function of Pressure for R11(1)+R22(2) System at 350 K and x(1)= 0.83

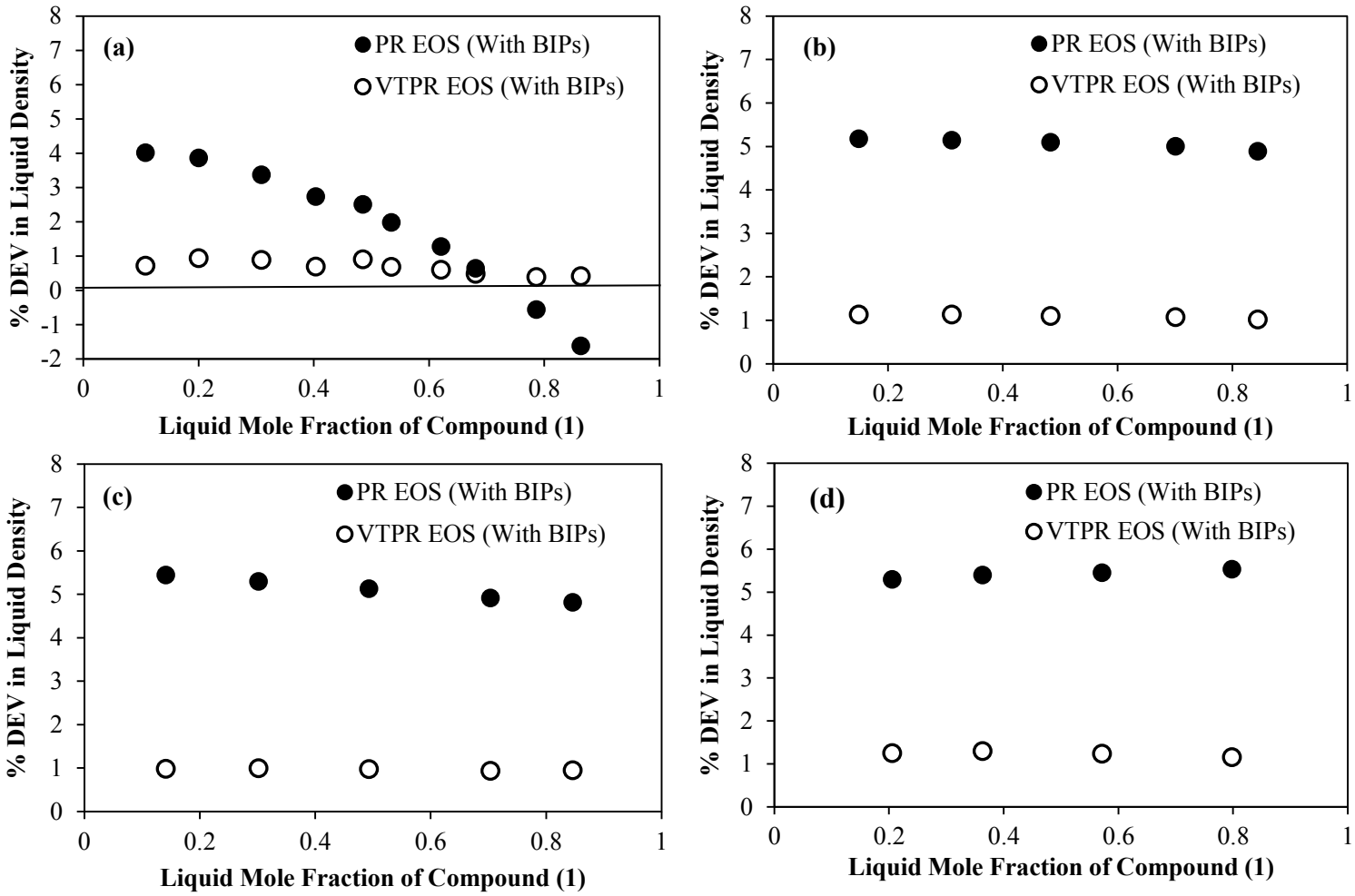

Figure 6.6. VTPR EOS Predictions for Saturated Liquid Densities of Light Hydrocarbon Systems at 288.75 K (Experimental Data from Kahre [97])
(a) Ethane(1)+Propane(2) (b) Propane(1)+Butane(2)
(c) Propane(1)+Isobutane(2) (d) Isobutane(1)+Butane(2)

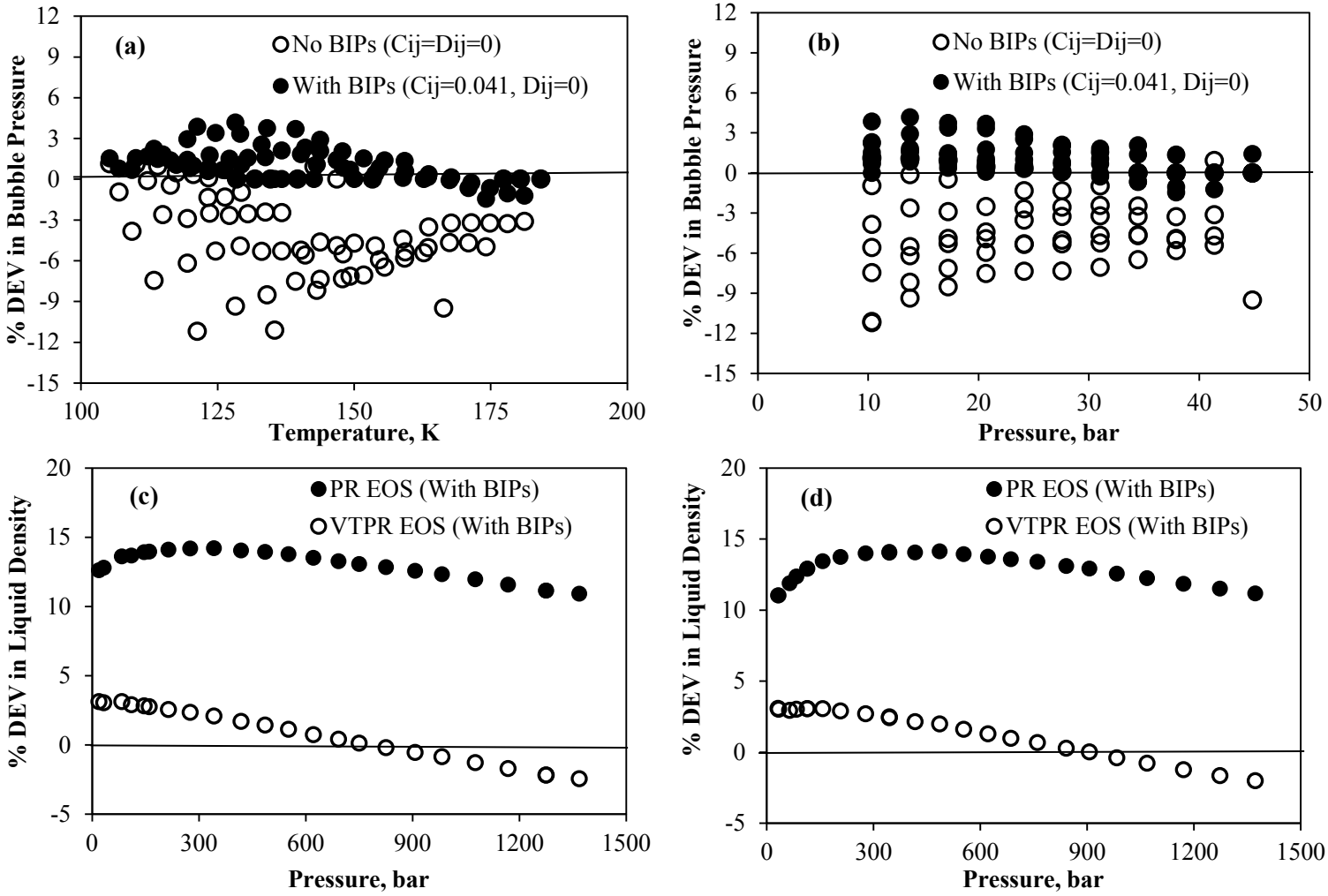

Figure 6.7. PR EOS Predictions for Bubble Pressure and VTPR EOS Predictions for Single-Phase Liquid Density of methane(1)+ nitrogen(2) System (Experimental Data from Bloomer and Parent [152] and Nunes Da Ponte et al.[144])
(a) Deviations in Bubble Pressure as a Function of Temperature
(b) Deviations in Bubble Pressure as a Function of Pressure
(c) Deviations in Liquid density as a Function of Pressure at T=110 K and x(1)=0.294
(d) Deviations in Liquid density as a Function of Pressure at T=120 K and x(1)=0.294

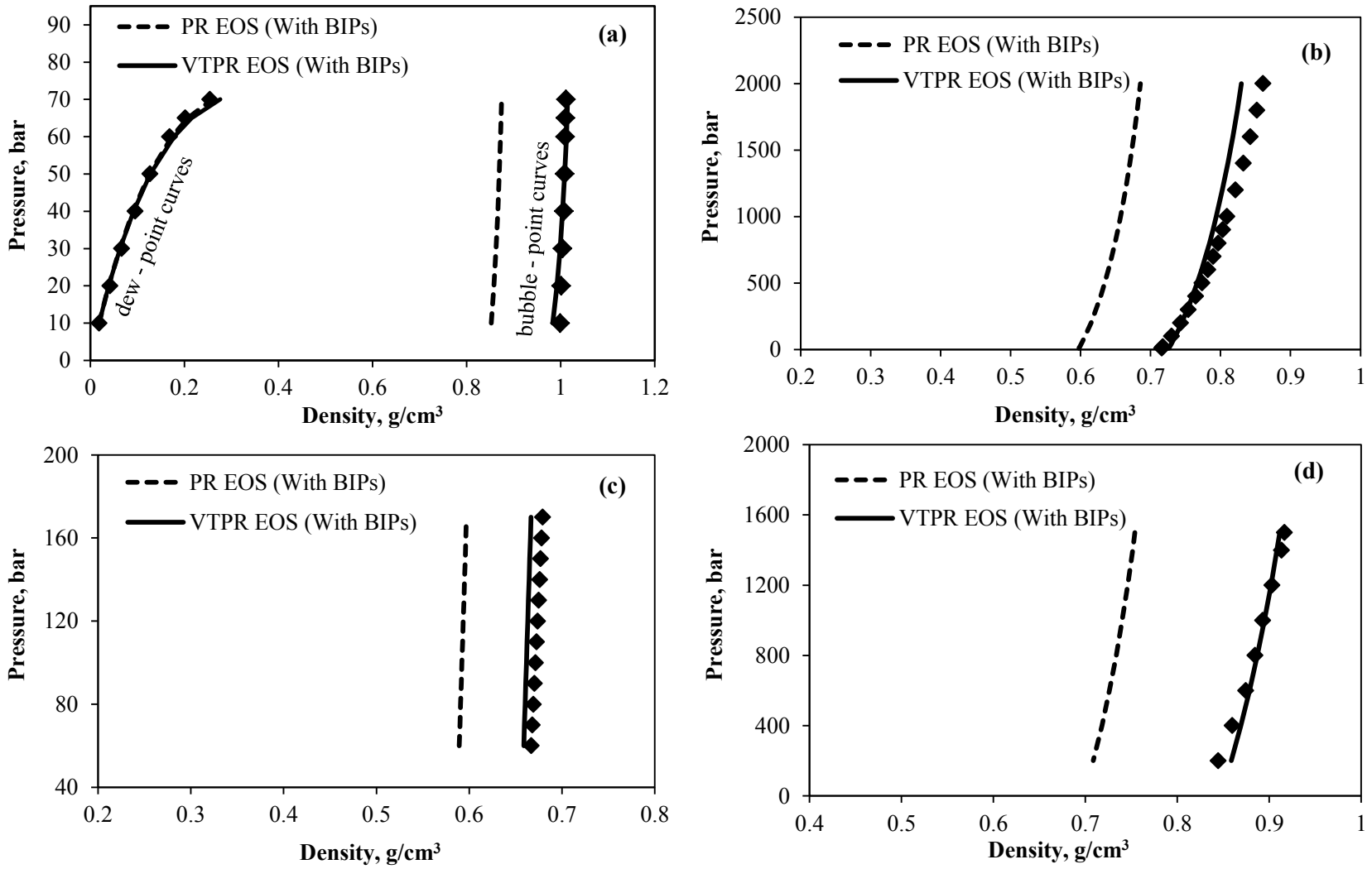

Figure 6.8. VTPR EOS Predictions for Liquid Densities of Systems Containing Water
(a) CO_2(1)+Water(2) system at 403 K (Experimental Data from Yaginuma et al.[37])
(b) Methanol(1)+Water(2) System at 400 K and x(1)= 0.8 (Experimental Data from Yokoyama and Uematsu [153])
(c) Ammonia(1)+Water(2) System at 400 K and x(1)= 0.6 (Experimental Data from Kondo et al.[67])
(d) Acetone(1)+Water(2) System at 433 K and x(1)= 0.1173 (Experimental Data from Mamedov and Guseinov [83])

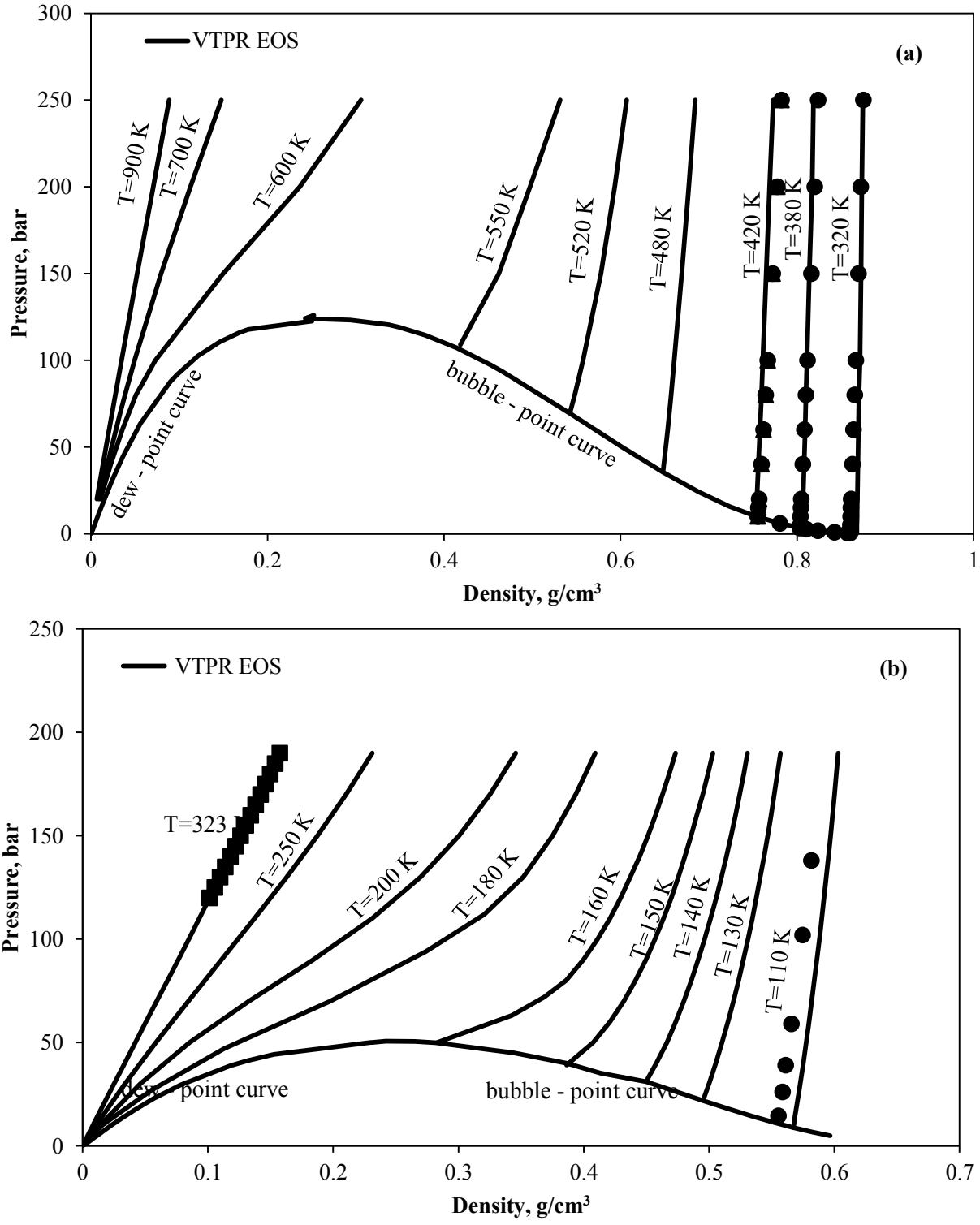

Figure 6.9. Phase Equilibrium Calculations and Volumetric Properties
(a) VTPR EOS Predictions for Methanol (0.4993) + Water (0.5007)
(Experimental Data from Osada et al. [54])
(b) VTPR EOS Predictions for Methane (0.497) + Nitrogen (0.503)
(Experimental Data from Nunes Da Ponte et al. [144] and Achtermann et al. [154])

REFERENCES

1. G. Soave, Equilibrium constants from a modified Redlich-Kwong equation of state, Chemical Engineering Science, 27 (1972) 1197-1203.
2. D.Y. Peng, D.B. Robinson, A new two-constant equation of state, Industrial & Engineering Chemistry Fundamentals, 15 (1976) 59-64.
3. J.J. Martin, Cubic equations of state-which?, Industrial & Engineering Chemistry Fundamentals, 18 (1979) 81-97.
4. A. Peneloux, E. Rauzy, R. Freze, A consistent correction for Redlich-Kwong-Soave volumes, Fluid Phase Equilibria, 8 (1982) 7-23.
5. J. Ahlers, J. Gmehling, Development of an universal group contribution equation of state: I. Prediction of liquid densities for pure compounds with a volume translated Peng–Robinson equation of state, Fluid Phase Equilibria, 191 (2001) 177-188.
6. H. Baled, R.M. Enick, Y. Wu, M.A. McHugh, W. Burgess, D. Tapriyal, B.D. Morreale, Prediction of hydrocarbon densities at extreme conditions using volume-translated SRK and PR equations of state fit to high temperature, high pressure PVT data, Fluid Phase Equilibria, 317 (2012) 65-76.
7. G.F. Chou, J.M. Prausnitz, A phenomenological correction to an equation of state for the critical region, AIchE Journal, 35 (1989) 1487-1496.
8. J.-C. de Hemptinne, P. Ungerer, Accuracy of the volumetric predictions of some important equations of state for hydrocarbons, including a modified version of the Lee-Kesler method, Fluid Phase Equilibria, 106 (1995) 81-109.

9. H.B. de Sant'Ana, P. Ungerer, J.C. de Hemptinne, Evaluation of an improved volume translation for the prediction of hydrocarbon volumetric properties, Fluid Phase Equilibria, 154 (1999) 193-204.

10. K. Frey, M. Modell, J. Tester, Density-and-temperature-dependent volume translation for the SRK EOS: 1. Pure fluids, Fluid Phase Equilibria, 279 (2009) 56-63.

11. H. Lin, Y.-Y. Duan, Empirical correction to the Peng–Robinson equation of state for the saturated region, Fluid Phase Equilibria, 233 (2005) 194-203.

12. K. Magoulas, D. Tassios, Thermophysical properties of normal-alkanes from C1 to C20 and their prediction for higher ones, Fluid Phase Equilibria, 56 (1990) 119-140.

13. P.M. Mathias, T. Naheiri, E.M. Oh, A density correction for the Peng—Robinson equation of state, Fluid Phase Equilibria, 47 (1989) 77-87.

14. J.-C. Tsai, Y.-P. Chen, Application of a volume-translated Peng-Robinson equation of state on vapor-liquid equilibrium calculations, Fluid Phase Equilibria, 145 (1998) 193-215.

15. P. Ungerer, C. Batut, Prédiction des propriétés volumétriques des hydrocarbures par une translation de volume améliorée, Oil & Gas Science and Technology - Rev. IFP, 52 (1997) 609-623.

16. P. Watson, M. Cascella, D. May, S. Salerno, D. Tassios, Prediction of vapor-pressures and saturated molar volumes with a simple cubic equation of state .2. The VanderWaals-711 EOS, Fluid Phase Equilibria, 27 (1986) 35-52.

17. A.M. Abudour, S.A. Mohammad, R.L. Robinson Jr., K.A.M. Gasem, Volume-translated Peng–Robinson equation of state for saturated and single-phase liquid densities, Fluid Phase Equilibria, 335 (2012) 74-87.

18. O. Pfohl, Evaluation of an improved volume translation for the prediction of hydrocarbon volumetric properties, Fluid Phase Equilibria, 163 (1999) 157-159.

19. P.M. Mathias, H.C. Klotz, J.M. Prausnitz, Equation-of-state mixing rules for multicomponent mixtures: the problem of invariance, Fluid Phase Equilibria, 67 (1991) 31-44.

20. J. Schwartzentruber, H. Renon, Equations of state: how to reconcile flexible mixing rules, the virial coefficient constraint and the "Michelsen-Kistenmacher syndrome" for multicomponent systems, Fluid Phase Equilibria, 67 (1991) 99-110.

21. S.K. Shibata, S.I. Sandler, Critical evaluation of equation of state mixing rules for the prediction of high-pressure phase equilibria, Industrial and Engineering Chemistry Research, 28 (1989) 1893-1898.

22. P.T. Eubank, G.-S. Shyu, N.S.M. Hanif, New procedures for application of the Wong-Sandler mixing rules to the prediction of vapor-liquid equilibria, Industrial and Engineering Chemistry Research, 34 (1995) 314–323.

23. H. Orbey, S.I. Sandler, Reformulation of Wong-Sandler mixing rule for cubic equations of state, AIChE Journal, 41 (1995) 683-690.

24. C.H. Twu, J.E. Coon, J.R. Cunningham, A new generalized alpha function for a cubic equation of state Part 1. Peng-Robinson equation, Fluid Phase Equilibria, 105 (1995) 49–59.

25. N. Trivedi, M. S. Thesis, in, Oklahoma State University, Stillwater, OK, 1996.

26. R.A. Heidemann, A.M. Khalil, The calculation of critical points, AIChE Journal, 26 (1980) 769-779.

27. P.L. Chueh, J.M. Prausnitz, Vapor-liquid equilibria at high pressures - calculation of critical temperatures volumes and pressures of nonpolar mixtures, AICHE Journal, 13 (1967) 1107.

28. K.A.M. Gasem, W. Gao, Z. Pan, R.L. Robinson Jr, A modified temperature dependence for the Peng–Robinson equation of state, Fluid Phase Equilibria, 181 (2001) 113-125.

29. J.M. Prausnitz, R.N. Lichtenthaler, E.G. Azevedo, Molecular thermodynamics of fluid-phase equilibria, 3rd ed., Prentice-Hall, New Jersey, 1999.

30. C. Tsonopoulos, J.L. Heidman, High-pressure vapor-liquid equilibria with cubic equations of state, Fluid Phase Equilibria, 29 (1986) 391–414.

31. J.W. Tester, M. Modell, Thermodynamics and Its Applications, 3rd ed., Prentice-Hall, New Jersey, 1997.

32. M. Aalto, K.I. Keskinen, J. Aittamaa, S. Liukkonen, An improved correlation for compressed liquid densities of hydrocarbons. Part 2. Mixtures, Fluid Phase Equilibria, 114 (1996) 21-35.

33. D.W. Marquardt, An algorithm for least-squares estimation of nonlinear parameters, Journal of the Society for Industrial and Applied Mathematics, 11 (1963) 431-441.

34. L.W. Jackson, A comparison of selected gradient methods for solving the nonlinear least squares problem, in: Computing and Information Sciences, Oklahoma State University, Stillwater, OK, 1978.

35. K.A.M. Gasem, GEOS, in, Oklahoma State university, Stillwater, OK, 1988-1999.

36. A.M. Abudour, S.A. Mohammad, K.A.M. Gasem, Modeling high-pressure phase equilibria of coalbed gases/water mixtures with the Peng–Robinson equation of state, Fluid Phase Equilibria, 319 (2012) 77-89.

37. R. Yaginuma, Y. Sato, D. Kodama, H. Tanaka, M. Kato, Saturated densities of carbon dioxide+water mixture at 304.1 K and pressures to 10 MPa, Journal of the Japan Institute of Energy, 79 (2000) 144-146

38. H. Teng, A. Yamasaki, M.K. Chun, H. Lee, Solubility of liquid CO_2 in water at temperatures from 278 K to 293 K and pressures from 6.44 MPa to 29.49 MPa and densities of the corresponding aqueous solutions, Journal of Chemical Thermodynamics, 29 (1997) 1301-1310.

39. M.B. King, A. Mubarak, J.D. Kim, T.R. Bott, The mutual solubilities of water with supercritical and liquid carbon-dioxide, Journal of Supercritical Fluids, 5 (1992) 296-302.

40. J.A. Nighswander, N. Kalogerakis, A.K. Mehrotra, Solubilities of carbon-dioxide in water and 1 wt-percent NaCl solution at pressures up to 10-MPa and temperatures from 80-degrees-C to 200-degrees-C, Journal of Chemical and Engineering Data, 34 (1989) 355-360.

41. Z.W. Li, M.Z. Dong, S.L. Li, L.M. Dai, Densities and solubilities for binary systems of carbon dioxide plus water and carbon dioxide plus brine at 59 degrees C and pressures to 29 MPa, Journal of Chemical and Engineering Data, 49 (2004) 1026-1031.

42. A. Hebach, A. Oberhof, N. Dahmen, Density of water plus carbon dioxide at elevated pressures: Measurements and correlation, Journal of Chemical and Engineering Data, 49 (2004) 950-953.

43. H. Kalra, T.R. Krishnana, D.B. Robinson, Equilibrium-phase properties of carbon dioxide-butane and nitrogen-hydrogen sulfide systems at subambient temperatures, Journal of Chemical & Engineering Data, 21 (1976) 222-225.

44. G.J. Besserer, D.B. Robinson, Equilibrium-phase properties of isobutane-carbon dioxide system, Journal of Chemical & Engineering Data, 18 (1973) 298-301.

45. N. Nagarajan, R.L. Robinson, Equilibrium phase compositions, phase densities, and interfacial tensions for carbon dioxide + hydrocarbon systems. 2. Carbon dioxide + n-decane, Journal of Chemical & Engineering Data, 31 (1986) 168-171.

46. R.D. Shaver, R.L. Robinson, K.A.M. Gasem, An automated apparatus for equilibrium phase compositions, densities, and interfacial tensions: data for carbon dioxide plus decane, Fluid Phase Equilibria, 179 (2001) 43-66.

47. C. Xiao, H. Bianchi, P.R. Tremaine, Excess molar volumes and densities of (methanol+water) at temperatures between 323 K and 573 K and pressures of 7.0 MPa and 13.5 MPa, The Journal of Chemical Thermodynamics, 29 (1997) 261-286.

48. H. Kubota, S. Tsuda, M. Murata, T. Yamamoto, Y. Tanaka, T. Makita, Specific volume and viscosity of methanol-water mixtures under high pressure, Rev. Phys. Chem. Jpn., 49 (1979) 59-69

49. H. Yokoyama, M. Uematsu, Thermodynamic properties of {xCH3OH+(1−x)H2O} at x=(1.0000,0.8005,0.4002,and 0.2034) in the temperature range from 320 K to 420 K at pressures up to 200 MPa, The Journal of Chemical Thermodynamics, 35 (2003) 813-823.

50. H. Kubota, Y. Tanaka, T. Makita, Volumetric behavior of pure alcohols and their water mixtures under high pressure, International Journal of Thermophysics, 8 (1987) 47-70.

51. P. Sentenac, Y. Bur, E. Rauzy, C. Berro, Density of methanol + water between 250 K and 440 K and up to 40 MPa and vapor−liquid equilibria from 363 K to 440 K, Journal of Chemical & Engineering Data, 43 (1998) 592-600.

52. T. Kuroki, N. Kagawa, H. Endo, S. Tsuruno, J.W. Magee, Specific heat capacity at constant volume for water, methanol, and their mixtures at temperatures from 300 K to 400 K and pressures to 20 MPa, Journal of Chemical & Engineering Data, 46 (2001) 1101-1106.

53. H. Kitajima, N. Kagawa, H. Endo, S. Tsuruno, J.W. Magee, Isochoric heat capacities of alkanols and their aqueous mixtures†, Journal of Chemical & Engineering Data, 48 (2003) 1583-1586.

54. O. Osada, M. Sato, M. Uematsu, Thermodynamic properties of {xCH3OH + (1−x)H2O} with x= (1.0000 and 0.4993) in the temperature range from 320 K to 420 K at pressures up to 200 MPa, The Journal of Chemical Thermodynamics, 31 (1999) 451-463.

55. C.M. Romero, M.S. Páez, D. Pérez, A comparative study of the volumetric properties of dilute aqueous solutions of 1-propanol, 1,2-propanediol, 1,3-propanediol, and 1,2,3-propanetriol at various temperatures, The Journal of Chemical Thermodynamics, 40 (2008) 1645-1653.

56. M.E. Friedman, H.A. Scheraga, Volume changes in hydrocarbon—water systems. partial molal volumes of alcohol—water solutions1, The Journal of Physical Chemistry, 69 (1965) 3795-3800.

57. D. Fenclová, S. Perez-Casas, M. Costas, V. Dohnal, Partial molar heat capacities and partial molar volumes of all of the isomeric (C3 to C5) alkanols at infinite dilution in water at 298.15 K, Journal of Chemical & Engineering Data, 49 (2004) 1833-1838.

58. H. Li, X.Y. Xu, C.J. Chi, M. Liu, Y.Y. Di, D.Z. Sun, Molar volumes and refractive indexes of hexane-1,2,3,4,5,6-hexol in aqueous solutions of 1-propanol and 2-propanol, Journal of Chemical & Engineering Data, 55 (2010) 2909-2913.

59. W. Marczak, M. Spurek, Compressibility and volume effects of mixing of 1-propanol with heavy water, Journal of Solution Chemistry, 33 (2004) 99-116.

60. F. Franks, H.T. Smith, Precision densities of dilute aqueous solutions of the isomeric butanols, Journal of Chemical & Engineering Data, 13 (1968) 538-541.

61. K. Nakanishi, Partial molal volumes of butyl alcohols and of related compounds in aqueous solution, Bulletin of the Chemical Society of Japan, 33 (1960) 793-797

62. J. Gregorowicz, A. Bald, A. Szejgis, A. Chmielewska, Gibbs energy of transfer and conductivity properties of NaI solutions in mixtures of water with butan-1-ol at 298.15 K, and some physicochemical properties of mixed solvent, Journal of Molecular Liquids, 84 (2000) 149-160.

63. H.N. Dunning, E.R. Washburn, Diffusion coefficients and some related properties of the butyl alcohols in aqueous solutions, The Journal of Physical Chemistry, 56 (1952) 235-237.

64. R. Lisi, C. Genova, R. Testa, V.T. Liveri, Thermodynamic properties of alcohols in a micellar phase. Binding constants and partial molar volumes of pentanol in sodium dodecylsulfate micelles at 15, 25, and 35°C, Journal of Solution Chemistry, 13 (1984) 121-150.

65. S. Muromachi, H. Miyamoto, M. Uematsu, The (p, ρ, T, x) properties for {xNH3+ (1-x)H2O} at T = (450 and 500) K over the pressure range from (10 to 200) MPa, The Journal of Chemical Thermodynamics, 40 (2008) 1594-1599.

66. T. Munakata, K. Kasahara, M. Uematsu, (p, ρ, T) measurements of (ammonia+ water) in the temperature range 310 K to 400 K at pressures up to 17 MPa. I. Measurements of { xNH3 + (1 − x)H2O } at x = (0.8952, 0.8041, 0.6985, 0.5052, and 0.1016), The Journal of Chemical Thermodynamics, 34 (2002) 807-819.

67. J. Kondo, Y. Yasukawa, M. Uematsu, (p, ρ, T) measurements of (ammonia + water) in the temperature range 310 K to 400 K at pressures up to 17 MPa. II. Measurements of{ xNH3 + (1 − x)H2O } at x = (1.0000, 0.8374, 0.6005, and 0.2973), The Journal of Chemical Thermodynamics, 34 (2002) 1045-1056.

68. S.K. Ogorodnikov, V.B. Kogan, M.S. Nemtsov, Liquid-vapor equilibrium in binary systems of hydrocarbons with acetone, Zh. Prikl. Khim. (Leningrad), 34 (1961) 323-331.

69. J. Acosta-Esquijarosa, I. Rodriguez-Donis, E. Pardillo-Fontdevila, Physical properties and their corresponding changes of mixing for the ternary mixture acetone + n-hexane +water at 298.15K., Thermochim. Acta, 443 (2006) 93-97.

70. G. Marino, M.M. Piñeiro, M. Iglesias, B. Orge, J. Tojo, Temperature dependence of binary mixing properties for acetone, methanol, and linear aliphatic alkanes (C6−C8), Journal of Chemical & Engineering Data, 46 (2001) 728-734.

71. K. Mulia, V.F. Yesavage, Isobaric heat capacity measurements for the n-pentane–acetone and the methanol–acetone mixtures at elevated temperatures and pressures, Fluid Phase Equilibria, 158–160 (1999) 1001-1010.

72. K. Holzapfel, G. Goetze, A.M. Demiriz, F. Kohler, Volume and isothermal compressibility of some normal alkanes (C5-C16) + 2,3-dimethylbutane, + methylcyclopentane, + butylcyclohexane, + benzene, + 2-propanone, or + tetrachloromethane, Int. Data Ser., Sel. Data Mixtures, Ser. A, 15 (1987) 30-56.

73. F. Vanden Kerchove, M. De Vijlder, Some physicochemical properties of the binary mixtures heptane-propanone and heptane-ethyl acetate, Journal of Chemical & Engineering Data, 22 (1977) 333-337.

74. A. Qin, D.E. Hoffman, P. Munk, Excess volumes of mixtures of alkanes with carbonyl compounds, Journal of Chemical & Engineering Data, 37 (1992) 55-61.

75. L.M. Casás, A. Touriño, B. Orge, G. Marino, M. Iglesias, J. Tojo, Thermophysical properties of acetone or methanol + n-alkane (C9 to C12) mixtures, Journal of Chemical & Engineering Data, 47 (2002) 887-893.

76. R.W. Hanks, A.C. Gupta, C.K.H. Yee, Liquid phase PVT data, excess volume data, constant volume excess thermodynamic functions, and thermal pressures for ten binary mixtures, Thermochimica Acta, 23 (1978) 57-71.

77. K.S. Howard, F.P. Pike, Viscosities and densities of acetone-benzene and acetone-acetic acid systems up to their normal boiling points, Journal of Chemical & Engineering Data, 4 (1959) 331-333.

78. A.C. Gupta, R.W. Hanks, Liquid phase PVT data for binary mixtures of toluene with nitroethane and acetone, and benzene with acetonitrile, nitromethane, and ethanol, Thermochimica Acta, 21 (1977) 143-152.

79. S. Enders, H. Kahl, J. Winkelmann, Surface tension of the ternary system water + acetone + toluene, Journal of Chemical & Engineering Data, 52 (2007) 1072-1079.

80. K. Rajagopal, S. Chenthilnath, Density and viscosity of ketones with toluene at different temperatures and at atmospheric pressure, Journal of Chemical & Engineering Data, 55 (2009) 1060-1063.

81. J.R. Lewis, he Viscosity of liquids containing dissolved gases., J. Am. Chem. Soc., 47 (1925) 626-640.

82. E. Ivanov, V. Abrosimov, E. Lebedeva, Volumetric properties of dilute solutions of water in acetone between 288.15 and 318.15 K, Journal of Solution Chemistry, 37 (2008) 1261-1270.

83. I.A. Mamedov, S.I. Guseinov, Experimental study of the P-V-T dependence and speed of sound in acetone-water binary mixtures, Izv. Vyssh. Uchebn. Zaved., Neft Gaz, 4 (1976) 110-112.

84. K. Tsuji, K. Ichikawa, H. Yamamoto, Solubilities of oxygen and nitrogen in acetone-water mixed solvent, Kagaku Kogaku Ronbunshu, 6 (1987) 825.

85. K.H.U. Ström, A study of liquid molar volumes for some pure halogenated hydrocarbons and their binary mixtures, The Canadian Journal of Chemical Engineering, 68 (1990) 645-652.

86. R. Castro-Gomez, W.J. Rogers, J.C. Holste, K.R. Hall, G.A. Iglesias-Silva, Experimental P−T−ρ and enthalpy-increment measurements of an equimolar mixture of trichlorofluoromethane (R-11) + dichlorodifluoromethane (R-12), Journal of Chemical & Engineering Data, 48 (2003) 1432-1434.

87. L. Yurttas, R. Castro-Gomez, W.J. Rogers, J.C. Holste, K.R. Hall, G.A. Iglesias-Silva, Experimental P−T−ρ and enthalpy-increment measurements of trichlorofluoromethane, R-11 (x = 0.83), + chlorodifluoromethane, R-22 (1 − x), Journal of Chemical & Engineering Data, 48 (2003) 1435-1439.

88. T.W. Phillips, K.P. Murphy, Liquid viscosity of halogenated refrigerants, ASHRAE Trans., 76 (1970) 146-156.

89. T. Takagi, K. Shiba, Liquid densities for binary mixtures of difluoromethane and pentafluoroethane, High Temperatures - High Pressures, 33 (2001) 303 – 309.

90. A. Matsuguchi, N. Kagawa, S. Koyama, Study on isochoric specific heat capacity of liquid R-410A and HFE-347pcf2, International Journal of Thermophysics, 31 (2010) 727-739.

91. A. Matsuguchi, K. Yamaya, N. Kagawa, Isochoric specific heat capacity of difluoromethane (R32) and a mixture of 51.11 mass% difluoromethane (R32) + 48.89 mass% pentafluoroethane (R125), International Journal of Thermophysics, 29 (2008) 1929-1938.

92. F. Weber, Simultaneous measurement of pressure, liquid and vapour density along the vapour–liquid equilibrium curve of binary mixtures of R32 and R125 of different composition, Fluid Phase Equilibria, 174 (2000) 165-173.

93. J.V. Widiatmo, T. Fujimine, H. Sato, K. Watanabe, Liquid densities of alternative refrigerants blended with difluoromethane, pentafluoroethane, and 1,1,1,2-tetrafluoroethane, Journal of Chemical & Engineering Data, 42 (1997) 270-277.

94. J.V. Widiatmo, H. Sato, K. Watanabe, Measurements of liquid densities of the binary HFC-32 + HFC-134a system, Fluid Phase Equilibria, 99 (1994) 199-207.

95. J.V. Widiatmo, T. Fujimine, H. Ohta, K. Watanabe, Bubble-point pressures and liquid densities of mixtures blended with difluoromethane, pentafluoroethane, and 1,1,1-trifluoroethane, Journal of Chemical & Engineering Data, 44 (1999) 1315-1320.

96. J.V. Widiatmo, H. Sato, K. Watanabe, Bubble-point pressures and liquid densities of binary R-125 + R-143a System, International Journal of Thermophysics, 16 (1995) 801-810.

97. L.C. Kahre, Liquid density of light hydrocarbon mixtures, Journal of Chemical & Engineering Data, 18 (1973) 267-270.

98. C.D. Holcomb, J.W. Magee, W.M. Haynes, Density measurements on natural gas liquids, in: Gas Processors Association Project 916, Tulsa OK, 1995.

99. W.R. Parrish, Compressed liquid densities of ethane-propane mixtures between 10 and 49°C at pressures up to 9.6 MPa, Fluid Phase Equilibria, 18 (1984) 279-297.

100. W.B. Kay, Vapor-liquid equilibrium relations of binary systems. Propane-n-alkane systems. n-Butane and n-pentane, Journal of Chemical & Engineering Data, 15 (1970) 46-52.

101. H. Miyamoto, M. Uematsu, The (p, ρ, T, x) properties of (x_1 propane + x_2 n-butane) with x_1 = (0.0000, 0.2729, 0.5021, and 0.7308) over the temperature range from (280 to 440) K at pressures from (1 to 200) MPa, The Journal of Chemical Thermodynamics, 40 (2008) 240-247.

102. H. Miyamoto, K. Shigetoyo, M. Uematsu, The (p, ρ, T, x) properties for {x propane + (1 − x) isobutane} with x = (1.0000, 0.2765, 0.5052, and 0.7468) in the temperature range from (280 to 440) K at pressures from (1 to 200) MPa, The Journal of Chemical Thermodynamics, 39 (2007) 1423-1431.

103. Y. Kayukawa, M. Hasumoto, Y. Kano, K. Watanabe, Liquid-phase thermodynamic properties for the binary and ternary systems of propane (1), n-butane (2), and isobutane (3), Journal of Chemical & Engineering Data, 50 (2005) 565-578.

104. S.W. Chun, J.C. Rainwater, W.B. Kay, Vapor-liquid equilibria of mixtures of propane and isomeric hexanes, Journal of Chemical & Engineering Data, 38 (1993) 494-501.

105. G.W. Swift, D.B. Manley, Relative volatility of propane-propene system by integration of general coexistence equation, Journal of Chemical & Engineering Data, 16 (1971) 301-307.

106. H.H. Reamer, B.H. Sage, Phase Equilibria in Hydrocarbon Systems. Phase behavior in the n-butane-n-decane system, Journal of Chemical & Engineering Data, 9 (1964) 24-28.

107. H. Miyamoto, T. Koshi, M. Uematsu, The (p, ρ, T, x) properties for (x_1 n-butane + x_2 isobutane) with x_1= (0.2625, 0.4913, and 0.7508) in the temperature range from (280 to 440) K at pressures from (1 to 200) MPa, The Journal of Chemical Thermodynamics, 40 (2008) 567-572.

108. K. Holzapfel, G. Goetze, F. Kohler, Volume and isothermal compressibility of some normal alkanes (C5-C16)+2,2,4-trimethylpentane,+cycloalkanes (C5,C6,C8), or methylcyclohexane., Int. Data Ser., Sel. Data Mixtures, Ser. A, 1 (1986) 38-65.

109. J. Balán, L. Morávková, J. Linek, Excess molar volumes of the (cyclohexane + pentane, or hexane, or heptane, or octane, or nonane) systems at the temperature 298.15 K, Chemical Papers, 61 (2007) 497-501.

110. K.-J. Lee, W.-K. Chen, J.-W. Ko, L.-S. Lee, C.-M.J. Chang, Isothermal vapor–liquid equilibria for binary mixtures of hexane, heptane, octane, nonane and cyclohexane at 333.15 K, 343.15K and 353.15K, Journal of the Taiwan Institute of Chemical Engineers, 40 (2009) 573-579.

111. D. Pečar, V. Doleček, Isothermal compressibilities and isobaric expansibilities of pentane, hexane, heptane and their binary and ternary mixtures from density measurements, Fluid Phase Equilibria, 211 (2003) 109-127.

112. J.L.E. Chevalier, P.J. Petrino, Y.H. Gaston-bonhomme, viscosity and density of some aliphatic, cyclic, and aromatic hydrocarbons binary liquid mixtures, Journal of Chemical & Engineering Data, 35 (1990) 206-212.

113. J.R. Goates, J.B. Ott, R.B. Grigg, Excess volumes of n-hexane +n-heptane, +n-octane, +n-nonane, and +n-decane at 283.15, 298.15, and 313.15 K, The Journal of Chemical Thermodynamics, 13 (1981) 907-913.

114. S.A. Beg, N.M. Tukur, D.K. Al-Harbi, Densities and excess volumes of cyclohexane + hexane between 298.15 K and 473.15 K, Fluid Phase Equilibria, 113 (1995) 173-184.

115. F.A. Namazov, M.M. Tagiev, Experimental study of the PVT dependence of binary mixtures of cyclohexane and n-hexane, Izv. Vyssh. Uchebn. Zaved., Neft Gaz, 19 (1976) 20.

116. J.S. Matos, J.L. Trenzado, E. González, R. Alcalde, Volumetric properties and viscosities of the methyl butanoate + n-heptane + n-octane ternary system and its binary constituents

in the temperature range from 283.15 to 313.15 K, Fluid Phase Equilibria, 186 (2001) 207-234.

117. T.M. Aminabhavi, V.B. Patil, M.I. Aralaguppi, H.T.S. Phayde, Density, viscosity, and refractive index of the binary mixtures of cyclohexane with hexane, heptane, octane, nonane, and decane at (298.15, 303.15, and 308.15) K, Journal of Chemical & Engineering Data, 41 (1996) 521-525.

118. W.A. Gherwi, A. Nhaesi, A.-F. Asfour, Densities and kinematic viscosities of ten binary liquid regular solutions at 308.15 and 313.15 K, Journal of Solution Chemistry, 35 (2006) 455-470.

119. A. Arimoto, H. Ogawa, S. Murakami, Temperature dependence of molar excess volumes and excess thermal expansion coefficients for binary mixtures of cyclohexane with some hydrocabons between 298.15 and 313.15 K, Thermochimica Acta, 163 (1990) 191-202.

120. S. Toscani, P. Figuiere, H. Szwarc, Measurements of (p,ρ,T) on c-C6H12 and on (0.501 c-C6H12 + 0.499n-C7H16) at pressures up to 100 MPa, Elsevier, Kidlington, ROYAUME-UNI, 1990.

121. M.V. Subnis, Application of Hammick and Andrews Equation to Binary Mixtures, in: Rheochor Part II, Univ. Rajputana Studies, Phys. Sci., 1952, pp. 121-127.

122. M.V. Sabnis, W.V. Bhagwat, H.G. Silawat, Application of mixture law to rheochor part III, J. Indian Chem. Soc., 26 (1949) 533-538.

123. W.J. Jones, S.T. Bowden, W.W. Yarnold, W.H. Jones, The viscosity of solutions of primary alcohols and fatty acids in benzene and in carbon tetrachloride, The Journal of Physical and Colloid Chemistry, 52 (1947) 753-760.

124. J. Smiljanić, M. Kijevčanin, B. Djordjević, D. Grozdanić, S. Šerbanović, Temperature dependence of densities and excess molar volumes of the ternary mixture (1-butanol + chloroform + benzene) and its binary constituents (1-butanol + chloroform and 1-butanol + benzene), International Journal of Thermophysics, 29 (2008) 586-609.

125. A. Ali, A.K. Nain, B. Lal, D. Chand, Densities, viscosities, and refractive indices of binary mixtures of benzene with isomeric butanols at 30°C, International Journal of Thermophysics, 25 (2004) 1835-1847.

126. O. Hiroyuki, Excess volumes of (1-pentanol + cyclohexane or benzene) at temperatures between 283.15 K and 328.15 K, The Journal of Chemical Thermodynamics, 34 (2002) 849-859.

127. J.M. Lenoir, G.K. Kuravila, H.G. Hipkin, Measured enthalpies of binary mixtures of hydrocarbons with pentane, Proc. - Am. Pet. Inst., Div. Refin., 49 (1969) 89-146.

128. S.A. Beg, N.M. Tukur, D.K. Al-Harbi, E.Z. Hamad, Densities and excess volumes of benzene + hexane between 298.15 and 473.15 K, Journal of Chemical & Engineering Data, 40 (1995) 74-78.

129. S.A. Sanni, C.J.D. Fell, H.P. Hutchison, Diffusion coefficients and densities for binary organic liquid mixtures, Journal of Chemical & Engineering Data, 16 (1971) 424-427.

130. L. Morávková, Z. Wagner, J. Linek, (p, Vm, T) measurements of (octane + benzene) at temperatures from (298.15 to 328.15) K and at pressures up to 40 MPa, The Journal of Chemical Thermodynamics, 40 (2008) 607-617.

131. J.G. Baragi, M.I. Aralaguppi, Excess and deviation properties for the binary mixtures of methylcyclohexane with benzene, toluene, p-xylene, mesitylene, and anisole at T = (298.15, 303.15, and 308.15) K, The Journal of Chemical Thermodynamics, 38 (2006) 1717-1724.

132. C.E. Linebarger, On the viscosity of mixtures of liquids, American Journal of Science, Series 4 Vol. 2 (1896) 331-340.

133. J.H. Mathews, R.D. Cook, On the existence of compounds in binary liquid mixtures, The Journal of Physical Chemistry, 18 (1913) 559-585.

134. T.S. Akhundov, F.G. Abdullaev, Y.A. Dzhabiev, Experimental study of specific volumes of a benzene + toluene solution with 50-50 percent molar composition, Izv. Vyssh. Uchebn. Zaved., Neft Gaz, 21 (1978) 59.

135. J. Janisch, G. Raabe, J. Köhler, Vapor−liquid equilibria and saturated liquid densities in binary mixtures of nitrogen, methane, and ethane and their correlation using the VTPR and PSRK GCEOS, Journal of Chemical & Engineering Data, 52 (2007) 1897-1903.

136. M.J. Hiza, W.M. Haynes, W.R. Parrish, Orthobaric liquid densities and excess volumes for binary mixtures of low molarmass alkanes and nitrogen between 105 and 140 K, The Journal of Chemical Thermodynamics, 9 (1977) 873-896.

137. J.R. Tomlinson, Liquid densities of ethane, propane, and ethane-propane mixtures, Nat. Gas Processors Assoc. Tech. Publ., TP-1 (1971).

138. A. Fenghour, J.P.M. Trusler, W.A. Wakeham, Phase behaviour and density of (methane+n-butane), Fluid Phase Equilibria, 163 (1999) 139-156.

139. W.M. Haynes, Orthobaric liquid densities and dielectric constants of (methane+2-methyl-propane) and (methane+n-butane) at low temperatures, The Journal of Chemical Thermodynamics, 15 (1983) 903-911.

140. B.H. Sage, H.H. Reamer, R.H. Olds, W.N. Lacey, Phase equilibria in hydrocarbon systems, Ind. Eng. Chem., 34 (1942) 1108–1117.

141. K. Chylinski, Apparatus for phase equilibrium measurements at high temperatures and pressures, The Journal of Chemical Thermodynamics, 34 (2002) 1703-1728.

142. H. Reamer, B. Sage, W. Lacey, Phase equilibria in hydrocarbon systems. Volumetric and phase behavior of the methane-cyclohexane system, Industrial & Engineering Chemistry Chemical & Engineering Data Series, 3 (1958) 240-245.

143. J.C.G. Calado, H.J.R. Guedes, M. Nunes da Ponte, W.B. Streett, Thermodynamic properties of liquid mixtures of carbon monoxide and methane, Fluid Phase Equilibria, 16 (1984) 185-204.

144. M. Nunes Da Ponte, W.B. Streett, L.A.K. Staveley, An experimental study of the equation of state of liquid mixtures of nitrogen and methane, and the effect of pressure on their excess thermodynamic functions, The Journal of Chemical Thermodynamics, 10 (1978) 151-168.

145. G. Raabe, J. Janisch, J. Koehler, Experimental studies of phase equilibria in mixtures relevant for the description of natural gases, Fluid Phase Equilibria, 185 (2001) 199-208.

146. T.S. Brown, V.G. Niesen, E.D. Sloan, A.J. Kidnay, Vapor-liquid equilibria for the binary systems of nitrogen, carbon dioxide, and n-butane at temperatures from 220 to 344 K, Fluid Phase Equilibria, 53 (1989) 7-14.

147. S.K. Shibata, S.I. Sandler, High pressure vapor-liquid equilibria of mixtures of nitrogen, carbon dioxide, and cyclohexane, Journal of Chemical & Engineering Data, 34 (1989) 419-424.

148. I.R. Krichevskii, G.D. Efremova, Phase and volume relations in liquid-gas systems at high pressures: III liquid-gas systems., Zh. Fiz. Khim., 25 (1951) 577-583.

149. I.R. Krichevskii, G.D. Efremova, Phase and volume relations in liquid - gas systems at high pressures. IV., Zh. Fiz. Khim., 26 (1952) 1117-1121.

150. D.M. Bailey, G.J. Esper, J.C. Holste, K.R. Hall, P.T. Eubank, K.M. Marsh, W.J. Rogers, Gas processors association properties of co2 mixtures with N2 and with CH4, in: RR-122, Tulsa, Oklahoma, 1989.

151. A.N. Shahverdiyev, J.T. Safarov, P-ρ-T and Ps-ρs-Ts properties of methanol + water and n-propanol + water solutions in wide range of state parameters, Physical Chemistry Chemical Physics, 4 (2002) 979-986.

152. O.T. Bloomer, J.D. Parent, Liquid-vapor phase behavior of the methane-nitrogen system, Chem. Eng. Prog. Symp. Ser., 49 (1953) 11-24.

153. H. Yokoyama, M. Uematsu, Thermodynamic properties of {xCH3OH+(1−x)H2O} at x=(1.0000,0.8005,0.4002 and 0.2034) in the temperature range from 320 K to 420 K at pressures up to 200 MPa, The Journal of Chemical Thermodynamics, 35 (2003) 813-823.

154. H.J. Achtermann, T.K. Bose, H. Rögener, J.M. St-Arnaud, Precise determination of the compressibility factor of methane, nitrogen, and their mixtures from refractive index measurements, International Journal of Thermophysics, 7 (1986) 709-720.

155. V.G. Niesen, (Vapor + liquid) equilibria and coexisting densities of (carbon dioxide + n-butane) at 311 to 395 K, The Journal of Chemical Thermodynamics, 21 (1989) 915-923.

156. J.J.C. Hsu, N. Nagarajan, R.L. Robinson, Equilibrium phase compositions, phase densities, and interfacial tensions for carbon dioxide + hydrocarbon systems. 1. Carbon dioxide + n-butane, Journal of Chemical & Engineering Data, 30 (1985) 485-491.

157. R.D. Shaver, R.L. Robinson Jr, K.A.M. Gasem, An automated apparatus for equilibrium phase compositions, densities, and interfacial tensions: data for carbon dioxide + decane, Fluid Phase Equilibria, 179 (2001) 43-66.

158. G. Bredig, R. Bayer, Vapor pressures of the binary system methyl alcohol + water, Z. Phys. Chem., 130 (1927).

159. S. Uchida, H. Kato, Studies on distillation: i-ii on the properties of methanol - water mixture, Kogyo Kagaku Zasshi, 37 (1934) 525-530.

160. H.E. Hughes, J.O. Maloney, The application of radioactive tracers to diffusional operations. Binary and ternary equilibrium data, Journal Name: Chem. Eng. Progress; Journal Volume: Vol: 48; Other Information: Orig. Receipt Date: 31-DEC-52, (1952) Medium: X; Size: Pages: 192-200.

161. J. Ocon, F. Rebolleda, Vapor-liquid equilibrium: VI. Study of the binary system methyl alcohol + water, An. Real. Soc. Espan. De Fis. Y Quim., 54B (1958) 525-530.

162. W. Schroeder, Measuring vapor-liquid equilibria at elevated pressure, Chem. Ing. Tech., 30 (1958) 523.

163. M.L. McGlashan, A.G. Williamson, Isothermal liquid-vapor equilibriums for system methanol-water, Journal of Chemical & Engineering Data, 21 (1976) 196-199.

164. H. Yokoyama, M. Uematsu, Thermodynamic properties of {xCH3OH+(1−x)H2O} at x=(1.0000,0.8005,0.4002, and 0.2034) in the temperature range from 320 K to 420 K at pressures up to 200 MPa, The Journal of Chemical Thermodynamics, 35 (2003) 813-823.

165. A.R. Bazaev, I.M. Abdulagatov, J.W. Magee, E.A. Bazaev, A.E. Ramazanova, A.A. Abdurashidova, PVTx measurements for a H2O + methanol mixture in the subcritical and supercritical regions, International Journal of Thermophysics, 25 (2004) 805-838.

166. A.V. Orchillés, P.J. Miguel, E. Vercher, A. Martínez-Andreu, Isobaric vapor−liquid equilibria for 1-propanol + water + 1-ethyl-3-methylimidazolium trifluoromethanesulfonate at 100 kPa, Journal of Chemical & Engineering Data, 53 (2008) 2426-2431.

167. E. Vercher, F.J. Rojo, A. Martínez-Andreu, Isobaric vapor−liquid equilibria for 1-propanol + water + calcium nitrate, Journal of Chemical & Engineering Data, 44 (1999) 1216-1221.

168. M.C. Iliuta, F.C. Thyrion, O.M. Landauer, Effect of calcium chloride on the isobaric vapor−liquid equilibrium of 1-propanol + water, Journal of Chemical & Engineering Data, 41 (1996) 402-408.

169. C. Gabaldón, P. Marzal, J.B. Montón, M.A. Rodrigo, Isobaric Vapor−liquid equilibria of the water + 1-propanol system at 30, 60, and 100 kPa, Journal of Chemical & Engineering Data, 41 (1996) 1176-1180.

170. U. Woerpel, P. Vohland, H. Schuberth, The effect of urea on the vapor-liquid equilibrium behavior of n-propanol/water at 60° C, Z. Phys. Chem. (Leipzig), 258 (1977) 905-912.

171. P. Murti, M. Van Winkle, Vapor-liquid equilibria for binary systems of methanol, ethyl alcohol, 1-propanol, and 2-propanol with ethyl acetate and 1-propanol-water, Industrial & Engineering Chemistry Chemical & Engineering Data Series, 3 (1958) 72-81.

172. W.E. Smith, Australian J. Phys., 12 (1959) 109.

173. M. Wrewsky, Uber zusammensetzung und spannung des dampfes bin'arer flussigkeitsgemische., Z. Phys. Chem., 81 (1913) 1-29.

174. F. Barr-David, B.F. Dodge, Vapor-liquid Equilibrium at high pressures. The systems ethanol-water and 2-propanol-water, Journal of Chemical & Engineering Data, 4 (1959) 107-121.

175. Q. Li, J. Zhang, Z. Lei, J. Zhu, B. Wang, X. Huang, Isobaric vapor−liquid equilibrium for (propan-2-ol + water + 1-butyl-3-methylimidazolium tetrafluoroborate), Journal of Chemical & Engineering Data, 54 (2009) 2785-2788.

176. A. Wilson, E.L. Simons, Vapor-liquid equilibria, Industrial & Engineering Chemistry, 44 (1952) 2214-2219.

177. E. Lladosa, J.B. Montón, M.C. Burguet, R. Muñoz, Phase equilibrium for the esterification reaction of acetic acid + butan-1-ol at 101.3 kPa, Journal of Chemical & Engineering Data, 53 (2007) 108-115.

178. J.S. Stockhardt, C.M. Hull, Vapor-liquid equilibria and boiling-point composition relations for systems n-butanol–water and Iisobutanol–water1,2, Industrial & Engineering Chemistry, 23 (1931) 1438-1440.

179. I.N. Bushmakin, A.P. Begetova, K.I. Kuchinskaya, The equilibrium between the liquid and vapor of the binary system butyl acohol + water, Sint. Kauch., 4 (1936).

180. T. Bylewski, On the form of isobars of mixtures of isobutyl alcohol with water, Rocznimi Chemii, 12 (1932) 311-326.

181. J.S. Stockhardt, C.M. Hull, Vapor-liquid equilibria and boiling-point composition relations for systems n-butanol–water and isobutanol–water1,2, Industrial & Engineering Chemistry, 23 (1931) 1438-1440.

182. A. Marshall, CXXXV.-The vapour pressures of binary mixtures. Part I. The possible types of vapour pressure curves, Journal of the Chemical Society, Transactions, 89 (1906) 1350-1386.

183. J.L. Guillevic, D. Richon, H. Renon, Vapor-liquid equilibrium data for the binary system water-ammonia at 403.1, 453.1, and 503.1 K up to 7.0 MPa, Journal of Chemical & Engineering Data, 30 (1985) 332-335.

184. T. Sako, T. Hakuta, H. Yoshitome, Chem. Eng. Jpn., 18 (1985) 420.

185. J. Polak, B.C.Y. Lu, Vapor-liquid equilibriums in system ammonia-water at 14.69 and 65 psia, Journal of Chemical & Engineering Data, 20 (1975) 182-183.

186. I.I. Clifford, E. Hunter, The system ammonia–water at temperatures up to 150°C. and at pressures up to twenty atmospheres, The Journal of Physical Chemistry, 37 (1932) 101-118.

187. T. Munakata, K. Kasahara, M. Uematsu, (p, ρ, T) measurements of (ammonia + water) in the temperature range 310 K to 400 K at pressures up to 17 MPa. I. Measurements of { xNH 3 + (1 − x) H 2O } at x = (0.8952, 0.8041, 0.6985, 0.5052, and 0.1016), The Journal of Chemical Thermodynamics, 34 (2002) 807-819.

188. P.C. Gillespie, W.V. Wilding, G.M. Wilson, Vapor-liquid equilibrium measurements on the ammonia-water system from 313 K to 589 K, AIChE Symp. Ser., 83 (1987) 97-127.

189. L.S. Kudryavtseva, M.P. Susarev, Liquid− vapor equilibriums in the systems acetone− hexane and hexane− ethyl alcohol at 35, 45, and 55° and 760mmHg, Zh. Prikl. Khim. (Leningrad), 36 (1963) 1471.

190. W. Rall, K. Schaefer, Thermodynamic investigations of liquid mixed systems of acetone and pentane and of acetone and hexane., Z. Elektrochem., 63 (1959) 1019-1024.

191. K. Schaefer, W. Rall, Vapor pressure and activity coefficients in the system acetone-hexane., Ber. Bunsen-Ges. Phys. Chem., 62 (1958) 1090.

192. J. Acosta, A. Arce, J. Martínez-Ageitos, E. Rodil, A. Soto, Vapor−liquid equilibrium of the ternary system ethyl acetate + hexane + acetone at 101.32 kPa, Journal of Chemical & Engineering Data, 47 (2002) 849-854.

193. S.W. Campbell, R.A. Wilsak, G. Thodos, Isothermal vapor-liquid equilibrium measurements for the n-pentane-acetone system at 372.7, 397.7, and 422.6 K, Journal of Chemical & Engineering Data, 31 (1986) 424-430.

194. T.C. Lo, H.H. Bieber, A.E. Karr, Vapor-liquid equilibrium of n-pentane-acetone, Journal of Chemical & Engineering Data, 7 (1962) 327-331.

195. S.K. Ogorodnikov, V.B. Kogan, M.S. Nemtsov, Liquid-vapor equilibrium in binary systems of hydrocarbons with acetone, Zh. Prikl. Khim.(Leningrad), 34 (1961) 323-331.

196. G. Kolasinska, M. Goral, J. Giza, Vapor-liquid equilibrium and excess gibbs free energy in binary systems of acetone with aliphatic and aromatic hydrocarbons, Z. Phys. Chem. (Leipzig), 263 (1982) 151.

197. V.O. Maripuri, G.A. Ratcliff, Measurement of isothermal vapor-liquid equilibriums for acetone-n-heptane mixtures using modified Gillespie still, Journal of Chemical & Engineering Data, 17 (1972) 366-369.

198. A. Zacharias, D. Srinivasan, M.G.S. Rau, Isobaric vapor-liquid equilibria for the systems acetone + n-heptane and n- hexane + trichloroethylene., Indian J. Technol., 14 (1976) 162.

199. K. Schaefer, W. Rall, F.C. Wirth-Lindemann, Thermodynamic experiments on the systems acetone + n-heptane and acetone + n-nonane., Z. Phys. Chem. (Munich), 14 (1958) 197-207.

200. U. Messow, U. Doye, S. Kuntzsch, D. Kuchenbecker, Thermodynamic studies on solvent/n-paraffin systems. V. The acetone/n- decane, acetone/n-dodecane, acetone/n-

tetradecane and acetone/n-hexadecane systems., Z. Phys. Chem. (Leipzig), 258 (1977) 90-106.

201. V.C. Maripuri, G.A. Ratcliff, Isothermal vapour-liquid equilibria in binary mixtures of ketones and alkanes, Journal of Applied Chemistry and Biotechnology, 22 (1972) 899-903.

202. J. Edwards, J.I. Rodriguez, Thermodynamics of the n-decane + acetone system: I, Monatsh. Chem., 100 (1969) 2066.

203. K. Kojima, K. Tochigi, K. Kurihara, M. Nakamichi, Isobaric vapor-liquid equilibria for acetone + chloroform + benzene and the three constituent binary systems, Journal of Chemical & Engineering Data, 36 (1991) 343-345.

204. M.R. Ebersole, Minimum boiling-points and vapor composition, II, The Journal of Physical Chemistry, 5 (1900) 239-255.

205. A.N. Campbell, R.M. Chatterjee, Vapor–liquid equilibria in the system acetone–benzene, Canadian Journal of Chemistry, 48 (1970) 277-285.

206. J. Kraus, J. Linek, Liquid-vapor equilibrium. XLVIII. The systems acetone-benzene, acetone-toluene, benzene-methyl ethyl ketone, methyl ethyl ketone-toluene and methyl ethyl ketone-ethylbenzene., Collect. Czech. Chem. Commun., 36 (1971) 2547−2567.

207. R.V. Orye, J.M. Prausnitz, Thermodynamic properties of some binary solutions containing hydrocarbons and polar organic solvents, Transactions of the Faraday Society, 61 (1965) 1338-1346.

208. M.R. Rao, R. Sitapathy, N.S.R. Anjaneyulu, G.J.V.J. Raju, C.V. Rao, J. Sci. Ind. Res. Sect. B, 15 (1956) 556.

209. G. Kortuem, H.-J. Freier, F. Woerner, The dynamic method of determining vapor-liquid equilibria., Chem. Ing. Tech., 25 (1953) 125.

210. M.A. Rosanoff, C.W. Bacon, R.H. White, A rapid laboratory method of measuring the partial vapor pressures of liquid mixtures, Journal of the American Chemical Society, 36 (1914) 1803-1825.

211. V. Bekarek, E. Hala, Liquid-vapor equilibrium. XXXIX. Liquid-vapor equilibrium in systems of components with widley differing volatilities., Collect. Czech. Chem. Commun., 33 (1968) 2598-2607.

212. J. Polednová, I. Wichterle, Vapour-liquid equilibrium in the acetone-water system at 101.325 kPa, Fluid Phase Equilibria, 17 (1984) 115-121.

213. N.D. Loi, Liquid-steam balance test plant and meter readings for an R12/Rll mixture, Luft Kaeltetech, 19 (1983) 37-40.

214. M. Meskel-Lesavre, D. Richon, H. Renon, Bubble pressures and saturated liquid molar volumes of trichlorofluoromethane—chlorodifluoromethane mixtures. Representation of refrigerant-mixtures vapor—liquid equilibrium data by a modified form of the Peng—Robinson equation of state, Fluid Phase Equilibria, 8 (1982) 37-53.

215. H. Kubota, T. Ikawa, Y. Tanaka, T. Makita, K. Miyoshi, Vapor-liquid equilibria of non-azeotropic halogenated hydrocarbon mixtures under high pressure, JOURNAL OF CHEMICAL ENGINEERING OF JAPAN, 23 (1990) 155-159.

216. Y.W. Kang, K.Y. Chung, Vapor−liquid equilibria for the systems difluoromethane + chlorodifluoromethane, difluoromethane + dichlorodifluoromethane, and difluoromethane + Chloromethane at 10.0 °C, Journal of Chemical and Engineering Data, 41 (1996) 443-445.

217. M. Nagel, K. Bier, Vapour-liquid equilibrium of ternary mixtures of the refrigerants R32, R125 and R134a, International Journal of Refrigeration, 18 (1995) 534-543.

218. B.G. Lee, J.Y. Park, J.S. Lim, S.Y. Cho, K.Y. Park, Phase equilibria of chlorofluorocarbon alternative refrigerant mixtures, Journal of Chemical & Engineering Data, 44 (1999) 190-192.

219. M. Kobayashi, H. Nishiumi, Vapor–liquid equilibria for the pure, binary and ternary systems containing HFC32, HFC125 and HFC134a, Fluid Phase Equilibria, 144 (1998) 191-202.

220. J.V. Widiamto, H. Sato, K. Watanabe, Saturated-liquid densities and bubble-point pressures of the binary system HFC-32 + HFC-125, Pion, London, ROYAUME-UNI, 1993.

221. R. Kato, H. Nishiumi, Vapor–liquid equilibria and critical loci of binary and ternary systems composed of CH2F2, C2HF5 and C2H2F4, Fluid Phase Equilibria, 249 (2006) 140-146.

222. E.-Y. Chung, M.S. Kim, Vapor−liquid equilibria for the difluoromethane (HFC-32) + 1,1,1,2-tetrafluoroethane (HFC-134a) system, Journal of Chemical & Engineering Data, 42 (1997) 1126-1128.

223. M.B. Shiflett, S.I. Sandler, Modeling fluorocarbon vapor–liquid equilibria using the Wong–Sandler model, Fluid Phase Equilibria, 147 (1998) 145-162.

224. C.N. Kim, Y.M. Park, Vapor−liquid equilibria for the difluoromethane (HFC-32) + 1,1,1-trifluoroethane (HFC-143a) system, Journal of Chemical & Engineering Data, 45 (1999) 34-37.

225. T. Fujimine, H. Sato, K. Watanabe, Bubble-point pressures and saturated- and compressed-liquid densities of the binary R-125 + R-143a system, International Journal of Thermophysics, 20 (1999) 911-922.

226. J. Mikšovský, I. Wichterle, Vapour-liquid equilibria in the ethane-propane system at high pressures, Collect. Czech. Chem. Commun., 40 (1975) 365-370.

227. Y. Kayukawa, K. Fujii, Y. Higashi, Vapor−liquid equilibrium (VLE) properties for the binary systems propane (1) + n-butane (2) and propane (1) + isobutane (3), Journal of Chemical & Engineering Data, 50 (2005) 579-582.

228. H. Hipkin, Experimental vapor-liquid equilibrium data for propane-isobutane, AIChE Journal, 12 (1966) 484-487.

229. R.H. Sage, B.L. Hicks, W.N. Lacey, Phase equilibria in hydrocarbon systems, Industrial & Engineering Chemistry, 32 (1940) 1085-1092.

230. J. Vejrosta, I. Wichterle, The propane-pentane system at high pressures, Collect. Czech. Chem. Commun., 39 (1974) 1246-1248.

231. H.H. Reamer, B.H. Sage, Volumetric and phase behavior of propene-propane system, Industrial & Engineering Chemistry, 43 (1951) 1628-1634.

232. M. Hirata, S.B. Suda, Equilibrium measurements by the vapor-liquid flow method vapor-liquid equilibrium measurements for three binary mixtures of n-butane at 0-31c., Jpn. Pet. Inst., 10 (1968) 20-27.

233. H. Myers, VL equilibrium for naphthenes and paraffins, Petroleum Refiner, 36 (1957) 175-180.

234. J.M. Lenoir, G.K. Kuravila, H.G. Hipkin, Enthalpies of cyclohexane and mixtures of n-pentane and cyclohexane, Journal of Chemical & Engineering Data, 16 (1971) 271-276.

235. E.H. Leslie, A.R. Carr, Vapor Pressure of Organic Solutions, Industrial & Engineering Chemistry, 17 (1925) 810-817.

236. K.N. Marsh, J.B. Ott, M.J. Costigan, Excess enthalpies, excess volumes, and excess Gibbs free energies for (n-hexane + n-decane) at 298.15 and 308.15 K, The Journal of Chemical Thermodynamics, 12 (1980) 343-348.

237. ChenChen, M. Tang, Y.-P. Chen, Vapor−liquid equilibria of binary and ternary mixtures of cyclohexane, 3-methyl-2-butanone, and octane at 101.3 kPa, Journal of Chemical & Engineering Data, 41 (1996) 557-561.

238. D.V.S. Jain, O.P. Yadav, Thermodynamics of n-alkane solutions: part III - vapour pressure and excess free energy for n-octane-cyclohexane system., Indian J. Chem., 9 (1971) 342.

239. L. Sieg, Vapor-liquid equilibria in binary systems of hydrocarbons of various types, Chem.-Ing.-Tech., 22 (1950) 322-326.

240. J. Ocon, J. Espantoso, Vapor-liquid equilibrium: IV methanol + benzene and carbon tetrachloride + toluene systems, An. R. Soc. Esp. Fis. Quim., B, 54 (1950) 421-430.

241. A.H. Wehe, J. Coates, Vapor-Liquid equilibrium relations predicted by thermodynamic examination of activity coefficients, Aiche Journal, 1 (1955) 241-246.

242. V. Nataraj, M.R. Rao, Isobaric Vapor-liquid equilibrium data for the binary systems benzene- cyclohexand, benzene-isobutranol, and cyclohexand-isobutanol, Indian J. Technol., 5 (1967) 212.

243. Y. De Mauduit, M. Enjalbert, Extension of dynamic ebulliometry to measurements under moderate pressures, Chim. Ind., Genie Chim., 102 (1969) 965.

244. J.L.H. Wang, B.C.Y. Lu, Vapor-liquid equilibrium data for the n-pentane - benzene system., J. Appl. Chem. Biotechnol., 21 (1971) 297.

245. H.S. Myers, Vapor-liquid equilibrium data for binary mixtures of paraffins and aromatics, Industrial & Engineering Chemistry, 47 (1955) 2215-2219.

246. F. Gotthard, I. Minea, Rev. Chim.(Bucharest), 11 (1960) 642.

247. M.S. Medani, M.A. Hasan, Thermodynamic properties of the n-hexane and benzene system at elevated temperatures, Journal of Applied Chemistry and Biotechnology, 27 (1977) 80-92.

248. S.R.M. Ellis, A new equilibrium still and binary equilibrium data, Trans. Inst. Chem. Eng., 30 (1952) 58.

249. I.M. Elshayal, B.C.Y. Lu, Isothermal Vapor-liquid equilibria for the binary system benzene-n-octane, J. Appl. Chem. Biotechnol., 18 (1968) 277-280.

250. S. Gu, Y. Zheng, W. Zhao, J. Shi, Study on the VLE for methylcyclohexane-benzene-DMF-Water system, Natural Gas Chemical Industry, 20 (1995) 56-59.

251. X. Huang, S. Xia, P. Ma, S. Song, B. Ma, Vapor–liquid equilibrium of N-formylmorpholine with toluene and xylene at 101.33 kPa, Journal of Chemical & Engineering Data, 53 (2007) 252-255.

252. P.M. Heertjes, Determination of vapor-liquid equilibria of binary mixtures, Chem. Process Eng. (London), 41 (1960) 385-387.

253. M.K. Gupta, G.C. Gardner, M.J. Hegarty, A.J. Kidnay, Liquid-vapor equilibriums for the N2 + CH4 + C2H6 system from 260 to 280 K, Journal of Chemical & Engineering Data, 25 (1980) 313-318.

254. H.H. Reamer, B.H. Sage, W.N. Lacey, Phase equilibria in hydrocarbon systems. volumetric and phase behavior of the methane-propane system, Industrial & Engineering Chemistry, 42 (1950) 534-539.

255. M.E. Kandil, E.F. May, B.F. Graham, K.N. Marsh, M.A. Trebble, R.D. Trengove, S.H. Huang, Vapor−liquid equilibria measurements of methane + 2-methylpropane (isobutane) at temperatures from (150 to 250) K and pressures to 9 MPa, Journal of Chemical & Engineering Data, 55 (2010) 2725-2731.

256. W.E. Reiff, P. Peters-Gerth, K. Lucas, A static equilibrium apparatus for (vapour + liquid) equilibrium measurements at high temperatures and pressures results for (methane + n-pentane), The Journal of Chemical Thermodynamics, 19 (1987) 467-477.

257. A. Toyama, P.S. Chappelear, T.W. Leland, R. Kobayashi, Vapor-liquid equilibria at low temperatures: the carbon monoxide + methane system, Adv. Cryog. Eng., 7 (1962) 125-136.

258. H.H. Reamer, B.H. Sage, Phase behavior in the nitrogen-ammonia system, Journal of Chemical & Engineering Data, 4 (1959) 303-305.

259. I.R. Krichevskii, N.E. Khazanova, L.S. Lesnevskaya, L.Y. Sandalova, Liquid-gas equilibrium in the nitrogen + carbon dioxide system under elevated pressures., Khim. Prom-st. (Moscow), 38 (1962) 169-171.

CHAPTER VII

CONCLUSIONS AND RECOMMENDATIONS

In this chapter, the conclusions and recommendations of the studies presented in Chapters 2-6 are summarized herein.

7.1 Quantitative structure-property relationship (QSPR) models for prediction of pure-fluid critical properties and acentric factor

The objective of this part of the study was to develop an accurate non-linear QSPR model to predict the critical properties (critical temperature, pressure and volume) and acentric factor using a database made up of diverse set of compounds. Following are the conclusions and recommendations of this specific study.

Conclusions

- Four reasonably accurate non-linear models for the prediction of the critical temperature, critical pressure, critical volume and acentric factor were developed using the QSPR methodology.
- The new QSPR models were capable of predicting the critical properties and acentric factor values of the diverse set of molecules with errors of 2%, 3%, 2% and 12%AAD for critical temperature, critical pressure, critical volume and acentric factor, respectively.
- Unlike models for predicting T_c, P_c and V_c, the developed model for predicting ω has higher prediction errors due mainly to the larger experimental uncertainties in the acentric factor data.

- The resulting models from this work can be used to predict *a priori* the critical temperature, critical pressure, critical volume and acentric factor of new molecules with reasonable accuracy.

Recommendations

- Restricted correlations that provide better predictions for a specific type of molecules (e.g., n-paraffins, n-olefins) should be used where they are applicable and more accurate, although the QSPR models developed in this work have wider ranges of capabilities.
- More accurate experimental data should be assembled for critical temperature, critical pressure, and vapor pressure since the acentric factor is a defined quantity determined from these properties. The use of these data will lead to better predictions for acentric factor for diverse set of compounds.

7.2 Modeling high-pressure phase equilibria of coalbed gases / water mixtures with the Peng-Robinson equation of state

The objective of this part of the work was to develop generalized expressions to describe the temperature dependence of the binary interaction parameters in the PR EOS for coalbed gases (methane, nitrogen and carbon dioxide) with water systems. Following are the conclusions and recommendations of this specific study.

Conclusions

- The PR EOS was successfully employed to model the high-pressure phase equilibria of coalbed gas + water mixtures (methane + water, nitrogen + water and carbon dioxide + water) at conditions encountered in coalbed methane work.
- New expressions were developed for the temperature dependence of interaction parameters in the PR EOS for the three systems.
- The generalized predictions for the liquid-phase compositions were within three times the

experimental uncertainties in the data employed in the analysis. However, the errors in predictions for the vapor-phase composition of water were noticeably higher (on a *percentage* basis), due to the low concentrations of water in the gas-rich phase.

Recommendations

- More data for vapor phase compositions should be assembled for the methane + water and nitrogen + water systems. Such data will lead to better predictions for the vapor-phase composition of these systems.

7.3 Generalized binary interaction parameters for the Peng-Robinson equation of state

The objective of this part of the work was to assess the representation capability of the PR EOS model and generalize the binary interaction parameters of the PR EOS using a QSPR modeling approach. The conclusions and recommendations from this work are presented below.

Conclusions

- The QSPR modeling approach was applied successfully to generalize the binary interaction parameters of the PR EOS model. The modeling effort involved 916 binary VLE systems comprised of diverse molecular species.
- The new QSPR models provided phase equilibria property predictions within two times the errors obtained through the data regression analyses.
- The PR-QSPR generalized model was capable for *a priori* predictions of VLE for diverse systems over wide conditions of pressure, temperature and composition.

Recommendations

- A database containing higher-pressure VLE data over a wider range of temperature for asymmetric binary systems should be assembled. The expand database would facilitate a more comprehensive generalized PR-QSPR model evaluations for the correlations of phase behavior.

- Other mixing rules such as Wong-Sandler mixing rules that are more theoretically based should be used in the CEOS to determine if they can represent more precisely highly non-ideal and aqueous systems.
- Further study should be focused on testing to see if including a temperature dependence of the binary interaction parameters of the PR EOS could lead to more accurate predictions for PR EOS.
- The generalization procedure, employed in this study for classical combining rule parameters, should be applied for conformal combining rule parameters so that the performance of different combining rules could be compared and the relative merits of one combining rule over the other could be explored.

7.4 Volume-translated Peng–Robinson equation of state for saturated and single-phase liquid densities

The objective of this part of the work was to develop a new volume-translation method for the PR EOS that can provide accurate and reliable predictions for *both* saturated and single-phase liquid densities of diverse chemical species over extended ranges of temperature and pressure. The conclusions and recommendations from this work are presented below.

Conclusions

- A volume-translation method for the PR EOS was developed for accurately predicting pure-fluid liquid densities in the saturated and the single-phase region of diverse classes of molecules.
- The generalized volume-translated Peng-Robinson equation-of-state (VTPR EOS) provided an overall %AAD of 0.8 and 1.8 for saturated and compressed liquid densities, respectively.
- Unlike other temperature-dependent volume-translation methods, the VTPR EOS did not

lead to thermodynamic inconsistency such as isotherm cross-overs in the compressed liquid region at higher pressures.

Recommendations

- Additional data should be assembled for chemical classes currently not represented in the database. Such data will enrich the structural representation of the QSPR model and widen its applicability domain.

7.5 Volume-translated Peng-Robinson equation of state for liquid densities of diverse binary mixtures

The objective of this part of the work was to extend the pure-fluid volume-translation function to mixture liquid densities predictions over large ranges of pressure and temperature. The conclusions and recommendations from this work are presented below.

Conclusions

- The pure-fluid volume-translation function was successfully extended to predicting liquid densities of mixtures comprised of diverse molecular species over large ranges of temperature and pressure.
- The new volume-translated PR EOS yielded errors that were three to five times lower than the corresponding predictions from the untranslated PR EOS of state.

Recommendations

- Other mixture critical point calculations methods such as Heidmann and Khalil's algorithm [1] that are more accurate should be used for estimating critical properties of mixtures as part of the volume translation for mixtures.

REFERENCES

1. R.A. Heidemann, A.M. Khalil, The calculation of critical points, AIChE Journal, 26 (1980) 769-779.

APPENDICES

Appendix A

GENERALIZED BINARY INTERACTION PARAMETERS FOR THE PENG-ROBINSON EQUATION OF STATE

Table A.1. Binary VLE Database Used in Model Development

NO.	System	Temperature range (K)	Pressure range (bar)	Component (1) liquid mole fraction range	Component (1) vapor mole fraction range	NDP
1	methyl teritiary butyl ether(1) + methanol(2)	298.15-417.85	0.17-10	0-1	0-1	99
2	methyl teritiary butyl ether(1) + tertiary butyl alcohol(2)	324.65-355.75	1.01-1.01	0-1	0-1	26
3	dimethyl ether(1) + methyl teritiary butyl ether(2)	298.15-348.15	0.34-19.8	0-1	0-1	16
4	methyl teritiary butyl ether(1) + butane(2)	273.15-373.15	0.11-15.18	0-1	0-1	40
5	methyl teritiary butyl ether(1) + isopentane(2)	288.15-421.95	0.22-18.35	0-1	0-1	36
6	methyl teritiary butyl ether(1) + methyl cyclohexane(2)	266.15-333.15	0.01-0.51	0-0.2716	0-0.7022	17
7	isobutene(1) + methyl teritiary butyl ether(2)	323.15-353.15	0.85-12.24	0-1	0-1	29
8	ethyl teritiary butyl ether(1) + ethanol(2)	343.15-363.15	0.94-2.42	0.057-0.884	0.161-0.795	22
9	tertiary butyl alcohol(1) + ethyl teritiary butyl ether(2)	323.15-423.15	0.24-8.68	0-1	0-1	39
10	isopentane(1) + ethyl teritiary butyl ether(2)	293.15-303.15	0.13-1.09	0-1	0-1	30
11	methyl cyclohexane(1) + ethyl teritiary butyl ether(2)	323.15-443.15	0.19-10.13	0-1	0-1	36
12	isobutene(1) + ethyl teritiary butyl ether(2)	323.15-373.15	0.46-18.38	0-1	0-1	16

Table A.1. Binary VLE Database Used in Model Development *(Continued)*

NO.	System	Temperature range (K)	Pressure range (bar)	Component (1) liquid mole fraction range	Component (1) vapor mole fraction range	NDP
13	methanol(1) + teritiary amyl methyl ether(2)	289.25-448.15	0.13-24.85	0-1	0-1	64
14	teritiary amyl methyl ether(1) + teritiary amyl alcohol(2)	363.15-393.15	0.65-1.89	0-0.045	-	22
15	teritiary amyl alcohol(1) + teritiary amyl methyl ether(2)	363.15-393.15	1.11-2.49	0-0.065	-	23
16	teritiary amyl methyl ether(1) + n-pentane(2)	343.15-383.15	0.6-7.38	0-1	0-1	99
17	teritiary amyl methyl ether(1) + methyl cyclohexane(2)	293.15-333.15	0.05-0.42	0-1	0-1	47
18	dimethyl ether(1) + methanol(2)	273.15-293.15	0.04-5.21	0-1	0-1	14
19	diethyl ether(1) + water(2)	273-323	0.25-1.76	0.627-1	0-1	30
20	methanol(1) + ethanol(2)	298.15-351.9	0.08-1.02	0-1	0-1	44
21	butane(1) + methanol(2)	273.15-373.15	0.04-17.18	0-1	0-1	44
22	methanol(1) + n-heptane(2)	331.95-371.55	1.01-1.01	0-1	0-1	22
23	isobutane(1) + methanol(2)	273.15-404.15	0.04-29.26	0-1	0-1	54
24	n-pentane(1) + methanol(2)	303.31-335.37	1-1.01	0.001-1	0.05-1	21
25	1-pentene(1) + methanol(2)	299.45-337.85	1.01-1.01	0-1	0-1	15
26	2-methyl 2-butene(1) + methanol(2)	306.2-337.85	1.01-1.01	0-1	0-1	12
27	Isoprene(1) + methanol(2)	303.15-337.85	0.99-1.01	0-1	0-1	21
28	Isoprene(1) + diethyl ether(2)	303.35-307.75	1.01-1.01	0.0008-0.4	0.0012-0.467	10
29	methanol(1) + 1-heptene(2)	331.75-366.75	1.01-1.01	0-1	0-1	13
30	methanol(1) + water(2)	307.11-373.15	0.27-1.01	0-1	0-1	63
31	butane(1) + ethanol(2)	298.45-345.65	0.08-8.81	0-1	0-1	72
32	ethanol(1) + water(2)	298.15-373.15	0.03-1.01	0-1	0-1	52
33	hexane(1) + tertiary butyl alcohol(2)	313.15-355.57	0.14-1.01	0-1	0-1	42
34	tertiary butyl alcohol(1) + n-heptane(2)	313.15-348.15	0.12-0.88	0-1	0-1	34
35	tertiary butyl alcohol(1) + n-octane(2)	313.15-313.15	0.04-0.14	0-1	-	16
36	tertiary butyl alcohol(1) + isopentane(2)	303.15-373.15	0.08-7.23	0-1	0-1	32
37	tertiary butyl alcohol(1) + 2-methyl 2-butene(2)	303.15-373.15	0.08-5.7	0-1	0-1	36

Table A.1. Binary VLE Database Used in Model Development *(Continued)*

NO.	System	Temperature range (K)	Pressure range (bar)	Component (1) liquid mole fraction range	Component (1) vapor mole fraction range	NDP
38	Isoprene(1) + tertiary butyl alcohol(2)	307.25-355.7	1.01-1.01	0-1	0-1	13
39	tertiary butyl alcohol(1) + water(2)	298.15-373.15	0.03-1.01	0-1	0-1	33
40	teritiary amyl alcohol(1) + n-pentane(2)	343.15-383.15	0.27-7.37	0-1	0-1	99
41	methyl teritiary butyl ether(1) + acetonitrile(2)	313.15-313.15	0.23-0.61	0-1	0-1	35
42	methyl teritiary butyl ether(1) + 1,3-butadiene(2)	273.15-323.15	0.11-5.62	0-1	0-1	16
43	methanol(1) + tertiary butyl alcohol(2)	298.15-355.55	0.06-1.01	0-1	0-1	63
44	methanol(1) + isobutene(2)	323.15-323.15	0.55-6.31	0-1	0-1	11
45	methanol(1) + acetonitrile(2)	298.15-354.75	0.13-1.01	0-1	0-1	115
46	methanol(1) + propionitrile(2)	337.85-370.5	1.01-1.01	0-1	0-1	17
47	ethanol(1) + tertiary butyl alcohol(2)	313.15-355.75	0.14-1.01	0-1	0-1	34
48	teritiary amyl alcohol(1) + water(2)	360.35-375.05	1.01-1.01	0.099-1	0.381-1	10
49	butane(1) + tertiary butyl alcohol(2)	333.15-433.15	3.65-38.89	0.0844-0.9305	0.3033-0.9816	23
50	butane(1) + n-pentane(2)	298.15-298.15	0.73-1.08	0.0176-0.187	0-0.594	12
51	n-pentane(1) + ethanol(2)	293.15-293.15	0.06-0.63	0-0.3	0-0.9227	7
52	n-pentane(1) + 2-methyl 2-butene(2)	273.15-298.15	0.21-0.68	0-1	-	54
53	n-pentane(1) + acetonitrile(2)	333.15-363.15	0.49-5.57	0-1	-	20
54	isobutane(1) + butane(2)	273.15-273.15	1.04-1.57	0-1	0-1	12
55	isobutene(1) + butane(2)	277.59-344.26	1.22-10.09	0-1	-	50
56	isobutene(1) + isobutane(2)	277.59-344.26	1.55-11.13	0-1	-	50
57	1-butene(1) + butane(2)	310.93-410.93	3.55-34.89	0-1	0-1	77
58	1-butene(1) + isobutane(2)	277.62-344.36	1.62-10.89	0.2517-0.7536	-	30
59	1-butene(1) + 1,3-butadiene(2)	277.61-344.38	1.46-9.88	0-1	0-1	62
60	cis, 2-butene(1) + butane(2)	278.15-358.15	1.14-11.21	0.1063-0.7358	-	20
61	trans, 2-butene(1) + butane(2)	278.15-358.15	1.22-11.3	0.0999-0.7512	-	19

Table A.1. Binary VLE Database Used in Model Development *(Continued)*

NO.	System	Temperature range (K)	Pressure range (bar)	Component (1) liquid mole fraction range	Component (1) vapor mole fraction range	NDP
62	2-methyl 1-butene(1) + methanol(2)	300.53-317.85	1.01-1.01	0.05-0.89	0.536-0.837	11
63	2-methyl 1-butene(1) + n-pentane(2)	273.15-298.15	0.25-0.81	0-1	-	48
64	2-methyl 1-butene(1) + 2-methyl 2-butene(2)	273.15-308.8	0.21-0.99	0-1	0-0.629	57
65	2-methyl 2-butene(1) + methanol(2)	305.8-337.85	1.01-1.01	0-1	0-1	23
66	2-methyl 2-butene(1) + ethanol(2)	309.95-351.83	1.01-1.01	0-1	-	13
67	2-methyl 2-butene(1) + acetonitrile(2)	309.25-416.96	1.01-5.23	0-1	0-1	46
68	acetonitrile(1) + ethanol(2)	313.15-313.15	0.18-0.28	0-1	0-1	17
69	acetonitrile(1) + tertiary butyl alcohol(2)	333.15-355.55	0.39-1.01	0-1	0-1	25
70	acetonitrile(1) + butane(2)	425.4-545.5	37.97-48.3	0-1	0-1	4
71	acetonitrile(1) + diisobutylene(2)	313.15-313.15	0.12-0.32	0-1	-	21
72	acetonitrile(1) + water(2)	323.15-333.15	0.12-0.56	0-1	0-1	32
73	propionitrile(1) + n-pentane(2)	467.7-553.7	36.3-45.7	0.1-0.958	-	7
74	propionitrile(1) + water(2)	359.15-371.05	1.01-1.01	0.0019-0.975	0.073-0.871	23
75	1,3-butadiene(1) + methanol(2)	323.15-323.15	0.55-5.82	0-1	0-1	11
76	1,3-butadiene(1) + butane(2)	310.93-338.71	3.55-8.36	0-1	0-1	33
77	1,3-butadiene(1) + isobutane(2)	277.54-344.04	1.63-10.99	0.2478-0.7475	-	30
78	1,3-butadiene(1) + cis, 2-butene(2)	278.15-338.15	1.1-7.83	0.0882-0.7498	-	12
79	1,3-butadiene(1) + trans, 2-butene(2)	278.15-338.15	1.2-8.19	0.0529-0.9515	-	20
80	1,3-butadiene(1) + acetonitrile(2)	304.71-330.18	0.73-6.4	0.056-0.913	-	38
81	cis, 1,3-pentadiene(1) + methanol(2)	311.15-337.85	1.01-1.01	0-1	0-1	13
82	trans, 1,3-pentadiene(1) + methanol(2)	309.63-337.85	1.01-1.01	0-1	0-1	23
83	trans, 1,3-pentadiene(1) + acetonitrile(2)	303.15-313.15	0.36-0.95	0.1-0.9	0.5913-0.9278	18
84	tertiary butyl alcohol(1) + 2-methyl 1-butene(2)	303.15-373.15	0.08-7.23	0-1	0-1	32
85	methyl mercaptan(1) + methanol(2)	269.15-288.15	0.03-1.43	0-1	0-1	30

Table A.1. Binary VLE Database Used in Model Development *(Continued)*

NO.	System	Temperature range (K)	Pressure range (bar)	Component (1) liquid mole fraction range	Component (1) vapor mole fraction range	NDP
86	dimethyl sulfide(1) + methanol(2)	263.15-288.15	0.02-0.46	0-1	0-1	30
87	Hydrogen Sulfide(1) + methanol(2)	298.15-348.15	0.17-58	0-1	0-1	26
88	methanol(1) + dimethyl disulfide(2)	310.95-335.95	0.07-0.96	0-1	0-1	21
89	methyl mercaptan(1) + water(2)	323.06-372.65	0.12-5.02	0-0.0081	0-0.9441	10
90	dimethyl disulfide(1) + methyl mercaptan(2)	273.15-373.15	0.01-14.45	0-1	0-1	30
91	Hydrogen Sulfide(1) + methyl mercaptan(2)	305.35-321.35	22.77-25.93	0.775-0.9914	0.9497-0.9995	27
92	Hydrogen Sulfide(1) + dimethyl sulfide(2)	313.71-313.71	5.37-16.21	0.221-0.619	0.813-0.962	4
93	methyl mercaptan(1) + dimethyl sulfide(2)	263.15-368.23	0.17-12.42	0.0819-0.9506	0.2089-0.9821	24
94	benzene(1) + toluene(2)	353.25-383.76	1.01-1.01	0-1	0-1	13
95	n-heptane(1) + ethylbenzene(2)	327.76-327.76	0.06-0.23	0-1	0-1	17
96	n-octane(1) + ethylbenzene(2)	398.85-409.35	1.01-1.01	0-1	0-1	21
97	1-heptene(1) + toluene(2)	328.15-328.15	0.15-0.27	0-1	0-1	13
98	n-heptane(1) + p-xylene(2)	313.11-313.11	0.03-0.12	0-1	0-1	15
99	benzene(1) + cyclohexane(2)	313.15-313.15	0.24-0.27	0-1	0-1	11
100	methyl cyclopentane(1) + benzene(2)	313.14-313.14	0.24-0.34	0-1	0-1	16
101	cyclohexane(1) + toluene(2)	298.15-298.15	0.04-0.13	0-1	0-1	13
102	Isoprene(1) + 2-methyl 2-butene(2)	307.22-311.72	1.01-1.01	0-1	0-1	11
103	hexafluorobenzene(1) + toluene(2)	303.15-303.15	0.05-0.14	0-1	0-1	12
104	tetrachloromethane(1) + benzene(2)	349.68-353.18	1.01-1.01	0-1	0-1	16
105	carbondisulfide(1) + cyclohexane(2)	298.15-298.15	0.13-0.48	0-1	0-1	12
106	carbondisulfide(1) + cyclopentane(2)	288.15-288.15	0.28-0.34	0-1	0-1	19
107	carbondisulfide(1) + tetrachloromethane(2)	298.15-298.15	0.17-0.47	0.0318-0.9626	0.1049-0.9838	14
108	hexafluorobenzene(1) + p-xylene(2)	313.15-313.15	0.03-0.22	0-1	0-1	12
109	hexafluorobenzene(1) + cyclohexane(2)	303.15-303.15	0.14-0.21	0-1	0-1	12
110	toluene(1) + 4-methyl 2-pentanone(2)	323.15-323.15	0.09-0.12	0-1	0-1	28
111	toluene(1) + 2-pentanone(2)	323.15-323.15	0.12-0.16	0-1	0-1	27

Table A.1. Binary VLE Database Used in Model Development *(Continued)*

NO.	System	Temperature range (K)	Pressure range (bar)	Component (1) liquid mole fraction range	Component (1) vapor mole fraction range	NDP
112	benzene(1) + acetone(2)	329.33-353.25	1.01-1.01	0-1	0-1	15
113	benzene(1) + 2-butanone(2)	389.65-392.75	3.08-3.08	0.1-0.9	0.109-0.885	9
114	benzene(1) + thiophene(2)	328.15-328.15	0.38-0.45	0-1	0-1	12
115	hexafluorobenzene(1) + diisopropyl ether(2)	298.13-298.13	0.11-0.2	0-1	0-1	29
116	tetrachloromethane(1) + 2-butanone(2)	346.85-352.7	1.01-1.01	0-1	0-1	14
117	cyclohexane(1) + 2-butanone(2)	344.75-353.95	1.01-1.01	0-1	0-1	23
118	n-heptane(1) + thiophene(2)	328.15-328.15	0.23-0.39	0-1	0-1	25
119	n-heptane(1) + 3-pentanone(2)	353.15-353.15	0.5-0.67	0-1	0-1	17
120	n-heptane(1) + 2-butanone(2)	350.15-371.45	1.01-1.01	0-1	0-1	19
121	n-decane(1) + acetone(2)	333.15-333.15	0.01-1.15	0-1	0-1	14
122	tetrachloromethane(1) + furfural(2)	350.15-434.85	1.01-1.01	0-1	0-1	11
123	tetrachloromethane(1) + acetone(2)	304.35-321.92	0.4-0.4	0-1	0-1	29
124	benzene(1) + 1,2-dichloroethane(2)	353.25-356.62	1.01-1.01	0-1	0-1	17
125	toluene(1) + 1,2-dichloroethane(2)	356.6-383.76	1.01-1.01	0-1	0-1	13
126	benzene(1) + diethylamine(2)	328.15-328.15	0.44-1	0-1	0-1	15
127	benzene(1) + Triethylamine(2)	353.15-353.15	0.76-1.01	0-1	0-1	22
128	ethylbenzene(1) + acrylonitrile(2)	282.95-330.85	0.07-0.07	0-1	0-1	10
129	toluene(1) + nitrobenzene(2)	373.15-373.15	0.03-0.75	0-1	0-1	8
130	n-heptane(1) + butylchloride(2)	323.15-323.15	0.19-0.39	0-1	0-1	15
131	cyclopentane(1) + chloroform(2)	298.15-298.15	0.26-0.42	0-1	0-1	14
132	n-heptane(1) + Triethylamine(2)	333.15-333.15	0.28-0.39	0-1	0-1	20
133	2,3-dimethylbutane(1) + chloroform(2)	328.65-333.95	1.01-1.01	0-1	0-1	11
134	ethylbenzene(1) + nitrobenzene(2)	373.15-373.15	0.03-0.34	0-1	0-1	8
135	benzene(1) + nitromethane(2)	318.15-318.15	0.13-0.3	0-1	0-1	15

Table A.1. Binary VLE Database Used in Model Development *(Continued)*

NO.	System	Temperature range (K)	Pressure range (bar)	Component (1) liquid mole fraction range	Component (1) vapor mole fraction range	NDP
136	benzene(1) + tertiary butyl alcohol(2)	318.15-318.15	0.18-0.34	0-1	0-1	13
137	benzene(1) + ethanol(2)	324.35-335.65	0.53-0.53	0-1	0-1	12
138	benzene(1) + 2-propanol(2)	344.28-355.53	1.01-1.01	0-1	0-1	30
139	n-heptane(1) + ethyl iodide(2)	323.15-323.15	0.19-0.47	0-1	0-1	18
140	cyclohexane(1) + pyridine(2)	353.15-388.45	1.01-1.01	0-1	0-1	13
141	n-octane(1) + pyridine(2)	353.15-353.15	0.23-0.39	0-1	0-1	15
142	n-octane(1) + methanol(2)	335.85-398.75	1.01-1.01	0-1	0-1	13
143	cyclohexane(1) + ethanol(2)	308.15-308.15	0.14-0.3	0-1	0-1	9
144	n-pentane(1) + 1-butanol(2)	303.15-303.15	0.01-0.82	0-1	0-1	15
145	tetrachloroethylene(1) + ethanol(2)	350.85-394.25	1.01-1.01	0-1	0-1	17
146	hexafluorobenzene(1) + 1-propanol(2)	288.15-288.15	0.02-0.08	0-1	0-1	10
147	hexafluorobenzene(1) + methanol(2)	288.15-288.15	0.07-0.15	0-1	0-1	11
148	propionic aldehyde(1) + acetone(2)	321.13-329.35	1.01-1.01	0-1	0-1	15
149	propionic aldehyde(1) + 2-butanone(2)	318.15-318.15	0.3-0.91	0-1	0-1	15
150	acetone(1) + vinyl acetate(2)	329.45-345.8	1.01-1.01	0-1	0-1	11
151	acetone(1) + propyl acetate(2)	330.85-372.15	1.01-1.01	0.02-0.96	0.09-0.99	15
152	acetaldehyde(1) + vinyl acetate(2)	293.5-345.71	1.01-1.01	0-1	0-1	28
153	acetaldehyde(1) + methyl acetate(2)	293.5-330.05	1.01-1.01	0-1	0-1	19
154	diethyl ether(1) + acetone(2)	303.15-303.15	0.38-0.86	0-1	0-1	13
155	acetaldehyde(1) + diethyl ether(2)	292.8-307.8	1.01-1.01	0-1	0-1	12
156	diethyl ether(1) + methyl iodide(2)	308.15-308.15	0.78-1.03	0-1	0-1	11
157	diethyl ether(1) + dichloromethane(2)	307.1-313.35	0.99-0.99	0-1	0-1	27
158	1,4-dioxane(1) + 2-propanol(2)	355.65-372.65	1.01-1.01	0.036-0.955	0.033-0.9	20
159	Ethyl propyl ether(1) + chloroform(2)	316.05-322.2	0.53-0.53	0-1	0-1	17
160	diethyl ether(1) + chloroform(2)	310.45-333.45	1-1	0.0566-0.874	0.0636-0.9719	10

Table A.1. Binary VLE Database Used in Model Development *(Continued)*

NO.	System	Temperature range (K)	Pressure range (bar)	Component (1) liquid mole fraction range	Component (1) vapor mole fraction range	NDP
161	acetone(1) + chloroform(2)	308.15-308.15	0.33-0.47	0-1	0-1	11
162	propyl acetate(1) + 1-propanol(2)	361.21-367.14	0.8-0.8	0-1	0-1	11
163	ethyl acetate(1) + 2-propanol(2)	333.15-333.15	0.42-0.58	0.0455-0.9225	0.1254-0.9	19
164	diethyl ether(1) + ethanol(2)	273.15-273.15	0.05-0.24	0.05-0.95	0.6787-0.9861	19
165	furfural(1) + ethanol(2)	338.15-338.15	0.07-0.56	0.0201-0.98	0.0048-0.351	9
166	acetone(1) + methanol(2)	328.15-328.15	0.69-1	0-1	0-1	12
167	1,4-dioxane(1) + methanol(2)	308.15-308.15	0.08-0.28	0-1	0-1	16
168	ethanol(1) + Triethylamine(2)	308-308	0.14-0.16	0-1	0-1	12
169	tertiary butyl alcohol(1) + 1-butanol(2)	312.57-343.06	0.13-0.13	0-1	0-1	11
170	1-propanol(1) + 2-methyl 1-propanol(2)	343.15-343.15	0.21-0.33	0-1	0-1	11
171	ethanol(1) + 2-propanol(2)	351.61-355.54	1.01-1.01	0-1	0-1	12
172	methanol(1) + 2-methyl 1-propanol(2)	323.15-323.15	0.07-0.56	0-1	0-1	11
173	ethanol(1) + 2-methyl 1-propanol(2)	333.15-333.15	0.13-0.47	0-1	0-1	11
174	butylamine(1) + 1-butanol(2)	313.15-313.15	0.03-0.25	0-1	0-1	10
175	diethylamine(1) + ethanol(2)	313.15-313.15	0.19-0.57	0-1	0-1	11
176	butylamine(1) + 1-propanol(2)	318.15-318.15	0.09-0.31	0-1	0-1	11
177	bromobenzene(1) + cyclohexanol(2)	383.15-383.15	0.17-0.28	0-1	0-1	11
178	1,2-dichloroethane(1) + 2-methyl 1-propanol(2)	323.15-323.15	0.07-0.31	0-1	0-1	11
179	methanol(1) + 1,2-dichloroethane(2)	313.15-313.15	0.2-0.44	0-1	0-1	11
180	water(1) + diethylamine(2)	311.5-311.5	0.07-0.54	0-1	0-1	13
181	water(1) + pyridine(2)	362.98-362.98	0.46-0.87	0-1	0-1	19
182	water(1) + methanol(2)	337.65-373.15	1.01-1.01	0-1	0-1	21
183	water(1) + 2-propanol(2)	308.93-323.86	0.13-0.13	0-1	0-1	24
184	water(1) + ethanol(2)	351.55-369.25	1.01-1.01	0.2606-0.985	0.105-0.8575	13
185	acetaldehyde(1) + propylene oxide(2)	293.15-308.15	1.01-1.01	0-1	0-1	18

Table A.1. Binary VLE Database Used in Model Development *(Continued)*

NO.	System	Temperature range (K)	Pressure range (bar)	Component (1) liquid mole fraction range	Component (1) vapor mole fraction range	NDP
186	propionic aldehyde(1) + cyclohexane(2)	318.15-318.15	0.3-0.92	0-1	0-1	18
187	chloroform(1) + furfural(2)	336.05-424.35	1.01-1.01	0.04-0.929	0.296-0.999	14
188	1-butene(1) + furfural(2)	310.95-324.85	1.01-5.27	0.0318-0.3121	0.984-0.999	18
189	toluene(1) + furfural(2)	384.45-426.45	1.01-1.01	0.027-0.9536	0.2507-0.983	20
190	ethylbenzene(1) + furfural(2)	405.45-427.65	0.96-0.96	0.035-0.979	0.1383-0.974	16
191	p-xylene(1) + furfural(2)	407.35-428.95	0.96-0.96	0.0223-0.962	0.096-0.954	20
192	n-pentane(1) + acetone(2)	238.15-322.3	0.01-1.01	0-1	0-1	49
193	furfural(1) + n-decane(2)	420.35-437.55	1.01-1.01	0.074-0.978	0.3-0.865	11
194	toluene(1) + benzaldehyde(2)	327.55-370.05	0.13-0.13	0.1-0.9	0.553-0.985	9
195	benzaldehyde(1) + benzyl acetate(2)	392.55-414.85	0.13-0.13	0.082-0.83	0.255-0.974	7
196	acetone(1) + tetrachloromethane(2)	304.35-349.85	0.4-1.01	0-1	0-1	103
197	carbondisulfide(1) + acetone(2)	298.15-302.35	0.43-0.6	0.074-0.951	0.286-0.806	10
198	acetone(1) + acetonitrile(2)	318.15-318.15	0.3-0.64	0.052-0.896	0.12-0.951	10
199	acetone(1) + 1,2-dichloroethane(2)	329.26-356.56	1-1.01	0-1	0-1	28
200	acetone(1) + ethyl iodide(2)	293.15-293.15	0.19-0.27	0.09-0.95	0.2991-0.9325	6
201	methyl acetate(1) + acetone(2)	328.55-329.45	1.01-1.01	0.105-0.933	0.125-0.912	9
202	acetone(1) + methyl acetate(2)	293.15-329.65	0.23-1.01	0.027-0.965	0.033-0.964	56
203	acetone(1) + 2-butanone(2)	330.05-395.15	1.01-3.45	0.019-0.95	0.037-0.972	39
204	acetone(1) + ethyl acetate(2)	329.75-348.45	1.01-1.01	0.046-0.98	0.102-0.989	16
205	diethyl ether(1) + acetone(2)	293.15-293.15	0.25-0.58	0-1	0-1	7
206	acetone(1) + pyridine(2)	329.25-388.45	1.01-1.01	0-1	0-1	13
207	Isoprene(1) + acetone(2)	307.05-329.55	1.01-1.01	0-1	0-1	11
208	2-methyl 2-butene(1) + acetone(2)	308.75-317.9	1.01-1.01	0.139-0.906	0.384-0.866	18
209	isopentane(1) + acetone(2)	298.73-317.5	1.01-1.01	0.0593-0.952	0.371-0.92	17
210	acetone(1) + 1,1,2-trichloroethane(2)	330.45-385.15	1.01-1.01	0.022-0.919	0.08-0.991	21

Table A.1. Binary VLE Database Used in Model Development *(Continued)*

NO.	System	Temperature range (K)	Pressure range (bar)	Component (1) liquid mole fraction range	Component (1) vapor mole fraction range	NDP
211	cyclohexane(1) + 4-methyl 2-pentanone(2)	338.4-383.95	0.53-1.01	0.055-0.965	0.1725-0.975	47
212	benzene(1) + 4-methyl 2-pentanone(2)	338.5-385.85	0.43-1.01	0.042-0.968	0.118-0.99	63
213	chloroform(1) + 4-methyl 2-pentanone(2)	335-386.6	1.01-1.01	0.0453-0.9774	0.0944-0.999	14
214	cyclohexane(1) + cyclohexanone(2)	323.15-348.15	0.1-0.83	0.065-0.96	0.662-0.9905	27
215	n-heptane(1) + 3-pentanone(2)	338.15-368.15	0.29-1.07	0-1	0-1	51
216	3-pentanone(1) + 4-methyl 2-pentanone(2)	375.67-387.55	1.01-1.01	0.126-0.951	0.161-0.972	19
217	ethyl acetate(1) + 3-pentanone(2)	350.25-374.85	1.01-1.01	0-1	0-1	11
218	methyl acetate(1) + 3-pentanone(2)	329.85-374.85	1.01-1.01	0-1	0-1	11
219	2-butanone(1) + ethylbenzene(2)	298.15-348.15	0.01-0.84	0-1	0-1	57
220	2-butanone(1) + n-octane(2)	338.15-338.15	0.23-0.61	0.058-0.97	0.472-0.968	9
221	2-butanone(1) + n-heptane(2)	323.15-371.45	0.28-1.01	0-1	0-1	35
222	2-butanone(1) + toluene(2)	323.15-383.75	0.12-1.01	0-1	0-1	96
223	2-butanone(1) + benzene(2)	323.15-421.95	0.36-5.65	0-1	0-1	74
224	benzene(1) + 2-butanone(2)	313.15-333.15	0.24-0.55	0-0.9197	0-0.908	45
225	2-methyl 2-butene(1) + 2-butanone(2)	311.69-352.65	1.01-1.01	0-1	0-1	13
226	ethyl acetate(1) + 2-butanone(2)	349.78-353.1	1.01-1.01	0-1	0-1	14
227	chloroform(1) + 2-butanone(2)	336.05-352.85	1.01-1.01	0.035-0.935	0.033-0.981	18
228	acetone(1) + n-decane(2)	313.15-333.15	0.01-1.15	0-1	0-1	25
229	diethyl ether(1) + benzene(2)	273.15-353.45	0.04-1.02	0-1	0-1	57
230	diethyl ether(1) + hexafluorobenzene(2)	298.13-298.13	0.11-0.71	0-0.9959	0-0.999	30
231	diethyl ether(1) + ethyl acetate(2)	273.15-303.15	0.03-0.87	0-1	0-1	33
232	1,4-dioxane(1) + n-octane(2)	353.15-353.15	0.25-0.53	0.021-0.981	0.098-0.967	8
233	1,4-dioxane(1) + toluene(2)	335.27-382.7	0.27-1.01	0-1	0-1	51
234	n-heptane(1) + 1,4-dioxane(2)	353.15-353.15	0.53-0.72	0.0173-0.977	0.063-0.951	12
235	benzene(1) + 1,4-dioxane(2)	298.15-373.21	0.05-1.01	0-1	0-1	118

Table A.1. Binary VLE Database Used in Model Development *(Continued)*

NO.	System	Temperature range (K)	Pressure range (bar)	Component (1) liquid mole fraction range	Component (1) vapor mole fraction range	NDP
236	diethylamine(1) + 1,4-dioxane(2)	328.45-374.55	1.01-1.01	0-1	0-1	18
237	ethyl acetate(1) + 1,4-dioxane(2)	350.05-374.55	1.01-1.01	0-1	0-1	39
238	carbondisulfide(1) + 1,4-dioxane(2)	293.15-293.15	0.03-0.4	0-1	0-1	13
239	tetrachloromethane(1) + 1,4-dioxane(2)	298.15-313.15	0.05-0.28	0-1	0-1	63
240	diisopropyl ether(1) + ethylbenzene(2)	323.15-343.15	0.08-1	0.048-0.95	0.345-0.993	40
241	diisopropyl ether(1) + toluene(2)	323.15-343.15	0.15-1	0.044-0.892	0.163-0.965	39
242	diisopropyl ether(1) + benzene(2)	323.15-353.25	0.36-1.07	0-1	0-1	59
243	diisopropyl ether(1) + hexafluorobenzene(2)	298.13-298.13	0.11-0.2	0-1	0-1	32
244	chloroform(1) + diisopropyl ether(2)	303.5-343.75	0.33-1.01	0-1	0-1	86
245	diisopropyl ether(1) + n-heptane(2)	342.35-388.85	1.01-2.21	0.197-0.932	0.36-0.972	18
246	acetaldehyde(1) + diethyl ether(2)	292.8-304.3	1.01-1.01	0.058-0.926	0.155-0.904	10
247	propionic aldehyde(1) + methyl acetate(2)	303.16-313.13	0.36-0.76	0-1	0-1	30
248	propionic aldehyde(1) + ethyl acetate(2)	303.16-313.15	0.16-0.76	0-1	0-1	36
249	propionic aldehyde(1) + benzene(2)	313.15-313.15	0.24-0.76	0-1	0-1	15
250	n-pentane(1) + propionic aldehyde(2)	313.15-313.15	0.76-1.36	0-1	0-1	26
251	Isoprene(1) + butyraldehyde(2)	307.25-337.35	1.01-1.01	0.1-1	0.3017-1	10
252	dichloromethane(1) + furfural(2)	312.3-434.95	1.01-1.01	0-1	0-1	21
253	1,2-dichloroethane(1) + furfural(2)	356.65-434.95	1.01-1.01	0-1	0-1	21
254	acetone(1) + furfural(2)	329.25-434.85	1.01-1.01	0-1	0-1	12
255	ethyl acetate(1) + furfural(2)	350.35-434.85	1.01-1.01	0-1	0-1	12
256	butane(1) + furfural(2)	310.95-324.85	1.02-4.63	0.0223-0.179	0.984-0.998	19
257	4-methyl 2-pentanone(1) + furfural(2)	368.09-368.09	0.11-0.53	0-1	0-1	19
258	tetrachloroethylene(1) + furfural(2)	393.8-434.95	1.01-1.01	0-1	0-1	26
259	ethylbenzene(1) + benzaldehyde(2)	348.15-368.15	0.03-0.29	0-1	0-1	54
260	diethyl ether(1) + tetrachloromethane(2)	298.15-308.15	0.15-1.03	0-1	0-1	69

Table A.1. Binary VLE Database Used in Model Development *(Continued)*

NO.	System	Temperature range (K)	Pressure range (bar)	Component (1) liquid mole fraction range	Component (1) vapor mole fraction range	NDP
261	diethyl ether(1) + cyclohexane(2)	298.15-298.15	0.13-0.71	0-1	0-1	16
262	diethyl ether(1) + toluene(2)	283.15-383.45	0.06-1.01	0.0031-0.9	0.0215-0.9933	21
263	isopentane(1) + diethyl ether(2)	300.95-307.75	1.01-1.01	0.0008-0.98	0.0012-0.9808	19
264	methyl teritiary butyl ether(1) + tetrachloromethane(2)	313.15-313.15	0.28-0.6	0-1	0-1	20
265	methyl teritiary butyl ether(1) + chloroform(2)	313.15-313.15	0.4-0.6	0-1	0-1	32
266	methyl teritiary butyl ether(1) + methyl acetate(2)	323.35-373.17	0.94-4.05	0-1	0-1	59
267	methyl teritiary butyl ether(1) + ethyl acetate(2)	353.15-373.17	1.11-3.64	0-1	0-1	33
268	methyl teritiary butyl ether(1) + benzene(2)	313.15-363.05	0.24-2.79	0-1	0-1	83
269	methyl teritiary butyl ether(1) + cyclohexane(2)	313.15-313.15	0.25-0.6	0-1	0-1	26
270	methyl teritiary butyl ether(1) + diisopropyl ether(2)	325.75-339.12	0.94-0.94	0-1	0-1	14
271	methyl teritiary butyl ether(1) + toluene(2)	325.6-381.04	0.29-1.01	0-1	0-1	41
272	methyl teritiary butyl ether(1) + n-heptane(2)	298.15-366.45	0.06-0.94	0-1	0-1	74
273	dichloromethane(1) + methyl teritiary butyl ether(2)	308.15-308.15	0.5-0.85	0-1	0-1	22
274	butane(1) + methyl teritiary butyl ether(2)	273.15-322.89	0.11-4.6	0-1	0-1	30
275	Isoprene(1) + methyl teritiary butyl ether(2)	307.23-328.15	1.01-1.01	0-1	0-1	13
276	2-methyl 2-butene(1) + methyl teritiary butyl ether(2)	311.75-328.15	1.01-1.01	0-1	0-1	13
277	isopentane(1) + methyl teritiary butyl ether(2)	288.15-322.9	0.22-1.95	0-1	0-1	27
278	isopentane(1) + ethyl teritiary butyl ether(2)	293.15-322.9	0.13-1.96	0-1	0-1	40
279	ethyl teritiary butyl ether(1) + toluene(2)	311.15-333.15	0.07-0.66	0-1	0-1	26
280	ethyl teritiary butyl ether(1) + n-octane(2)	323.15-323.15	0.07-0.47	0-1	0-1	20
281	dimethyl ether(1) + methylamine(2)	273.15-273.15	1.34-2.68	0-1	0-1	21
282	dimethyl ether(1) + butane(2)	282.96-297.86	1.47-5.79	0-1	0-1	35
283	dimethyl ether(1) + methyl teritiary butyl ether(2)	298.15-298.15	0.34-5.91	0-1	0-1	8
284	chloroform(1) + benzene(2)	293.15-373.15	0.1-2.74	0-1	0-1	22
285	carbondisulfide(1) + benzene(2)	353.15-353.15	1.01-2.71	0-1	0-1	11

Table A.1. Binary VLE Database Used in Model Development *(Continued)*

NO.	System	Temperature range (K)	Pressure range (bar)	Component (1) liquid mole fraction range	Component (1) vapor mole fraction range	NDP
286	butylamine(1) + benzene(2)	323.15-343.15	0.36-0.81	0-1	0-1	29
287	diethylamine(1) + benzene(2)	308.15-353.25	0.2-1.01	0-1	0-1	46
288	benzene(1) + acetonitrile(2)	293.15-364.25	0.04-1.01	0.015-0.991	0.039-0.972	131
289	benzene(1) + pyridine(2)	293.15-382.7	0.02-1.01	0-1	0-1	75
290	benzene(1) + hexafluorobenzene(2)	303.15-343.15	0.14-0.74	0-1	0-1	109
291	benzene(1) + bromobenzene(2)	303.15-353.15	0.01-1.01	0-1	0-1	49
292	benzene(1) + nitrobenzene(2)	298.15-343.15	0.01-0.71	0-1	0-1	27
293	benzene(1) + ethylbenzene(2)	353.53-409.33	1.01-1.01	0-1	0-1	13
294	benzene(1) + p-xylene(2)	356.75-402.15	1.01-1.01	0.086-0.886	0.285-0.979	26
295	toluene(1) + nitroethane(2)	318.15-318.15	0.08-0.11	0-1	0-1	14
296	toluene(1) + ethylenediamine(2)	376.15-386.45	1.01-1.01	0.027-0.96	0.095-0.909	29
297	toluene(1) + pyridine(2)	293.15-388.32	0.02-1.01	0-1	0-1	84
298	chloroform(1) + toluene(2)	334.48-382.07	0.99-1.01	0-1	0-1	36
299	carbondisulfide(1) + toluene(2)	283.15-363.15	0.02-3.48	0-1	0-1	74
300	acetonitrile(1) + toluene(2)	313.15-381.45	0.1-1.01	0-1	0-1	77
301	1,2-dichloroethane(1) + toluene(2)	303.15-383.76	0.05-1.01	0-1	0-1	78
302	tetrachloromethane(1) + ethylbenzene(2)	303.15-407.25	0.02-1.02	0-1	0-1	84
303	acetonitrile(1) + ethylbenzene(2)	354.9-405.9	1.01-1.01	0.01-0.97	0.115-0.978	15
304	diethylamine(1) + ethylbenzene(2)	308.15-308.15	0.02-0.48	0-1	0-1	8
305	tetrachloromethane(1) + p-xylene(2)	273.15-409.55	0.0013-1.01	0-1	0-1	42
306	acetonitrile(1) + p-xylene(2)	354.96-408.65	1.01-1.01	0.01-0.9775	0.095-0.9825	21
307	1,2-dichloroethane(1) + p-xylene(2)	303.15-303.15	0.01-0.13	0-1	0-1	13
308	acetaldehyde(1) + toluene(2)	293.95-383.95	1.01-1.01	0-1	0-1	14
309	butyraldehyde(1) + toluene(2)	349.85-378.35	1.01-1.01	0.083-0.917	0.197-0.956	15
310	2-methyl 1-butene(1) + acetone(2)	303.25-329.55	1.01-1.01	0-1	0-1	11

Table A.1. Binary VLE Database Used in Model Development *(Continued)*

NO.	System	Temperature range (K)	Pressure range (bar)	Component (1) liquid mole fraction range	Component (1) vapor mole fraction range	NDP
311	propylene oxide(1) + acetone(2)	307.4-329.65	1.01-1.01	0-1	0-1	38
312	3-hexanone(1) + 4-heptanone(2)	396.55-417.25	1.01-1.01	0-1	0-1	17
313	toluene(1) + cyclohexanone(2)	383.55-427.95	1.01-1.01	0-1	0-1	10
314	hexane(1) + 3-pentanone(2)	338.15-338.15	0.46-0.92	0.126-0.937	0.43-0.951	11
315	3-pentanone(1) + 4-heptanone(2)	374.55-417.25	1.01-1.01	0-1	0-1	12
316	hexane(1) + 2-butanone(2)	333.15-338.15	0.67-1.03	0.055-0.961	0.175-0.917	21
317	hexane(1) + 1,4-dioxane(2)	341.95-358.05	0.61-1.43	0.03-0.977	0.198-0.977	21
318	acetaldehyde(1) + acetone(2)	293.35-348.15	0.3-5.4	0-1	0-1	56
319	propylene oxide(1) + propionic aldehyde(2)	307.93-319.9	1-1	0.0368-0.9418	0.0532-0.9646	13
320	methyl acetate(1) + butyraldehyde(2)	313.15-323.15	0.29-0.79	0-1	0-1	34
321	butyraldehyde(1) + propyl acetate(2)	323.15-333.15	0.15-0.62	0-1	0-1	28
322	butyraldehyde(1) + benzene(2)	313.15-393.15	0.24-3.14	0-1	0-1	49
323	butyraldehyde(1) + n-heptane(2)	298.15-343.15	0.06-0.89	0-1	0-1	63
324	ethyl teritiary butyl ether(1) + n-heptane(2)	353.55-366.93	0.57-2.21	0-1	0-1	26
325	1,3-butadiene(1) + N,N-dimethylformide(2)	323.15-323.15	0.02-5.72	0-1	0-1	11
326	1,3-butadiene(1) + vinylacetylene(2)	305.65-316.76	3.43-4.75	0.9087-0.9872	0.9146-0.9877	8
327	hexane(1) + 2,4-Dimethylpyridine(2)	283.15-313.15	0.07-0.36	0.1279-0.91	0.1886-0.9379	52
328	2,4-Dimethylpyridine(1) + n-octane(2)	283.15-313.15	0.01-0.25	0-1	0-1	60
329	2-methyl 2-butene(1) + N,N-dimethylformide(2)	323.15-323.15	0.02-1.39	0-0.9	0-0.9921	11
330	isopentane(1) + hexane(2)	300.92-341.75	1.01-1.01	0-1	0-1	34
331	isopentane(1) + N,N-dimethylformide(2)	300.95-323.15	0.02-1.94	0-1	0-1	24
332	isopentane(1) + toluene(2)	301.05-383.85	1.01-1.01	0.0001-0.9905	0.0005-0.9995	20
333	cis, 2-butene(1) + N,N-dimethylformide(2)	323.15-323.15	0.02-4.45	0-1	0-1	11
334	cis, 2-butene(1) + vinylacetylene(2)	277.98-316.76	1.08-3.86	0.8523-0.9804	0.8243-0.9751	11
335	cyclopentane(1) + cyclooctane(2)	288.15-308.15	0.03-0.55	0.1032-0.885	0.8397-0.9982	36

Table A.1. Binary VLE Database Used in Model Development *(Continued)*

NO.	System	Temperature range (K)	Pressure range (bar)	Component (1) liquid mole fraction range	Component (1) vapor mole fraction range	NDP
336	cyclopentane(1) + N,N-dimethylformide(2)	313.15-313.15	0.01-0.74	0-1	0-1	9
337	1-chloropropane(1) + cyclohexane(2)	308.15-318.15	0.2-0.96	0-1	0-1	26
338	cyclohexane(1) + chlorobenzene(2)	348.15-348.15	0.16-0.85	0-1	0-1	28
339	cyclohexane(1) + cycloheptane(2)	298.15-298.15	0.04-0.12	0.1302-0.8937	0.4083-0.9735	13
340	cyclohexane(1) + cyclooctane(2)	298.15-298.15	0.02-0.11	0.0893-0.8621	0.6358-0.9909	13
341	cyclohexane(1) + n-heptane(2)	278.15-313.15	0.02-0.25	0-1	0-1	108
342	hexane(1) + cyclohexane(2)	278.15-353.85	0.05-1.01	0-1	0-1	150
343	methyl cyclopentane(1) + cyclohexane(2)	344.97-353.91	1.01-1.01	0-1	0-1	5
344	cyclohexane(1) + methyl cyclohexane(2)	308.15-308.15	0.1-0.2	0-1	0-1	15
345	cyclohexane(1) + nitroethane(2)	318.15-318.15	0.08-0.34	0.0022-0.9983	0.0656-0.9951	45
346	cyclohexane(1) + nitromethane(2)	318.15-318.15	0.13-0.41	0.0005-0.9392	0.0293-0.6957	30
347	cyclohexane(1) + N,N-dimethylformide(2)	298.15-348.15	0.03-0.85	0-1	0-1	56
348	cyclohexane(1) + n-octane(2)	298.15-313.15	0.02-0.25	0-1	0-1	61
349	acetonitrile(1) + methyl cyclohexane(2)	344.25-366.65	1.01-1.01	0.018-0.988	0.209-0.932	14
350	benzene(1) + methyl cyclohexane(2)	303.15-323.15	0.08-0.36	0-1	0-1	52
351	methyl cyclohexane(1) + ethylbenzene(2)	303.15-323.15	0.02-0.18	0-1	0-1	47
352	n-heptane(1) + methyl cyclohexane(2)	320.65-320.65	0.17-0.17	0.064-0.8842	0.066-0.8925	14
353	methyl cyclohexane(1) + p-xylene(2)	313.15-348.15	0.03-0.46	0-1	0-1	46
354	methyl cyclohexane(1) + toluene(2)	303.15-323.15	0.05-0.19	0-1	0-1	56
355	benzene(1) + n-decane(2)	313.15-353.15	0.005-1.01	0-1	0-1	43
356	carbondisulfide(1) + n-decane(2)	298.15-298.15	0.08-0.44	0.1501-0.8982	0.9814-0.9995	10
357	hexane(1) + n-decane(2)	308.15-308.15	0.03-0.28	0.0846-0.9028	0.8875-0.9988	12
358	butane(1) + ethylamine(2)	218.15-273.15	0.02-1.1	0-1	0-1	104
359	butane(1) + N,N-dimethylformide(2)	323.15-323.15	0.02-4.96	0-1	0-1	5
360	n-pentane(1) + benzene(2)	323.15-323.15	0.36-1.59	0-1	0-1	15
361	1-pentene(1) + n-pentane(2)	273.15-298.15	0.25-0.85	0-1	0-1	53

Table A.1. Binary VLE Database Used in Model Development *(Continued)*

NO.	System	Temperature range (K)	Pressure range (bar)	Component (1) liquid mole fraction range	Component (1) vapor mole fraction range	NDP
362	hexane(1) + benzene(2)	298.15-403.15	0.13-5.02	0-1	0-1	109
363	hexane(1) + chlorobenzene(2)	338.2-338.2	0.07-0.9	0.0014-0.998	0.0204-0.9996	55
364	carbondisulfide(1) + hexane(2)	298.15-298.15	0.26-0.47	0.1304-0.9005	0.3523-0.9334	13
365	hexane(1) + nitrobenzene(2)	342.15-483.15	1.01-1.01	0-1	0-1	22
366	hexane(1) + N,N-dimethylformide(2)	343.15-343.15	0.05-1.06	0-1	0-1	16
367	hexane(1) + n-octane(2)	319.85-372.35	0.08-0.65	0-1	0-1	24
368	1,2-dichloroethane(1) + n-heptane(2)	303.15-343.15	0.08-0.74	0-1	0-1	47
369	1-heptene(1) + n-heptane(2)	343.15-371.59	0.4-1.01	0-0.933	0-0.9399	40
370	benzene(1) + n-heptane(2)	298.15-428.15	0.06-6.28	0-1	0-1	96
371	n-heptane(1) + N,N-dimethylformide(2)	373.15-373.15	0.19-1.09	0-1	0-1	18
372	n-heptane(1) + m-xylene(2)	348.15-348.15	0.12-0.48	0-1	0-1	29
373	n-heptane(1) + toluene(2)	298.15-383.85	0.04-1.01	0-1	0-1	162
374	trans, 2-butene(1) + vinylacetylene(2)	276.04-316.76	1.08-4.12	0.856-0.9852	0.8358-0.981	11
375	1-propanol(1) + 1-butanol(2)	313.15-387.35	0.03-1.02	0-1	0-1	33
376	benzene(1) + 1-propanol(2)	313.15-370.23	0.24-1.01	0-1	0-1	54
377	chloroform(1) + 1-propanol(2)	303.15-328.15	0.04-0.81	0-1	0-1	21
378	carbondisulfide(1) + 1-propanol(2)	303.15-303.15	0.06-0.58	0.01-0.995	0.362-0.9956	15
379	cyclohexane(1) + 1-propanol(2)	347.69-370.23	1.01-1.01	0-1	0-1	23
380	butane(1) + 1-propanol(2)	330.18-330.19	3.87-5.54	0.2434-0.7469	1-1	12
381	hexane(1) + 1-propanol(2)	298.15-361.75	0.03-1.01	0-1	0-1	32
382	1-propanol(1) + n-heptane(2)	357.35-371.55	1.01-1.01	0-1	0-1	21
383	1-propanol(1) + p-xylene(2)	313.15-313.15	0.03-0.07	0-0.5296	0-0.7079	10
384	1-propanol(1) + toluene(2)	313.15-313.15	0.08-0.11	0-0.5341	0-0.4461	11
385	ethanol(1) + 1-butanol(2)	313.15-403.15	0.03-5.62	0-1	0-0.994	72
386	ethanol(1) + 1-propanol(2)	298.15-313.15	0.04-0.18	0-1	-	16
387	ethanol(1) + 2-butanone(2)	298.15-298.15	0.08-0.13	0-1	0-1	14

Table A.1. Binary VLE Database Used in Model Development *(Continued)*

NO.	System	Temperature range (K)	Pressure range (bar)	Component (1) liquid mole fraction range	Component (1) vapor mole fraction range	NDP
388	acetone(1) + ethanol(2)	372.7-372.7	2.23-3.67	0-1	0-1	11
389	ethanol(1) + n-decane(2)	351.45-355.45	1.01-1.01	0.405-1	0-0.989	15
390	hexane(1) + ethanol(2)	313.15-318.15	0.18-0.61	0-1	0-1	55
391	ethanol(1) + n-octane(2)	313.15-372.55	0.04-1.01	0-1	-	24
392	ethanol(1) + toluene(2)	313.15-380.95	0.08-1.01	0-1	0-1	90
393	methanol(1) + 1-butanol(2)	284.85-370.65	0.03-1.01	0-1	-	25
394	methanol(1) + 1-propanol(2)	313.15-370.15	0.07-1.01	0-1	0-1	33
395	methanol(1) + benzene(2)	308.2-353.4	0.2-1.01	0-1	0-1	162
396	carbondisulfide(1) + methanol(2)	303.15-337.15	0.6-1.03	0.0055-0.999	0.028-0.978	16
397	methanol(1) + cyclohexane(2)	293.15-313.15	0.1-0.57	0-1	-	41
398	diethyl ether(1) + methanol(2)	298.15-338.17	0.17-2.74	0-1	0-1	79
399	methanol(1) + hexane(2)	293.15-341.85	0.13-1.01	0-1	0-1	121
400	methanol(1) + toluene(2)	313.15-313.15	0.08-0.31	0-0.1143	0-0.7588	21
401	methanol(1) + vinyl acetate(2)	331.95-345.45	1.01-1.01	0-1	0-1	29
402	butane(1) + 2-butanone(2)	283.15-313.15	1.01-1.01	0.1121-0.3885	-	3
403	2-butanone(1) + p-xylene(2)	349.45-411.45	0.91-1.01	0-1	0-1	61
404	vinyl acetate(1) + 2-butanone(2)	333.2-393.2	0.53-3.84	0.0288-0.987	0.0378-0.988	20
405	cyclohexane(1) + 3-pentanone(2)	298.15-298.15	0.05-0.13	0-1	-	19
406	hexane(1) + 4-heptanone(2)	338.15-338.15	0.34-0.88	0.255-0.928	0.864-0.988	6
407	acetone(1) + cyclohexane(2)	273.15-342.15	0.04-1.01	0-1	0-1	48
408	acetone(1) + hexane(2)	283.15-330.85	0.1-1.01	0-1	0-1	66
409	acetone(1) + n-heptane(2)	273.15-371.35	0.02-1.01	0-1	0-1	34
410	acetone(1) + n-octane(2)	313.15-313.15	0.04-0.57	0-1	0-1	21
411	acetone(1) + toluene(2)	330.35-374.55	1.01-1.01	0.034-0.953	0.222-0.986	11
412	p-xylene(1) + cyclohexanone(2)	380.05-426.35	0.4-0.99	0-1	0-1	34

Table A.1. Binary VLE Database Used in Model Development *(Continued)*

NO.	System	Temperature range (K)	Pressure range (bar)	Component (1) liquid mole fraction range	Component (1) vapor mole fraction range	NDP
413	acetaldehyde(1) + 1-pentene(2)	313.2-353.2	1.57-6.62	0.0181-0.993	0.064-0.986	16
414	butyraldehyde(1) + 2-butanone(2)	329.2-352.55	0.53-1.01	0.019-0.993	0-0.919	40
415	n-octane(1) + furfural(2)	393.45-421.75	1.01-1.01	0.03-0.952	0.31-0.902	13
416	propionic aldehyde(1) + toluene(2)	313.15-313.15	0.08-0.76	0-1	0-1	9
417	2-methyl 2-butene(1) + 1-Pentyne(2)	310.92-313.1	1.01-1.01	0.1-1	0.125-1	9
418	cyclohexane(1) + Fluorobenzene(2)	348.15-348.15	0.74-0.91	0-1	0-1	30
419	hexane(1) + Triethylamine(2)	298.15-298.15	0.09-0.2	0-1	-	9
420	Triethylamine(1) + n-octane(2)	298.15-298.15	0.02-0.09	0-1	-	8
421	acetaldehyde(1) + Isoprene(2)	292.25-307.25	1.01-1.01	0-1	-	11
422	Isoprene(1) + Isobutyr Aldehyde(2)	307.25-330.15	1.01-1.01	0.1-1	-	10
423	Isoprene(1) + Crotonaldehyde(2)	307.25-375.55	1.01-1.01	0-1	0-1	13
424	Isobutyr Aldehyde(1) + n-heptane(2)	318.15-335	0.15-0.93	0-1	0-1	37
425	butyraldehyde(1) + cyclohexane(2)	298.15-298.15	0.13-0.19	0-1	-	16
426	methanol(1) + tetrachloromethane(2)	293.15-293.15	0.12-0.21	0-1	-	22
427	dichloromethane(1) + methanol(2)	310.95-331.75	1.01-1.01	0.05-0.973	0.276-0.897	11
428	Dimethylamine(1) + methanol(2)	293.15-293.15	0.99-1.19	0.669-0.748	-	4
429	carbondisulfide(1) + Isobutyl chloride(2)	293.15-293.15	0.17-0.4	0-1	0-1	9
430	methyl iodide(1) + carbondisulfide(2)	314.35-319.45	1.01-1.01	0-1	-	19
431	carbondisulfide(1) + tetrachloroethylene(2)	298.15-318.15	0.1-0.91	0.1024-0.9285	0.72-0.9937	35
432	carbondisulfide(1) + nitromethane(2)	293.65-293.65	0.04-0.43	0-1	0-1	7
433	acetonitrile(1) + chlorobenzene(2)	293.15-402.65	0.01-2.98	0-1	0-0.988	81
434	chlorobenzene(1) + bromobenzene(2)	404.85-404.85	0.58-0.93	0.114-0.837	0.2-0.912	10
435	butylamine(1) + chlorobenzene(2)	333.15-353.15	0.09-1.12	0-1	0-1	42
436	chloroform(1) + chlorobenzene(2)	337.95-399.85	1.01-1.01	0.022-0.868	0.159-0.988	17
437	butylchloride(1) + chlorobenzene(2)	298.17-398.21	0.02-3.54	0-1	-	45

Table A.1. Binary VLE Database Used in Model Development *(Continued)*

NO.	System	Temperature range (K)	Pressure range (bar)	Component (1) liquid mole fraction range	Component (1) vapor mole fraction range	NDP
438	chlorobenzene(1) + Cyclohexaylamine(2)	383.15-403.15	0.5-0.97	0-1	0-1	22
439	chlorobenzene(1) + 1,2-Dibromoethane(2)	348.15-373.15	0.16-0.41	0.0786-0.8316	0.0947-0.8119	12
440	diethylamine(1) + chlorobenzene(2)	308.15-333.15	0.04-1.19	0-1	0-1	43
441	1-Nitropropane(1) + chlorobenzene(2)	348.15-393.15	0.16-0.8	0.156-0.904	0.196-0.882	16
442	Triethylamine(1) + chlorobenzene(2)	343.15-363.15	0.13-1.04	0-1	0-1	44
443	chloroform(1) + acetonitrile(2)	313.15-354.15	0.23-1.01	0-1	0-0.976	49
444	dichloromethane(1) + chloroform(2)	312.88-333.95	0.58-1.21	0-1	0-1	39
445	chloroform(1) + 2-Methylpyridine(2)	308.15-308.15	0.02-0.33	0.0599-0.935	-	20
446	chloroform(1) + Methyl ethyl sulfide(2)	331.75-339.75	0.93-0.93	0-1	0-1	10
447	chloroform(1) + tetrachloroethylene(2)	335.25-389.95	1.01-1.01	0.03-0.9275	0.15-0.991	16
448	Hydrogen cyanide(1) + 3-Chloro-1-propene(2)	296.35-318.15	1.01-1.01	0-1	0-1	22
449	Isopropyl chloride(1) + 3-Chloro-1-propene(2)	308.55-317.2	1.01-1.01	0.0518-0.923	-	17
450	tetrachloromethane(1) + 1,2-Dibromoethane(2)	293.15-388.15	0.01-1.01	0-1	0-1	29
451	acetonitrile(1) + 1,2-dichloroethane(2)	333.15-333.15	0.47-0.52	0.0467-0.9785	0.0674-0.9717	21
452	dichloromethane(1) + 1,2-dichloroethane(2)	293.15-323.15	0.1-0.99	0.037-0.715	0.2-0.92	24
453	1,2-dichloroethane(1) + tetrachloroethylene(2)	357.35-390.95	1.01-1.01	0.02-0.938	0.115-0.97	16
454	Vinyl chloride(1) + 1,2-dichloroethane(2)	285.15-323.15	1.01-1.01	0.109-0.388	0.711-0.966	17
455	1,1-Dichloroethylene(1) + acrylonitrile(2)	305.45-344.85	1.01-1.01	0.05-0.95	0.255-0.98	11
456	Vinyl chloride(1) + 1,1-Dichloroethylene(2)	293.15-293.15	0.75-3.21	0.05-0.95	0.235-0.991	11
457	dichloromethane(1) + acetonitrile(2)	298.23-398.13	0.12-10.25	0-1	-	45
458	dichloromethane(1) + Dibromomethane(2)	312.65-369.65	1.01-1.01	0-1	0-1	25
459	dichloromethane(1) + pyridine(2)	303.15-303.15	0.04-0.7	0-1	-	25
460	dichloromethane(1) + methyl iodide(2)	298.15-298.15	0.55-0.58	0.088-0.93	0.106-0.927	11
461	dichloromethane(1) + tetrachloroethylene(2)	316.25-378.25	1.01-1.01	0.05-0.863	0.321-0.993	10
462	dichloromethane(1) + Triethylamine(2)	283.15-283.15	0.06-0.29	0.074-0.9206	0.3096-0.9891	9

Table A.1. Binary VLE Database Used in Model Development *(Continued)*

NO.	System	Temperature range (K)	Pressure range (bar)	Component (1) liquid mole fraction range	Component (1) vapor mole fraction range	NDP
463	water(1) + 2-Methylpyridine(2)	298.15-308.15	0.02-0.06	0-0.9531	-	22
464	water(1) + cyclohexanone(2)	330.05-360.15	0.2-0.2	0.05-0.4301	0.5308-0.8746	5
465	diisopropyl ether(1) + water(2)	336.15-373.15	1.01-1.01	0-1	0-1	13
466	Triethylamine(1) + water(2)	278.15-278.15	0.01-0.04	0.0055-1	-	16
467	water(1) + 2,4-Dimethylpyridine(2)	344.65-344.65	0.06-0.35	0-0.976	0-0.9258	6
468	ethylamine(1) + water(2)	290.85-374.55	0.93-1.07	0-1	0-1	24
469	water(1) + ethylenediamine(2)	422.64-436.58	3.7-3.7	0.0832-0.7817	0.0888-0.9025	10
470	water(1) + Ethylbutylamine(2)	283.15-313.1	0.01-0.12	0-0.9968	-	34
471	Hydrogen cyanide(1) + water(2)	291.15-370.05	0.17-1.01	0.003-1	0-0.989	37
472	Isobutyr Aldehyde(1) + water(2)	333.55-335.25	1.02-1.02	0.862-0.958	0.811-0.888	7
473	Isopropylamine(1) + water(2)	308.25-367.05	1.01-1.01	0.0058-0.87	0.192-0.989	16
474	water(1) + Isopropylbenzene(2)	368.15-425.45	1.01-1.01	0-1	-	9
475	Propylamine(1) + water(2)	324.95-348.25	1.01-1.01	0.184-0.809	0.651-0.964	8
476	Ethyl Bromide(1) + benzene(2)	314.64-348.01	1.01-1.01	0.074-0.866	0.206-0.967	9
477	ethyl iodide(1) + benzene(2)	293.15-293.15	0.13-0.15	0.2-0.8	-	4
478	benzene(1) + Fluorobenzene(2)	352.5-356.7	1.01-1.01	0.09-1	0.1-1	11
479	benzene(1) + Isopropylbenzene(2)	354.75-409.55	1.01-1.01	0.1-0.9	0.446-0.981	9
480	methyl mercaptan(1) + benzene(2)	313.15-313.15	0.25-3.28	0-1	-	22
481	methyl iodide(1) + benzene(2)	308.15-308.15	0.2-0.78	0-1	-	13
482	benzene(1) + nitroethane(2)	298.15-298.15	0.03-0.13	0-1	0-1	12
483	benzene(1) + 1-Nitropropane(2)	298.15-298.15	0.01-0.13	0-1	0-1	9
484	benzene(1) + tetrachloroethylene(2)	354.75-379.05	1.01-1.01	0.198-0.958	-	21
485	chlorobenzene(1) + ethylbenzene(2)	293.15-293.15	0.01-0.01	0-1	-	13
486	1,2-dichloroethane(1) + ethylbenzene(2)	356.55-401.8	0.98-0.98	0.08-0.98	0.168-0.997	17
487	ethylbenzene(1) + Isopropylbenzene(2)	409.75-424.85	1.01-1.01	0.036-0.966	0.05-0.978	18

Table A.1. Binary VLE Database Used in Model Development *(Continued)*

NO.	System	Temperature range (K)	Pressure range (bar)	Component (1) liquid mole fraction range	Component (1) vapor mole fraction range	NDP
488	tetrachloromethane(1) + Isopropylbenzene(2)	303.15-303.15	0.01-0.19	0-1	-	21
489	toluene(1) + bromobenzene(2)	303.15-303.15	0.01-0.05	0-1	-	12
490	toluene(1) + chlorobenzene(2)	303.15-343.15	0.02-0.25	0-1	0-0.912	23
491	diethylamine(1) + toluene(2)	308.15-308.15	0.06-0.48	0-1	0-1	10
492	toluene(1) + Dimethyl sulfoxide(2)	323.15-323.15	0.004-0.13	0-1	-	11
493	toluene(1) + ethylbenzene(2)	298.15-298.15	0.02-0.04	0-1	-	6
494	toluene(1) + 2-Methylpyridine(2)	383.78-402.55	1.01-1.01	0-1	-	13
495	chlorobenzene(1) + p-xylene(2)	401.05-407.65	0.91-0.91	0-1	0-1	20
496	p-xylene(1) + N,N-dimethylformide(2)	407.25-421.65	1.01-1.01	0.025-0.985	0.095-0.982	14
497	methyl iodide(1) + tetrachloromethane(2)	298.15-298.15	0.2-0.51	0.084-0.903	0.301-0.961	14
498	methylamine(1) + tetrachloromethane(2)	253.15-293.15	0.01-2.92	0-1	-	66
499	tetrachloromethane(1) + tetrachloroethylene(2)	333.15-343.15	0.15-0.79	0.043-0.935	0.16-0.984	33
500	tetrachloromethane(1) + Trichloethylene(2)	349.85-360.05	1.01-1.01	0-1	0-1	36
501	tetrachloromethane(1) + acetonitrile(2)	318.15-352.25	0.33-1.01	0.021-0.993	0.098-0.945	58
502	ethyl iodide(1) + tetrachloromethane(2)	323.14-323.14	0.41-0.47	0-0.4983	0-0.5237	13
503	tetrachloromethane(1) + nitroethane(2)	298.15-298.15	0.03-0.15	0-1	0-1	22
504	tetrachloromethane(1) + Dimethyl sulfoxide(2)	293.15-313.15	0.0005-0.28	0-1	-	42
505	tetrachloromethane(1) + acrylonitrile(2)	303.15-323.15	0.18-0.57	0-1	-	30
506	tetrachloromethane(1) + thiophene(2)	343.15-343.15	0.67-0.82	0.0758-0.9366	0.1111-0.94	12
507	diethylamine(1) + tetrachloromethane(2)	293.15-313.15	0.12-0.58	0-1	0-1	39
508	tetrachloromethane(1) + nitrobenzene(2)	298.15-298.15	0.03-0.15	0.1-1	0.984-1	14
509	tetrachloromethane(1) + Triethylamine(2)	293.15-293.15	0.07-0.12	0-1	0-1	22
510	Tribromomethane(1) + Dimethyl sulfoxide(2)	298.15-298.15	0.0008-0.01	0-1	-	14
511	pyridine(1) + Tribromomethane(2)	303.15-313.15	0.01-0.05	0-1	-	29
512	methyl iodide(1) + chloroform(2)	298.15-308.15	0.28-0.78	0-1	0-0.955	25

Table A.1. Binary VLE Database Used in Model Development *(Continued)*

NO.	System	Temperature range (K)	Pressure range (bar)	Component (1) liquid mole fraction range	Component (1) vapor mole fraction range	NDP
513	chloroform(1) + Triethylamine(2)	283.14-283.14	0.04-0.13	0.1159-0.9485	0.0955-0.9958	11
514	Dibromomethane(1) + Dimethyl sulfoxide(2)	298.15-308.15	0.0008-0.1	0-1	-	39
515	tetrachloromethane(1) + nitromethane(2)	318.15-318.15	0.23-0.4	0.0512-0.9541	0.4717-0.8704	12
516	Trichloethylene(1) + nitromethane(2)	353.45-369.45	1.01-1.01	0.025-0.865	0.155-0.76	11
517	acetonitrile(1) + nitromethane(2)	298.15-398.17	0.05-3.38	0-1	0-0.9737	55
518	ethyl iodide(1) + nitromethane(2)	333.15-338.15	0.42-0.84	0.0806-0.926	-	17
519	nitromethane(1) + nitroethane(2)	307.25-363.75	0.07-0.53	0.118-0.888	0.195-0.917	28
520	nitromethane(1) + N,N-dimethylformide(2)	313.15-313.15	0.01-0.1	0-1	-	17
521	thiophene(1) + nitromethane(2)	318.15-318.15	0.13-0.26	0-1	0-1	11
522	butylchloride(1) + nitromethane(2)	298.18-398.16	0.05-3.78	0-1	-	45
523	nitromethane(1) + Glutaronitrile(2)	293.15-293.15	0.02-0.04	0.444-1	-	4
524	nitromethane(1) + chlorobenzene(2)	298.15-398.26	0.02-2.05	0-1	-	45
525	nitromethane(1) + nitrobenzene(2)	376.95-445.85	1.01-1.01	0.1-0.9	-	9
526	methylamine(1) + methyl mercaptan(2)	313.15-313.15	3.31-5.64	0-0.9535	-	21
527	methyl mercaptan(1) + acetonitrile(2)	313.15-313.15	0.24-3.26	0-1	-	22
528	methyl mercaptan(1) + N,N-dimethylformide(2)	313.15-313.15	0.01-3.23	0-1	-	22
529	methylamine(1) + Trimethylamine(2)	233.15-293.15	0.14-2.95	0-1	-	108
530	carbondisulfide(1) + acetonitrile(2)	293.65-293.65	0.09-0.47	0-1	0-1	8
531	Trichloethylene(1) + Diethyl sulfide(2)	357.35-362.65	0.93-0.93	0-1	0-1	10
532	acetonitrile(1) + Trichloethylene(2)	347.45-358.55	1.01-1.02	0.011-0.971	0.066-0.925	37
533	butylchloride(1) + acetonitrile(2)	298.69-397.89	0.12-4.53	0-1	-	45
534	acetonitrile(1) + 2-Methylpyridine(2)	354.75-402.55	1.01-1.01	0-1	0-1	21
535	1,2-dichloroethane(1) + Trichloethylene(2)	355.35-358.85	1.01-1.01	0.05-0.948	0.072-0.94	16
536	Ethyl Bromide(1) + ethyl iodide(2)	303.15-303.15	0.31-0.72	0.1747-0.9594	0.4154-0.993	19
537	ethyl iodide(1) + nitrobenzene(2)	293.15-293.15	0.06-0.13	0.17-0.79	-	5

Table A.1. Binary VLE Database Used in Model Development *(Continued)*

NO.	System	Temperature range (K)	Pressure range (bar)	Component (1) liquid mole fraction range	Component (1) vapor mole fraction range	NDP
517	acetonitrile(1) + nitromethane(2)	298.15-398.17	0.05-3.38	0-1	0-0.9737	55
518	ethyl iodide(1) + nitromethane(2)	333.15-338.15	0.42-0.84	0.0806-0.926	-	17
519	nitromethane(1) + nitroethane(2)	307.25-363.75	0.07-0.53	0.118-0.888	0.195-0.917	28
520	nitromethane(1) + N,N-dimethylformide(2)	313.15-313.15	0.01-0.1	0-1	-	17
521	thiophene(1) + nitromethane(2)	318.15-318.15	0.13-0.26	0-1	0-1	11
522	butylchloride(1) + nitromethane(2)	298.18-398.16	0.05-3.78	0-1	-	45
523	nitromethane(1) + Glutaronitrile(2)	293.15-293.15	0.02-0.04	0.444-1	-	4
524	nitromethane(1) + chlorobenzene(2)	298.15-398.26	0.02-2.05	0-1	-	45
525	nitromethane(1) + nitrobenzene(2)	376.95-445.85	1.01-1.01	0.1-0.9	-	9
526	methylamine(1) + methyl mercaptan(2)	313.15-313.15	3.31-5.64	0-0.9535	-	21
527	methyl mercaptan(1) + acetonitrile(2)	313.15-313.15	0.24-3.26	0-1	-	22
528	methyl mercaptan(1) + N,N-dimethylformide(2)	313.15-313.15	0.01-3.23	0-1	-	22
529	methylamine(1) + Trimethylamine(2)	233.15-293.15	0.14-2.95	0-1	-	108
530	carbondisulfide(1) + acetonitrile(2)	293.65-293.65	0.09-0.47	0-1	0-1	8
531	Trichloethylene(1) + Diethyl sulfide(2)	357.35-362.65	0.93-0.93	0-1	0-1	10
532	acetonitrile(1) + Trichloethylene(2)	347.45-358.55	1.01-1.02	0.011-0.971	0.066-0.925	37
533	butylchloride(1) + acetonitrile(2)	298.69-397.89	0.12-4.53	0-1	-	45
534	acetonitrile(1) + 2-Methylpyridine(2)	354.75-402.55	1.01-1.01	0-1	0-1	21
535	1,2-dichloroethane(1) + Trichloethylene(2)	355.35-358.85	1.01-1.01	0.05-0.948	0.072-0.94	16
536	Ethyl Bromide(1) + ethyl iodide(2)	303.15-303.15	0.31-0.72	0.1747-0.9594	0.4154-0.993	19
537	ethyl iodide(1) + nitrobenzene(2)	293.15-293.15	0.06-0.13	0.17-0.79	-	5
538	dichloromethane(1) + Dimethyl sulfoxide(2)	298.15-298.15	0.0008-0.58	0-1	-	18
539	Ethanethiol(1) + Dimethyl sulfoxide(2)	308.15-310.45	1.01-1.01	0-1	0-1	9
540	Ethanethiol(1) + N,N-dimethylformide(2)	298.15-298.15	0.03-0.11	0.023-0.09	-	4
541	ethylamine(1) + diethylamine(2)	283.15-293.15	0.16-1.16	0-1	-	20

Table A.1. Binary VLE Database Used in Model Development *(Continued)*

NO.	System	Temperature range (K)	Pressure range (bar)	Component (1) liquid mole fraction range	Component (1) vapor mole fraction range	NDP
542	ethylamine(1) + Triethylamine(2)	273.15-283.15	0.03-0.77	0-1	-	18
543	acrylonitrile(1) + tetrachloroethylene(2)	303.15-323.15	0.12-0.4	0.2005-1	-	20
544	acrylonitrile(1) + propionitrile(2)	350.45-370.45	1.01-1.01	0-1	0-1	28
545	N,N-dimethylformide(1) + Dimethyl sulfoxide(2)	373.15-373.15	0.05-0.19	0-1	-	11
546	thiophene(1) + N,N-dimethylformide(2)	358.85-406.85	1.01-1.01	0.0905-0.885	0.414-0.983	10
547	tetrachloromethane(1) + 1-Nitropropane(2)	298.15-298.15	0.01-0.15	0-1	0-1	41
548	1-Nitropropane(1) + 1,2-Dibromoethane(2)	348.15-393.15	0.15-0.82	0-1	0-1	23
549	Isopropylamine(1) + Diisopropylamine(2)	305.45-353.65	1.01-1.01	0.0208-0.981	0.118-0.996	23
550	Trimethylamine(1) + tetrachloromethane(2)	253.15-293.15	0.01-1.85	0-1	-	63
551	thiophene(1) + pyridine(2)	357.8-387.3	1.01-1.01	0.013-0.951	0.026-0.977	14
552	butylchloride(1) + Buthyl Bromide(2)	323.15-323.15	0.17-0.39	0-1	0-1	16
553	pyridine(1) + 2-Methylpyridine(2)	388.4-402.57	1.01-1.01	0-1	0-1	13
554	hexafluorobenzene(1) + Triethylamine(2)	283.15-283.15	0.05-0.06	0.0777-0.9616	0.1652-0.9379	12
555	methanol(1) + benzaldehyde(2)	293.15-293.15	0.07-0.12	0.005-0.03	-	6
556	1-propanol(1) + propionic aldehyde(2)	321.18-370.35	1.01-1.01	0-1	0-1	40
557	1-propanol(1) + butyraldehyde(2)	343.65-353.15	0.34-1.19	0-1	0-1	23
558	2-methyl 1-propanol(1) + butyraldehyde(2)	347.85-380.95	1.01-1.01	0-1	0-1	22
559	2-methyl 1-propanol(1) + Isobutyr Aldehyde(2)	336.45-380.95	1.01-1.01	0-1	0-1	52
560	teritiary amyl alcohol(1) + propionic aldehyde(2)	333.15-333.15	0.17-1.51	0-1	0-1	43
561	ethanol(1) + propionic aldehyde(2)	298.15-351.42	0.08-1.01	0-1	0-1	97
562	ethanol(1) + butyraldehyde(2)	323.15-353.15	0.3-1.31	0-1	0-1	65
563	1-butanol(1) + butyraldehyde(2)	347.85-390.85	1.01-1.01	0-1	0-1	22
564	1-butanol(1) + Isobutyr Aldehyde(2)	337.35-390.85	1.01-1.01	0-1	0-1	17
565	Isobutyr Aldehyde(1) + butyraldehyde(2)	323.8-348.7	0.53-1.07	0-1	0-1	94
566	Isoprene(1) + n-pentane(2)	303.11-323.19	0.84-1.72	0.043-0.982	0-0.983	94
567	1,3-butadiene(1) + cyclohexane(2)	303.15-413.15	0.16-9.49	0-1	0-1	62

Table A.1. Binary VLE Database Used in Model Development *(Continued)*

NO.	System	Temperature range (K)	Pressure range (bar)	Component (1) liquid mole fraction range	Component (1) vapor mole fraction range	NDP
568	1-Pentyne(1) + n-pentane(2)	308-311.45	1.01-1.01	0.1-1	0.151-1	11
569	Isoprene(1) + trans, 1,3-pentadiene(2)	307.15-314.35	1.01-1.01	0.225-0.9934	0.3068-0.9958	10
570	N,N-dimethylformide(1) + tertiary butyl alcohol(2)	353.85-423.95	0.94-0.95	0-1	0-1	33
571	methanol(1) + N,N-dimethylformide(2)	293.15-426.55	0.004-1.01	0-1	0-1	121
572	N,N-dimethylformide(1) + 1-propanol(2)	313.15-425.63	0.02-1.14	0-1	0-1	108
573	2-propanol(1) + N,N-dimethylformide(2)	325-408.65	0.08-1	0-1	0-1	49
574	N,N-dimethylformide(1) + 1-butanol(2)	338.15-424.75	0.05-1.31	0-1	0-1	170
575	N,N-dimethylformide(1) + 2-methyl 1-propanol(2)	379.76-425.63	0.95-1.01	0-1	0-1	41
576	N,N-dimethylformide(1) + benzaldehyde(2)	378-398	0.1-0.45	0-1	0-1	31
577	N,N-dimethylformide(1) + Isobutyr Aldehyde(2)	313.15-333.15	0.01-0.88	0-1	0-1	24
578	N,N-dimethylformide(1) + Triethylamine(2)	323.15-353.15	0.02-0.78	0-1	0-1	42
579	N,N-dimethylformide(1) + ethylenediamine(2)	353.15-353.15	0.12-0.25	0.2002-0.8994	-	8
580	N,N-dimethylformide(1) + Cyclohexaylamine(2)	373-393	0.19-0.69	0-1	0-1	35
581	tertiary butyl alcohol(1) + bromobenzene(2)	335.39-416.15	0.4-1.01	0.018-0.9239	0.3037-0.9806	28
582	ethanol(1) + bromobenzene(2)	298.15-303.17	0.01-0.1	0-1	0-1	30
583	1-butanol(1) + bromobenzene(2)	367.06-420.18	0.4-1.01	0.0342-0.9657	0.2374-0.9705	28
584	2-methyl 1-propanol(1) + bromobenzene(2)	358.03-418.76	0.4-1.01	0-1	0.2693-0.9873	27
585	bromobenzene(1) + N,N-dimethylformide(2)	418.45-427.05	0.95-0.95	0-1	0-1	27
586	N,N-dimethylformide(1) + Fluorobenzene(2)	360.95-416.95	1.01-1.01	0.084-0.9732	0.026-0.8939	12
587	bromobenzene(1) + Fluorobenzene(2)	360.1-413.8	0.99-1	0.093-0.918	0.012-0.618	9
588	benzene(1) + isobutene(2)	298.15-298.15	0.27-1.02	0.769-0.97	-	5
589	benzene(1) + 1-butene(2)	298.15-298.15	0.41-1.02	0.755-0.934	-	4
590	benzene(1) + 1-heptene(2)	328.14-328.14	0.27-0.44	0-1	0-1	13
591	benzene(1) + vinylacetylene(2)	278.55-352.42	0.99-0.99	0-1	0-1	14
592	p-xylene(1) + vinylacetylene(2)	278.55-410.73	0.99-0.99	0-1	0-1	23
593	Isobutyr Aldehyde(1) + toluene(2)	338.82-378.13	1.01-1.01	0.061-0.917	0.182-0.982	14

Table A.1. Binary VLE Database Used in Model Development *(Continued)*

NO.	System	Temperature range (K)	Pressure range (bar)	Component (1) liquid mole fraction range	Component (1) vapor mole fraction range	NDP
594	n-octane(1) + water(2)	363.04-398.38	1.01-1.01	0.0001-0.9999	0.0086-0.9867	22
595	toluene(1) + vinylacetylene(2)	293.24-363.32	0.99-0.99	0.478-0.952	-	8
596	butylamine(1) + water(2)	350.12-368.52	1.01-1.01	0.006-0.955	0.159-0.968	16
597	Cyclohexaylamine(1) + water(2)	333.15-407.43	0.08-1.01	0-1	0-1	39
598	m-xylene(1) + water(2)	367.16-408.15	1.01-1.01	0-0.9978	0.0103-0.8784	22
599	methyl teritiary butyl ether(1) + water(2)	326.7-327.7	1.01-1.01	0.451-0.967	0.919-0.934	4
600	Dimethyl sulfoxide(1) + nitrobenzene(2)	458.15-483.05	0.95-0.95	0-1	0-1	10
601	benzene(1) + Tribromomethane(2)	303.14-313.14	0.01-0.22	0-1	0-1	24
602	benzene(1) + Dibromomethane(2)	308.14-308.14	0.09-0.19	0-1	0-1	10
603	benzene(1) + 1,2-Dibromoethane(2)	282.99-405.8	0.01-1.02	0-1	0-1	295
604	benzene(1) + Buthyl Bromide(2)	343.13-343.13	0.37-0.73	0-1	0-1	29
605	ethylbenzene(1) + Buthyl Bromide(2)	343.13-343.13	0.11-0.37	0-1	0-1	27
606	p-xylene(1) + 1,2-Dibromoethane(2)	298.15-308.15	0.01-0.03	0-1	0-1	23
607	1,2-Dibromoethane(1) + m-xylene(2)	298.15-308.15	0.01-0.03	0-1	0-1	22
608	tertiary butyl alcohol(1) + tetrachloroethylene(2)	353.95-391.05	0.95-0.95	0-1	0-1	11
609	methanol(1) + tetrachloroethylene(2)	335.15-391.75	0.95-1.01	0-1	0-1	23
610	1-propanol(1) + tetrachloroethylene(2)	327.65-394.15	0.2-1.01	0-1	0-1	94
611	2-propanol(1) + tetrachloroethylene(2)	318.35-394.15	0.2-1	0-1	0-1	72
612	1-butanol(1) + tetrachloroethylene(2)	311.95-391.52	0.06-1.01	0-1	0-1	109
613	2-methyl 1-propanol(1) + tetrachloroethylene(2)	376.02-388.02	1.01-1.01	0.048-0.925	0.208-0.845	16
614	methanol(1) + Vinyl chloride(2)	253.15-273.15	0.12-0.93	0.678-0.9825	-	23
615	tertiary butyl alcohol(1) + 3-Chloro-1-propene(2)	319.49-345.18	1.01-1.01	0.2124-0.9018	0.1045-0.627	10
616	3-Chloro-1-propene(1) + methanol(2)	312.14-327.64	1-1	0.05-0.933	-	11
617	methanol(1) + 1,1-Dichloroethylene(2)	302.04-337.53	1.01-1.01	0-1	0-1	17
618	ethanol(1) + 1,1-Dichloroethylene(2)	303.84-351.43	1.01-1.01	0-1	0-1	17

Table A.1. Binary VLE Database Used in Model Development *(Continued)*

NO.	System	Temperature range (K)	Pressure range (bar)	Component (1) liquid mole fraction range	Component (1) vapor mole fraction range	NDP
619	tertiary butyl alcohol(1) + Trichloethylene(2)	348.85-358.83	0.95-1.01	0-1	0-1	32
620	methanol(1) + Trichloethylene(2)	330.75-357.55	0.95-0.95	0-1	0-1	10
621	ethanol(1) + Trichloethylene(2)	343.82-357.65	0.95-1.01	0-1	0-1	9
622	1-propanol(1) + Trichloethylene(2)	312.05-369.75	0.2-1.01	0-1	0-1	89
623	2-propanol(1) + Trichloethylene(2)	308.55-359.55	0.2-1.01	0-1	0-1	81
624	1-butanol(1) + Trichloethylene(2)	313-390.25	0.2-1.01	0-1	0-1	88
625	2-methyl 1-propanol(1) + Trichloethylene(2)	357.05-379.32	0.95-1.01	0-1	0-1	25
626	acetaldehyde(1) + ethylene-oxide(2)	273-333	0.44-5.23	0-1	0-1	49
627	diethyl ether(1) + nitromethane(2)	293.64-293.64	0.04-0.6	0-1	0-1	13
628	nitromethane(1) + 1,4-dioxane(2)	303.13-371.12	0.06-0.96	0-1	0-1	56
629	diethyl ether(1) + nitrobenzene(2)	293.14-293.14	0.19-0.45	0.25-0.75	-	5
630	chlorobenzene(1) + ethyl acetate(2)	313.14-393.12	0.04-3.47	0-1	0-1	45
631	chlorobenzene(1) + 1,4-dioxane(2)	374.32-405.22	1.01-1.01	0-1	0-1	14
632	diisopropyl ether(1) + chlorobenzene(2)	341.33-410.32	1.01-1.01	0-1	0-1	12
633	acetone(1) + chlorobenzene(2)	313.14-404.92	0.04-5.21	0-1	0-1	120
634	2-butanone(1) + chlorobenzene(2)	351.25-403.05	0.95-1.01	0-1	0-1	23
635	4-methyl 2-pentanone(1) + chlorobenzene(2)	388.82-405.22	1.01-1.01	0-1	0-1	19
636	1,2-Dibromoethane(1) + Fluorobenzene(2)	358.4-405.4	1.02-1.02	0-1	0-1	21
637	acetonitrile(1) + bromobenzene(2)	352.55-427.05	0.95-0.95	0-1	0-1	16
638	nitrobenzene(1) + bromobenzene(2)	385.32-481.15	0.27-0.95	0-1	0-1	54
639	Dimethyl sulfoxide(1) + bromobenzene(2)	424.65-460.95	0.95-0.95	0-1	0-1	10
640	ethyl iodide(1) + toluene(2)	308.15-363.18	0.06-1.57	0-1	0-1	37
641	toluene(1) + thiophene(2)	353.38-379.44	0.9-1.01	0-1	0-1	29
642	propylene oxide(1) + water(2)	306.98-373.07	1.01-1.01	0-1	0-1	17
643	ethylene-oxide(1) + water(2)	278.15-345.87	0.03-4.48	0.0043-1	0-1	107
644	propylene oxide(1) + ethyl acetate(2)	308.14-348.13	0.5-3.43	0.089-0.9433	0.1798-0.9712	30

Table A.1. Binary VLE Database Used in Model Development *(Continued)*

NO.	System	Temperature range (K)	Pressure range (bar)	Component (1) liquid mole fraction range	Component (1) vapor mole fraction range	NDP
645	pyridine(1) + ethyl acetate(2)	323.45-423.15	0.1-6.96	0-1	0-1	119
646	2-Methylpyridine(1) + ethyl acetate(2)	303.15-303.15	0.02-0.16	0-1	0-1	13
647	ethyl iodide(1) + ethyl acetate(2)	323.12-323.12	0.37-0.48	0-1	0-1	25
648	acetonitrile(1) + ethyl acetate(2)	313.14-393.12	0.23-3.6	0-1	0-1	61
649	nitromethane(1) + ethyl acetate(2)	298.15-398.14	0.05-3.94	0-1	0-1	66
650	nitrobenzene(1) + ethyl acetate(2)	293.14-293.14	0.03-0.09	0.1-0.75	-	6
651	nitroethane(1) + ethyl acetate(2)	350.28-387	1.01-1.01	0-1	0-1	21
652	Dimethyl sulfoxide(1) + ethyl acetate(2)	298.14-318.14	0.002-0.31	0-1	0-1	33
653	tetrachloromethane(1) + propyl acetate(2)	349.89-374.68	1.01-1.01	0-1	0-1	30
654	tetrachloromethane(1) + methyl acetate(2)	329.97-349.89	1.01-1.01	0-1	0-1	64
655	chloroform(1) + methyl acetate(2)	298-337.82	0.21-1.01	0-0.941	0-0.968	72
656	dichloromethane(1) + methyl acetate(2)	298-303.14	0.29-0.7	0-1	0-1	46
657	1,1-Dichloroethylene(1) + vinyl acetate(2)	303.99-344.98	1.01-1.01	0-1	0-1	24
658	propylene oxide(1) + methyl acetate(2)	308.14-348.13	0.5-3.43	0.089-0.9433	0.1798-0.9712	30
659	methyl acetate(1) + 1,2-epoxybutane(2)	298-348	0.24-1.79	0-1	0-1	182
660	methyl acetate(1) + ethyl acetate(2)	273.15-373.17	0.03-3.66	0-1	0-1	286
661	methyl iodide(1) + methyl acetate(2)	315.24-326.14	1.01-1.01	0.103-0.942	0.22-0.943	8
662	acetonitrile(1) + propyl acetate(2)	354.53-374.62	1.01-1.01	0-1	0-1	21
663	acetonitrile(1) + methyl acetate(2)	323.14-354.63	0.34-1.01	0-1	0-1	34
664	acetonitrile(1) + vinyl acetate(2)	345.21-353.33	1.01-1.01	0.059-0.965	0.07-0.931	24
665	acrylonitrile(1) + vinyl acetate(2)	341.13-350.63	1.01-1.01	0-1	0-1	24
666	nitromethane(1) + propyl acetate(2)	371.3-374.69	1.01-1.01	0-1	0-1	21
667	nitroethane(1) + propyl acetate(2)	374.69-387	1.01-1.01	0-1	0-1	21
668	propyl acetate(1) + pyridine(2)	374.55-388.15	1.01-1.01	0-1	0-1	21
669	vinyl acetate(1) + water(2)	339.03-373.12	1.01-1.01	0-1	0-1	25
670	methyl acetate(1) + water(2)	298.14-429.47	0.03-11.72	0-1	0-1	150

Table A.1. Binary VLE Database Used in Model Development *(Continued)*

NO.	System	Temperature range (K)	Pressure range (bar)	Component (1) liquid mole fraction range	Component (1) vapor mole fraction range	NDP
671	Ethanethiol(1) + toluene(2)	323.13-372.85	0.22-1.47	0.0511-0.1421	-	9
672	methyl mercaptan(1) + toluene(2)	323.07-372.65	0.29-2.33	0.0394-0.1392	-	10
673	thiophene(1) + ethyl teritiary butyl ether(2)	333.15-343.15	0.45-0.93	0-1	0-1	35
674	methanol(1) + thiophene(2)	308.14-353.67	0.17-1.01	0-1	0-1	165
675	ethanol(1) + thiophene(2)	308.14-318.14	0.14-0.38	0-1	0-1	48
676	1-propanol(1) + thiophene(2)	308.14-318.14	0.05-0.28	0-1	0-1	51
677	2-propanol(1) + thiophene(2)	308.14-318.14	0.11-0.33	0-1	0-1	48
678	thiophene(1) + isobutene(2)	308.11-336.85	0.17-8.55	0-1	0-1	52
679	thiophene(1) + trans, 2-butene(2)	308.13-335.88	0.17-6.66	0-1	0-1	52
680	butane(1) + Hydrogen Sulfide(2)	182.33-182.33	0.06-0.15	0.3577-1	0-1	7
681	Dimethyl sulfoxide(1) + water(2)	296.08-441.51	0.0008-0.73	0-1	0-1	478
682	tetrachloromethane(1) + N,N-dimethylformide(2)	303.13-333.12	0.02-0.57	0.0372-0.9667	0.5415-0.9953	67
683	N,N-dimethylformide(1) + 1,2-dichloroethane(2)	355.15-421.15	0.95-0.95	0-1	0-1	21
684	chloroform(1) + N,N-dimethylformide(2)	335.4-408.9	1.01-1.01	0.0412-0.9158	0.3551-0.9841	14
685	N,N-dimethylformide(1) + butylchloride(2)	313.15-323.15	0.05-0.34	0.1591-0.9223	0-0.1139	20
686	N,N-dimethylformide(1) + Trichloethylene(2)	359.18-425	0.99-0.99	0-1	0-1	13
687	N,N-dimethylformide(1) + chlorobenzene(2)	402.85-424.35	0.95-0.95	0-1	0-1	34
688	N,N-dimethylformide(1) + ethyl acetate(2)	350.24-426.3	1.01-1.01	0-1	0-1	32
689	N,N-dimethylformide(1) + 1,4-dioxane(2)	302.98-332.97	0.01-0.23	0.0469-0.9778	0.0108-0.8072	50
690	N,N-dimethylformide(1) + diisopropyl ether(2)	339.65-420.85	0.95-0.95	0-1	0-1	17
691	acetone(1) + N,N-dimethylformide(2)	293.14-426.01	0.004-1.01	0-1	0-1	69
692	N,N-dimethylformide(1) + cyclohexanone(2)	318.65-426.27	0.02-1.01	0.105-0.935	0-0.892	18
693	N,N-dimethylformide(1) + acrylonitrile(2)	349.5-425	0.99-0.99	0-1	0-1	13
694	N,N-dimethylformide(1) + pyridine(2)	389.33-423.87	1.01-1.01	0.046-0.98	0.022-0.948	32
695	N,N-dimethylformide(1) + toluene(2)	313.14-422.41	0.01-3.65	0-1	0-1	203

Table A.1. Binary VLE Database Used in Model Development *(Continued)*

NO.	System	Temperature range (K)	Pressure range (bar)	Component (1) liquid mole fraction range	Component (1) vapor mole fraction range	NDP
696	N,N-dimethylformide(1) + water(2)	367.52-426.24	0.8-1.02	0-1	0-1	145
697	chlorobenzene(1) + 2-Methylpyridine(2)	303.15-303.15	0.02-0.02	0-1	0-1	15
698	Dimethyl sulfoxide(1) + chlorobenzene(2)	402.35-460.95	0.95-0.95	0-1	0-1	10
699	benzene(1) + propyl acetate(2)	353.23-374.62	1.01-1.01	0-1	0-1	37
700	benzene(1) + methyl acetate(2)	273.15-363.12	0.04-3	0-1	0-1	281
701	methyl acetate(1) + o-xylene(2)	332.45-414.25	1.01-1.01	0.0144-0.9333	0.141-0.9851	15
702	benzene(1) + vinyl acetate(2)	345-353.25	1.01-1.01	0-1	0-1	17
703	p-xylene(1) + vinyl acetate(2)	344.68-410	0.97-0.97	0-1	0-1	20
704	Isopropylbenzene(1) + vinyl acetate(2)	345.46-421.85	0.97-0.97	0.0317-0.995	0.0063-0.9437	23
705	benzene(1) + ethyl acetate(2)	323.14-353.13	0.37-1.01	0.05-0.984	0.049-0.98	71
706	ethylbenzene(1) + ethyl acetate(2)	323.14-343.13	0.05-0.67	0.179-0.984	0.032-0.927	42
707	p-xylene(1) + ethyl acetate(2)	351.04-409.67	1.01-1.01	0.035-0.994	0.008-0.952	20
708	o-xylene(1) + ethyl acetate(2)	351.55-414.35	1.01-1.01	0.0239-0.9861	0.0012-0.8739	12
709	methanol(1) + Hydrogen cyanide(2)	273.15-348.15	0.04-4.82	0-1	0-1	30
710	Hydrogen cyanide(1) + acrylonitrile(2)	288.04-351.12	0.53-1.01	0.005-0.9973	0.0153-0.9989	81
711	bromobenzene(1) + n-heptane(2)	371.4-428.8	1.01-1.01	0-1	0-1	14
712	bromobenzene(1) + cyclohexane(2)	288.14-308.13	0.004-0.2	0-1	0-1	94
713	bromobenzene(1) + n-decane(2)	427.15-445.25	0.96-0.96	0-1	0-1	7
714	butane(1) + ethyl acetate(2)	318.4-318.41	0.31-4.37	0-1	0-1	26
715	isobutane(1) + ethyl acetate(2)	318.38-318.4	0.31-6.08	0-1	0-1	26
716	n-pentane(1) + ethyl acetate(2)	309.3-350.15	1.01-1.01	0-1	0-1	25
717	hexane(1) + ethyl acetate(2)	319.08-350.15	0.33-1.01	0-1	0-1	58
718	ethyl acetate(1) + n-heptane(2)	323.14-371.56	0.19-1.01	0-1	0-1	85
719	n-octane(1) + ethyl acetate(2)	339.77-398.83	0.71-1.01	0-1	0-1	63
720	cyclohexane(1) + ethyl acetate(2)	293.15-350.62	0.1-1.01	0-1	0-1	75

Table A.1. Binary VLE Database Used in Model Development *(Continued)*

NO.	System	Temperature range (K)	Pressure range (bar)	Component (1) liquid mole fraction range	Component (1) vapor mole fraction range	NDP
721	n-decane(1) + ethyl acetate(2)	350.15-433.02	1.01-1.01	0-0.974	0-0.68	20
722	Trichloethylene(1) + ethyl acetate(2)	332.97-360.02	0.42-1.01	0-1	0-1	173
723	tetrachloromethane(1) + ethyl acetate(2)	293.14-350.52	0.1-1.01	0-1	0-1	285
724	1,2-dichloroethane(1) + ethyl acetate(2)	313.15-313.15	0.21-0.24	0.1523-0.9782	0.1146-0.9814	18
725	chloroform(1) + ethyl acetate(2)	313.14-350.92	0.24-1.01	0-1	0-1	78
726	dichloromethane(1) + ethyl acetate(2)	298.2-398.14	0.13-10.28	0-1	0-1	57
727	butylchloride(1) + ethyl acetate(2)	298.14-398.15	0.13-3.96	0-1	0-1	45
728	Dibromomethane(1) + ethyl acetate(2)	313.15-313.15	0.14-0.24	0.071-0.9154	0.0315-0.8192	14
729	Trimethylamine(1) + ethyl acetate(2)	273-362.98	0.03-11.6	0-1	0-1	32
730	1,3-butadiene(1) + ethyl acetate(2)	298.19-298.19	0.13-1.04	0-0.3242	0-0.911	8
731	isobutene(1) + ethyl acetate(2)	318.4-318.41	0.31-5.38	0-1	0-1	26
732	toluene(1) + benzyl acetate(2)	324.99-483.26	0.13-0.93	0-1	0-1	33
733	1-Nitropropane(1) + water(2)	367.92-376.02	1.01-1.01	0.0135-0.8041	0.1525-0.3735	11
734	nitromethane(1) + water(2)	294.2-356.82	0.03-1.01	0-1	0-1	52
735	1,2-Dibromoethane(1) + bromobenzene(2)	404.6-429.4	1.02-1.02	0-1	0-1	24
736	2-butanone(1) + bromobenzene(2)	327.14-427.25	0.4-0.95	0-1	0-1	38
737	pyridine(1) + 1,4-dioxane(2)	308.64-323.14	0.05-0.15	0.035-0.9805	0.0225-0.9556	73
738	methyl mercaptan(1) + dimethyl ether(2)	313.14-313.14	3.26-8.9	0-1	0-1	23
739	acetone(1) + methyl mercaptan(2)	313.14-313.14	0.57-3.24	0-1	0-1	22
740	acetone(1) + nitromethane(2)	298.18-397.16	0.05-6.64	0-1	0-1	60
741	acetone(1) + nitrobenzene(2)	293.14-293.14	0.05-0.17	0.25-0.75	-	5
742	2-butanone(1) + nitrobenzene(2)	327.54-481.65	0.4-0.95	0-1	0-1	38
743	acetone(1) + water(2)	283.15-503.16	0.02-34.47	0-1	0-1	952
744	3-pentanone(1) + water(2)	342.98-342.98	0.31-0.62	0-1	0-1	22

Table A.1. Binary VLE Database Used in Model Development *(Continued)*

NO.	System	Temperature range (K)	Pressure range (bar)	Component (1) liquid mole fraction range	Component (1) vapor mole fraction range	NDP
745	2-butanone(1) + water(2)	293.14-515.37	0.02-34.47	0-1	0-1	538
746	4-methyl 2-pentanone(1) + water(2)	298.14-389.12	0.03-1.01	0-1	0-1	79
747	propylene oxide(1) + methyl teritiary butyl ether(2)	303.14-363.13	0.4-5.45	0-1	0-1	40
748	propylene oxide(1) + toluene(2)	308.44-368.43	1.01-1.01	0.0417-0.9325	0.3806-0.995	13
749	methyl mercaptan(1) + hexane(2)	223.16-372.68	0.002-4.67	0-1	0-1	185
750	methyl mercaptan(1) + n-decane(2)	313.14-313.14	0.01-3.28	0-1	0-1	22
751	Ethanethiol(1) + isopentane(2)	298.34-370.22	1.01-5.88	0-1	0-1	36
752	Ethanethiol(1) + butane(2)	323.15-373.15	1.68-15.26	0-1	0-1	32
753	Ethanethiol(1) + n-pentane(2)	303.24-371.42	1.01-5.88	0-1	0-1	41
754	Ethanethiol(1) + hexane(2)	323.18-372.65	0.67-2.92	0.0489-0.0897	-	9
755	Ethanethiol(1) + n-decane(2)	323.09-372.91	0.12-1.01	0.049-0.148	-	8
756	methyl acetate(1) + propyl acetate(2)	313.14-333.13	0.1-1.08	0-1	0-1	32
757	vinyl acetate(1) + propyl acetate(2)	345.7-374.4	1.01-1.01	0-1	0-1	21
758	methyl acetate(1) + vinyl acetate(2)	329.84-345.69	1.01-1.01	0-1	0-1	65
759	propyl acetate(1) + Diethyl sulfide(2)	363.15-363.15	0.71-0.96	0-1	0-1	11
760	carbondisulfide(1) + methyl acetate(2)	313.39-329.74	1.01-1.01	0-1	0-1	48
761	methyl acetate(1) + toluene(2)	330.98-379.68	1.01-1.01	0.018-0.95	0.115-0.986	24
762	vinyl acetate(1) + toluene(2)	347.33-379.16	1.01-1.01	0.048-0.923	0-0.939	19
763	tetrachloromethane(1) + propylene oxide(2)	299.99-319.99	0.29-1.57	0.0028-0.9964	0.0008-0.9774	36
764	ethylene-oxide(1) + 1,2-dichloroethane(2)	284.94-356.42	1.01-1.01	0-1	0-1	17
765	1,2-epoxybutane(1) + chloroform(2)	288.15-313.15	0.11-0.48	0-1	0-1	50
766	1,2-epoxybutane(1) + butylchloride(2)	313.15-333.15	0.26-0.91	0-1	0-1	28
767	Ethyl Bromide(1) + water(2)	310.24-311.54	1.01-1.01	0.9299-0.9997	0.9456-0.9995	9
768	3-Chloro-1-propene(1) + water(2)	316.14-373.12	1.01-1.01	0-1	0-1	9

Table A.1. Binary VLE Database Used in Model Development *(Continued)*

NO.	System	Temperature range (K)	Pressure range (bar)	Component (1) liquid mole fraction range	Component (1) vapor mole fraction range	NDP
769	Dibromomethane(1) + toluene(2)	308.14-308.14	0.06-0.09	0-1	0-1	10
770	1,2-Dibromoethane(1) + toluene(2)	298.15-405.5	0.02-1.02	0-1	0-1	44
771	toluene(1) + Buthyl Bromide(2)	343.13-343.13	0.27-0.37	0-1	0-1	58
772	Trichloethylene(1) + toluene(2)	320.84-383.72	0.27-1.01	0-1	0-1	160
773	pyridine(1) + tetrachloroethylene(2)	323.14-373.12	0.09-0.7	0.0301-0.9797	0-0.9677	74
774	Trichloethylene(1) + chlorobenzene(2)	358.25-402.55	0.95-1.01	0-1	0-1	17
775	acetone(1) + tetrachloroethylene(2)	273.15-393.33	0.01-0.99	0-1	0-1	35
776	2-butanone(1) + tetrachloroethylene(2)	298.15-391.45	0.02-0.95	0-1	0-1	23
777	acetone(1) + Vinyl chloride(2)	281.15-339.13	0.14-11.47	0-1	0-1	44
778	2-butanone(1) + 3-Chloro-1-propene(2)	323.14-348.13	1.01-1.01	0.186-0.926	0.063-0.884	8
779	acetone(1) + Trichloethylene(2)	273.15-273.15	0.03-0.09	0-1	0-1	12
780	2-butanone(1) + Trichloethylene(2)	288.15-359.02	0.06-1.01	0-1	0-1	66
781	Trichloethylene(1) + 4-methyl 2-pentanone(2)	360.13-388.72	1.01-1.01	0-1	0-1	21
782	1,4-dioxane(1) + tetrachloroethylene(2)	303.15-390.12	0.03-1.01	0-1	0-1	28
783	Trichloethylene(1) + 1,4-dioxane(2)	303.15-303.15	0.06-0.12	0-1	0-1	10
784	chlorobenzene(1) + Fluorobenzene(2)	357.7-405.4	1.01-1.02	0-1	0-1	10
785	chlorobenzene(1) + isobutene(2)	298.15-343.15	1.52-8.75	0.1321-0.8165	-	11
786	chlorobenzene(1) + 1-pentene(2)	280-359.98	0.01-5.15	0-1	0-1	42
787	tertiary butyl alcohol(1) + chlorobenzene(2)	334.3-404.82	0.4-1.01	0-1	0-1	63
788	methanol(1) + chlorobenzene(2)	293.15-404.92	0.01-5.07	0-1	0-1	126
789	teritiary amyl alcohol(1) + chlorobenzene(2)	374.85-404.05	1-1	0-1	0-1	23
790	ethanol(1) + chlorobenzene(2)	298.14-405.12	0.02-5.05	0-1	0-1	166
791	1-propanol(1) + chlorobenzene(2)	331.15-449.25	0.2-3	0-1	0-1	186
792	2-propanol(1) + chlorobenzene(2)	328.14-404.05	0.16-1.01	0-1	0-1	74
793	1-butanol(1) + chlorobenzene(2)	293.15-449.25	0.01-3	0-1	0-1	236

Table A.1. Binary VLE Database Used in Model Development *(Continued)*

NO.	System	Temperature range (K)	Pressure range (bar)	Component (1) liquid mole fraction range	Component (1) vapor mole fraction range	NDP
794	2-methyl 1-propanol(1) + chlorobenzene(2)	355.77-402.5	0.4-1.01	0-1	0-1	80
795	chlorobenzene(1) + cyclohexanol(2)	383.12-403.12	0.17-0.96	0-1	0-1	21
796	methanol(1) + ethyl iodide(2)	293.15-383.12	0.13-6.22	0-1	0-1	35
797	ethanol(1) + ethyl iodide(2)	303.13-343.32	0.1-1.01	0-1	0-1	43
798	1-butanol(1) + ethyl iodide(2)	293.14-293.14	0.09-0.16	0-0.83	-	12
799	methyl iodide(1) + acetaldehyde(2)	293-314.8	1-1	0-1	0-1	23
800	Tribromomethane(1) + methyl acetate(2)	293.14-293.14	0.02-0.2	0.1-0.9	-	9
801	diethyl ether(1) + Tribromomethane(2)	293.14-293.14	0.04-0.52	0.1-0.9	-	9
802	1,2-Dibromoethane(1) + 1,4-dioxane(2)	293-293	0.01-0.03	0-1	0-1	13
803	acetone(1) + Ethyl Bromide(2)	312.14-328.84	1.01-1.01	0.026-0.9953	0.0192-0.9701	17
804	propylene oxide(1) + ethylbenzene(2)	307.79-386.52	1.01-1.01	0.0537-0.945	0.51-0.9981	9
805	pyridine(1) + hexafluorobenzene(2)	343.13-343.13	0.22-0.72	0-1	0-1	19
806	tetrachloromethane(1) + hexafluorobenzene(2)	278.68-323.06	0.04-0.43	0-1	0-1	90
807	tetrachloromethane(1) + Fluorobenzene(2)	322.16-343.08	0.32-0.8	0-1	0-1	32
808	acetone(1) + diethylamine(2)	298.02-398.07	0.31-7.65	0-1	0-1	58
809	acetone(1) + Triethylamine(2)	318.14-318.14	0.22-0.68	0-1	0-1	28
810	2-butanone(1) + diethylamine(2)	501.48-527.81	38.01-41.19	0.1589-0.8824	-	13
811	2-butanone(1) + Triethylamine(2)	293.15-373.12	0.07-2	0-1	0-1	56
812	cyclohexanone(1) + Triethylamine(2)	313.14-333.13	0.01-0.4	0-1	0-1	58
813	tetrachloromethane(1) + 1,3-butadiene(2)	298.19-298.19	0.15-0.78	0.7865-1	0.163-1	6
814	dichloromethane(1) + 1,3-butadiene(2)	298.19-298.19	0.58-1.26	0.7278-1	0.349-1	9
815	Vinyl chloride(1) + 1,3-butadiene(2)	213.8-253.07	0.06-0.74	0.0917-0.8479	-	40
816	nitromethane(1) + Isoprene(2)	307.23-330.22	1.01-1.01	0-0.9	-	10
817	nitromethane(1) + 1,3-butadiene(2)	298.19-298.19	0.05-1.26	0.8652-1	0.036-1	7
818	Dimethyl sulfoxide(1) + Isoprene(2)	293.15-323.14	0.0006-1.7	0-1	0-1	50

Table A.1. Binary VLE Database Used in Model Development *(Continued)*

NO.	System	Temperature range (K)	Pressure range (bar)	Component (1) liquid mole fraction range	Component (1) vapor mole fraction range	NDP
819	carbondisulfide(1) + 1,3-butadiene(2)	298.19-298.19	0.48-1.23	0.7959-1	0.331-1	8
820	Dimethyl sulfoxide(1) + trans, 1,3-pentadiene(2)	293.15-323.14	0.0006-1.32	0-1	0-1	45
821	acetonitrile(1) + diethylamine(2)	297.99-398.3	0.12-7.03	0-1	0-1	89
822	Dimethyl sulfoxide(1) + ethylenediamine(2)	353.13-353.13	0.04-0.25	0.1006-0.9043	-	9
823	tertiary butyl alcohol(1) + pyridine(2)	313.14-313.14	0.06-0.14	0-1	0-1	29
824	methanol(1) + pyridine(2)	298.14-413.17	0.03-10.62	0-1	0-1	139
825	ethanol(1) + pyridine(2)	313.14-347.98	0.06-0.89	0-1	0-1	66
826	1-propanol(1) + pyridine(2)	313.14-362.98	0.06-0.77	0-1	0-1	72
827	2-propanol(1) + pyridine(2)	298.14-348.13	0.03-0.75	0-1	0-1	97
828	1-butanol(1) + pyridine(2)	293.14-362.98	0.02-0.46	0-1	0-1	77
829	2-methyl 1-propanol(1) + pyridine(2)	313.14-313.14	0.04-0.06	0-1	0-1	25
830	tertiary butyl alcohol(1) + 2-Methylpyridine(2)	313.14-313.14	0.03-0.14	0-1	0-1	15
831	methanol(1) + 2-Methylpyridine(2)	298.14-318.14	0.02-0.44	0-1	0-1	85
832	ethanol(1) + 2-Methylpyridine(2)	313.14-313.14	0.03-0.18	0-1	0-1	16
833	1-propanol(1) + 2-Methylpyridine(2)	313.14-313.14	0.03-0.07	0-1	0-1	16
834	2-propanol(1) + 2-Methylpyridine(2)	313.14-313.14	0.03-0.14	0-1	0-1	13
835	1-butanol(1) + 2-Methylpyridine(2)	313.14-313.14	0.02-0.03	0-1	0-1	18
836	2-methyl 1-propanol(1) + 2-Methylpyridine(2)	313.14-313.14	0.03-0.04	0-1	0-1	16
837	dimethyl sulfide(1) + isobutene(2)	312.59-312.6	1.07-4.65	0-1	0-1	26
838	isobutene(1) + dimethyl disulfide(2)	350.43-350.44	0.36-11.54	0-1	0-1	26
839	isobutene(1) + Diethyl sulfide(2)	312.6-312.6	0.15-4.66	0-1	0-1	26
840	nitromethane(1) + 2-methyl 1-butene(2)	304.13-315.13	1.01-1.01	0-0.9	-	10
841	nitromethane(1) + 2-methyl 2-butene(2)	311.28-320.63	1.01-1.01	0-0.9	-	10
842	methyl acetate(1) + 1-pentene(2)	323.15-323.15	0.79-1.94	0-1	0-1	59
843	propylene oxide(1) + n-pentane(2)	300.39-308.89	1.01-1.01	0-1	0-1	12

Table A.1. Binary VLE Database Used in Model Development *(Continued)*

NO.	System	Temperature range (K)	Pressure range (bar)	Component (1) liquid mole fraction range	Component (1) vapor mole fraction range	NDP
844	propylene oxide(1) + hexane(2)	307.3-341.54	1.01-1.01	0-1	0-1	12
845	propylene oxide(1) + n-heptane(2)	307.3-371.43	1.01-1.01	0-1	0-1	12
846	ethylene-oxide(1) + isobutane(2)	298-348	1.75-13.14	0-1	0-1	28
847	1,2-epoxybutane(1) + hexane(2)	313.15-333.15	0.37-1.02	0-1	0-1	30
848	1,2-epoxybutane(1) + n-heptane(2)	313.15-333.15	0.12-0.91	0-1	0-1	27
849	propylene oxide(1) + tertiary butyl alcohol(2)	307.8-339.22	0.24-2.18	0.0525-0.9801	0-0.9967	78
850	methanol(1) + propylene oxide(2)	307.69-335.9	1.01-1.01	0.0838-0.99	0.0694-0.9458	18
851	2-propanol(1) + propylene oxide(2)	307.39-355.37	1.01-1.01	0-1	0-1	44
852	methanol(1) + 1,2-epoxybutane(2)	298.15-298.15	0.19-0.28	0.017-0.973	0.05-0.886	24
853	ethanol(1) + 1,2-epoxybutane(2)	298.15-298.15	0.09-0.24	0.019-0.983	0.02-0.88	25
854	1-propanol(1) + 1,2-epoxybutane(2)	298.15-298.15	0.04-0.23	0.061-0.985	0.014-0.906	27
855	2-propanol(1) + 1,2-epoxybutane(2)	298.15-298.15	0.07-0.23	0.035-0.983	0.019-0.894	24
856	methanol(1) + nitromethane(2)	293.64-388.21	0.05-5.58	0-1	0-1	84
857	ethanol(1) + nitromethane(2)	298.17-398.14	0.05-5.04	0-1	0-1	92
858	1-propanol(1) + nitromethane(2)	333.15-362.42	0.2-1.01	0-1	0-1	26
859	2-propanol(1) + nitromethane(2)	298.14-298.14	0.05-0.09	0-1	0-1	13
860	1-butanol(1) + nitromethane(2)	293.15-313.14	0.01-0.11	0-1	0-1	34
861	methanol(1) + nitrobenzene(2)	293.14-423.15	0.002-14.13	0-1	0-1	41
862	ethanol(1) + nitrobenzene(2)	356.12-376.62	1.01-1.01	0.15-0.67	-	4
863	tertiary butyl alcohol(1) + nitroethane(2)	355.47-387.16	1.01-1.01	0-1	0-1	21
864	methanol(1) + nitroethane(2)	337.58-387.16	1.01-1.01	0-1	0-1	21
865	ethanol(1) + nitroethane(2)	351.17-387.16	1.01-1.01	0-1	0-1	22
866	1-propanol(1) + nitroethane(2)	367.78-387.16	1.01-1.01	0-1	0-1	21
867	2-propanol(1) + nitroethane(2)	354.86-387.16	1.01-1.01	0-1	0-1	23
868	Vinyl chloride(1) + acetaldehyde(2)	293.15-293.15	0.98-3.33	0-1	0-1	13

Table A.1. Binary VLE Database Used in Model Development *(Continued)*

NO.	System	Temperature range (K)	Pressure range (bar)	Component (1) liquid mole fraction range	Component (1) vapor mole fraction range	NDP
869	ethanol(1) + Ethyl Bromide(2)	303.13-303.13	0.1-0.76	0-1	0-1	15
870	methanol(1) + Tribromomethane(2)	303.14-308.13	0.01-0.28	0-1	0-1	33
871	ethanol(1) + Tribromomethane(2)	303.14-308.13	0.01-0.14	0-1	0-1	25
872	Dibromomethane(1) + tertiary butyl alcohol(2)	330.1-367.41	0.4-1.01	0.0161-0.9806	0.0299-0.9059	30
873	1-propanol(1) + Dibromomethane(2)	313.15-313.15	0.07-0.16	0-1	0-1	14
874	1-butanol(1) + Dibromomethane(2)	341.2-386.75	0.4-1.01	0.0295-0.9761	0.0409-0.8828	23
875	Dibromomethane(1) + 2-methyl 1-propanol(2)	339.8-380.06	0.4-1.01	0.0159-0.9777	0.0488-0.9511	27
876	tertiary butyl alcohol(1) + 1,2-Dibromoethane(2)	333.76-394	0.4-1.01	0.018-0.9247	0.2439-0.9539	25
877	1-butanol(1) + 1,2-Dibromoethane(2)	361.67-400.15	0.4-1.01	0.028-0.9689	0.1052-0.9266	24
878	2-methyl 1-propanol(1) + 1,2-Dibromoethane(2)	355.03-398.26	0.4-1.01	0.04-0.9374	0.1904-0.9152	23
879	tertiary butyl alcohol(1) + Buthyl Bromide(2)	298.15-368.63	0.07-1.01	0.0329-0.9617	0-0.9464	89
880	methanol(1) + Buthyl Bromide(2)	303.11-323.2	0.07-0.61	0-1	0-1	57
881	ethanol(1) + Buthyl Bromide(2)	278.15-323.15	0.03-0.36	0.0494-0.8942	-	120
882	1-butanol(1) + Buthyl Bromide(2)	278.15-388.09	0.01-1.01	0-1	0-1	143
883	2-methyl 1-propanol(1) + Buthyl Bromide(2)	278.15-379.01	0.01-1.01	0.0424-0.9534	0-0.8896	133
884	Ethyl Bromide(1) + n-heptane(2)	303.13-303.13	0.08-0.76	0-1	0-1	11
885	Tribromomethane(1) + hexane(2)	303.14-313.14	0.01-0.36	0-1	0-1	24
886	1,2-Dibromoethane(1) + cyclohexane(2)	293-298.15	0.01-0.13	0-1	0-1	25
887	Buthyl Bromide(1) + hexane(2)	341.95-365.85	0.95-0.95	0.1079-0.9012	-	9
888	Buthyl Bromide(1) + n-heptane(2)	323.13-371.55	0.17-0.95	0-1	0-1	34
889	propyl acetate(1) + n-heptane(2)	273.15-374.55	0.01-1.01	0-1	0-1	131
890	propyl acetate(1) + cyclohexane(2)	263.15-363.15	0.01-1.33	0-1	0-1	108
891	methyl acetate(1) + n-pentane(2)	298.14-298.15	0.35-0.75	0.0245-0.9834	0-0.8008	30
892	methyl acetate(1) + hexane(2)	303.09-303.09	0.36-0.37	0.991-1	0-1	19
893	methyl acetate(1) + n-heptane(2)	329.61-370.13	1.01-1.01	0.0024-0.9935	0.0193-0.9918	25

Table A.1. Binary VLE Database Used in Model Development *(Continued)*

NO.	System	Temperature range (K)	Pressure range (bar)	Component (1) liquid mole fraction range	Component (1) vapor mole fraction range	NDP
894	methyl acetate(1) + cyclohexane(2)	308.14-347.42	0.3-1.01	0.028-0.952	0.182-0.915	31
895	vinyl acetate(1) + hexane(2)	333.18-393.17	0.67-4.88	0.086-0.9867	0-0.9846	31
896	vinyl acetate(1) + cyclohexane(2)	340.43-346.63	1.01-1.01	0.098-1	0.343-1	11
897	vinyl acetate(1) + n-decane(2)	346.05-444.85	1.01-1.01	0.0103-0.9944	0.1327-0.9997	44
898	hexane(1) + tetrachloroethylene(2)	333.12-333.12	0.23-0.7	0.113-0.882	0.497-0.971	6
899	tetrachloroethylene(1) + n-heptane(2)	369.75-393.72	0.96-1.01	0-1	0-1	27
900	cyclohexane(1) + tetrachloroethylene(2)	283.15-323.15	0.01-0.35	0.0433-0.9383	-	108
901	tetrachloroethylene(1) + cyclopentane(2)	297.99-297.99	0.07-0.4	0.0638-0.9157	0.0053-0.3393	15
902	Vinyl chloride(1) + hexane(2)	259.05-308.14	0.03-5.32	0-1	0-1	46
903	Trichloethylene(1) + hexane(2)	333.12-356.63	0.48-1.01	0.098-0.9112	0.072-0.8141	15
904	Trichloethylene(1) + cyclohexane(2)	351.65-359.62	0.95-1.01	0-1	0-1	27
905	dichloromethane(1) + 1-butene(2)	303-363	1.3-11.8	0.3003-0.8751	0.073-0.643	16
906	diisobutylene(1) + butylchloride(2)	293.15-313.14	0.05-0.26	0-1	0-1	96
907	water(1) + 1,4-dioxane(2)	283.14-374.52	0.01-1.01	0-1	0-1	517
908	furfural(1) + water(2)	298.14-434.81	0.002-1.01	0-1	0-1	231
909	ethyl acetate(1) + water(2)	344.6-373	1.01-1.01	0.0006-0.986	0.0406-0.954	18
910	benzene(1) + water(2)	294.15-374.01	0.1-2.09	0-1	0-1	56
911	water(1) + 1-butanol(2)	299.15-385.65	0.01-1.02	0-0.999	0-0.981	46
912	hexane(1) + water(2)	373.11-494.15	3.43-24.52	0.9674-0.998	0.4745-0.977	6
913	propyl acetate(1) + water(2)	327.83-375.68	0.25-1.01	0-1	0-1	42
914	Trimethylamine(1) + water(2)	283-373.15	0.04-2.03	0-0.9733	0-0.9493	83
915	acrylonitrile(1) + water(2)	308.25-360.65	0.2-1.01	0-1	0-1	31
916	1-propanol(1) + water(2)	333.15-368.15	0.23-1.01	0.039-0.95	0.28-0.855	28

Table A.2. The Optimized Binary Parameters (C_{ij} and D_{ij}) of PR EOS with Summary Results for PR EOS Bubble-point Pressure Representations for the 916 Systems

NO.	System	NDP	Case 2		Case 3		
			C_{ij}	%AAD	C_{ij}	D_{ij}	%AAD
1	methyl teritiary butyl ether(1) + methanol(2)	99	-0.0256	4.7	0.1917	-0.2349	3.0
2	methyl teritiary butyl ether(1)+tertiary butyl alcohol(2)	26	0.0246	5.5	0.1512	-0.1519	5.5
3	dimethyl ether(1) + methyl teritiary butyl ether(2)	16	-0.0006	1.8	0.0140	-0.0159	1.8
4	methyl teritiary butyl ether(1) + butane(2)	40	0.0115	1.9	-0.0037	0.0180	1.8
5	methyl teritiary butyl ether(1) + isopentane(2)	36	0.0087	1.2	0.0369	-0.0340	1.1
6	methyl teritiary butyl ether(1)+methyl cyclohexane(2)	17	0.0146	5.6	0.0323	-0.0192	5.6
7	isobutene(1) + methyl teritiary butyl ether(2)	29	0.0055	2.2	-0.0169	0.0271	2.2
8	ethyl teritiary butyl ether(1) + ethanol(2)	22	0.0376	6.8	0.1803	-0.1655	5.7
9	tertiary butyl alcohol(1)+ethyl teritiary butyl ether(2)	39	0.0340	5.1	0.1680	-0.1593	3.8
10	isopentane(1) + ethyl teritiary butyl ether(2)	30	0.0048	1.8	0.0070	-0.0025	1.8
11	methyl cyclohexane(1)+ethyl teritiary butyl ether(2)	36	-0.0011	2.0	0.0250	-0.0310	1.8
12	isobutene(1) + ethyl teritiary butyl ether(2)	16	0.0024	1.0	-0.0131	0.0183	1.0
13	methanol(1) + teritiary amyl methyl ether(2)	64	-0.0097	5.2	0.1909	-0.2233	4.1
14	teritiary amyl methyl ether(1)+teritiary amyl alcohol(2)	22	-0.0527	4.8	0.1400	-0.2500	4.2
15	teritiary amyl alcohol(1)+teritiary amyl methyl ether(2)	23	-0.0352	0.9	0.1499	-0.2353	0.9
16	teritiary amyl methyl ether(1) + n-pentane(2)	99	0.0073	0.6	-0.0015	0.0114	0.5
17	teritiary amyl methyl ether(1)+methyl cyclohexane(2)	47	-0.0002	1.4	0.0295	-0.0337	1.3
18	dimethyl ether(1) + methanol(2)	14	-0.0132	4.7	0.0800	-0.0983	4.7
19	diethyl ether(1) + water(2)	30	-0.0525	1.2	0.0104	-0.0740	1.2
20	methanol(1) + ethanol(2)	44	0.0081	4.1	-0.0180	0.0299	4.0
21	butane(1) + methanol(2)	44	-0.0041	19.6	0.1768	-0.1627	12.9
22	methanol(1) + n-heptane(2)	22	0.0343	12.6	0.0891	-0.0511	12.6
23	isobutane(1) + methanol(2)	54	-0.0383	17.0	0.1732	-0.1906	13.4
24	n-pentane(1) + methanol(2)	21	0.0219	8.7	0.1725	-0.1505	8.5
25	1-pentene(1) + methanol(2)	15	0.0296	13.1	0.1432	-0.1227	8.7
26	2-methyl 2-butene(1) + methanol(2)	12	0.0257	13.8	0.1897	-0.1723	9.5
27	Isoprene(1) + methanol(2)	21	0.0233	7.0	0.1303	-0.1129	6.3
28	Isoprene(1) + diethyl ether(2)	10	0.0321	1.5	0.0202	0.0142	1.5
29	methanol(1) + 1-heptene(2)	13	0.0538	14.7	0.0692	-0.0171	14.7
30	methanol(1) + water(2)	63	-0.0772	4.1	0.0160	-0.0933	3.6
31	butane(1) + ethanol(2)	72	0.0583	14.4	0.2114	-0.1701	7.7
32	ethanol(1) + water(2)	52	-0.1047	7.4	0.0391	-0.1376	4.0
33	hexane(1) + tertiary butyl alcohol(2)	42	0.0698	5.0	0.2290	-0.1874	3.6
34	tertiary butyl alcohol(1) + n-heptane(2)	34	0.0627	7.3	0.1843	-0.1422	6.9

Table A.2. The Optimized Binary Parameters (C_{ij} and D_{ij}) of PR EOS with Summary Results for PR EOS Bubble-point Pressure Representations for the 916 Systems *(Continued)*

NO.	System	NDP	Case 2		Case 3		
			C_{ij}	%AAD	C_{ij}	D_{ij}	%AAD
35	tertiary butyl alcohol(1) + n-octane(2)	16	0.0470	12.2	0.1532	-0.1209	12.2
36	tertiary butyl alcohol(1) + isopentane(2)	32	0.0649	7.6	0.2047	-0.1601	4.1
37	tertiary butyl alcohol(1) + 2-methyl 2-butene(2)	36	0.0617	6.5	0.1690	-0.1233	3.4
38	Isoprene(1) + tertiary butyl alcohol(2)	13	0.0724	3.3	0.1481	-0.1005	3.3
39	tertiary butyl alcohol(1) + water(2)	33	-0.2621	13.8	-0.0073	-0.2067	9.1
40	teritiary amyl alcohol(1) + n-pentane(2)	99	0.0616	4.3	0.1750	-0.1464	1.6
41	methyl teritiary butyl ether(1) + acetonitrile(2)	35	0.0628	2.2	0.0275	0.0414	2.1
42	methyl teritiary butyl ether(1) + 1,3-butadiene(2)	16	-0.0150	4.0	-0.0189	0.0033	4.0
43	methanol(1) + tertiary butyl alcohol(2)	63	-0.0743	7.1	-0.0001	-0.0791	6.9
44	methanol(1) + isobutene(2)	11	0.0383	16.2	0.1803	-0.1554	8.8
45	methanol(1) + acetonitrile(2)	115	0.0426	2.5	0.0432	-0.0006	2.5
46	methanol(1) + propionitrile(2)	17	0.0301	4.6	0.0932	-0.0724	4.6
47	ethanol(1) + tertiary butyl alcohol(2)	34	-0.0447	4.2	0.0032	-0.0532	4.2
48	teritiary amyl alcohol(1) + water(2)	10	-0.1878	7.1	0.0417	-0.2115	5.1
49	butane(1) + tertiary butyl alcohol(2)	23	0.1173	2.6	0.1781	-0.0809	1.8
50	butane(1) + n-pentane(2)	12	0.0136	0.6	0.0239	-0.0117	0.6
51	n-pentane(1) + ethanol(2)	7	0.0344	16.3	0.2192	-0.1896	2.8
52	n-pentane(1) + 2-methyl 2-butene(2)	54	0.0104	1.3	0.0170	-0.0076	1.3
53	n-pentane(1) + acetonitrile(2)	20	0.1826	6.8	0.1679	0.0224	6.8
54	isobutane(1) + butane(2)	12	-0.0071	0.9	-0.0316	0.0293	0.8
55	isobutene(1) + butane(2)	50	0.0087	0.9	0.0018	0.0086	0.9
56	isobutene(1) + isobutane(2)	50	0.0052	1.2	0.0058	-0.0007	1.2
57	1-butene(1) + butane(2)	77	-0.0008	0.6	-0.0212	0.0263	0.5
58	1-butene(1) + isobutane(2)	30	-0.0005	0.3	-0.0202	0.0245	0.3
59	1-butene(1) + 1,3-butadiene(2)	62	0.0023	0.6	-0.0431	0.0572	0.6
60	cis, 2-butene(1) + butane(2)	20	0.0018	0.3	0.0142	-0.0153	0.3
61	trans, 2-butene(1) + butane(2)	19	0.0011	0.5	0.0142	-0.0160	0.5
62	2-methyl 1-butene(1) + methanol(2)	11	0.0145	14.0	0.1618	-0.1578	9.3
63	2-methyl 1-butene(1) + n-pentane(2)	48	0.0054	1.2	-0.0224	0.0326	1.2
64	2-methyl 1-butene(1) + 2-methyl 2-butene(2)	57	0.0015	1.4	-0.0379	0.0461	1.4
65	2-methyl 2-butene(1) + methanol(2)	23	0.0240	15.8	0.1877	-0.1723	11.1
66	2-methyl 2-butene(1) + ethanol(2)	13	0.0553	9.4	0.1923	-0.1538	5.3
67	2-methyl 2-butene(1) + acetonitrile(2)	46	0.1324	3.4	0.1390	-0.0091	3.3
68	acetonitrile(1) + ethanol(2)	17	0.0735	2.9	0.1233	-0.0581	2.6
69	acetonitrile(1) + tertiary butyl alcohol(2)	25	0.0622	1.2	0.1479	-0.1027	1.1
70	acetonitrile(1) + butane(2)	4	0.1000	0.2	0.1579	0.0184	0.1
71	acetonitrile(1) + diisobutylene(2)	21	0.1027	7.6	0.0867	0.0184	7.6

Table A.2. The Optimized Binary Parameters (C_{ij} and D_{ij}) of PR EOS with Summary Results for PR EOS Bubble-point Pressure Representations for the 916 Systems *(Continued)*

NO.	System	NDP	Case 2		Case 3		
			C_{ij}	%AAD	C_{ij}	D_{ij}	%AAD
72	acetonitrile(1) + water(2)	32	-0.1984	19.8	0.0967	-0.2498	9.6
73	propionitrile(1) + n-pentane(2)	7	0.1000	1.5	0.1713	-0.0534	1.3
74	propionitrile(1) + water(2)	23	-0.2196	11.1	0.0111	-0.1815	9.8
75	1,3-butadiene(1) + methanol(2)	11	0.0441	12.4	0.1302	-0.0984	8.4
76	1,3-butadiene(1) + butane(2)	33	0.0119	0.8	0.0255	-0.0171	0.8
77	1,3-butadiene(1) + isobutane(2)	30	0.0149	0.3	0.0230	-0.0100	0.3
78	1,3-butadiene(1) + cis, 2-butene(2)	12	-0.0007	0.2	-0.0075	0.0084	0.2
79	1,3-butadiene(1) + trans, 2-butene(2)	20	0.0004	0.4	-0.0071	0.0092	0.4
80	1,3-butadiene(1) + acetonitrile(2)	38	0.0841	3.7	0.0941	-0.0115	3.4
81	cis, 1,3-pentadiene(1) + methanol(2)	13	0.0491	10.2	0.1245	-0.0843	8.8
82	trans, 1,3-pentadiene(1) + methanol(2)	23	0.0464	11.2	0.1264	-0.0891	9.4
83	trans, 1,3-pentadiene(1) + acetonitrile(2)	18	0.0835	2.7	0.1173	-0.0405	2.3
84	tertiary butyl alcohol(1) + 2-methyl 1-butene(2)	32	0.0784	11.2	0.1954	-0.1311	7.0
85	methyl mercaptan(1) + methanol(2)	30	0.0706	13.5	0.1725	-0.1067	9.5
86	dimethyl sulfide(1) + methanol(2)	30	0.0507	10.2	0.1811	-0.1431	7.4
87	Hydrogen Sulfide(1) + methanol(2)	26	0.0619	3.9	0.0549	0.0057	3.9
88	methanol(1) + dimethyl disulfide(2)	21	0.1037	3.8	0.1406	-0.0440	3.8
89	methyl mercaptan(1) + water(2)	10	-0.0442	17.5	0.0188	-0.0491	16.4
90	dimethyl disulfide(1) + methyl mercaptan(2)	30	0.0062	2.7	0.0142	-0.0082	2.5
91	Hydrogen Sulfide(1) + methyl mercaptan(2)	27	-0.1391	3.1	-0.1768	0.0765	3.0
92	Hydrogen Sulfide(1) + dimethyl sulfide(2)	4	-0.0325	1.4	-0.0900	0.0697	1.4
93	methyl mercaptan(1) + dimethyl sulfide(2)	24	0.0025	2.4	0.0097	-0.0085	2.4
94	benzene(1) + toluene(2)	13	-0.0048	0.7	-0.0531	0.0571	0.7
95	n-heptane(1) + ethylbenzene(2)	17	0.0075	0.6	0.0194	-0.0138	0.6
96	n-octane(1) + ethylbenzene(2)	21	-0.0020	0.3	0.0426	-0.0530	0.2
97	1-heptene(1) + toluene(2)	13	0.0161	4.4	0.0615	-0.0519	4.2
98	n-heptane(1) + p-xylene(2)	15	0.0049	1.0	0.0065	-0.0018	1.0
99	benzene(1) + cyclohexane(2)	11	0.0126	1.6	0.0417	-0.0334	1.6
100	methyl cyclopentane(1) + benzene(2)	16	0.0123	1.0	0.0595	-0.0544	0.9
101	cyclohexane(1) + toluene(2)	13	0.0145	3.1	0.0250	-0.0119	3.1
102	Isoprene(1) + 2-methyl 2-butene(2)	11	-0.0032	1.0	0.0047	-0.0094	1.0
103	hexafluorobenzene(1) + toluene(2)	12	-0.0360	2.6	-0.0807	0.0501	2.2
104	tetrachloromethane(1) + benzene(2)	16	0.0039	0.4	0.0494	-0.0537	0.4
105	carbondisulfide(1) + cyclohexane(2)	12	-0.0086	1.8	-0.0594	0.0587	1.8
106	carbondisulfide(1) + cyclopentane(2)	19	0.0018	1.6	-0.0707	0.0820	1.4
107	carbondisulfide(1) + tetrachloromethane(2)	14	0.0001	1.3	0.0147	-0.0164	1.3
108	hexafluorobenzene(1) + p-xylene(2)	12	-0.0431	2.9	-0.0585	0.0171	2.6

Table A.2. The Optimized Binary Parameters (C_{ij} and D_{ij}) of PR EOS with Summary Results for PR EOS Bubble-point Pressure Representations for the 916 Systems *(Continued)*

NO.	System	NDP	Case 2		Case 3		
			C_{ij}	%AAD	C_{ij}	D_{ij}	%AAD
109	hexafluorobenzene(1) + cyclohexane(2)	12	0.0660	1.0	0.0371	0.0341	1.0
110	toluene(1) + 4-methyl 2-pentanone(2)	28	-0.0107	1.9	0.0544	-0.0730	1.9
111	toluene(1) + 2-pentanone(2)	27	0.0038	0.6	0.0421	-0.0434	0.5
112	benzene(1) + acetone(2)	15	0.0288	0.8	-0.0018	0.0368	0.7
113	benzene(1) + 2-butanone(2)	9	0.0260	0.3	0.0249	0.0014	0.3
114	benzene(1) + thiophene(2)	12	-0.0017	0.7	0.0010	-0.0031	0.7
115	hexafluorobenzene(1) + diisopropyl ether(2)	29	0.0127	1.4	-0.0306	0.0511	1.4
116	tetrachloromethane(1) + 2-butanone(2)	14	0.0360	0.8	0.0820	-0.0552	0.8
117	cyclohexane(1) + 2-butanone(2)	23	0.0751	1.0	0.1215	-0.0567	1.0
118	n-heptane(1) + thiophene(2)	25	-0.0027	0.8	0.0373	-0.0448	0.8
119	n-heptane(1) + 3-pentanone(2)	17	0.0498	1.2	0.0637	-0.0167	1.2
120	n-heptane(1) + 2-butanone(2)	19	0.0753	2.5	0.0370	0.0470	2.5
121	n-decane(1) + acetone(2)	14	0.0743	3.7	0.0030	0.0865	1.5
122	tetrachloromethane(1) + furfural(2)	11	0.0793	6.6	0.1729	-0.1078	3.3
123	tetrachloromethane(1) + acetone(2)	29	0.0543	1.1	0.0575	-0.0048	1.0
124	benzene(1) + 1,2-dichloroethane(2)	17	0.0126	2.3	-0.0029	0.0184	2.3
125	toluene(1) + 1,2-dichloroethane(2)	13	0.0172	3.7	-0.0095	0.0317	3.7
126	benzene(1) + diethylamine(2)	15	-0.0163	1.4	-0.0121	-0.0048	1.4
127	benzene(1) + Triethylamine(2)	22	-0.0132	0.7	-0.0144	0.0014	0.7
128	ethylbenzene(1) + acrylonitrile(2)	10	0.0495	12.6	-0.0376	0.0958	12.6
129	toluene(1) + nitrobenzene(2)	8	0.0135	7.4	-0.0155	0.0300	7.4
130	n-heptane(1) + butylchloride(2)	15	0.0041	2.6	-0.0566	0.0704	2.4
131	cyclopentane(1) + chloroform(2)	14	0.0215	0.8	-0.0188	0.0470	0.6
132	n-heptane(1) + Triethylamine(2)	20	-0.0036	0.5	-0.0211	0.0203	0.5
133	2,3-dimethylbutane(1) + chloroform(2)	11	0.0107	0.4	-0.0073	0.0211	0.4
134	ethylbenzene(1) + nitrobenzene(2)	8	0.0171	7.7	0.0643	-0.0599	7.7
135	benzene(1) + nitromethane(2)	15	0.0451	1.8	0.0082	0.0421	1.8
136	benzene(1) + tertiary butyl alcohol(2)	13	0.0588	3.7	0.0732	-0.0102	3.6
137	benzene(1) + ethanol(2)	12	0.0917	2.9	0.0238	0.0816	2.9
138	benzene(1) + 2-propanol(2)	30	0.0929	1.2	0.0491	0.0540	1.2
139	n-heptane(1) + ethyl iodide(2)	18	-0.0261	5.3	-0.1013	0.0832	5.2
140	cyclohexane(1) + pyridine(2)	13	0.0522	0.9	0.0842	-0.0387	0.7
141	n-octane(1) + pyridine(2)	15	0.0184	2.0	0.1524	-0.1502	1.7
142	n-octane(1) + methanol(2)	13	-0.0100	21.6	0.0823	-0.0412	18.8
143	cyclohexane(1) + ethanol(2)	9	0.0863	7.2	0.2170	-0.1500	6.0
144	n-pentane(1) + 1-butanol(2)	15	0.0405	11.4	0.1874	-0.1444	7.4
145	tetrachloroethylene(1) + ethanol(2)	17	0.1229	6.9	-0.0903	0.2590	3.9

Table A.2. The Optimized Binary Parameters (C_{ij} and D_{ij}) of PR EOS with Summary Results for PR EOS Bubble-point Pressure Representations for the 916 Systems *(Continued)*

NO.	System	NDP	Case 2		Case 3		
			C_{ij}	%AAD	C_{ij}	D_{ij}	%AAD
146	hexafluorobenzene(1) + 1-propanol(2)	10	0.0557	8.0	-0.0025	0.0646	8.0
147	hexafluorobenzene(1) + methanol(2)	11	0.0321	10.2	-0.0146	0.0506	10.2
148	propionic aldehyde(1) + acetone(2)	15	0.0464	6.7	-0.0067	0.0644	6.7
149	propionic aldehyde(1) + 2-butanone(2)	15	0.0461	9.8	0.0848	-0.0457	9.7
150	acetone(1) + vinyl acetate(2)	11	0.0052	0.5	0.0118	-0.0078	0.5
151	acetone(1) + propyl acetate(2)	15	0.0175	2.4	0.0220	-0.0053	2.4
152	acetaldehyde(1) + vinyl acetate(2)	28	0.0119	3.5	0.0210	-0.0112	3.3
153	acetaldehyde(1) + methyl acetate(2)	19	0.0120	3.4	0.0396	-0.0328	3.1
154	diethyl ether(1) + acetone(2)	13	0.0355	1.0	0.0399	-0.0051	0.9
155	acetaldehyde(1) + diethyl ether(2)	12	0.0573	3.2	0.0310	0.0317	3.2
156	diethyl ether(1) + methyl iodide(2)	11	-0.0095	2.4	-0.0750	0.0758	2.0
157	diethyl ether(1) + dichloromethane(2)	27	-0.0685	1.6	-0.1461	0.0880	1.4
158	1,4-dioxane(1) + 2-propanol(2)	20	0.0248	1.2	0.1559	-0.1546	1.0
159	Ethyl propyl ether(1) + chloroform(2)	17	-0.0739	0.6	-0.1127	0.0434	0.6
160	diethyl ether(1) + chloroform(2)	10	-0.0941	1.3	-0.1013	0.0085	1.3
161	acetone(1) + chloroform(2)	11	-0.0597	0.9	-0.0323	-0.0307	0.9
162	propyl acetate(1) + 1-propanol(2)	11	0.0160	1.1	0.1255	-0.1269	0.8
163	ethyl acetate(1) + 2-propanol(2)	19	0.0257	1.6	0.1088	-0.0965	1.2
164	diethyl ether(1) + ethanol(2)	19	-0.0160	7.3	0.1228	-0.1451	2.5
165	furfural(1) + ethanol(2)	9	0.0761	7.8	-0.0107	0.0923	2.8
166	acetone(1) + methanol(2)	12	0.0047	0.8	0.1391	-0.1539	0.8
167	1,4-dioxane(1) + methanol(2)	16	0.0461	2.4	0.1367	-0.1015	2.4
168	ethanol(1) + Triethylamine(2)	12	-0.0448	1.9	0.1105	-0.1655	1.3
169	tertiary butyl alcohol(1) + 1-butanol(2)	11	-0.0480	8.0	-0.0399	-0.0091	8.0
170	1-propanol(1) + 2-methyl 1-propanol(2)	11	-0.0239	2.9	-0.0071	-0.0189	2.8
171	ethanol(1) + 2-propanol(2)	12	-0.0093	0.4	-0.0044	-0.0057	0.4
172	methanol(1) + 2-methyl 1-propanol(2)	11	-0.0045	4.9	0.0250	-0.0323	4.6
173	ethanol(1) + 2-methyl 1-propanol(2)	11	-0.0021	3.0	0.0132	-0.0152	2.8
174	butylamine(1) + 1-butanol(2)	10	-0.0598	7.2	0.0375	-0.1051	6.6
175	diethylamine(1) + ethanol(2)	11	-0.1127	3.6	-0.0343	-0.0849	3.6
176	butylamine(1) + 1-propanol(2)	11	-0.1064	3.9	0.0024	-0.1183	3.1
177	bromobenzene(1) + cyclohexanol(2)	11	0.0089	7.8	0.0125	-0.0042	7.8
178	1,2-dichloroethane(1) + 2-methyl 1-propanol(2)	11	0.0786	8.6	0.1308	-0.0608	8.0
179	methanol(1) + 1,2-dichloroethane(2)	11	0.1040	5.4	0.0936	0.0125	5.4
180	water(1) + diethylamine(2)	13	-0.3928	9.3	-0.2606	-0.1014	3.6
181	water(1) + pyridine(2)	19	-0.1108	2.7	-0.0640	-0.0448	2.3
182	water(1) + methanol(2)	21	-0.0737	2.0	0.0134	-0.0933	1.3

Table A.2. The Optimized Binary Parameters (C_{ij} and D_{ij}) of PR EOS with Summary Results for PR EOS Bubble-point Pressure Representations for the 916 Systems *(Continued)*

NO.	System	NDP	Case 2		Case 3		
			C_{ij}	%AAD	C_{ij}	D_{ij}	%AAD
183	water(1) + 2-propanol(2)	24	-0.1800	9.3	0.0297	-0.1818	3.5
184	water(1) + ethanol(2)	13	-0.1025	5.9	0.0391	-0.1376	2.0
185	acetaldehyde(1) + propylene oxide(2)	18	0.0270	4.0	0.0353	-0.0145	3.9
186	propionic aldehyde(1) + cyclohexane(2)	18	0.1375	8.7	0.1161	0.0260	8.7
187	chloroform(1) + furfural(2)	14	-0.0147	6.3	0.0397	-0.0585	4.6
188	1-butene(1) + furfural(2)	18	0.0343	6.0	0.0351	-0.0008	6.0
189	toluene(1) + furfural(2)	20	0.0334	2.9	0.0450	-0.0196	2.9
190	ethylbenzene(1) + furfural(2)	16	0.0420	3.3	0.0383	0.0044	3.3
191	p-xylene(1) + furfural(2)	20	0.0373	2.9	0.0614	-0.0283	2.8
192	n-pentane(1) + acetone(2)	49	0.0926	4.6	0.1568	-0.0750	3.6
193	furfural(1) + n-decane(2)	11	0.0407	6.4	0.1119	-0.0789	5.6
194	toluene(1) + benzaldehyde(2)	9	-0.0036	1.8	0.0107	-0.0162	1.6
195	benzaldehyde(1) + benzyl acetate(2)	7	0.0004	9.0	-0.0850	0.0976	8.6
196	acetone(1) + tetrachloromethane(2)	103	0.0586	1.6	0.0575	0.0014	1.6
197	carbondisulfide(1) + acetone(2)	10	0.0970	2.7	-0.0028	0.1195	2.3
198	acetone(1) + acetonitrile(2)	10	0.0065	1.1	-0.0222	0.0334	0.9
199	acetone(1) + 1,2-dichloroethane(2)	28	0.0034	2.1	0.0000	0.0042	2.1
200	acetone(1) + ethyl iodide(2)	6	0.0489	2.5	0.0503	-0.0017	2.5
201	methyl acetate(1) + acetone(2)	9	0.0112	0.3	0.0228	-0.0138	0.3
202	acetone(1) + methyl acetate(2)	56	0.0041	0.8	0.0228	-0.0218	0.7
203	acetone(1) + 2-butanone(2)	39	0.0006	1.3	0.0092	-0.0107	1.3
204	acetone(1) + ethyl acetate(2)	16	0.0081	0.6	0.0318	-0.0280	0.6
205	diethyl ether(1) + acetone(2)	7	0.0035	1.0	0.0078	-0.0051	1.0
206	acetone(1) + pyridine(2)	13	-0.0013	1.3	0.0247	-0.0291	1.1
207	Isoprene(1) + acetone(2)	11	0.0487	1.1	0.0775	-0.0351	1.0
208	2-methyl 2-butene(1) + acetone(2)	18	0.0805	3.3	0.1310	-0.0620	3.0
209	isopentane(1) + acetone(2)	17	0.1022	3.0	0.1353	-0.0414	2.7
210	acetone(1) + 1,1,2-trichloroethane(2)	21	-0.0209	3.2	0.0025	-0.0275	2.8
211	cyclohexane(1) + 4-methyl 2-pentanone(2)	47	0.0404	2.8	0.0886	-0.0539	2.4
212	benzene(1) + 4-methyl 2-pentanone(2)	63	-0.0170	2.0	0.0423	-0.0683	2.0
213	chloroform(1) + 4-methyl 2-pentanone(2)	14	-0.0761	2.0	0.0028	-0.0882	1.7
214	cyclohexane(1) + cyclohexanone(2)	27	0.0477	2.7	0.0937	-0.0520	1.9
215	n-heptane(1) + 3-pentanone(2)	51	0.0493	1.2	0.0637	-0.0172	1.2
216	3-pentanone(1) + 4-methyl 2-pentanone(2)	19	-0.0197	1.4	-0.0258	0.0071	1.4
217	ethyl acetate(1) + 3-pentanone(2)	11	0.0018	0.8	0.0049	-0.0037	0.8
218	methyl acetate(1) + 3-pentanone(2)	11	0.0285	1.4	0.0222	0.0075	1.4
219	2-butanone(1) + ethylbenzene(2)	57	0.0171	2.9	-0.0421	0.0662	2.9

Table A.2. The Optimized Binary Parameters (C_{ij} and D_{ij}) of PR EOS with Summary Results for PR EOS Bubble-point Pressure Representations for the 916 Systems *(Continued)*

NO.	System	NDP	Case 2		Case 3		
			C_{ij}	%AAD	C_{ij}	D_{ij}	%AAD
220	2-butanone(1) + n-octane(2)	9	0.0729	2.7	0.0253	0.0561	1.9
221	2-butanone(1) + n-heptane(2)	35	0.0750	3.3	0.0370	0.0462	3.2
222	2-butanone(1) + toluene(2)	96	0.0146	1.1	-0.0006	0.0179	1.0
223	2-butanone(1) + benzene(2)	74	0.0079	1.1	0.0171	-0.0110	1.1
224	benzene(1) + 2-butanone(2)	45	0.0033	0.7	0.0249	-0.0249	0.7
225	2-methyl 2-butene(1) + 2-butanone(2)	13	0.0551	1.2	0.1105	-0.0673	1.0
226	ethyl acetate(1) + 2-butanone(2)	14	0.0072	0.6	0.0138	-0.0078	0.6
227	chloroform(1) + 2-butanone(2)	18	-0.0636	0.8	-0.0304	-0.0382	0.7
228	acetone(1) + n-decane(2)	25	0.0732	3.5	-0.0021	0.0883	2.0
229	diethyl ether(1) + benzene(2)	57	-0.0274	2.1	-0.0124	-0.0172	2.1
230	diethyl ether(1) + hexafluorobenzene(2)	30	0.0118	0.8	-0.0686	0.0938	0.8
231	diethyl ether(1) + ethyl acetate(2)	33	-0.0070	1.2	-0.0165	0.0108	1.1
232	1,4-dioxane(1) + n-octane(2)	8	0.0315	2.0	-0.0151	0.0533	2.0
233	1,4-dioxane(1) + toluene(2)	51	0.0100	0.7	0.0145	-0.0052	0.7
234	n-heptane(1) + 1,4-dioxane(2)	12	0.0373	1.4	-0.0164	0.0623	1.4
235	benzene(1) + 1,4-dioxane(2)	118	-0.0034	1.9	0.0281	-0.0361	1.9
236	diethylamine(1) + 1,4-dioxane(2)	18	0.0055	1.5	-0.0128	0.0215	1.2
237	ethyl acetate(1) + 1,4-dioxane(2)	39	-0.0099	0.5	0.0097	-0.0229	0.5
238	carbondisulfide(1) + 1,4-dioxane(2)	13	0.0633	3.2	-0.0049	0.0766	2.3
239	tetrachloromethane(1) + 1,4-dioxane(2)	63	0.0019	1.9	0.0216	-0.0224	1.9
240	diisopropyl ether(1) + ethylbenzene(2)	40	-0.0080	0.8	0.0088	-0.0183	0.8
241	diisopropyl ether(1) + toluene(2)	39	-0.0142	0.5	0.0260	-0.0459	0.5
242	diisopropyl ether(1) + benzene(2)	59	-0.0178	1.7	0.0205	-0.0444	1.7
243	diisopropyl ether(1) + hexafluorobenzene(2)	32	0.0131	1.4	-0.0306	0.0511	1.4
244	chloroform(1) + diisopropyl ether(2)	86	-0.0913	1.8	-0.0926	0.0015	1.8
245	diisopropyl ether(1) + n-heptane(2)	18	0.0116	3.6	0.0157	-0.0099	3.5
246	acetaldehyde(1) + diethyl ether(2)	10	0.0573	2.6	0.0259	0.0378	2.6
247	propionic aldehyde(1) + methyl acetate(2)	30	0.0497	8.6	0.0804	-0.0365	8.6
248	propionic aldehyde(1) + ethyl acetate(2)	36	0.0410	10.4	0.0727	-0.0368	10.2
249	propionic aldehyde(1) + benzene(2)	15	0.0511	11.8	-0.0177	0.0795	11.8
250	n-pentane(1) + propionic aldehyde(2)	26	0.1193	3.5	0.1302	-0.0133	3.5
251	Isoprene(1) + butyraldehyde(2)	10	0.0474	1.5	0.0461	0.0019	1.5
252	dichloromethane(1) + furfural(2)	21	-0.0090	1.6	-0.0273	0.0204	1.3
253	1,2-dichloroethane(1) + furfural(2)	21	0.0122	3.0	0.0226	-0.0122	2.7
254	acetone(1) + furfural(2)	12	-0.0079	1.3	-0.0212	0.0198	1.1
255	ethyl acetate(1) + furfural(2)	12	-0.0290	1.3	-0.0110	-0.0205	1.3
256	butane(1) + furfural(2)	19	0.0586	1.5	0.0775	-0.0158	1.5

Table A.2. The Optimized Binary Parameters (C_{ij} and D_{ij}) of PR EOS with Summary Results for PR EOS Bubble-point Pressure Representations for the 916 Systems *(Continued)*

NO.	System	NDP	Case 2		Case 3		
			C_{ij}	%AAD	C_{ij}	D_{ij}	%AAD
257	4-methyl 2-pentanone(1) + furfural(2)	19	-0.0347	2.9	-0.0144	-0.0223	2.9
258	tetrachloroethylene(1) + furfural(2)	26	0.0650	2.1	0.0817	-0.0201	1.8
259	ethylbenzene(1) + benzaldehyde(2)	54	0.0118	1.1	0.0226	-0.0124	1.0
260	diethyl ether(1) + tetrachloromethane(2)	69	-0.0218	1.0	-0.0302	0.0097	1.0
261	diethyl ether(1) + cyclohexane(2)	16	0.0120	2.2	0.0321	-0.0235	2.2
262	diethyl ether(1) + toluene(2)	21	0.0271	5.1	-0.0155	0.0464	5.0
263	isopentane(1) + diethyl ether(2)	19	0.0107	0.7	0.0286	-0.0213	0.7
264	methyl teritiary butyl ether(1) + tetrachloromethane(2)	20	-0.0250	2.0	-0.0284	0.0041	1.9
265	methyl teritiary butyl ether(1) + chloroform(2)	32	-0.1044	2.8	-0.1111	0.0073	2.8
266	methyl teritiary butyl ether(1) + methyl acetate(2)	59	0.0206	0.9	0.0245	-0.0048	0.9
267	methyl teritiary butyl ether(1) + ethyl acetate(2)	33	0.0118	0.6	-0.0056	0.0215	0.5
268	methyl teritiary butyl ether(1) + benzene(2)	83	-0.0199	1.5	0.0105	-0.0354	1.5
269	methyl teritiary butyl ether(1) + cyclohexane(2)	26	0.0031	1.9	0.0378	-0.0408	1.9
270	methyl teritiary butyl ether(1) + diisopropyl ether(2)	14	-0.0075	1.2	-0.0391	0.0375	1.2
271	methyl teritiary butyl ether(1) + toluene(2)	41	-0.0063	1.3	0.0015	-0.0091	1.3
272	methyl teritiary butyl ether(1) + n-heptane(2)	74	0.0034	2.4	0.0009	0.0028	2.4
273	dichloromethane(1) + methyl teritiary butyl ether(2)	22	-0.0718	2.5	-0.1436	0.0799	2.5
274	butane(1) + methyl teritiary butyl ether(2)	30	0.0147	1.0	-0.0005	0.0180	1.0
275	Isoprene(1) + methyl teritiary butyl ether(2)	13	-0.0040	1.5	-0.0079	0.0046	1.5
276	2-methyl 2-butene(1)+methyl teritiary butyl ether(2)	13	0.0023	0.9	0.0091	-0.0082	0.9
277	isopentane(1) + methyl teritiary butyl ether(2)	27	0.0102	1.7	0.0369	-0.0319	1.6
278	isopentane(1) + ethyl teritiary butyl ether(2)	40	0.0074	2.6	0.0253	-0.0213	2.5
279	ethyl teritiary butyl ether(1) + toluene(2)	26	-0.0186	2.1	0.0264	-0.0501	2.1
280	ethyl teritiary butyl ether(1) + n-octane(2)	20	0.0014	2.7	0.0173	-0.0178	2.7
281	dimethyl ether(1) + methylamine(2)	21	0.0178	1.8	0.0391	-0.0257	1.7
282	dimethyl ether(1) + butane(2)	35	0.0427	0.8	0.0056	0.0462	0.6
283	dimethyl ether(1) + methyl teritiary butyl ether(2)	8	0.0017	1.6	0.0140	-0.0130	1.6
284	chloroform(1) + benzene(2)	22	-0.0173	3.4	-0.0124	-0.0056	3.4
285	carbondisulfide(1) + benzene(2)	11	0.0013	0.5	-0.0039	0.0062	0.5
286	butylamine(1) + benzene(2)	29	0.0025	2.0	0.0668	-0.0745	1.9
287	diethylamine(1) + benzene(2)	46	-0.0147	2.6	-0.0121	-0.0030	2.6
288	benzene(1) + acetonitrile(2)	131	0.0583	4.3	0.0318	0.0480	3.9
289	benzene(1) + pyridine(2)	75	-0.0019	3.5	0.0199	-0.0272	3.3
290	benzene(1) + hexafluorobenzene(2)	109	-0.0248	2.8	-0.0748	0.0569	2.8
291	benzene(1) + bromobenzene(2)	49	-0.0086	3.2	-0.0058	-0.0032	3.2
292	benzene(1) + nitrobenzene(2)	27	-0.0053	6.4	-0.0292	0.0352	6.1

Table A.2. The Optimized Binary Parameters (C_{ij} and D_{ij}) of PR EOS with Summary Results for PR EOS Bubble-point Pressure Representations for the 916 Systems *(Continued)*

NO.	System	NDP	Case 2		Case 3		
			C_{ij}	%AAD	C_{ij}	D_{ij}	%AAD
293	benzene(1) + ethylbenzene(2)	13	-0.0051	1.1	-0.0760	0.0840	1.1
294	benzene(1) + p-xylene(2)	26	-0.0052	0.9	-0.0444	0.0457	0.8
295	toluene(1) + nitroethane(2)	14	0.0481	2.7	-0.0003	0.0559	2.5
296	toluene(1) + ethylenediamine(2)	29	0.0841	1.6	0.1174	-0.0397	1.6
297	toluene(1) + pyridine(2)	84	-0.0020	2.9	-0.0199	0.0191	2.9
298	chloroform(1) + toluene(2)	36	-0.0218	1.5	-0.0280	0.0073	1.5
299	carbondisulfide(1) + toluene(2)	74	-0.0012	3.7	-0.0972	0.1064	2.6
300	acetonitrile(1) + toluene(2)	77	0.0778	1.9	0.0252	0.0624	1.8
301	1,2-dichloroethane(1) + toluene(2)	78	0.0108	3.8	-0.0165	0.0317	3.8
302	tetrachloromethane(1) + ethylbenzene(2)	84	-0.0061	2.1	-0.0297	0.0268	2.0
303	acetonitrile(1) + ethylbenzene(2)	15	0.0842	1.5	0.0010	0.0995	1.2
304	diethylamine(1) + ethylbenzene(2)	8	-0.0111	4.3	-0.0722	0.0673	4.3
305	tetrachloromethane(1) + p-xylene(2)	42	-0.0158	4.9	0.0123	-0.0307	4.9
306	acetonitrile(1) + p-xylene(2)	21	0.0854	1.7	0.0279	0.0679	1.5
307	1,2-dichloroethane(1) + p-xylene(2)	13	0.0130	6.4	-0.0409	0.0553	6.4
308	acetaldehyde(1) + toluene(2)	14	-0.1326	3.9	-0.2235	0.1009	3.5
309	butyraldehyde(1) + toluene(2)	15	0.0274	3.8	-0.0110	0.0460	3.8
310	2-methyl 1-butene(1) + acetone(2)	11	0.0769	1.4	0.0856	-0.0108	1.4
311	propylene oxide(1) + acetone(2)	38	0.0033	1.0	0.0316	-0.0338	0.9
312	3-hexanone(1) + 4-heptanone(2)	17	-0.0123	1.0	-0.0620	0.0590	1.0
313	toluene(1) + cyclohexanone(2)	10	-0.0594	12.6	0.0589	-0.1147	11.7
314	hexane(1) + 3-pentanone(2)	11	0.0505	3.4	0.1300	-0.0955	2.3
315	3-pentanone(1) + 4-heptanone(2)	12	-0.0246	1.3	-0.0717	0.0554	1.3
316	hexane(1) + 2-butanone(2)	21	0.0694	2.4	0.1465	-0.0931	2.0
317	hexane(1) + 1,4-dioxane(2)	21	0.0440	2.0	0.0964	-0.0614	1.1
318	acetaldehyde(1) + acetone(2)	56	0.0114	4.6	0.0379	-0.0313	4.4
319	propylene oxide(1) + propionic aldehyde(2)	13	0.0469	5.9	0.0230	0.0299	5.8
320	methyl acetate(1) + butyraldehyde(2)	34	0.0238	3.7	-0.0084	0.0382	3.5
321	butyraldehyde(1) + propyl acetate(2)	28	0.0232	5.5	-0.0216	0.0517	5.5
322	butyraldehyde(1) + benzene(2)	49	0.0175	4.5	-0.0834	0.1188	4.5
323	butyraldehyde(1) + n-heptane(2)	63	0.0847	4.7	0.0528	0.0376	4.7
324	ethyl teritiary butyl ether(1) + n-heptane(2)	26	0.0377	4.5	0.0472	-0.0117	4.5
325	1,3-butadiene(1) + N,N-dimethylformide(2)	11	0.0478	5.5	0.0876	-0.0418	3.6
326	1,3-butadiene(1) + vinylacetylene(2)	8	-0.0189	0.5	0.0177	-0.0464	0.5
327	hexane(1) + 2,4-Dimethylpyridine(2)	52	0.0804	5.2	0.0774	0.0037	5.2
328	2,4-Dimethylpyridine(1) + n-octane(2)	60	0.2100	36.3	0.2464	-0.0404	35.8
329	2methyl 2butene(1)+N,N-dimethylformide(2)	11	0.0813	5.3	0.1326	-0.0530	3.0

Table A.2. The Optimized Binary Parameters (C_{ij} and D_{ij}) of PR EOS with Summary Results for PR EOS Bubble-point Pressure Representations for the 916 Systems *(Continued)*

NO.	System	NDP	Case 2		Case 3		
			C_{ij}	%AAD	C_{ij}	D_{ij}	%AAD
330	isopentane(1) + hexane(2)	34	0.0000	0.4	-0.0401	0.0478	0.4
331	isopentane(1) + N,N-dimethylformide(2)	24	0.0941	7.6	0.1216	-0.0296	7.4
332	isopentane(1) + toluene(2)	20	0.0132	3.3	-0.0115	0.0223	3.3
333	cis, 2-butene(1) + N,N-dimethylformide(2)	11	0.0988	4.9	0.1157	-0.0189	3.8
334	cis, 2-butene(1) + vinylacetylene(2)	11	0.0065	0.6	0.0206	-0.0172	0.5
335	cyclopentane(1) + cyclooctane(2)	36	-0.0046	0.9	-0.0146	0.0106	0.9
336	cyclopentane(1) + N,N-dimethylformide(2)	9	0.1172	3.8	0.1298	-0.0147	3.8
337	1-chloropropane(1) + cyclohexane(2)	26	0.0273	1.2	0.0628	-0.0421	0.9
338	cyclohexane(1) + chlorobenzene(2)	28	0.0201	0.7	0.0284	-0.0095	0.7
339	cyclohexane(1) + cycloheptane(2)	13	-0.0136	2.3	-0.0823	0.0793	1.9
340	cyclohexane(1) + cyclooctane(2)	13	-0.0072	1.7	-0.0280	0.0224	1.5
341	cyclohexane(1) + n-heptane(2)	108	-0.0155	3.5	-0.0565	0.0495	3.3
342	hexane(1) + cyclohexane(2)	150	-0.0089	1.3	-0.0449	0.0408	1.3
343	methyl cyclopentane(1) + cyclohexane(2)	5	-0.0059	0.8	-0.0149	0.0108	0.8
344	cyclohexane(1) + methyl cyclohexane(2)	15	-0.0125	2.0	-0.0507	0.0433	2.0
345	cyclohexane(1) + nitroethane(2)	45	0.1089	4.3	0.1782	-0.0783	3.8
346	cyclohexane(1) + nitromethane(2)	30	0.1312	3.0	0.2088	-0.0821	2.4
347	cyclohexane(1) + N,N-dimethylformide(2)	56	0.1168	5.7	0.1453	-0.0315	4.9
348	cyclohexane(1) + n-octane(2)	61	-0.0170	2.4	-0.0650	0.0528	2.1
349	acetonitrile(1) + methyl cyclohexane(2)	14	0.1671	6.0	0.1043	0.0783	5.5
350	benzene(1) + methyl cyclohexane(2)	52	0.0095	1.4	0.0445	-0.0398	1.4
351	methyl cyclohexane(1) + ethylbenzene(2)	47	0.0083	1.6	0.0287	-0.0228	1.6
352	n-heptane(1) + methyl cyclohexane(2)	14	-0.0095	0.4	-0.0200	0.0118	0.4
353	methyl cyclohexane(1) + p-xylene(2)	46	0.0088	1.5	0.0036	0.0060	1.4
354	methyl cyclohexane(1) + toluene(2)	56	0.0080	1.2	0.0339	-0.0294	1.2
355	benzene(1) + n-decane(2)	43	-0.0203	1.9	0.0084	-0.0316	1.9
356	carbondisulfide(1) + n-decane(2)	10	-0.0649	0.6	-0.0631	-0.0015	0.6
357	hexane(1) + n-decane(2)	12	-0.0028	0.4	-0.0500	0.0479	0.4
358	butane(1) + ethylamine(2)	104	0.0470	5.9	0.0821	-0.0392	5.3
359	butane(1) + N,N-dimethylformide(2)	5	0.1262	4.2	0.1347	-0.0081	4.2
360	n-pentane(1) + benzene(2)	15	0.0118	1.0	0.0209	-0.0106	1.0
361	1-pentene(1) + n-pentane(2)	53	0.0103	0.8	-0.0124	0.0266	0.8
362	hexane(1) + benzene(2)	109	0.0048	1.1	0.0538	-0.0565	1.1
363	hexane(1) + chlorobenzene(2)	55	0.0045	2.2	0.0443	-0.0470	2.2
364	carbondisulfide(1) + hexane(2)	13	-0.0325	0.3	-0.0532	0.0224	0.3
365	hexane(1) + nitrobenzene(2)	22	-0.0065	10.9	0.0900	-0.1030	3.8
366	hexane(1) + N,N-dimethylformide(2)	16	0.1246	4.4	0.1668	-0.0442	4.4

Table A.2. The Optimized Binary Parameters (C_{ij} and D_{ij}) of PR EOS with Summary Results for PR EOS Bubble-point Pressure Representations for the 916 Systems *(Continued)*

NO.	System	NDP	Case 2		Case 3		
			C_{ij}	%AAD	C_{ij}	D_{ij}	%AAD
367	hexane(1) + n-octane(2)	24	-0.0202	4.1	-0.1082	0.1017	3.7
368	1,2-dichloroethane(1) + n-heptane(2)	47	0.0527	1.9	-0.0476	0.1151	1.6
369	1-heptene(1) + n-heptane(2)	40	0.0131	2.0	0.0063	0.0052	1.9
370	benzene(1) + n-heptane(2)	96	0.0000	1.3	0.0427	-0.0488	1.2
371	n-heptane(1) + N,N-dimethylformide(2)	18	0.1010	3.5	0.0801	0.0218	3.5
372	n-heptane(1) + m-xylene(2)	29	0.0050	0.5	0.0021	0.0033	0.5
373	n-heptane(1) + toluene(2)	162	0.0010	1.2	0.0462	-0.0509	1.1
374	trans, 2-butene(1) + vinylacetylene(2)	11	0.0039	0.7	0.0220	-0.0287	0.7
375	1-propanol(1) + 1-butanol(2)	33	-0.0263	6.2	-0.0265	0.0002	6.2
376	benzene(1) + 1-propanol(2)	54	0.0853	1.8	0.0667	0.0229	1.8
377	chloroform(1) + 1-propanol(2)	21	0.0397	7.2	0.0964	-0.0641	6.1
378	carbondisulfide(1) + 1-propanol(2)	15	0.0863	4.8	0.0426	0.0459	4.8
379	cyclohexane(1) + 1-propanol(2)	23	0.1057	3.9	0.2191	-0.1396	3.0
380	butane(1) + 1-propanol(2)	12	0.0871	8.0	0.1797	-0.1339	2.7
381	hexane(1) + 1-propanol(2)	32	0.0392	11.9	0.2246	-0.2024	6.6
382	1-propanol(1) + n-heptane(2)	21	0.0780	5.9	0.1491	-0.0817	5.5
383	1-propanol(1) + p-xylene(2)	10	0.0589	7.9	-0.0180	0.0885	7.3
384	1-propanol(1) + toluene(2)	11	0.0734	4.2	0.0161	0.0670	4.1
385	ethanol(1) + 1-butanol(2)	72	-0.0083	3.1	0.0163	-0.0279	2.8
386	ethanol(1) + 1-propanol(2)	16	-0.0130	4.3	0.0025	-0.0174	4.3
387	ethanol(1) + 2-butanone(2)	14	0.0242	1.6	0.1416	-0.1311	1.4
388	acetone(1) + ethanol(2)	11	0.0197	0.4	0.1040	-0.1028	0.4
389	ethanol(1) + n-decane(2)	15	0.0388	3.6	0.0605	-0.0250	3.6
390	hexane(1) + ethanol(2)	55	0.0443	12.0	0.2093	-0.1763	8.3
391	ethanol(1) + n-octane(2)	24	0.0461	9.0	0.0967	-0.0565	9.0
392	ethanol(1) + toluene(2)	90	0.0946	5.5	0.0014	0.0923	4.7
393	methanol(1) + 1-butanol(2)	25	-0.0107	9.3	0.0135	-0.0262	8.9
394	methanol(1) + 1-propanol(2)	33	-0.0018	4.4	0.0046	-0.0073	4.4
395	methanol(1) + benzene(2)	162	0.0989	8.4	-0.0137	0.1345	8.3
396	carbondisulfide(1) + methanol(2)	16	0.1490	9.4	0.0447	0.1236	9.4
397	methanol(1) + cyclohexane(2)	41	0.0751	16.8	0.1771	-0.1114	16.2
398	diethyl ether(1) + methanol(2)	79	-0.0277	7.0	0.1878	-0.2289	3.5
399	methanol(1) + hexane(2)	121	0.0150	14.1	0.1553	-0.1424	12.2
400	methanol(1) + toluene(2)	21	0.1559	8.9	-0.0558	0.2258	6.7
401	methanol(1) + vinyl acetate(2)	29	0.0401	2.9	0.0996	-0.0708	2.9
402	butane(1) + 2-butanone(2)	3	0.0637	5.6	0.1095	-0.0512	3.4
403	2-butanone(1) + p-xylene(2)	61	0.0262	2.6	-0.0134	0.0469	2.6

Table A.2. The Optimized Binary Parameters (C_{ij} and D_{ij}) of PR EOS with Summary Results for PR EOS Bubble-point Pressure Representations for the 916 Systems *(Continued)*

NO.	System	NDP	Case 2		Case 3		
			C_{ij}	%AAD	C_{ij}	D_{ij}	%AAD
404	vinyl acetate(1) + 2-butanone(2)	20	-0.0060	2.0	-0.0013	-0.0056	2.0
405	cyclohexane(1) + 3-pentanone(2)	19	0.0560	1.8	0.1030	-0.0549	1.8
406	hexane(1) + 4-heptanone(2)	6	0.0260	2.7	0.0133	0.0153	2.7
407	acetone(1) + cyclohexane(2)	48	0.1040	2.1	0.1288	-0.0302	2.1
408	acetone(1) + hexane(2)	66	0.0997	4.1	0.1479	-0.0581	4.0
409	acetone(1) + n-heptane(2)	34	0.0963	4.4	0.0326	0.0751	3.8
410	acetone(1) + n-octane(2)	21	0.1005	6.8	0.0214	0.0924	4.5
411	acetone(1) + toluene(2)	11	0.0475	3.5	-0.0364	0.1025	1.9
412	p-xylene(1) + cyclohexanone(2)	34	-0.0764	15.0	-0.0132	-0.0710	15.0
413	acetaldehyde(1) + 1-pentene(2)	16	0.0926	3.0	0.0808	0.0151	3.0
414	butyraldehyde(1) + 2-butanone(2)	40	0.0239	4.5	-0.0541	0.0932	4.5
415	n-octane(1) + furfural(2)	13	0.0292	12.2	0.1087	-0.0873	10.1
416	propionic aldehyde(1) + toluene(2)	9	0.1293	15.0	-0.0587	0.2597	14.6
417	2-methyl 2-butene(1) + 1-Pentyne(2)	9	-0.0017	1.9	-0.0054	0.0044	1.9
418	cyclohexane(1) + Fluorobenzene(2)	30	0.0322	0.4	0.0653	-0.0397	0.4
419	hexane(1) + Triethylamine(2)	9	0.0159	1.5	-0.0402	0.0645	1.3
420	Triethylamine(1) + n-octane(2)	8	0.0112	1.1	-0.0148	0.0295	1.0
421	acetaldehyde(1) + Isoprene(2)	11	0.0624	2.4	0.0596	0.0034	2.4
422	Isoprene(1) + Isobutyr Aldehyde(2)	10	0.0381	2.1	0.0410	-0.0033	2.1
423	Isoprene(1) + Crotonaldehyde(2)	13	0.0459	1.6	0.0800	-0.0411	1.6
424	Isobutyr Aldehyde(1) + n-heptane(2)	37	0.0752	3.3	0.0350	0.0481	3.1
425	butyraldehyde(1) + cyclohexane(2)	16	0.0863	3.4	0.1149	-0.0340	3.4
426	methanol(1) + tetrachloromethane(2)	22	0.0595	8.9	0.0034	0.0612	8.9
427	dichloromethane(1) + methanol(2)	11	0.0721	5.5	0.0031	0.0814	5.5
428	Dimethylamine(1) + methanol(2)	4	-0.1624	0.5	-0.1335	-0.0659	0.3
429	carbondisulfide(1) + Isobutyl chloride(2)	9	0.0097	1.1	-0.0569	0.0749	0.9
430	methyl iodide(1) + carbondisulfide(2)	19	0.0387	2.4	-0.0145	0.0628	2.4
431	carbondisulfide(1) + tetrachloroethylene(2)	35	0.0140	1.2	-0.0244	0.0417	1.2
432	carbondisulfide(1) + nitromethane(2)	7	0.1462	10.9	0.0515	0.1098	8.9
433	acetonitrile(1) + chlorobenzene(2)	81	0.0752	2.8	-0.0343	0.1260	2.8
434	chlorobenzene(1) + bromobenzene(2)	10	-0.0028	0.4	0.0364	-0.0456	0.4
435	butylamine(1) + chlorobenzene(2)	42	0.0087	0.9	0.0133	-0.0053	0.9
436	chloroform(1) + chlorobenzene(2)	17	0.0026	2.3	-0.0177	0.0228	2.3
437	butylchloride(1) + chlorobenzene(2)	45	-0.0192	4.5	-0.0182	-0.0011	4.5
438	chlorobenzene(1) + Cyclohexaylamine(2)	22	0.0078	1.4	-0.0111	0.0222	1.4
439	chlorobenzene(1) + 1,2-Dibromoethane(2)	12	0.1066	9.6	0.0338	0.0810	9.6
440	diethylamine(1) + chlorobenzene(2)	43	-0.0163	2.4	-0.0333	0.0194	2.2

Table A.2. The Optimized Binary Parameters (C_{ij} and D_{ij}) of PR EOS with Summary Results for PR EOS Bubble-point Pressure Representations for the 916 Systems *(Continued)*

NO.	System	NDP	Case 2		Case 3		
			C_{ij}	%AAD	C_{ij}	D_{ij}	%AAD
441	1-Nitropropane(1) + chlorobenzene(2)	16	0.0338	1.9	-0.0488	0.0967	1.6
442	Triethylamine(1) + chlorobenzene(2)	44	-0.0151	0.8	0.0056	-0.0238	0.6
443	chloroform(1) + acetonitrile(2)	49	0.0233	0.9	-0.0090	0.0383	0.8
444	dichloromethane(1) + chloroform(2)	39	-0.0019	1.0	-0.0704	0.0803	0.9
445	chloroform(1) + 2-Methylpyridine(2)	20	-0.1461	18.2	-0.0918	-0.0562	17.9
446	chloroform(1) + Methyl ethyl sulfide(2)	10	-0.0585	1.9	-0.0531	-0.0062	1.9
447	chloroform(1) + tetrachloroethylene(2)	16	0.0204	2.5	0.0091	0.0130	2.5
448	Hydrogen cyanide(1) + 3-Chloro-1-propene(2)	22	0.1014	3.1	-0.0596	0.1946	2.7
449	Isopropyl chloride(1) + 3-Chloro-1-propene(2)	17	-0.0208	2.3	-0.0065	-0.0167	2.3
450	tetrachloromethane(1) + 1,2-Dibromoethane(2)	29	-0.0087	19.0	0.0530	-0.0658	19.0
451	acetonitrile(1) + 1,2-dichloroethane(2)	21	0.0407	1.7	-0.0077	0.0573	1.6
452	dichloromethane(1) + 1,2-dichloroethane(2)	24	0.0057	3.0	-0.0546	0.0674	2.4
453	1,2-dichloroethane(1) + tetrachloroethylene(2)	16	0.0517	2.4	0.0409	0.0129	2.4
454	Vinyl chloride(1) + 1,2-dichloroethane(2)	17	-0.0236	3.0	-0.0329	0.0099	3.0
455	1,1-Dichloroethylene(1) + acrylonitrile(2)	11	0.0496	5.0	0.0700	-0.0244	4.7
456	Vinyl chloride(1) + 1,1-Dichloroethylene(2)	11	-0.0035	1.0	-0.0064	0.0034	0.9
457	dichloromethane(1) + acetonitrile(2)	45	0.0154	2.3	-0.0503	0.0764	2.3
458	dichloromethane(1) + Dibromomethane(2)	25	-0.0574	14.2	0.0479	-0.1202	12.9
459	dichloromethane(1) + pyridine(2)	25	-0.0372	1.4	-0.0508	0.0152	1.3
460	dichloromethane(1) + methyl iodide(2)	11	0.0160	2.3	-0.0584	0.0847	2.1
461	dichloromethane(1) + tetrachloroethylene(2)	10	0.0265	0.6	-0.0453	0.0791	0.6
462	dichloromethane(1) + Triethylamine(2)	9	-0.0500	2.1	-0.1125	0.0669	2.1
463	water(1) + 2-Methylpyridine(2)	22	-0.2731	20.0	-0.1490	-0.0969	20.0
464	water(1) + cyclohexanone(2)	5	-0.2083	10.1	0.0126	-0.1931	9.4
465	diisopropyl ether(1) + water(2)	13	-0.4367	12.9	-0.0369	-0.2579	12.2
466	Triethylamine(1) + water(2)	16	-0.4695	27.1	-0.1201	-0.2328	10.7
467	water(1) + 2,4-Dimethylpyridine(2)	6	-0.2231	7.6	-0.1043	-0.1000	7.1
468	ethylamine(1) + water(2)	24	-0.3132	10.0	-0.2609	-0.0480	10.0
469	water(1) + ethylenediamine(2)	10	-0.2215	4.5	0.0135	-0.2312	3.5
470	water(1) + Ethylbutylamine(2)	34	-0.5000	67.8	-0.3144	-0.2022	67.8
471	Hydrogen cyanide(1) + water(2)	37	-0.2164	19.4	-0.0373	-0.1465	5.9
472	Isobutyr Aldehyde(1) + water(2)	7	-0.0900	13.0	0.0081	0.0090	2.9
473	Isopropylamine(1) + water(2)	16	-0.3146	6.0	-0.2599	-0.0475	6.0
474	water(1) + Isopropylbenzene(2)	9	-0.2909	19.7	-0.2149	-0.0586	19.6
475	Propylamine(1) + water(2)	8	-0.2697	3.3	-0.1855	-0.0881	2.1
476	Ethyl Bromide(1) + benzene(2)	9	-0.0129	0.4	0.0116	-0.0285	0.4
477	ethyl iodide(1) + benzene(2)	4	0.0159	1.5	-0.0104	0.0298	1.5

Table A.2. The Optimized Binary Parameters (C_{ij} and D_{ij}) of PR EOS with Summary Results for PR EOS Bubble-point Pressure Representations for the 916 Systems *(Continued)*

NO.	System	NDP	Case 2		Case 3		
			C_{ij}	%AAD	C_{ij}	D_{ij}	%AAD
478	benzene(1) + Fluorobenzene(2)	11	0.0032	0.3	0.0267	-0.0278	0.3
479	benzene(1) + Isopropylbenzene(2)	9	-0.0042	0.8	-0.0429	0.0457	0.8
480	methyl mercaptan(1) + benzene(2)	22	0.0120	2.5	-0.0014	0.0155	2.5
481	methyl iodide(1) + benzene(2)	13	0.0129	3.9	0.0010	0.0134	3.9
482	benzene(1) + nitroethane(2)	12	0.0360	4.9	-0.0193	0.0622	3.9
483	benzene(1) + 1-Nitropropane(2)	9	0.0247	8.3	0.0356	-0.0127	8.0
484	benzene(1) + tetrachloroethylene(2)	21	0.0052	1.4	-0.0040	0.0113	1.4
485	chlorobenzene(1) + ethylbenzene(2)	13	-0.0106	1.4	-0.0585	0.0524	1.4
486	1,2-dichloroethane(1) + ethylbenzene(2)	17	0.0105	3.7	-0.0518	0.0728	3.7
487	ethylbenzene(1) + Isopropylbenzene(2)	18	-0.0029	0.4	-0.0542	0.0612	0.4
488	tetrachloromethane(1) + Isopropylbenzene(2)	21	-0.0148	1.3	-0.0005	-0.0154	1.3
489	toluene(1) + bromobenzene(2)	12	-0.0128	1.9	-0.0125	-0.0003	1.9
490	toluene(1) + chlorobenzene(2)	23	-0.0099	0.8	-0.0085	-0.0018	0.8
491	diethylamine(1) + toluene(2)	10	-0.0135	3.7	-0.0305	0.0195	3.5
492	toluene(1) + Dimethyl sulfoxide(2)	11	0.0447	7.4	-0.0074	0.0549	7.4
493	toluene(1) + ethylbenzene(2)	6	0.0105	2.5	-0.0522	0.0699	2.1
494	toluene(1) + 2-Methylpyridine(2)	13	-0.0327	8.5	0.0155	-0.0561	8.5
495	chlorobenzene(1) + p-xylene(2)	20	-0.0104	0.5	-0.0147	0.0050	0.5
496	p-xylene(1) + N,N-dimethylformide(2)	14	0.0712	1.6	0.0267	0.0562	1.6
497	methyl iodide(1) + tetrachloromethane(2)	14	0.0178	3.3	0.0989	-0.0915	2.9
498	methylamine(1) + tetrachloromethane(2)	66	0.0244	6.9	-0.0759	0.1049	3.3
499	tetrachloromethane(1) + tetrachloroethylene(2)	33	-0.0110	1.7	0.0369	-0.0548	1.3
500	tetrachloromethane(1) + Trichloethylene(2)	36	-0.0117	1.3	0.1002	-0.1307	1.2
501	tetrachloromethane(1) + acetonitrile(2)	58	0.1223	2.6	0.0566	0.0813	2.6
502	ethyl iodide(1) + tetrachloromethane(2)	13	-0.0127	1.2	0.0917	-0.1191	1.2
503	tetrachloromethane(1) + nitroethane(2)	22	0.0600	4.3	0.0612	-0.0018	4.3
504	tetrachloromethane(1) + Dimethyl sulfoxide(2)	42	0.0463	7.7	0.0360	0.0103	7.7
505	tetrachloromethane(1) + acrylonitrile(2)	30	0.1013	1.9	0.1358	-0.0417	1.8
506	tetrachloromethane(1) + thiophene(2)	12	0.0048	0.4	0.0913	-0.1006	0.3
507	diethylamine(1) + tetrachloromethane(2)	39	-0.0403	3.7	-0.0420	0.0021	3.7
508	tetrachloromethane(1) + nitrobenzene(2)	14	0.0262	1.7	0.0333	-0.0069	1.5
509	tetrachloromethane(1) + Triethylamine(2)	22	-0.0377	1.1	-0.0782	0.0446	1.1
510	Tribromomethane(1) + Dimethyl sulfoxide(2)	14	-0.0747	17.6	-0.1471	0.0756	16.7
511	pyridine(1) + Tribromomethane(2)	29	-0.0674	9.0	-0.0792	0.0127	9.0
512	methyl iodide(1) + chloroform(2)	25	0.0096	3.0	0.0176	-0.0092	3.0
513	chloroform(1) + Triethylamine(2)	11	-0.1153	5.9	-0.0230	-0.0974	5.3
514	Dibromomethane(1) + Dimethyl sulfoxide(2)	39	-0.1049	42.7	-0.2179	0.1330	34.2

Table A.2. The Optimized Binary Parameters (C_{ij} and D_{ij}) of PR EOS with Summary Results for PR EOS Bubble-point Pressure Representations for the 916 Systems *(Continued)*

NO.	System	NDP	Case 2		Case 3		
			C_{ij}	%AAD	C_{ij}	D_{ij}	%AAD
515	tetrachloromethane(1) + nitromethane(2)	12	0.0946	4.9	0.1096	-0.0172	4.6
516	Trichloethylene(1) + nitromethane(2)	11	0.0848	1.9	0.0491	0.0483	1.9
517	acetonitrile(1) + nitromethane(2)	55	-0.0147	4.3	-0.0123	-0.0028	4.3
518	ethyl iodide(1) + nitromethane(2)	17	0.0736	3.7	0.0745	-0.0011	3.7
519	nitromethane(1) + nitroethane(2)	28	0.0139	4.4	-0.0384	0.0601	4.2
520	nitromethane(1) + N,N-dimethylformide(2)	17	-0.0514	5.2	0.0571	-0.1158	4.6
521	thiophene(1) + nitromethane(2)	11	0.0502	1.3	0.0609	-0.0124	1.3
522	butylchloride(1) + nitromethane(2)	45	0.0320	4.3	0.1213	-0.1003	3.8
523	nitromethane(1) + Glutaronitrile(2)	4	-0.0078	2.6	-0.0172	0.0113	2.3
524	nitromethane(1) + chlorobenzene(2)	45	0.0567	4.0	-0.0824	0.1600	3.3
525	nitromethane(1) + nitrobenzene(2)	9	0.0145	3.4	-0.0757	0.1018	2.9
526	methylamine(1) + methyl mercaptan(2)	21	0.0201	1.2	-0.0065	0.0331	1.2
527	methyl mercaptan(1) + acetonitrile(2)	22	0.0679	2.2	0.0452	0.0263	2.0
528	methyl mercaptan(1) + N,N-dimethylformide(2)	22	0.0126	2.5	0.0324	-0.0202	2.0
529	methylamine(1) + Trimethylamine(2)	108	-0.0069	3.0	0.0727	-0.0894	2.7
530	carbondisulfide(1) + acetonitrile(2)	8	0.1562	4.8	-0.0114	0.2003	2.6
531	Trichloethylene(1) + Diethyl sulfide(2)	10	-0.0270	1.5	-0.0458	0.0219	1.5
532	acetonitrile(1) + Trichloethylene(2)	37	0.0819	1.4	-0.0435	0.1543	1.4
533	butylchloride(1) + acetonitrile(2)	45	0.0700	3.8	0.0337	0.0488	3.8
534	acetonitrile(1) + 2-Methylpyridine(2)	21	0.0040	4.8	0.0175	-0.0159	4.7
535	1,2-dichloroethane(1) + Trichloethylene(2)	16	0.0318	3.1	-0.0129	0.0537	3.0
536	Ethyl Bromide(1) + ethyl iodide(2)	19	-0.0058	0.7	0.0201	-0.0301	0.6
537	ethyl iodide(1) + nitrobenzene(2)	5	0.0494	4.4	0.0252	0.0255	1.9
538	dichloromethane(1) + Dimethyl sulfoxide(2)	18	-0.0400	6.7	-0.0778	0.0396	5.1
539	Ethanethiol(1) + Dimethyl sulfoxide(2)	9	0.1303	19.0	0.0652	0.0689	17.9
540	Ethanethiol(1) + N,N-dimethylformide(2)	4	0.0275	6.9	0.0272	0.0001	6.9
541	ethylamine(1) + diethylamine(2)	20	-0.0126	3.4	0.0156	-0.0315	3.2
542	ethylamine(1) + Triethylamine(2)	18	0.0028	3.5	0.0607	-0.0585	3.5
543	acrylonitrile(1) + tetrachloroethylene(2)	20	0.0992	6.3	0.0628	0.0443	6.3
544	acrylonitrile(1) + propionitrile(2)	28	0.0059	3.1	0.0098	-0.0047	3.1
545	N,Ndimethylformide(1)+Dimethyl sulfoxide(2)	11	-0.0315	5.6	-0.0439	0.0139	5.6
546	thiophene(1) + N,N-dimethylformide(2)	10	0.0319	3.0	0.0733	-0.0490	2.6
547	tetrachloromethane(1) + 1-Nitropropane(2)	41	0.0527	6.7	0.0742	-0.0239	6.5
548	1-Nitropropane(1) + 1,2-Dibromoethane(2)	23	0.1261	20.3	0.1016	0.0270	20.3
549	Isopropylamine(1) + Diisopropylamine(2)	23	0.0164	2.2	0.0191	-0.0032	2.2
550	Trimethylamine(1) + tetrachloromethane(2)	63	-0.0577	2.4	-0.0303	-0.0299	2.4
551	thiophene(1) + pyridine(2)	14	0.0170	0.4	0.0253	-0.0099	0.4

Table A.2. The Optimized Binary Parameters (C_{ij} and D_{ij}) of PR EOS with Summary Results for PR EOS Bubble-point Pressure Representations for the 916 Systems *(Continued)*

NO.	System	NDP	Case 2		Case 3		
			C_{ij}	%AAD	C_{ij}	D_{ij}	%AAD
552	butylchloride(1) + Buthyl Bromide(2)	16	-0.0089	5.2	0.0031	-0.0132	5.2
553	pyridine(1) + 2-Methylpyridine(2)	13	-0.0563	9.8	-0.1017	0.0521	9.8
554	hexafluorobenzene(1) + Triethylamine(2)	12	0.0313	1.1	0.0015	0.0340	1.1
555	methanol(1) + benzaldehyde(2)	6	0.2000	55.4	-0.0680	0.2730	26.3
556	1-propanol(1) + propionic aldehyde(2)	40	0.0289	9.9	0.1344	-0.1256	9.5
557	1-propanol(1) + butyraldehyde(2)	23	-0.0079	5.3	0.1280	-0.1579	4.9
558	2-methyl 1-propanol(1) + butyraldehyde(2)	22	0.0422	7.7	0.1582	-0.1399	7.3
559	2-methyl 1-propanol(1) + Isobutyr Aldehyde(2)	52	0.0219	4.0	0.1462	-0.1465	2.9
560	teritiary amyl alcohol(1) + propionic aldehyde(2)	43	0.0515	17.2	0.1699	-0.1370	15.2
561	ethanol(1) + propionic aldehyde(2)	97	-0.0038	14.4	0.1230	-0.1441	12.9
562	ethanol(1) + butyraldehyde(2)	65	0.0304	6.6	0.1564	-0.1464	6.3
563	1-butanol(1) + butyraldehyde(2)	22	0.0254	4.9	0.1613	-0.1626	3.0
564	1-butanol(1) + Isobutyr Aldehyde(2)	17	0.0279	6.0	0.1481	-0.1466	3.4
565	Isobutyr Aldehyde(1) + butyraldehyde(2)	94	0.0431	4.4	-0.0150	0.0704	4.3
566	Isoprene(1) + n-pentane(2)	94	0.0034	1.2	0.0323	-0.0346	1.2
567	1,3-butadiene(1) + cyclohexane(2)	62	0.0000	2.9	0.0394	-0.0445	2.4
568	1-Pentyne(1) + n-pentane(2)	11	0.0101	4.3	0.0068	0.0129	4.3
569	Isoprene(1) + trans, 1,3-pentadiene(2)	10	-0.0162	2.2	-0.0095	-0.0079	2.2
570	N,N-dimethylformide(1)+tertiary butyl alcohol(2)	33	0.0041	5.0	0.0361	-0.0527	4.6
571	methanol(1) + N,N-dimethylformide(2)	121	-0.0510	7.2	0.0733	-0.1258	4.7
572	N,N-dimethylformide(1) + 1-propanol(2)	108	-0.0331	2.8	0.0323	-0.0723	2.8
573	2-propanol(1) + N,N-dimethylformide(2)	49	-0.0199	2.1	0.0299	-0.0552	2.1
574	N,N-dimethylformide(1) + 1-butanol(2)	170	-0.0350	3.8	0.0311	-0.0745	3.7
575	N,N-dimethylformide(1)+ 2-methyl 1-propanol(2)	41	-0.0194	2.5	0.0435	-0.0741	2.5
576	N,N-dimethylformide(1) + benzaldehyde(2)	31	-0.0102	3.2	-0.0791	0.0790	2.9
577	N,N-dimethylformide(1) + Isobutyr Aldehyde(2)	24	0.0344	7.7	0.0378	-0.0045	7.7
578	N,N-dimethylformide(1) + Triethylamine(2)	42	0.0704	5.5	0.0627	0.0085	5.5
579	N,N-dimethylformide(1) + ethylenediamine(2)	8	0.0295	6.2	0.1729	-0.1617	5.7
580	N,N-dimethylformide(1) + Cyclohexaylamine(2)	35	0.0503	3.8	0.0544	-0.0048	3.8
581	tertiary butyl alcohol(1) + bromobenzene(2)	28	0.0720	3.2	-0.0599	0.1492	3.2
582	ethanol(1) + bromobenzene(2)	30	0.0997	14.1	-0.1438	0.2723	6.3
583	1-butanol(1) + bromobenzene(2)	28	0.0686	3.4	-0.0679	0.1643	2.8
584	2-methyl 1-propanol(1) + bromobenzene(2)	27	0.0753	3.9	-0.0561	0.1562	2.6
585	bromobenzene(1) + N,N-dimethylformide(2)	27	0.0337	6.0	-0.0449	0.0945	5.9
586	N,N-dimethylformide(1) + Fluorobenzene(2)	12	0.0155	2.1	0.0076	0.0094	1.9
587	bromobenzene(1) + Fluorobenzene(2)	9	0.0075	0.5	0.0071	0.0006	0.5
588	benzene(1) + isobutene(2)	5	0.0175	0.2	0.0023	0.0156	0.2

Table A.2. The Optimized Binary Parameters (C_{ij} and D_{ij}) of PR EOS with Summary Results for PR EOS Bubble-point Pressure Representations for the 916 Systems *(Continued)*

NO.	System	NDP	Case 2		Case 3		
			C_{ij}	%AAD	C_{ij}	D_{ij}	%AAD
589	benzene(1) + 1-butene(2)	4	0.0116	0.5	-0.0192	0.0321	0.5
590	benzene(1) + 1-heptene(2)	13	0.0076	3.4	0.0284	-0.0238	3.4
591	benzene(1) + vinylacetylene(2)	14	-0.0055	4.3	-0.0200	0.0171	3.8
592	p-xylene(1) + vinylacetylene(2)	23	0.0070	5.2	-0.0577	0.0652	2.7
593	Isobutyr Aldehyde(1) + toluene(2)	14	0.0237	4.3	-0.0126	0.0429	4.3
594	n-octane(1) + water(2)	22	-0.4412	24.4	-0.0878	-0.2344	23.6
595	toluene(1) + vinylacetylene(2)	8	0.0050	4.4	-0.0549	0.0634	1.9
596	butylamine(1) + water(2)	16	-0.2572	4.4	-0.1879	-0.0570	3.8
597	Cyclohexaylamine(1) + water(2)	39	-0.1865	6.6	-0.1123	-0.0663	6.4
598	m-xylene(1) + water(2)	22	-0.1937	24.0	-0.1357	-0.0446	23.7
599	methyl teritiary butyl ether(1) + water(2)	4	-0.1517	1.3	0.0550	-0.2359	1.3
600	Dimethyl sulfoxide(1) + nitrobenzene(2)	10	0.0632	4.4	-0.1050	0.2055	4.1
601	benzene(1) + Tribromomethane(2)	24	-0.0231	9.8	-0.0732	0.0546	9.5
602	benzene(1) + Dibromomethane(2)	10	-0.1454	25.3	-0.1121	0.0162	25.2
603	benzene(1) + 1,2-Dibromoethane(2)	295	-0.0044	21.2	-0.0078	0.0047	21.1
604	benzene(1) + Buthyl Bromide(2)	29	0.0078	2.5	0.0255	-0.0244	2.4
605	ethylbenzene(1) + Buthyl Bromide(2)	27	0.0137	4.0	0.0098	0.0043	4.0
606	p-xylene(1) + 1,2-Dibromoethane(2)	23	0.0461	20.2	0.0025	0.0437	20.2
607	1,2-Dibromoethane(1) + m-xylene(2)	22	0.0506	20.3	0.0313	0.0300	20.3
608	tertiary butyl alcohol(1) + tetrachloroethylene(2)	11	0.0664	3.3	-0.0675	0.1666	2.4
609	methanol(1) + tetrachloroethylene(2)	23	0.1323	19.5	-0.0764	0.2361	16.0
610	1-propanol(1) + tetrachloroethylene(2)	94	0.0939	6.2	-0.0758	0.2047	6.2
611	2-propanol(1) + tetrachloroethylene(2)	72	0.0992	6.9	-0.0881	0.2272	6.3
612	1-butanol(1) + tetrachloroethylene(2)	109	0.0575	5.5	-0.0463	0.1193	5.5
613	2-methyl 1-propanol(1) + tetrachloroethylene(2)	16	0.0883	2.2	-0.0387	0.1522	2.1
614	methanol(1) + Vinyl chloride(2)	23	-0.0123	12.2	0.1198	-0.1233	3.3
615	tertiary butyl alcohol(1) + 3-Chloro-1-propene(2)	10	0.0625	4.9	0.1469	-0.1056	3.9
616	3-Chloro-1-propene(1) + methanol(2)	11	0.0517	5.2	0.0871	-0.0410	4.5
617	methanol(1) + 1,1-Dichloroethylene(2)	17	0.0755	10.9	0.0652	0.0103	10.9
618	ethanol(1) + 1,1-Dichloroethylene(2)	17	0.0779	10.2	0.0700	0.0068	10.2
619	tertiary butyl alcohol(1) + Trichloethylene(2)	32	0.0614	2.0	0.0430	0.0222	2.0
620	methanol(1) + Trichloethylene(2)	10	0.1080	6.8	-0.0117	0.1453	6.6
621	ethanol(1) + Trichloethylene(2)	9	0.0087	6.0	-0.0905	0.1163	6.0
622	1-propanol(1) + Trichloethylene(2)	89	0.0701	3.3	0.0212	0.0577	3.3
623	2-propanol(1) + Trichloethylene(2)	81	0.0774	4.5	0.0165	0.0727	4.5
624	1-butanol(1) + Trichloethylene(2)	88	0.0640	3.8	0.0720	-0.0093	3.8
625	2-methyl 1-propanol(1) + Trichloethylene(2)	25	0.0674	2.5	0.0646	0.0035	2.5

Table A.2. The Optimized Binary Parameters (C_{ij} and D_{ij}) of PR EOS with Summary Results for PR EOS Bubble-point Pressure Representations for the 916 Systems *(Continued)*

NO.	System	NDP	Case 2		Case 3		
			C_{ij}	%AAD	C_{ij}	D_{ij}	%AAD
626	acetaldehyde(1) + ethylene-oxide(2)	49	0.0093	2.9	-0.0158	0.0297	2.9
627	diethyl ether(1) + nitromethane(2)	13	0.0169	1.0	0.1021	-0.0920	1.0
628	nitromethane(1) + 1,4-dioxane(2)	56	-0.0081	2.8	0.0831	-0.1027	2.7
629	diethyl ether(1) + nitrobenzene(2)	5	-0.0352	3.1	-0.0453	0.0127	1.6
630	chlorobenzene(1) + ethyl acetate(2)	45	-0.0045	0.9	0.0050	-0.0108	0.9
631	chlorobenzene(1) + 1,4-dioxane(2)	14	-0.0029	1.1	-0.0062	0.0039	1.1
632	diisopropyl ether(1) + chlorobenzene(2)	12	-0.0218	1.8	-0.0192	-0.0030	1.8
633	acetone(1) + chlorobenzene(2)	120	0.0203	2.3	-0.0566	0.0871	2.3
634	2-butanone(1) + chlorobenzene(2)	23	0.0140	3.2	-0.0173	0.0375	3.1
635	4-methyl 2-pentanone(1) + chlorobenzene(2)	19	-0.0179	1.9	0.0120	-0.0338	1.9
636	1,2-Dibromoethane(1) + Fluorobenzene(2)	21	0.0546	19.7	-0.0034	0.0663	16.4
637	acetonitrile(1) + bromobenzene(2)	16	0.0571	5.0	-0.0880	0.1804	2.2
638	nitrobenzene(1) + bromobenzene(2)	54	0.0107	7.6	0.0001	0.0133	7.5
639	Dimethyl sulfoxide(1) + bromobenzene(2)	10	0.0552	4.9	-0.0901	0.1761	4.9
640	ethyl iodide(1) + toluene(2)	37	-0.0269	4.3	-0.0868	0.0678	3.7
641	toluene(1) + thiophene(2)	29	0.0025	2.9	-0.0565	0.0605	2.3
642	propylene oxide(1) + water(2)	17	-0.2320	13.2	0.0023	-0.1889	8.8
643	ethylene-oxide(1) + water(2)	107	-0.1630	21.8	0.0178	-0.1440	7.8
644	propylene oxide(1) + ethyl acetate(2)	30	0.0748	6.4	-0.0140	0.1118	5.3
645	pyridine(1) + ethyl acetate(2)	119	-0.0215	2.7	0.0434	-0.0756	2.5
646	2-Methylpyridine(1) + ethyl acetate(2)	13	-0.0481	15.0	0.0115	-0.0657	14.4
647	ethyl iodide(1) + ethyl acetate(2)	25	-0.0103	2.5	0.0326	-0.0488	2.5
648	acetonitrile(1) + ethyl acetate(2)	61	0.0255	1.2	-0.0239	0.0586	1.1
649	nitromethane(1) + ethyl acetate(2)	66	-0.0228	1.7	0.0892	-0.1278	1.7
650	nitrobenzene(1) + ethyl acetate(2)	6	-0.0236	4.8	-0.0623	0.0451	2.5
651	nitroethane(1) + ethyl acetate(2)	21	-0.0102	1.2	0.0589	-0.0818	1.2
652	Dimethyl sulfoxide(1) + ethyl acetate(2)	33	0.0165	4.7	-0.0127	0.0301	4.7
653	tetrachloromethane(1) + propyl acetate(2)	30	0.0228	0.8	0.0952	-0.0863	0.8
654	tetrachloromethane(1) + methyl acetate(2)	64	0.0366	0.5	0.0624	-0.0309	0.5
655	chloroform(1) + methyl acetate(2)	72	-0.0579	3.6	-0.0234	-0.0391	3.5
656	dichloromethane(1) + methyl acetate(2)	46	-0.0476	0.9	-0.0800	0.0366	0.8
657	1,1-Dichloroethylene(1) + vinyl acetate(2)	24	0.0264	2.8	0.0270	-0.0007	2.8
658	propylene oxide(1) + methyl acetate(2)	30	0.0053	0.6	0.0008	0.0054	0.6
659	methyl acetate(1) + 1,2-epoxybutane(2)	182	0.0033	2.3	0.0101	-0.0079	2.3
660	methyl acetate(1) + ethyl acetate(2)	286	0.0146	3.2	0.0153	-0.0008	3.2
661	methyl iodide(1) + methyl acetate(2)	8	0.0463	1.8	0.0009	0.0539	1.8
662	acetonitrile(1) + propyl acetate(2)	21	0.0338	0.8	-0.0237	0.0690	0.8

Table A.2. The Optimized Binary Parameters (C_{ij} and D_{ij}) of PR EOS with Summary Results for PR EOS Bubble-point Pressure Representations for the 916 Systems *(Continued)*

NO.	System	NDP	Case 2		Case 3		
			C_{ij}	%AAD	C_{ij}	D_{ij}	%AAD
663	acetonitrile(1) + methyl acetate(2)	34	0.0182	1.4	-0.0255	0.0528	1.4
664	acetonitrile(1) + vinyl acetate(2)	24	0.0333	0.4	-0.0400	0.0881	0.3
665	acrylonitrile(1) + vinyl acetate(2)	24	0.0469	4.5	0.0143	0.0396	4.4
666	nitromethane(1) + propyl acetate(2)	21	-0.0260	1.8	0.0953	-0.1377	1.5
667	nitroethane(1) + propyl acetate(2)	21	0.0031	0.7	0.0779	-0.0881	0.7
668	propyl acetate(1) + pyridine(2)	21	-0.0144	0.4	0.0422	-0.0658	0.3
669	vinyl acetate(1) + water(2)	25	-0.2064	12.3	-0.0404	-0.1273	11.8
670	methyl acetate(1) + water(2)	150	-0.2339	20.6	-0.0010	-0.1747	11.8
671	Ethanethiol(1) + toluene(2)	9	0.0075	2.0	-0.0423	0.0517	1.6
672	methyl mercaptan(1) + toluene(2)	10	0.0018	2.9	-0.0533	0.0523	2.6
673	thiophene(1) + ethyl teritiary butyl ether(2)	35	-0.0363	0.9	-0.0139	-0.0253	0.9
674	methanol(1) + thiophene(2)	165	0.1060	6.6	0.0668	0.0342	5.8
675	ethanol(1) + thiophene(2)	48	0.0974	6.1	0.0558	0.0483	6.1
676	1-propanol(1) + thiophene(2)	51	0.0742	4.2	0.0545	0.0224	4.2
677	2-propanol(1) + thiophene(2)	48	0.0821	3.6	0.0521	0.0377	3.6
678	thiophene(1) + isobutene(2)	52	0.0133	2.3	0.0290	-0.0175	2.0
679	thiophene(1) + trans, 2-butene(2)	52	0.0118	1.2	0.0067	0.0058	1.1
680	butane(1) + Hydrogen Sulfide(2)	7	0.0584	16.3	-0.0940	0.1636	7.5
681	Dimethyl sulfoxide(1) + water(2)	478	-0.2605	14.8	-0.0559	-0.1733	11.7
682	tetrachloromethane(1)+N,N-dimethylformide(2)	67	0.0402	5.8	0.0799	-0.0425	4.0
683	N,N-dimethylformide(1)+ 1,2-dichloroethane(2)	21	-0.0069	4.1	0.0468	-0.0637	3.2
684	chloroform(1) + N,N-dimethylformide(2)	14	0.0305	4.0	0.0452	-0.0168	3.6
685	N,N-dimethylformide(1) + butylchloride(2)	20	0.0229	3.8	0.0272	-0.0048	3.8
686	N,N-dimethylformide(1) + Trichloethylene(2)	13	0.0208	2.5	0.0190	0.0022	2.5
687	N,N-dimethylformide(1) + chlorobenzene(2)	34	0.0395	3.4	-0.0166	0.0678	3.4
688	N,N-dimethylformide(1) + ethyl acetate(2)	32	-0.0001	3.9	0.0013	-0.0017	3.9
689	N,N-dimethylformide(1) + 1,4-dioxane(2)	50	0.0123	2.5	0.0385	-0.0289	2.1
690	N,N-dimethylformide(1) + diisopropyl ether(2)	17	0.0545	6.2	0.0182	0.0409	6.2
691	acetone(1) + N,N-dimethylformide(2)	69	0.0080	2.3	0.0026	0.0059	2.3
692	N,N-dimethylformide(1) + cyclohexanone(2)	18	-0.0619	13.4	-0.0749	0.0143	13.4
693	N,N-dimethylformide(1) + acrylonitrile(2)	13	-0.0253	3.9	-0.0055	-0.0238	3.6
694	N,N-dimethylformide(1) + pyridine(2)	32	-0.0005	0.7	0.0094	-0.0117	0.7
695	N,N-dimethylformide(1) + toluene(2)	203	0.0306	7.2	0.0238	0.0071	7.2
696	N,N-dimethylformide(1) + water(2)	145	-0.2245	4.0	-0.0553	-0.1522	4.0
697	chlorobenzene(1) + 2-Methylpyridine(2)	15	-0.0923	20.6	-0.1041	0.0129	20.5
698	Dimethyl sulfoxide(1) + chlorobenzene(2)	10	0.0193	2.7	-0.0865	0.1262	1.1
699	benzene(1) + propyl acetate(2)	37	-0.0122	0.6	0.0233	-0.0416	0.6

Table A.2. The Optimized Binary Parameters (C_{ij} and D_{ij}) of PR EOS with Summary Results for PR EOS Bubble-point Pressure Representations for the 916 Systems *(Continued)*

NO.	System	NDP	Case 2		Case 3		
			C_{ij}	%AAD	C_{ij}	D_{ij}	%AAD
700	benzene(1) + methyl acetate(2)	281	0.0260	2.7	0.0370	-0.0128	2.7
701	methyl acetate(1) + o-xylene(2)	15	0.0253	1.9	-0.0026	0.0312	1.9
702	benzene(1) + vinyl acetate(2)	17	0.0282	0.6	0.0335	-0.0063	0.6
703	p-xylene(1) + vinyl acetate(2)	20	0.0722	6.2	0.0306	0.0509	5.2
704	Isopropylbenzene(1) + vinyl acetate(2)	23	0.0455	3.0	0.0111	0.0408	1.9
705	benzene(1) + ethyl acetate(2)	71	-0.0048	0.7	0.0375	-0.0493	0.6
706	ethylbenzene(1) + ethyl acetate(2)	42	0.0102	2.4	-0.0060	0.0176	2.4
707	p-xylene(1) + ethyl acetate(2)	20	0.0404	1.5	0.0112	0.0349	0.9
708	o-xylene(1) + ethyl acetate(2)	12	0.0172	1.8	0.0074	0.0120	1.8
709	methanol(1) + Hydrogen cyanide(2)	30	-0.0239	10.3	-0.0110	-0.0142	10.3
710	Hydrogen cyanide(1) + acrylonitrile(2)	81	-0.0196	4.2	-0.0301	0.0141	4.1
711	bromobenzene(1) + n-heptane(2)	14	-0.0010	2.1	-0.0114	0.0119	2.1
712	bromobenzene(1) + cyclohexane(2)	94	0.0222	2.1	-0.0128	0.0350	2.1
713	bromobenzene(1) + n-decane(2)	7	-0.0163	1.4	0.0372	-0.0615	1.3
714	butane(1) + ethyl acetate(2)	26	0.0689	0.5	0.0759	-0.0083	0.5
715	isobutane(1) + ethyl acetate(2)	26	0.0643	0.5	0.0704	-0.0067	0.5
716	n-pentane(1) + ethyl acetate(2)	25	0.0636	1.1	0.0879	-0.0296	1.0
717	hexane(1) + ethyl acetate(2)	58	0.0637	1.0	0.1160	-0.0637	0.8
718	ethyl acetate(1) + n-heptane(2)	85	0.0599	1.5	0.0585	0.0017	1.5
719	n-octane(1) + ethyl acetate(2)	63	0.0609	1.9	0.0471	0.0165	1.8
720	cyclohexane(1) + ethyl acetate(2)	75	0.0651	0.9	0.0900	-0.0298	0.9
721	n-decane(1) + ethyl acetate(2)	20	0.0743	3.2	0.0301	0.0505	2.0
722	Trichloethylene(1) + ethyl acetate(2)	173	-0.0232	1.6	-0.0115	-0.0135	1.5
723	tetrachloromethane(1) + ethyl acetate(2)	285	0.0125	1.3	0.0907	-0.0913	1.1
724	1,2-dichloroethane(1) + ethyl acetate(2)	18	-0.0101	3.7	-0.0110	0.0011	3.7
725	chloroform(1) + ethyl acetate(2)	78	-0.0787	1.5	-0.0304	-0.0541	1.4
726	dichloromethane(1) + ethyl acetate(2)	57	-0.0613	1.8	-0.0714	0.0111	1.8
727	butylchloride(1) + ethyl acetate(2)	45	-0.0012	3.5	0.0374	-0.0453	3.3
728	Dibromomethane(1) + ethyl acetate(2)	14	-0.1426	12.7	-0.1344	0.0010	12.3
729	Trimethylamine(1) + ethyl acetate(2)	32	0.0189	1.2	0.0197	-0.0008	1.2
730	1,3-butadiene(1) + ethyl acetate(2)	8	0.0054	0.7	0.0092	-0.0041	0.6
731	isobutene(1) + ethyl acetate(2)	26	0.0398	1.2	0.0442	-0.0054	1.0
732	toluene(1) + benzyl acetate(2)	33	-0.0379	4.0	-0.0914	0.0606	3.4
733	1-Nitropropane(1) + water(2)	11	-0.1516	9.7	0.0240	-0.1543	7.2
734	nitromethane(1) + water(2)	52	-0.0884	13.8	0.0563	-0.1289	12.4
735	1,2-Dibromoethane(1) + bromobenzene(2)	24	0.1868	11.5	0.0408	0.1814	11.5
736	2-butanone(1) + bromobenzene(2)	38	0.0188	1.2	-0.0578	0.0910	1.2

Table A.2. The Optimized Binary Parameters (C_{ij} and D_{ij}) of PR EOS with Summary Results for PR EOS Bubble-point Pressure Representations for the 916 Systems *(Continued)*

NO.	System	NDP	Case 2		Case 3		
			C_{ij}	%AAD	C_{ij}	D_{ij}	%AAD
737	pyridine(1) + 1,4-dioxane(2)	73	-0.0052	1.9	0.0255	-0.0344	1.9
738	methyl mercaptan(1) + dimethyl ether(2)	23	0.0012	0.7	-0.0552	0.0710	0.7
739	acetone(1) + methyl mercaptan(2)	22	0.0227	1.5	0.0358	-0.0157	1.3
740	acetone(1) + nitromethane(2)	60	-0.0298	1.9	0.0502	-0.0898	1.9
741	acetone(1) + nitrobenzene(2)	5	-0.0344	1.7	-0.0742	0.0428	1.7
742	2-butanone(1) + nitrobenzene(2)	38	-0.0056	3.2	-0.0852	0.0877	3.2
743	acetone(1) + water(2)	952	-0.2577	20.4	0.0165	-0.2209	9.8
744	3-pentanone(1) + water(2)	22	-0.2600	18.8	0.0343	-0.2195	15.9
745	2-butanone(1) + water(2)	538	-0.2591	36.0	0.0251	-0.2200	12.9
746	4-methyl 2-pentanone(1) + water(2)	79	-0.3539	25.6	0.0094	-0.2556	22.6
747	propylene oxide(1)+methyl teritiary butyl ether(2)	40	0.0097	1.6	0.0085	0.0014	1.6
748	propylene oxide(1) + toluene(2)	13	0.0340	3.5	-0.0178	0.0603	3.2
749	methyl mercaptan(1) + hexane(2)	185	0.0348	4.9	0.0216	0.0138	4.4
750	methyl mercaptan(1) + n-decane(2)	22	0.0061	2.4	-0.0589	0.0677	2.4
751	Ethanethiol(1) + isopentane(2)	36	0.0345	1.2	0.0299	0.0061	1.2
752	Ethanethiol(1) + butane(2)	32	0.0363	0.4	0.0031	0.0422	0.4
753	Ethanethiol(1) + n-pentane(2)	41	0.0335	1.1	-0.0031	0.0448	1.0
754	Ethanethiol(1) + hexane(2)	9	0.0353	1.4	-0.0039	0.0444	1.3
755	Ethanethiol(1) + n-decane(2)	8	0.0104	5.3	-0.0608	0.0590	4.2
756	methyl acetate(1) + propyl acetate(2)	32	0.0202	2.2	0.0322	-0.0138	2.1
757	vinyl acetate(1) + propyl acetate(2)	21	-0.0032	0.6	0.0088	-0.0142	0.6
758	methyl acetate(1) + vinyl acetate(2)	65	-0.0054	0.8	-0.0114	0.0070	0.8
759	propyl acetate(1) + Diethyl sulfide(2)	11	0.0130	0.3	0.0029	0.0120	0.3
760	carbondisulfide(1) + methyl acetate(2)	48	0.0856	0.6	0.0206	0.0784	0.6
761	methyl acetate(1) + toluene(2)	24	0.0327	1.5	0.0076	0.0299	1.2
762	vinyl acetate(1) + toluene(2)	19	0.0186	0.8	0.0281	-0.0111	0.8
763	tetrachloromethane(1) + propylene oxide(2)	36	0.0226	1.0	-0.0389	0.0709	1.0
764	ethylene-oxide(1) + 1,2-dichloroethane(2)	17	0.0014	7.7	-0.0953	0.1090	5.6
765	1,2-epoxybutane(1) + chloroform(2)	50	-0.0936	4.3	-0.0755	-0.0198	4.3
766	1,2-epoxybutane(1) + butylchloride(2)	28	-0.0218	3.2	-0.0428	0.0240	3.2
767	Ethyl Bromide(1) + water(2)	9	0.0833	1.0	-0.0675	0.1947	1.0
768	3-Chloro-1-propene(1) + water(2)	9	-0.2377	12.6	-0.1678	-0.0521	10.6
769	Dibromomethane(1) + toluene(2)	10	-0.1509	35.6	-0.1476	0.0237	34.3
770	1,2-Dibromoethane(1) + toluene(2)	44	0.0255	20.6	-0.0002	0.0263	20.6
771	toluene(1) + Buthyl Bromide(2)	58	0.0132	3.6	0.0290	-0.0183	3.6
772	Trichloethylene(1) + toluene(2)	160	-0.0198	1.4	-0.0741	0.0627	1.2
773	pyridine(1) + tetrachloroethylene(2)	74	0.0213	2.2	0.0377	-0.0187	2.1

Table A.2. The Optimized Binary Parameters (C_{ij} and D_{ij}) of PR EOS with Summary Results for PR EOS Bubble-point Pressure Representations for the 916 Systems *(Continued)*

NO.	System	NDP	Case 2		Case 3		
			C_{ij}	%AAD	C_{ij}	D_{ij}	%AAD
774	Trichloethylene(1) + chlorobenzene(2)	17	-0.0313	2.8	-0.0407	0.0110	2.8
775	acetone(1) + tetrachloroethylene(2)	35	0.0981	9.7	-0.0081	0.1252	9.5
776	2-butanone(1) + tetrachloroethylene(2)	23	0.0492	2.7	0.0042	0.0518	2.7
777	acetone(1) + Vinyl chloride(2)	44	0.0008	2.7	-0.0022	0.0028	2.6
778	2-butanone(1) + 3-Chloro-1-propene(2)	8	-0.0198	2.7	-0.0157	-0.0048	2.7
779	acetone(1) + Trichloethylene(2)	12	0.0103	1.9	-0.0179	0.0319	1.8
780	2-butanone(1) + Trichloethylene(2)	66	-0.0008	2.3	-0.0109	0.0108	2.2
781	Trichloethylene(1) + 4-methyl 2-pentanone(2)	21	-0.0227	2.0	-0.0318	0.0106	2.0
782	1,4-dioxane(1) + tetrachloroethylene(2)	28	0.0136	2.5	-0.0059	0.0223	2.5
783	Trichloethylene(1) + 1,4-dioxane(2)	10	-0.0471	3.9	-0.0902	0.0478	3.7
784	chlorobenzene(1) + Fluorobenzene(2)	10	0.0054	0.6	0.0120	-0.0079	0.6
785	chlorobenzene(1) + isobutene(2)	11	0.0177	2.6	-0.0006	0.0202	2.6
786	chlorobenzene(1) + 1-pentene(2)	42	0.0052	0.7	-0.0080	0.0129	0.7
787	tertiary butyl alcohol(1) + chlorobenzene(2)	63	0.0737	3.0	-0.0148	0.1067	2.6
788	methanol(1) + chlorobenzene(2)	126	0.0980	15.2	-0.0975	0.2160	11.2
789	teritiary amyl alcohol(1) + chlorobenzene(2)	23	0.0360	2.5	0.0107	0.0306	2.3
790	ethanol(1) + chlorobenzene(2)	166	0.0910	8.0	-0.1001	0.2239	6.8
791	1-propanol(1) + chlorobenzene(2)	186	0.0810	4.1	-0.0582	0.1686	4.0
792	2-propanol(1) + chlorobenzene(2)	74	0.0973	4.7	-0.0395	0.1630	3.5
793	1-butanol(1) + chlorobenzene(2)	236	0.0424	8.3	-0.0191	0.0693	8.3
794	2-methyl 1-propanol(1) + chlorobenzene(2)	80	0.0639	3.5	-0.0095	0.0917	3.3
795	chlorobenzene(1) + cyclohexanol(2)	21	0.0236	5.4	0.0472	-0.0280	5.3
796	methanol(1) + ethyl iodide(2)	35	0.1029	6.5	0.0861	0.0195	6.5
797	ethanol(1) + ethyl iodide(2)	43	0.0886	6.8	0.1028	-0.0136	6.8
798	1-butanol(1) + ethyl iodide(2)	12	0.0881	1.9	0.1143	-0.0313	1.9
799	methyl iodide(1) + acetaldehyde(2)	23	0.0764	4.9	0.0251	0.0621	4.9
800	Tribromomethane(1) + methyl acetate(2)	9	-0.0562	4.7	-0.1005	0.0468	4.0
801	diethyl ether(1) + Tribromomethane(2)	9	-0.0951	6.6	-0.1634	0.0712	1.8
802	1,2-Dibromoethane(1) + 1,4-dioxane(2)	13	0.0000	24.2	0.0011	0.0245	17.6
803	acetone(1) + Ethyl Bromide(2)	17	0.0149	1.4	0.0099	0.0059	1.4
804	propylene oxide(1) + ethylbenzene(2)	9	0.0109	1.9	-0.0425	0.0585	1.9
805	pyridine(1) + hexafluorobenzene(2)	19	-0.0070	2.1	-0.0361	0.0327	1.8
806	tetrachloromethane(1) + hexafluorobenzene(2)	90	0.0109	1.5	0.0268	-0.0182	1.5
807	tetrachloromethane(1) + Fluorobenzene(2)	32	0.0106	0.9	0.1087	-0.1141	0.8
808	acetone(1) + diethylamine(2)	58	0.0313	1.7	0.1136	-0.0982	1.5
809	acetone(1) + Triethylamine(2)	28	0.0752	3.3	0.0481	0.0325	3.2
810	2-butanone(1) + diethylamine(2)	13	0.0000	1.3	0.0651	-0.0992	0.1

Table A.2. The Optimized Binary Parameters (C_{ij} and D_{ij}) of PR EOS with Summary Results for PR EOS Bubble-point Pressure Representations for the 916 Systems *(Continued)*

NO.	System	NDP	Case 2		Case 3		
			C_{ij}	%AAD	C_{ij}	D_{ij}	%AAD
811	2-butanone(1) + Triethylamine(2)	56	0.0492	1.6	0.0445	0.0055	1.6
812	cyclohexanone(1) + Triethylamine(2)	58	0.0359	6.6	0.0919	-0.0664	5.7
813	tetrachloromethane(1) + 1,3-butadiene(2)	6	0.0038	0.6	0.0612	-0.0596	0.6
814	dichloromethane(1) + 1,3-butadiene(2)	9	-0.0135	0.9	-0.0102	-0.0037	0.8
815	Vinyl chloride(1) + 1,3-butadiene(2)	40	-0.0339	3.9	0.0008	-0.0389	3.9
816	nitromethane(1) + Isoprene(2)	10	0.0601	3.8	0.1117	-0.0604	1.9
817	nitromethane(1) + 1,3-butadiene(2)	7	0.0453	0.6	0.0590	-0.0128	0.6
818	Dimethyl sulfoxide(1) + Isoprene(2)	50	0.0457	6.4	0.0673	-0.0180	6.0
819	carbondisulfide(1) + 1,3-butadiene(2)	8	-0.0095	0.6	-0.0145	0.0054	0.6
820	Dimethyl sulfoxide(1)+ trans, 1,3-pentadiene(2)	45	0.0581	6.2	0.0613	-0.0028	6.2
821	acetonitrile(1) + diethylamine(2)	89	0.0662	3.1	0.0748	-0.0101	3.1
822	Dimethyl sulfoxide(1) + ethylenediamine(2)	9	0.0060	14.5	0.1948	-0.2069	9.5
823	tertiary butyl alcohol(1) + pyridine(2)	29	-0.0450	7.2	-0.0145	-0.0331	7.2
824	methanol(1) + pyridine(2)	139	-0.0149	3.0	0.0005	-0.0170	2.9
825	ethanol(1) + pyridine(2)	66	-0.0039	0.9	-0.0100	0.0068	0.9
826	1-propanol(1) + pyridine(2)	72	-0.0244	2.3	-0.0186	-0.0051	2.3
827	2-propanol(1) + pyridine(2)	97	-0.0154	3.2	-0.0199	0.0051	3.2
828	1-butanol(1) + pyridine(2)	77	-0.0234	9.0	0.0259	-0.0550	8.9
829	2-methyl 1-propanol(1) + pyridine(2)	25	-0.0531	7.1	-0.0200	-0.0359	7.1
830	tertiary butyl alcohol(1) + 2-Methylpyridine(2)	15	-0.0939	19.4	-0.0623	-0.0341	19.4
831	methanol(1) + 2-Methylpyridine(2)	85	-0.0788	14.6	-0.0300	-0.0512	14.2
832	ethanol(1) + 2-Methylpyridine(2)	16	-0.0500	18.8	-0.0028	-0.0830	18.8
833	1-propanol(1) + 2-Methylpyridine(2)	16	-0.0350	31.3	-0.1033	-0.0097	16.5
834	2-propanol(1) + 2-Methylpyridine(2)	13	-0.0745	18.4	-0.0043	-0.0760	18.3
835	1-butanol(1) + 2-Methylpyridine(2)	18	-0.1000	24.9	-0.1012	-0.0482	21.9
836	2-methyl 1-propanol(1) + 2-Methylpyridine(2)	16	-0.1000	32.0	-0.1029	-0.0549	28.3
837	dimethyl sulfide(1) + isobutene(2)	26	0.0161	2.0	0.0262	-0.0129	1.8
838	isobutene(1) + dimethyl disulfide(2)	26	0.0102	0.9	0.0259	-0.0172	0.8
839	isobutene(1) + Diethyl sulfide(2)	26	0.0161	2.2	0.0280	-0.0134	1.6
840	nitromethane(1) + 2-methyl 1-butene(2)	10	0.0717	7.0	0.1268	-0.0653	4.1
841	nitromethane(1) + 2-methyl 2-butene(2)	10	0.0816	8.0	0.1624	-0.0929	4.6
842	methyl acetate(1) + 1-pentene(2)	59	0.0592	0.6	0.0834	-0.0293	0.4
843	propylene oxide(1) + n-pentane(2)	12	0.0699	2.0	0.0427	0.0329	2.0
844	propylene oxide(1) + hexane(2)	12	0.0738	2.2	0.0379	0.0431	1.9
845	propylene oxide(1) + n-heptane(2)	12	0.0633	3.1	-0.0056	0.0826	2.0
846	ethylene-oxide(1) + isobutane(2)	28	0.0585	1.9	0.0123	0.0567	1.9
847	1,2-epoxybutane(1) + hexane(2)	30	0.0407	1.6	0.0389	0.0020	1.6

Table A.2. The Optimized Binary Parameters (C_{ij} and D_{ij}) of PR EOS with Summary Results for PR EOS Bubble-point Pressure Representations for the 916 Systems *(Continued)*

NO.	System	NDP	Case 2		Case 3		
			C_{ij}	%AAD	C_{ij}	D_{ij}	%AAD
848	1,2-epoxybutane(1) + n-heptane(2)	27	0.0352	2.2	-0.0036	0.0449	1.9
849	propylene oxide(1) + tertiary butyl alcohol(2)	78	0.0240	2.2	0.1340	-0.1294	1.9
850	methanol(1) + propylene oxide(2)	18	0.0136	5.4	0.1613	-0.1766	3.4
851	2-propanol(1) + propylene oxide(2)	44	0.0284	1.9	0.1267	-0.1132	0.6
852	methanol(1) + 1,2-epoxybutane(2)	24	0.0128	2.6	0.1776	-0.1798	1.6
853	ethanol(1) + 1,2-epoxybutane(2)	25	0.0229	2.4	0.1520	-0.1441	2.4
854	1-propanol(1) + 1,2-epoxybutane(2)	27	0.0142	3.6	0.1243	-0.1191	3.6
855	2-propanol(1) + 1,2-epoxybutane(2)	24	0.0241	3.3	0.1353	-0.1250	3.3
856	methanol(1) + nitromethane(2)	84	0.0991	8.4	0.0280	0.0850	7.9
857	ethanol(1) + nitromethane(2)	92	0.0939	2.3	0.0107	0.1000	2.0
858	1-propanol(1) + nitromethane(2)	26	0.0861	1.4	0.0162	0.0834	1.4
859	2-propanol(1) + nitromethane(2)	13	0.0895	1.7	0.0105	0.0920	1.3
860	1-butanol(1) + nitromethane(2)	34	0.0860	6.9	0.0432	0.0478	6.9
861	methanol(1) + nitrobenzene(2)	41	0.0921	13.5	-0.0621	0.1587	9.8
862	ethanol(1) + nitrobenzene(2)	4	0.0901	6.9	-0.0116	0.1125	2.9
863	tertiary butyl alcohol(1) + nitroethane(2)	21	0.0690	1.7	0.0508	0.0222	1.7
864	methanol(1) + nitroethane(2)	21	0.0925	5.3	0.0007	0.1103	3.5
865	ethanol(1) + nitroethane(2)	22	0.0913	1.4	0.0208	0.0861	0.7
866	1-propanol(1) + nitroethane(2)	21	0.0846	0.8	0.0537	0.0379	0.8
867	2-propanol(1) + nitroethane(2)	23	0.0830	1.5	0.0687	0.0175	1.5
868	Vinyl chloride(1) + acetaldehyde(2)	13	0.0163	1.6	-0.0199	0.0468	1.5
869	ethanol(1) + Ethyl Bromide(2)	15	0.0885	4.9	0.1606	-0.0832	2.6
870	methanol(1) + Tribromomethane(2)	33	0.0872	12.8	-0.0871	0.2023	8.8
871	ethanol(1) + Tribromomethane(2)	25	0.0788	9.2	-0.0702	0.1688	5.7
872	Dibromomethane(1) + tertiary butyl alcohol(2)	30	-0.0515	13.9	-0.1335	0.0922	13.9
873	1-propanol(1) + Dibromomethane(2)	14	-0.0090	24.0	-0.1581	0.1894	22.3
874	1-butanol(1) + Dibromomethane(2)	23	-0.0501	24.7	-0.1503	0.1327	23.6
875	Dibromomethane(1) + 2-methyl 1-propanol(2)	27	-0.0436	19.1	-0.1409	0.1260	18.1
876	tertiary butyl alcohol(1)+1,2-Dibromoethane(2)	25	0.0621	12.0	0.0441	0.0193	11.7
877	1-butanol(1) + 1,2-Dibromoethane(2)	24	0.1320	12.9	0.1297	0.0026	12.9
878	2-methyl 1-propanol(1)+ 1,2-Dibromoethane(2)	23	0.1125	11.3	0.0949	0.0198	11.3
879	tertiary butyl alcohol(1) + Buthyl Bromide(2)	89	0.0783	6.5	0.1501	-0.0849	6.5
880	methanol(1) + Buthyl Bromide(2)	57	0.1095	11.9	0.0891	0.0253	11.9
881	ethanol(1) + Buthyl Bromide(2)	120	0.1083	8.3	0.1455	-0.0433	8.3
882	1-butanol(1) + Buthyl Bromide(2)	143	0.0790	11.9	0.1765	-0.1090	10.3
883	2-methyl 1-propanol(1) + Buthyl Bromide(2)	133	0.0859	9.7	0.1794	-0.1072	8.9
884	Ethyl Bromide(1) + n-heptane(2)	11	-0.0113	1.2	-0.0467	0.0383	0.8

Table A.2. The Optimized Binary Parameters (C_{ij} and D_{ij}) of PR EOS with Summary Results for PR EOS Bubble-point Pressure Representations for the 916 Systems *(Continued)*

NO.	System	NDP	Case 2		Case 3		
			C_{ij}	%AAD	C_{ij}	D_{ij}	%AAD
885	Tribromomethane(1) + hexane(2)	24	-0.0052	9.9	-0.0306	0.0264	9.9
886	1,2-Dibromoethane(1) + cyclohexane(2)	25	-0.0050	13.0	-0.0530	0.0451	12.9
887	Buthyl Bromide(1) + hexane(2)	9	0.0117	1.8	0.0306	-0.0225	1.7
888	Buthyl Bromide(1) + n-heptane(2)	34	0.0122	2.4	-0.0792	0.1054	1.9
889	propyl acetate(1) + n-heptane(2)	131	0.0473	1.0	0.0274	0.0232	1.0
890	propyl acetate(1) + cyclohexane(2)	108	0.0462	1.9	0.0431	0.0037	1.9
891	methyl acetate(1) + n-pentane(2)	30	0.0915	2.5	0.1163	-0.0294	2.5
892	methyl acetate(1) + hexane(2)	19	0.0607	0.3	0.1349	-0.0833	0.3
893	methyl acetate(1) + n-heptane(2)	25	0.0744	1.3	0.0442	0.0368	1.0
894	methyl acetate(1) + cyclohexane(2)	31	0.0937	1.3	0.1174	-0.0287	1.3
895	vinyl acetate(1) + hexane(2)	31	0.0660	1.4	0.1260	-0.0735	1.3
896	vinyl acetate(1) + cyclohexane(2)	11	0.0802	0.7	0.0966	-0.0201	0.7
897	vinyl acetate(1) + n-decane(2)	44	0.0553	3.8	0.0693	-0.0157	3.8
898	hexane(1) + tetrachloroethylene(2)	6	-0.0109	0.7	0.0063	-0.0195	0.5
899	tetrachloroethylene(1) + n-heptane(2)	27	-0.0268	1.7	-0.0599	0.0384	1.7
900	cyclohexane(1) + tetrachloroethylene(2)	108	-0.0025	2.6	-0.0289	0.0281	2.6
901	tetrachloroethylene(1) + cyclopentane(2)	15	0.0067	1.0	-0.0361	0.0474	1.0
902	Vinyl chloride(1) + hexane(2)	46	0.0202	3.5	0.0295	-0.0104	3.5
903	Trichloethylene(1) + hexane(2)	15	-0.0146	1.4	0.0179	-0.0379	1.2
904	Trichloethylene(1) + cyclohexane(2)	27	-0.0011	1.8	-0.0206	0.0229	1.8
905	dichloromethane(1) + 1-butene(2)	16	-0.0001	1.6	-0.0563	0.0701	1.6
906	diisobutylene(1) + butylchloride(2)	96	-0.0402	6.4	-0.0317	-0.0095	6.4
907	water(1) + 1,4-dioxane(2)	517	-0.1706	17.6	-0.0266	-0.1172	14.7
908	furfural(1) + water(2)	231	-0.0286	15.1	-0.1080	0.0752	14.8
909	ethyl acetate(1) + water(2)	18	-0.2693	6.0	-0.0702	-0.1534	6.0
910	benzene(1) + water(2)	56	-0.1729	13.4	-0.2118	0.0314	13.4
911	water(1) + 1-butanol(2)	46	-0.1597	13.3	0.0312	-0.1586	8.6
912	hexane(1) + water(2)	6	-0.1200	14.7	0.0312	-0.1586	14.7
913	propyl acetate(1) + water(2)	42	-0.2997	10.7	-0.0373	-0.1878	9.6
914	Trimethylamine(1) + water(2)	83	-0.4389	20.4	-0.1781	-0.1844	16.8
915	acrylonitrile(1) + water(2)	31	-0.2294	13.8	-0.0426	-0.1499	8.5
916	1-propanol(1) + water(2)	28	-0.1171	6.2	0.0589	-0.1641	2.9

Appendix B

VOLUME-TRANSLATED PENG-ROBINSON EQUATION OF STATE FOR LIQUID DENSITIES OF DIVERSE BINARY MIXTURES

Table B.1. Binary VLE Database for the Systems Used in PR EOS

System	Temperature Range (K)	Pressure Range (bar)	Compound (1) Mole Fraction Range	NDP	Ref.
CO_2(1)+Water(2)	278.15–293.15	64.4–294.9	0.025-0.0331	24	[38]
CO_2(1)+Water(2)	288.15–298.15	6.08–20.27	0.0244-0.0301	25	[39]
CO_2(1)+Water(2)	352.85–393.4	21.1–101.8	0.0034-0.0166	18	[40]
CO_2(1)+Water(2)	332.15	33.4-198.9	0.00946-0.0249	6	[41]
CO_2(1)+Butane(2)	311.1-394.6	3.57-80.61	0.0108-0.8866	101	[155]
CO_2(1)+Butane(2)	319.3-377.6	21.8-80.8	0.088-0.873	51	[156]
CO_2(1)+Butane(2)	283.1	3.578-41.334	0.0296-0.9254	10	[43]
CO_2(1)+Isobutane(2)	310.9-394.3	5.03-48.33	0.0251-0.8845	32	[44]
CO_2(1)+Decane(2)	344.3-377.6	63.845-164.65	0.457-0.925	45	[45]
CO_2(1)+Decane(2)	344.3	13.8-127.1	0.108-0.935	28	[157]
Methanol(1)+Water(2)	340.1-366.1	1.0132	0.0531-0.8741	20	[158]
Methanol(1)+Water(2)	337.9-372.6	1.0132	0.0028-0.9869	29	[159]
Methanol(1)+Water(2)	337.8-369.6	1.0132	0.0321-0.996	32	[160]
Methanol(1)+Water(2)	337.8-372.6	1.0132	0.0017-0.9885	34	[161]
Methanol(1)+Water(2)	413.1	5.0956-10.585	0.096-0.946	6	[162]
Methanol(1)+Water(2)	338.1	0.3903-0.9696	0.0854-0.903	10	[163]
Methanol(1)+Water(2)	424.1-442.1	6.65-20.93	0.1061-0.9061	10	[51]
Methanol(1)+Water(2)	373.1-523.1	1.907-86.124	0.25-0.75	21	[151]
Methanol(1)+Water(2)	320-420	0.231-7.3	0.2034-0.8005	20	[164]
Methanol(1)+Water(2)	523.1-583.1	71.4-147	0.36	20	[165]
1-Propanol(1)+Water(2)	360.5-368.6	1	0.008-0.956	25	[166]
1-Propanol(1)+Water(2)	360.4-367.6	1	0.019-0.95	32	[167]
1-Propanol(1)+Water(2)	360.9-368.0	1.0132	0.053-0.952	18	[168]
1-Propanol(1)+Water(2)	360.3-371.9	1	0.001-0.987	26	[169]
1-Propanol(1)+Water(2)	333.1	0.2273-0.312	0.05-0.95	20	[170]
1-Propanol(1)+Water(2)	333.1	0.226-0.308	0.039-0.95	18	[171]
1-Propanol(1)+Water(2)	329.8-338.7	0.2666	0.003-0.73	11	[172]

Table B.1. Binary VLE Database for the Systems Used in PR EOS *(Continued)*

System	Temperature Range (K)	Pressure Range (bar)	Compound (1) Mole Fraction Range	NDP	Ref.
1-Propanol(1)+Water(2)	323.1-352.9	0.1617-0.7313	0.0856-0.8201	18	[173]
2-Propanol(1)+Water(2)	423-473	5.171-28.062	0.004-0.934	37	[174]
2-Propanol(1)+Water(2)	353.3-356.6	1.013	0.082-0.911	10	[175]
2-Propanol(1)+Water(2)	393.6-414.1	4.115	0.006-0.9845	15	[176]
Butanol(1)+Water(2)	365.6-390.5	1.013	0.005-0.989	17	[177]
Butanol(1)+Water(2)	365.9-384.6	1.01	0.001-0.961	25	[178]
Butanol(1)+Water(2)	366.1-372.3	1.0132	0.0042-0.844	21	[179]
Isobutanol(1)+Water(2)	362.8-411	1.0132	0.0076-0.9582	82	[180]
Isobutanol(1)+Water(2)	362.1-372.1	1.01	0.002-9.865	38	[181]
Pentanol(1)+Water(2)	367.8-373	1.008	0.0075-0.015	5	[182]
Ammonia(1)+Water(2)	403.1-503.1	19-57.5	0.076-0.696	18	[183]
Ammonia(1)+Water(2)	372.4-373.2	1.013	0.000009 -0.00198	12	[184]
Ammonia(1)+Water(2)	363.9-420.1	1.0132-4.481	0.00094-0.04248	23	[185]
Ammonia(1)+Water(2)	303.2-443.2	10.13	0.036-0.876	15	[186]
Ammonia(1)+Water(2)	313.1-360.0	0.312-42.019	0.1016-0.8952	25	[187]
Ammonia(1)+Water(2)	313.1-519.3	0.0738-217.85	0.0092-0.9885	214	[188]
Acetone(1)+Hexane(2)	308.1-328.1	0.4421-1.2068	0.0862-0.909	27	[189]
Acetone(1)+Hexane(2)	268.1-293.1	0.07773-0.319	0.0839-0.9768	25	[190]
Acetone(1)+Hexane(2)	253.2-318.1	0.03285-0.8527	0.0822-0.9658	22	[191]
Acetone(1)+Hexane(2)	322.7-340.1	1.0132	0.0106-0.995	24	[192]
Acetone(1)+Pentane(2)	238.2-298.1	0.0382-0.7782	0.0713-0.9906	31	[190]
Acetone(1)+Pentane(2)	372.7-422.6	4.781-16.358	0.044-0.956	27	[193]
Acetone(1)+Pentane(2)	305.1-318.9	1.013	0.047-0.939	7	[194]
Acetone(1)+Heptane(2)	328.3-337.6	0.997-1.03	0.202-0.886	6	[195]
Acetone(1)+Heptane(2)	313.1	0.2623-0.57545	0.0569-0.9496	14	[196]
Acetone(1)+Heptane(2)	338	0.775-1.3745	0.118-0.867	8	[197]
Acetone(1)+Heptane(2)	329.4-360.1	1.01	0.0422-0.8937	9	[198]
Acetone(1)+Octane(2)	313.1	0.4538-0.5535	0.3513-0.9417	16	[196]
Acetone(1)+Nonane(2)	313.1	0.36705-0.5660	0.2241-0.9462	20	[196]
Acetone(1)+Nonane(2)	302.2-324.5	0.292-0.8566	0.281-0.9733	16	[199]
Acetone(1)+Decane(2)	313.1-333.1	0.3116-0.9897	0.2355-0.7322	22	[200]
Acetone(1)+Decane(2)	338.1	0.85166-1.3419	0.345-0.985	9	[201]
Acetone(1)+Decane(2)	321.1	0.2306-0.7433	0.13-0.9956	23	[202]
Acetone(1)+Benzene(2)	329.3-353.3	1.013	0.139-0.883	21	[203]

Table B.1. Binary VLE Database for the Systems Used in PR EOS *(Continued)*

System	Temperature Range (K)	Pressure Range (bar)	Compound (1) Mole Fraction Range	NDP	Ref.
Acetone(1)+Benzene(2)	328.9-352.6	0.987	0.1857-0.9624	35	[204]
Acetone(1)+Benzene(2)	373-544.7	2.1106-46.5994	0.093-0.872	159	[205]
Acetone(1)+Toluene(2)	318-328	0.1349-0.91783	0.0356-0.9257	30	[206]
Acetone(1)+Toluene(2)	318.1	0.0989-0.6824	0.0125-0.961	20	[207]
Acetone(1)+Toluene(2)	329.9-381.1	1.01	0.01-0.981	28	[208]
Acetone(1)+Toluene(2)	346.6-350.6	1.0132	0.361-0.393	6	[209]
Acetone(1)+Toluene(2)	329.6-382.6	1.002	0.1499-0.8999	8	[210]
Acetone(1)+Sulfur dioxide(2)	293-313	0.2563-0.924	0.7098-0.9675	22	[211]
Acetone(1)+Water(2)	329.2-373.1	1.0132	0.0006-0.9995	31	[212]
R11(1)+R12(2)	253.2-323.1	0.28-10.83	0.052-0.935	47	[213]
R11(1)+R22(2)	298.1-323.1	3.1-19.5	0.1296-0.8432	16	[214]
R12(1)+R114(2)	253.2-313.1	0.57-8.96	0.061-0.882	25	[215]
R12(1)+R114(2)	277.6-372.3	3.5-14.5	0.087-0.945	40	[85]
R12(1)+R32(2)	283	4.204-11.362	0.0282-0.9195	16	[216]
R32(1)+R125(2)	204.8-345.5	0.3824-50.49	0.2414-0.9512	74	[217]
R32(1)+R125(2)	303.9-323.8	18.357-29.59	0.4161-0.8807	44	[92]
R32(1)+R125(2)	303.1-323.1	15.73-31.4	0.2128-0.9678	17	[218]
R32(1)+R125(2)	273.1-318.1	6.9-27.71	0.055-0.895	21	[219]
R32(1)+R125(2)	280-310.0	8.84-23.05	0.2042-0.9021	24	[220]
R32(1)+R134a(2)	202.9-368.9	0.1482-54.19	0.2124-0.7719	106	[217]
R32(1)+R134a(2)	313.1-350.1	13.76-28.48	0.034-0.829	28	[221]
R32(1)+R134a(2)	273.1-363.4	3.1-48.1	0.041-0.881	45	[219]
R32(1)+R134a(2)	263.1-323.1	1.997-31.361	0.2079-0.7599	35	[222]
R32(1)+R143a(2)	303.1-323.1	14.38-31.5	0.1188-0.9592	16	[218]
R32(1)+R143a(2)	256	3.505-4.592	0.074-0.902	13	[223]
R32(1)+R143a(2)	263.1-313.1	4.501-24.81	0.0996-0.8858	60	[224]
R32(1)+R143a(2)	280-320	7.64-22.93	0.2483-0.7497	34	[95]
R125(1)+R134a(2)	303.8-363.1	9.2-39.2	0.045-0.871	48	[221]
R125(1)+R134a(2)	263.1-303.1	2.01-15.73	0.1786-0.8136	35	[224]
R125(1)+R134a(2)	268.1-293.1	2.54-11.58	0.032-0.944	29	[219]
R125(1)+R143a(2)	280-320	7.62-22.15	0.00007-0.7369	38	[225]
R125(1)+R143a(2)	280-321	7.74-23.11	0.0726-0.8631	32	[96]
Ethane(1)+Propane(2)	240.4-354.6	2.96-50.1	0.069-0.782	94	[98]
Ethane(1)+Propane(2)	303.1	10.822-46.64	0.0245-0.9947	22	[226]

Table B.1. Binary VLE Database for the Systems Used in PR EOS *(Continued)*

System	Temperature Range (K)	Pressure Range (bar)	Compound (1) Mole Fraction Range	NDP	Ref.
Propane(1)+Butane(2)	270.0-310	1.426-7.206	0.1692-0.8704	17	[227]
Propane(1)+Isobutane(2)	266.5-394.3	1.2342-41.71	0.00095-0.9839	80	[228]
Propane(1)+Pentane(2)	344.3-444.3	4.14-44.82	0.013-0.962	66	[229]
Propane(1)+Pentane(2)	336.6-383.1	3.344-38.828	0.055-0.982	79	[230]
Propane(1)+Hexane(2)	348.1-495.4	4.497-49.802	0.144-0.922	74	[104]
Propane(1)+Propylene(2)	260.9-360.9	3.247-42.83	0.153-0.825	74	[231]
Propane(1)+Propylene(2)	244-310	1.758-14.905	0.167-0.9999	60	[105]
Butane(1)+Decane(2)	310.9-510.9	0.00503-49.229	0.0324-0.9751	72	[106]
Isobutane(1)+Butane(2)	273.1	1.0872-1.5345	0.0895-0.9321	24	[232]
Pentane(1)+Cyclohexane(2)	309.2-353.9	1.0132	0.008-0.876	32	[233]
Pentane(1)+Cyclohexane(2)	407.3-520.7	10.342-34.474	0.197-0.793	20	[234]
Hexane(1)+Heptane(2)	287.1-371.8	0.123-1.013	0.1144-0.9128	66	[235]
Hexane(1)+Octane(2)	287.1-397.4	0.123-1.014	0.1284-0.9227	66	[235]
Hexane(1)+Decane(2)	308.1	0.02828-0.2757	0.0846-0.9028	12	[236]
Hexane(1)+Cyclohexane(2)	342-353.9	1.0132	0.008-0.969	36	[233]
Heptane(1)+Octane(2)	312.6-397.4	0.123-1.013	0.1124-0.9112	66	[235]
Cyclohexane(1)+Octane(2)	355.2-396.3	1.0132	0.0372-0.9491	28	[237]
Cyclohexane(1)+Octane(2)	298.1-328.1	0.03656-0.4146	0.1526-0.9226	32	[238]
Cyclohexane(1)+Nonane(2)	333.1-353.2	0.118-0.922	0.103-0.901	11	[110]
Cyclohexane(1)+Heptane(2)	354.8-369.3	1.0132	0.107-0.919	17	[239]
Cyclohexane(1)+Heptane(2)	354.3-371.1	1.0132	0.016-0.973	25	[233]
Benzene(1)+Methanol(2)	331.1-351	1.01	0.0051-0.998	45	[240]
Benzene(1)+Butanol(2)	353.2-388	1.01	0.0026-0.9846	30	[241]
Benzene(1)+Isobutanol(2)	352.9-376.6	1.01	0.042-0.962	10	[242]
Benzene(1)+Isobutanol(2)	352.6-411.3	0.9807-3.4324	0.062-0.947	173	[243]
Benzene(1)+Pentanol(2)	353.2-409.3	1.01	0.0103-0.9684	39	[241]
Benzene(1)+Pentane(2)	308-323	0.27598-1.2775	0.1-0.9686	53	[244]
Benzene(1)+Pentane(2)	309.2-353.3	1.01	0.024-0.994	42	[245]
Benzene(1)+Hexane(2)	341.9-352.6	1.0132	0.018-0.976	29	[246]
Benzene(1)+Hexane(2)	363.1-463.1	1.475-15.106	0.0898-0.9613	60	[247]
Benzene(1)+Heptane(2)	353.3-371.6	1.0132	0.088-0.985	36	[239]
Benzene(1)+Heptane(2)	353.4-371.3	1.01	0.0085-0.986	36	[245]
Benzene(1)+Octane(2)	358.1-393.1	1.01	0.062-0.796	24	[248]
Benzene(1)+Octane(2)	328-348	0.16879-0.8378	0.1833-0.957	67	[249]
Benzene(1)+Methylcyclohexane(2)	353.4-368.6	1.013	0.138-0.9815	24	[250]

Table B.1. Binary VLE Database for the Systems Used in PR EOS *(Continued)*

System	Temperature Range (K)	Pressure Range (bar)	Compound (1) Mole Fraction Range	NDP	Ref.
Benzene(1)+Toluene(2)	355.3-382.3	1.01	0.0374-0.9148	16	[251]
Benzene(1)+Toluene(2)	353.3-383.8	1.01	0.042-0.941	17	[252]
Methane(1)+Ethane(2)	260-280	17.02-62.92	0.007-0.4615	40	[253]
Methane(1)+Ethane(2)	140-270.1	4.908-66.263	0.0504-0.9408	15	[135]
Methane(1)+Propane(2)	277.6-360.9	5.447-99.973	0.0049-0.6891	127	[254]
Methane(1)+Butane(2)	294.3-394.3	2.16-131	0.0029-0.7152	120	[229]
Methane(1)+Isobutane(2)	151.4-251.4	10.65-83.78	0.5494-0.9223	10	[255]
Methane(1)+Pentane(2)	310.9-411	6.93-161	0.0224-0.7124	56	[256]
Methane(1)+Hexane(2)	348.1	22.7-115.6	0.0901-0.3996	10	[141]
Methane(1)+Cyclohexane(2)	294.3-444.3	4.275-275.79	0.0148-0.735	95	[142]
Methane(1)+Carbon monoxide(2)	113.7-185.9	6.895-49.642	0.384-0.9829	20	[257]
Methane(1)+Nitrogen(2)	105.3-184.2	10.34-44.82	0.0485-0.9389	72	[152]
Nitrogen(1)+Ethane(2)	150-270	5.597-101.04	0.0236-0.3581	36	[135]
Nitrogen(1)+Ethane(2)	150-271	10.12-101.04	0.0305-0.3581	14	[145]
Nitrogen(1)+Butane(2)	311.1-344.4	7.77-130.6	0.004-0.2678	28	[146]
Nitrogen(1)+Cyclohexane(2)	366.3-410.9	17.99-275.93	0.0169-0.2906	18	[147]
Nitrogen(1)+Methanol(2)	298	253.3-755.9	0.0534-0.123	11	[148]
Nitrogen(1)+Ammonia(2)	277-394	5.054-308.42	0.0422-0.9395	50	[258]
Nitrogen(1)+CO_2(2)	288.1-301.1	50.66-101.33	0.025-0.161	23	[259]
Overall Statistics				**5298**	

Table B.2. Summary Results for PR EOS Bubble-point Pressure Representations: Systems Containing CO_2

System	NDP	Binary Interaction Parameters (BIPs) (C_{ij}, D_{ij})		% AAD in Bubble Pressure	
		C_{ij}	D_{ij}	No BIPs*	With BIPs**
CO_2(1)+Water(2)	24	0.00106*T- 0.08943	-0.2	17	4.5
CO_2(1)+Water(2)	25			59	6.2
CO_2(1)+Water(2)	18			63	7.2
CO_2(1)+Water(2)	6			68	7.7
CO_2(1)+Butane(2)	101	0.1433	0	13	3.5
CO_2(1)+Butane(2)	51			26	2.0
CO_2(1)+Butane(2)	10			25	4.3
CO_2(1)+Isobutane(2)	32	0.12	0	8	1.5
CO_2(1)+Decane(2)	45	0.096	0	8	1.9
CO_2(1)+Decane(2)	28			15	3.9
Overall Statistics	**340**			**22**	**3.5**

* No BIPs: $C_{ij} = D_{ij} = 0$ ** With BIPs: C_{ij} = Constant or C_{ij} (T), D_{ij}=0 or Constant

Table B.3. Summary Results of PR EOS Bubble-point Pressure Representations: Systems Containing Mixtures of Alcohols or Ammonia with Water

System	NDP	Binary Interaction Parameters (BIPs) (C_{ij}= Constant, D_{ij}=0)	%AAD in Bubble Pressure	
		C_{ij}	No BIPs	With BIP
Methanol(1)+Water(2)	20	-0.066	53	4.5
Methanol(1)+Water(2)	29		36	3.6
Methanol(1)+Water(2)	32		58	5.5
Methanol(1)+Water(2)	34		40	3.3
Methanol(1)+Water(2)	6		23	3.3
Methanol(1)+Water(2)	10		60	5.4
Methanol(1)+Water(2)	5		25	4.9
Methanol(1)+Water(2)	5		14	2.0
Methanol(1)+Water(2)	21		19	4.8
Methanol(1)+Water(2)	20		36	3.7
Methanol(1)+Water(2)	20		30	1.7
1-Propanol(1)+Water(2)	25	-0.11	87	6.3
1-Propanol(1)+Water(2)	32		77	6.7
1-Propanol(1)+Water(2)	18		86	5.6
1-Propanol(1)+Water(2)	26		88	5.8
1-Propanol(1)+Water(2)	20		67	5.8
1-Propanol(1)+Water(2)	18		78	5.1
1-Propanol(1)+Water(2)	11		77	5.6
1-Propanol(1)+Water(2)	9		74	5.0
1-Propanol(1)+Water(2)	9		67	3.9
2-Propanol(1)+Water(2)	18	-0.13	86	5.8
2-Propanol(1)+Water(2)	19		76	6.6
2-Propanol(1)+Water(2)	10		65	5.9
2-Propanol(1)+Water(2)	15		85	7.2
Butanol(1)+Water(2)	17	-0.135	77	5.1
Butanol(1)+Water(2)	25		86	6.4
Butanol(1)+Water(2)	21		65	5.2
Isobutanol(1)+Water(2)	82	-0.16	75	6.0
Isobutanol(1)+Water(2)	38		88	5.2
Pentanol(1)+Water(2)	5	-0.17	55	3.6

Table B.3. Summary Results of PR EOS Bubble-point Pressure Representations: Systems Containing Mixtures of Alcohols or Ammonia with Water *(Continued)*

System	NDP	Binary Interaction Parameters (BIPs) (C_{ij}= Constant, D_{ij}=0)	% AAD in Bubble Pressure	
		C_{ij}	No BIPs	With BIP
Ammonia(1)+Water(2)	18	-0.265	63	5.9
Ammonia(1)+Water(2)	12		15	5.1
Ammonia(1)+Water(2)	23		88	6.4
Ammonia(1)+Water(2)	15		60	4.2
Ammonia(1)+Water(2)	25		72	1.9
Ammonia(1)+Water(2)	214		88	5.2
Overall Statistics	**927**		**71**	**5**

Table B.4. Summary Results of PR EOS Bubble-point Pressure Representations: Systems Containing Acetone

System	NDP	Binary Interaction Parameters (BIPs) (C_{ij}= Constant, D_{ij}=0)	%AAD in Bubble Pressure	
		C_{ij}	No BIPs	With BIP
Acetone(1)+Pentane(2)	31	0.1	32	5.5
Acetone(1)+Pentane(2)	27		17	2.2
Acetone(1)+Pentane(2)	7		28	2.4
Acetone(1)+Hexane(2)	27	0.093	26	2.8
Acetone(1)+Hexane(2)	25		28	2.9
Acetone(1)+Hexane(2)	22		26	4.3
Acetone(1)+Hexane(2)	24		21	3.0
Acetone(1)+Heptane(2)	6	0.088	26	4.4
Acetone(1)+Heptane(2)	14		28	4.2
Acetone(1)+Heptane(2)	8		25	2.8
Acetone(1)+Heptane(2)	9		24	3.7
Acetone(1)+Octane(2)	16	0.075	15	1.7
Acetone(1)+Nonane(2)	20	0.07	23	3.3
Acetone(1)+Nonane(2)	16		15	4.2
Acetone(1)+Decane(2)	22	0.066	28	4.4
Acetone(1)+Decane(2)	9		16	2.0
Acetone(1)+Decane(2)	23		21	4.9
Acetone(1)+Benzene(2)	21	0.018	6	1.8
Acetone(1)+Benzene(2)	35		4	0.8
Acetone(1)+Benzene(2)	159		10	1.5
Acetone(1)+Toluene(2)	30	0.04	11	2.2
Acetone(1)+Toluene(2)	20		15	2.0
Acetone(1)+Toluene(2)	28		11	1.9
Acetone(1)+Toluene(2)	6		15	2.4
Acetone(1)+Toluene(2)	8		7	2.8
Acetone(1)+Sulfur dioxide(2)	22	-0.1663	84	1.4
Acetone(1)+Water(2)	31	-0.237	76	2.9
Overall Statistics	**666**		**22**	**3**

Table B.5. Summary Results of PR EOS Bubble-point Pressure Representations: Systems Containing Refrigerants

System	NDP	Binary Interaction Parameters (BIPs) (C_{ij}= Constant, D_{ij}=0)	%AAD in Bubble Pressure	
		C_{ij}	No BIPs	With BIP
R11(1)+R12(2)	47	0.0092	3.1	2.0
R11(1)+R22(2)	16	0.0459	9	1.4
R12(1)+R114(2)	25	0.005	2.5	1.7
R12(1)+R114(2)	40		2.2	2.1
R12(1)+R32(2)	16	0.1279	15	2.0
R32(1)+R125(2)	74	0.001	0.79	0.79
R32(1)+R125(2)	44		1.34	1.32
R32(1)+R125(2)	17		0.36	0.31
R32(1)+R125(2)	21		1.52	1.44
R32(1)+R125(2)	24		0.33	0.25
R32(1)+R134a(2)	106	-0.002	0.6	0.5
R32(1)+R134a(2)	28		1.6	1.5
R32(1)+R134a(2)	45		2.0	1.7
R32(1)+R134a(2)	35		1.5	1.3
R32(1)+R143a(2)	16	0.009	1.1	1.1
R32(1)+R143a(2)	13		2.7	1.3
R32(1)+R143a(2)	60		1.4	0.6
R32(1)+R143a(2)	34		1.3	0.7
R125(1)+R134a(2)	48	-0.003	1.3	1.1
R125(1)+R134a(2)	35		0.6	0.3
R125(1)+R134a(2)	29		0.7	0.4
R125(1)+R143a(2)	38	-0.014	2.0	0.5
R125(1)+R143a(2)	32		1.6	0.6
Overall Statistics	**843**		**1.8**	**1.0**

Table B.6. Summary Results of PR EOS Bubble-point Pressure Representations: Systems Containing Alkanes and/or Cycloalkanes

System	NDP	Binary Interaction Parameters (BIPs) (C_{ij}= Constant, D_{ij}=0)	%AAD in Bubble Pressure	
		C_{ij}	No BIPs	With BIP
Ethane(1)+Propane(2)	94	0.009	1.9	1.3
Ethane(1)+Propane(2)	22		0.9	0.8
Propane(1)+Butane(2)	17	0.0003	1.7	1.7
Propane(1)+Isobutane(2)	80	-0.007	1.5	1.0
Propane(1)+Pentane(2)	66	0.022	3.8	1.0
Propane(1)+Pentane(2)	79		3.7	1.1
Propane(1)+Hexane(2)	74	0.003	1.9	0.9
Propane(1)+Propylene(2)	74	0.008	1.2	0.5
Propane(1)+Propylene(2)	60		2.4	1.1
Butane(1)+Decane(2)	72	0.0078	2.4	1.5
Isobutane(1)+Butane(2)	24	-0.0021	0.5	0.2
Pentane(1)+Cyclohexane(2)	32	-0.002	0.9	0.5
Pentane(1)+Cyclohexane(2)	20		1.1	1.1
Hexane(1)+Heptane(2)	66	-0.009	2.9	1.3
Hexane(1)+Octane(2)	66	-0.0405	11	2.7
Hexane(1)+Decane(2)	12	-0.0043	2.4	0.8
Hexane(1)+Cyclohexane(2)	36	-0.008	2.3	0.8
Heptane(1)+Octane(2)	66	-0.002	1.8	1.3
Cyclohexane(1)+Octane(2)	28	-0.015	4.9	0.9
Cyclohexane(1)+Octane(2)	32		5.9	1.9
Cyclohexane(1)+Nonane(2)	11	0.0221	6.8	2.9
Cyclohexane(1)+Heptane(2)	17	-0.012	3.3	0.5
Cyclohexane(1)+Heptane(2)	25		2.6	0.5
Overall Statistics	**1073**		**3.0**	**1.2**

Table B.7. Summary Results of PR EOS Bubble-point Pressure Representations: Systems Containing Benzene

System	NDP	Binary Interaction Parameters (BIPs) (C_{ij}= Constant, D_{ij}=0)	% AAD in Bubble Pressure	
		C_{ij}	No BIPs	With BIP
Benzene(1)+Methanol(2)	45	0.0917	18	4.3
Benzene(1)+Butanol(2)	30	0.0755	18	1.3
Benzene(1)+Isobutanol(2)	10	0.078	15	1.8
Benzene(1)+Isobutanol(2)	173		19	2.7
Benzene(1)+Pentanol(2)	39	0.0552	14	1.9
Benzene(1)+Pentane(2)	53	0.0125	4.4	1.1
Benzene(1)+Pentane(2)	42		2.6	0.7
Benzene(1)+Hexane(2)	29	-0.002	1.2	1.1
Benzene(1)+Hexane(2)	60		1.5	1.4
Benzene(1)+Heptane(2)	36	-0.003	0.9	0.7
Benzene(1)+Heptane(2)	36		1.4	0.8
Benzene(1)+Octane(2)	24	-0.009	3.8	1.1
Benzene(1)+Octane(2)	67		2.9	1.2
Benzene(1)+ Methylcyclohexane(2)	24	0.0113	2.9	0.7
Benzene(1)+Toluene(2)	16	-0.006	2.1	0.7
Benzene(1)+Toluene(2)	17		1.5	0.8
Overall Statistics	**701**		**9.0**	**1.7**

Table B.8. Summary Results of PR EOS Bubble-point Pressure Representations: Systems Containing Methane or Nitrogen

System	NDP	Binary Interaction Parameters (BIPs) (C_{ij}= Constant, D_{ij}=0)	% AAD in Bubble Pressure	
		C_{ij}	No BIPs	With BIP
Methane(1)+Ethane(2)	40	0.0108	1.0	0.8
Methane(1)+Ethane(2)	15		2.5	0.9
Methane(1)+Propane(2)	127	0.0205	2.6	0.9
Methane(1)+Butane(2)	120	0.023	3.4	1.3
Methane(1)+Isobutane(2)	10	0.01	2.9	1.4
Methane(1)+Pentane(2)	56	0.018	3.7	1.6
Methane(1)+Hexane(2)	10	0.023	8.1	1.3
Methane(1)+Cyclohexane(2)	95	0.0285	8.3	3.0
Methane(1)+Carbon monoxide(2)	20	0.023	3.3	1.3
Methane(1)+Nitrogen(2)	72	0.041	6.0	1.3
Nitrogen(1)+Ethane(2)	36	0.051	11.5	3.0
Nitrogen(1)+Ethane(2)	14		12.5	3.0
Nitrogen(1)+Butane(2)	28	0.0791	12.4	2.0
Nitrogen(1)+Cyclohexane(2)	18	0.094	15.8	2.7
Nitrogen(1)+Methanol(2)	11	-0.1587	4.7	1.0
Nitrogen(1)+Ammonia(2)	50	-0.42	9.6	1.3
Nitrogen(1)+CO_2(2)	23	-0.027	1.0	0.6
Overall Statistics	**745**		**5.6**	**1.6**

VITA

Agelia M. Abudour

Candidate for the Degree of

Doctor of Philosophy

Thesis: DEVELOPMENT OF A PREDICTIVE EQUATION OF STATE FOR EQUILIBRIUM AND VOLUMETRIC PROPERTIES OF DIVERSE MOLECULES AND THEIR MIXTURES

Major Field: Chemical Engineering

Biographical:

Education:

Completed the requirements for the Doctor of Philosophy in Chemical Engineering at Oklahoma State University, Stillwater, Oklahoma in December/2014.

Completed the requirements for the Master of Science in Chemical Engineering at Tripoli University, Tripoli, Libya in 2007.

Completed the requirements for the Bachelor of Science in Chemical Engineering at Alzawia University, Subrata, Libya in 2001.

Experience:

- Research Assistant, Oklahoma State University, Stillwater, Oklahoma, June 2010 – December 2014
- Instructor, Tripoli University, Tripoli, Libya, June 2007 – June 2008
- Teaching Assistant, Tripoli University, Tripoli, Libya, January 2004 – June 2006
- Graduate Assistant, Tripoli University, Tripoli, Libya, January 2002 – June 2004

Professional Memberships:

- American Institute of Chemical Engineers (AIChE), 2010-Present